Lecture Notes in Civil Engineering

Krishna R. Reddy
P. T. Ravichandran
R. Ayothiraman
Anil Joseph *Editors*

Recent Advances in Civil Engineering

Select Proceedings of ICC-IDEA 2023

Springer

Lecture Notes in Civil Engineering

Volume 398

Lecture Notes in Civil Engineering (LNCE) publishes the latest developments in Civil Engineering—quickly, informally and in top quality. Though original research reported in proceedings and post-proceedings represents the core of LNCE, edited volumes of exceptionally high quality and interest may also be considered for publication. Volumes published in LNCE embrace all aspects and subfields of, as well as new challenges in, Civil Engineering. Topics in the series include:

- Construction and Structural Mechanics
- Building Materials
- Concrete, Steel and Timber Structures
- Geotechnical Engineering
- Earthquake Engineering
- Coastal Engineering
- Ocean and Offshore Engineering; Ships and Floating Structures
- Hydraulics, Hydrology and Water Resources Engineering
- Environmental Engineering and Sustainability
- Structural Health and Monitoring
- Surveying and Geographical Information Systems
- Indoor Environments
- Transportation and Traffic
- Risk Analysis
- Safety and Security.

To submit a proposal or request further information, please contact the appropriate Springer Editor:

– Pierpaolo Riva at pierpaolo.riva@springer.com (Europe and Americas);
– Swati Meherishi at swati.meherishi@springer.com (Asia—except China, Australia, and New Zealand);
– Wayne Hu at wayne.hu@springer.com (China).

All books in the series now indexed by Scopus and EI Compendex database!

Krishna R. Reddy · P. T. Ravichandran ·
R. Ayothiraman · Anil Joseph
Editors

Recent Advances in Civil Engineering

Select Proceedings of ICC-IDEA 2023

Springer

Editors
Krishna R. Reddy
University of Illinois
Chicago, USA

P. T. Ravichandran
SRM Institute of Science and Technology
Kattankulathur, India

R. Ayothiraman
Indian Institute of Technology Delhi
New Delhi, India

Anil Joseph
Geostructurals Pvt. Ltd
Cochin, Kerala, India

ISSN 2366-2557 ISSN 2366-2565 (electronic)
Lecture Notes in Civil Engineering
ISBN 978-981-99-6228-0 ISBN 978-981-99-6229-7 (eBook)
https://doi.org/10.1007/978-981-99-6229-7

Preface

I am delighted to present to you the book "Recent Advances in Civil Engineering." As the editor of this compilation, it gives me immense pleasure to share with you the latest advancements and breakthroughs in the field of civil engineering.

Civil engineering plays a crucial role in shaping our modern world. It encompasses a wide range of disciplines, from structural engineering to geotechnical engineering, transportation systems, environmental engineering, and beyond. This book aims to provide a comprehensive overview of the recent developments and innovations within these areas.

The field of civil engineering is constantly evolving, driven by new technologies, materials, and methodologies. This book brings together a collection of chapters contributed by leading experts and researchers who have made significant contributions to their respective areas of specialization. Their insightful and thought-provoking work provides valuable insights into the current trends and future directions of civil engineering.

Throughout the pages of this book, you will find a diverse range of topics covered, including but not limited to sustainable construction practices, advanced materials in structural engineering, smart transportation systems, resilient infrastructure design, and innovative approaches to environmental conservation. The chapters offer a blend of theoretical analysis, practical case studies, and experimental findings, thus making this book a valuable resource for researchers and practitioners.

I would like to extend my deepest appreciation to all the contributors who have generously shared their knowledge and expertise in the form of chapters for this book. Their dedication and commitment to the advancement of the field of civil engineering are commendable. I am grateful for their valuable contributions that have enriched this publication.

I would also like to express my gratitude to the editorial and publishing team for their support and professionalism throughout the production process. Their efforts have been instrumental in ensuring this book's high quality and coherence.

Finally, I extend my heartfelt gratitude to you, the reader. By choosing to explore "Recent Advances in Civil Engineering," you demonstrate your commitment to staying up to the latest developments in the field. I hope this book serves as a valuable resource, inspiring new ideas and fostering innovation in civil engineering practices.

Thank you for joining me on this exciting journey into the world of recent advances in civil engineering. The knowledge shared within these pages will contribute to the progress and growth of the field, ultimately benefiting society as a whole.

New Delhi, India Dr. P. T. Ravichandran

Contents

Editors and Contributors

About the Editors

Dr. Krishna R. Reddy is University Scholar, Distinguished Researcher, and Professor of Civil and Environmental Engineering, Director of both the Sustainable Engineering Research Laboratory (SERL) and the Geotechnical and Geo-Environmental Engineering Laboratory (GAGEL) in the Department of Civil, Materials, and Environmental Engineering (CME) at the University of Illinois at Chicago (UIC). He has received Ph.D. in Civil Engineering from the Illinois Institute of Technology, Chicago. He has over 28 years of research, teaching, and consulting experience in civil, geotechnical, materials, environmental, and sustainable/resilient engineering, addressing the nexus of sustainability, resiliency, infrastructure, water, energy, and the environment. His research is funded by the US National Science Foundation, the US Environmental Protection Agency, several prominent state and local government agencies, and industries. He is Author of four books, 297 journal papers, 32 edited books/conference proceedings, and 25 chapters. He has served as Associate Editor or Editorial Board Member of over ten different journals.

Dr. P. T. Ravichandran is currently working as Professor and Head of the Department of Civil Engineering, Kattankulathur Campus, SRM Institute of Science and Technology. He graduated with B.E. (Civil) from Madurai Kamaraj University, M.E. (Soil Mechanics and Foundation Engineering), and Ph.D. from CEG, Anna University, Chennai. He actively collaborates with industry partners to apply his research to real-world projects. His research focuses are study of soils characteristics under different loading conditions, improving the design and stability of structures, and retaining structures, Bio-Geo technology, concrete technology, and sustainable construction materials. In addition to his academic pursuits, he is dedicated to mentoring and advising students interested in pursuing careers in various fields of civil engineering research. He has published over 100+ research articles in refereed journals, two patents publications, and three books. He is Fellow Member of IE (I)

and IGS. He is Founder Chairman of Institution of Engineers (I) Kattankulathur Local Centre.

Dr. R. Ayothiraman is currently working as Professor in the Department of Civil Engineering, Indian Institute of Technology Delhi. He completed his graduation in Civil Engineering from Madurai Kamaraj University and PostgGraduation from College of Engineering, Guindy, Chennai. He obtained his Ph.D. in the area of Soil Dynamics from IIT Madras. His areas of research interest include soil dynamics, pile foundations, tunneling in soils and rocks, and ground improvement. He has published around 105 papers in reputed journals and conferences. His research findings have contributed to the advancement of knowledge in the field of soil mechanics and have practical implications in the construction industry. He is Recipient of the Young Engineer Award from IE (I) and DST and DAAD Fellowship. His research is funded by several prominent state and central government agencies and industries.

Dr. Anil Joseph is Managing Director of Geostructurals (P) Ltd., a leading foundation and structural consultancy firm based at Cochin. He obtained his graduation and postgraduation in Civil Engineering from NIT, Surat. He was awarded Ph.D. from NIT, Calicut. He has provided the technical solutions in the field of foundation and structures for more than 3000 high-rise structures, including many landmark multi-storied and infrastructure projects in India and abroad in the last 30 years. He is Managing Director of CECONS (P) Ltd., a construction firm specialized in the execution of pile foundations and also Director of Engineers Diagnostic Centre (P) Ltd., a firm specialized in geotechnical investigation and retrofitting works. He owns the ICI-UltraTech award for outstanding concrete structure of Kerala in the building category in the year 2012, 2017, 2018, and 2020. He is President of the Indian Geotechnical Society and National Council Member of the Institution of Engineers (I) in Civil Division.

Contributors

K. Abhinesh Department of Civil Engineering, KPR Institute of Engineering and Technology, Coimbatore, Tamil Nadu, India

Wesam Al Agha Department of Civil Engineering, Delhi Technological University, Delhi, India;
Department of Engineering and Geology, University G. d'Annunzio of Chieti-Pescara, Pescara, Italy

G. Dheeran Amarapathi Department of Civil Engineering, Kongu Engineering College, Erode, India

S. K. Amaya Department of Civil Engineering, Faculty of Engineering and Technology, SRM Institute of Science and Technology, Kattankulathur, Tamilnadu, India

Geever Alwin Ambaden Department of Civil Engineering, School of Engineering, Cochin University of Science and Technology, Eattappilly, India

S. Anandaraj Department of Civil Engineering, KPR Institute of Engineering and Technology, Coimbatore, India

K. S. Anandh Department of Civil Engineering, Faculty of Engineering and Technology, SRM Institute of Science and Technology, Kattankulathur, Tamil Nadu, India

S. Anandh Department of Civil Engineering, Faculty of Engineering and Technology, SRM Institute of Science and Technology, Kattankulathur, Tamil Nadu, India

R. Annadurai Department of Civil Engineering, Faculty of Engineering and Technology, SRM Institute of Science and Technology, Kattankulathur, Tamil Nadu, India

M. Durai Aravindh Department of Civil Engineering, Faculty of Engineering and Technology, SRM Institute of Science and Technology, Kattankulathur, Tamil Nadu, India

S. Archana Jyothi Engineering College, Thrissur, India

A. Arokiaprakash Department of Civil Engineering, Faculty of Engineering and Technology, SRM Institute of Science and Technology, Kattankulathur, Tamil Nadu, India

A. P. Arthi Department of Civil Engineering, Faculty of Engineering and Technology, SRM Institute of Science and Technology, Kattankulathur, Tamil Nadu, India

Sujitha Arumugam Department of Civil Engineering, SRM Institute of Science and Technology, Changalpattu, Tamil Nadu, India

Md Asad Ahmad Department of Civil and Construction Engineering, National Taiwan University of Science and Technology, Taipei, Taiwan

K. Athiappan Department of Civil Engineering, Thiagarajar College of Engineering, Madurai, India

Bhaskar Babu Sree Gnanesh Civil Department, SASTRA Deemed to be University, Thanjavur, India

Aparna S. Bhaskar Department of Civil Engineering, Faculty of Engineering and Technology, SRM Institute of Science and Technology, Kattankulathur, Tamil Nadu, India

Niharika Bindal Department of Civil Engineering, Faculty of Engineering and Technology, SRM Institute of Science and Technology, Kattankulathur, Tamilnadu, India

S. Prakash Chandar Department of Civil Engineering, Easwari Engineering College, Ramapuram, Chennai, India

L. Chandrakanthamma Department of Civil Engineering, Easwari Engineering College, Ramapuram, Chennai, India

Umabharathi Chandrasekar Department of Civil Engineering, Kongu Engineering College, Perundurai, India

Ashish Chauhan Department of Civil Engineering, Faculty of Engineering and Technology, SRM Institute of Science and Technology, Kattankulathur, Tamil Nadu, India

Ashwini Chauhan Department of Civil Engineering, Faculty of Engineering and Technology, SRM Institute of Science and Technology, Kattankulathur, Tamil Nadu, India

Augustine Crispin Department of Civil Engineering, Faculty of Engineering and Technology, SRM Institute of Science and Technology, Kattankulathur, Tamil Nadu, India

M. Danish Department of Civil Engineering, Aligarh Muslim University, Aligarh, India

Surojit Das Department of Civil Engineering, Central Institute of Technology, Kokrajhar, Assam, India

D. Deepa Civil Department, SASTRA Deemed to be University, Thanjavur, India

R. Devanathan Department of Civil Engineering, Faculty of Engineering and Technology, SRM Institute of Science and Technology, Kattankulathur, Tamil Nadu, India

S. Dhansekar Department of Civil Engineering, Faculty of Engineering and Technology, SRM Institute of Science and Technology, Kattankulathur, Tamilnadu, India

K. Divya Krishnan Department of Civil Engineering, Faculty of Engineering and Technology, SRM Institute of Science and Technology, Chennai, Tamil Nadu, India

R. Anna Durai Department of Civil Engineering, Faculty of Engineering and Technology, SRM Institute of Science and Technology, Kattankulathur, Tamil Nadu, India

S. Durgadevagi Department of Civil Engineering, Faculty of Engineering and Technology, SRM Institute of Science and Technology, Tamil Nadu, Kattankulathur, India

P. Eshanthini Department of Civil Engineering, Sathyabama Institute of Science and Technology, Chennai, Tamil Nadu, India

Jeeva Ra Ga Department of Civil Engineering, SRM Institute of Science and Technology, Kattankulathur, Tamilnadu, India

Senthil kumar Ganapathy Environmental Engineering Laboratory, Annamalai University, Chidambaram, India

N. Ganapathy Ramasamy Department of Civil Engineering, Faculty of Engineering and Technology, SRM Institute of Science and Technology, Kattankulathur, Tamil Nadu, India

Anupam Ghosh Department of Civil Engineering, Faculty of Engineering and Technology, SRM Institute of Science and Technology, Kattankulathur, Tamil Nadu, India

N. Giridharan Department of Civil Engineering, College of Engineering and Technology, SRM Institute of Science and Technology, Kattankulathur, Chengalpattu, Tamil Nadu, India

Minna Gopi Krishna Civil Department, SASTRA Deemed to be University, Thanjavur, India

S. Gopinath Department of Civil Engineering, Faculty of Engineering and Technology, SRM Institute of Science and Technology, Kattankulathur, Tamil Nadu, India

D. Harish Department of Civil Engineering, SRM Institute of Science and Technology, Kattankulathur, Chengalpattu, India

S. Hariswaran Department of Civil Engineering, Sri Venkateswara College of Engineering, Sriperumbudur, India

Rajashekar Hubballi Department of Civil Engineering, Central Institute of Technology, Kokrajhar, Assam, India

B. Indhu Department of Civil Engineering, Faculty of Engineering and Technology, SRM Institute of Science and Technology, Kattankulathur, Tamil Nadu, India

Waseem Ahmad Ismaeel Department of Civil Engineering, Faculty of Engineering and Technology, SRM Institute of Science and Technology, Kattankulathur, Tamil Nadu, India

P. Jagatheswari Department of Civil Engineering, Faculty of Engineering and Technology, SRM Institute of Science and Technology, Tamil Nadu, Kattankulathur, India

V. Jaladevi Department of Civil Engineering, Puducherry Technological University, Puducherry, India

Jijo James College of Engineering Guindy, Anna University, Chennai, Tamil Nadu, India

S. Jayakumar Civil Engineering, SMVEC, Puducherry, India

R. Jino Department of Civil Engineering, Vels Institute of Science, Technology & Advanced Studies, Pallavaram, Chennai, India

N. Jothilakshmi Department of Civil Engineering, Kongu Engineering College, Perundurai, India

Priyanka Kale Project Management Division, CBRE, Pune, India

M. Kalidhas Department of Civil Engineering, College of Engineering and Technology, SRM Institute of Science and Technology, Kattankulathur, Tamil Nadu, India

Raja Kanagaraju Department of Civil Engineering, Sona College of Technology, Salem, India

P. R. Kannan Rajkumar Department of Civil Engineering, Faculty of Engineering and Technology, SRM Institute of Science and Technology, Kattankulathur, Tamil Nadu, India

Uma Maheswari Kannapiran Department of Civil Engineering, Faculty of Engineering and Technology, SRM Institute of Science and Technology, Kattankulathur, Tamil Nadu, India

S. Karunamoorthy Department of Civil Engineering, Easwari Engineering College, Chennai, India

R. Kaviraja Department of Civil Engineering, Faculty of Engineering and Technology, SRM Institute of Science and Technology, Kattankulathur, Tamil Nadu, India

R. Kavitha Department of Civil Engineering, KPR Institute of Engineering and Technology, Coimbatore, Tamil Nadu, India

Syed Mohamed Ibrahim Khutpudeen Department of Civil Engineering, Kongu Engineering College, Perundurai, India

Vineesh Kotni Civil Department, SASTRA Deemed to be University, Thanjavur, India

M. Kowsalya Department of Civil Engineering, Faculty of Engineering and Technology, SRM Institute of Science and Technology, Kattankulathur, India

V. M. V. Sai Krishna Department of Civil Engineering, College of Engineering and Technology, SRM Institute of Science and Technology, Kattankulathur, Tamilnadu, India

L. Krishnaraj Department of Civil Engineering, Faculty of Engineering and Technology, SRM Institute of Science and Technology, Kattankulathur, Tamil Nadu, India

J. Satish Kumar Department of Civil Engineering, Faculty of Engineering and Technology, SRM Institute of Science and Technology, Kattankulathur, Tamil Nadu, India

Praveen Kumar Department of Civil Engineering, Faculty of Engineering and Technology, SRM Institute of Science and Technology, Kattankulathur, Tamil Nadu, India

Vishwa Kumar Department of Civil Engineering, Kongu Engineering College, Perundurai, India

S. Manikandaprabhu Department of Civil Engineering, SRM Institute of Science and Technology, Kattankulathur, Chengalpattu, India

Asaithambi Manimaran Department of Civil Engineering, Faculty of Engineering and Technology, SRM Institute of Science and Technology, Kattankulathur, Tamil Nadu, India

A. Meenachi Department of Civil Engineering, Sona College of Technology (Anna University), Salem, Tamil Nadu, India

Krantikumar V. Mhetre Civil Engineering Department, COEP Tech University (Formerly College of Engineering Pune), Pune, Maharashtra, India

Taha Ahmed Ghaleb Mohammed Department of Civil Engineering, Cyprus International University, via Mersin 10, Haspolat, North Cyprus, Turkey

B. Mohan Kumar Sri Sivasubramaniya Nadar College of Engineering, Kalavakkam, Tamil Nadu, India

S. Mohanakrishna Department of Civil Engineering, Faculty of Engineering and Technology, SRM Institute of Science and Technology, Kattankulathur, Tamil Nadu, India

R. Monishkumar Department of Civil Engineering, KPR Institute of Engineering and Technology, Coimbatore, Tamil Nadu, India

V. Murugaiyan Department of Civil Engineering, Puducherry Technological University, Puducherry, India

Balasubramanian Murugesan Department of Civil Engineering, Faculty of Engineering and Technology, SRM Institute of Science and Technology, Kattankulathur, Tamil Nadu, India

D. Muthu Civil Department, SASTRA Deemed to be University, Thanjavur, India

S. Nagaraj Department of Civil Engineering, Faculty of Engineering and Technology, SRM Institute of Science and Technology, Kattankulathur, Tamil Nadu, India

Mohanad Ali Ishaq Najajra Department of Civil Engineering, Cyprus International University, via Mersin 10, Haspolat, North Cyprus, Turkey

G. Nakkeeran Department of Civil Engineering, Faculty of Engineering and Technology, SRM Institute of Science and Technology, Kattankulathur, Tamil Nadu, India

Rinkal Kishor Nakrani Department of Civil Engineering, Faculty of Engineering and Technology, SRM Institute of Science and Technology, Kattankulathur, Tamil Nadu, India

Sachikanta Nanda Department of Civil Engineering, Faculty of Engineering and Technology, SRM Institute of Science and Technology, Kattankulathur, Tamil Nadu, India

Vishnuvardan Narayanamurthi Department of Civil Engineering, Faculty of Engineering and Technology, SRM Institute of Science and Technology, Kattankulathur, Tamil Nadu, India

T. C. Natesh Department of Civil Engineering, Faculty of Engineering and Technology, SRM Institute of Science and Technology, Kattankulathur, Tamil Nadu, India

K. S. Navaneethan Department of Civil Engineering, Kongu Engineering College, Perundurai, India

S. Nithiyanantham Post Graduate and Research Department of Physics (Applied Energy Resources/Bio-Physics Divisions), Thiru. Vi. Kalyanasundaram Govt Arts and Science College (Affiliated to Bharathidasan University, Tiruchirapalli), Thiruvarur, Tamil Nadu, India

Abdilahi Bashir Omer Lincoln University College, Borama, Somaliland

Ye Min Paing Department of Civil Engineering, Faculty of Engineering and Technology, SRM Institute of Science and Technology, Kattankulathur, Tamil Nadu, India

N. Pannirselvam Department of Civil Engineering, Faculty of Engineering and Technology, SRM Institute of Science and Technology, Kattankulathur, Tamil Nadu, India

Purushothaman Parthasarathy Department of Civil Engineering, Faculty of Engineering and Technology, SRM Institute of Science and Technology, Kattankulathur, Tamil Nadu, India

Vaishali Patankar Department of Civil Engineering, Institute of Technical Education and Research, Siksha 'O' Anusandhan (Deemed to be University), Bhubaneswar, Odisha, India

N. Pavithra Department of Civil Engineering, SRM Institute of Science and Technology, Kattankulathur, Chengalpattu, India

K. Perumal Department of Civil Engineering, Faculty of Engineering and Technology, SRM Institute of Science and Technology, Kattankulathur, Tamil Nadu, India

K. Prasanna Department of Civil Engineering, Faculty of Engineering and Technology, SRM Institute of Science and Technology, Kattankulathur, Tamilnadu, India

K. Pushpa Civil Engineering, Women's Polytechnic College, Puducherry, India

Natta Charan Raj Department of Civil Engineering, Sathyabama Institute of Science and Technology, Chennai, Tamil Nadu, India

K. Raja Department of Civil Engineering, Sona College of Technology, Salem, India

M. Ram Vivekananthan Department of Civil Engineering, KPR Institute of Engineering and Technology, Coimbatore, Tamil Nadu, India

Annadurai Ramasamy Department of Civil Engineering, Faculty of Engineering and Technology, SRM Institute of Science and Technology, Kattankulathur, Tamil Nadu, India

R. Ramasubramani Department of Civil Engineering, Faculty of Engineering and Technology, SRM Institute of Science and Technology, Tamil Nadu, Kattankulathur, India

S. Ramesh Department of Civil Engineering, Faculty of Engineering and Technology, SRM Institute of Science and Technology, Kattankulathur, Tamilnadu, India

Sathyanathan Rangarajan Department of Civil Engineering, Faculty of Engineering and Technology, SRM Institute of Science and Technology, Kattankulathur, Tamil Nadu, India

Tejaswi Ratnakaran Department of Civil Engineering, Faculty of Engineering and Technology, SRM Institute of Science and Technology, Kattankulathur, Tamil Nadu, India

Abishek Rauniyar Department of Civil Engineering, Faculty of Engineering and Technology, SRM Institute of Science and Technology, Kattankulathur, Tamil Nadu, India

Monisha Ravi Department of Civil Engineering, Faculty of Engineering and Technology, SRM Institute of Science and Technology, Kattankulathur, Tamil Nadu, India

Sujitha Ravi Environmental Engineering Laboratory, Annamalai University, Chidambaram, India

P. T. Ravichandran Department of Civil Engineering, Faculty of Engineering and Technology, SRM Institute of Science and Technology, Kattankulathur, Tamil Nadu, India

K. Sri Chaitanya Reddy Department of Civil Engineering, Faculty of Engineering and Technology, SRM Institute of Science and Technology, Kattankulathur, Tamil Nadu, India

Peketi Sai Sasidhar Reddy Department of Civil Engineering, Faculty of Engineering and Technology, SRM Institute of Science and Technology, Kattankulathur, Tamil Nadu, India

Y. Sivananda Reddy Department of Civil Engineering, Faculty of Engineering and Technology, SRM Institute of Science and Technology, Kattankulathur, Tamil Nadu, India

R. Rohithraman Department of Civil Engineering, Faculty of Engineering and Technology, SRM Institute of Science and Technology, Kattankulathur, Tamil Nadu, India

Shristi Sah Department of Civil Engineering, Faculty of Engineering and Technology, SRM Institute of Science and Technology, Kattankulathur, Tamil Nadu, India

D. R. Sakthi Kiran Civil Department, SASTRA Deemed to be University, Thanjavur, India

V. Sampathkumar Department of Civil Engineering, Kongu Engineering College, Erode, India

P. Samundeeswari Sri Sivasubramaniya Nadar College of Engineering, Kalavakkam, Tamil Nadu, India

R. Santhosh Ram Department of Civil Engineering, Faculty of Engineering and Technology, SRM Institute of Science and Technology, Kattankulathur, Tamil Nadu, India

Rakesh Sarma Department of Civil Engineering, Central Institute of Technology, Kokrajhar, Assam, India

Srinivasa Sathyanarayana Reddy Department of Civil Engineering, Sathyabama Institute of Science and Technology, Chennai, Tamil Nadu, India

R. Senthamil Selvi Sri Sivasubramaniya Nadar College of Engineering, Kalavakkam, Tamil Nadu, India

Manoj Shanmugamoorthy Department of Civil Engineering, Kongu Engineering College, Perundurai, India

Durgadevagi Shanmugavel Department of Civil Engineering, Faculty of Engineering and Technology, SRM Institute of Science and Technology, Kattankulathur, Tamil Nadu, India

C. Sharan Department of Civil Engineering, Faculty of Engineering and Technology, SRM Institute of Science and Technology, Kattankulathur, Tamilnadu, India

Mohd Sheob Department of Civil and Construction Engineering, National Taiwan University of Science and Technology, Taipei, Taiwan

Ali Shkera Department of Civil Engineering, Institute of Technical Education and Research, Siksha 'O' Anusandhan (Deemed to be University), Bhubaneswar, Odisha, India

S. Sindhu Nachiar Department of Civil Engineering, Faculty of Engineering and Technology, SRM Institute of Science and Technology, Kattankulathur, India

N. Singh Ministry of Environment, Forest and Climate Change, New Delhi, India

A. Siranjeevinathan Department of Civil Engineering, Faculty of Engineering and Technology, SRM Institute of Science and Technology, Kattankulathur, Tamil Nadu, India

Kurupati Sireesha Department of Civil Engineering, Faculty of Engineering and Technology, SRM Institute of Science and Technology, Kattankulathur, Tamil Nadu, India

A. R. Sivakumar Department of Civil Engineering, Faculty of Engineering and Technology, SRM Institute of Science and Technology, Kattankulathur, Tamil Nadu, India

R. Sivakumar Department of Civil Engineering, College of Engineering and Technology, SRM Institute of Science and Technology, Kattankulathur, Chengalpattu, Tamil Nadu, India

S. Sivakumar Department of Civil Engineering, Easwari Engineering College, Chennai, India

M. Soundararajan Department of Civil Engineering, Sona College of Technology (Anna University), Salem, Tamil Nadu, India

K. J. Sowmiya Narayanan Department of Civil Engineering, Faculty of Engineering and Technology, SRM Institute of Science and Technology, Kattankulathur, Tamil Nadu, India

C. Sreejith Department of Civil Engineering, Vels Institute of Science, Technology & Advanced Studies, Pallavaram, Chennai, India

S. Srinivasan Department of Civil Engineering, KPR Institute of Engineering and Technology, Coimbatore, Tamil Nadu, India

B. Srisaran Department of Civil Engineering, Kongu Engineering College, Erode, India

M. Subbulakshmi Department of Civil Engineering, Faculty of Engineering and Technology, SRM Institute of Science and Technology, Kattankulathur, Tamil Nadu, India

Chidambaranathan Subramanian Manufacturing Engineering, Annamalai University, Chidambaram, India

J. S. Sudarsan School of Energy and Environment, NICMAR University [National Institute of Construction Management and Research (NICMAR)], Balewadi, Pune, India

C. K. Suma Abhivandya Sri Sivasubramaniya Nadar College of Engineering, Kalavakkam, Tamil Nadu, India

C. S. Surya Jyothi Engineering College, Thrissur, India

V. A. Sushma Department of Civil Engineering, Easwari Engineering College, Chennai, India

Andinet Kebede Tekile Adama Science and Technology University, Adama, Ethiopia

Aruna D. Thube Civil Engineering Department, COEP Tech University (Formerly College of Engineering Pune), Pune, Maharashtra, India

N. Umamaheswari Department of Civil Engineering, Faculty of Engineering and Technology, SRM Institute of Science and Technology, Kattankulathur, Tamil Nadu, India

N. Umashankar Department of Civil Engineering, Sona College of Technology (Anna University), Salem, Tamil Nadu, India

Sampathkumar Velusamy Department of Civil Engineering, Kongu Engineering College, Perundurai, India

C. Vinodhini Department of Civil Engineering, KPR Institute of Engineering and Technology, Coimbatore, Tamil Nadu, India

M. VishnuPriyan Department of Civil Engineering, Faculty of Engineering and Technology, SRM Institute of Science and Technology, Kattankulathur, Tamil Nadu, India

S. Vismaya Department of Civil Engineering, Faculty of Engineering and Technology, SRM Institute of Science and Technology, Chennai, Tamil Nadu, India

D. Yuvaraj Department of Civil Engineering, Faculty of Engineering and Technology, SRM Institute of Science and Technology, Kattankulathur, Tamil Nadu, India

Geotechnical Engineering

Enhance the Engineering Properties of Low Load Carrying Capacity of Expansive Soil by Using Alccofine-1203 and Phosphogypsum

V. Jaladevi and V. Murugaiyan

Abstract Extensive soil originates in dry and semi-arid parts of the globe. One of the issues associated with such expansive soils is their tendency to inflate in accordance with an upsurge in their natural moisture content. Numerous issues with substructure, including houses, roadways, breast walls, etc., are imposed by the various swell-shrink performance of soils. Civil engineers have put forth a lot of effort to comprehend the performance of clay soil and apply proper control techniques. The aim of study is to determine the effectiveness of alccofine-1203 (3, 6, 9, and 12%) and phosphogypsum (PG) (0.25, 0.5, 0.75, and 1.0%), enhancing the engineering characteristics of soil, such as swelling behaviour and low load-carrying capacity, which includes the benefits of civil engineers. The experiments are LL, PL, SL, PI, optimum moisture content (OMC), unconfined compressive strength (UCS), maximum dry density (MDD), SEM, XRD, along with other important soil characteristics that were calculated using an experimental program. These additives were applied separately and merged into the soil. The results reveal that the LL, PI, optimal moisture level, and swelling behaviour of soil significantly declined with the accumulation of additives. With the combined effect of 12% alccofine + 1.0% phosphogypsum of expansive soil, UCS improved from 46.4 to 155 kPa. The strength improved owing to the growth of calcium silicate hydrate (C–S–H), calcium aluminate hydrates (C–A–H), and other cementitious complexes observed in SEM and XRD studies. As a consequence of results, it has been observed that the accumulation of 12% alccofine + 1% phosphogypsum acted as a valuable additive on the highly expansive soil, and that through the inclusion of additive, an undesirable soil was transformed into a superior.

Keywords Atterberg's limits · Expansive soil · Phosphogypsum · Swelling · UCS

V. Jaladevi (✉) · V. Murugaiyan
Department of Civil Engineering, Puducherry Technological University, Puducherry 605014, India
e-mail: jaladevi@pec.edu

K. R. Reddy et al. (eds.), *Recent Advances in Civil Engineering*, Lecture Notes in Civil Engineering 398, https://doi.org/10.1007/978-981-99-6229-7_1

1 Introduction

The inherent mineralogical behaviour of expansive/extensive soils is universally recognized for their volume change behaviour under moisture changes. It usually consumes the predictable effect, resulting in undesired engineering behaviour, and high permeability to moisture [1, 2]. These soils are most common in semi-arid and dry regions of the land. They consist of a broad geographic region of around the globe, includes Canada, China, India, and the USA, which suffered infrastructural damage caused by expansive soil. Gujarat, Karnataka, Madhya Pradesh, Maharashtra, Tamil Nadu, and Puducherry have wide tracks of expanding soil recognized as black cotton soil that shelter almost 20% of India's entire surface area. Among the most problematic soils for civil engineers is to build structures on extensive soil, which swells and shrinks in accordance with variations in the flow of water [3]. The footings of structures constructed on expansive soil are in grave danger. Because of its inherent expanding and contracting behaviour [4] when it interacts with water, this soil may produce uplift forces which considerably destroy lightly loaded structures such as pavements and basement [5, 6]. As an outcome, the difficult soil is distinguished via their stiffness while drying and significant swelling potential when wet, and damage from expanding soils is quite mutual in arid and semi-arid places where yearly loss exceeds annual rainfall [7]. It has been displayed to be a potential natural hazard, if not addressed properly, can inflict catastrophic damage to structures and destruction to human life. Mechanical stabilization, especially compaction, and a natural additive method was employed to reinforce the mud characteristics and reclaim its engineering characteristics of the soil, in addition to its expanding and contracting features, to achieve the required strength. A study carried out with [8] employed different concentrations of $CaCl_2$ and alccofine to alleviate the soil as CNS-cohesive non-swelling soils beneath the lightweight constructions, with 6% alccofine and 1% $CaCl_2$ providing the best expansive soil strength. On the other hand, $CaCl_2$ and $MgCl_2$ are hygroscopic minerals perfect for stabilizing expansive soils due to their ability to attract humidity from the atmosphere and avoid contraction forming in extensive soil throughout the straw-hat. Furthermore, by combining waste materials and fibres with chemical agents, the strength and stiffness of soft soils can be improved [9, 10]. According to the study by [11], utilizing bagasse ash and hydrated lime to stabilize expansive soils improves strength and ameliorate to manage conservational matters by eliminating dissipate from the sugar cane manufacturing. Manikandan and Maganraj [12] discovered that adding bagasse ash and hydrated lime tranquil is further effective than adding bagasse ash alone in managing the association of soil. As a result, 3% lime and 0.75% sisal fibre content [13] are optimal proportions for clay soil to boost CBR value. Several studies utilize industrial by-product material such as alccofine [14, 15], using pond ash and alccofine [16], cement kiln dust, alccofine-1101 [17], marble dust, alccofine-1108 [18], as chemicals have become more prevalent because of their comparatively less price; additionally, CO_2 emissions may be substantially decreased through the consumption of supplemental cementing

Table 1 Geotechnical characteristics of soil

Properties of soil	Unit	Result	Properties of soil	Unit	Result	Properties of soil	Unit	Result
G_s		2.27	SL	(%)	01.82	S	(%)	57.74
Clay	(%)	67.9	PI	(%)	65.22	CEC	meq/100 g	26.27
Silt	(%)	28.49	OMC	(%)	36	SSA	m^2/g	01.021
Sand	(%)	03.61	FSI	(%)	125	USCS		CH
LL	(%)	103	FSR		02.25	UCS	kPa	46.44
PL	(%)	37.78	W_A	(%)	93.73	MDD	KN/m^3	13.8

components [19] that are currently thrown in lagoons and landfill sites. The capability of the additive to give an adequate quantity of calcium is the most significant aspect of clayey soils. The purpose of this work is to strengthen the expansive soil by improving its engineering characteristics with a mixture of phosphogypsum (PG) and alccofine to serve as binding agents while preventing the serious environmental and health problems that may occur from discarding it. As a result, combining the two elements as a stabilizing agent may be more useful than utilizing them separately. Still, no studies on the combined action of phosphogypsum (PG) and alccofine as soil stabilizers have been published thus far. The admixtures were chosen with a focus on waste reduction, economic benefits, and environmental friendliness in mind.

2 Materials and Methodology

2.1 Black Cotton Soil

Due to its tendency of highly swelling soil gathered at a depth 1.5 m below ground level from a location in India's Puducherry district be utilized for this experiment. It is dried and screened using a 4.75 mm sieve to eliminate any remaining gravel fraction. And it is saved in the lab. According to IS Classification (IS 1498: 1970), the soil is classed as 'CH,' with inorganic clay of high plasticity [20]. Table 1 shows the geotechnical characteristics of expansive soil.

2.2 Alccofine

Alccofine-1203 is an extremely well cementitious material attained from Counto Micro-Fine Product Private Limited, Goa, India, and that exceeds all other mineral

Table 2 Physical and chemical properties of ultrafine slag

Physical properties	Results	Chemical properties	Results (%)
G_s	2.9	CaO	32.9
γ (kg/m^3)	680	Fe_2O_3	1.9
D10	1.5	MgO	7.98
D50	5.0	Al_2O_3	21.6
D90	9.0	SO_3	0.21
D95	11.5	SiO_2	35.41

admixtures used. The vast majority of ultrafine slag products be utilized in high-performance soil stabilization. The physical and chemical properties of ultrafine slag are shown in Table 2.

2.3 Phosphogypsum (PG)

PG is a calcium sulphate hydrate produced as a consequence of phosphate rock compost manufacture. It is primarily composed of gypsum ($CaSO_4 2H_2O$). However, it also contains environmentally hazardous contaminants like residual acids, fluoride, heavy metals, and obviously happening radionuclides. PG contamination structure differs substantially based on the availability of phosphate rock used in phosphoric acid production and by treating phosphate ore (apatite) with sulfuric acid according to the reaction:

$$\begin{aligned} Ca_5(PO_4)_3X + 5H_2SO_4 + 10H_2O \rightarrow 3H_3PO_4 \\ + 5(CaSO_4 \cdot 2H_2O) + HX \end{aligned}$$

where X may include OH, F, Cl, or Br. For every tonne of phosphoric acid produced, approximately 4–6 tonnes of PG. Only 15% of the globe's PG output is recycled [21] into building products such cement retarder, building gypsum powder, gypsum board, papermaking filler, fibre plaster board, mine filling agent, and roadbed substance [22, 23]. Around 85% of this by-product is dumped into the marine or stream or held untreated in lagoons or springs. This method of dumping is quite polluting. Reducing the exclusion of this by-product offers both monetary and eco-friendly rewards. Table 3 displays the oxide configuration of phosphogypsum.

Table 3 Oxide configuration of phosphogypsum

Elements	Results	Elements	Results	Elements	Results	Elements	Results
SO_3	44.7	Na_2O	0.13	SiO_2	0.43	Fe_2O_3	0.07
CaO	32.04	Cl	0.72	Al_2O_3	0.24	LOI	21.06
F	0.79	P_2O_5	0.67	MgO	0.14		

2.4 Testing Methodology

The present investigation examines geotechnical characteristics, like compaction, strength, and swell or shrink performance of extensive soil, and tests were performed with various amounts of phosphogypsum (0.25, 0.50, 0.75, 1.0%) and alccofine − 1203 (3, 6, 9, 12%). Specific gravity, Atterberg limits, compaction, UCS, and swelling parameters of the expansive soil sample had been measured rendering to Indian Standards. The absorption of water (W_A) in soil is mixed with the above-mentioned additives which were measured alone, then combined with expansive soil. Mokeagus [24] develops and recommends a water absorption (W_A) equation, and its formula is:

$$W_A = 0.91\text{LL} \tag{1}$$

A Specific Surface Area is established and recommended by [25] to determine the Specific Surface Area (SSA) of the soil–binders mixture. The CEC of the additive mixed soil samples was measured. It was formed and is recommended by [20].

3 Result and Discussion

The influence of admixtures on expansive soil characteristics was assessed using Indian standards and detailed in the segments below.

3.1 Atterberg Limits

The effect of alccofine and phosphogypsum is on the Atterberg limits of expansive soil. The results demonstrate that the liquid and plastic limits gradually reduced while the SL increased; henceforth, the variance between the plastic and shrinkage limits is referred to as the shrinkage index (SI). When compared to individual admixtures, the PI is lowered by approximately 66%, and the SI is enhanced by about 53% in which the soil sample is mixed via 12% A + 1% PG due to the pozzolanic response and the ability of positive ion conversation, as shown in Table 4. Based on IS (1498)–1970 classification, the laboratory experiments have been conducted in

Table 4 Effects on index and strength properties of soil combined with admixtures

Admixtures (%)	LL (%)	PL (%)	SL (%)	PI (%)	SI (%)	G_S	FSI (%)	FSR	UCS (kPa)	S (%)	W_A (%)
0	103	37.78	1.82	65.22	35.96	2.27	125	2.25	46.4	57.74	93.73
A3	77.8	29.17	7.05	48.63	22.12	2.44	81.25	1.81	89.5	28.21	70.79
A6	68	28.78	5.4	39.22	23.38	2.46	25	1.25	118	16.69	61.88
A9	60.5	20.44	11.32	40.06	9.12	2.42	13.63	1.13	150	17.58	55.06
A12	42	31.18	17.95	10.82	13.23	2.64	4.5	1.05	172	0.72	38.22
PG 0.25	68.2	26.41	5.85	41.79	20.56	2.45	70.59	1.71	94	19.49	62.06
PG 0.50	60.5	32.18	0.97	28.32	31.21	2.53	66.67	1.67	110	7.54	55.06
PG 0.75	42	22.82	8.77	19.18	14.05	2.95	38.89	1.39	128	2.91	38.22
PG 1	66	29.09	5.93	36.91	23.16	2.88	44.4	1.44	83	14.39	60.06
A3 + PG 0.25	77.8	29.17	7.05	48.63	22.12	2.31	82.35	1.82	81	28.21	70.79
A6 + PG 0.50	68	35.09	14.14	32.91	20.95	2.79	66.67	1.67	120	10.88	61.88
A9 + PG 0.75	53.5	34.28	9.06	19.22	25.22	2.61	44.4	1.44	135	2.93	48.69
A12 + PG 1	48	26.14	9.16	21.86	16.98	2.68	16.67	1.17	155	4.01	43.68

Note LL = Liquid limit; PL = Plastic limit; SL = Shrinkage limit; PI = Plasticity index; G_S = Specific gravity; S = Swell potential

Geotechnical Engineering Lab, Civil Engineering Department, PTU. And the results demonstrated that the deposition of 12% alccofine + 1% phosphogypsum modified the geotechnical properties of untreated soil from high-to-medium swell potential [26]. It has been recommended that plasticity is a better predictor of swell potential; a lower PI indicates a lower swell potential.

Figures 1 and 2 depict the compaction parameters like MDD and OMC of treated soils. With a concentration of 12% alccofine and 1% phosphogypsum, the maximum dry density increases from 13.8 to 17.5 kN/m^3, and the ideal moisture content drops from 36 to 15.6%; hence, for the specimen with the greatest strength. When the GGBS admixture was utilized as alleviating materials, MDD and OMC behaved similarly [27, 28]. The rise in dry density for a certain compaction impact is advantageous for usage as building constituents since it implies soil enhancement [29, 30].

3.2 Free Swell Index (FSI)

Table 4 illustrates the swelling behaviour of soil combined with various amounts of alccofine and phosphogypsum. The presence of montmorillonite minerals has a massive impact on the swelling characteristics of soils. Individually applying these

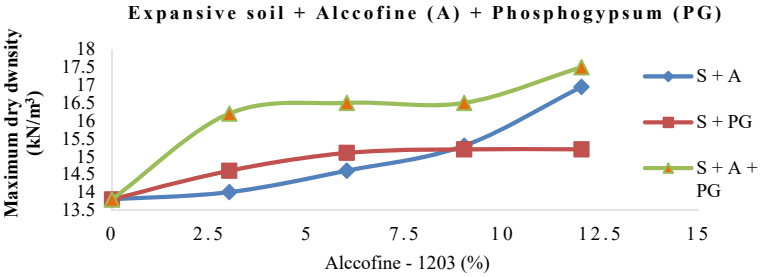

Fig. 1 Effect of MDD on treated soil

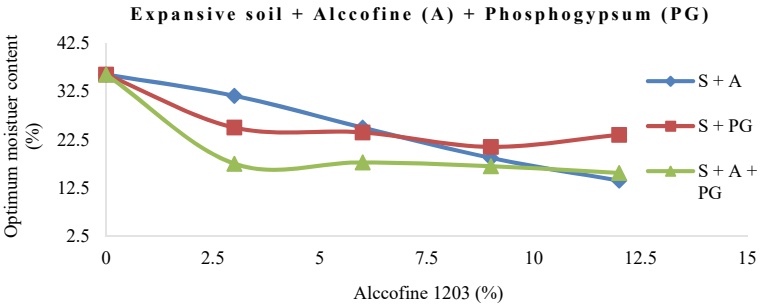

Fig. 2 Effect of OMC on treated soil

compounds reduces the FSI from 125 to 4.5% at 12% alccofine and 38.89% at 0.75% phosphogypsum. According to an outcome, both admixtures diminished the swell potential of the soil from high to low, while the same result is obtained at the combined action of 12% A + 1% PG as per IS 1498–1970.

3.3 Free Swell Ratio (FSR)

The FSR approach is extremely aggressive for predicting a soil's swell potential because it involves a relatively simple procedure. It has defined as the ratio of the equilibrium sediment volume of 10 g oven-dried soil passing through a 425 m sieve in distilled water to the equilibrium sediment volume in kerosene.

$$\text{FSR} = V_d / V_k \tag{2}$$

The results show that adding 12% alccofine + 1% phosphogypsum reduces the FSR value from 2.25 to 1.17, indicating that soil swelling is reduced from high to low. Furthermore, the major clay mineral shifts from montmorillonite to a mix of kaolinite and montmorillonite [31].

3.4 Cation-Exchange Capacity

Soil clay minerals have a negatively charged surface that holds exchangeable cations. C^{++}, Mg^{++}, H^{+}, K^{+}, NH_4^{+}, and Na^{+} are the most common exchangeable cations occurring in the order of general relative abundance. The ability of clay to absorb ions from the solution indicates the presence of such charges. Cations (positive ions) absorb faster than anions (negative ions). A cation such as Na^{+} is easily attracted to a clay surface from a salt solution. The adsorbed Na^{+} ion, however, is not permanently connected; it can be replaced by K^{+} ions if the clay has immersed in a potassium chloride (KCL) solution. Cation exchange is the activity of replacing excess cations [32]. Ca, Mg, Na, and K were measured by transferring them from soil colloids using NH4. Asian Enviro Labs Pvt. Ltd., Pallavaram, Chennai, performs it.

3.5 Unconfined Compressive Strength (UCS)

The soil specimen was prepared by using admixtures, which applied separately, then unified with the expanding soil. It was done with equally treated and untreated soil. Untreated specimen has a UCS value of 46.4 kPa. The percentage of phosphogypsum and alccofine in the soil is estimated based on its dry weight, and the influence of curing time was studied for intervals ranging from 0 to 56 days. The UCS values are shown in Fig. 3. Table 5 shows that the highest strength was achieved at 12% A with 1% PG, and it steadily increased from 46.4 to 948 kPa over 56 days. In contrast to previous experiments, the strength decreased when more binder was added than 7% alccofine. When the stabilizer content surpasses a certain threshold, the compressive strength of the soil reduced gradually. Similar findings were made by [33], demonstrating that the best strength was obtained using natural soil and an alccofine concentration of 8 and 1% $CaCl_2$. Related research has been done [34]. Utilization of calcium chloride and rice husk ash (RHA) with a ratio of 8% RHA to 1% $CaCl_2$ in soil made of black cotton.

4 Mineralogical and Microstructural Analysis

4.1 SEM Analysis

Among the most effective devices for examining the microstructure of soil molecules is the scanning electron microscope (SEM). A sample surface emits secondary electrons, which are seen as three-dimensional pictures [35]. SEM and EDAX technologies were applied to measure variations in the exterior background and chemical composition between the interactions of soil minerals. In this research, EVO 18 Carl Zeiss is used for the SEM and EDAX study. The experiment was conducted to track

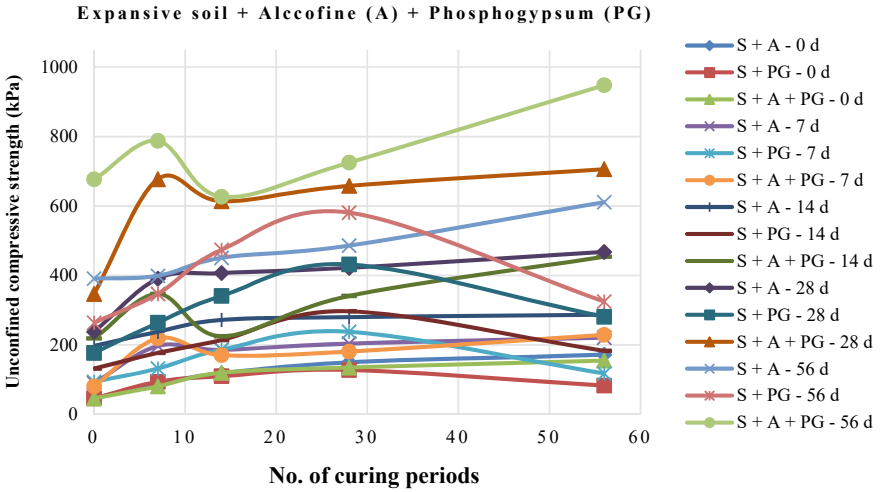

Fig. 3 UCS of soil + alccofine – 1203 + phosphogypsum at various days (d)

Table 5 Optimum result obtained on soil (S) + alccofine (A) + phosphogypsum (PG)

Properties	87% S + 12% A + 1% PG	Properties	87% S + 12% A + 1% PG
G_S	2.68	FSI (%)	16.67
LL (%)	48	FSR	1.17
PL (%)	26.14	W_A (%)	43.68
SL (%)	9.16	CEC (meq/100 g)	45.52
PI (%)	21.86	OMC (%)	15.6
SI (%)	16.98	MDD (kN/m^3)	17.5
USCS	CI	UCS (kPa)	155

the changes in an intrinsic soil, and the results are presented in Fig. 5 for soil + alccofine + phosphogypsum. These tests were conducted to examine the distinct, and a modification in soil is mixed through admixtures of 0 and 56 days curing. Ca, Mg, and Si are recognized as prominent peaks in Fig. 4.

The main purpose of the test was to identify the different cementations compounds on the clay soil stabilized with 12% alccofine + 1% phosphogypsum mixture, or for the sample that exhibits the highest level of strength. Therefore, the key factor reducing swelling in expansive soil is the development of aggregation [36]. If hydration of cement ingredients like C–S–H gel are combined with calcium hydroxide, particles can be detected in the SEM micrograph. Most often, hydration products are combined with tiny pores which remain vacant but are filled by cured epoxy glue [37].

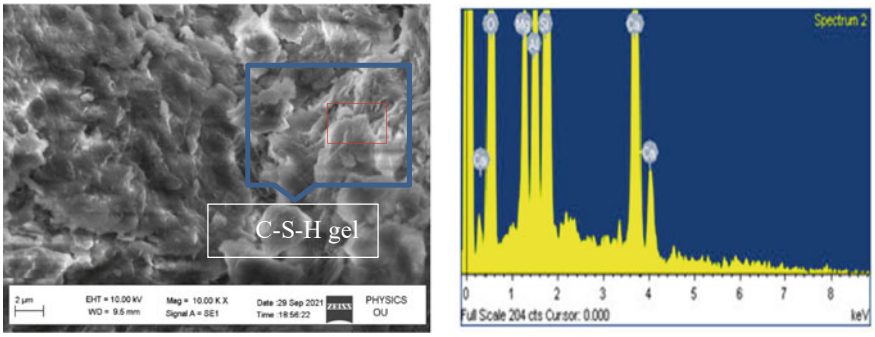

Fig. 4 SEM with EDAX analysis for soil + 12% alccofine + 1% phosphogypsum

4.1.1 X-Ray Diffraction

X-ray diffraction analysis has become a widely recognized approach for determining the mineralogy of soil with fine grains. The bulk of soil elements have crystal shapes, and their structure is determined by a specific geometry. The diffraction pattern of the soil samples according to its crystal structure is then investigated for the quantitative as well as qualitative analysis of elements [35]. The soil + 12% alccofine + 1% phosphogypsum and natural soil are identified by the X-ray diffraction peaks. According to Fig. 5, the most significant peak traced was associated with calcium hydroxide (CH) and was located at $2\theta = 26°–39°$ [37]. It was done to support the development of new minerals that have the potential to significantly improve soil admixture behaviour while also strengthening the existing minerals. The X-ray findings clearly demonstrate that the intensity of radiation is higher for alccofine and phosphogypsum material injected when compared to the expanding soil. The primary hydration products of pozzolanic reactions are C–S–H gel and CH [38]. The utmost significant peak outlined was connected to CH and was found at $2 = 26°–39°$.

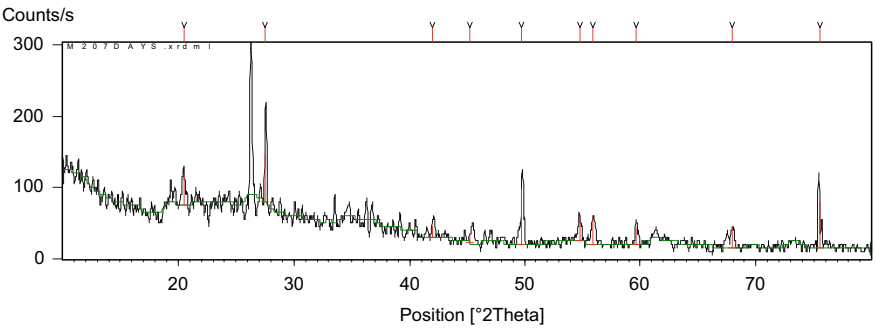

Fig. 5 XRD analysis for soil + 12% alccofine + 1% phosphogypsum

5 Conclusion

This study performed several tests to assess the influence of admixture on expanding features and durability performance. The following are the findings of the data analysis for this study:

Alccofine-1203 and phosphogypsum buildup in the soil raised the SL while decreasing the LL and plasticity index. The accumulation of binder's grounds the agglomeration of clay elements and an increase in the sum of coarse units, decreasing the Atterberg limits. With a binding content, the optimal moisture content (OMC) dropped from 36 to 15.6%, whereas the MDD increased from 13.8 to 17.5 kN/m^3. The UCS of alccofine-1203 and phosphogypsum injected separately and mixed with the expanding soils was tested. It was carried out on both treated and intrinsic soil. The UCS value of untreated soil is 46.4 kPa. After 56 days of curing, the strength grew from 46.4 to 948 kPa.

Soil swelling behaviour; the FSI is lowered from 125 to 16.67%, demonstrating that the addition of 12% A + 1% PG reduces soil swelling from high to low. Studies using SEM and XRD demonstrate that reaction products like Si, Ca, and Mg are formed and greatly contribute to strength. The above-mentioned 2ϴ is a CH-related peak that appears in XRD as a result of the accumulation of admixtures to the expansive soil. Based on the favourable results, the extensive soil containing alccofine and phosphogypsum can be described as a beneficial cohesive non-swelling soil (CNS) for roads, pavements, and floorings. As a consequence of results, it has been observed that the addition of 12% A + 1% PG acted as a valuable additive on the highly expansive soil, and that through the inclusion of additive, an undesirable soil was transformed into a superior.

Acknowledgements I want to express my appreciation to the Vice Chancellor and Head of the Civil Engineering Department of Puducherry Technological University in Puducherry, India, for providing unflinching dedication in conducting this study. I'd like to thank the TEQIP-III Research Assistantship for Ph.D. Scholars at PTU for the assistance with funding. And also, I am very grateful to lab assistance who helped me to accomplish my research well and on schedule.

References

1. Chen FH (1988) Foundation on expansive soils. Elsevier, Oxford
2. Chen FH (1975) Foundations on expansive soils. The Netherland, Elsevier Amsterdam
3. Azam S, Ito M, Chowdhury R (2013) Engineering properties of an expansive soil. In: Proceedings of the 18th international conference on soil mechanics and geotechnical engineering, Paris
4. Mishra AK, Dhawan S, Rao SM (2008) Analysis of swelling and shrinkage behaviour of compacted clays. Geotech Eng 26(3):289–298
5. Subba Rao KS (2000) Swell-shrink behaviour of expansive soils—geotechnical challenges. Indian Geotechn J 30(1)

6. Selvamsagayaradja M, Murugaiyan V, Sundarajan T (2021) Geotechnical mapping of expansive soil problems associated with damages in low rise buildings along south east coast of India. Int J Sci Eng Manage (IJSEM) 6(4)
7. Suresh R, Murugaiyan V (2018) Amelioration of highly sensitive clay using natural fiber and chemical admixture. In: IEEE international conference on system computation automation and networking (ICSCAN)
8. Suresh R, Murugaiyan V (2019) Experimental studies on influence of alccofine and calcium chloride on geotechnical properties of expansive soil. Indian Geotechn Conf GeoIndus 19(21):1389–4380
9. Fatahi B, Khabbaz H (2012) Mechanical characteristics of soft clay treated with fibre and cement. Geosynth Int 19(3):252–262
10. Fatahi B, Thu Minh Le, Fatahi B, Khabbaz H (2013) Shrinkage properties of soft clay treated with cement and geofibers. Geotechn Geol Eng 31(5):1421–1435
11. Hasan H, Dang L, Khabbaz H, Fatahi B, Terzaghi S (2016) Remediation of expansive soils using agricultural waste bagasse ash. In: Advances in transportation geotechnics, the 3rd international conference on transportation geotechnics (ICTG 2016), vol 143, pp 1368–1375
12. Manikandan AT, Maganraj M (2014) Consolidation and rebound characteristics of expansive soil by using lime and bagasse ash. Int J Res Eng Technol 3(4):403–411
13. Manjunath KR, Venugopal G, Rudresh AN (2013) Effect of random inclusion of sisal fibre on strength behavior of black cotton soil. Int J Eng Res Technol (IJERT) 2(7):2227–2232
14. Shukla RP, Parihar NS (2016) Stabilization of black cotton soil using micro-fine slag. J Inst Eng Ser A
15. Dutta RK, Khatri VN, Thakur V, Das PP (2019) Effect of alccofine addition on the index and engineering properties of bentonite. J Geotechn Eng JOGE STM J 6(1)
16. Tahir MF, Tripti Goyal E (2019) Improvement of engineering properties of soil using pond ash and alccofine. Int Res J Eng Technol (IRJET) 6(3)
17. Talgotra A, Neeraj Sharma E (2017) Stabilization of clayey soil with cement kiln dust and alccofine 1101. Int J Adv Res Sci Eng (IJARSE) 6(12):1220–1228
18. Soni MK, Singh S (2019) Statistical interpretation of marble dust and alccofine for soil stabilization. Int J Innov Technol Explor Eng (IJITEE) 8(7)
19. Tayibi H, Choura M, Alguacil FJ (2009) Environmental impact and management of phospho-gypsum. Review: 1–38
20. Sridharan A, Nagaraj HB (2009) Absorption water content and liquid limit of soils. Geotechn Testing J
21. Rashad AM (2017) Phosphogypsum as a construction material. J Clean Prod: 1–54
22. do Carmo Holanda F, Schmidt H, Quarcioni VA (2017) Influence of phosphorus from phosph-ogypsum on the initial hydration of Portland cement in the presence of superplasticizers. Cem Concr Compos: 384–393
23. Zhao S, Ma L, Yang J, Zheng D, Liu H, Yang J (2017) Mechanism of CO_2 capture technology based on phosphogypsum reduction thermal decomposition process. Energy Fuels Am Chem Soc: 1–27
24. Mokeagus JA (ed) (1978) Manual on soil sampling and methods of analysis, 2nd edn. Canada Soil Society Suite, 907, 151 later st., Ottawn, Ontario
25. Amy B, Cerato, Alan J (2002) Determination of surface area of fine-grained soils by the ethylene glycol monoethyl ether (EGME) method. Geotechn Test J 25(3)
26. Mitchell J (1993) Fundamentals of soil behaviour. Wiley, New York
27. Phani Kumar BR, Sharma RS (2004) Effect of fly ash on engineering properties of expansive soils. J Geotechn Geoenviron Eng: 764–767
28. Cokca E (2001) Use of class C fly ashes for the stabilization of an expansive soil. J Geotechn Geoenviron Eng: 568–573
29. Shukla RP, Singh N, Yadav P, Mankotia N (2015) Problems and treatment of black cotton soil. In: 50th Indian geotechnical conference
30. Sivapullaiah PV, Subba Rao KS, Gurumurthy JV (2004) Stabilization of rice husk ash for use as cushion below foundation on expansive soils. Ground Improvement 8(4):37–149

31. Prakash K, Sridharan A, Prasanna HS, Manjunatha K (2009) Identification of soil clay mineralogy by free swell ratio method. GEOTIDE Indian Geotechnical Society, IGC, Guntur, India, pp 27–30
32. Grim RE (1968) Clay mineralogy. McGraw-Hill, New York
33. Suresh R, Murugaiyan V (2021) Influence of chemical admixtures on geotechnical properties of expansive soil. Int J Eng 34(1):19–25
34. Ramanamurty V, Praveen GV (2008) Use of chemically stabilized soil as cushion material below light weight structures founded on expansive soils. J Mater Civ Eng ASCE 20(5):392–400
35. Sekhar DC, Nayak S (2017) SEM and XRD investigations on lithomargic clay stabilized using granulated blast furnace slag and cement. Int J Geotechn Eng: 1–15
36. Al Rawas AA (2002) Microfabric and mineralogical studies on the stabilization of an expansive soil using cement by-pass dust and some type of slags. Can Geotechn J 39(5):1150–1167
37. Bahmani S et al (2016) The effect of size and replacement content of nano silica on strength development of cement treated residual soil. Constr Build Mater 118:294–306
38. Diamond S (2004) The microstructure of cement paste and concrete- a visual primer. Cem Concr Compos 26(8):919–933

Early Strength of an Expansive Soil Stabilized Using a Blend of Hydrated Lime, Unrefined Brown Sugar and Ground Gallnut Dust Under Varying Curing Conditions

Jijo James, B. Mohan Kumar, P. Samundeeswari, R. Senthamil Selvi, and C. K. Suma Abhivandya

Abstract The present investigation attempts to use a traditional blend of unrefined brown sugar (UBS) and ground gallnut dust (GGD) with lime in augmenting the strength of a virgin soil of swelling nature. A swelling soil from Thaiyur area in Chengalpattu district was collected and characterized in the laboratory. The least lime dose needed to alter the characteristics of the soil known as the lime modification optimum (LMO) was determined as 5% using the Eades-Grim pH test as per ASTM code D6276. For evaluating the unconfined compression strength (UCS), cylindrical soil samples of size 3.8 cm × 7.6 cm were formed to evaluate the strength of all blends. All test specimens were kept aside for curing for a duration of three days to evaluate the strength. Soil cylinders were moulded to a target density and water content identified from mini compaction test. The ideal ratio of lime, UBS and GGD came out to be 5:1:1. The specimens stabilized with ideal dosage were exposed to air curing, moisture curing and thermal curing for a period of three days. The ideal blend was also subjected to 0, 1 and 2 cycles of wetting–drying (WD) to get a preliminary indication of its durability. The outcome of the work indicated that temperature curing was the most conducive for the progress of initial strength of the combination. WD results in loss of strength in the first cycle. However, the loss of strength in the second cycle was similar to first cycle. The study concluded that the usage of this traditional blend has potential in treatment of swelling soils, but more detailed investigations as to the role of the individual components need to be probed further.

Keywords Swelling/expansive soil · Brown sugar · Ground gallnut dust · Lime · Early strength · Wetting–drying

J. James (✉)
College of Engineering Guindy, Anna University, Chennai, Tamil Nadu 600025, India
e-mail: jijojames@annauniv.edu

B. Mohan Kumar · P. Samundeeswari · R. Senthamil Selvi · C. K. Suma Abhivandya
Sri Sivasubramaniya Nadar College of Engineering, Kalavakkam, Tamil Nadu 603110, India

K. R. Reddy et al. (eds.), *Recent Advances in Civil Engineering*, Lecture Notes in Civil Engineering 398, https://doi.org/10.1007/978-981-99-6229-7_2

1 Introduction

Geotechnical engineers face problematic and difficult soils all around the globe. One such type of difficult soil is expansive soil. As the name indicates, these soils have high volume change with moisture variation. They are usually treated with lime, which has proven to be an effective technique for mitigating the disastrous effects of this type of soil. Of late, there has been a move towards sustainable and eco-friendly methods of improving poor and problematic soils.

There have been investigations using natural materials, organic materials as well as biopolymers both in the form of standalone stabilizers as well as subsidiary admixtures to primary stabilizers. There have been investigations using natural polymers including xanthan gum [1], lignosulphonate [2], molasses [3], sugarcane mulch [4] to name a few. One such natural polymer that is obtained from sugarcane is unrefined brown sugar (UBS), also called as jaggery. The use of UBS as a building material in Chola dynasty structures [5] and in Madras plaster [6] is well-documented. UBS addition to lime plaster is for enhancing its binding capacity [7]. The conventional lime-based plasters use the combination of UBS for friction and ground gallnut dust (GGD), the powdered form of the gallnut as a bonding agent [8]. There are multiple records of the usage of this combo of lime, UBS and GGD in ancient South Indian architecture [9, 10]. This combination of lime, UBS and GGD has received a renewed interest in recent times. There have been a good number of investigations involving lime mortar using UBS and GGD for enhancing its performance. However, the utilization of the combo in soil engineering and soil treatment has not been given the same depth of investigation. Very limited number of investigations have been carried out in this area. James and Pandian [9] attempted the use of the combination of lime, UBS and GGD (1:1:1 and 2:3:1) in their investigation to stabilize an expansive soil. James et al. [10], attempted the use of the combination for an expansive soil with a different mix ratio of 1:4:2. Later on, James et al. [11], fixed the lime dose using the Eades-Grim pH test [12] and then varied the dosage of UBS and GGD with a fixed lime dose in all dosages including 8:2:2, 8:1:2 and 8:2:1. This work attempts to study the same combination for the stabilization of a swelling soil by fixing the lime dose using the pH test, followed by optimizing the UBS and GGD content based on unconfined compression strength (UCS) tests along with variation in curing environment for the optimized combo and response to wetting–drying (WD) of the stabilized soil.

2 Materials and Methods

A virgin soil of swelling nature, high-grade industrial quality hydrated lime, UBS and GGD was utilized in the investigation. Figure 1 shows the materials utilized in the investigation. The swelling soil was sampled from Thaiyur, near Kelambakkam, Tamil Nadu. Table 1 displays the properties of the expansive soil evaluated in the

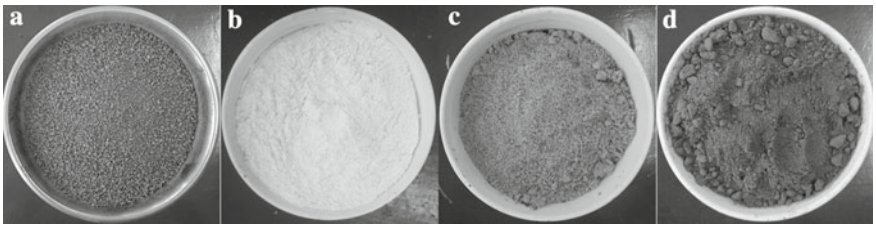

Fig. 1 **a** Virgin soil; **b** Hydrated lime; **c** UBS; **d** GGD

laboratory and the typical proportions of the chemical constituents of lime, UBS and GGD. Lime supplied by the manufacturer in packages was used as delivered. UBS, also commonly called as jaggery, is a traditional sweetener used in India. It is obtained by heating clarified cane juice. It contains a mixture of sugar and molasses.

UBS is commonly available in solid, liquid and granulated forms in the market [13]. The major composition of UBS is 65–85% sucrose, 10–15% reducing sugars and 3–10% moisture. Powdered UBS was utilized in the investigation. GGD was purchased as a powder from a herbal medicine store. Gallnut is indigenous to South Asia including India, falling under the evergreen classification. It is long known to be used in the construction of ancient structures in South India, particularly in the state of Tamil Nadu.

The swelling soil was prepared [21], tested, and classified [22] in the geotechnical laboratory based on relevant codes of Bureau of Indian Standards (BIS). The UBS purchased in solid form was crushed to smaller clods, grated and dried in an oven at 50 °C for 30 min, then pulverized manually using fingers, sieved through BIS 150 μ sieve and stored in air tight containers. The GGD was sieved through BIS 150 μ sieve and stored in air tight containers for later use. The lowest lime dosage needed for the alteration of soil characteristics, commonly known as the lime modification

Table 1 Material properties

Geo-mechanical properties of soil		Chemical constitution			
Property	Value	Oxide (%)	Lime [14]	UBS [11]	GGD [11]
Liquid limit [15]	75.8%	CaO	81.051	11.743	21.199
Plastic limit [15]	23.5%	SiO_2	4.728	34.945	18.140
Plasticity index	52.3%	Al_2O_3	0.382	4.996	3.867
Shrinkage limit [16]	11.2%	Fe_2O_3	0.079	2.280	5.133
Specific gravity [17]	2.76	Na_2O	7.994	20.062	11.042
Optimum water content [18]	28.2%	K_2O	0.000	6.754	13.311
Maximum unit weight [18]	13.09 kN/m^3	MgO	3.217	4.178	8.887
UCS [19]	47.3 kPa	TiO_2	0.045	0.667	1.614
Free swell index [20]	100%	P_2O_5	0.175	1.468	2.828
Classification [22]	CH	SO_3	2.328	12.803	13.571

optimum (LMO), was evaluated from the Eades-Grim pH test [12] as per the standard procedure laid down in ASTM code [23]. The compaction behaviour of the modified soil with lime was evaluated using the mini compaction apparatus developed by Sridharan and Sivapullaiah [24]. The test was carried out based on the specification given in BIS code [25] for stabilized soils. For this investigation, soil cylinders of dimension 3.8 cm × 7.6 cm were moulded in a UCS split cast and statically compacted for the different blends of lime, UBS and GGD. Since the variations in UBS and GGD contents were very small, all the test cylinders were moulded to a set dry density of 12.05 kN/m^3 and corresponding water content of 31.1% obtained for the lime modified soil. A similar approach has also been followed by previous investigators [26, 27]. The prepared cylinders were then mellowed for a duration of three days in closed polythene bags. To evaluate the ideal quantum of UBS, the dosage of UBS was varied from 0.5 to 2% in additions of 0.5%. Three soil cylinders were moulded for each combination of UBS. All the cylinders were allowed to cure for three days. At the end of the resting period, the cylinders were taken out of their bags and loaded axially at a rate of 1.6% per minute until failure to find the strengths of the specimens. The UBS content that developed the highest strength was taken to be the ideal dose. A similar procedure was used to determine the ideal dosage of GGD, varied in additions of 0.25% up to 1%, along with the LMO and ideal dosage of UBS in the soil. Both UBS and GGD being materials of organic origin, their quantities were limited to small dosages as it is a well-known fact that too much organic content interferes with the progression of pozzolanic reactions. To study the influence of varying curing conditions, three different curing regimes were adopted: (1) air curing with the test cylinders placed in air tight polythene covers, (2) moisture curing with the cylinders sandwiched between two soaking wet beds of cotton rolls and (3) thermal curing with the specimens maintained at an elevated temperature of 122 °F in an oven. This temperature was chosen to simulate ground temperature conditions in semi-arid regions in India which can range between 90 and 135 °F in summer [28]. All curing conditions were maintained for a resting period of three days. The air cured soil cylinders were then exposed to WD cycles to evaluate its initial response to cyclic changes in water content based on the procedure followed in earlier investigations [29, 30]. The test cylinders were exposed to 0, 1 and 2 cycles of WD to study their initial wet–dry response. The samples subjected to the wetting–drying cycles were then strained axially to determine their UCS and study their loss/gain in strength in the aftermath of WD.

3 Results and Discussion

The results of the pH test indicated an LMO of 5% wherein the pH crosses 12.4. In a similar investigation, James et al. [11] fixed the lime dose using the Eades-Grim pH test before using UBS and GGD in the mixture. Their soil had an LMO of 4%.

3.1 Optimization of UBS and GGD

Figure 2 shows the variation of the strength of the lime modified soil with increasing content of UBS. From the figure, the first inference that can be gauged is that the addition of UBS along with lime can increase the early UCS of the modified soil at three days of curing. The strength of the virgin soil increased from 47.7 to 61 kPa for 0.5% addition of UBS with lime. On further increase in the UBS content to 1%, the strength further increased to 77 kPa, achieving peak strength. Any additional dosage of UBS resulted in a reduction in the strength of the modified soil. At 1.5% UBS content, the UCS reduced to 43.6 kPa and increasing the UBS dosage to 2% resulted in the strength reducing to 30.6 kPa. Thus, it can be inferred that 1% UBS was the ideal dosage for the soil under investigation stabilized at its LMO content. James et al. [11] found that 1% UBS along with 4% lime was the ideal dosage for their soil. Furthermore, it is noticed that addition of small dosages of UBS alone results in augmenting the strength of the virgin soil along with lime. Higher dosages of UBS were detrimental to the strength development of the soil. This was also evident from an earlier investigation wherein the strength of the modified soil was lower than the virgin soil, when the proportions of UBS and GGD together were higher than lime in the mix [10]. This can be attributed to the organic nature of the additives. Tremblay et al. [31] state that presence of high organic content is detrimental for stabilization reactions.

From the figure, it can also be understood that the addition of GGD results in a loss in the UCS of the modified soil at three days of curing. With the inclusion of 0.25% GGD, there is a drop in the UCS of the untreated soil from 47.7 to 34.4 kPa. With increase in the GGD content, there was no big variation in the strength of the modified soil until 0.75% GGD with the strength ranging between 34.4 and 35 kPa. However, on addition of 1% GGD, the strength increases from 35 to 52.5 kPa. Though, this was only marginally greater than the UCS of the untreated soil, this was considered

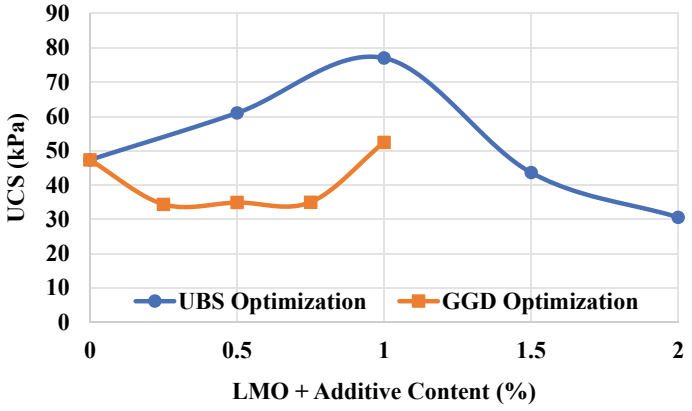

Fig. 2 Optimization of UBS content

as the ideal dosage of GGD content. However, there are inherent limitations to this inference. One is the limitation of the test programme leading to the GGD content variation being stopped at 1% and the second one is the investigation limiting itself to only early strength at three days of resting. Increased GGD contents as well as curing periods may or may not change the ideal dosage of the GGD content. Thus, the ideal blend of lime, UBS and GGD (LUG) came out to be 5:1:1 for the soil under investigation.

3.2 Influence of Curing Condition

The influence of curing condition on the ideal dosage of LUG was studied by considering air, water, and thermal curing for a duration of three days. Figure 3 displays the strengths of the modified specimens developed due to the different curing regimes. Moisture curing had the least beneficial effect on the strength development. Moisture curing for a period of three days resulted in a strength of only 34.8 kPa. This was lower than the UCS of the untreated soil. The exposure of the sample to soaking conditions has led to absorption of moisture by the modified specimen resulting in the softening of the sample. As already mentioned, curing of the samples in air inside sealed polythene covers developed a strength of 52.5 kPa. Curing of the combination in the oven at a temperature of 122 °F for three days more than doubled the strength of the specimen to 95.8 kPa. Similar results were also reported by James et al. [11] in their investigation where moisture curing produced the least strength, followed by air curing and thermal curing. The figure also shows the strength ratio (SR) of different curing regimens computed with the strength of air cured samples as reference. The SR values computed from the study of James et al. [11] are also included for comparison. The SR of water cured samples in relation to air cured samples in the present study was 0.66, whereas the SR of thermally cured samples was 1.83. Thus, there in an 83% increase in strength due to change in curing condition to thermal curing, whereas there is a loss in strength of 34% due to moisture curing. Comparing this with the outcome derived by James et al. [11], thermal curing developed an SR of 3.67, whereas moisture curing developed an SR of 0.14. This may be due to the difference in soil, the dosage of LUG (8:1:2) in their investigation and the curing period considered (seven days). To better understand the standing of the results of the present investigation among similar investigations, the results of the investigation were compared with that of earlier similar investigations.

Figure 4 shows the comparison of this study with previous studies. The strength of all the combinations was reduced as a ratio of the UCS of the modified soil to virgin soil, thereby obtaining the strength gain ratio (SGR). From the figure, it is clear that the SGR in this study for an UBS/GGD ratio of 1 was very close to that of the study conducted by James et al. [11]. This may be due to similar lime content, wherein the LMO value for the soil in their study was 4% whereas the LMO value for the soil in this study was 5%. The SGR was the least for the investigation by James et al. [10] in the year 2014. This was primarily due to very low lime content

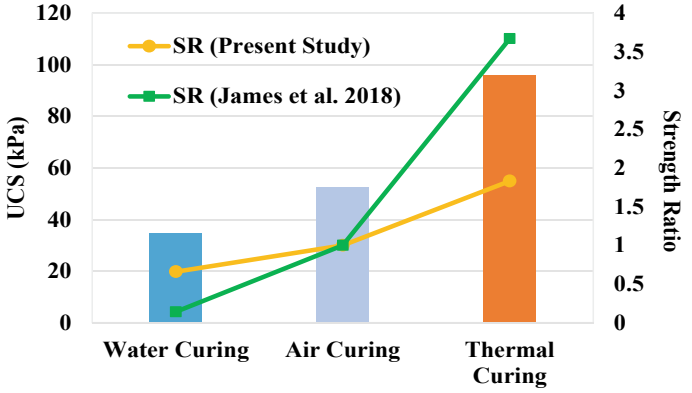

Fig. 3 Influence of curing condition on strength

and comparatively higher dosage of UBS and GGD. There was not enough lime content for the combination to be effective. The highest SGR of all the studies was that reported by James and Pandian [9], however, the lime content in their study was lower than that of the present study as well as the study done by James et al. [11]. Though, superficially, Fig. 4 seems to indicate that there is an increase in SGR value with increase in UBS/GGD ratio, the inference does not actually hold good when a lower lime content is able to achieve higher SGR. Another important point to be noted is that the curing periods of the four different studies are not the same, which may be another limitation in attempting to bring all similar work under one roof. Thus, a more critically designed experimental programme is needed to study the influence of lime content, UBS content and GGD content in developing significant strength of the modified soil.

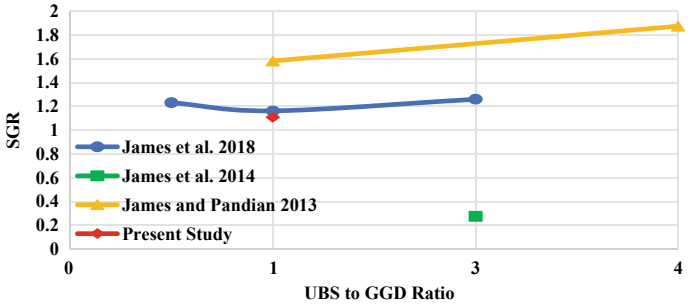

Fig. 4 Comparison of the present study with earlier work

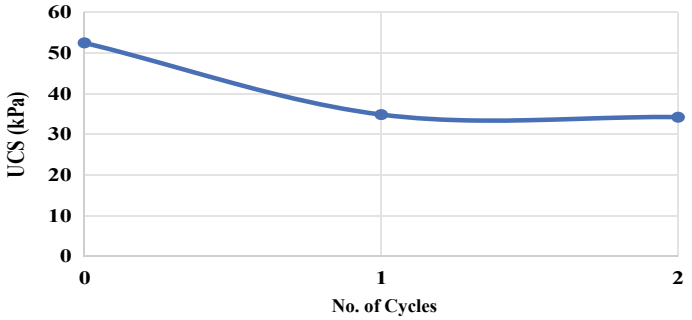

Fig. 5 Influence of WD cycles

3.3 Wet–Dry Response

The wet–dry response of the ideal blend treated soil was assessed by exposing the cylindrical samples to one and two cycles of WD. Figure 5 presents the wet–dry response of the ideal combination air cured for three days. WD leads to a loss in UCS of the modified soil after first and second cycles. However, it can be noticed that there seems to be no big loss in the UCS of the soil after the first cycle of WD. Loss in strength after WD cycles has been reported by earlier investigators. This may be due to the softening of the specimens due to immersion, followed by cracking of the specimens due to loss in moisture. After the first WD cycle, the average strength of the modified samples drops to 34.8 kPa, a loss of 33.64%. After the second cycle, the strength reduces to 34.22 kPa, a loss in strength of 34.82%. Thus, the loss in strength of the specimen after the first WD cycle is not significant. The present study does not carry out enough cycles to put forward a concrete conclusion; however, there seems to be an indication that the modified specimens are withstanding the effects of alternate cycles of WD after the second cycle. However, multiple cycles need to be analyzed before a concrete conclusion can be inferred on this front.

4 Conclusions and Recommendations

The present investigation endeavoured to identify the ideal dosage of UBS and GGD that needs to be added to the LMO content for successfully modifying the soil using the traditional blend of lime, UBS and GGD. Based on the outcomes, the following conclusions can be drawn.

i. The least lime dose required for altering the soil under investigation was 5%. Based on the dosage optimization carried out using strength tests, the ideal dosage of LUG was 5:1:1 for the soil under investigation.

ii. Considering the curing conditions, thermal curing was capable of more than doubling the UCS of the virgin soil when compared with the other curing conditions. Hence, thermal curing of the specimens was the ideal environment for development of strength of the modified soil, followed by air curing and water curing.
iii. The initial response to WD showed a loss in strength of the samples. However, after the second cycle, there was no big variation in the UCS of the modified soil when compared with the virgin soil. Thus, it can be stated that the WD response of LUG modified soil samples resemble that of lime treated soil.

Thus, the present study reinforces the potential of the blend of lime, UBS and GGD. However, it only studied the early strength at three days. Future investigations can attempt different ratios of LUG with higher curing periods and a greater number of wetting–drying cycles. A comparison of the performance of LMO- and lime stabilization optimum (LSO)-modified soil with UBS and GGD can also be attempted in the future investigations to understand the role of lime in the success of the combination.

Acknowledgements The authors are indebted to the management of Sri Sivasubramaniya Nadar College of Engineering, Chennai for the facilities provided.

References

1. Chang I, Im J, Kharis A, Cho G (2015) Effects of Xanthan gum biopolymer on soil strengthening. Constr Build Mater 74:65–72
2. Blanck G, Cuisinier O, Masrouri F (2013) Soil treatment with organic non-traditional additives for the reduction of environmental impact of earthworks. Waste Biomass Valorization 4:703–708. https://doi.org/10.1007/s12649-013-9243-x
3. Ravi E, Sharma A, Manikandan AT, Karthick G, Jameel AA (2015) Study on effect of molasses on strength of soil. Int J Adv Res Trends Eng Technol 2:57–61
4. Moghadam BK, Jamili T, Nadian H, Shahbazi E (2015) The influence of sugarcane mulch on sand dune stabilization in Khuzestan, the southwest of Iran article history. Iran Agric Res 34:71–80
5. Kulke H, Kesavapany K, Sakhuja V (2009) Excavation at Gangaikondacholapuram, the imperial capital of Rajendra Chola and its significance. In: Nagapattinam to Suvarnadwipa: reflections on the Chola Naval expeditions to Southeast Asia. ISEAS–Yusof Ishak Institute, pp 96–101
6. Varghese PC (2009) Building construction. PHI Learning Pvt. Ltd., New Delhi, India
7. Kapoor S (2002) Indian encyclopaedia, vol 1. Genesis Publishing Pvt. Ltd.
8. Radhakrishnan S, Priya RS (2014) Eco friendly materials used in traditional buildings of Chettinadu in Tamil Nadu, India. Am J Sustain Cities Soc 1:335–344
9. James J, Pandian PK (2013) Performance study on soil stabilisation using natural materials. Int J Earth Sci Eng 6:194–203
10. James J, Lakshmi SV, Pandian PK, Vanitha S (2014) Engineering performance of lime stabilized soil admixed with natural materials. Int J Appl Environ Sci 9:1209–1217

11. James J, Karthickeyan S, Chidambaram S, Dayanandan B, Karthick K (2018) Effect of curing conditions and freeze-thaw cycles on the strength of an expansive soil stabilized with a combination of lime, jaggery, and gallnut powder. Adv Civ Eng 2018. https://doi.org/10.1155/2018/1813563
12. Eades JL, Grim RE (1966) A quick test to determine lime requirements for lime stabilization. Highw Res Rec 139:61–72
13. Rao PVKJ, Das M, Das SK (2007) Jaggery—a traditional Indian sweetener. 6:95–102
14. James J, Pandian PK, Switzer AS (2017) Egg shell ash as auxiliary addendum to lime stabilization of an expansive soil. J Solid Waste Technol Manag 43:15–25
15. BIS: IS (1985) 2720 methods of test for soils: part 5 determination of liquid and plastic limit, India
16. BIS: IS (1972) 2720 methods of test for soils: part 6 determination of shrinkage factors, India
17. Bureau of Indian Standard (BIS): IS (1997) 2720 (part III/I) determination of specific gravity of fine grained soil
18. BIS: IS (1980) 2720 methods of test for soils: part 7 determination of water content-dry density relation using light compaction, India
19. BIS: IS (1991) 2720 methods of test for soils: part 10—determination of unconfined compressive strength, India
20. BIS: IS (1977) 2720 methods of test for soils: part 40 determination of free swell index of soils, India
21. BIS: IS (1983) 2720 methods of test for soils: part 1—preparation of dry soil sample for various tests, India
22. BIS: IS (1970) 1498 classification and identification of soils for general engineering purposes, India
23. ASTM (2019) D6276 standard test method for using pH to estimate the soil-lime proportion requirement, United States
24. Sridharan A, Sivapullaiah PV (2005) Mini compaction test apparatus for fine grained soils. Geotech Test J 28:240–246. https://doi.org/10.1520/gtj12542
25. BIS: IS (1967) 4332 methods of test for stabilized soils: part 3 test for determination of moisture density relations for stabilized soil mixtures, India
26. Bagheri Y, Ahmad F, Ismail MAM (2014) Strength and mechanical behavior of soil–cement–lime–rice husk ash (soil–CLR) mixture. Mater Struct 47:55–66. https://doi.org/10.1617/s11527-013-0044-2
27. Wild S, Kinuthia JM, Jones GI, Higgins DD (1998) Effects of partial substitution of lime with ground granulated blast furnace slag (GGBS) on the strength properties of lime-stabilised sulphate-bearing clay soils. Eng Geol 51:37–53. https://doi.org/10.1016/S0013-7952(98)00039-8
28. Patil MN, Sinha S (2006) Soil temperature distribution with vegetation and rainfall over semi-arid region of Western India. Mausam 57:688–694
29. James J, Saraswathy R (2020) Performance of fly ash—lime stabilized lateritic soil blocks subjected to alternate cycles of wetting and drying. Civ Environ Eng 16:30–38. https://doi.org/10.2478/cee-2020-0004
30. James J, Kirubhakaran JA, Balamurukan R, Jawahar V, Soorya SS (2021) Wetting-drying resistance of a lime stabilized soil amended with steel slag and reinforced with fibres. Rev Iteckne 18. https://doi.org/10.15332/iteckne.v18i1.2490
31. Tremblay H, Duchesne J, Locat J, Leroueil S (2002) Influence of the nature of organic compounds on fine soil stabilization with cement. Can Geotech J 39:535–546. https://doi.org/10.1139/t02-002

A Study on the Strength Characteristics of Expansive Soil Blended with Rice Husk Ash

Asaithambi Manimaran and P. T. Ravichandran

Abstract Expansive soils are continuously creating a problem for geotechnical engineers because their intrinsic performance is too high under moisture conditions to alter the efficiency of swelling or shrinking. This alternate shrink-swell behavior of soft soil causes a decrease in soil shear strength, resulting in significant damage to the minimally loaded structural elements such as pavements, retaining walls, foundations, residential buildings, and canal beds. Hence, for mitigating the bearing capacity and volume change problems, waste additives are used with expansive soil for stabilization. Various additives on expansive soils have also gained recognition for their stabilizing properties. The current study investigates the effects of using agro-waste admixture as an additive for improving the strength characteristics of expansive soil using the UCC and CBR tests. The significant results show that adding rice husk ash content increases the optimal level of moisture content and highest dry density. The study results show that enhancing the rice husk ash content increased the unconfined compressive stress and California bearing ratio significantly. The UCS improved up to 817 kPa from 142 kPa as well as the CBR peak values improved to 17.29% from 2.41% and were reported at 12% RHA. It confirms that the optimum strength was attained at 12% RHA for strength advancement on expansive soil. The free swell index of expansive soil started to decrease the swell potential corresponding in proportion to the increase in the percentage of rice husk ash used to stabilize the expansive soil. However, the cost-benefits effectiveness can be attained in the subgrade soil of flexible pavement stabilized on the optimum percentage of RHA.

Keywords Expansive soil · Rice husk ash · Unconfined compressive stress · California bearing ratio · Free swell index

A. Manimaran (✉) · P. T. Ravichandran
Department of Civil Engineering, Faculty of Engineering and Technology, SRM Institute of Science and Technology, Kattankulathur, Tamil Nadu 603203, India
e-mail: manimara@srmist.edu.in

K. R. Reddy et al. (eds.), *Recent Advances in Civil Engineering*, Lecture Notes in Civil Engineering 398, https://doi.org/10.1007/978-981-99-6229-7_3

1 Introduction

Soil improvement could be made either by stabilization or modification or by a combination of both. To decide the soil problem, the engineering attributions of the soil need to be changed by implementing soil modification techniques that involve the addition of different modifiers like lime, cement, GGBS, fly ash, etc., in the expansive soil [1, 2]. It is essential to change the behavior of soils by applying soil stabilization techniques to improve the strength and durability of expansive soils [3], so that the developed soil is entirely appropriate for construction beyond their creative classification. Stabilized soil is indeed a composite, long-lasting material made up of soil and stabilizing agents in the right proportions, altering the soil characteristics [4]. Over the years, both solid and liquid waste dumping in open land areas is increasing. If it is improperly disposed of, it leads to contamination at various levels. In order to challenge this problem, several scholars originated different advancements to evaluate the use of these excess wastes in soil stabilization [5–7].

With the enhancements using solid waste in the engineering properties of expansive soil, the maximum dry density was increased and an addition in the percentage of raise of unwanted solid waste materials mixed with the optimum moisture content was decreased [8]. For the enhancement and stabilization of the subgrade of lightly trafficked roads, different admixtures can be used [9]. However, few stabilizers that have a high ignition loss should be avoided to stabilize the expansive soil [5, 10]. It was found that the usage of industrial solid waste to stabilize expansive soil had a stabilizing effect in which different percentages of addictive prepared to be better than the stabilizing effect achieved with optimum percentage usage of different addictive [11]. Stabilization of expansive soils using industrial and agro-waste admixture effectively resolved that as the percentage of various admixture increases, the maximum dry density and unconfined compressive strength increases to an exact optimum proportion and further percentage value decreases [12–15].

As different stabilizers increase in percentage, the flexibility of the clay stabilizer mixture decreases. The engineering properties of expansive soil values increase with different stabilizers, and beyond the optimum percentage corresponding strength values decreases [16]. An exemplary powder material portion consists of calcium oxide facilitating the pozzolanic reactions. The free calcium oxide and the silica content of different waste materials were significant record parameters for the efficiency of the stabilization near with different intervals of the healing period [17, 18]. Thus in this work, an investigational study was conducted in the soil using rice husk ash (RHA) as an additive to improve the soil characteristics with varying percentages, and its strength and swelling characteristics was studied at the age of 28 days.

2 Materials Used

2.1 Soil

The natural soil utilized in this investigation has been gathered at 1.5–2.5 m depth from the ground level by using the method of disturbed sampling from a site in Madhavacheri (road), Kallakurichi. The soil sample was collected, air-dried at room temperature, then pulverized with a pulverizer machine, and stored in the laboratory with a shield cover [19]. Before being used for conducting laboratory tests according to Indian standards, the pulverized soil sample has been sieved through a 425-micron sieve [20–25]. The following are the physical properties of soil that have been identified and classified: optimum moisture content 21%, free swell index 240%, unconfined strength properties 142 kPa, and California bearing value 2.41 percent at 2.5 mm penetration. Hence, the soil was found highly expansive. So, it is classified under as CH-group.

2.2 Rice Husk Ash

Among the various waste materials, rice husk ash is among the resources available, which is used in this study as a stabilizer. For the stabilization of soil, the additive RHA is attained from flaming nearby obtainable rice husk at 660 °C temperature in a closed furnace for around 24 h. The additive substance is then allowed to dry after throughout flaming; after which the burnt substance was sieved through 425-micron sieve as per Indian Standard and it is used in this study. The rice husk ash chemical composition analysis showed the presence of silica (87.87%), calcium oxide (3.04%), and others (9.09%). Due to pozzolanic reaction it is very reactive because of its physical and chemical properties.

3 Sample Preparation and Tests on Soil

The soil sample for the basic test was prepared as per the requirement for the test. The soil samples pulverized were sieved through the required sieve as per IS and the test samples were weighed out for the test as required quantum of soil. The additive substance to be added to the soil was also sieved through an appropriate sieve as per IS and then the required quantum was weighed based on the ratio to be added to the soil for the test. Before testing, the soil and the additive substance were then mixed thoroughly in dry conditions. As per Indian Standards, the soil and additive mixed sample were used for performing the various tests. After obtaining the compaction characteristics, test results on untreated soil samples and testing of treated soil samples were performed on unconfined compressive strength (UCS)

strength variation and California Bearing Ratio (CBR) at 28 days curing period with different proportions like 3, 6, 9, 12, and 15% RHA in soil. Likewise in IS 2720 (Part VII), the OMC and MDD of expansive soil were attained using the Standard Proctor Compaction test. After the test, the tested UCS untreated and treated samples were dried, powdered for finding the swell characteristics.

4 Results and Discussions

The test outcomes are analyzed and discussed below, followed by the compaction characteristics, unconstrained compressive strength (UCS), and California bearing ratio (CBR) that have been determined for the expansive soil, along with the corresponding increment in the proportion of rice husk ash.

4.1 Compaction Characteristics Behavior of Soil

In sequence of the study, the solid unwanted waste additive material on the characteristics of expansive soil compaction, on the soil with only an increasing proportion of rice husk ash on a weight basis a standard proctor compaction test was performed. The results variation of the MDD and OMC with increasing percentages of rice husk ash was obtained for the soil with 0, 3, 6, 9, 12, and 15% mixes as shown in the figure. It is found that the OMC increases with an increased percentage of rice husk ash content. Figure 1 shows the change in maximum dry density as the proportion of RHA content increases.

Figure 1 illustrates the soil moisture density with untreated and 12% RHA treated. The adding of rice husk ash tends to increase the OMC and reduce the MDD

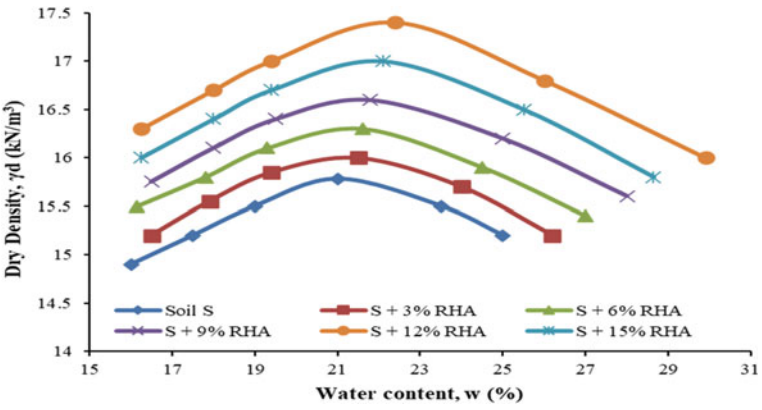

Fig. 1 Compaction characteristics variation of soil treated with RHA

significantly. This change is considered as an indication in the improvement of the compaction characteristics of the RHA-stabilized soil samples. The dry density reduction happens because the flocculated and agglomerated elements of soil occupy large gaps, and the cause for increasing optimum moisture content is that the rice husk ash needs additional water for the pozzolanic reactions [26].

4.2 Unconfined Compressive Strength

The effect of RHA on the expansive soil's stress–strain behavior was studied, UCS direct shear testing was performed. The study result attained from UCS does not imply that the very shear strength limitations of the soil are upgraded. Instead, direct shear test was carried out on the soil with increasing percentages of rice husk ash on weight basis and the test results of stress–strain behavior characteristics were attained for expansive soil with 0, 3, 6, 9, 12, and 15% respectively.

Figure 2 shows the graph results on stress–strain behavior of untreated and RHA treated at 28 days curing period. The untreated soil failed at the UCS of 142 kPa, whereas treated soil at 28 days curing period failed at higher values of the UCS. The raise in the percentage of rice husk ash has a considerable impact on the UCS of the expansive soil stabilized with RHA. On adding RHA up to 12%, the UCS of soil improves to 817 kPa from 142 kPa and at a continued addition of rice husk ash to 15%, the graph result showed a reduction in the UCS of the soil to 744 kPa [27, 28].

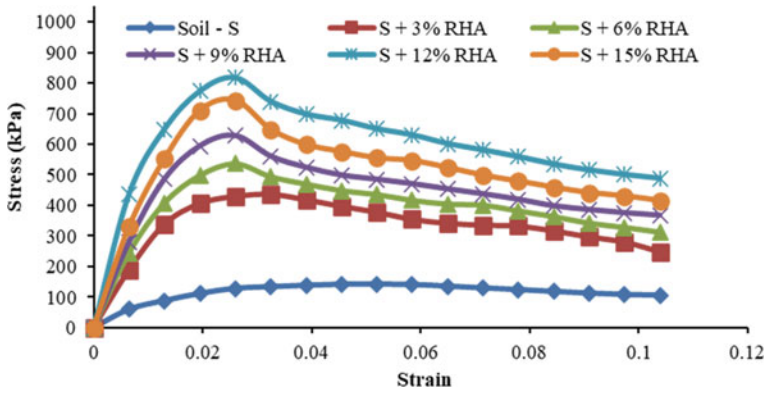

Fig. 2 Stress–strain behavior of soil treated with RHA at the curing period of 28 days

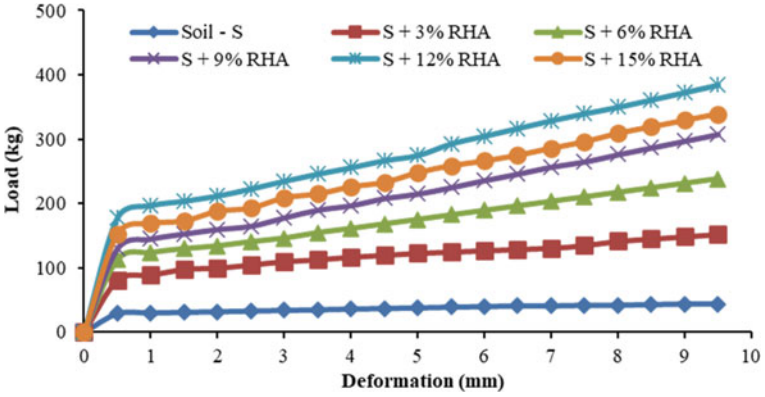

Fig. 3 Load-deformation curve for soil treated with RHA at 28 days curing period

4.3 California Bearing Ratio

In sequence of the study, the strength of subgrades of the rigid-flexible pavement thickness is a main activity to perform the results of CBR values. From the test results, it is certain that the maximum dry density of soil retained increases incessantly with the percentage of RHA for expansive soil and the OMC decreases with the same, which implies that such soil's strength increases, respectively. CBR tests were carried out for the expansive soil with 0, 3, 6, 9, 12, and 15% RHA.

Figure 3 illustrates the load-deformation difference curve of RHA on CBR values. The CBR value for RHA mixed with expansive soil improved as a result of the graph results [29]. The soil treated with 12% RHA for expansive soil of CBR value is 17.29%, and this increased from 2.41%, respectively. It occurs since the rice husk ash particles occupy void spaces between the expansive soil particles [30]. Hence, the California bearing ratio value of expansive soil improved significantly.

4.4 Free Swell Index

Before and after the treatment, the free swelling percent of the expansive soil was studied, as shown in Fig. 4. In the initial study, results presented that the free swelling ratio value of the expansive soil was 240%. The graph result presented that the free swelling percentage value after 28 days of curing and 15% rice husk ash led to decreased free swelling percent from 240 to 70%.

A reduction in the free swell index values was observed while comparing the treated and untreated soil sample with RHA. From the free swell index values, it was strong evidence that the combination of rice husk ash reduced free swell index values from 240 to 70% over a 28-day period with a 12% RHA. This is mainly due to the consumption of minerals from the additive by the soil due to the hydration reactions

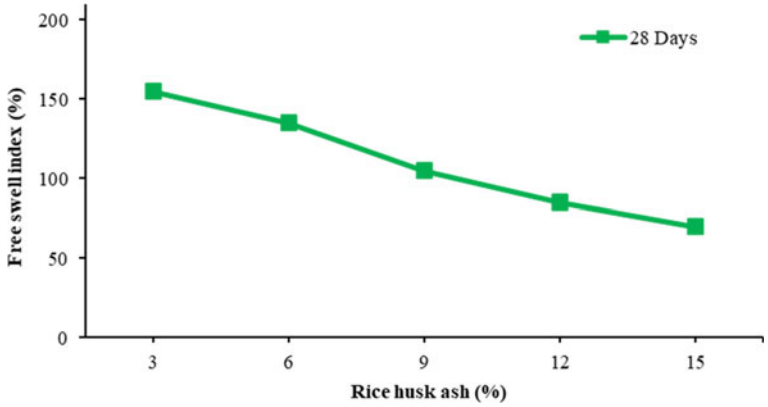

Fig. 4 Effect of RHA on FSI value of treated soil for 28 days curing period

[31, 32]. Additionally, the reaction of CSH with expansive soil led to a formation of an aggregate of various sizes with a low ability for swelling [33]. Based on the swelling results, it seems that RHA is a better additive to modify the expansive soil properties.

5 Conclusions

The following conclusions are drawn from the research results of this investigation.

From the standard proctor test results, the addition of 12 percent RHA increased OMC and decreased MDD, and the maximum dry density was 17 kN/m^3 with the addition of 12 percent RHA.

After the stress strain characteristics of soil, the UCS value improved nearly by 817 kPa in treated soil after adding 12% rice husk ash from an untreated strength value of 142 kPa after a 28-day curing time. The treated soil's CBR value increased from 2.41 to 17.29% with the addition of 12% RHA after a 28-day curing period, indicating a similar trend of improvement in CBR value. Furthermore, the addition of rice husk ash lowers the UCS and CBR values slightly but improves the strength of the soil more than stabilized soils.

The addition of rice husk ash led to a decrease in the free swelling values from 240 to 70% at a period of 28 day with 12% RHA. The reduction in free swell index values indicates that the soil minerals are consuming minerals from the additive by hydration reactions and thus forming the cementitious compounds.

Based on this research, it was discovered that adding RHA to soil increases its characteristics in a better direction. As an outcome, it can be used as one of the soil stabilizers to lower costs and effectively dispose of agricultural RHA waste.

References

1. Nelson JD, Miller DJ (1992) Expansive soils problems and practice in foundation and pavement engineering. Int J Numer Anal Meth Geomech 17(10):745–746
2. Bell FG (1988) Stabilization and treatment of clay soils with lime. Ground Eng 21(1):12–15
3. Nalbantoglu Z, Tawfiq S (2006) Evaluation of the effectiveness of olive cake residue as an expansive soil stabilizer. Environ Geol 50:803–807
4. Mishra ENK (2012) Strength characteristics of clayey sub-grade soil stabilized with fly ash and lime for road works. Indian Geotechn J 42:206–211
5. Bhasin NK, Goswami NK, Oli P, Krishan N, Lal NB (1988) A laboratory study on the utilisation of waste materials for the construction of roads in black cotton soil areas. Highw Res Bull 36:1–11
6. Basha EA, Hashim R, Muntohar AS (2003) Effect of the cement-rice husk ash on the plasticity and compaction of soil. Electron J Geotechn Eng 8(A)
7. El-Sayed MdA, El-Samni TM (2006) Physical and chemical properties of rice straw ash and its effect on the cement paste produced from different cement types. J King Saud Univ Eng Sci 19(01):21–30
8. Albino V, Cioffi R, de Vito B, Santoro Albino L (1996) Evaluation of solid waste stabilization processes by means of leaching tests. Environ Technol 17(3):309–315
9. Muntohar AS, Hantoro G (2000) Influence of rice husk ash and lime on engineering properties of a clayey subgrade. Electron J Geotechn Eng: 5
10. George SZ, Ponniah DA, Little JA (1992) Effect of temperature on lime-soil stabilization. Constr Build Mater 6(4):247–252
11. Sabat AK (2012) Utilization of bagasse ash and lime sludge for construction of flexible pavements in expansive soil areas. Electron J Geotechn Eng 17(H):1037–1046
12. Anupam AK, Kumar P, Ransinchung RN (2013) Use of various agricultural and industrial waste materials in road construction. Procedia Soc Behav Sci 104:264–273
13. Sabat AK, Nanda RP (2011) Effect of marble dust on strength and durability of rice husk ash stabilised expansive soil. Int J Civ Struct Eng 1(4):939–948
14. Sabat AK (2012) Effect of polypropylene fiber on engineering properties of rice husk ash-lime stabilized expansive soil. Electron J Geotechn Eng 17(E):651–660
15. Sabat AK (2013) Engineering properties of an expansive soil stabilized with rice husk ash and lime sludge. Int J Eng Technol 5(6):4826–4833
16. Ijimdiya TS, Ashimiyu AL, Abubakar DK (2012) Stabilization of black cotton soil using groundnut shell ash. Electron J Geotech Eng 17:3645–3652
17. Ravichandran PT, Divyakrishnan K, Janani V, Annadurai R, Gunturi M (2015) Soil stabilization with phosphogypsum and fly ash—a micro level study. Int J Chem Tech Res 7(2):622–628
18. Lekha BM, Ravi Shankar AU, Sarang G (2013) Fatigue and engineering properties of chemically stabilized soil for pavements. Indian Geotechn J 43:96–104
19. IS: 2720 (1983) Part 1: methods of test for soil—preparation of dry soil sample for various tests. Bureau of Indian Standards, New Delhi
20. IS: 2720 (1980) Part 3: methods of tests for soil—determination of specific gravity. Bureau of Indian Standards, New Delhi
21. IS: 2720 (1985, 1972) Part 5&6: methods of tests for soil—determination of Atterberg's limits. Bureau of Indian Standards, New Delhi
22. IS: 2720 (1980) Part 7: methods of tests for soil—determination of water content-dry density relation using light compaction. Bureau of Indian Standards, New Delhi
23. IS: 2720 (1973) Part 10: methods of tests for soil-determination of unconfined compressive strength. Bureau of Indian Standards, New Delhi
24. IS: 2720 (1987) Part 16: methods of tests for soil-laboratory determination of CBR. Bureau of Indian Standards, New Delhi
25. IS: 2720 (1987) Part 40: methods of tests for soil-determination of free swell index of soils. Bureau of Indian Standards, New Delhi

26. Hossain KMA, Mol L (2011) Some engineering properties of stabilized clayey soils incorporating natural pozzolans and industrial wastes. Constr Build Mater 25(8):3495–3501
27. Rahman ZA, Ashari HH, Sahibin AR, Tukimat L, Razi IWM (2014) Effect of rice husk ash addition on geotechnical characteristics of treated residual soil. Am Eurasian J Agric Environ Sci 14(12):1368–1377
28. Divya Krishnan K, Ravichandran PT (2020) Investigation on industrial waste material for stabilizing the expansive soil. IOP Conf Ser Mater Sci Eng 912:1–8
29. Mukherjee S, Ghosh P (2021) Soil behavior and characterization: effect of improvement in CBR characteristics of soil subgrade on design of bituminous pavements. Indian Geotech J 51:567–582
30. Divya Krishnan K, Kiruthika P, Ravichandran PT (2020) Use of wood ash waste to stabilise soils. Int J Environ Waste Manage 25(1):112–120
31. Oviya R, Manikandan R (2016) An experimental investigation on stabilizing the soil using rice husk ash with lime as admixture. Int J Inform Futuristic Res 03(09):3511–3519
32. Divya Krishnan K, Ravichandran PT (2018) Geotechnical properties of soil stabilised with wood ash. J Mines Metals Fuels SRM IST Spec Issue Part II: 191–194
33. Divya Krishnan K, Ravichandran PT (2017) Microstructural characterisation and quantitative enhancement in strength properties of stabilised soil. Int J Control Theor Appl 10(12):367–376

Study on Performance of Expansive Soil Using Agro Waste as a Sustainable Stabilizer

S. Vismaya, K. Divya Krishnan, and P. T. Ravichandran

Abstract For a safe construction of diminutive and edifice structures in soil, the foundation soil should be keenly observed and improved before the construction activities. To improve the soil characteristics, replacing the traditional methods of soil stabilization can be done by utilizing the agriculture wastes as one of the best cost-effective and sustainable method. For this study, agriculture waste wheat husk ash (WHA) of different percentages (3, 6, 9 and 12%) were mixed to the problematic soil at varying curing periods (3, 7, 14 and 28 days) and tests like standard proctor compaction, unconfined compressive strength and free swell index test were done in order to know the optimum percentage of additive to develop the improved characteristics of the soil. According to the test results, wheat husk ash of 9% showed an enhancement of 150% in strength at 28 days of curing, indicating it as the optimum dosage and there is a volume reduction in soil by 50% with the addition of WHA compared with untreated soil. Wheat husk waste which is one of the agricultural wastes produced abundantly causing waste disposal problem and threat to the surroundings can be utilized in soils for strength enhancement which leads to a sustainable eco-friendlier environment by reducing the environmental impacts.

Keywords Stabilization · Wheat husk ash · Soil · Unconfined compressive strength · Compaction

1 Introduction

Foundation is the portion of a building that should be strong enough to transmit load efficiently to the soil which is available beneath it. The quality of soil has larger impact on the structures to be constructed. Expansive soil is a kind of problematic soil which shows undesirable properties making it a weak soil because of the volumetric change behavior. Excessive swelling and shrinking of the clay soil are seen

S. Vismaya · K. Divya Krishnan (✉) · P. T. Ravichandran
Department of Civil Engineering, Faculty of Engineering and Technology, SRM Institute of Science and Technology, Chennai, Tamil Nadu 603203, India
e-mail: divyakrk@srmist.edu.in

K. R. Reddy et al. (eds.), *Recent Advances in Civil Engineering*, Lecture Notes in Civil Engineering 398, https://doi.org/10.1007/978-981-99-6229-7_4

whenever soil is in contact with the moisture leading to failure of the structures, thus indicating that the bearing ability of the soil is not enough to support loads. In order to improve the soil properties and to rectify the problem of swelling and shrinking, ground improvement techniques are required. Soil stabilization is one among that will enhance and modify the soil properties by improving strength and reducing the swell-shrink properties. Mechanical stabilization is one of the technique available which depends on particle gradation, aggregate as well as plasticity characteristics, making this method suitable in construction of embankments of railways, roads, etc. The other technique is chemical stabilization which has many advantages which includes uniformity in quality and performance, this will reduce the volume increase. The chemical stabilization includes alteration of soil performance using lime, Portland cement, fly ash, sodium chloride, calcium chloride, or materials such as bitumen.

The traditional method of lime stabilization is done by many methods which include usage of high calcium quick lime, hydrated high calcium lime, dolomite lime, normal hydrated as well as pressure hydrated dolomite lime. Researchers like Pongsivasathit and Sreekrishnavilasam [1, 2] studied how traditional stabilizers like cement, cement kiln dust improved the mechanical strength and Saride [3] initiated to understand the behavioral mechanisms of lime and cement stabilized in eight different organic soils. Authors like Vakili et al. [4] combined cement with sodium silicate, GGBFS and performed tests to increase shear strength, whereas the study [5] investigated on effects of nanoparticles on consistency, compaction, hydraulic conductivity and compressive strength of cement-treated residual soil on improving pozzolanic reaction. Some of the main advantages of chemical stabilization are that the setting and curing time are controllable. But researchers are searching for alternate admixtures because of the cost and environment concerns. There are many kinds of wastes such as industrial wastes, agricultural wastes, domestic wastes and mineral wastes. There is an ongoing trend in utilization of waste materials and locally available materials in soil stabilization for a sustainable eco-friendly environment.

Industrialization has led to production of huge number of waste generation which is useless materials generated during manufacturing process in mills, factories and industries. Researchers like Gidley and Sack [6] used many methods to utilize industrial wastes in the construction which improved soil strength. The wastes include fly ash, bottom ash, red mud, copper slag ash, waste paper sludge, etc. These wastes come in large quantities and their problem of disposal is a main problem. Adding industrial wastes like beverage can of aluminum affected significantly the compaction, strength as well as swell properties of the clay [7]. Incorporating industrial wastes like high-density polyethylene (HDPE) and glass to the soil is found satisfactory to be used as stabilizer in subgrade modification for road structure by resolving disposal issues by promoting sustainability in highway construction [8]. Divya Krishnan K studied strength characteristics of two different expansive clayey soils using phospho gypsum in varying percentages at different curing periods. The outcomes show that addition of certain percentage of phospho gypsum showed optimum dosage in both the soils by exhibited maximum compressive strength [9]. The studies are done by tests performed on strength behavior of black cotton soil using coal bottom ash

(CBA). CBA as a cementitious material, enhanced the strength of the soil and also reduced swelling and shrinkage property. Coal bottom ash was added at 0, 10, 20, 30 and 40% as an additive and conducted various tests such as UCS, CBR, MDD and OMC. It was observed that the optimum condition is reached by 30% addition of coal bottom ash.

At present, the method of soil stabilization is also slowly taken up by the use of various agricultural wastes. Research on combining those wastes with chemical additive showed an increase in rate of stabilization. As E. A. Basha who studied in using rice husk ash as a stabilizer combining with cement said, agriculture wastes from rice, wheat, sunflower and tobacco plants have silica in cuticle parts. Plants get enough minerals during their growth from Earth and it is also available in large quantity, so that it can be utilized to bring down construction cost, specifically in the rural regions of developing countries [10]. Agricultural wastes which are produced in 350 million tons in India are a result of agricultural operations from fields, poultry and farm wastes. Utilization of agricultural wastes will reduce many problems associated with it, such as waste disposal, land availability making it a very cost-effective method and by reducing carbon footprints caused by chemicals usage present in traditional stabilizers. Apart from rice husk ash, researchers used two types of fly ash in soft soil stabilization. The optimum content of the high calcium fly ash along with the effect of palm oil fuel ash resulted in pozzolanic reaction and altering the engineering properties of the soil [11]. In an economic point of view, the improved characteristics of soil using the combination of wheat husk ash and coir fibre increases the California Bearing Ratio which indicates the enhancement in the strength characteristics of soil [12]. With increased olive waste production in Jordan [13] burned olive waste and used as a soil stabilizer to reduce the problem. Based on the effects of various wastes in soil as a stabilizer, the wheat husk ash (WHA) is used in this study as an additive to enhance the soil characteristics in a cost-effective approach and to reduce waste disposal problems.

2 Materials and Methodology

2.1 Soil

Expansive soil of 1 m depth is considered for this study which is collected from Taramani area, Chennai and the quantity of soil required is sun-dried and pulverized and used for further experimental work. In order to get the swell and strength characteristics, basic tests like Atterberg's limit, compaction and unconfined compressive strength tests were done in accordance with IS standards [14–18]. Table 1 gives the geotechnical properties of the soil. From the test results, the plasticity index of 31.37% and the other test results indicate that the soil is classified under high compressible-high plasticity clays according to unified soil and Indian Standard Classification system. Light compaction [19] is done in untreated soil and an optimum moisture

Table 1 Basic properties of expansive clay

Free swell index (%)	Specific gravity	Atterberg's limit			Plasticity index (%)	Soil classification	Unconfined compressive strength (UCS) (kPa)
		Liquid limit (%)	Plastic limit (%)	Shrinkage limit (%)			
85	2.51	55.6	24.23	10.4	31.37	CH	125.20

content of 22% and a maximum dry density of 14.90 kN/m^3 is obtained indicating it as a weak soil.

2.2 Wheat Husk Ash (WHA)

Wheat husk, which is an agricultural waste produced in abundant quantity and locally available, is taken and burnt in a temperature of 600 °C and is passed through 425-micron sieve which is taken for the study. The ash produced by this process is a silicious material which will help in pozzolanic reaction to take place along with the soil and moisture content. Elemental composition of WHA includes silicon of 60.44%. Here, the investigation is done according to the strength and swell characteristics and the chemical characteristics impart the alteration in the soil. The chemical composition for wheat husk ash includes 85% of SiO_2, 2.51% of CaO and 24.23% of MgO. As per Lin et al., by mixing additives pozzolanic reactions will be quicker if calcium is more [20]. The additive silica is of sufficient amount and available for the reaction to take place producing cementitious compound like silicate hydrate or calcium silicate [21].

3 Sample Preparation and Tests

For the present study, experiments are carried out with adding different percentages of WHA to the soil (3–12%). After the basic tests, in order to obtain the strength value, compaction characteristics of the soil–binders' mixtures, moisture density relations are found out that is using light compaction. In accordance with IS: 1970 (Part 10) (1973), unconfined compressive strength (UCS) was tested for untreated soil as well as soil-additive mixtures of different percentages (3, 6, 9 and 12%) was done [20]. For the UCS tests, samples of 38 mm and 76 mm in diameter and length, respectively, are made according to the optimum conditions. The wet sample obtained by mixing the soil with dry WHA of varying percentage with optimum water content is placed in cylindrical mold and compacted from both the ends. The extruded sample is kept for curing (3, 7, 14 and 28 days). Microstructural analysis is done in order to know the microstructural characteristics of the specimen after oven drying of soil with and without the additive.

4 Results and Discussion

4.1 Effect of Additive in Strength Characteristics of the Soil

In this study, unconfined compressive strength tests were done to analyze the strength characteristics of various combination of soil-additive mix. Strength development is studied at varying curing periods of 3, 7, 14 as well as 28 days. Figures 1 and 2 show the typical stress–strain behavior of the treated soil with varying percentages of additive at 7 and 28 days period of curing.

From the graphs, it was observed that strength develops with number of days of curing. Treating soil with 9% WHA showed optimum value indicating the maximum

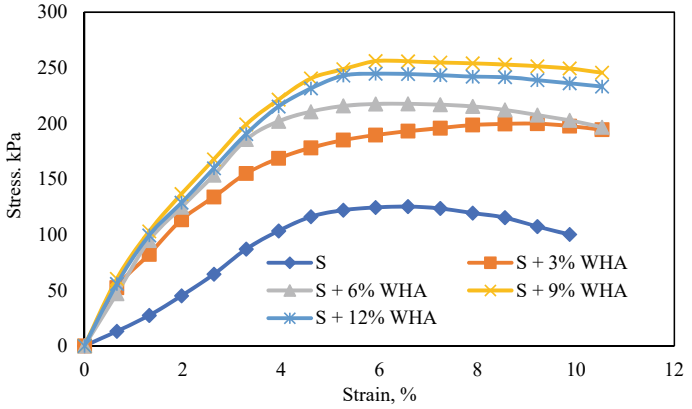

Fig. 1 Stress–strain variation of stabilized soil with WHA at 7 days curing period

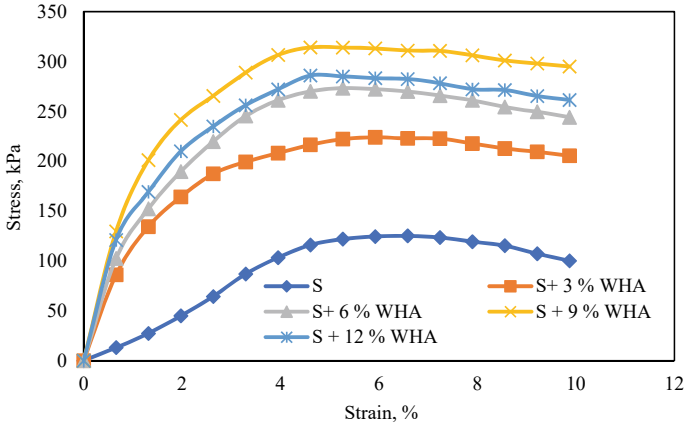

Fig. 2 Stress–strain variation of stabilized soil with WHA at 28 days curing period

Table 2 UCS values of unstabilized and stabilized soil with WHA

Soil + WHA%	Curing period (days)			
	Unconfined compressive strength (UCS), kPa			
	3	7	14	28
SS + 3%	155.60	199.78	214.66	223.98
SS + 6%	180.56	217.57	247.94	273.35
SS + 9%	192.96	255.98	294.66	314.14
SS + 12%	177.09	244.65	276.44	285.92

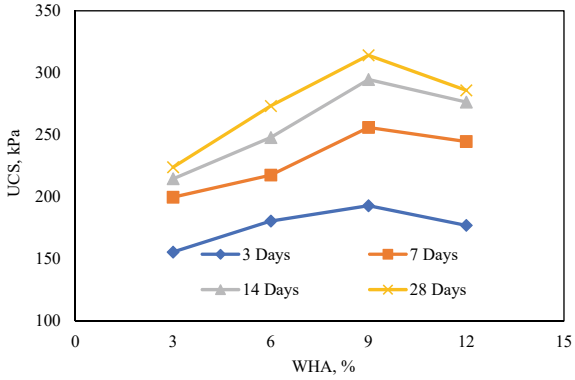

Fig. 3 Effect of UCS value of soil with varying percentage of WHA

strength. After 14 days and 28 days of curing, strength development to a value of 294.66 and 314.14 kPa, respectively, is observed and then reduces thereafter with increase in additive percentage and the same was observed in other curing days. The stress was increased and reached peak at lesser strain in case of WHA-treated sample compared with untreated sample. Table 2 and Fig. 3 show the results and the variation of effects of UCS with varying percentages of WHA by treating the soil. Here the strength of same percentage is always proportional to curing days [22].

Calcium-silicate, calcium-aluminate and calcium-aluminum-silicate hydrates are the compounds which are cementitious, resulting in strength in the sample. As it is a time depending process, it increases with curing days. However, the value decreases after addition of additive after 9%, because in stabilized soil with the extra additive content, there is no pozzolanic reactions to take place with the binder content and they remain as unbonded reducing the overall strength [23].

4.2 Effect of Additive in Swell Characteristics of the Soil

Sample for free swell tests is prepared from the tested UCS samples and Table 3 gives the tested results of free swell index of untreated and treated soil with varying

Table 3 FSI values of unstabilized and stabilized soil with WHA

Soil + WHA%	Curing period (days)			
	FSI, %			
	3	7	14	28
SS + 3%	70	65	60	55
SS + 6%	60	55	55	50
SS + 9%	60	55	50	45
SS + 12%	55	50	50	45

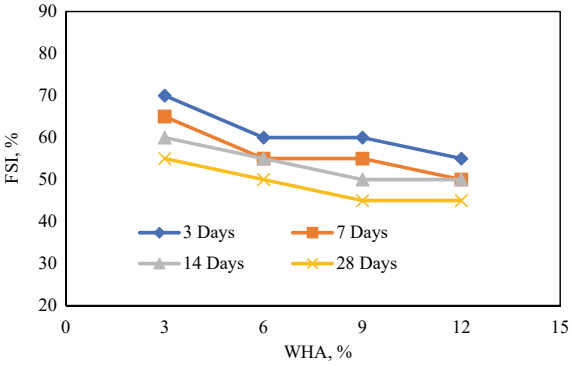

Fig. 4 Variation of FSI values with different percentages of WHA

percentage of WHA at different curing periods. Increasing the additive proportion of WHA in untreated soil results in the decrease of the swell value. At 28 days, the FSI value got reduced to 45% from 85% of the soil by increasing the WHA content. It was a conclusion that the chemical composition of stabilizer will give an evidence of the effectiveness in stabilization in expansive soil [24]. The calcium ions reduce the intensity of swelling potential of clay having Smectite and Illite clay minerals. Thus, expansive nature of a soil can be determined using free swell index test to know the swelling potential.

Figure 4 gives the variation of FSI with WHA at varying curing periods, indicating the volume change by lowering the swelling character of the expansive soil. The soil is made less expansive irrespective of the percentage addition of wheat husk ash.

4.3 Microstructural Analysis of the Soil

The strength and swell characteristics show that WHA is suitable for soil stabilization. Based upon the test results, the values are compared in order for detailed observation with the help of SEM and EDS analysis. Figure 5 shows the SEM image and EDS spectra of untreated soil, WHA and soil treated with 9% WHA at 14 days curing

period. From the figure, it is evident that there is alteration in soil structure giving a compact and dense structure of uniform matrix by number of curing days [25]. The void spaces in untreated soil are more when compared with treated sample because of the chemical reactions taking place with curing days [26]. The elemental composition is easily analyzed with the help of EDS and it was seen that elements, like silica, calcium and aluminum are increased with WHA when compared with untreated soil.

5 Conclusion

From the study of soil modified with WHA in order to observe the strength and swell characteristics enhancement, following conclusions are observed:

- The unconfined compressive strength was improved with the addition of stabilizer with longer curing days. The soil showed maximum strength of 314.14 kPa in 28 days curing period, resulting in an effective stabilization at the optimum content of 9% of WHA. The strength was enhanced by 150% when bonded with the additive comparing it with the untreated soil, having less unconfined compressive strength of 125.20 kPa.
- The volume change behavior of getting less swell potential is observed with the addition of additive. Thus, swelling behavior problem was reduced by improving the strength characteristics and FSI value of 45% was obtained for soil with 9% WHA from the untreated soil FSI of 85%.
- SEM images confirm that there is formation of calcium hydroxide, silicon hydroxide and C–S–H reactions imparting the strength in the expansive soil.
- Thus, by utilizing WHA as a sustainable stabilizer can save significant amounts of costs and it was considered as an eco-friendlier stabilizer to improve the strength and swell characteristics.

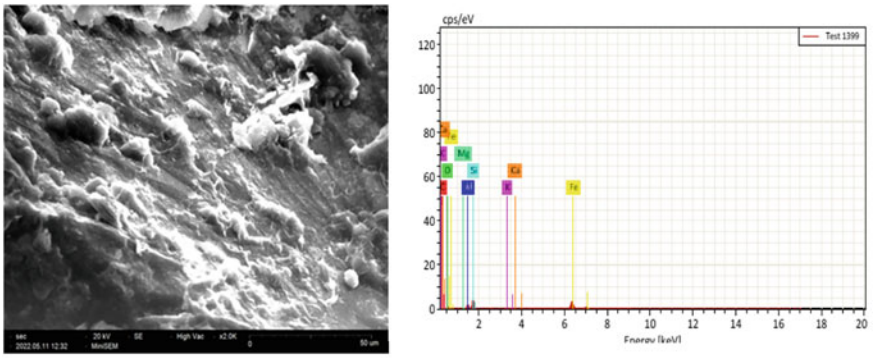

(a) Untreated Soil

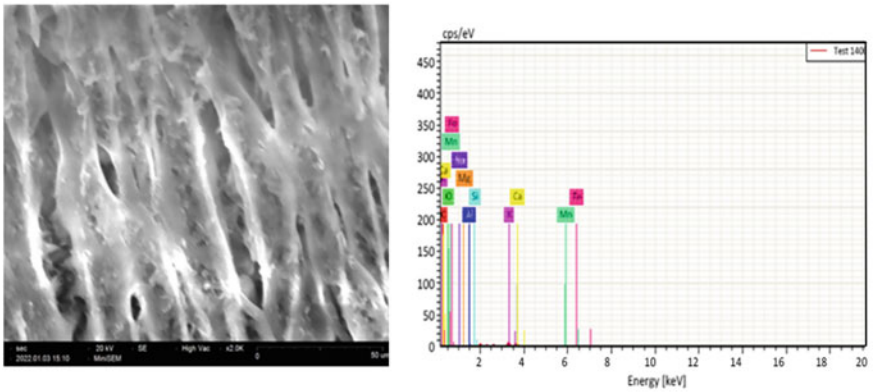

(b) Wheat Husk Ash

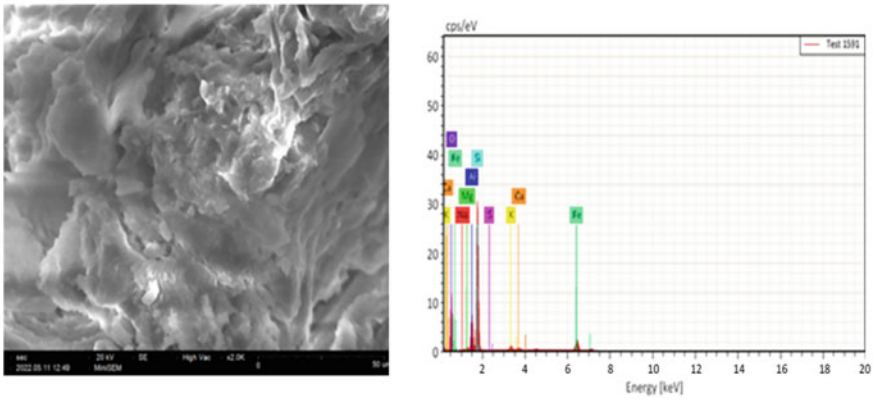

(c) Soil treated with 9 % WHA

Fig. 5 SEM micrograph and EDS spectra of untreated, WHA and treated sample at 14 days curing

References

1. Pongsivasathit S, Horpibulsuk S, Piyaphipat S (2019) Assessment of mechanical properties of cement stabilized soils. Case Stud Constr Mater 11:1–15
2. Sreekrishnavilasam A, Rahardja S, Kmetz R, Santagata M (2007) Soil treatment using fresh and landfilled cement kiln dust. Constr Build Mater 21(2):318–327
3. Saride S, Puppala AJ, Chikyala SR (2013) Swell-shrink and strength behaviors of lime and cement stabilized expansive organic clays. Appl Clay Sci 85(1):39–45
4. Vakili MV, Chegenizadeh A, Nikraz H, Keramatikerman M (2018) Investigation on shear strength of stabilised clay using cement, sodium silicate and slag. Appl Clay Sci: 124–125:243–251
5. Bahmani SH, Huat BBK, Asadi A, Farzadnia N (2014) Stabilization of residual soil using SiO_2 nanoparticles and cement. Constr Build Mater 64:350–359
6. Gidley James S, Sack WA (1984) Environmental aspects of waste utilization in construction. J Environ Eng 110(6):1117–1133
7. Canakci H, Celik F, Bizne MOA, Bizne MOA (2016) Stabilization of clay with using waste beverage can. Procedia Eng 161:595–599
8. Fauzi A, Mohd W, Wan N, Rahman A, Jauhari Z (2013) Utilization waste material as stabilizer on Kuantan clayey soil stabilization. Procedia Eng 53:42–47
9. Divya Krishnan K, Ravichandran PT (2020) Investigation on industrial waste material for stabilizing the expansive soil. IOP Conf Ser Mater Sci Eng 912:062062
10. Basha EA, Hashim R, Mahmud HB, Muntohar AS (2005) Stabilization of residual soil with rice husk ash and cement. Constr Build Mater 19:448–453
11. Jafer H, Atherton W, Sadique M, Ruddock F, Loffill E (2018) Stabilisation of soft soil using binary blending of high calcium fly ash and palm oil fuel ash. Appl Clay Sci 152:323–332
12. Ahmed, Sharma A (2019) Use of coir fiber and wheat husk ash to improve the characteristics of clayey soil. Int J Eng Trends Technol 67(10):85–89
13. Attom MF, Al-sharif MM (1998) Soil stabilization with burned olive waste. Appl Clay Sci 13:219–230
14. IS 2720 Part XL (2002) Methods of tests for soil determination of free swell index of soils. Bureau of Indian Standards, New Delhi
15. IS 2720 Part III (1987) Methods of tests for soil determination of specific gravity. Bureau of Indian Standards, New Delhi
16. IS 2720 Part V (1985) Methods of tests for soil determination of Atterberg's limits. Bureau of Indian Standards, New Delhi
17. IS 2720 Part VI (1972) Methods of tests for soil determination of shrinkage factors. Bureau of Indian Standards, New Delhi
18. IS 2720 Part VII (1980) Methods of tests for soil determination of water content dry density relation using light compaction. Bureau of Indian Standards, New Delhi
19. Locat J, Berube MA, Choquet M (1990) Laboratory investigations on the lime stabilization of sensitive clays: shear strength development. Can Geotech J 27(3):294–304
20. Sharman AK, Sivapullaiah PV (2016) Ground granulated blast furnace slag amended fly ash as an expansive soil stabilizer. Soils Found 56(2):205–212
21. IS 2720 Part X (1973) Methods of tests for soil determination of unconfined compressive strength. Bureau of Indian Standards, New Delhi
22. Horpibulsukn S, Phetchuay C, Chinkulkijniwat A, Cholaphatsorn A (2013) Strength development in silty clay stabilized with calcium carbide residue and fly ash. Soils Found 53(4):477–486
23. Kate JM (2005) Strength and volume change behavior of expansive soils treated with fly ash. American Society of Civil Engineers geo-frontiers congress—innovations in grouting and soil improvement, 1–15
24. Al-Rawas AA, Taha R, Nelson JD, Al-Shab TB, Al-Siyabi H (2002) A comparative evaluation of various additives used in the stabilization of expansive soils. Geotech Testing J 25(2):199–209

25. Jha K, Sivapullaiah P (2015) Mechanism of improvement in the strength and volume change behavior of lime stabilized soil. Eng Geol 198:53–64
26. Al-Mukhtar M, Khattab S, Alcover J-F (2012) Microstructure and geotechnical properties of lime-treated expansive clayey soil. Eng Geol 139–140:17–27

Artificial Intelligence in the Construction Industry: A Status Update, Prospects, and Potential Application and Challenges

Sujitha Arumugam and P. T. Ravichandran

Abstract The expansion of the construction industry is significantly hampered by complicated issues such as health and safety, cost and project overruns, productivity, and labour insufficiency. Furthermore, this business is among the least technologically savvy on the planet, making it difficult to find answers to the problems it is now facing. Artificial intelligence (AI) is a cutting-edge computer-generated technology transforming the manufacturing, merchandising, and public relations industries. Machine learning, computer vision, knowledge-based systems, optimisation, and robotics are artificial intelligence subfields that have been successfully deployed to improve production, safety, efficiency, and security in a variety of sectors. Despite the ease of AI applications, the construction industry continues to face a number of AI-related challenges. This study intends to decipher AI applications, investigate AI methodologies, and identify potential and challenges for AI applications in the construction sector. Resources, properties, and cost-effectiveness were considered when we examined the literature on artificial intelligence applications in the building industry. This research also emphasises and covers the opportunities and limitations of using artificial intelligence in construction. This study explores the most significant AI applications connected to the construction industry, as well as the challenges and road to achieving the potential advantages of AI in the area.

Keywords Structural analysis · Artificial intelligence · Systematic review

1 Introduction

Artificial intelligence is when a machine does human work. AI is a computing technology that mimics human intelligence by performing a function. AI can improve iteratively based on the data it has collected [1, 2]. Various engineering fields use artificial intelligence. AI is thought capable of impersonating every field of engineering

S. Arumugam (✉) · P. T. Ravichandran
Department of Civil Engineering, SRM Institute of Science and Technology, Changalpattu, Tamil Nadu 603203, India
e-mail: sa8831@srmist.edu.in

K. R. Reddy et al. (eds.), *Recent Advances in Civil Engineering*, Lecture Notes in Civil Engineering 398, https://doi.org/10.1007/978-981-99-6229-7_5

and engineers. This computing technology helps machines solve complex problems with more human-like intelligence. AI generally necessitates taking characters from human intelligence and appertaining them as an algorithm in a favourable computer way. Depending on the needs, a more or less flexible and effective method may be employed, influencing how artificially intelligent the conduct looks [3].

1.1 The Conference that Started the Reign

The logic theorists Allen Newell, Herbert Simon, and Cliff Shaw suggested a programme supported by the Research and Development (RAND) Corporation to imitate a human's problem-solving abilities. The phrase "artificial intelligence" was coined by the first stone foundation. This momentous event served as the impetus for the following 20 years (From a Harvard University paper) [4].

1.2 Aim of the Review

This study aims to acknowledge the various attributes of AI in building technology. A systemic literature review is necessary as it provides a valuable research benchmark. The aim of this review

1. Pick out the research reported on construction technology and the contribution of AI.
2. Examine the practical execution of AI in construction technology.
3. Identify the future possibility of AI research in construction engineering.

2 Previous Systematic Literature Review in Civil Engineering

Despite increasing research on AI, it is asserted that there needs to be more ground research on how AI is incorporated into construction technology. Civil engineering projects are unique and require high human creativity and experience for a successful project [5]. In this review, we claim and identify the gap in the AI technology used in construction engineering. We acknowledged three previous studies and highlighted their limitation in these studies (Table 1).

Table 1 SLRS from the past in construction technology compared

Comparing section	Objective	Years incorporated	Number of citations
Manzoor [6]	AI towards sustainability by automation in construction	1995–2020	10
Mohammed Hamza Momade et al. [21]	AI application tools in construction technology	1991 to 2010	2
Sofiat O. Abioye [22]	Present status of AI in construction filed	1969–2019	7

3 Research Methodology

An overview of the systematic review procedure used in this review is provided in this session. A systematic literature review "identifies, evaluates, and analyses currently available research on a specific research question, issue, or phenomenon of interest" [7]. This methodical technique was adopted in order to give high-quality, transparent, and facsimile reviews [8].

3.1 Construction of Literature Review

Okoli [8, 9] proposed a methodical evaluation procedure that incorporates eight steps, including two steps of planning, two steps of selection, two steps of extraction, and two steps of execution which primarily consists of four phases. These four phases and eight steps were talked through in this session. This session's primary goal is to answer the indagated query in Table 2.

The quality of the literature review is dependent on a thorough search procedure. The ideal way to construct a search strategy is by an indagation query. The key objective is to review as innumerable papers to find the answers to indagation queries. The first step in the literature search process is using a keyword in a search engine to find the proper study [10]. In this process, articles were limited to the English language only.

Table 2 Indagation query

ID	Indagation query
RQ1	Elucidate AI?
RQ2	How many scholarly works on AI from the AEC have been published?
RQ3	What is the application of AI in the building business?
RQ4	What role does AI play in the building sector?
RQ5	What are the challenges overlooked in the application of AI in building technology?

Table 3 Definitions expressing artificial intelligence

Source cited	Definition
McCarthy [10]	AI refers to the science and engineering that makes machines intelligent
Carbonell [11]	ML is built on memorising facts and learning broad concepts from examples of data ranges to provide correct results
Cross [12]	Defined it as information technology that programmes the task and performs it on the user's behalf
Russell [13]	Artificial intelligence is which enables machines to exhibit human intelligence

4 Research and Analysis

The outcomes of the primary analysis of the studies published in the literature are presented to us in this session. This analysis is only based on (1) a year of research, (2) a definition of artificial intelligence, and (3) a published article, (4) the research method adopted, and (5) types of AI.

4.1 RQ1 Elucidate AI?

The main aim of this research question is to identify the accurate and absolute definition of AI in construction technology. However, when AI has impacted almost all engineering filed, and despite being studied for almost 70 years, no article cited provides a clear definition of AI. Here are a few precise definitions expressing artificial intelligence in Table 3.

4.2 RQ2 How Many Scholarly Works on AI from the AEC Have Been Published?

This powerful tool is used in Architecture Engineering and Construction (AEC) to combat complex and challenging problems. A record of 41,827 allied bibliographies was received from Scopus in qualitative analysis of the science mapping method. Some of AEC's most popular AI techniques include genetic algorithms, neural networks, fuzzy sets, fuzzy logic, and machine learning. The most prevalent subjects and issues using AI methods and concepts include upgrading, simulating uncertainty, project managing, and bridging [14].

4.3 RQ3 What is the Application of AI in the Building Business?

AI is an influential mechanism with many achievements now evident in almost every industrial technology. However, the escalation approval of AI in the building industry has been bounded compared to other business provinces.

This research aims to comprehensively review AI applications in the building quarters. This study divulges that (a) artificial intelligence (AI) is used in building planning, design, (b) the construction lifecycle, and (c) AI can be applied to construction projects that require an accurate risk assessment, cost forecasting, and event management. (d) Adopting AI, reducing time spent and improving the work on construction sites are beneficial. Table 4 demonstrates some benefits and shortcomings of adopting AI in structural sectors.

4.4 RQ4 What is the Future of AI in the Building Sectors?

Estimation and Scheduling

BIM is now state-of-the-art for increasing the construction industry's precision of cost and time estimates [30]. Integrating schedule (4D) and capital (5D) into BIM enables advancements in project programming and cost evaluation at the early design stage [31].

In order to profit from improved accuracy, this involves merging cutting-edge AI techniques like DL with BIM for price arrangement prediction. Deep learning methods may thus also aid in more precise forecasting of other essential factors, such as triumphant, energy, negligence, carbon coherence, as well as trash [20].

Construction Site Analytics

Construction sites quickly evolve into innovative working environments as IoT sensors and other computer-generated mechanisms become increasingly prevalent. Building site analytics aims to generate, amass, stock, and analyse data from building sites to provide intelligent visualisations [25, 26, 28].

Job Creation

By the mid-2030s, the preponderance of construction vocations with moderate to stunted educational requirements would almost certainly be mechanised (38–45%) [19]. However, the use of such technology may result in the creation of whole new vocations in order to integrate and retrain displaced workers in the sector. As a result of the usage of computer-based technologies such as AI in the building business, new job categories will arise [26, 30].

Table 4 Benefits and shortcomings of using AI in structural sectors

Subfield	Benefits in structural sectors	Shortcomings in structural sectors	References
Machine learning	• Lower costs • Increased safety • More practical use of resources • Fewer errors and omissions	• Incomplete data • Commencement with high-structural data, learning from streaming data, scaling of models, and distributed computing	[15, 16]
Planning and scheduling automation	• Cost savings as a result of enhanced operations, such as logistics • Enhanced output • Decreased planning effort • Easier management and monitoring • Optimal scheduling and plans	• Expensive to implement • Complex • Needed models' • Knowledge representations, monitoring problems, integration problems, synthesis approaches, etc.	[16]
Optimisation	• Increased productivity as a result of streamlined operations • Increased effectiveness • Time and money savings	• Demands a lot of CPU power • Scalability problems	[17]
Natural language processing	• Enhanced productivity • Economical use of resources • Effective use of time • Enhance collaboration between stakeholders	Speech recognition problems include construction site noise, homonyms, accent variations, etc.; appropriate representation of fragmented, prolonged, and incorrect language • Concerns with data security and privacy	[18]

Health and Safety Analytics

Health and safety analytics (HSA) uses cutting-edge data inquisitive approaches to anticipate and prevent workplace accidents. One of the most recent applications of artificial intelligence in health and safety is wearable technology for monitoring construction safety. Identification and reduction of fall hazards using BIM, as well

as the use of BIM and sensor-based technologies, are to improve construction safety [25, 27].

4.5 RQ5 What Are the Challenges Overlooked in Applying AI in Building Technology?

This study has identified certain emerging trends as well as prospective uses of AI in the building sector. Recognising and discussing the main obstacles to further enhancing this field of study are critical.

Issues of Culture and Comprehensible AI

It is common knowledge that the building sector is among the least digitalised and among the last to accept new technology. This might be a result of the risky and expensive nature of the majority of construction procedures, where even small mistakes can have big effects. Established methods are chosen in the building industry over new, untested technologies that claim to produce outstanding outcomes [23, 24].

Security

While artificial intelligence (AI) may improve security and ascertain breaches, it is also a prominent earmark for exploitation by hackers, cybercriminals, and seclusion intruders. This serious issue has significant economic and financial ramifications.

High Upfront Price

The advantages of AI-driven solutions for the building industry are undeniable. However, the primary costs of AI technology, such as robots, are sometimes rather costly.

Talent Shortage

AI developers with the skills required to spur substantial advancements across industries are now in short supply. It may be difficult to locate AI professionals with building industry knowledge who can offer customised answers to the sector's many problems [29].

5 Conclusion

This paper acknowledges the growth of artificial intelligence in the construction industry and provides a systemic review.

- This paper provides a thorough tutorial on creating a systematic literature review in this essay. Here, outline the procedures to guarantee a thorough review that thoroughly summarises and examines the available literature on an important research subject.
- This paper emphasises that such a review be explicit in identifying the methodologies used so that other researchers conducting the same review process might replicate the findings.

References

1. Cockburn IM et al (2018) The impact of artificial intelligence on innovation [online]. Available http://www.nber.org/papers/w24449
2. Lu P, Chen S, Zheng Y (2012) Artificial intelligence in civil engineering. Math Probl Eng 2012. https://doi.org/10.1155/2012/145974
3. Turing AM (1950) Mind a quarterly review of psychology and philosophy I.—computing machinery and intelligence [online]. Available https://academic.oup.com/mind/article/LIX/236/433/986238
4. Ali A, Qadir J, Rasool RU, Sathiaseelan A, Zwitter A, Crowcroft J (2016) Big data for development: applications and techniques. Big Data Anal 1(1). https://doi.org/10.1186/s41044-016-0002-4
5. Manzoor B, Othman I, Durdyev S, Ismail S, Wahab MH (2021) Influence of artificial intelligence in civil engineering toward sustainable development—a systematic literature review. Appl Syst Innov 4(3). https://doi.org/10.3390/asi4030052
6. Salehi H, Burgueño R (2018) Emerging artificial intelligence methods in structural engineering. Eng Struct 171:170–189. https://doi.org/10.1016/j.engstruct.2018.05.084
7. Leidner DE, Kayworth T (2006) Review: a review of culture in information systems research: toward a theory of information technology culture conflict. MIS Q Manage Inf Syst 30(2):357–399. https://doi.org/10.2307/25148735
8. Okoli C (2015) A guide to conducting a standalone systematic literature review. Commun Assoc Inf Syst 37(1):879–910. https://doi.org/10.17705/1cais.03743
9. Levy Y, Ellis TJ (2006) A systems approach to conduct an effective literature review in support of information systems research. Inform Sci J
10. Mccarthy DJ. Session 1 paper 3 programs with common sense
11. Carbonell JG, Michalski RS, Mitchell TM. An overview of machine learning
12. Cross SR (2003) Agency, contract and intelligent software agents. Int Rev Law Comput Technol 17(2):175–189. https://doi.org/10.1080/1360086032000122556
13. Russell SJ, Norvig P. Instructor's manual: exercise solutions for artificial intelligence a modern approach, 2nd edn. [online]. Available http://aima.cs.berkeley.edu
14. Darko A, Chan APC, Adabre MA, Edwards DJ, Hosseini MR, Ameyaw EE (2020) Artificial intelligence in the AEC industry: scientometric analysis and visualisation of research activities. Autom Constr 112. https://doi.org/10.1016/j.autcon.2020.103081
15. Kotsiantis SB (2007) Supervised machine learning: a review of classification techniques
16. Najafabadi MM, Villanustre F, Khoshgoftaar TM, Seliya N, Wald R, Muharemagic E (2015) Deep learning applications and challenges in big data analytics. J Big Data 2(1). https://doi.org/10.1186/s40537-014-0007-7
17. Roy R, Hinduja S, Teti R (2008) Recent advances in engineering design optimisation: challenges and future trends. CIRP Ann Manuf Technol 57(2):697–715. https://doi.org/10.1016/j.cirp.2008.09.007

18. Bates M, Weischedel RM (1993) Challenges in natural language processing. Cambridge University Press
19. Will robots really steal our jobs? [online]. Available www.pwc.co.uk/economics
20. Bhatnagar S et al (2018) Mapping intelligence: requirements and possibilities. In: Studies in applied philosophy, epistemology and rational ethics. Springer International Publishing, pp 117–135. https://doi.org/10.1007/978-3-319-96448-5_13
21. Momade MH, Durdyev S, Estrella D, Ismail S (2021) Systematic review of application of artificial intelligence tools in architectural, engineering and construction. Front Eng Built Environ 1(2):203–216. https://doi.org/10.1108/febe-07-2021-0036
22. Abioye SO et al (2021) Artificial intelligence in the construction industry: a review of present status, opportunities and future challenges. J Build Eng 44. https://doi.org/10.1016/j.jobe.2021.103299
23. Czarnecki S, Sadowski Ł, Hoła J (2020) Artificial neural networks for non-destructive identification of the interlayer bonding between repair overlay and concrete substrate. Adv Eng Softw 141. https://doi.org/10.1016/j.advengsoft.2020.102769
24. Asteris PG, Skentou AD, Bardhan A, Samui P, Lourenço PB (2021) Soft computing techniques for the prediction of concrete compressive strength using non-destructive tests. Constr Build Mater 303. https://doi.org/10.1016/j.conbuildmat.2021.124450
25. Garrett JC, Mei H, Giurgiutiu V (2022) An artificial intelligence approach to fatigue crack length estimation from acoustic emission waves in thin metallic plates. Appl Sci 12(3). https://doi.org/10.3390/app12031372
26. Ghiasi R, Ghasemi MR, Chan THT (2021) Optimum feature selection for SHM of benchmark structures using efficient AI mechanism. Smart Struct Syst 27(4):623–640. https://doi.org/10.12989/sss.2021.27.4.623
27. Seo J, Han S, Lee S, Kim H (2015) Computer vision techniques for construction safety and health monitoring. Adv Eng Inform 29(2):239–251. https://doi.org/10.1016/j.aei.2015.02.001
28. Neelamkavil J (2009) Automation in the prefab and modular construction industry, June 2009. https://doi.org/10.22260/ISARC2009/0018
29. Bogue R (2018) What are the prospects for robots in the construction industry? Ind Robot 45(1):1–6. https://doi.org/10.1108/IR-11-2017-0194
30. Patil D (2018) Building information modelling (BIM) application in construction industry. Int J Sci Res.https://doi.org/10.21275/SR20525213518
31. Liu Z, Osmani M, Demian P, Baldwin A (2015) A BIM-aided construction waste minimisation framework. Autom Constr 59:1–23. https://doi.org/10.1016/j.autcon.2015.07.020

Prediction of Diaphragm Wall Deflection by Using Different Models for Deep Excavation in Sands

Mohd Sheob, M. Danish, and Md Asad Ahmad

Abstract The purpose of this investigation is to assess and contrast findings from analyses of deep excavations in an undrained condition using the most used three soil models. In this research, three distinct soil models were employed to predict the ground surface settlement and diaphragm wall deflection for deep excavation in sands. These models included the Mohr–Coulomb model (MC model), the hardening soil model (HS model), and the hardening soil small strain model (HSS model). A case study of a deep excavation that actually takes place in layers upon layers of sand in Kaohsiung city, Taiwan, and had well-documented monitoring data is employed for the analysis in this study, and soil investigation results compiled for the construction project served as the basis for selecting the geotechnical parameters. The results show that the wall deflections predicted by the Hardening soil with small strain model are relatively close to those results, which were derived from field measurements. The hardening soil model produces superior results, when compared to the Mohr–Coulomb model. The ground settlement results predicted by any of the three soil models were poor. To anticipate the wall deflection and compare the results of the 2D analysis, a 3D analysis in PLAXIS was also carried out in this study, and the outcomes of the 3D analyses were nearly identical below the excavated depth to those of the 2D analyses. This research shows that HS and HSS models in numerical calculations are useful for predicting the soil behaviour during excavation, and researchers and engineers can use the findings of this work to improve the accuracy of their numerical studies using constitutive soil models.

Keywords Deep excavation · Mohr–Coulomb model · Numerical modelling · Surface settlement · Hardening soil small strain model · Wall deflection

M. Sheob (✉) · M. Asad Ahmad
Department of Civil and Construction Engineering, National Taiwan University of Science and Technology, Taipei, Taiwan
e-mail: mohdsheobamu@gmail.com

M. Danish
Department of Civil Engineering, Aligarh Muslim University, Aligarh, India

K. R. Reddy et al. (eds.), *Recent Advances in Civil Engineering*, Lecture Notes in Civil Engineering 398, https://doi.org/10.1007/978-981-99-6229-7_6

1 Introduction

Densely populated urban and suburban areas necessitate frequent deep excavations for the construction of tall buildings, MRT systems, road tunnels, among many other facilities. When working in soft ground, deep excavation might cause unfavourable ground deformations that may compromise nearby buildings. Therefore, it is essential to foresee these shifts so that some safety measures can be implemented to lessen the effects of the ground deformation [1]. Many studies have explored the diaphragm wall and ground movements caused by deep excavations with different models [2–6]. However, the proper selection of the constitutive model for the soil, which has a direct impact on the design, has not been thoroughly examined in 2D and 3D simulation on FEM-based software, and this issue is investigated in present study; the selected models are MC model, the HS model, and the HSS model due its widely acceptability and consideration of unloading effect in simulation. Some researchers have developed empirical approaches to estimate the settlement amplitude and profile by using feedback from a number of historically well-documented excavations [6]. With PLAXIS, more settlement and lateral deformation were computed than had been determined by local surveys [7]. The study, which was based on the measured data gathered from 296 case histories, provided support for earlier research by showing that the stiffness of the retaining system has no effect on the deformations in non-cohesive soil or stiff clay, while in soft clay, there is a low correlation between the stiffness and wall deflections [8]. The maximum surface settlement caused by excavation ranges from 0.1 to 0.35% of H_e (depth of excavation), and the maximum surface settlement is located between 0.33 and 0.5 H_e from the margin of the excavation [9].

As the safety of nearby structures must always be taken into account, there is still a lot of work to be done to improve the accuracy of finite element analysis in urban excavation design. Accuracy is determined by the formulation of the model, and parameters. Some of the most widely applied constitutive models are linear and nonlinear stress–strain models, which have emerged over the past five decades [10–13]. Predicting movements caused by deep excavations by using numerical calculations is still difficult. Numerous choices, including boundary condition, comprehensibility of geometry, constitutive models, input parameters, and mesh generation; affect the precision of a numerical analysis. Soil input parameters can be determined through experimentation in the lab or in the field, or they can be calculated using empirical equations. Engineers' familiarity with numerical methods and soil constitutive models is crucial for accurate results from numerical analysis [14].

This research aims to evaluate the efficacy of three soil models in PLAXIS software to anticipating the actions, generated by a deep excavation in sands. The numerical calculations in this scrutiny are based on a case study of deep excavation that has been thoroughly documented in Kaohsiung city, Taiwan.

2 Case Study Overview

In this study, numerical assessments are based on a case study of Kaohsiung city, Taiwan. Culture Center Station, of MRT system in Kaohsiung, was closed by the construction site. The location was about 3 km east of Kaohsiung bay, in the middle of Kaohsiung city. The site was in rectangular shape with dimension of 70 m by 20 m. Diaphragm walls, that were used to contain the excavation while it was being excavated by the bottom-up technique of excavation, were 0.9 m thick, and height was 32 m; excavation took place over the course of five phases, with the deepest reaching 16.8 m; Table 1 outlines the stages of the construction process. Steel struts were used to support the retaining wall at four different heights, with an average horizontal distance of 5.5 m between each pair of struts. Figure 1 exhibits the cross section of site and existing ground condition. Figure 1 shows that the three clay layers (CL type) have negligible effects on excavation behaviour since they are so thin. The site excavation thus represents a prototypical instance of a deep excavation in sand, all of the soil parameters were obtained from a study that had previously analysed the wall deflection and settlement using a two-dimensional analysis [14]. The additional parameters required have been calculated by the given equations in each subsection. On the other hand, the purpose of this investigation is to contrast the findings obtained from 2D analysis with those obtained from 3D analysis.

Table 1 Excavation process of site

Excavation activities	Stage
Dewatering till 3.5 m	1
Excavated to the depth of 2.5 m below the GL	
Install first struts H400 × 400 × 13 × 21 at the depth of 1.5 m below the GL. Preload of each strut is 900 kN	2
Dewatering till 8.3 m	
Excavated to the depth of 7.3 m below the GL	
Install second struts H400 × 400 × 13 × 21 at the depth of 6.3 m below the GL. Preload of each strut is 2000 kN	
Dewatering till 11.65 m	3
Excavated to the depth of 10.65 m below the GL	
Install third struts H400 × 400 × 13 × 21 at the depth of 9.65 m below the GL. Preload of each strut is 2800 kN	
Dewatering till 15 m	4
Excavated to the depth of 14 m below the GL	
Install fourth struts H400 × 400 × 13 × 21 at the depth of 13 m below the GL. Preload of each strut is 2800 kN	
Dewatering till 17.80 m	5
Excavated to the depth of 16.80 m below the GL	
Construct the base slab	

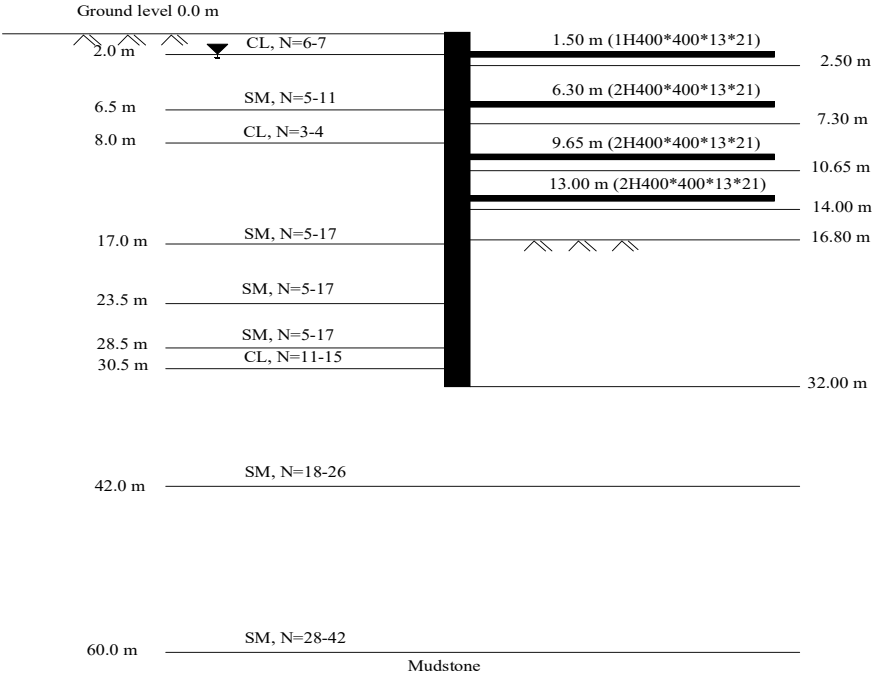

Fig. 1 Soil profile of excavation site

The reported groundwater level (GWL) before excavation was 2.0 m, and before the beginning of each phase of excavation, the GWL was nethered to a depth of 1 m below the planned excavation level to facilitate the work. Figure 1 describes the stratigraphic of site condition based on data gathered throughout the investigation: Clay (CL) makes up the initial layer to a depth of 2 m. It has an N value of somewhere between 6 and 7, which places it in the middle of the range for clay. The second layer, consisting of silty sand (SM) with N values of 5–11 and $\varphi\prime = 32°$ and a thickness of 2–6.5 m. Again, clay (CL) with an N value of about 3–4 makes up the third layer, which extends from 6.5 to 8 m deep. The fourth layer, from 8 to 17 m deep, consists of compact silty sand (SM) with an N value of 5–17, and $\varphi\prime = 32°$. The fifth layer consists of a medium-density silty sand (SM) that is from 17 to 23.5 m thick, with an N value of between 5 and 17, and $\varphi\prime = 32°$. Between 23.5 and 28.5 m deep, with a density of medium-to-dense silt sand and N value lies between 5 and 17 and $\varphi\prime = 33°$, lies the sixth layer. From 28.5 to 30.5 m beneath the sixth layer is more clayey soil, with N value of 11–15. Eighth layer properties are identical to those of the sixth layer from 30.5 to 42 m in depth, with N values of 18–26 and $\varphi\prime = 34°$. From 42 to 60 m down, a layer of compact silty sand (SM) with an N value of 28–42 and $\varphi\prime = 34°$.

The displacement of the ground and surrounding structures was observed by ground instrumentation. During the process of excavation, inclinometers had been

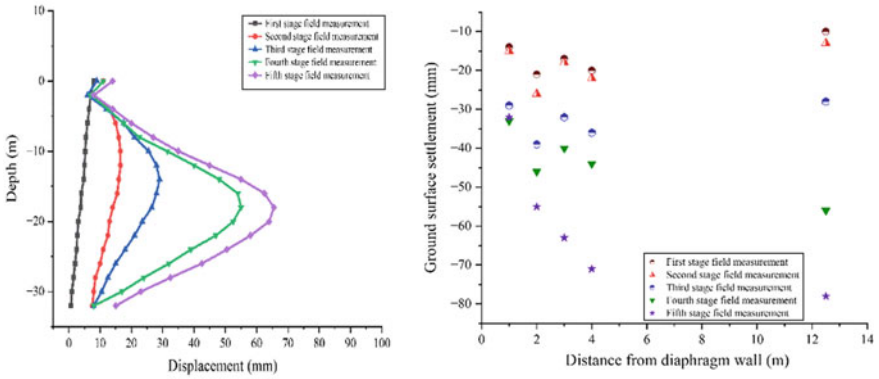

Fig. 2 Wall deflection and surface settlement by inclinometers and settlement observation instrumentation, respectively

used to monitor the wall deflections and settlement observation sections were used to monitor the surface settlements. In order to make sure that movements were acceptable, measurements acquired by the equipment were utilized to study the response of walls and nearby structures. They also contributed to provide the data that was used to support the accuracy of the numerical modelling in this research. Figure 2 depicts the actual wall deflections and ground surface settlements.

Figure 2 shows that during the first phase of excavation, the wall is meant to behave as a cantilever before the first-level steel struts have been erected and preloaded. Later excavation levels show the wall displaying deep inward shifts. At the end of excavation, the maximum value of wall deflection was reported as 0.39% of the total excavation depth (H_e). Consequently, this number agrees with the range of 0.2% H_e to 0.5% H_e discovered by a researcher [2]. It was difficult to see the entire extent of settlement beyond the retaining wall, because of the proximity of the excavation to the busy road. However, reported maximum values of surface settlement (δ_{vm}) in the end of excavation was around 0.125–0.1785% of H_e, or the ratio δ_{vm}/H_e is equivalent to 0.12–0.18%. Excavations in stiff clays and sands resulted in maximum surface settlements of around 0.15% of H_e [6].

3 Numerical Modelling

The evaluation software PLAXIS was employed in this study. The thin clay layers have no appreciable effect on excavation behaviour. As a counterexample, sand layers have a significant impact on excavation behaviour. In this work, three different soil models were used to replicate the sand layers in order to compare how well they predicted the surface settlements and wall deflections caused by the excavation of site. In the numerical computations, it was assumed that all sand layers included drained

materials. To ensure the consistent evaluation, a total stress undrained analysis of the clay strata was undertaken using the MC model; shear strength S_u, internal friction angle $\varphi_u = 0$, and undrained Young's modulus E_u were utilized for a total stress study of the clay layers in an undrained state. The empirical equation $E_u = 500\ S_u$ has been proposed to calculate the value of E_u [4, 5, 15]. The numerical difficulties associated with exceptionally low compressibility of water led to the adoption of Poisson's ratio $\nu_u = 0.495$ to model the behaviour of water. Clay layer input parameters utilized for analysis are listed in Table 2.

Plate element has been used in this study to simulate the diaphragm wall, while fixed-end anchor was used to simulate the steel struts; the steel struts and diaphragm walls were modelled using a linear elastic constitutive relationship. Young's modulus along with Poisson's ratio are the two input parameters needed for this model. The Poisson's ratio of steel struts and diaphragm wall was used as 0.2. The ACI Committee 318 (1995) formula was used to determine the diaphragm wall's Young's modulus:

$$E = 4700\sqrt{f_c}\ (\text{MPa})$$

In which f_c is the characteristic compressive strength of the concrete employed in the diaphragm walls. The Young's modulus of steel struts was considered to be 210 GPa. It is recommended to reduce the rigidity of the diaphragm wall by 30% and the steel struts by 40% from their standard values to account for cracks caused by bending forces in the diaphragm wall and to account for multiple uses and steel struts that were installed incorrectly, respectively [3]. The input parameters utilized in the numerical computations for the diaphragm wall are listed in Table 3 and for the steel strut are listed in Table 4.

Figure 3 shows the resulting numerical study of the site based on the finite element model. It was only necessary to reproduce half geometry of the site in order to excavate it because of its symmetry. The ideal distance between the lateral boundary

Table 2 Clayey soil parameters

Layer	Depth (m)	γ_t (kN/m^3)	S_u (kPa)	ν_u	E_u (kPa)
1	0.0–2.0	19.3	28	0.495	14,000
3	6.5–8.0	19.7	21	0.495	10,500
7	28.0–30.5	18.6	84	0.495	42,000

Table 3 Related parameters of diaphragm wall

Specifications	Value
Thickness Weight	0.9 m 4.95 kN/m/m
Axial stiffness 70%	15.66×10^6 kN/m
Poisson's ratio	0.2
Flexural stiffness 70%	1.057×10^6 kN-m^2/m

Table 4 Related parameters of steel struts

Strut level	Identification	Section area (m^2)	EA (kN)	Preload (kN)	60% EA (kN)
1	1H400 × 400 × 13 × 21	0.0219	4.59×10^6	900	2.75×10^6
2	2H400 × 400 × 13 × 21	0.0437	9.18×10^6	2000	5.50×10^6
3	3H400 × 400 × 13 × 21	0.0437	9.18×10^6	2800	5.50×10^6
4	4H400 × 400 × 13 × 21	0.0437	9.18×10^6	2800	5.50×10^6

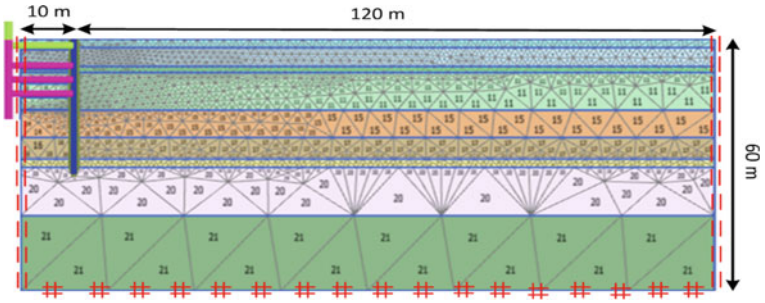

Fig. 3 Mesh used in this study

of the model and the diaphragm wall is seven times the depth of the excavation, i.e. 120 m [5]. The horizontal motion of model was restricted at its side boundaries. Vertical and horizontal mobility was limited at the bottom boundary of the model.

3.1 Mohr–Coulomb Model (MC Model)

In the field of geotechnical engineering, the MC model is commonly employed for the purpose of design because of its simplicity as a linear elastic-perfectly plastic model used to predict the material behaviour under monotonic loads. The relative simplicity of the model and necessity of only the most fundamental soil parameters, i.e. friction and dilation of soils, have made it a favourite among those interested in simulating the behaviour of soils. Sand layers were supposed to have zero effective cohesion (c') values; however, to keep PLAXIS calculations simple, layers of sand were assigned the extremely low value of $c' = 0.5$ kPa. Numerous studies assumed a drained Poisson's ratio of 0.3 for sand layers [5]. A study suggested the following method for determining the dilatancy angle for sands [16].

$$\text{If, } \Phi' \leq 30^\circ: \Psi' = 0, \text{ or } \Phi' > 30^\circ: \Psi' = \Phi' - 30^\circ.$$

The following formula, derived by a study, can be used to determine the coefficient of lateral earth pressure at rest.

$$K_0 = 1 - \sin \Phi'$$

The sand stiffness parameter E' is notoriously difficult to obtain an exact value from test results. This is because Φ' is closely associated with characteristics of the sand particles themselves, such as their surface roughness, compaction, and shape, all of which are seldom affected by the sample disturbance. Furthermore, the Young's modulus E' of sand is significantly affected by the sample disturbance since it is dependent on the physical qualities of sand and the intergranular force between the grains. Therefore, the E' is typically derived from empirical equations, this can be discovered through calibration studies of field-scale load testing or deep excavation case histories. In recent years, many geotechnical engineers now employ the standard penetration test (SPT) since it is reliable and inexpensive. As a result, several nations now routinely employ connections between SPT or N values and soil qualities. Scientists have proposed empirical links between the E' and N for sands in the form of $E' = A \times N$, where A is a correlation ratio [17]. This study similarly employed the following relation between E' and N: $E' = 2000N$ (kPa).

A researcher utilized an identical equation to describe the excavation of sands at the O6 station, located roughly 0.6 km from the actual excavation site [1].

3.2 Hardening Soil Model (HS Model)

A legitimate second-order model for soils is the HS model; the HS model uses the same failure criterion as the MC model and is a more sophisticated model. Before the primary loading reaches the fracture surface, the HS model uses the hyperbolic stress–strain relationship between vertical strain and deviatoric stress; plastic shear strain under deviatoric loading and cap hardening characteristics is modelled by using frictional hardening characteristics, while plastic volumetric strain under primary compression is modelled. Nine parameters are needed for the hardening soil model, i.e. three reference stiffness; triaxial unloading/reloading stiffness $E_{\text{ur}}^{\text{ref}}$, triaxial loading secant stiffness ref E_{50}^{ref}, and oedometer loading tangent stiffness $E_{\text{oed}}^{\text{ref}}$, along with a reference pressure p^{ref}, the value of p^{ref} typically taken to be 100 kPa (1 bar). The strain level to failure is determined by the failure ratio (R_{f}), the pure elastic Poisson's ratio or unloading/reloading Poisson's ratio (ν_{ur}); the Mohr–Coulomb strength parameters cohesion (c') and angle of internal friction (φ'); a power (m) for the stress-dependent stiffness; the fundamental one-dimensional compression K_0 value (K_0^{nc}). By using three reference stiffness, the HS model measures soil stiffness much more precisely.

$$\text{For sand } \boldsymbol{E}_{50} = \boldsymbol{E}_{50}^{\mathbf{ref}} \left(\frac{\boldsymbol{c'\cos\Phi\prime + \sigma_3\prime \sin\Phi\prime}}{\boldsymbol{c'\cos\Phi' + p^{ref}\sin\Phi\prime}} \right)^{\boldsymbol{m}} = \boldsymbol{E}_{50}^{\mathbf{ref}} \left(\frac{\boldsymbol{\sigma'_3}}{\boldsymbol{p^{ref}}} \right)^{\boldsymbol{m}}.$$

In which $\sigma_3\prime$ is the effective minor principal stress. The Mohr–Coulomb strength parameters and K_0 were identical to those in the MC model in every way. For sands, the values of m and ν_{ur} were set to 0.5 and 0.2, respectively [18]. As a default value in the PLAXIS, the R_f was taken to be 0.9. The E_{ur}^{ref} and E_{oed}^{ref} stiffness parameters were adjusted to $3E_{50}^{ref}$ and E_{50}^{ref} for sands, respectively. The back analysis between E_{50}^{ref} and N for the sand layers yielded the following best-fit relation [14].

$$E_{50}^{ref} = 1200N \text{ (kPa)}$$

3.3 Hardening Soil Small Strain Model (HSS Model)

The original hardening soil model has been improved with the hardening soil small strain (HSS) model, which consider the small strain properties of soil [19]. The HSS model comprises two extra parameters beyond the requirements for the hardening soil model, reference shear modulus at very low strain (G_0^{ref}) and the shear strain ($\gamma_{0.7}$) at which the secant shear modulus equals around 70% of its beginning value are the two additional parameters ($G_s = 0.722G_o = 0.722G_{max}$). The input parameters of HSS model were identical to those used in the HS model in every way. The PLAXIS user manual suggests the following equation to obtain the $\gamma_{0.7}$ value.

$$\gamma_{0.7} = \frac{1}{9G_0}\left[2c'\left(1 + \cos 2\varphi'\right) - \sigma_1\prime(1 + K_0)\sin 2\varphi'\right]$$

In which $\sigma_1\prime$ is effective vertical stress. The HSS model predicts far smaller wall deflections and surface settlements than those observed in the field when $\gamma_{0.7}$ was estimated according to the given equation, the estimation of $\gamma_{0.7}$ from above equation should be adjusted accordingly. However, the value of strain as 10^{-4} is typically considered to be a small strain. Consequently, $\gamma_{0.7}$ was assumed to be 10^{-4} instead of utilizing the above equation.

4 Results

4.1 MC Model

The sand layer input parameters of MC model are listed in Table 5.

Table 5 Sandy soil parameters of MC model

Layer	Depth (m)	Soil type	γ_t (kN/m^3)	N value	φ' (°)	c' (kPa)	E' (kPa)	ν'	ψ (°)	K_0
2	2.0–6.5	SM	20.9	5–11	32	0.5	16,000	0.3	2	0.47
4	8.0–17.0	SM	20.6	5–17	32	0.5	22,000	0.3	2	0.47
5	17.0–23.5	SM	18.6	5–17	32	0.5	22,000	0.3	2	0.47
6	23.5–28.5	SM	19.6	5–17	33	0.5	22,000	0.3	3	0.46
8	30.5–42.0	SM	19.6	18–26	34	0.5	44,000	0.3	4	0.44
9	42.0–60.0	SM	19.9	28–42	34	0.5	70,000	0.3	4	0.44

The findings of the MC model, i.e. predictions of ground surface settlement and wall deflection, are shown in Fig. 4; the projected outcomes are also compared to the observed outcomes. Figure 4 demonstrates that during first, second, and third stages of excavation, the wall deflections anticipated by the model are often larger than those observed in actual. This is due to the fact that the MC model disregards the small strain features and the high stiffness modulus behaviour of soil under low strain levels. It follows that the sands used in the MC model have a too-low Young's modulus, because the range of small strain soil area was higher in the beginning stages of excavation. In later excavation stages of excavation, i.e. fourth and fifth stages, predicted wall deflections are larger than field measurements at upper wall parts, but are comparable to actual measurements at lower wall parts. Both the field measurements and the predicted findings show that the greatest deflection occurs at the excavation level. However, the expected values are larger than what was actually measured in the field. One possible explanation could be that the MC model only uses one Young's modulus and does not distinguish between stiffness during loading and unloading. This occurs as a result of the MC model ignoring the behaviour of strain-dependent stiffness. Since the majority of the strains in the secondary influence zone (SIZ) are at low strain levels, the single Young's modulus used in the MC model was inaccurate.

4.2 HS Model

Table 6 provides the sand layer parameters for the HS model analysis. The predicted and observed ground surface settlements and wall deflections for the excavation by HS model are compared in Fig. 5. The findings of the HS model are significantly superior than those of the MC model, as shown in Fig. 5.

Thus, the HS model calculates the unloading stiffness. The HS model predicts that the largest ground surface settlement will occur between 0.6 and 1.0% of H_e away from the wall, with a value of approximately 0.47% of H_e. However, at the upper stages of excavation, the anticipated wall displacements are still more than the actual measurements. Settlements in the SIZ are still considered to be larger

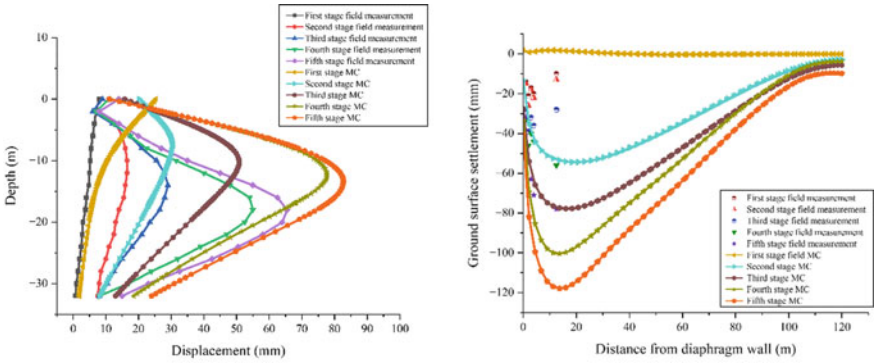

Fig. 4 Wall deflection and ground surface settlement by MC model

Table 6 Sandy soil parameters of HS model

Layer	Depth (m)	γ_t (kN/m^3)	N value	φ' (°)	c' (kPa)	ψ (°)	E_{50}^{ref}	E_{oed}^{ref}	E_{ur}^{ref}	K_0
2	2.0–6.5	20.9	5–11	32	0.5	2	9600	9600	28,800	0.47
4	8.0–17.0	20.6	5–17	32	0.5	2	13,200	13,200	39,600	0.47
5	17.0–23.5	18.6	5–17	32	0.5	2	13,200	13,200	39,600	0.47
6	23.5–28.5	19.6	5–17	33	0.5	3	13,200	13,200	39,600	0.46
8	30.5–42.0	19.6	18–26	34	0.5	4	26,400	26,400	79,200	0.44
9	42.0–60.0	19.9	28–42	34	0.5	4	42,000	42,000	126,000	0.44

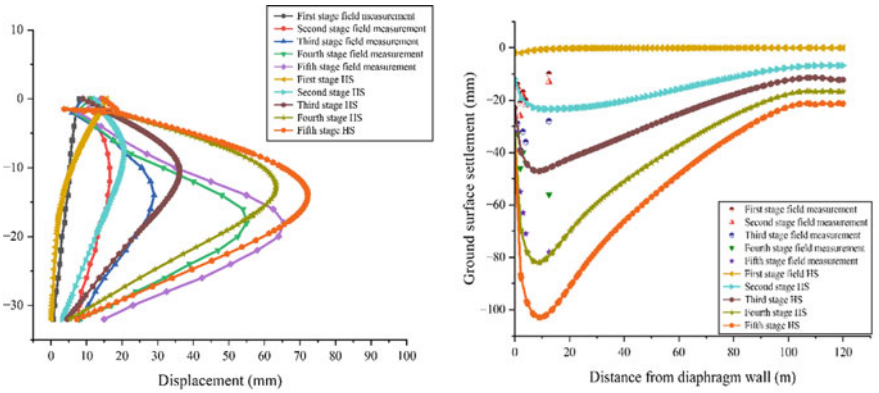

Fig. 5 Wall deflection and ground surface settlement by HS model

and wider than what was discovered in earlier studies. This is due to the fact that the HS model does not account for strain-dependent stiffness behaviour or small strain properties of soil. HS model are clearly superior to those of the MC model, as

shown in Fig. 5, particularly in terms of the prediction of surface settlements. The HS model calculates the unloading stiffness. The HS model predicts that the largest ground surface settlement will occur between 0.6 and 1.0% of $H_{e.}$

4.3 HSS Model

The results are displayed in Fig. 6, where $\gamma_{0.7}$ was considered as 10^{-4}. The required sand layer parameters used in the HSS model under analysis are displayed in Table 7.

Figure 6 compares and contrasts the surface settlements and wall deflections that occurred during excavation using the HSS model. Figure 6 illustrates how the HSS model significantly improves the MC model and the HS model in terms of ground surface settlements and wall deflections. The HSS model does not depict the significant wall toe displacements at later stages of excavation or the excessive wall deflection predictions at later stages of excavation. The greatest settlement in the HSS model is also around 0.6–1.0% of H_e from the wall and has a value of about 0.59% H_e, making it slightly smaller than the largest settlement in the HS model.

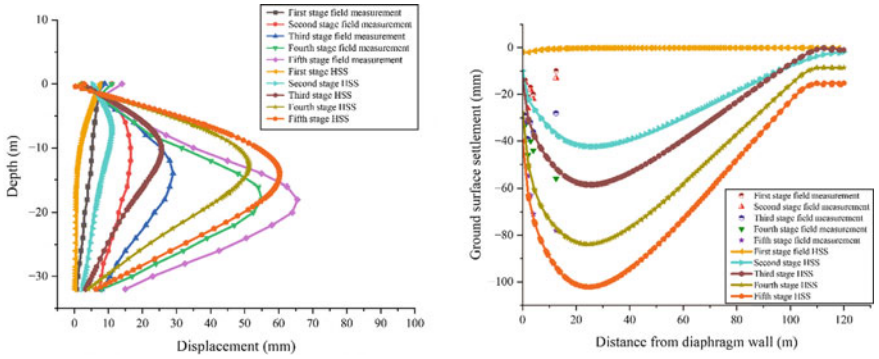

Fig. 6 Wall deflection and ground surface settlement by HSS model

Table 7 Sandy soil parameters of HSS model

Layer	Depth (m)	N value	V_s (m/s)	σ_3' (kPa)	G_0 (kPa)	G_0^{ref} (kPa)	$\gamma_{0.7}$
2	2.0–6.5	5–11	161	63	55,343	69,657	10^{-4}
4	8.0–17.0	5–17	183	150	69,974	57,153	10^{-4}
5	17.0–23.5	5–17	183	226	63,180	42,069	10^{-4}
6	23.5–28.5	5–17	183	278	66,577	39,966	10^{-4}
8	30.5–42.0	18–26	239	374	114,480	59,204	10^{-4}
9	42.0–60.0	28–42	287	518	167,115	73,412	10^{-4}

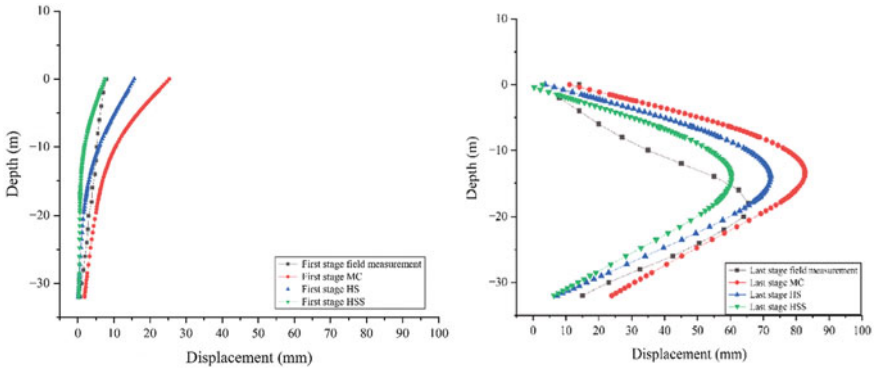

Fig. 7 Wall deflection at first stage and last stage by different models

4.4 Comparing of Results from Different Soil Models

Figure 7 depicts the comparison in the results of wall deflection between first and last stage of excavation by MC model, HS model, HSS model, and field observations; fourth stage wall deflection results by all models and field measurements are depicted by Fig. 8; in addition, results of ground surface settlement of last stage are also compared by different models, and field observations are depicted by Fig. 9. The anticipated wall deflections from both MC and HS models slightly surpass than the actual deflection. However, the projected wall deflections from the HSS model are reasonably equal to the field data during the first stage of excavation. The last stage results of HSS model are quite close to the actual results. However, the findings of HS model and MC model are overestimated as compared to actual data. All three models have surface settlements that are more than the fields observation data. While the settlement profiles of the HS and HSS models are more in line with field observations, those of the MC model are far off the mark.

4.5 Numerical Analysis in 3D

The numerical simulations are carried out in this section by using the geotechnical software PLAXIS 3D. In above subsection, study demonstrates that the best result was given by HSS model while contrasted to the MC and HS models. Consequently, in this section HSS model has been used for the analyses. According to Fig. 10, the study employed a finite element mesh with a total of 386,692 nodes and 268,067 elements.

Figure 11 compares and contrasts wall deflections that occurred during excavation using the HSS model in 2D and 3D analyses. It can be seen that the results from 3D are quite same below the excavation depth. In all stages, the wall deflection predicted by

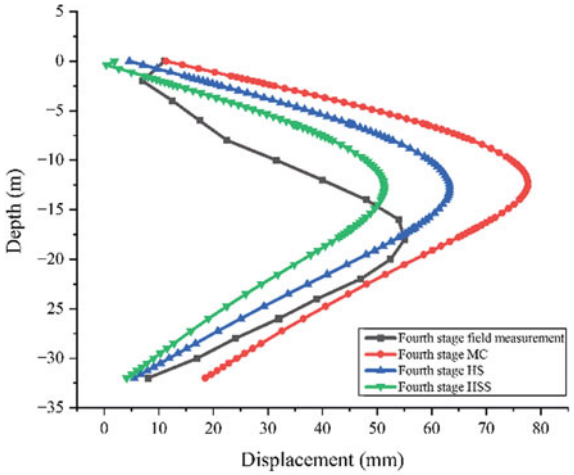

Fig. 8 Wall deflection at fourth stage by different models

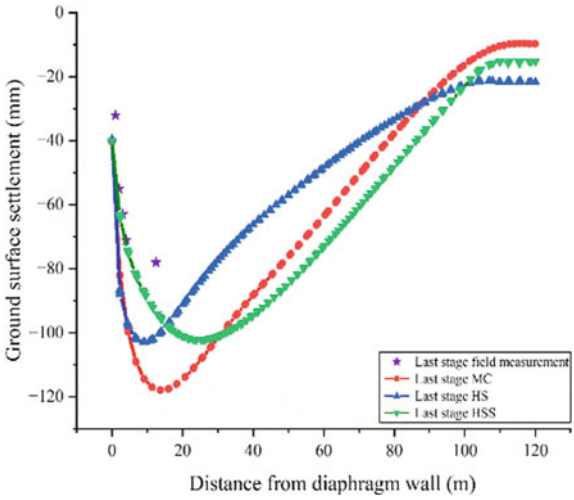

Fig. 9 Ground surface settlement at last stage by different models

3D analyses was slightly overestimated to some degree as compared to 2D analyses. However, it can be seen that the maximum value of deflection occurs at the same depth in twain 2D and 3D analysis, i.e. excavated depth. Lateral wall deflections calculated using 2D and 3D analysis are slightly underestimated and overestimated, respectively, when compared to actual wall deflections. However, predictions and actual outcomes have similar patterns.

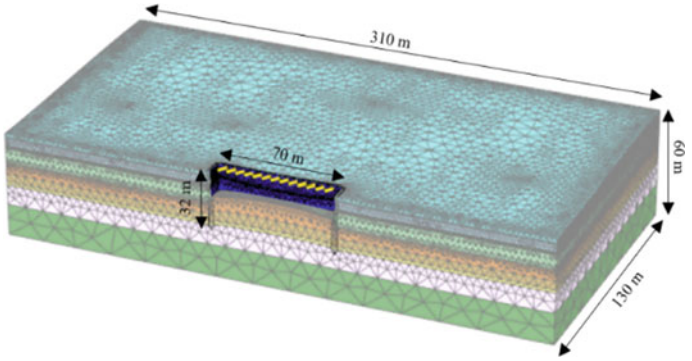

Fig. 10 Half mesh model from PLAXIS 3D

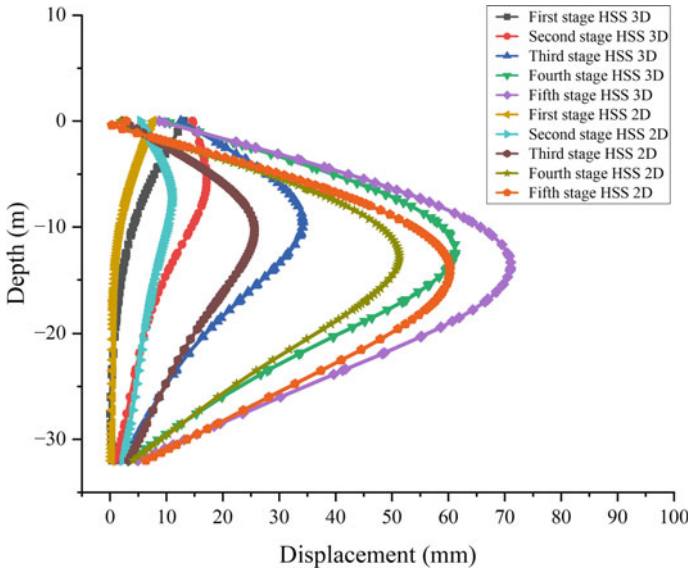

Fig. 11 Wall deflection by HSS model in 2D and 3D

5 Conclusion

- It has been found that using a more complex soil model in numerical computations leads to more accurate predictions of wall deflection and surface settlement, when compared to the HS model, which is better than the MC model, the HSS model is clearly the best option.
- The HSS model's predicted wall deflections are extremely similar to the actual field measurements, whereas those prediction by the MC and HS models are slightly bigger. The settlement profiles of the HS and HSS models are more in line with the field results than that of the MC model, which deviates by a large margin.
- In the case of a deep excavation in sand, the predictions for maximum wall deflection in both 2D and 3D modelling were found at the same depth approximately of each stage. However, the prediction by 3D model was slightly overestimated as compared to 2D model. So rather than 3D analysis, PLAXIS 2D analyses would be appropriate. Unlike 3D analyses, it doesn't require as much calculating time and is less tedious.

References

1. Hsiung B-CB (2009) A case study on the behaviour of a deep excavation in sand. Comput Geotech 36(4):665–675. https://doi.org/10.1016/j.compgeo.2008.10.003
2. Ou C-Y, Hsieh P-G, Chiou D-C (1993) Characteristics of ground surface settlement during excavation. Can Geotech J 30(5):758–767. https://doi.org/10.1139/t93-068
3. Ou C-Y (2006) Deep excavation: theory and practices. Taylor Francis, Netherlands
4. Lim A, Ou C-Y, Hsieh P-G (2010) Evaluation of clay constitutive models for analysis of deep excavation under undrained condition. J Geoeng 5(1):9–20
5. Khoiri M, Ou C-Y (2013) Evaluation of deformation parameter for deep excavation in sand through case histories. Comput Geotech 47:57–67. https://doi.org/10.1016/j.compgeo.2012.06.009
6. Hsieh P-G, Ou C-Y (1998) Shape of ground surface settlement profiles caused by excavation. Can Geotech J 35(6):1004–1017. https://doi.org/10.1139/t98-056
7. Pakbaz MS, Imanzadeh S, Bagherinia KH (2013) Characteristics of diaphragm wall lateral deformations and ground surface settlements: case study in Iran-Ahwaz metro. Tunn Undergr Sp Technol 35:109–121. https://doi.org/10.1016/j.tust.2012.12.008
8. Long M (2001) Database for retaining wall and ground movements due to deep excavations. J Geotech Geoenviron Eng 127(3):203–224. https://doi.org/10.1061/(ASCE)1090-0241(2001)127:3(203)
9. Aswathy MS, Vinoth M, Mittal A, Behera S (2020) Prediction of surface settlement due to deep excavation in indo-gangetic plain: a case study. Indian Geotech J 50(4):620–633. https://doi.org/10.1007/s40098-019-00399-x
10. Ou C-Y, Shiau B-Y, Wang I-W (2000) Three-dimensional deformation behavior of the Taipei National Enterprise Center (TNEC) excavation case history. Can Geotech J 37(2):438–448. https://doi.org/10.1139/t00-018
11. Calvello M, Finno RJ (2004) Selecting parameters to optimize in model calibration by inverse analysis. Comput Geotech 31(5):410–424. https://doi.org/10.1016/j.compgeo.2004.03.004

12. Nikolinakou MA, Whittle AJ, Savidis S, Schran U (2011) Prediction and interpretation of the performance of a deep excavation in Berlin sand. J Geotech Geoenviron Eng 137(11):1047–1061. https://doi.org/10.1061/(ASCE)GT.1943-5606.0000518
13. Ou C-Y, Lai C-H (1994) Finite-element analysis of deep excavation in layered sandy and clayey soil deposits. Can Geotech J 31(2):204–214. https://doi.org/10.1139/t94-026
14. Hsiung B-CB, Dao S-D (2014) Evaluation of constitutive soil models for predicting movements caused by a deep excavation in sands. Electron J Geotech Eng 19:17325–17344
15. Likitlersuang S, Surarak C, Wanatowski D, Oh E, Balasubramaniam A (2013) Finite element analysis of a deep excavation: a case study from the Bangkok MRT. Soils Found 53(5):756–773. https://doi.org/10.1016/j.sandf.2013.08.013
16. Bolton MD (1986) The strength and dilatancy of sands. Geotech 36:65–78
17. Schmertmann JH (1970) Static cone to compute static settlement over sand. J Soil Mech Found Div 96(3):1011–1043. https://doi.org/10.1061/JSFEAQ.0001418
18. Schanz T, Vermeer PA, Bonnier PG (1999) The hardening soil model: Formulation and verification. Beyond 2000 Comput Geotech 10 Years PLAXIS. Balkema, Rotterdam
19. Hardin BO, Drnevich VP (1972) Shear modulus and damping in soils: design equations and curves. J Soil Mech Found Div 98(7):667–692. https://doi.org/10.1061/JSFEAQ.0001760

Geomatics, Geosciences, Remote Sensing, Geographical Information Systems

A Comparative Study on Various Water Index Methods Through Satellite Image Processing for Pre- and Post-flood Monitoring of 2021—A Case Study of Chengalpattu Taluk, India

M. Kalidhas and R. Sivakumar

Abstract Flood is the most hazardous, widespread, and significant natural disaster, leading to more damage to all resources, specifically the highly affected urbanized area. Remote sensing is a useful technique for studying flood-prone area detection. The purpose of this research is to delineate pre- and post-flooded areas in Chengalpattu taluk during 2021. In this research, various water index methods, like Water Ratio Index (WRI), Modified Normalized Difference Water Index (MNDWI), and Normalized Difference Water Index (NDWI), were computed using spectral bands from selected visible to SWIR wavelengths of satellite images. This spectral band-based index provides a better understanding of the identification of flooded areas. The results indicated that the pre-flood was estimated as 3.11 km^2, 7.79 km^2, and 4.91 km^2 by NDWI, MNDWI, and WRI, respectively. Further, the post-flood area was estimated as 4.98 km^2, 15.43 km^2, and 6.15 km^2 by NDWI, MNDWI, and WRI, respectively. Also, a comparative study of the results was conducted for the above various methods, and this approach could be very helpful to delineate in mapping flooded areas with better accuracy. Analysis and results show that the MNDWI method can be used for better water separation and flood area delineation compared to NDWI and WRI.

Keywords NDWI · MNDWI · WRI · Flood · Remote sensing

1 Introduction

Environmental monitoring and nature conservation have benefited significantly from remote sensing, a fast-expanding space technology. These remote sensing technologies have made it possible to update surface water data accurately and often [1].

M. Kalidhas · R. Sivakumar (✉)
Department of Civil Engineering, College of Engineering and Technology, SRM Institute of Science and Technology, Kattankulathur, Tamil Nadu 603203, India
e-mail: sivakumr@srmist.edu.in

K. R. Reddy et al. (eds.), *Recent Advances in Civil Engineering*, Lecture Notes in Civil Engineering 398, https://doi.org/10.1007/978-981-99-6229-7_7

Floods are one of the most common natural disasters in the world, resulting in both economic harm and fatalities [2]. In everyday life, surface water is a vital resource. It can be used for aquaculture, irrigation, drinking, and thermoelectric cooling, among other things [3]. Surface water is yet another reliable evidence of how the places are impacted by humans, climate, anthropogenic, and environmental factors. Rivers, lakes, water reservoirs, and other surface waterways can be observed for current conditions and spatial and temporal changes using remote sensing and a geographic information system [4]. Satellite image processing has emerged as a competitively low-cost alternative for element identification and hydrogeological system knowledge in areas with adequate field data, in addition to acting as the mainstay of hydrogeological exploration in regions lacking thorough field data and overall map coverage [5]. The formation of water-logged areas has been observed worldwide due to natural and artificial sources. Rural areas treat water logging as a natural or nearly natural hazard. Water logging is an issue for the environment that affects many parts of the world [6–8]. For the past 30 years, the Landsat satellites have been collecting multispectral, 30 m resolution images of the globe every 16 days. Although it is true that surface water movement can change drastically between Landsat acquisitions and move quickly, the data can acts as a useful long-term, wide-area, multi-temporal reference for water and land monitoring [9]. It has long been identified to delineate water bodies from remotely sensed images using extraction techniques. The methods mainly included single-band and multi-band techniques, which involved respect with the number of bands used [10]. Efficient water-logged area mapping is now made possible by the use of water index-based algorithms. Due to its specific spectral properties in the visible and infrared regions, water bodies have been frequently identified using water index- and threshold-based methods [11]. The surface area of a water body to receive near-infrared radiation (NIR) while still allowing visible green radiation to pass through it is termed the spectral characteristics of water, and McFetters [12] created a new approach based on these qualities to distinguish water bodies. In order to solve the issue of the McFetters' zero (0) criterion for separating a water body from its surroundings, Xu [13] created this new indicator, NDWI [14]. The use of the middle-infrared band (MIR) in place of the near infrared, Xu [13] presented a modified NDWI index. The author [13] claims that MNDWI can more precisely distinguish between features that are near or in water. The Water Ratio Index is another well-known multi-band water index (WRI). The WRI provides a water range more prominent greater than one [15] due to the green and red bands' dominance of the spectral properties over the NIR and MIR bands.

Index methods like the Normalized Difference Water Index [12], Modified Normalized Difference Water Index [13], and Water Ratio Index [16] are widely used to estimate surface water, which uses a threshold value to separate the water from the background. Generally, thresholds usually have a set value of either 0 or 1. However, problematic situations include shades, hills, forests, urban regions, and even coastal lines [17].

2 Study Area

The study area is one of the taluk of Chengalpattu district, Tamil Nadu, India [18]. Its headquarters, Chengalpattu taluk, lies within the northern latitudes from $12^0 37' 47.331''$ to $12^0 50' 31.596''$ and eastern longitudes from $79^0 52' 52.056''$ to $80^0 5' 13.596''$. The area spans 254 km^2 and shares its northern border with the Chennai district. The region experiences a tropical environment with both wet and dry seasons and experiences minimal temperature changes throughout the year due to its proximity to the thermal equator and location along the coast. January, which has an annual average temperature of roughly 25 °C, is the coldest month.

The majority of taluk's 1400 mm of yearly precipitation, which falls between October and November during the northeast monsoon season, occurs during this time. River Palar runs through the district, serving as one of the major rivers in the state. The district's economy heavily relies on agriculture, especially rice farming, and benefits from its proximity to Chennai. In 2011, 571,254 people lived in the area, including 288,411 men and 282,843 women. The literacy rate in the taluk was 77.56%. Among children under six, there were 29,492 boys and 28,476 girls. See Fig. 1 for the study area's location. In addition to its strong agricultural sector, Chengalpattu taluk is also known for its historical and cultural significance. The region has been inhabited for centuries and has played a significant role in the political and social history of Tamil Nadu. The taluk boasts several notable landmarks and tourist attractions, including the Vedanthangal Bird Sanctuary, home to various migratory birds. Other famous sites include the Varadharaja Perumal Temple, the Marundeeswarar Temple, and the Kanchipuram Siva Temple, all offering unique insights into the region's rich cultural heritage. Despite its vital cultural and economic contributions, Chengalpattu taluk faces several challenges, including environmental degradation and urbanization. The area has seen significant growth in recent years, leading to concerns over sustainable development and preservation of natural resources.

Efforts are underway to address these challenges and promote sustainable development, including implementing eco-friendly initiatives and promoting responsible tourism practices. Overall, Chengalpattu taluk is a region of great importance and potential, offering a unique blend of historical, cultural, and natural attractions. Its rich heritage and strong agricultural sector makes it a valuable contributor to the broader economy and culture of Tamil Nadu. At the same time, its commitment to sustainability and responsible development bode well for its future.

3 Data Collection

Remote sensing data is one of the main sources for analyzing environmental processes at both the local and global scales. These statistics have made it possible to identify changes that have taken place in recent decades.

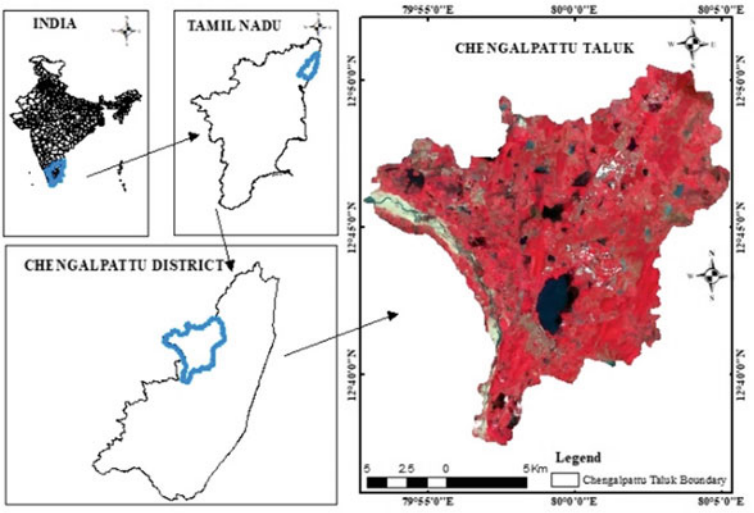

Fig. 1 Study area map

It is now simpler to visualize, categorize, and analyze various locations thanks to remote sensing data from satellites like Landsat, Sentinel, Spot, and others [16]. These data can be categorized using the resolution, number of bands, imaging medium electromagnetic spectrum, and energy source. How well the categorization can be done depends on the level of detail provided by the satellite data in terms of radiometric resolution, spectral resolution, spatial resolution, and temporal resolution [14]. Table 1 presents the collected Landsat 8 and Landsat 9 images and data sources that can be used for various classifications. Classification of Landsat data is usually based on the wavelength of its multiple bands, including blue, green, red, infrared, thermal, and panchromatic. Using a panchromatic band helps improve the resolution of the data. For instance, Landsat 8 provides 11 bands, but only four bands, including green, red, NIR, and SWIR, are used for the analysis of the Water Ratio Index, Normalized Difference Water Index, and Modified Normalized Difference Water Index [17].

Table 1 Data sources

S. No.	Data	Sources
1	Open series map (1:50,000)	Survey of India
2	Landsat 8 (pre-flood 19.10.2021)	USGS Earth Explorer
3	Landsat 9 (post-flood 21.01.2022)	USGS Earth Explorer

4 Methodology

The satellite images like Universal Transverse Mercator (UTM) Projection WGS 84, 44 N were projected to the Landsat images before GIS software processing [19]. The three index approaches—the Water Ratio Index, Normalized Difference Water Index, and Modified Normalized Difference Water Index—were used to analyze surface water bodies. These indexes make the measurement of temporal changes in surface water bodies easier. The methodology flowchart is illustrated in Fig. 2.

4.1 Data

The study employed images from Landsat 8 and Landsat 9, with each test site having an Operational Land Image (OLI) captured during pre- and post-flood periods. The United States Geological Survey provided Level 1 Terrain Corrected (L1T) data, then pre-georeferencing images using the WGS 84 datum. Images were chosen based on pre- and post-season dates to flood conditions. The OLI design produces imagery with spectral, spatial, radiometric, and geometric properties consistent with earlier Landsat data. The maximum ground sampling distance (GSD), including for all bands, including in-track and cross-track provided by OLI, is 30 m (98 ft), except the panchromatic band, which has a GSD of 15 m (49 ft). OLI offers both internal calibration sources and the capability to conduct solar and lunar calibrations to guarantee radiometric accuracy and stability.

4.2 Image Preprocessing

Before calculating the water index, the collected pre- and post-images underwent preprocessing steps: this featured attenuation adjustment, sub-setting, and radiometric calibration. Radiometric calibration was carried out using the Environment

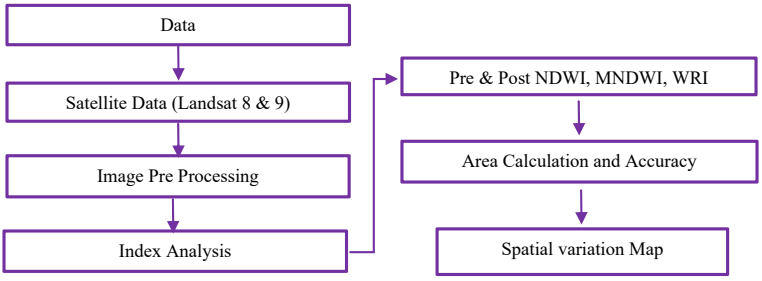

Fig. 2 Methodology flowchat

Table 2 Water index

Index methods	Equation	Remarks	References
NDWI	NDWI = (Green − NIR)/(Green + NIR)	Positive value	[20]
MNDWI	MNDWI = (Green − SWIR)/(Green + SWIR)	Positive value	[2]
WRI	WRI = (Green + Red)/(NIR − SWIR)	Value is > 1	[21]

for Visualizing Images (ENVI) version 5.1 software, which translated the image's digital number into a top-of-atmosphere reflectance. The software used the Landsat header MTL metadata file information during the conversion. All test locations' multispectral and panchromatic images were then divided into smaller groups and eliminated to allow for focused processing during the radiometric calibration phase, as shown in Fig. 1. Each sub-setted multispectral image underwent atmospheric correction using the dark object subtraction (DOS) technique.

4.3 Index Analysis

Surface water extraction using NDWI, MNDWI, and WRI from each image simultaneously serves as the index method for change detection analysis in this context [19]. The threshold value and water index were computed for the binary classification of background water and non-water [2] based on the equation displayed in Table 2.

4.4 Normalized Difference Water Index (NDWI)

A popular index for examining surface water bodies is the Normalized Difference Water Index (NDWI). In most circumstances, it effectively enhances water information using satellite images, green and near-infrared bands. The NDWI, however, might be sensitive to populated areas and lead to an overestimation of water bodies. To more accurately evaluate apparent change areas in their context, NDVI change items can be combined with NDWI products. Water bodies have poor reflectivity and mostly reflect electromagnetic radiation in the visible spectrum. Blue light is generally reflected more strongly by liquid water than green or red light. Water appears blue because it reflects the most light in the visible spectrum's blue area. Contrarily, murky water reflects more light in the visible spectrum. Beyond the near infrared, there is no reflection. NDWI was created by Gao (1996) using the short-wave infrared (SWIR) bands and near infrared (NIR) to improve water-related landscape features. Table 3 contains the NDWI calculation formula, and the NDWI value ranges from − 1 to 1. It is simple to discriminate between vegetation and water bodies since vegetation typically has NDWI values that are significantly smaller than 0.5. Surface water

bodies usually have values between pre-flood from − 0.84 to 0.81 and post-flood from − 0.58 to 0.28.

The spatial variation of pre- and post-NDWI is shown in Figs. 3 and 4, respectively. According to the estimate, the surface area of water bodies will grow by 32% between the pre- and post-flood seasons of 2021 and 2022. After preprocessing the gathered photographs, which included radiometric calibration, sub-setting, and atmospheric correction, the NDWI results were produced. Radiometric calibration was performed with ENVI version 5.1 software, and atmospheric adjustments were made to each sub-setting multispectral image using the dark object subtraction (DOS) technique. The USGS portal provided the Landsat 8 and Landsat 9 pictures utilized in the study, and Table 1 lists their parameters.

Table 3 Pre- and post-flood area calculations

Index method	Pre-flood	Post-flood
	Area calculations (km^2)	Area calculations (km^2)
NDWI	3.9186	4.9816
MNDWI	7.7949	15.4305
WRI	4.9122	6.1569

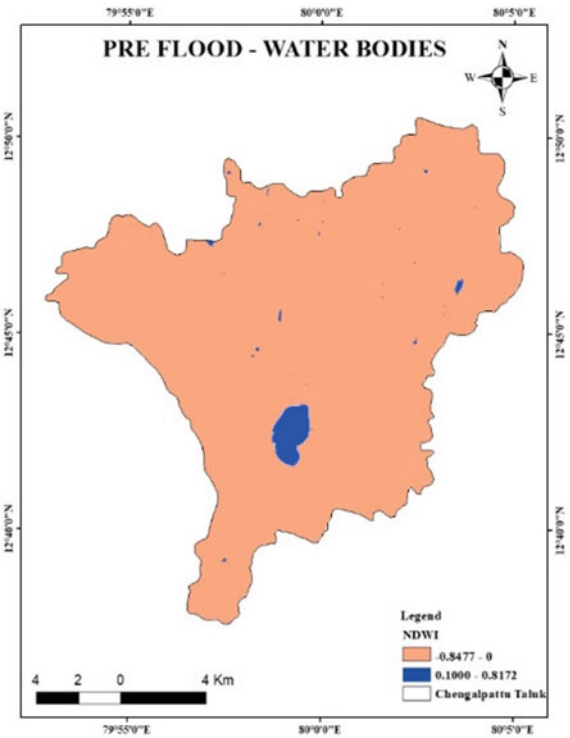

Fig. 3 NDWI pre-flood—waterbodies

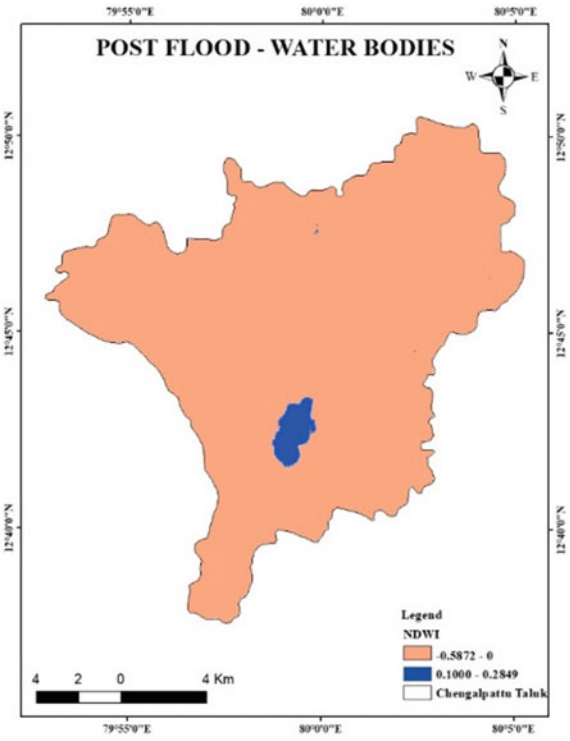

Fig. 4 NDWI post-flood—waterbodies

4.5 Modified Normalized Difference Water Index (MNDWI)

This index method makes use of the SWIR and green bands to highlight open water features [22, 23]. Additionally, it lessens characteristics of built-up areas that are usually connected to open water in other indices [24]. MNDWI index can be calculated by the formula shown in Table 3. This calculation was applied to the pre- and post-Landsat satellite images in 2021 and 2022. The resultant of waterbodies maps for pre- and post-flood ranges from − 0.82 to 0.39 and − 0.72 to 0.33, as shown in Figs. 5 and 6. The area of surface water bodies in 2022 will have grown by 98% compared to the pre-flood season of 2021.

4.6 Water Ratio Index (WRI)

The Water Ratio Index (WRI) is the proportion of the total of the green and red bands' spectral reflectance to the total of their near-infrared (NIR) and short-wave infrared bands (SWIR) [25]. Calculating the index is possible using the formula in Table 3. Figures 7 and 8 depict the identified water bodies found using this technique on pre-

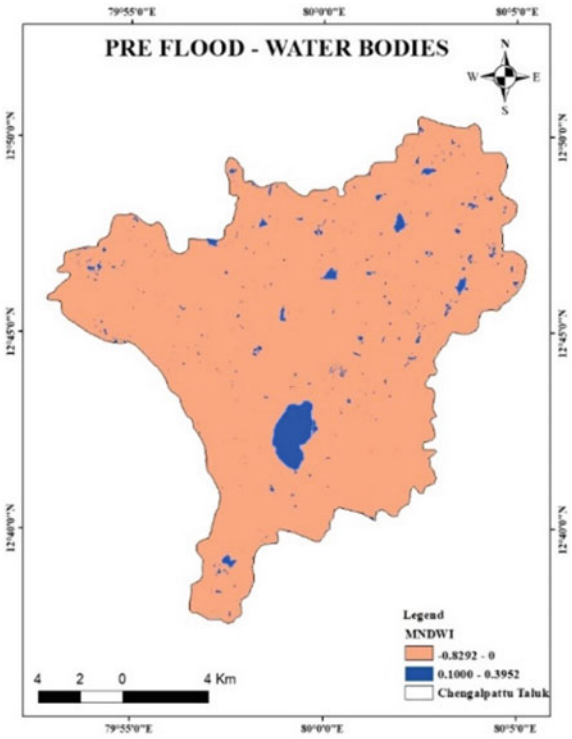

Fig. 5 MNDWI pre-flood—waterbodies

and post-flood satellite pictures from 2021 and 2022. Index value ranges from 0.20 to 1.83 and 0.27 to 1.58 for pre- and post-flood. The area of surface water bodies is 68% more in 2022 than in the pre-flood season of 2021. This year has seen an average rainfall of 2006 mm per year. Area calculation for three water index methods is shown in Table 3.

5 Accuracy Assessment

Although the indices are designed to generate quick and precise water maps, it is essential to conduct an accuracy assessment to evaluate their performance. The approach used in this work is confusion matrix-based, as shown in Table 4. When the extracted water and non-water value is compared to the reference data, three different types of pixels are produced.

i. True positive (TP): The number of correctly extracted water pixels.
ii. False negative (FN): The number of undetected water pixels.
iii. False positive (FP): The number of incorrectly extracted water pixels.
iv. True negative (TN): The number of correctly rejected non-water pixels.

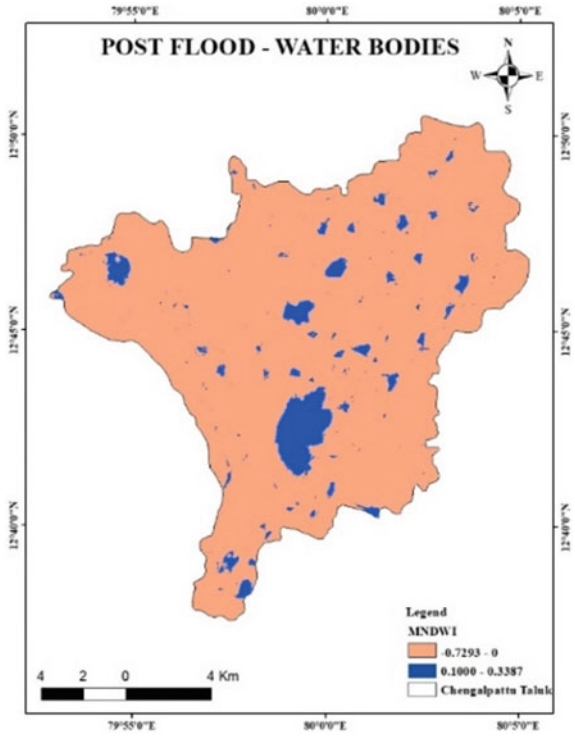

Fig. 6 MNDWI post-flood—waterbodies

The overall accuracy (OA) and kappa coefficient (kappa) were used to evaluate the accuracy of the created maps with various water indices based on the aforementioned four results. You can compute these as

$$\text{Producer's accuracy} = \frac{\text{TP}}{\text{TP} + \text{FN}} \tag{1}$$

$$\text{User's accuracy} = \frac{\text{TP}}{\text{TP} + \text{FP}} \tag{2}$$

$$\text{Overall accuracy} = \frac{\text{TP} + \text{TN}}{T} \tag{3}$$

$$\text{Kappa coefficient} = \frac{T(\text{TP} + \text{TN}) - \sum}{T^2 - \sum} \tag{4}$$

where $\sum$ is the accuracy of the change indicated by

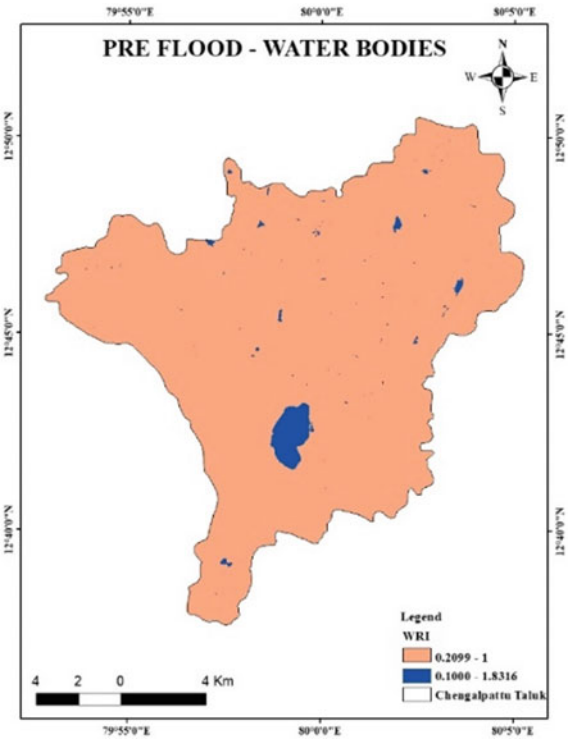

Fig. 7 WRI pre-flood—waterbodies

(TP + FP) (TP + FN) + (FN + TN)(FP + TN)(TP + FP)(TP + FN) + (FN + TN)(FP + TN) and T is the total number of pixels considered for evaluating accuracy.

Because chance agreements between datasets are not taken into consideration, the performance of classification accuracy measures like PA, UA, and OA can be constrained. The kappa statistic is therefore frequently employed in conjunction with these measurements to solve this restriction. Kappa is a metric that assesses how closely two rasters agree. It ranges from − 1 to + 1, with 0 signifying the level of agreement that could be predicted by chance alone and 1 signifying complete agreement. The values of PA, UA, OA, and kappa for the water and non-water maps are presented in Table 5.

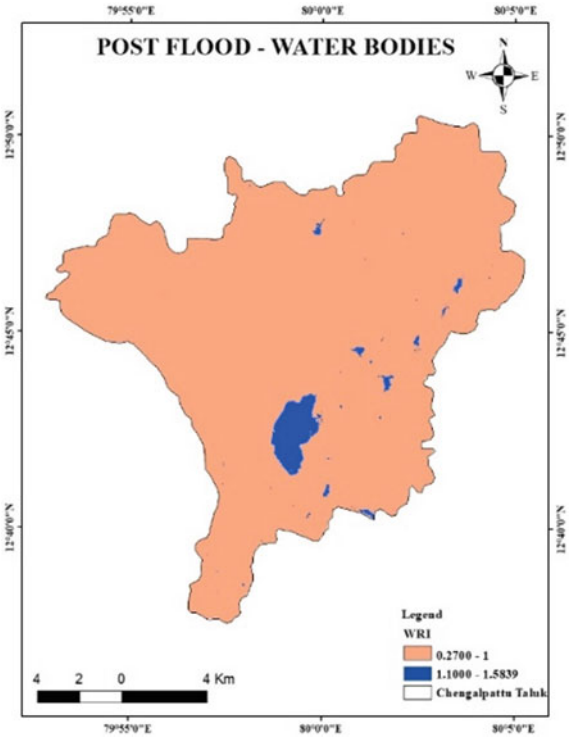

Fig. 8 WRI post-flood—waterbodies

Table 4 Confusion matrix

		Reference data	
		Water	Non-water
Classified data	Water	True positive	False negative
	Non-water	False negative	True positive

Table 5 Pre-/post-flood accuracy assessment

	Accuracy assessment					
	Water index	Threshold	PA	UA	OA	Kappa
Pre-flood	NDWI	0.39	0.698	0.846	0.862	0.812
	MNDWI	0.81	0.871	0.812	0.832	0.862
	WRI	1.83	0.921	0.521	0.713	0.784
Post-flood	NDWI	0.33	0.762	0.847	0.810	0.801
	MNDWI	0.28	0.861	0.896	0.873	0.928
	WRI	1.58	0.798	0.578	0.728	0.794

6 Conclusion

Because chance agreements between datasets are not taken into consideration, the performance of classification accuracy measures like PA, UA, and OA can be constrained. The kappa statistic is therefore frequently employed in conjunction with these measurements to solve this restriction. Kappa measures the degree of agreement between raster and goes from − 1 to + 1, where + 1 represents total agreement and 0 the degree of understanding that would be determined by chance alone, and the results showed that MNDWI at threshold 0 was the most effective for water separation compared to the other indices. The study also conducted an accuracy assessment using a confusion matrix-based approach and found the overall accuracy satisfactory. The study's findings demonstrate the potential of remote sensing and indices like NDWI and MNDWI in mapping surface water accurately and efficiently, which can be of great value for flood management and disaster risk reduction efforts. The study's methodology can be replicated in other regions prone to flooding to monitor and assess changes in surface water over time.

Acknowledgements I appreciate the support and facilities provided by the SRM Institute of Science and Technology at Kattankulathur for this research work.

Conflict of Interest There is no conflict of interest.

References

1. Al Kafy A, Al Rakib A, Akter KS, Rahaman ZA, Jahir DM, Subramanyam G, Michel OO, Bhatt A (2021) The operational role of remote sensing in assessing and predicting land use/land cover and seasonal land surface temperature using machine learning algorithms in Rajshahi, Bangladesh. Appl Geomatics 13(4):793–816. https://doi.org/10.1007/s12518-021-00390-3
2. Mukherjee NR, Samuel C (2016) Assessment of the temporal variations of surface water bodies in and around Chennai using Landsat imagery. Indian J Sci Technol 9. https://doi.org/10.17485/ijst/2016/v9i18/92089
3. Aldiansyah S (2023) Evaluation of flood susceptibility prediction based on a resampling method using machine learning. J Water Clim Change 14:937–961. https://doi.org/10.2166/wcc.2023.494
4. Fatemi M, Narangifard M (2019) Monitoring LULC changes and its impact on the LST and NDVI in District 1 of Shiraz City. Arab J Geosci 12(4). https://doi.org/10.1007/s12517-019-4259-6
5. Acharya TD, Subedi A, Huang H, Lee DH (2019) Application of water indices in surface water change detection using Landsat imagery in Nepal. Sens Mater 31(5):1429–1447. https://doi.org/10.18494/SAM.2019.2264
6. Sahu A (2014) Identification and mapping of the water-logged areas in Purba Medinipur part of Keleghai river basin, India: RS and GIS methods. Int J Adv Geosci 2(2). https://doi.org/10.14419/ijag.v2i2.2452
7. Chowdary VM (2008) Assessment of surface and sub-surface waterlogged areas in irrigation command areas of Bihar state using remote sensing and GIS. Agric Water Manag 95:754–766
8. Choubey VK (1998) Assessment of waterlogging in Sriram Sagar Command Area, India, by remote sensing. Water Resour Manag 12(5):343–357

9. Fisher A, Flood N, Danaher T (2016) Comparing Landsat water index methods for automated water classification in eastern Australia. Remote Sens Environ 175:167–182. https://doi.org/10.1016/j.rse.2015.12.055
10. Mondejar JP, Tongco AF (2019) Near infrared band of Landsat 8 as water index: a case study around Cordova and Lapu-Lapu City, Cedu, Philippines. Sustain Environ Res 5:1–15
11. Liu H, Hu H, Liu X, Jiang H, Liu W, Yin X (2022) A comparison of different water indices and band downscaling methods for water bodies mapping from Sentinel-2 imagery at 10-M resolution. Water (Switzerland) 14(17). https://doi.org/10.3390/w14172696
12. McFeeters SK (1996) The use of the Normalized Difference Water Index (NDWI) in the delineation of open water features. Int J Remote Sens 17(7):1425–1432. https://doi.org/10.1080/01431169608948714
13. Xu H (2006) Modification of normalised difference water index (NDWI) to enhance open water features in remotely sensed imagery. Int J Remote Sens 27(14):3025–3033. https://doi.org/10.1080/01431160600589179
14. Șerban C, Maftei C, Dobrică G (2022) Surface water change detection via water indices and predictive modeling using remote sensing imagery: a case study of Nuntasi-Tuzla Lake, Romania. Water (Switzerland) 14(4). https://doi.org/10.3390/w14040556
15. Shen L, Li C (2010) Water body extraction from Landsat ETM+ imagery using Adaboost algorithm. In: 2010 18th international conference on geoinformatics, Geoinformatics 2010, pp 3–6. https://doi.org/10.1109/GEOINFORMATICS.2010.5567762
16. Acharya TD, Subedi A, Yang IT, Lee DH (2017) Combining water indices for water and background threshold in Landsat image, p 143. https://doi.org/10.3390/ecsa-4-04902
17. Acharya TD, Lee DH, Yang IT, Lee JK (2016) Identification of water bodies in a Landsat 8 OLI image using a J48 decision tree. Sensors (Switzerland) 16(7):1–16. https://doi.org/10.3390/s16071075
18. Kalidhas M, Sivakumar R (2022) Image processing and supervised classification of LANDSAT data for flood impact assessment on land use and land cover. In: Proceedings of the international conference on technological advancements in computational sciences (ICTACS 2022), pp 437–440. https://doi.org/10.1109/ICTACS56270.2022.9988164
19. Xu H (2018) Modification of Normalised Difference Water Index (NDWI) to enhance open water features in remotely sensed imagery. Int J Remote Sens 14:3025–3033
20. Yue H, Li Y, Qian J, Liu Y (2020) A new accuracy evaluation method for water body extraction. Int J Remote Sens 41(19):1–32. https://doi.org/10.1080/01431161.2020.1755740
21. Lee JK, Acharya TD, Lee DH (2018) Exploring land cover classification accuracy of Landsat 8 image using spectral index layer stacking in hilly region of South Korea. Sens Mater 30(12):2927–2941
22. Xu H (2007) Extraction of urban built-up land features from Landsat imagery using a thematic-oriented index combination technique. Photogramm Eng Remote Sens 73:1381–1391
23. Zhao X, Chen H (2005) Use of normalized difference bareness index in quickly mapping bare areas from TM/ETM+. In: Proceedings. IEEE international geoscience and remote sensing symposium, 2005. IGARSS '05, vol 3, pp 1666–1668
24. Xie D, Zhao Y, He C, Shi P (2010) Improving the normalized difference build-up index to map urban built-up areas using a semiautomatic segmentation approach. Remote Sens Lett 1(4):213–221
25. Xu H (2005) A study on information extraction of water body with the Modified Normalized Difference Water Index (MNDWI). J Remote Sens 9:589–595

Metro Route Selection Using Quantum GIS

L. Chandrakanthamma, S. Sivakumar, V. A. Sushma, and S. Karunamoorthy

Abstract With a growing population, grows different modes of transport, metro trains has becoming a popular mode of travel in recent times. It has become the backbone of any Public Transport System. Using Quantum Geographical Information System, we can analyse the metro route of Chennai airport and Parandur airport. The interspace of Chennai and Parandur is of 70 km and the working Chennai airport be 57 km, is about 1 h and 50 min as road transport. Using this metro route, they can reach the airport within 30–45 min. Metro serves as the best mode of public transport by eliminating traffic. GIS is incorporated here to make this tedious process, easy and minimize human errors. Here QGIS plays a vital role in making the tedious process easy. We are focusing on giving a modelled data map about metro routing from the existing Chennai airport to the upcoming airport in Parandur using Quantum GIS. By using this data map, we can analyse the routes, type of foundation, and whether the metro is elevated or underground section. Traditional surveying methods require manpower which is a tedious process but incorporating QGIS, makes the process easy, and fast and helps us to make better decisions.

Keywords Geomorphological map · Mapping · Road map · Shapefile · Slope map · Soil map

1 Introduction

The art of choosing the optimal way for a metro trains is add on with geospatial techniques. The major principle of the study is to take opportunity of the available technology which offers right circumstances to impose maps, integrate them, and perform 2 and 3D spatial analysis on various layers of source. It will be applied to a real-life case study for a new path [2] between Chennai airport and Parandur airport.

By using data map, we can analyse the routes, type of foundation, if the metro is elevated or underground section. Traditional surveying methods require manpower

L. Chandrakanthamma (✉) · S. Sivakumar · V. A. Sushma · S. Karunamoorthy
Department of Civil Engineering, Easwari Engineering College, Chennai 600089, India
e-mail: chandrakanthamma.1@eec.srmrmp.edu.in

K. R. Reddy et al. (eds.), *Recent Advances in Civil Engineering*, Lecture Notes in Civil Engineering 398, https://doi.org/10.1007/978-981-99-6229-7_8

which is tedious process but by incorporating QGIS, it makes the process easy, fast, and helps us to make better decisions.

2 Methodology

The traditional highway selecting process is altered using GIS in a joined model. The procedure has five essential phases, which are correlated. The database come into one phase of the procedure will be helpful in the upcoming phases.

The primary process is creating a site map (marking the study area) for creating the maps. The data maps will be road map, slope map, geomorphological map, soil map, population map. The phases of metro route selection process are given by below (refer Fig. 1).

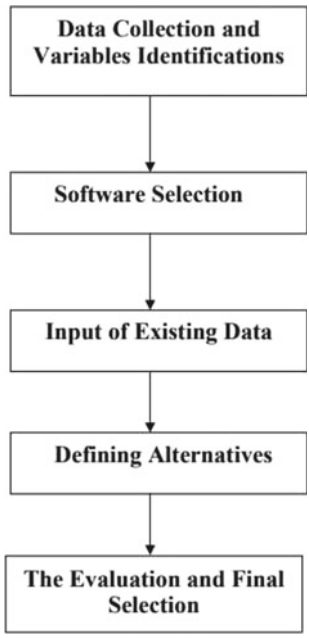

Fig. 1 Phases of metro route selection

3 QGIS Modelling Process

3.1 Creating Shape File

Geographic features in shapefiles can be picturized as geometric shapes. In this study, there are three different shape files. For road map, geomorphology map, and slope map, the shape file covers 96,000 ha. For soil map, the shape file covers 760,000 ha. For population map, the shape file covers 57,794.241 ha (Figs. 2 and 3).

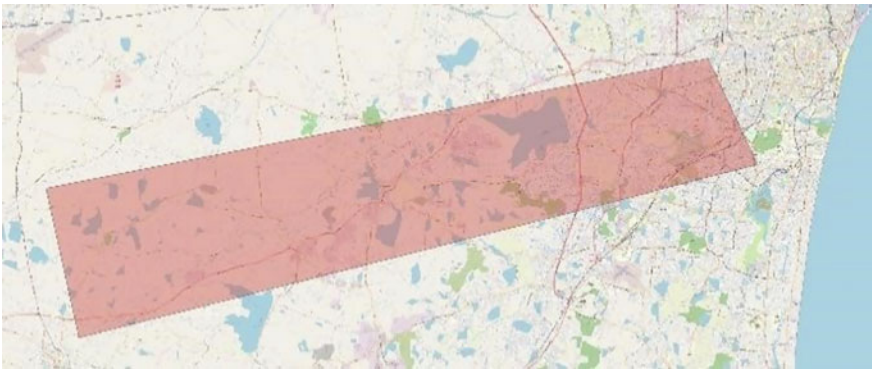

Fig. 2 Shape file of 96,000 ha

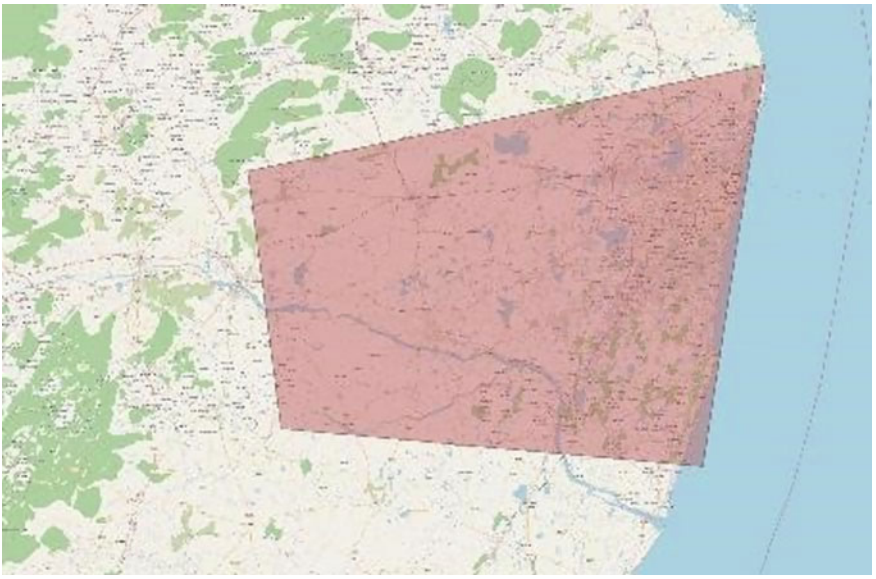

Fig. 3 Shape file of 760,000 ha

Fig. 4 Coordinates

1. Lat: 12° 57' 55" N, Lon: 079° 41' 43" E
2. Lat: 13° 03' 32" N, Lon: 080° 11' 03" E
3. Lat: 12° 58' 56" N, Lon: 080° 13' 13" E
4. Lat: 12° 51' 28" N, Lon: 079° 43' 09" E
5. Lat: 12° 51' 30" N, Lon: 079° 43' 10" E

As shapes antecede every shapes, ESRI shapefile is empirically used to occupying different geometry. Ability of different shape types must be restricted to interspersing null shapes with the uni-shape is decided in file nature. A ESRI shapefile can neither be polyline or polygon data.

3.2 Creating Road Map

QGIS only has one base map that is included by default, Open Street Map. However, QGIS does have the functionality to support many different types of base map sources and services. Base maps can be added to QGIS by. The three ways to add base maps to QGIS project. Default OpenStreetMap, Web Map Service (WMS), and XYZ Tiles.

Data are extracted from Bhukosh a spatial data portal and a geophysical data repository. The coordinates of the shapefile (Fig. 4) play a vital role in creating the road map. The coordinates are tabulated below.

The coordinates are measured in QGIS using the created shape file. The extracted coordinates are entered in Bhukosh data site. The shape file gets generated and a zip file will be created. The created zip file must be buffered and values are obtained. The generated values are entered in QGIS which is saved as a layer. The layer forms a line in the base map of QGIS. By using the road map (Fig. 5), we can analyse the route so that the road will not be a barrier to decide if the route of metro has to elevated or underground, the image is attached below.

3.3 Geomorphology Map

Geomorphology map is used to show the roads, railways, land use, buildings in the chosen study area. The legends shows the black line as roads, red line as railways, blue as natural water body, green as land use, and black as buildings. The data extracted from USGS and place on base map and clipped (refer Fig. 6). In this the roads and railways are majorly taken into account for route selection.

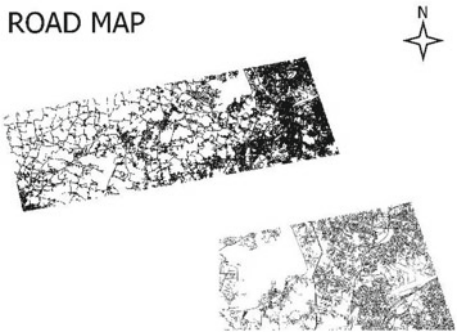

Fig. 5 Road map

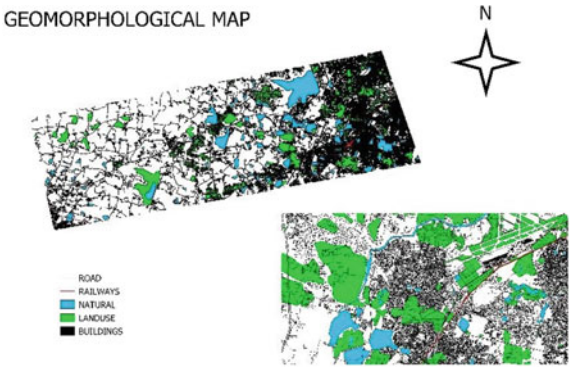

Fig. 6 Geomorphology map

3.4 Soil Map

Soil data of India is extracted from fao.gov and by layering it with the shape of 6,700,000 ha is placed the data are buffered and soil data for the desirable land is achieved.

From the attribute table the legend of the soil (Fig. 7) is identified and from the legend given by FAO, the name of the soil is identified.

The soil types available in the given study area are 4 types which is based on the legends given by FAO (Figs. 8 and 9). The main characteristic of luvisols, a subsurface zone with higher clay content than the material above it are: Chromic luvisols, Orthic luvisols, Dystric regosols, and Chromic vertisols.

Vertisols are coloured mineral soils with a high content of expansive clays that form deep and wide vertical cracks in the dry season. Its main component is clay, which have a laminar structure. Chromic vertisol are very dark in colour, with a wide variable organic matter content (1–6%).

Regosols are characterized by shallow, unconsolidated material that may be of alluvial origin and by the lack of a significant soil horizon (layer) formation because of dry or cold climatic conditions.

Fig. 7 Legends of soil data

Fig. 8 Soil data of India

Dystric regosols are deep mineral soils, poorly developed, with a superficial horizon on the original material not yet consolidated. The presence of this thick material in most of the profile gives it good drainage due to its high porosity.

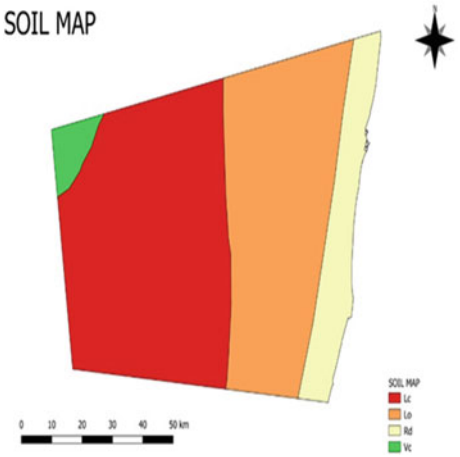

Fig. 9 Soil map

3.5 Slope Map

Slope map is used to decide the routing to be in elevation or underground. Based on the slope data the decision in made.

The slope data of this study is extracted as four different images covering separate parts of study area. These four different maps gives different layers to make it uniform it is merged to one data with uniform scaling and colouring is chosen. In this slope stepness is coloured yellow if it is low, orange if it is moderate and red if it is high. By using this we can identify the specific high slope area.

Layer 8 image is converted into spectral form since, the data are in 4 different squares each square will have a range starting with zero (Figs. 10 and 11). To avoid this, the four separate data are merged into one data so that single value is produced (Fig. 12).

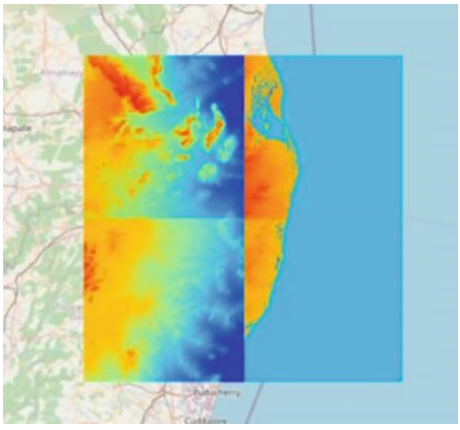

Fig. 10 Slope data before merging

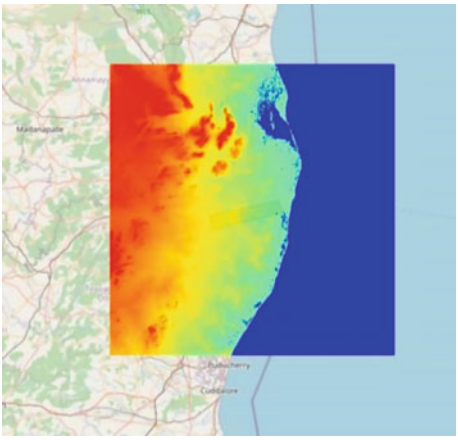

Fig. 11 Slope data after merging

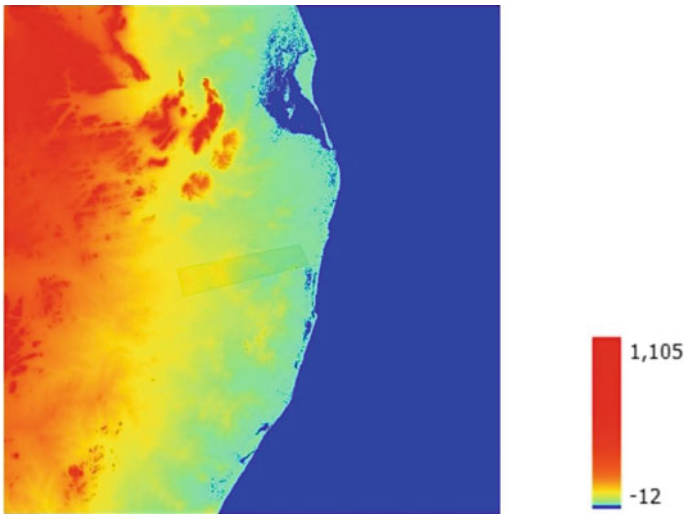

Fig. 12 Slope map

4 Results and Discussion

Based on the data of maps, routes can be generated using ORS tools in QGIS. Two ways of routing is extracted which is fastest and shortest. Out of these extracted routes, based on geomorphological map we can analyse the building height, railway lines, and waterbodies. By analysing these, common route in fastest and shortest is pinned. Then commercial zones are pinned and an economical route is given (Fig. 13). Based on this elevated or underground is decided.

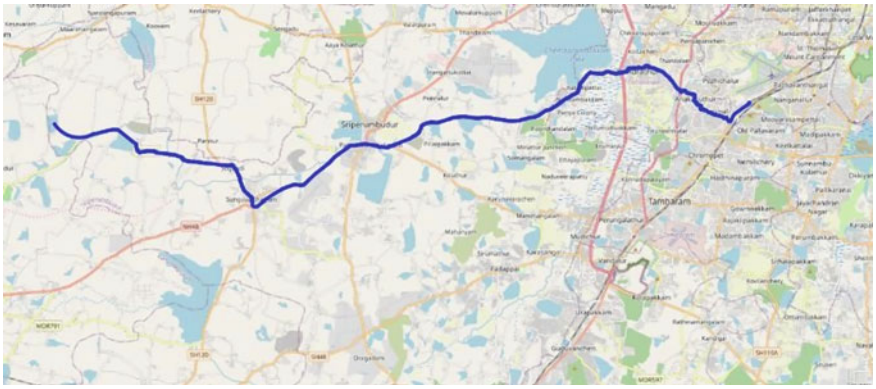

Fig. 13 Final route

5 Conclusions

By the soil data report, the soil is identified and by the characteristics of the soil. From the soil data gathered for the existing metro, they both have similar soils with similar properties. So, the foundation for the study area can be applied as same as the existing metro. The foundation laid in the existing metro is pile foundation as it supports heavy load and based on soil conditions. The data of the existing metro was taken to check the soil data of the study area.

References

1. Longley P, Goodchild M, Maguire D, Rhind D (2015) Geographic information systems and science. Wiley, pp 200–220
2. O'Sullivan D, Unwin D (2018) Geographic information analysis. Wiley, pp 145–147
3. Yang X (2019) Introduction to GIS programming and fundamentals with Python and ArcGIS. CRC Press, pp 56–60
4. Graser A (2016) Learning QGIS, 3rd edn. Packt Publishing, pp 23–27
5. Muenchow J, Hurt J (2017) QGIS map design, 2nd edn. Packt Publishing, pp 178–180
6. Anselin L, Rey S (2014) Modern spatial econometrics in practice: a guide to GeoDa, GeoDaSpace and PySAL. GeoDa Press, pp 560–601
7. Rogerson P (2019) Statistical methods for geography: a student's guide. Sage Publications, pp 796–809
8. Mitchell A (2017) The ESRI guide to GIS analysis, vol 3: modeling suitability, movement, and interaction. ESRI Press, pp 145–150
9. Lídia B, Domingos X (2019) GIS-based analysis of coastal Lidar time-series data: strategies for coastal monitoring. Springer, pp 123–135
10. Bivand R, Pebesma E, Gomez-Rubio V (2013) Applied spatial data analysis with R. Springer, pp 800–830
11. Barry R, Chorley R (2019) Atmosphere, weather and climate. Routledge, pp 568–608

12. Wang F (2018) Quantitative methods and applications in GIS. CRC Press, pp 78–90
13. Anand SP (2017) GIS-based studies in the humanities and social sciences. Springer, pp 790–812
14. Gorsevski P, Gessler P (2013) Visualization in GIS. CRC Press, pp 560–590
15. Kang-Tsung C, Thill J (2020) Advanced spatial modeling with stochastic partial differential equations. CRC Press, pp 90–99

Groundwater Potential Zone Identification Through Remote Sensing GIS Technology in Part of Dharmapuri District, Tamil Nadu

N. Umashankar, M. Soundararajan, and A. Meenachi

Abstract To raise and promote public understanding of groundwater resources, the Ford Foundation assisted in the publication of the groundwater status of Tamil Nadu. The fact that it defines rules for addressing farmers' requests, industrial water needs, and drinking water needs benefits administrators, planners, financial institutions, and the general public. Dharmapuri is a place with a lot of natural resources. One an overview of integrated studies from the ongoing research, covering lineament theme geographical exploration, soil, drainage, land use/land cover, geology, and geomorphology. Modern technologies were used by both this research study's geographic information system (GIS) and remote sensing (RS). The study outcomes can guide policymakers, water resource managers, and stakeholders in implementing effective strategies for groundwater utilization and conservation. Hence, considerable work has been done on the origin and evolution of the high-grade terrain in which the hypersthene bearing rock viz., charnockite forms the major component. Land use/land cover features are more related to groundwater quantity as well as quality. The study area's hill and woodland are the next most prominent features, followed by more cropland. A woodland is, broadly speaking, terrain that is covered in trees. A woodland is, broadly speaking, terrain that is covered in trees. In a more specific sense, a woodland is synonymous with wood, and it is a low-density forest that creates open environments with little to no cover from the sun and lots of sunshine. A light canopy of trees and plants forms in some grasslands, such as savanna woodlands.

Keywords Ground water · Remote sensing and GIS · Soil map · Land use/land cover map

N. Umashankar (✉) · M. Soundararajan · A. Meenachi
Department of Civil Engineering, Sona College of Technology (Anna University), Salem, Tamil Nadu 636005, India
e-mail: Umashankarcivil6@gmail.com

K. R. Reddy et al. (eds.), *Recent Advances in Civil Engineering*, Lecture Notes in Civil Engineering 398, https://doi.org/10.1007/978-981-99-6229-7_9

1 Introduction

Water is essential to plant and animal life as well as human existence. To sustain the body's vital fluids, each individual needs 3litters of drinking water each day. Despite two the worrisome rate of global population growth, rainfall on land remains largely stable. The world's oceans contain 97.20%t of the world's fresh water, according to a study of the water supply. 2.80% of the total are in land areas. Groundwater that is at least 13,000 ft below the surface makes up 61% of the total, whereas glaciers and ice caps only hold 2.14%. 0.0005% of soil moisture, 0.009% of freshwater lakes, 0.0001% of rivers, and 0.008% of salty lakes are found in the world's oceans. Saline or glacial ice traps more than 75% of the land's water. Humans may access freshwater, which makes up a small portion of the total amount of water in the planet. About 90% of the freshwater resource of the earth consists of groundwater accumulated in regionally extensive aquifers. Much information is obtainable in shortest possible time about the orientation, shape, distribution, and type of groundwater bearing belts [1]. Every year on March 22, World Water Day, a particular problem or facet of freshwater conservation is highlighted. The Food and Agriculture Organization (FAO) is the organizing partner for World Water Day 2012, which has as its subject "Food and Security: We are hungry because the world is thirsty" [2]. To increase and broaden public understanding of groundwater resources, the Ford Foundation assisted in the publication of the groundwater status of TN.

1.1 Climate and Rainfall

The coldest months are December and January, with March, April, and May being the hottest. From November to February, the weather is generally nice. The highest temperature is between 25 and 40 °C, while the minimum is between 12 and 20 °C, between 60 and 90% of the relative humidity is present. The South-West Monsoon season saw the highest relative humidity readings [3]. The wind speed indicates faster speed during the SW monsoon and lower speed during the NE monsoon season. The range is 5–20 km/h. The mean number of sunlight hours ranges from 9.7 to 2.5. In general, evaporation is highest in March, April, and May and lowest in the months when it rains [4].

1.2 Population

The district covers a total size of 4659.40 km^2 (3.46% of Tamil Nadu geographical area). Compared to the hilly and forested areas, the aerial extended plain area is 3313.15 km^2 larger [5]. One of the regions with natural resources is Dharmapuri. Dharmapuri district is twenty fourth ranks of population overall Tamil Nadu State.

Total population of the Dharmapuri district is of about 1,506,843 of which 774,303 are males and 732,540 are females. The total scheduled castes are 245,392 out of which 124,706 are males and 120,686 are females [6]. The total scheduled tribes are 63,044 out of which, 32,130 are males and 30,914 are females (Census 2011).

1.3 Communication

Dharmapuri district is well connected with all the districts. It is lying in Kanyakumari-Bangalore. Salem-Bangalore railway line cut across the study area in South to North direction and Coimbatore to Chennai railway line cut across the study area in South to Northeast direction. Villages around this are also connected by metal roads. Many of the villages are interconnected by unmetalled cart, tracks and foot paths [7–9]. The impact of communication in a groundwater potential study conducted through remote sensing GIS technology in a specific part of Dharmapuri District, Tamil Nadu, is significant. Effective communication plays a crucial role in ensuring that the study's findings, implications, and recommendations are understood and utilized by relevant stakeholders.

1.4 Vegetation

The flora is rich and varied. The trees that are Common in the study area are *Acacia Arabica* (Karuvelan); *Agattiground flora* (Agathi); *Strychnos nux Vomica* (etti); *Cocos nucifera* (coconut); *Barassos plabellifer* (palmyra); *Mangifera indica* (mango); *psidium Guajava* (Guava); *Moringe* (Murungai); *Azadirachla indica* (Neem); *Bassia lattifolia* (Iluppai); *Eriodendron pentandrum* (Silk Cotton); *Ficus Bengalengis* (Banyan Tree) [10].

1.5 Crops

Most of the study area is used for growing various Crops. Some of them are food crops and some other cash Crops. The chief food crops grown are Paddy: Ragi, Black gram, Horse gram, red gram. The Chief cash Crops are Cotton, Tobacco, and Gingelly [11]. The chief plantation Groundnut, Crops are coconuts and mangoes.

1.6 Hydrogeology

The rock types are hard and compact. Topsoil varies from 1 to 10 ft, weathered rock thickness ranges from 3 to 30 ft, rock is seen below average of 30 ft. The water level is up to 50 ft. In summer, few wells are dry, and the average water level is 6 ft.

2 Materials and Methods

2.1 Base Map Generation

Base map prepared from Dharmapuri district; Taluk boundary map scale is 1:75,000. The study area is part of Dharmapuri district, with the following five Taluks namely Dharmapuri, Harur, Palacode, Pennagaram and Pappireddipatti. Drainage map is prepared from toposheets, scale 1:50,000 [12].

2.2 Remote Sensing

Landsat 8 land satellite image (March-2020) was downloaded from www.glcf.com website. These 8 lands are merged in ERDAS IP (Earth Resources Data Analysis System Image Processing) software. Creating themed maps using supervised categorization, such as a map of land usage and land cover [13]. Geomorphological map and Lineament map prepared using edge enhancement analysis (Fig. 1).

3 Study Area Details and Groundwater Possibility

3.1 Study Area Description

The Dharmapuri district is located between latitudes N 11°45′49″ and 12°30′54″ and longitudes E 77°40′38″ to 78°44′49″, according to Fig. 2. The district spans 4659.40 km^2 overall (3.46% of TN geographical area). Aerial extended plain area is 3313.15 km^2, while hill and forest area is 1346.25 km^2. One of the resource-rich regions is Dharmapuri. Blocks made of Pennagaram, Palacode, and Harur high quality black granite are offered. In Kendiganapalli Village of Pennagaram Taluk, quartz minerals are on display [14]. Another mineral with high economic potential is molybdenum, which is renowned for being a superb conductor. It's accessible in Harur. On October 10, 1965, Dharmapuri District was created from Salem District. The district has 1.507 million residents (2011 Census). It is surrounded by the districts

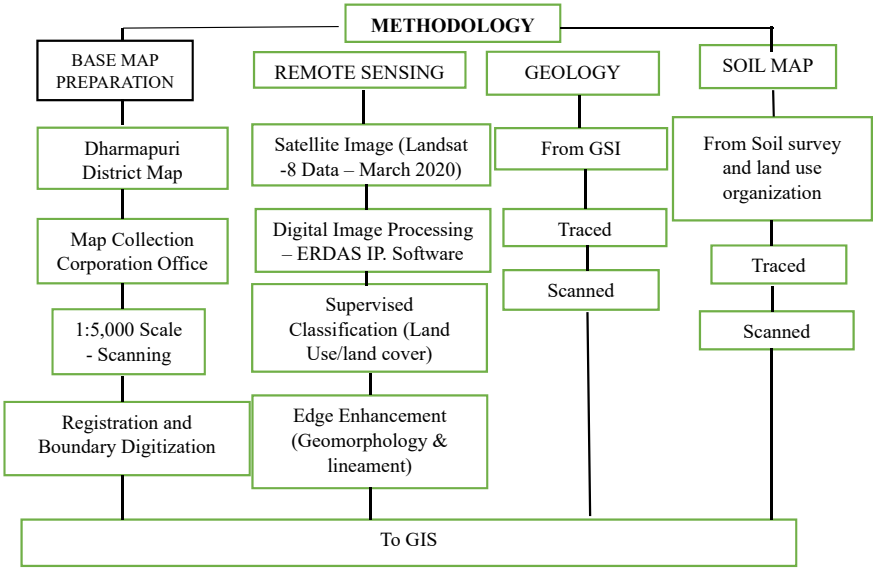

Fig. 1 Methodology

of Salem District on the south, Krishna Giri District on the north, Tiruvannamalai and Villupuram on the east, and Chamarajanagar District in Karnataka State on the west. Hills and trees surround the district. The Dharmapuri district of South India is in a noteworthy geographic area. Five Taluks, Dharmapuri, Harur, Palacode, Pennagaram, and Pappireddipatti, make up the Dharmapuri district [15].

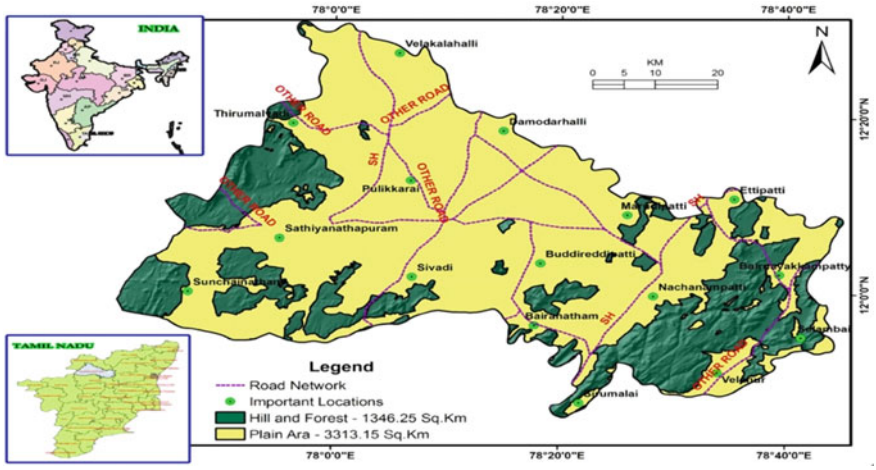

Fig. 2 Study area map

3.2 Soil

Seven different types of soil were identified in the Dharmapuri district.

Red Soil, Black Soil, Brown Soil, Forest Soil, Red Loamy Soil, Red Calcareous Soil, Red Non-calcareous Soil.

The few major soil series encountered in the study area given in Fig. 3.

Spatial analyses are results (Table 1), and spatial map are given below: red soil is a most dominating land in India. Soil type in India Red soil is a most important soil type because of from crystalline rocks (Study area is fully covered by crystalline rocks) [16]. The red colour due to high Fe^{2+} ionic concentration. Black soil is commonly called as black cotton soil. This type of soil covers a small portion in Dharmapuri District. Forest soil is a high nutrient component so; this is eco-friendly soil type and soil thickness is more. The forest soil derived from physical and chemical weathering of rock and minerals. This type of soil mostly underlies by mountain region.

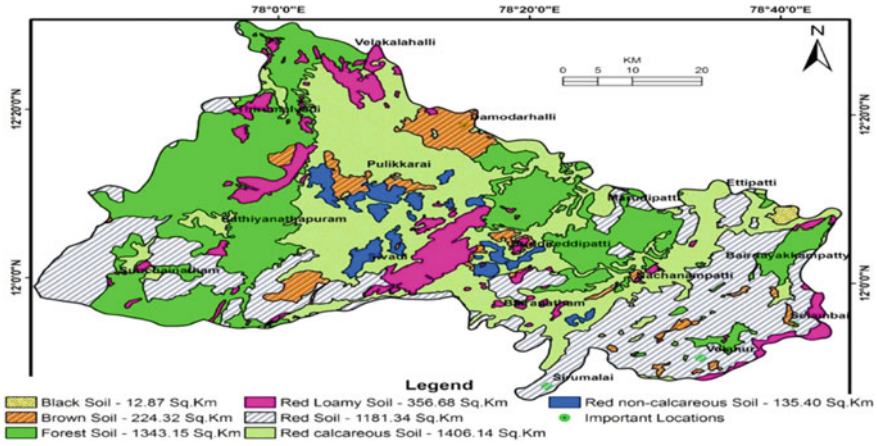

Fig. 3 Study area map

Table 1 Spatial results of soil

S. No.	Soil type	Area in km^2	Percentage of area
1	Black soil	12.87	0.28
2	Brown soil	224.32	4.81
3	Forest soil	1343.15	28.82
4	Red loamy soil	356.68	7.65
5	Red soil	1181.34	25.35
6	Red calcareous soil	1406.14	30.18
7	Red non-calcareous soil	135.4	2.91

Table 2 Spatial results of rock types

S. No.	Rock type	Area in km^2	Percentage of area
1	Amphibolite	0.93	0.02
2	Charnockite	2676.87	57.44
3	Epidote–hornblende gneiss	899.23	19.3
4	Gabbro	21.37	0.46
5	Pyroxene granulite	42.29	0.91
6	Granite	0.96	0.02
7	Hornblende–biotite gneiss	514.56	11.04
8	Kyanite quartzite	2.93	0.06
9	Pink migmatite	342.73	7.35
10	Pyroxene granulite	96.66	2.07
11	Syenite	61.39	1.32

3.3 Geology

A thorough field survey of the area reveals a fascinating igneous connection placed amidst Precambrian-aged rural rocks. Precambrian country rock includes dolerites, hornblende-biotite gneiss, charnockites, and pyroxene granulites (Table 2). Older ultramafics are also found as enclaves inside charnockites and gneisses, in addition to these. The related alkaline rocks and magnesite-bearing ultramafics make up the igneous association, which is similarly Precambrian in age.

3.4 Drainage Patterns and Drainage Density

The drainage system that develops there is impacted by the sorts and inclinations of the subsurface rocks as well as the slope of the local surface. In varying degrees, drainage patterns, which are readily visible on satellite photographs and images, reflect a region's lithology and structure. The arrangement of zones or lines of weakness, the distribution and pattern of the surface rocks, etc. Are the key determinants of drainage patterns in each location? Without examining the local drainage characteristics, no survey of natural resources is complete. The drainage density is defined as the ratio of a basin's total area to its full stream length. It is related to several landscape dissection elements, such as valley density [17], channel head source area [15], climate and vegetation [14], soil and rock properties [12], relief [16], and processes of landscape evolution. According to Strahler, low drainage density is favoured when basin relief is low and vice versa [18].

Table 3 GIS results of land use/land cover

S. No.	Class	Area in km^2	Percentage
1	Agricultural plantations	236.61	5.08
2	Built-up land	63.33	1.36
3	Crop land	1794.58	38.51
4	Fallow land	284.96	6.12
5	Hill and Forest	1414.35	30.35
6	Land with scrub	531.30	11.40
7	Land without scrub	234.27	5.03
8	Mining process	0.24	0.01
9	River	43.44	0.93
10	Tanks	56.84	1.22

Table 4 GIS results of slope

S. No.	Slope	Area in km^2	Percentage
1	Near to surface	3265.97	70.09
2	Gentle slope	725.18	15.56
3	Steep slope	434.39	9.32
4	Very steep slope	234.36	5.03

3.5 Land Use/Land Cover

NRSA created the categories of land use and land cover initially [19]. This categorization was used in the current stud. Using supervised classification, digital image processing was done. The spatial land use/land cover map preparation (Table 3).

3.6 Slope

Check the topographical map again after viewing the slope map created using SRTM satellite data. Slope toward the northeast and northwest was seen in the study area (Table 4) results provide a slope variation map [19].

3.7 GIS Analysis

To use GIS overlay analysis to determine the potential groundwater zones. This approach is used to a number of thematic layers, such as land use/cover, landforms, drainage density, lineament density, and slope, geology, and soil spatial maps [20].

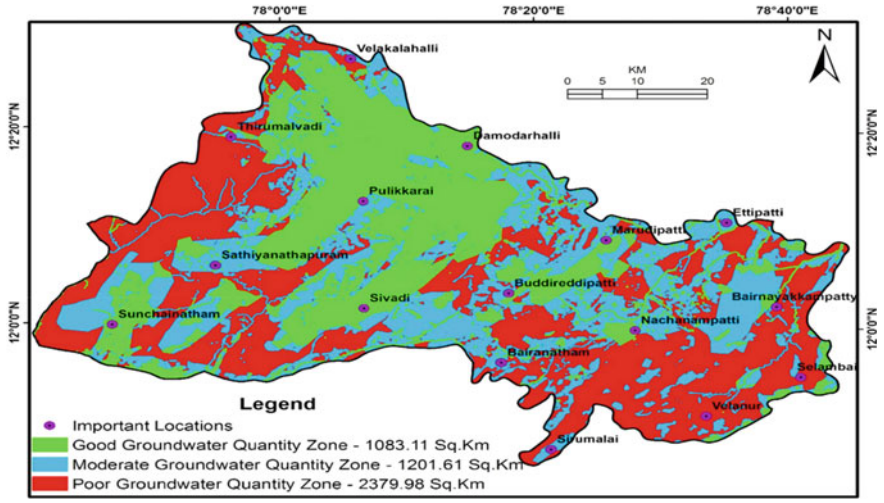

Fig. 4 Groundwater possible spatial map

Each feature of a themed map should be given the appropriate weight. GIS overlay analysis is present on all spatial maps.

3.8 Groundwater Possible Studies

To get all this information harmonised, it is essential to combine these data with the appropriate component [18]. As a result, the use of GIS allows for the integration of this information statistically. There are 3 combinations, as shown by the final (Groundwater quantity spatial map) (Fig. 4). The optimal groundwater quantity zone can be determined using this process. The following combinations, such as a potential zone with poor groundwater, encompass an area of around 2379.98 km^2. While the "Good Groundwater Quantity Zone" is 1083.11 km^2 in size.

4 Conclusion

Two stages of retrogression of charnockite and related rocks are shown by thorough geological and petrographic studies. The charnockite retrogrades to hornblende-biotite gneiss in the first stage of retrogression, while the basic-ultrabasic components form amphibolites, and this stage is typically encountered in any high-grade terrain. The second stage of retrogression is intimately associated with major shears traversing the area around which there is a profuse influx of carbonate and formation of highly epidotised hornblende-biotite gneisses, while pyroxenitee is reduced to

talc-actinolitee-chlorite schist [21]. These are essentially confined to the proximity of well-defined shear zone and lineaments which have probably served as favorable channels for the carbonate-rich solution. Study of charnockite and high grade epidotised hornblende-biotite gneisses, and hornblende-biotite gneisses have been of utmost importance for the geoscientists from time immemorial, due to the fact that these rocks are regarded as a crucial component of the earliest Earth's crust as well as the ancient continent nuclei around which the modern continents have accreted. As a result, extensive research has been done on the formation and evolution of the high-grade terrain, a key component of which is the hypersthene-bearing rock known as charnockite. Eighteen landforms occur in the study area, the dominating landforms like shallow buried Pedi plain and ridge type structural hills are area extended 1566.72 and 1326.72 km^2. Land use/land cover features are more related to groundwater quantity as well as quality. The research area's dominant features include hills and forests, followed by crops. This procedure can be used to identify the ideal groundwater quantity zone. The following combinations, such as a potential zone with poor groundwater, encompass an area of around 2379.98 km^2. While the "Good Groundwater Quantity Zone" spans 1083.11 km^2 [17].

References

1. Adhikary PP, Dash CJ, Chandrasekharan H, Rajput TBS, Dubey SK (2012) Evaluation of groundwater quality for drinking and irrigation using GIS and geostatistics in a peri-urban area of Delhi, India. Arab J Geosci 5:1423–1434
2. Wills A (2009) Innovative techniques in groundwater recharge—hard rock areas of Olakkur block of Villupuram district, Tamil Nadu. Unpublished M.Tech thesis of SRM University, Kattankulathur, pp 1–8
3. Anantha Iyer GV (1976) Mineral chemistry investigations of charnockites and associated rocks of North Arcot District, Tamil Nadu, South India. J Geol Soc India 17:162 p
4. APHA (1995) Standard methods for the examination of water and waste water, 19th edn. APHA, Washington, DC
5. Central Groundwater board technical report (2009) Government of India, Ministry of Water Resources, Central Ground Water Board, South Eastern Coastal Region, Chennai. Report prepared by A. Balachandran, Scientist-D
6. Chebotarev II (1955) Matamorphism of natural waters in the crust of weathering. Geochim Cosmochim Acta 8
7. Diersing, Nancy (2009) Water quality: frequently asked questions. Florida Keys National Marine Sanctuary, National Oceanic Atmospheric Administration, U.S. Dept. of Commerce
8. Gupta S, Nayek S, Chakraborty D (2016) Hydrochemical evaluation of Rangitriver, Sikkim, India: using Water Quality Index and multivariate statistics. Environ Earth Sci. https://doi.org/10.1007/s12665-015-5223-8,75:567
9. Hem JD (1991) Study and interpretation of the chemical characteristics of natural water. USGS water supply paper 2254, 264p
10. Johnson DL, Ambrose SH, Bassett TJ, Bowen ML, Crummey DE, Isaacson JS, Johnson DN, Lamb P, Saul M, Winter-Nelson AE (1997) Meanings of environmental terms. J Environ Qual 26(3):581–589
11. Karthikeyan A, Senthil Kumar GR (2011) Groundwater level fluctuation studies in part of Tindivanam taluk, Villupuram District, Tamil Nadu. Int J Recent Sci Res 2(11):271

12. Kelson KI, Wells SG (1989) Geologic influences on fluvial hydrology and bedload transport in small mountainous watersheds, northern New Mexico, USA. Earth Surf Process Landforms 14:671–690
13. Lawrence JF (1995) Digital evaluation of ground water resources in Ramanathapuram District, Tamil Nadu. Unpublished PhD Thesis, M.S. University, Tirunelveli, 291 p
14. Moglen GE, Eltahir EAB, Bras RL (1998) On the sensitivity of drainage density to climate change. Water Resour Res 34(4):855–862
15. Montgomery DR, Dietrich WE (1988) Where do channels begin? Nature 336:232–234
16. Montgomery DR, Dietrich WE (1989) Source areas, drainage density, and channel initiation. Water Resour Res 25(8):1907–1918
17. Tucker GE, Bras RL (1998) Hillslope processes, drainage density, and landscape morphology. Water Resour Res 34(10):2751–2764. U.S. Salinity Laboratory STAFF (1954) Diagnosis and improvement of saline and alkali soils. U.S. Dept. Agriculture Hand Book, 60p
18. Strahler AN (1964) Quantitative geomorphology of drainage basins and channel networks. In: Chow VT (ed) Handbook of applied hydrology. McGraw-Hill, New York, pp 439–476
19. NRSA (1996) Integrated mission for sustainable development. Technical guidelines, National Remote Sensing Agency, Department of Space, India
20. Radha Krishna BP (1971) Problems confronting the occurrence of groundwater rock. Proc Geol Soc India Sem 27–44
21. Sugavanam EB (1976) Multiphase basic and ultramafic activity in granulite terrain of North Arcot District, Tamil Nadu. J Geol Soc India 17:159 p

Watershed Monitoring Application for Sub-watersheds of Lower Palar River Reach Using Remote Sensing Data and Google Earth Engine Platform

S. Nagaraj and Purushothaman Parthasarathy

Abstract Watershed monitoring is critical for long-term water resource management, drought measures, and flood mitigation planning. Based on satellite data and a cloud-based platform, this study aimed to deploy a web-based application to monitor the sub-watersheds of the lower Palar River reach, which drain part of the Chengalpattu and Kanchipuram districts that are rapidly urbanizing. The geophysical parameters, terrain characteristics, meteorological parameters, and hydrological components of the watersheds were extracted from satellite data in this study. The satellite data was analyzed using the predefined algorithms through the advanced GIS tool Google Earth Engine (GEE). Much research is currently being conducted on revealing surface water potential and fluctuation monitoring using remotely sensed geospatial data and GIS tools. However, the traditional method involves collecting a large number of satellite-sensed images taken from the study area and then processing them in GIS software. The GEE is working on the cloud server, which is dedicated to the processing of satellite image data using machine learning code. GEE does not require image saving or collection, which are simple analyses of satellite data and mapping capabilities. The current study is intended to overcome technical limitations by providing a near real-time, cloud-based, and simple method for mapping hydrological components. Following that, a web-based application was created to provide access to geographical information to the government and other stakeholders. The dynamics of agricultural areas and townships and the state of the stream drainage system were identified without a site inspection. Post-flood information will be monitored, and it should direct the earliest and most beneficial relief operations. By selecting the flood event from the dropdown menu, users can obtain the extent of the flooded area. The web-based watershed monitoring application was deployed successfully.

Keywords GEE · GIS · Lower Palar · Remote sensing · Watershed

S. Nagaraj · P. Parthasarathy (✉)
Department of Civil Engineering, Faculty of Engineering and Technology, SRM Institute of Science and Technology, Kattankulathur, Tamil Nadu 603203, India
e-mail: Purushop1@srmist.edu.in

K. R. Reddy et al. (eds.), *Recent Advances in Civil Engineering*, Lecture Notes in Civil Engineering 398, https://doi.org/10.1007/978-981-99-6229-7_10

1 Introduction

In South India, watershed management is very much needed for sustainable irrigation and domestic water supply, particularly in the catchments of rivers with seasonal flows like the Palar River [1–3]. It is especially susceptible to the changing precipitation patterns and land cover in the lower Palar River's sub-catchments. Changes in land cover, excessive groundwater use, and dwindling yearly precipitation are to be monitored for sustainable watershed management. The data and knowledge dissemination will lead to better water resources management and the future.

The monitoring components of the watershed system considered were precipitation, land use, land cover, flood inundation, and surface water potential. GEE combines planetary-scale analytical capabilities with a multi-petabyte catalog of satellite data and geospatial datasets. GEE is used by climate researchers, investigators, and programmers to detect changes, map trends, and quantify variations on the planet's surface. GEE is now commercially available but free for research and educational purposes [4–10]. The application fields ranged from landscape and vegetation research findings to clinical sectors such as corona. Landsat remained the most widely known dataset; it is an essential element of the GEE data portal, with data available for use and download ranging from the earliest to the latest Landsat extended editions. Data analysis also demonstrated that developed-country institutions dominated usage, with study sites primarily in developed countries. Very few studies began in or were directed at emerging regions. Earlier studies were aimed on specific parameter of the watershed. This study aimed to integrate the major hydrological parameters in one application. And, it is very new to the study area. The conventional approach is much more time-consuming and inefficient for such time series analysis on hydrological components. In this sense, the GEE application has made it easier to access satellite data immediately.

This study aims to deploy a web-based application to monitor the watersheds to improve watershed sustainability. The interpretations of this study will lead to a better understanding of the watershed and its spatial and temporal variations for policymakers, researchers, watershed management planning experts, and other stakeholders. The study was carried out for the sub-catchment of the lower Palar River basin in the Kanchipuram and Chengalpattu districts of Tamil Nadu, India. The area was chosen because of its growing water problem.

The web-based watershed monitoring application's scope is to understand better the facts of various hydrological and influencing components of the watershed. It will reduce the analysis time and be economically good, which is required for developing countries like India. Different and multiple hypotheses can be tested within a short period which leads to a sustainable watershed management system [9, 11, 12].

2 Study Area

Sub-catchments of the lower Palar River are draining a part of the Kanchipuram and Chengalpattu districts of Tamil Nadu, India. Its geographical extent is 12.4699° to 12.9813° in the north and 79.5697° to 80.1618° the east (Fig. 1). This area receives 70% of its annual rainfall during the northeast monsoon (October to December). The average annual rainfall is 957.7 mm, and the temperature ranges from 20.9 to 34.5 °C. There are semi-arid and arid areas in the region, with varying climates. The region's geography is characterized by a consistent, extremely moderate slope, while the eastern portion has rolling undulations. With a gradual gradient from west to east, the research area's relief was 240 m above mean sea level.

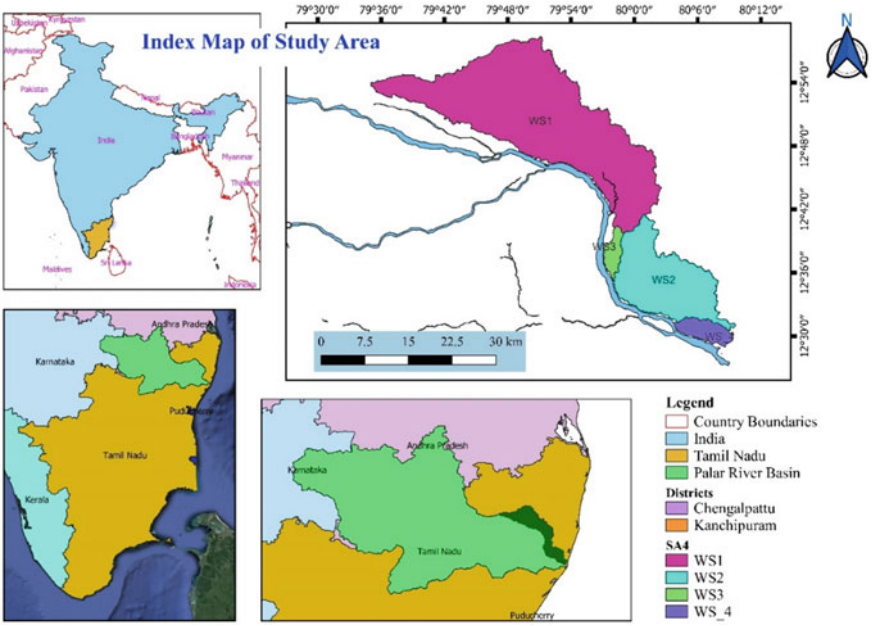

Fig. 1 Index map of sub-watersheds [sub-watershed 1 (WS1), sub-watershed 2 (WS2), sub-watershed 3 (WS3), and sub-watershed 4 (WS4)] of lower Palar River reach

Table 1 Details of the data and sources

Data	Resolution	Source
Sentinel-2 MSI	30 m	European Space Agency
Gridded rainfall	0.05°	Climate Hazards Center, UC Santa Barbara
SRTM DEM	30 m	Open Topography
Data	Resolution	Source
Sentinel-2 MSI	30 m	European Space Agency

3 Material and Methods

3.1 Data Used

Open-source satellite data and field observation data were used in this study. The satellite data was available for the last three decades, sufficient for the watershed trend analysis. The various satellite images were used, which are listed in Table 1.

3.2 Watershed Delineation

The study area was delineated based on the surface water flow draining points. The 30 m resolution SRTM digital elevation model was used [7, 13]. The four sub-watersheds, Neenjal Maduvu sub-watershed (WS1), Kazhuvalayar Maduvu sub-watershed (WS2), P. V. Kalathur sub-watershed (WS3), and Vasavasamuthram sub-watershed (WS4), were delineated in the lower Palar River reach. These four sub-watersheds drained in the lower Palar River get at various locations.

3.3 Rainfall Estimation

Climate Hazards Group Infrared Precipitation with Station Data (CHIRPS) is a 30-year quasi-global rainfall dataset. CHIRPS creates gridded rainfall time series for trend analysis and seasonal drought monitoring by combining rainfall analysis satellite data with in-situ station data. The code was used to add a monthly rainfall chart for a user-specified location to this study. These data were available every five days, and the mean, median, and annual rainfall were estimated [4].

3.4 Land Use Land Cover Classification

Sentinel-2 will make a significant contribution to land supervision by providing input data for both land cover and land cover change mapping, as well as assisting in the estimation of biogeophysical characteristics such as Leaf Area Index (LAI), Leaf Chlorophyll Content (LCC), and Leaf Cover (LC). The source for training and prediction in this land use land cover classification is a Sentinel-2 surface reflectance image with selected reflectance bands. Using the ESA WorldCover land cover map as a label source in classifier training, this study added land cover as a band to the reflectance image and sampled 100 pixels at a 10 m scale from each land cover class within a study area. The sample was subjected to a random value field, which was used to divide roughly 80% of the features into a training set and 20% into a validation set [14, 15].

3.5 Surface Water Mapping

The available global surface water datasets are intended to reveal various aspects of surface water, both temporal and spatial distribution, over the last 38 years [5, 16, 17]. Some datasets are intended to be mapped, while others are designed to demonstrate the temporal change at designated points [5]. Furthermore, some datasets include metadata on the number of observations and valid observations used that can be utilized to estimate the data's levels of confidence [15, 18, 19].

3.6 Flood Mapping

The flood mapping and web application were created in Python using GEE, a cloud-based analysis platform. A flood-inundated map was generated based on pre- and post-flood images of Synthetic Aperture Radar (SAR) from the Sentinel-1 satellite. It provides data by continuous observation during the flood because it can penetrate the cloud. SAR can operate in all weather conditions and provide timely and critical information about flooding, one of the most frequently occurring and devastating natural calamities. Too often, lacking technical expertise separates the disaster-affected community from the required information. The current study is intended to overcome technological limitations by providing a near real-time, cloud-based, and simple method for flood extent mapping [11, 20].

3.7 Web-Based Application

The web-based application was developed to allow the government and other stakeholders to access post-flood information. With the base geographic map, this application will display the water-inundated areas. Without a field visit, cropland damage, waterlogged settlements, damaged transportation routes, and the status of stream drainage capacity were identified. It should direct the earliest and most effective relief operations following a flood event. Users can get the area of water-inundated extent by selecting any flood event from the dropdown menu. GEE is a Google open cloud platform for geoscience data processing and analysis [14, 21–23].

It supports online programming and interactive display and can process data from remote sensing without retrieving images [13, 24–27]. Because of its powerful computing capabilities, it can process high-level remote sensing data, making it suitable for large-scale and long-term research projects. Furthermore, GEE's extensive API documentation incorporates numerous superior remote sensing image processing algorithms, which are extremely useful for people who focus on data processing rather than programming [12, 19, 27–29].

4 Results and Discussion

The average monthly rainfall was estimated, which ranged between 1500 and 2700 mm. The estimated rainfall was integrated in the GEE application which enables the user to visualize the monthly rainfall for any given point of the watershed in graphical user interface. Land use land cover was predicted by the classification of Sentinel images with five groups of spectral signatures, which were named later built-up area, waterbody, agricultural land, barren land, and forest; then, it was validated by 100 field observations. The surface water spread was estimated based on the global surface water datasets, and the area calculation was done by multiplying the number of pixels by the area of the single pixel, which is 30 m.

The watershed monitoring application based on the results obtained from satellite data analysis was made and shown in Fig. 2. This application will allow the user to get the rainfall series by selecting any location in the study area. Here the default time series was chosen as June 2018 to May 2019. The water spread of the individual watersheds was presented in a separate dialogue box with a dropdown box. By clicking on the dropdown, user can choose the watershed. The water spread map and calculated area were shown in the graphical area and toolbox area, respectively (Fig. 3).

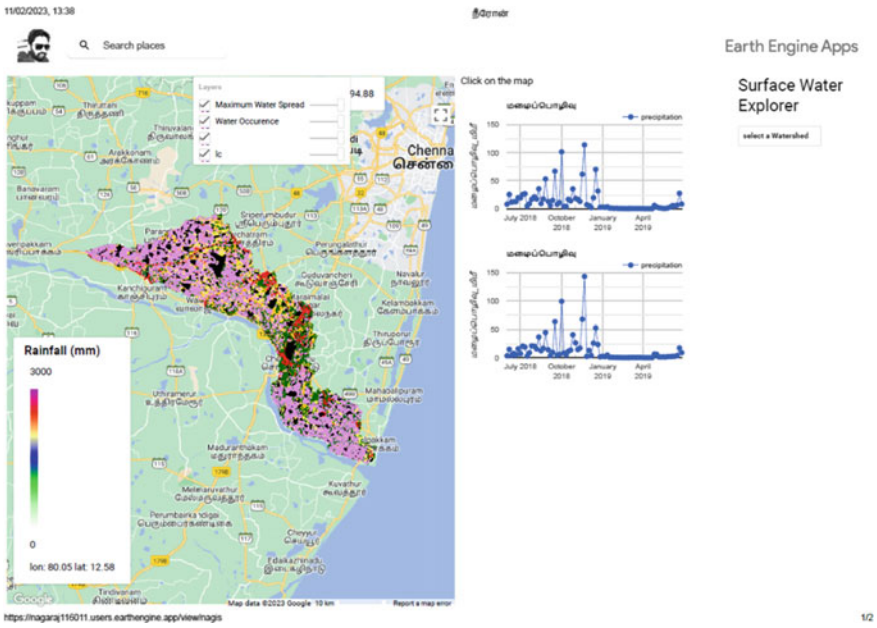

Fig. 2 GUI structure of web-based application for watershed monitoring

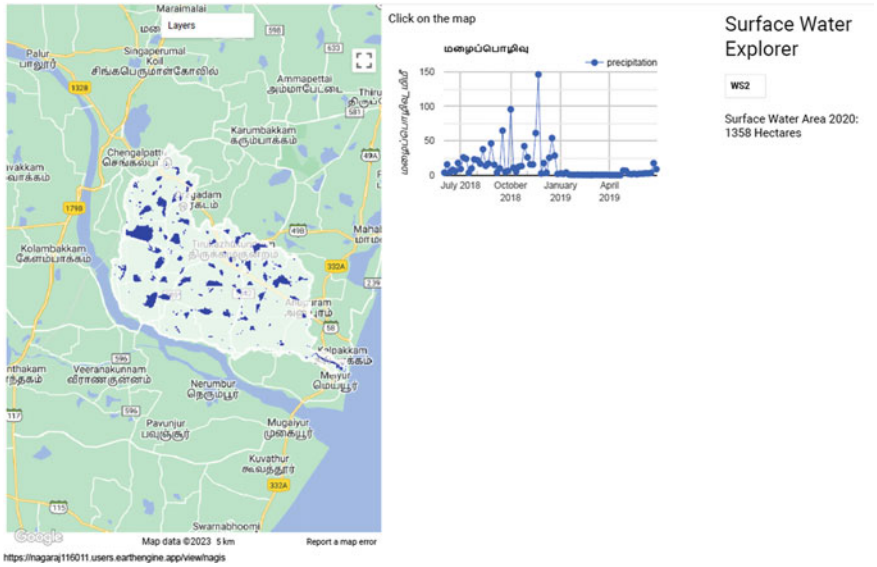

Fig. 3 GUI structure of sub-watershed-wise surface water potential and rainfall

5 Conclusion

Based on satellite data, the rainfall distribution, land use land cover, flood inundation, and surface water potential of lower Palar River reach sub-watersheds were estimated, and a web-based application was deployed using the GEE platform and machine language. The user can access the watershed information with the 30 m spatial accuracy by using the graphical user interface. The findings show that water potential and its influencing factors are linked. The web-based application is the best solution for getting immediate solutions to watershed issues, particularly in suburban areas with increasing demand and flood susceptibility. The findings in this study are entirely based on satellite images and predefined algorithms used in previous studies published in Scopus peer-reviewed journals. Proper validation and calibration must be performed to scale the study to other watersheds.

References

1. Thangamani V. Water Balance of the Palar Basin, India [Online]. Available at: https://www.researchgate.net/publication/339617763
2. Resmi MR, Achyuthan H (2018) Lower Palar River sediments, southern Peninsular, India: geochemistry, source-area weathering, provenance, and tectonic setting. J Geol Soc India 92(1):83–91. https://doi.org/10.1007/s12594-018-0956-0
3. Narayanan M, Thirukumaran V (2021) An impact of rain fall in ground water level fluctuation and prediction of rainfall at Kanchipuram District, Tamil Nadu, India. View project Identification of groundwater potential zones using time series analysis and GIS applications in Palar River Basin, Tamil Nadu, India. Novyi MIR Res J 6 [Online]. Available at: https://www.researchgate.net/publication/351834468
4. Kumar L, Mutanga O (2018) Google Earth Engine applications since inception: usage, trends, and potential. Remote Sens (Basel) 10(10). https://doi.org/10.3390/rs10101509
5. Liu C et al (2022) Monitoring water level and volume changes of lakes and reservoirs in the Yellow River Basin using ICESat-2 laser altimetry and Google Earth Engine. J Hydro-Environ Res 44:53–64. https://doi.org/10.1016/j.jher.2022.07.005
6. Zeng H et al (2019) Spatiotemporal analysis of precipitation in the sparsely gauged Zambezi River Basin using remote sensing and Google Earth Engine. Remote Sens (Basel) 11(24). https://doi.org/10.3390/rs11242977
7. Şener M, Arslanoğlu MC (2023) Morphometric analysis in Google Earth Engine: an online interactive web-based application for global-scale analysis. Environ Model Softw 105640. https://doi.org/10.1016/j.envsoft.2023.105640
8. Li K, Xu E (2021) High-accuracy continuous mapping of surface water dynamics using automatic update of training samples and temporal consistency modification based on Google Earth Engine: a case study from Huizhou, China. ISPRS J Photogramm Remote Sens 179:66–80. https://doi.org/10.1016/j.isprsjprs.2021.07.009
9. Habibie MI (2022) The application of machine learning using Google Earth Engine for remote sensing analysis [Online]. Available at: https://ejurnal.teknokrat.ac.id/index.php/teknoinfo/index
10. Kılıç M (2022) Drought monitoring on Google Earth Engine with remote sensing: a case study of Ş. Levantine J Appl Sci. https://doi.org/10.56917/ljoas.13
11. Mobariz M, Kaplan G (2021) Monitoring Amu Darya river channel dynamics using remote sensing data in Google Earth Engine, p 8012. https://doi.org/10.3390/ecws-5-08012

12. Tripathi RN, Ramachandran A, Hussain SA, Tripathi V, Badola R (2022) Development of a Google Earth Engine based application to monitor the seasonal water spread area of river Ganga. Int Arch Photogramm Remote Sens Spat Inf Sci ISPRS Arch 43(B3):1287–1292. https://doi.org/10.5194/isprs-archives-XLIII-B3-2022-1287-2022
13. Gorelick N, Hancher M, Dixon M, Ilyushchenko S, Thau D, Moore R (2017) Google Earth Engine: planetary-scale geospatial analysis for everyone. Remote Sens Environ 202:18–27. https://doi.org/10.1016/j.rse.2017.06.031
14. Ghorbanpour AK et al (2022) Crop water productivity mapping and benchmarking using remote sensing and google earth engine cloud computing. Remote Sens (Basel) 14(19). https://doi.org/10.3390/rs14194934
15. Liu Y et al (2022) Vietnam wetland cover map: using hydro-periods Sentinel-2 images and Google Earth Engine to explore the mapping method of tropical wetland. Int J Appl Earth Observ Geoinf 115. https://doi.org/10.1016/j.jag.2022.103122
16. Wang C, Jia M, Chen N, Wang W (2018) Long-term surface water dynamics analysis based on Landsat imagery and the Google Earth Engine Platform: a case study in the middle Yangtze River Basin. Remote Sens (Basel) 10(10). https://doi.org/10.3390/rs10101635
17. Kandekar VU et al (2021) Surface water dynamics analysis based on sentinel imagery and Google Earth Engine Platform: a case study of Jayakwadi dam. Sustain Water Resour Manag 7(3). https://doi.org/10.1007/s40899-021-00527-7
18. Donchyts G et al (2022) High-resolution surface water dynamics in Earth's small and medium-sized reservoirs. Sci Rep 12(1). https://doi.org/10.1038/s41598-022-17074-6
19. Thottolil R. Cloud computing for big geospatial data analysis with Google Earth Engine—urban research applications coastal zone management of Mangalore region view project [Online]. Available at: https://www.researchgate.net/publication/367253329
20. Farhadi H, Najafzadeh M (2021) Flood risk mapping by remote sensing data and random forest technique. Water (Switzerland) 13(21). https://doi.org/10.3390/w13213115
21. Attaf D, Djerriri K, Mansour D, Hamdadou D (2019) Mapping of burned area using presence and background learning framework on the google earth engine platform. Int Arch Photogramm Remote Sens Spat Inf Sci ISPRS Arch 42(3/W8):37–41. https://doi.org/10.5194/isprs-archives-XLII-3-W8-37-2019
22. Piralilou ST et al (2022) A Google Earth Engine approach for wildfire susceptibility prediction fusion with remote sensing data of different spatial resolutions. Remote Sens (Basel) 14(3). https://doi.org/10.3390/rs14030672
23. Ejaz N, Bahrawi J, Alghamdi KM, Rahman KU, Shang S (2023) Drought monitoring using Landsat derived indices and Google Earth Engine Platform: a case study from Al-Lith Watershed, Kingdom of Saudi Arabia. Remote Sens (Basel) 15(4):984. https://doi.org/10.3390/rs15040984
24. Abdul Rahaman S, Venkatesh R (2020) Application of remote sensing and google earth engine for monitoring environmental degradation in the Nilgiri biosphere reserve and its ecosystem of Western Ghats, India. Int Arch Photogram Remote Sens Spat Inf Sci ISPRS Arch 43(B3):933–940. https://doi.org/10.5194/isprs-archives-XLIII-B3-2020-933-2020
25. Hansen CH, Google Earth Engine as a platform for making remote sensing of water resources a reality for monitoring inland waters. Spatiotemporal variability of water quality in the Utah Lake-GSL system, and its implication for remote sensing model. Development View project NOAA National Water Center Summer Institute View project. https://doi.org/10.13140/RG.2.1.3688.1047
26. Panidi E, Rykin I, Kikin P, Kolesnikov A (2020) Cloud-desktop remote sensing data management to ensure time series analysis, integration of QGIS and google earth engine. Int Arch Photogram Remote Sens Spat Inf Sci ISPRS Arch 43(B4):553–557. https://doi.org/10.5194/isprs-archives-XLIII-B4-2020-553-2020
27. Rahmawati AD, Asy'ari R. Google Earth Engine: utilization of cloud computing-based mapping platform in detecting Mangrove distribution with Sentinel-2 images in Jakarta City [Online]. Available at: https://www.researchgate.net/publication/359426627

28. Aghlmand M, Kaplan G (2021) Monitoring urban expansion using remote-sensing data aided by Google Earth Engine. Eur J Geosci 3(1):1–8. https://doi.org/10.34154/2021-ejgs-0012/euraass
29. Ghosh S, Kumar D, Kumari R (2022) Cloud-based large-scale data retrieval, mapping, and analysis for land monitoring applications with Google Earth Engine (GEE). Environ Chall 9. https://doi.org/10.1016/j.envc.2022.100605

Using Decision Risk and Decision Accuracy Metrics for Decision Making for Remote Sensing and GIS Applications

K. J. Sowmiya Narayanan and Asaithambi Manimaran

Abstract A confusion matrix or error matrix or contingency table is the most widely used evaluation technique for assessing the difference in actuals with the results of spatial data processing. The confusion matrix provides the basis for computing various metrics such as accuracy, precision, prevalence, sensitivity, and specificity for quantifying the effectiveness of a data classification or a model or an algorithm applied to various applications of remote sensing and Geographic Information System. Since most of these metrics are based on both chance and occurrence but not on the absolute occurrence, in this paper, a set of new metrics is used that are reliably based on the absolute outcomes of the decisions. Decision risk metrics are defined based on errors variable over differentially among different classification groups for decision making. Decision accuracy metrics are defined in terms of decision risk, and absolute accuracy metrics are defined in terms of absolute occurrence that provides with the information for the evaluation of fuzziness in different classification groups and for the comparison among models, algorithms, and datasets.

Keywords Remote sensing · Geographic Information System · Confusion matrix · Decision metrics

1 Introduction

Spatial data classification, prediction, and estimation are generic problem in different application fields of remote sensing and Geographic Information Systems. In remote sensing, different supervised and unsupervised methods are applied for classification of Earth Observation and Satellite data into various classes [1, 2]; similarly in Geographic Information Systems, different models, methods, and algorithms are applied to generate thematic [3] and geostatistical maps. In many of these applications, it is essential to accurately assess and validate the accuracy of the processed

K. J. Sowmiya Narayanan · A. Manimaran (✉)
Department of Civil Engineering, Faculty of Engineering and Technology, SRM Institute of Science and Technology, Kattankulathur, Tamil Nadu 603203, India
e-mail: manimara@srmist.edu.in

K. R. Reddy et al. (eds.), *Recent Advances in Civil Engineering*, Lecture Notes in Civil Engineering 398, https://doi.org/10.1007/978-981-99-6229-7_11

spatial data for further processing and decision making. It is often the case that there are, in parallel, several different methods to perform spatial data processing, and it is required to compare them for the similarities and differences in the process of decision making. A confusion matrix is the most general representation of differences between the results of spatial data processing. There are several metrics used across the scientific community for making appropriate decisions based on the confusion matrix. Since most of these metrics are based on both the chance and occurrence but not on the absolute occurrences, in this paper, a set of new metrics is used that are reliably based on the absolute outcomes of the decisions. Decision risk metrics area defined based on errors variable over differentially among different classification groups for decision making. Decision accuracy metrics are defined in terms of decision risk, and absolute accuracy metrics are defined in terms of absolute occurrence that provides with the information for the evaluation of fuzziness in different classification groups and for the comparison between models, methods, algorithms, datasets, and so on.

1.1 Confusion Matrix

A confusion matrix ($M_{n,n}$) is an $n \times n$ square matrix showing the frequency of actual observation of a class or group against the prediction or classification or estimated occurrence of the class. There are several standard well-established metrics such as sensitivity, specificity, precision, and overall accuracy [1–5] that are defined mostly, based on a binary confusion matrix ($n = 2$). However, in this research, the focus is on a non-binary confusion matrix with $n > 2$. Table 1 shows the general structure of a non-binary confusion matrix with n classes or groups, C_i is the ith class, and $M_{i,j}$ represents the number actual match of ith class with respect to jth class as a matrix element in the confusion matrix.

Standard Metrics. There are several standard metrics developed based on an $n \times n$ confusion matrix that can be categorized under different two groups. A set of metrics is defined globally for all the classes from C_1 to C_n, and there are those that are defined individually for each class C_i. Some of the global metrics used widely in

Table 1 Confusion matrix

		Classification				
		C_1	C_2	C_3	…	C_n
Actual	C_1	$M_{1,1}$	$M_{1,2}$	$M_{1,3}$	…	$M_{1,n}$
	C_2	$M_{2,1}$				$M_{2,n}$
	C_3	$M_{3,1}$				$M_{3,n}$
	…	…				…
	C_n	$M_{n,1}$	$M_{n,2}$	$M_{n,3}$	…	$M_{n,n}$

remote sensing and GIS applications are overall accuracy A_o and kappa statistic κ [6] given in Eqs. (1) and (2), respectively, below for reference.

$$\text{Overall accuracy, } A_o = \frac{\sum_{i=1}^{n} M_{i,i}}{\sum_{i=1,j=1}^{n} M_{i,j}} \tag{1}$$

$$\text{Kappa statistic, } \kappa = \frac{A_o - P_c}{1 - P_c}, \tag{2}$$

where $P_c = \left(\frac{1}{\sum_{i=1,j=1}^{n} M_{i,j}^2}\right) * \left(\sum_{i=1}^{n} \left(\sum_{j=1}^{n} M_{i,j} * \sum_{j=1}^{n} M_{j,i}\right)\right)$.

Similarly, class producer's accuracy PA_C and class user's accuracy UA_C [3, 7] are used to determine the accuracy of an individual class given in Eqs. (3) and (4), respectively, below for reference.

$$\text{Class Producer}'\text{s Accuracy, } \text{PA}_{Ci} = \frac{M_{i,i}}{\sum_{j=1}^{n} M_{i,j}} \tag{3}$$

$$\text{Class User}'\text{s Accuracy, } \text{UA}_{Ci} = \frac{M_{i,i}}{\sum_{j=1}^{n} M_{j,i}} \tag{4}$$

2 Research Background

The confusion matrix and its related standard metrics are widely used for assessing the accuracy and for comparison of different methods of classification, parametric estimation, and prediction; however, first, they do not sufficiently consider the statistical distribution of the population; second, there is no metric to assess the fuzziness among different classes; third, there is no metric defined to assess the risk of misclassification based on the errors in classification; fourth, there is no single metric that combines both the producer's accuracy and user's accuracy to sufficiently represent the differences in results of classification. Further, there are arguments [7, 8] that overall accuracy is not a good representation of the map accuracy, and the proportions of different classes are not considered in determining the accuracy of classes. The kappa coefficient or statistic is unsuitable for assessing the similarity of different classification datasets [6]. Also, [9] emphasizes the need for standard reference datasets for ascertaining accuracy metrics and argues on the errors in validation data. In addition to these concerns, the problem of imbalanced datasets [2] on classification algorithms adversely affects the interpretation of standard metrics, and the fuzziness in discretizing entities [3] is the other challenges. In this context, it is required to standardize and define a set of metrics that can be reliably used to assess a classification or prediction.

3 Decision Metrics

A new set of decision metrics is proposed in contrast with the standard metrics to determine the risk and accuracy of the different classes and of the classifications. These decision metrics are defined by considering a set of three underlying criteria; error, population proportions, and fuzziness. First, a misclassification or an error classification can be treated as a risk of further identifying the class correctly. Second, the occurrence of a class and its identification by a classifier depend proportionately on its statistical population. Third, the distinguishability of a class or group from another depends on the fuzziness of the class or group in relation to the other. An illustration of the three criteria described is shown in Fig. 1, with (a) showing the proportions of classes or groups C_1 to C_6 along the diagonal and misclassification errors across, (b) showing the population proportions, and (c) showing the fuzziness of the classes or groups C_1 to C_6.

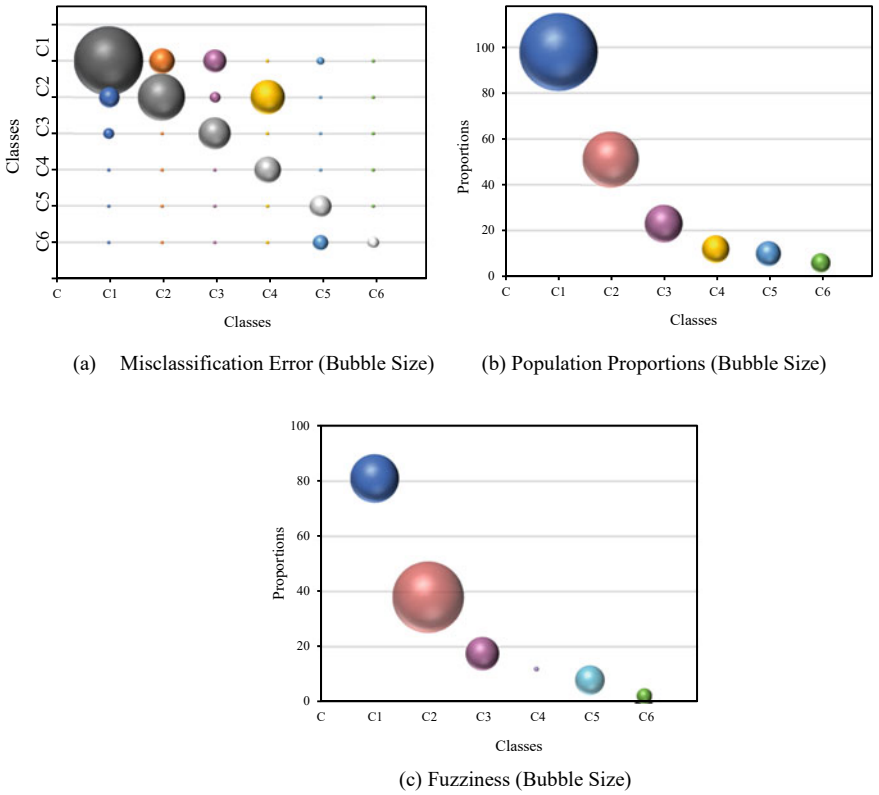

(a) Misclassification Error (Bubble Size)

(b) Population Proportions (Bubble Size)

(c) Fuzziness (Bubble Size)

Fig. 1 Illustration of **a** misclassification error (colored), **b** population proportions, and **c** fuzziness of different classes

3.1 Absolute Accuracy

The absolute accuracy metric (AA) provides the differential accuracy of the classification of a class or group based on the absolute occurrence by considering the third criteria and, hence, can be used for its comparison in determining the fuzziness. The absolute accuracy AA_{C1} of a class '1' $C1$ is given in Eq. (5), as the ratio of actual occurrence of the class $C1$ to the sum of actual occurrence of all the classes from $C1$ to Cn.

$$\text{Absolute accuracy, } \text{AA}_{C1} = \frac{M_{1,1}}{\sum_{i=1}^{n} M_{i,i}} \tag{5}$$

Similarly, Eq. (6) gives the absolute accuracy AA_{Cn} for class Cn.

$$\text{Absolute accuracy, } \text{AA}_{Cn} = \frac{M_{n,n}}{\sum_{i=1}^{n} M_{i,i}} \tag{6}$$

The absolute accuracy follows the condition that $\sum_{i=1}^{n} \text{AA}_{Ci}$ equals to one.

3.2 Decision Risk

The decision risk metric (DR) provides the risk of misclassification of a class or group based on its total classification error for appropriate decision making. The decision risk metric is defined based on the first and third criteria. The second criterion is not considered for the computation of the metric, given that general population statistic is unavailable. The decision risk DR_{C1} of a class '1' $C1$ is given in Eq. (7), as the ratio of sum of actual occurrence and the actual errors of all the other classes $C2$ to Cn to the sum of actual occurrence of all the classes $C1$ to Cn and the sum of the actual errors of all the other classes $C2$ to Cn.

$$\text{Decision risk, } \text{DR}_{C1} = \frac{\sum_{i=1}^{n} M_{1,i} + \sum_{i=1}^{n} M_{i,1} - 2 * M_{1,1}}{\sum_{i=1}^{n} M_{1,i} + \sum_{i=1}^{n} M_{i,1} - M_{1,1}} \tag{7}$$

Similarly, the decision risk DR_{Cn} for the class Cn is given, in Eq. (8). The decision risk metric value ranges in the closed interval of 0–1, with a minimum value of 0 representing no risk and a maximum value of 1 representing a high or complete risk.

$$\text{Decision risk, } \text{DR}_{Cn} = \frac{\sum_{i=1}^{n} M_{n,i} + \sum_{i=1}^{n} M_{i,n} - 2 * M_{n,n}}{\sum_{i=1}^{n} M_{n,i} + \sum_{i=1}^{n} M_{i,n} - M_{n,n}} \tag{8}$$

3.3 Decision Accuracy

The decision accuracy metric (DA) provides the accuracy of classification of a class or group based on the absolute accuracy and differentially on the decision risk taking all the three criteria in consideration. The decision accuracy DA_{C1} of a class '1' $C1$ is given in Eq. (9), as the ratio of actual occurrence to the sum of actual occurrences of all the classes $C1$ to Cn and sum of all errors of all the other classes $C2$ to Cn. Similarly, the decision risk DA_{Cn} for the class Cn is given, in Eq. (10). The decision accuracy (DA) is given by the summation of the class decision accuracy of all the classes or groups given in Eq. (11).

$$\text{Decision accuracy, } \mathrm{DA}_{C1} = \frac{M_{1,1}}{\sum_{i=1}^{n} M_{i,i} + \sum_{i=1}^{n} M_{1,i} + \sum_{i=1}^{n} M_{i,1} - 2 * M_{1,1}} \tag{9}$$

$$\text{Decision accuracy, } \mathrm{DA}_{Cn} = \frac{M_{n,n}}{\sum_{i=1}^{n} M_{i,i} + \sum_{i=1}^{n} M_{n,i} + \sum_{i=1}^{n} M_{i,n} - 2 * M_{n,n}} \tag{10}$$

The decision accuracy metric value ranges in the closed interval of 0–1 and takes a minimum value of 0 for total inaccuracy and a value of 1 for maximum accuracy.

$$\text{Decision accuracy, DA} = \sum_{i=1}^{n} \mathrm{DA}_{Ci} \tag{11}$$

4 Decision Metrics Interpretation

The decision metrics can be effectively used in interpretation of results of prediction, classification or an estimation, and for comparison of different types of predictors, classifiers, and estimators in the process of decision making.

4.1 Decision Making for Classifier or Predictor or Estimator

The decision accuracy metric is for the interpretation accuracy of different classifiers. Absolute accuracy provides for interpreting the fuzziness of classification among different classifiers, which however requires developing appropriate metrics based on the metric.

Table 2 Selected set of literatures with confusion matrix metadata

Title of the article	Description	Metrics used	Decision making
Good practices for object-based accuracy assessment [10]	Comparison for two methods area based and count based method	Overall accuracy, kappa statistic, producers accuracy, users accuracy, allocation disagreement, and quantity disagreement	Classification and classifier
A multidisciplinary approach for evaluating spatial and temporal variations in water quality [11]	Determining water quality using different classifiers considering spatial variability	Overall accuracy, mean absolute error, root mean squared error, relative absolute error, and root relative squared error	Classification and classifier

4.2 Decision Making for Classification or Prediction or Estimation

The absolute accuracy metric is for the interpretation of population proportions and fuzziness. The decision risk metric is applied for interpreting the risk of misclassification among different classes or groups. The class decision accuracy indicates the share of accurate classification among different classes.

5 Research Methodology

The research methodology involves a careful, systematic selection of literature with metadata on classification, prediction, and estimations in the form of confusion matrix for remote sensing, earth observation, and Geographic Information System applications. The selected set of literature with appropriate metadata (see Appendix) is provided in Table 2.

The derived decision metrics are computed for the metadata in each of the selected literature and is compare against the standard metrics. The results are critically evaluated and discussed.

6 Result and Discussion

The decision metrics are computed for the selected set of literature and are tabulated under two categories of interpretation. The computed results from the comparison tables are then interpreted, and the results are discussed for the two categories of interpretation: classification and classifier.

6.1 Classification

Table 3 lists out the absolute accuracy, decision risk, and decision accuracy in comparison with the standard metrics user's accuracy and producer's accuracy for different classes or groups.

High absolute accuracy and low decision risk of a class indicate that the classification accuracy is better for the class as with C_1. In case of the class C_5, it can be seen that even though the user's and producer's accuracy is high, a relatively high decision risk for the classification indicates that only around 4 of 10 (0.5982) on ground verification are likely to be correct. Further, a high class decision risk and low absolute accuracy for the class C_{12} indicate that the classification results are not dependable for the class. The class M_2 has low decision accuracy and high class decision risk that indicates a high fuzziness. The decision risk and class decision accuracy of class M_1 shows that the classification is highly accurate and represents the majority of the classification data. In this special case, where the class decision risk of M_1 is zero, it equals to absolute accuracy.

Table 3 Decision metrics comparison with standard metrics for the classifications from the literature metadata

Article reference	Classifier method	No. of classes	Total no. of obs.	Class or group	Absolute accuracy	Decision risk	Decision accuracy (class)	User accuracy	Producer accuracy
[10]	Count-based method	13	746	C_1	**0.2176**	**0.1437**	0.2099	0.89	0.95
				C_2	0.0167	0.5	0.0164	0.69	0.65
				C_3	0.0350	0.4523	0.0340	0.6	0.91
				C_4	0.1628	0.1705	0.1575	0.86	0.96
				C_5	0.0684	**0.5982**	**0.0681**	**0.98**	**0.96**
				C_6	0.0228	0.4642	0.0223	0.75	0.68
				C_7	0.0319	0.4166	0.0312	0.87	0.74
				C_8	0.0136	0.7	0.0132	0.69	0.33
				C_9	0.0045	0.1358	0.3304	0.92	0.93
				C_{10}	0.0030	0.3333	0.0030	1	0.62
				C_{11}	0.0684	**0.0816**	**0.0680**	**0.96**	**0.95**
				C_{12}	**0.0015**	**0.875**	**0.0015**	1	0.11
				C_{13}	0.0091	0.25	0.0091	1	0.72
[11]	Multilayer perceptron (MLP)	3	258	M_1	**0.6359**	**0**	**0.6359**	1	1
				M_2	**0.0414**	**0.82**	**0.0348**	0.30	0.31
				M_3	0.3225	0.3693	0.2713	0.7777	0.7692

6.2 Classifier

Table 4 lists the decision accuracy with overall accuracy and kappa statistic for comparison with different classifiers.

The overall accuracy and kappa statistic comparatively show that multilayer perceptron classifier performs better that naïve Bayes classifier; however, the decision accuracy shows that they are more or less similar with naïve Bayes classifier slightly performing better than the multilayer perceptron classifier. In case of the count- and area-based methods of classification, it is seen that the decision accuracy shows that the difference in classification results is similar to the differences between the overall accuracy and kappa statistic.

7 Conclusion

Assessing the accuracy of spatial data processing of remotely sensed and geographic data has always been challenging in the scientific community. There are several standard metrics available and have been used in practice based on a confusion matrix, which, however, does not sufficiently address some of the problems such as fuzziness, proportions of population, and absolute occurrence. In this research, a new set of decision metrics is defined based on the confusion matrix for interpretation and for use by the scientific community addressing some of these problems. A limitation of this research work is that only a few selected metadata was considered, and the further scope of this research includes exploration of the decision solution space with

Table 4 Decision accuracy comparison with standard metrics for the classifiers from the literature metadata

Article reference	Number of classifiers	Classifier method	Decision accuracy	Overall accuracy	Kappa statistic	Total number of observations
[10]	2	Count based	**94.2**	84.1	0.8677	746
		Area based	**97.4**	91.3	0.9013	1047.2 (area)
[11]	5	Multilayer perceptron	**94.2**	**84.1**	**0.7249**	258
		Radial basis function	99.2	86.8	0.7585	
		Decision tree	97.5	85.6	0.7485	
		Support vector machine	93.5	77.1	0.5855	
		Naïve Bayes classifier	**94.4**	**79.84**	**0.6638**	

the decision metrics, validation with simulated and real datasets, and comparison with several other standard metrics.

Appendix: Reference Confusion Matrix

The following is the confusion matrix from the source literatures for computations in Sect. 6.

Confusion Matrix (Count-Based Method) *[10]*

Class	C_1	C_2	C_3	C_4	C_5	C_6	C_7	C_8	C_9	C_{10}	C_{11}	C_{12}	C_{13}
C_1	143	5	1	0	0	0	0	2	7	0	0	1	1
C_2	3	11	1	0	0	0	0	0	1	0	0	0	0
C_3	1	1	23	0	0	0	1	2	8	0	2	0	0
C_4	0	0	1	107	0	7	5	4	0	0	0	0	1
C_5	0	0	0	1	45	0	0	0	0	0	0	0	0
C_6	0	0	0	2	2	15	1	0	0	0	0	0	0
C_7	0	0	0	1	0	1	21	1	0	0	0	0	0
C_8	0	0	1	0	0	0	2	9	1	0	0	0	0
C_9	3	0	0	0	0	0	3	8	229	1	0	4	0
C_{10}	0	0	0	0	0	0	0	0	0	2	0	0	0
C_{11}	0	0	0	0	0	0	0	0	0	0	45	2	0
C_{12}	0	0	0	0	0	0	0	0	0	0	0	1	0
C_{13}	0	0	0	0	0	0	0	0	0	0	0	0	6

***Confusion Matrix (Area-Based Method)* [10]**

Class	C_1	C_2	C_3	C_4	C_5	C_6	C_7	C_8	C_9	C_{10}	C_{11}	C_{12}	C_{13}
C_1	301	7	0.4	0	0	0	0	4	6	0	0	0.9	0.5
C_2	3	7	0.2	0	0	0	0	0	0.3	0	0	0	0
C_3	0.3	0.2	22	0	0	0	1	4	6	0	2	0	0
C_4	0	0	0.5	122	0	9	4	9	0	0	0	0	0.2
C_5	0	0	0	2	78	0	0	0	0	0	0	0	0

(continued)

(continued)

Class	C_1	C_2	C_3	C_4	C_5	C_6	C_7	C_8	C_9	C_{10}	C_{11}	C_{12}	C_{13}
C_6	0	0	0	0.7	2	15	0.5	0	0	0	0	0	0
C_7	0	0	0	1	0	1	21	1	0	0	0	0	0
C_8	0	0	0.6	0	0	0	2	7	0.6	0	0	0	0
C_9	5	0	0	0	0	0	5	6	338	0.8	0	3	0
C_{10}	0	0	0	0	0	0	0	0	0	2	0	0	0
C_{11}	0	0	0	0	0	0	0	0	0	0	36	1	0
C_{12}	0	0	0	0	0	0	0	0	0	0	0	0.5	0
C_{13}	0	0	0	0	0	0	0	0	0	0	0	0	7

Confusion Matrices (Algorithms) **[11]**

Class	Multilayer perceptron			Radial basis function			Decision tree			Support vector machine			Naïve Bayes classifier		
	M_1	M_2	M_3	M_1	M_2	M_3	M_1	M_2	M_3	M_1	M_2	M_3	M_1	M_2	M_3
M_1	138	0	0	137	0	1	137	0	1	127	0	11	134	0	4
M_2	0	9	21	6	0	24	0	7	23	2	1	27	0	16	14
M_3	0	20	70	3	0	87	13	7	77	15	4	71	0	34	56

References

1. Bush WS, Edwards TL, Dudek SM, McKinney BA, Ritchie MD (2008) Alternative contingency table measures improve the power and detection of multifactor dimensionality reduction. BMC Bioinform 9(1):1–17
2. Luque A, Carrasco A, Martin A, de Las HA (2019) The impact of class imbalance in classification performance metrics based on the binary confusion matrix. Pattern Recogn 91:216–231
3. Maxwell AE, Warner TA (2020) Thematic classification accuracy assessment with inherently uncertain boundaries: an argument for center-weighted accuracy assessment metrics. Remote Sens 12(12):1905. https://doi.org/10.3390/rs12121905
4. Vujovic Z (2021) Classification model evaluation metrics. Int J Adv Comput Sci Appl 12(6):599–606
5. Valero-Carreras D, Alcaraz J, Landete M (2023) Comparing two SVM models through different metrics based on the confusion matrix. Comput Oper Res 152:106131. https://doi.org/10.1016/j.cor.2022.106131
6. Garcia Garcia-Balboa JL, Alba-Fernandez MV, Ariza-Lopez FJ, Rodriguez-Avi J (2018) Analysis of thematic similarity using confusion matrices. ISPRS Int J Geo Inf 7(6):233. https://doi.org/10.3390/ijgi7060233

7. Shao G, Tang L, Liao J (2019) Overselling overall map accuracy misinforms about research reliability. Landsc Ecol 34:2487–2492
8. Stehman SV, Wickham J (2020) A guide for evaluating and reporting map data quality: affirming Shao et al. "Overselling overall map accuracy misinforms about research reliability". Landsc Ecol 35:1263–1267
9. Radoux J, Bogaert P (2020) About the pitfall of erroneous validation data in the estimation of confusion matrices. Remote Sens 12(24):4128
10. Radoux J, Bogaert P (2017) Good practices for object-based accuracy assessment. Remote Sens 9(7):646. https://doi.org/10.3390/rs9070646
11. Le VT, Quan NH, Loc HH, Thanh Duyen NT, Dung TD, Nguyen HD, Do QH (2019) A multidisciplinary approach for evaluating spatial and temporal variations in water quality. Water 11:853. https://doi.org/10.3390/w11040853

Potential Hafir Dam Site Selection Using GIS and Remote Sensing Techniques in Gabiley District, Somaliland

Abdilahi Bashir Omer and Andinet Kebede Tekile

Abstract Rainwater harvesting systems have been utilized recently in Somaliland, especially in dry areas. Locating a suitable site for the rainwater harvesting structure is a decisive task for better design and planning. To guarantee water supply and to reduce the consequences of flood events, the hydrological analysis for the Hafir dam site location is done by using a geographic information system (GIS) and remote sensing (RS). The first aim of this research was thus to select a suitable site for Hafir dam construction using GIS and RS tools. The research utilized three consecutive steps to propose the suitable Hafir dam site. First, feasibility study or physical observation of the water infrastructures in ten villages of Biji and Waheen catchments in Somaliland was done. This had the plan of selecting three villages of serious water scarcity. The second step was further evaluation of the three villages to find out the most vulnerable village. The third step was to locate appropriate site of the selected village. The baseline study result showed Ijaara village to be the most vulnerable based on water scarcity. The soil type of the locations was loam, except Location 4, which has sandy soil. Based on the GIS and RS hydrological analysis, considering the catchment yield, its soil type and slope, of the four locations of the selected village, the most suitable one is located at 9.561809° and 43.637782°, latitude and longitude, respectively.

Keywords GIS and RS · Hafir dam · Site selection · Somaliland · Water harvesting

A. B. Omer (✉)
Lincoln University College, Postal Code 00000, Borama, Somaliland
e-mail: abdilahi819@gmail.com

A. K. Tekile
Adama Science and Technology University, P.O. Box 1888, Adama, Ethiopia

K. R. Reddy et al. (eds.), *Recent Advances in Civil Engineering*, Lecture Notes in Civil Engineering 398, https://doi.org/10.1007/978-981-99-6229-7_12

1 Introduction

Globally, there are a number of technological options that can improve water supply systems in rural villages. Specifically, in the semi-arid regions, which the raining season only covered few months, the surface water storage is preferable. Collection of the surface water during the raining season is been used since roman time with roof catchments. The earliest time used surface water harvesting technology in the continent of Africa were seen in Northern Egypt since 2000 years, with tanks which its volume between 200 and 2000 cubic meters a lot of these are still in used today [1]. Rainwater harvesting systems in African countries are increasing in recent decades. Although the expansion is rapid, the progress of the system is slow due to the construction cost of the surface water harvesting system based on the income of households. The lack of construction material in Africa, the absence of water for the production industry, and other factors affect the total cost [2].

Somaliland is a water-scarce country as it regularly experiences water shortages and recurrent droughts during the dry season. Inadequate water is the largest constraint to sustainable livelihood throughout the country [3]. In Somaliland, surface water harvesting is with many technologies for collecting surface water to villagers, but it contributes to other sources of water, such as groundwater. The rainwater harvesting system in Somaliland has been used since time immemorial [4]. Due to the rainfall shortage in recent decades, the Somaliland government lacks the capacity to respond to the existing water scarcity and recurrent drought issues in the country. As the result, lack of access to reliable water becomes the main cause for preventable diseases, recurrent droughts, and resulting in more people struggling with food security.

Due to the lack of the surface water harvesting structures in Gabiley district of the country, which is located at east west of Hargeisa city, large number of people are vulnerable to drought and hunger. Hence, there is a critical need to ease water scarcity and recurrent droughts by providing effective rain water harvesting infrastructures to the villages of the district. This research study therefore aimed to contribute to the solution by locating the most suitable site for construction of water harvesting structures using the integrated technique of GIS and RS.

A geographic information system—GIS, is application program which is used for the analysis, mapping, and sorting of spatial and non-spatial information in a digital form. Remote sensing (RS), on the other hand, is a science and art of finding an information or data about the objects on the earth or earth features without physical contacts with that object [5]. GIS technology program tool is used to analysis a spatial data that collected from remote sensing and field surveys with different structures and resolution. The usage of GIS in the department of water catchments and water resource management is advanced in the last twenty years [6].

Application of GIS and remote sensing techniques for site selection of the Hafir dam has reached an incredible role in hydrological analysis. Remote sensing application in hydrological modeling is fast, less personal engagement. The automated generation of topographic watershed data and maps using GIS is keen significant

effort in recent decades for the site selections, planning, and design. Arc GIS provides an efficiency of analysis of watershed data in the process of the site selection [7].

To achieve the main objective of identifying the potential location of Hafir dam for a most seriously affected village, among ten villages of Gabiley district, three specific objectives were used as operational steps. (1) To study the current condition of water harvesting structures in ten villages of Gabiley district and Hargeisa city to propose most realistic villages to construct a Hafir dam construction. (2) To identify and select a potential location for Hafir dam at the selected village by considering the village most vulnerable to water scarcity. (3) To present the hydrological suitability of the pre-selected locations and to suggest final location for the Hafir dam at the selected village by GIS and RS.

2 Study Area and Methodology

2.1 Research Area

Somaliland is located in the eastern Africa. Somaliland is confirmed in north by the Gulf of Aden, in the east by federal republic of Somalia, in the north-west the Republic of Djibouti and in the south west by the Federal Republic of Ethiopia. It lies between 08°N and 11°30′N and between 42°30′E and 49°00′E [8]. Ijaara village admiration under Gabiley district, Maroodijeex region, Somaliland. Ijaara village locates at 9°35′1.86″N and 43°37′40.60″E latitude and longitude, respectively. The seasons of Somaliland are divided in four seasons; in the spring, it has Hagaa and GU, and in the summer, it has Jilaal and Deyr. The major raining season ranges from April to June and called Gu, which is 60% of the total rain in the year, and the second major rainy season is in between August and November which called (Deyr). Most raining season in Somaliland is GU and Deyr. Jilaal and Hagaa are the two dry seasons in the country; they occur between December and March and July and August, respectively. Somaliland is situated northern part of the Equator, and the Somaliland climates are semi-arid [9]. It has been found that the average daily temperatures of the Somaliland is from 25 to 35 °C. The annual rainfall in Somaliland ranges 200 mm in coastal area to 600 mm in mountains area [3].

Somaliland consists of four large drainage basins that are determined by the surface runoff and drainage pattern with sediment transportation systems. The major basins are Ogaden Basin, Darror Basin, Nugal Basin, and Gulf of Aden Basin. Among the catchments in Somaliland, four main catchments have been identified: Salel catchment, Durdur Add catchment, Biji catchment, and Waheen catchment. This research study is main concern of the upper part of the Biji catchment among those catchments [10]. Generally, the definition of Hafir dam differs from place to place and from state to state. In Somaliland, Hafir dam is an improved earth dam with additional components for efficient service provision includes the geomembrane lining systems and water treatment system [11].

2.2 Dam Site Selection Criteria

An empirical study carried out by Ghoraba on the hydrological modeling of the simply dam watershed of Pakistan using GIS and SWAT model. The study also discovered that, using GIS-SWAT appropriately adjusted, could be refer professionally in regions which have semi-arid climate to manage water resource schemes [12]. On the other hand, Choo et al. have proposed Suitable Dam Site based on Geographic Information using AHP. Their study was carried out to help a dam construction that could secure water resources and reduce the drought and floods. It was found out the most governor criteria for the site selection to be land cover, hydrological geology and slope [13].

Globally, the stress on water resources increased by the change of the climate, cyclic droughts, with a rising demand of the urban development; those countries located in semi-arid zones are experiencing a water scarcity for both human and livestock consumption. Somaliland is part of the countries which faces a shortage of water, as the main water resources which the country owned are the rainwater and ground water. In 2003, FAO produced a guideline on site selection criteria for the identification of potential rainwater harvesting sites with more related to the agricultural bases [14]. Adhama and Riksen carried out a review of the Identification of Suitable Sites for rainwater harvesting structures in arid and semi-arid regions based on the biophysical criteria including slope, soil type, rainfall, land use, and drainage network [15]. Lalhmingliana and Goutam-Saha conducted research on the Identification of Suitable Dam Site considering Multi-criteria Analysis GIS and remote sensing based to the biophysical characteristics and socio-economic criteria. This study showed the most effective criteria for choosing the best location which the rainfall, land use/cover, soil type, slope, and settlement distance [16].

2.3 Steps of Site Selection

The feasibility assessment had carried out in ten villages in Gabiley district and Hargeisa city based on the level of water scarcity and recurrent droughts (Fig. 1). This feasibility is to explore the potential for rainwater harvesting in structure. These villages located in Biji catchment and Waheen catchment. The description consists of two parts: first part was the overall information of the villages including population clusters, livelihood of the community, and second part was existing rainwater harvesting structures and boreholes in both public and private. It has been acknowledged a significant water runoff goes to waste in Gulf of Aden basin to red sea. This concern is to mitigate the rainwater by providing rainwater harvesting infrastructure. The common water harvesting and other water storage currently in place include earth dam construction, berkad construction, and shallow wells had recorded and physically observed.

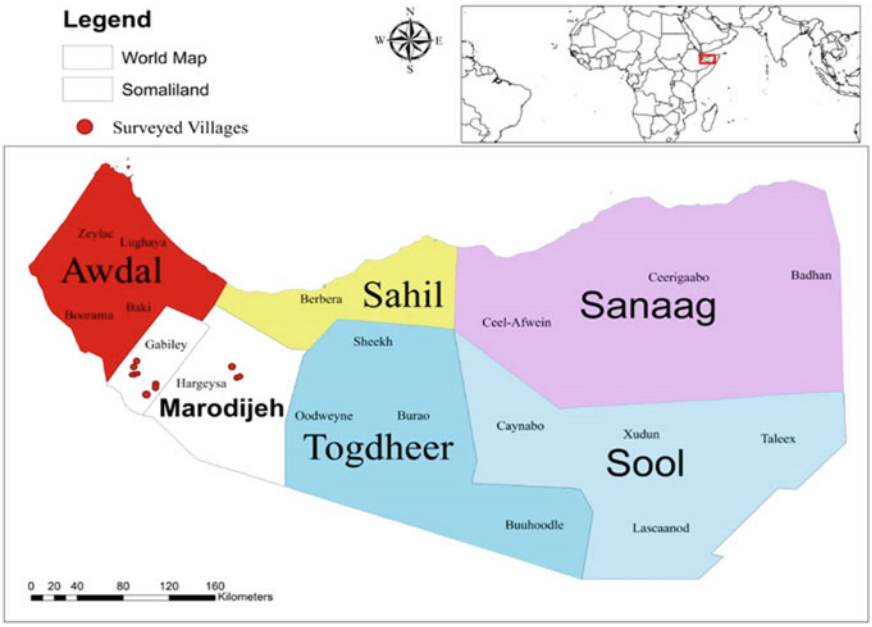

Fig. 1 Map of study location

After having completed the feasibility study, it has carried out a baseline study narratively in the pre-selected villages. This baseline study was household interviews and a participatory interview guide with key community informants as well as field observations to gather varied information. This method was used to gather, compile, assess, and analysis data on water infrastructures and water availability.

This research used various data, those collected from file by visual, physical, and remotely, and the data composed of different resolutions and scales in raster and vector data. The study used a selection criteria which was composed in the environment of GIS technology to decide better location for Hafir dam implementation. The study methodology which was used for this research was divided in phases in GIS and remote sensing including the determination of criteria which comprises the Hafir dam location and the assembly of all essential information by the determined criteria. Finally, the effect of each criterion was established and confirmed using GIS/RS. GIS and RS analysis was also carried out based on the watershed size, length and yield, slope, soil layers, and land use (Fig. 2).

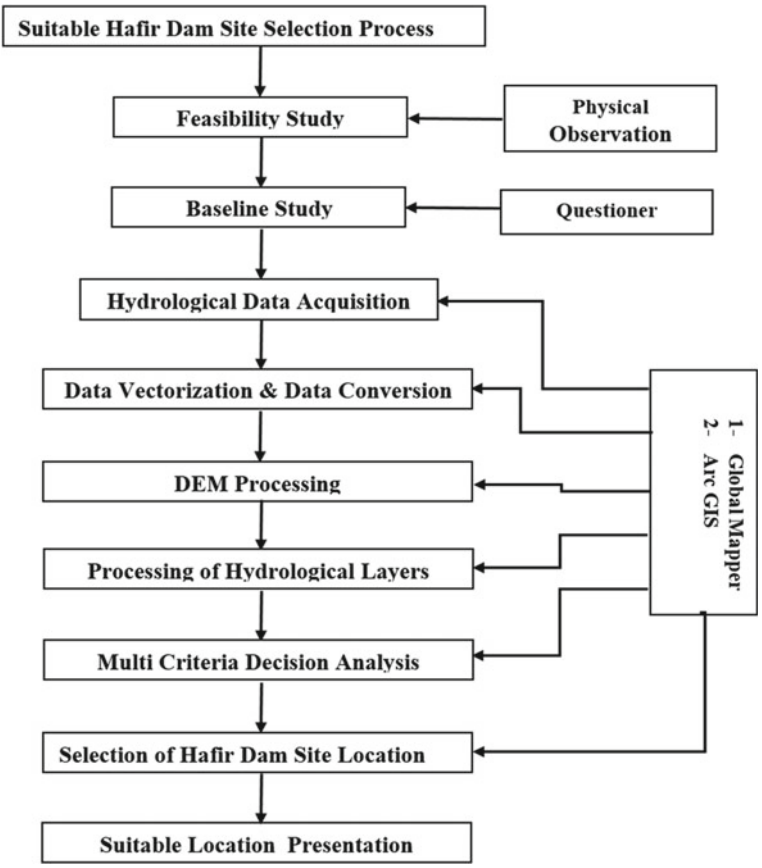

Fig. 2 Flowchart of the study

3 Results and Discussions

The feasibility study is carried out in ten villages in Maroodijeex region, Somaliland. The ten villages located in two catchments were: 6 villages are in Biji catchment (Illinta, Bottor, Boodhley, Gorey, Taysa, and Ijaara) and 4 villages in Waheen catchment (Awbarkhadle, Xunba-Wayne, Darar-Weyne, and Jaleelo); both catchments drain in to Aden Golf basin. During the feasibility study, the selection criteria were to assess water scarcity of the villages and rank them accordingly. The ranking system used for this research study is 1–4 starting from worst-case scenario to the excellent case for the all criteria except that the population goes highest to lowest. Based on the village analysis charts, the Biji catchment villages show the highest rank of the analysis system, while the Waheen catchment villages show the lowest rank of the analysis base on water scarcity. The villages, which are located in Biji catchment (Ijaara, Boodhley, Tays, and Gorey), are in high potential for Hafir dam construction.

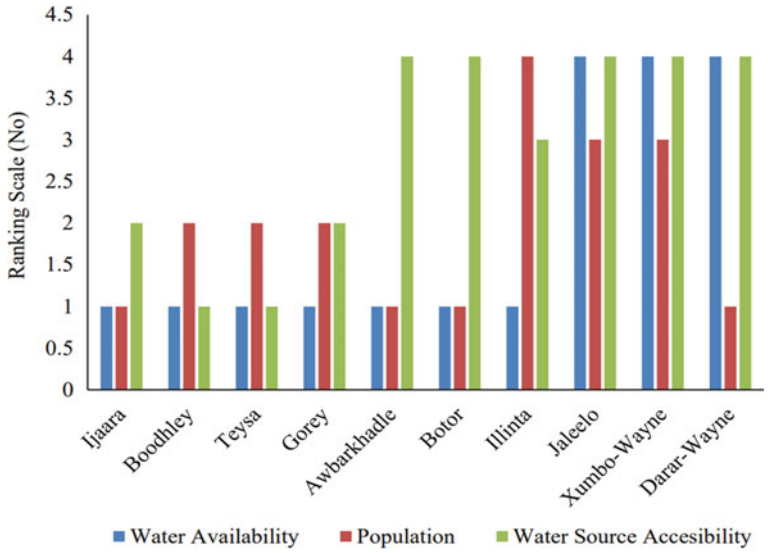

Fig. 3 Feasibility analysis result

The first priority of the assessment was based on the water availability on existing water harvesting infrastructure, and second priority was based on population of those villages, while the third priority was based on distance travel to the water source. The result of the analysis is shown in Fig. 3. Based on the evaluation criteria, the result of the feasibility study recommended the Biji catchment villages to be potential for further study.

Based on the recommendation for the feasibility study, a baseline study is carried out in three villages (Taysa, Boodhley, and Ijaara) in Gabiley district, Somaliland. The three villages are located in Biji catchment, which drain in to Aden Golf basin. This is to identify particular village in Gabiley district and address water scarcity through water storage structures with population of the village and distance travel to the water sources in dray seasons. It has been concluded that the Ijaara has more population than the other two villages, has less access of the access of the clean water, and has the longest distance to travel. So that Ijaara has recommended to the water interventions to reduce the distance and make water to be available and accessible for the Ijaara community (Fig. 4).

Based on the result of the baseline study, a GIS and RS analysis was carried out in four location in Ijaara villages to select suitable site for the Hafir dam construction. The result of the GIS and RS analysis of the four locations shows that the four locations shared similar hydrological information, while some hydrological information are different. Based on the GIS and RS analysis of the four locations at Ijaara village, the first three locations have loam soil. The loam soil has a low permeability, and it allows minimum water to pass through it which is good for the earth dams to hold water for long time. From the GIS and RS analysis, Location 4 has the highest yield

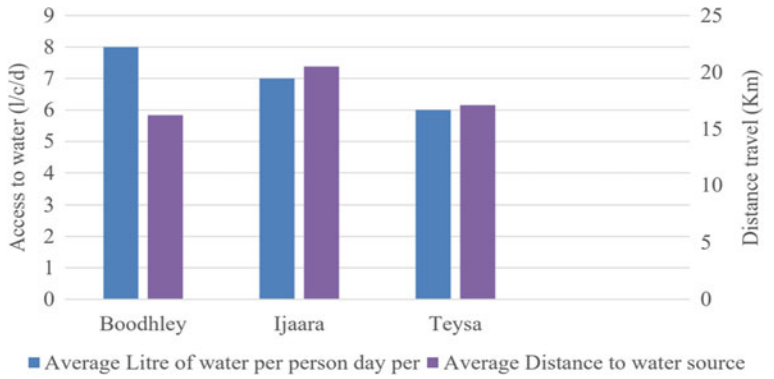

Fig. 4 Baseline analysis result

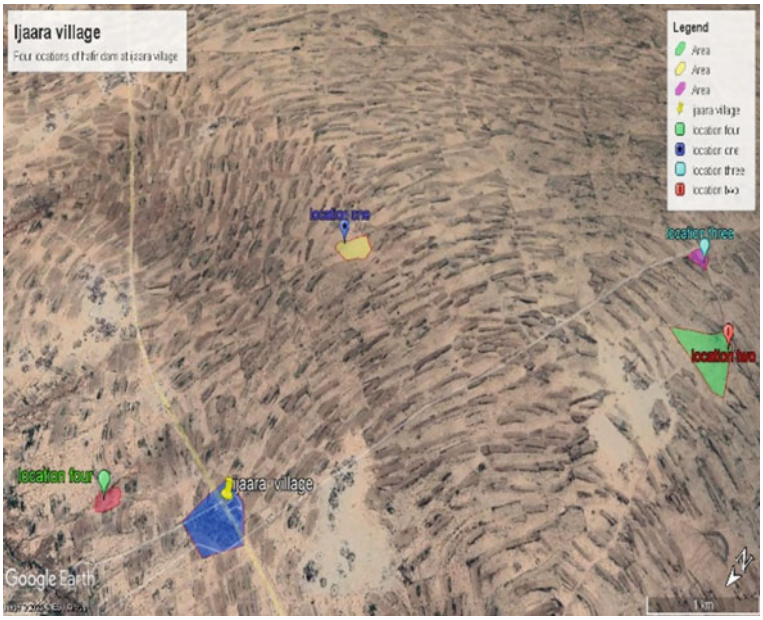

Fig. 5 Potential locations for the Hafir dam

capacity, but the soil is loam with sand, and the slope is 3%, which is the steepest among the four locations. The ideal location is Location 2, which has the second highest yield, gentle slope, and loam soil, but Locations 2 and 3 have lower yield capacity than water demand for the Ijaara village. Therefore, Location 1 was the suitable site for the Hafir dam construction site (Figs. 5, 6, 7, and 8).

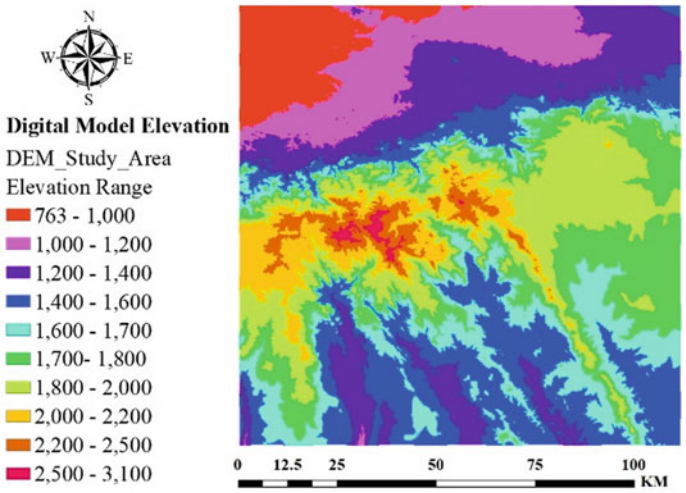

(a)

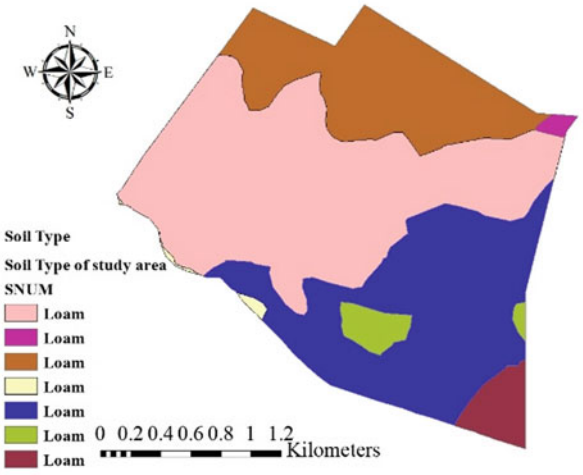

(b)

Fig. 6 RS analysis **a** digital model elevation, **b** soil type, **c** slope, and **d** land use and land cover of the study area

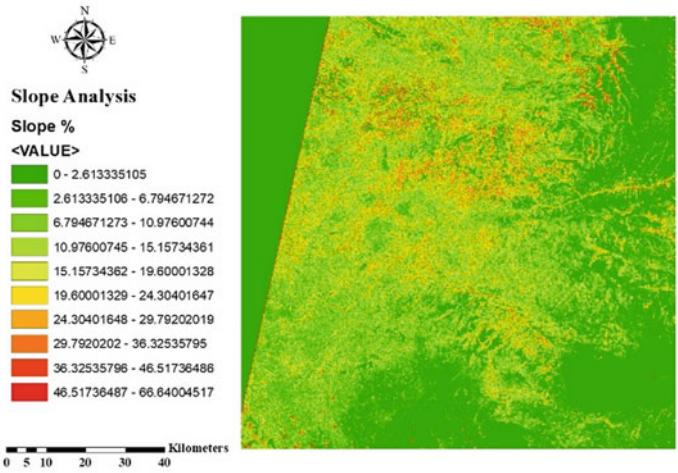

(c)

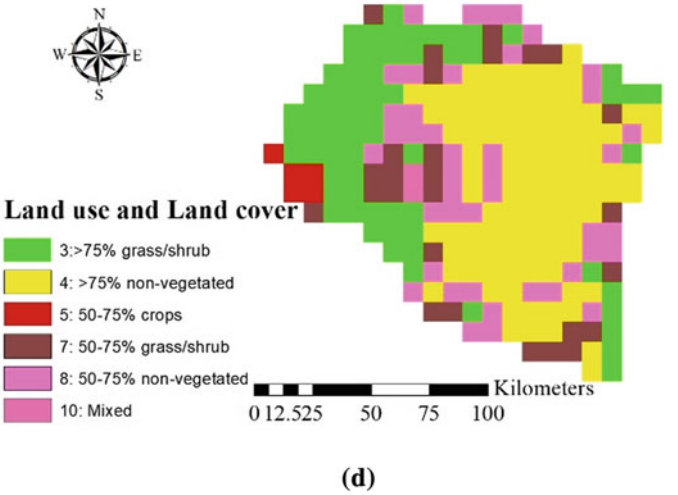

(d)

Fig. 6 (continued)

4 Conclusion

The main objective of the research is intended to select the Hafir dam site location from ten villages. Three different methods were applied to select the Hafir dam location; the first method was feasibility study or physical observation of the ten villages to know the current water availability of the each villages and the village population with current water sources. It has found the Ijaara, Boodhley, and Taysa.

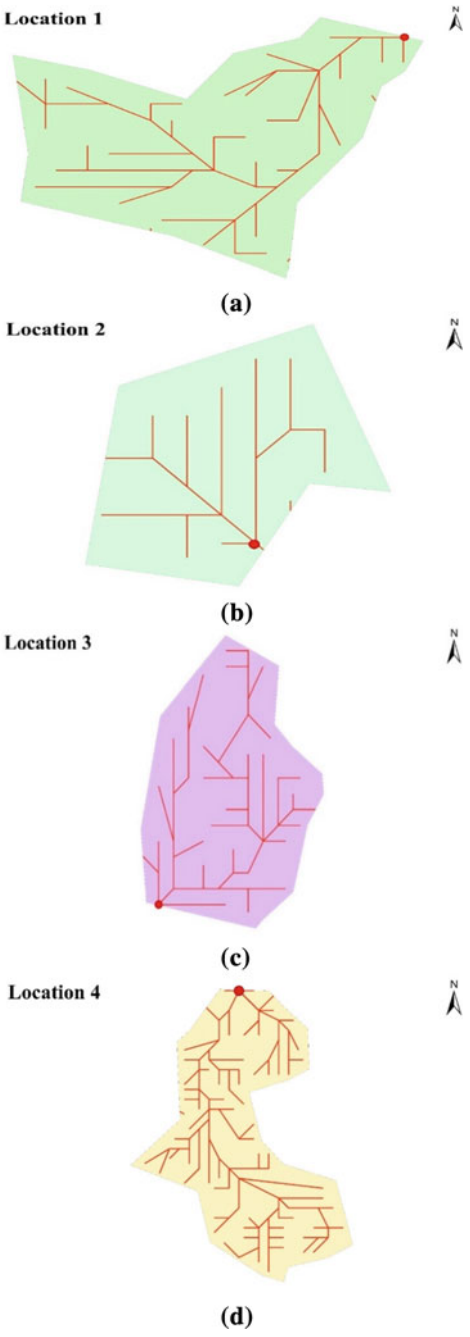

Fig. 7 GIS watershed map **a** Location 1, **b** Location 2, **c** Location 3, and **d** Location 4

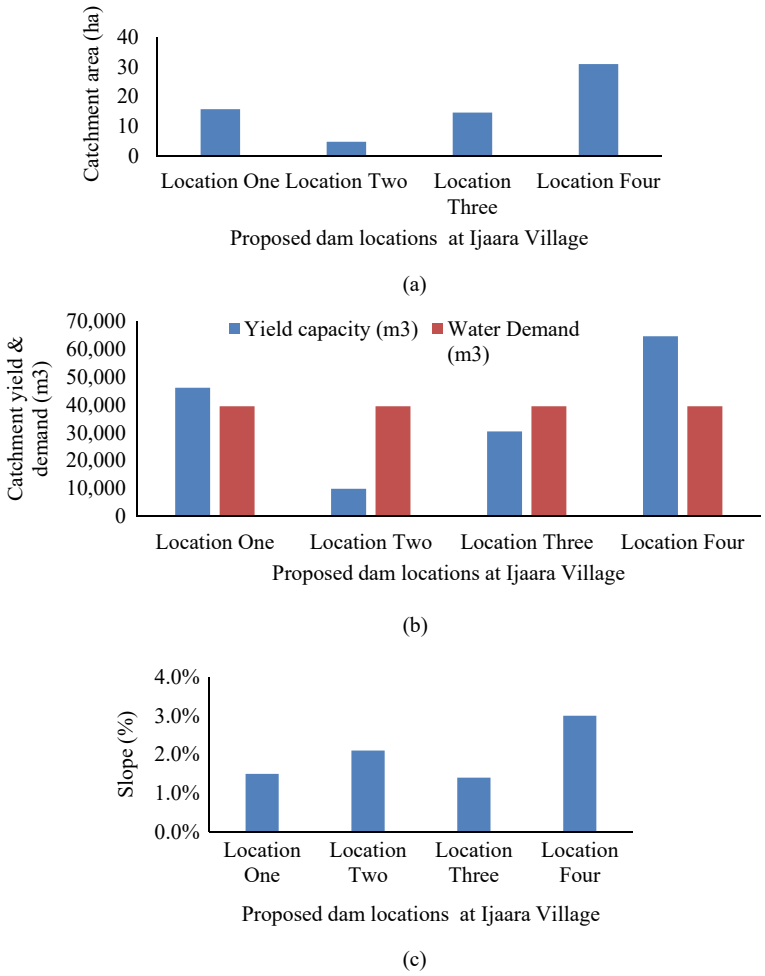

Fig. 8 GIS analysis **a** catchment area, **b** capacity yield and demand, and **c** slope

The second method was the baseline study of the selected three villages for the further analysis; this study was a census that was interviewed to all community of these three villages. The result shows that Ijaara village was the most populated and farther distance to the water sources up to 20.5 km away from the water sources. This study suggested that Ijaara village is the most vulnerable village and most appropriate for the Hafir dam construction. The third method that has applied during this research study was GIS applications. After the selection of the Ijaara villages, the community proposed four locations as public land for the Hafir dam construction. A Global Mapper and Arc GIS had been used for the hydrological analysis of the four locations to select the most suitable site based on the watershed size, slope, and soil type. The result of the GIS analysis showed that Location 1 is the most

suitable for the Hafir dam construction. This case study offers a reference to the GIS future researcher for choosing the Hafir dam location in Gabiley district in which the feasibility data and baseline data with GIS hydrological analysis were displayed.

Acknowledgements I would also like to thank the Pharo Foundation for their facilitation for me to do this research on the current programs in the foundation, especially Water Development Department and the Research and Evaluation Department.

References

1. UN-HABITAT (2005) Rainwater harvesting and utilisation. Blue drop series. Book 2: Beneficiaries & capacity builders. UN-HABITAT: Mtwapa, Kenya, p 77
2. Leggett DJ, Brown R, Brewer D, Stanfield G, Holliday E (2001) Rainwater and greywater use in buildings: best practice guidance. CIRIA Report C539, CIRIA, London, UK, p 134
3. Somaliland Vision 2030 (2011) Somaliland food & water security strategy
4. FAO-SWALIM (2007) Potential of rainwater harvesting in Somalia. Technical Report No. W-09, Oct 2007
5. Kumar H, Singh K (2018) Water resources: role of GIS and remote sensing. Int J Eng Res Technol. Special issue of RTCEC—2018 conference
6. Jehanzeb MM, Bastiaanssen GM (2017) Remote sensing and GIS applications in water resources management. Water resources management, pp 351–373 (chap. 16)
7. Thanoon HAM, Ahmed KA (2012) Hydrological information extraction for dams site selection using remote sensing techniques and geographical information system. Al-Rafidain Eng 21(5):102–114
8. Republic of Somaliland (2021) Country Profile 2021
9. National Development Plan II (2007)
10. MoAD (2020) Research, development and capacity building for sustainable agricultural development in Somaliland. Somaliland Ministry of Agricultural Development
11. Somalia (2017) WASH cluster—Somalia Minimum Wash Technical Guidelines
12. Ghoraba SM (2015) Hydrological modelling of the Simply Dam watershed (Pakistan) using GIS and SWAT model. Alexandria Eng J 54(3):583–594
13. Choo TH, Ahn SI, Yang DU, Yun GS (2017) A study on the estimating dam suitable site based on geographic information using AHP. In: 6th international conference on developments in engineering and technology (ICDET-2017)
14. FAO (2003) Land and water digital media series, 26. Training course on RWH (CDROM). Planning of 12 water harvesting schemes, unit 22. Food and Agriculture Organization of the United Nations, Rome
15. Adhama A, Riksen M, Ouessar M, Ritsema C (2016) Review paper identification of suitable sites for rainwater harvesting structures in arid and semi-arid regions: a review. Int Soil Water Conserv Res 4:108–120
16. Lalhmingliana G-S (2016) Identification of suitable dam site: a survey. Int J Comput Eng Technol 7(5):56–64

Surveying and Geospatial Engineering

Spatial Analysis of Physical Characteristics of Slums in Tiruchirappalli City

D. Deepa, D. Muthu, D. R. Sakthi Kiran, Bhaskar Babu Sree Gnanesh, Minna Gopi Krishna, and Vineesh Kotni

Abstract This study examines the state of slums in Tiruchirappalli city, Tamil Nadu, India, with a particular focus on basic services and infrastructure. Utilizing GIS technology, the researchers conducted site visits and mapped the collected data to prioritize each slum based on the significance of essential infrastructure elements. Parameters such as toilet facilities, street lighting, and water availability were analyzed and ranked, following UN-Habitat guidelines, which categorized the wards into three groups: satisfactory, above satisfactory, and below satisfactory. The GIS software also facilitated the creation of models to predict future development needs based on current trends. The study provides valuable insights into the living conditions of slums in Trichy city, enabling the formulation and implementation of effective strategies for improvement. Emphasis is placed on addressing the below satisfactory wards to uplift their living conditions, while acknowledging the progress achieved in above satisfactory wards as potential models for successful interventions. This analysis contributes to understanding disparities and variations in slum conditions and guides efforts to enhance overall living conditions in slums.

Keywords Slum · Slum upgradation · GIS · Spatial data · ArcMap · Slum clearance

1 Introduction

The population of current urban areas is becoming increasingly concentrated as a result of urbanization in developing nations like India. Such concentration, which is particularly noticeable in metropolitan areas, has put strain on urban services and infrastructure, causing the physical environment to deteriorate and the quality of life of citizens to decline. Due to the unplanned construction and urban sprawl that surround these cities, the enormous potential of the regions nearby major

D. Deepa (✉) · D. Muthu · D. R. Sakthi Kiran · B. Babu Sree Gnanesh · M. Gopi Krishna · V. Kotni
Civil Department, SASTRA Deemed to be University, Thanjavur, India
e-mail: deepa@src.sastra.edu

K. R. Reddy et al. (eds.), *Recent Advances in Civil Engineering*, Lecture Notes in Civil Engineering 398, https://doi.org/10.1007/978-981-99-6229-7_13

metropolitan areas also stays mostly untapped. This report uses the term "slum" in a broad sense to refer to a variety of low-income settlements and/or unfavorable living conditions [1, 2]. A "slum" or "slum area" is a small community of at least 20 homes that is made up of a number of shoddily constructed, primarily temporary, tenements that are packed close together and frequently lack basic sanitary and drinking water services. The inner-city slums of several towns and cities in both developed and developing nations serve as common examples. Slums also include the sizable informal settlements, such as squatter colonies and illegal subdivisions that are swiftly becoming as the most obvious manifestation of urban poverty in developing world cities [3]. So, using the appropriate socioeconomic data, background checks, etc., a database may be created and tagged. Government must create a database that contains all the necessary data about these slums' facilities and way of life in order to lessen the effects they have [4]. The slums must be evaluated in order to demonstrate their state. Thus, appropriate plans and recommendations for improving the slum neighborhoods can be established. In a quickly expanding urban area, the slum maps can be updated with the help of a suitable database and utilized as a basis map for many government and semi-government organizations [5].

The concentration of population in metropolitan cities has put a strain on existing urban infrastructure and services, resulting in a decline in the quality of life for residents. Unplanned urban development around these cities has also prevented the exploration of the potential of surrounding regions. The solution proposed by Dhanabalan [6] is the creation of "New Planned Self-Sufficient Cities" that prioritize sustainable infrastructure and reduce the pressure on existing cities. This approach emphasizes the importance of planning and developing new urban centers that can support a high quality of life for residents and promote sustainable growth. Such planned cities can incorporate features such as efficient transportation systems, green spaces, and state-of-the-art technology to ensure sustainable development. Additionally, they can prioritize inclusive and equitable access to housing, health care, education, and other basic services, which are essential for improving the quality of life of residents [7, 8].

The use of the term "slum" in this context refers to a wide range of low-income settlements and poor living conditions. Slums are characterized by informal settlements that are rapidly becoming the most visible form of urban poverty in developing countries [9, 10]. These settlements range from simple shacks to permanent structures and are often referred to by various names. The physical factors of developed slums can be compared with those of undeveloped slums to determine the severity of the problem [11, 12]. This comparison can reveal the extent of the lack of access to basic services and infrastructure in slums, such as water, electricity, and sanitation. Creating a map to show the severity of slums can help to better understand the extent of the problem and identify areas that need the most attention. Such a map can also be used to track the progress of slum upgrading efforts and evaluate their effectiveness in improving the living conditions of residents [13].

A comprehensive database is necessary to accurately understand the conditions of slums in a rapidly growing urban area like Tiruchirappalli city. This database can be created by collecting and labeling necessary socioeconomic information and

conducting ground checks. By doing so, the government can have a complete understanding of the lifestyle and facilities available to slum residents [14]. To address the challenges posed by slums, the database should include information that can be used to grade the condition of each slum. This will enable the government to make informed plans and suggestions for improving the living conditions in slum areas [15].

1.1 Role of GIS and Remote Sensing in Slum Mapping

GIS technology enables us to analyze and visualize spatial data in a meaningful way by combining it with socioeconomic information. This makes GIS an important tool for addressing the challenges posed by urban poverty and improving the living conditions of slum residents [16]. By incorporating satellite data, GIS provides valuable information for the implementation of development schemes and the monitoring of spatial variability at different locations. In the present study, GIS is used to map the slums in Tiruchirappalli city, India, and gather information about their physical characteristics, such as population density, number of kutcha houses, and access to toilets. The information collected during field work is used to create slum maps that highlight the key physical parameters. The resulting maps are a valuable tool for decision-makers and development organizations as they work to improve the living conditions of slum residents [17].

2 Study Area

Tiruchirappalli, also known as Trichy, is situated in the central region of Tamil Nadu state in India. The city is located along the banks of the Cauvery River and has a latitude of 10°48′38″N, longitude of 78°40′52″E, and an altitude of 85 m above sea level. The city covers an area of 167.23 km^2 and is divided into four zones—Srirangam, Ariyamangalam, Ponmalai (Golden rock), and Ko. Abhishekapuram [18]. The details of the zones are given in Table 1. The Cauvery River flows through the city and provides a source of irrigation and water supply. The district of Tiruchirappalli has an area of 4404 km^2 and is surrounded by other districts such as Salem, Namakkal, Perambalur, Ariyalur, Thanjavur, Pudukottai, Madurai, Sivagangai, Dindigul, and Karur. The city has 65 wards, out of which 11, 12, 13, 16, 17, 18, 22, 24, 32, and 34 do not have any slums. A significant portion of the population in Tiruchirappalli is served by slums, and the city's geographical location with access to the Kaveri River and its proximity to various other districts make it an important location for further development efforts.

Tiruchirappalli is an industrial city in Tamil Nadu, known for its manufacturing of engineering goods, automobile spares, and other products. The city also boasts a rich historical and cultural heritage with numerous temples and monuments attracting

Table 1 Details of zones, wards, households, population, and area of wards in Tiruchirappalli

S. no.	Zone	Wards	Total wards	Total slums	Household	Population	Total area (km^2)
1	Srirangam	1–6, 8–13, 16–18	15	65	7820	29,578	19.78
2	Ariyamangalam	7, 14, 15, 19–29, 33, 61, 62, 64	8	80	8741	35,814	27.08
3	Ponmalai (Golden rock)	30–32, 34–39, 42–44, 46–48, 63, 65	17	59	7054	29,934	56.75
4	Ko. Abhishekapuram	40, 41, 45, 49, 60	15	60	5400	18,211	63.67
Total			65	264	29,015	113,537	167.23

Source Census 2011

tourists. Despite its development, the presence of slums and inadequate housing for low-income populations remains a pressing issue. Improving the quality of life for residents necessitates affordable housing, better infrastructure, and improved access to basic services like water, electricity, and sanitation. Mapping and documenting the slums in Tiruchirappalli, along with socioeconomic data, will enhance understanding of the challenges faced by these communities and facilitate the development of effective solutions. The study aims to demarcate slum areas, prioritize them for phased development, and create thematic maps using geospatial technology. By analyzing slums and their physical characteristics, strategies for slum upgrading can be recommended to enhance the socioeconomic conditions of residents. This study's objectives center around utilizing GIS technology to understand and address the slum-related challenges in Tiruchirappalli.

3 Methodology

3.1 Mapping and Assessment of Slum Using GIS

The mapping and assessment of slums using GIS involves a systematic process to analyze and understand the spatial distribution and characteristics of slum areas. The step-by-step procedure is as follows:

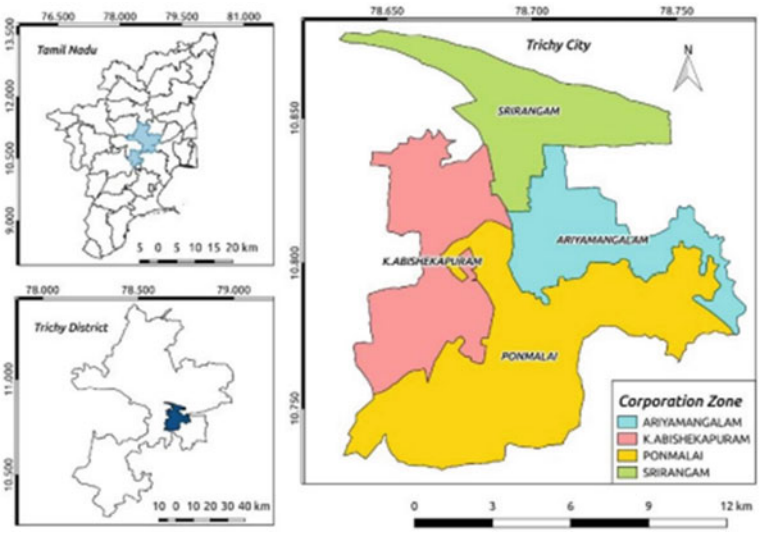

Fig. 1 Study area map. *Source* Action Plan for Control of Air Pollution with Respect to PM10 in Non-Attainment City/Million plus city—Trichy U A in Tamil Nadu

The process of mapping and assessing slums using GIS begins with gathering relevant data through field surveys, satellite imagery, and existing databases. This data includes information on slum locations, boundaries, infrastructure, socioeconomic indicators, and other pertinent attributes. Once collected, the data is organized and prepared for integration into a GIS environment, which involves tasks like digitizing maps, georeferencing satellite images, and converting data into suitable formats such as shapefiles or geodatabases. Next, GIS software like ArcGIS or QGIS is utilized to set up a new project. The base map or satellite imagery of the study area is imported as a reference for spatial context (Fig. 1). The prepared slum data, comprising location coordinates, attributes, and boundaries, is then integrated into the GIS software. This can be accomplished by adding shapefiles, CSV files, or connecting to a database. Spatial analysis techniques are employed to derive insights and patterns from the slum data. Proximity analysis, density analysis, clustering analysis, and overlay analysis with other relevant spatial datasets, such as infrastructure and land use, are performed to gain a comprehensive understanding of the slum areas.

Thematic maps are created using the visualization capabilities of the GIS software to represent the slum locations, boundaries, and attributes. Symbology and labeling are applied to effectively communicate the information depicted in the maps. The socioeconomic conditions, infrastructure accessibility, and other relevant factors within the slum areas are analyzed through data assessment. This may involve overlaying census data, income levels, access to basic services, and any additional information collected during the process. The results of the mapping and assessment are interpreted to gain insights into the slum conditions, identify challenges, and

prioritize interventions. This analysis aids in formulating strategies and policies for slum development and improvement.

The creation of slum maps based on different parameters allows for easier analysis and comprehension of the conditions in the slums. The maps were generated after conducting both qualitative and quantitative analyses on various aspects. The current study focuses on one slum but can be extended to all the slums in the city, helping to prioritize areas for development by the government. The slum maps can also be used for conducting relocation studies. The system is made more efficient and user-friendly by incorporating the slum maps, making it easier for users to update and add necessary information. The locations of the slums were determined through field surveys and satellite imagery, and field data was collected to understand the available facilities in each of Trichy's 65 wards.

3.2 Mapping Through ArcMap

The procedure for mapping data into a GIS environment involves several steps. Firstly, data is collected through field surveys and various websites such as smartcities.data.govt.in and censusindia.gov.in. Once the data is collected, it is saved in a CSV or Excel format. Next, the ArcMap software is opened, and the base map shape file is added. This shape file can be obtained from sources like Google Earth Pro or other reliable sources. After adding the base map, the necessary folders containing the collected data are added to the list of tables available in ArcMap. This allows the data to be incorporated into the GIS environment. To integrate the non-spatial data collected with the spatial data in the main layer, the data is joined. This is done by selecting the "Join Data" option and choosing a field that can correlate the existing data with the non-existing data. The table that serves as the basis for the join is selected, and the data collected is added to the attribute table. At this stage, further analysis and manipulation of the data can be performed.

4 Results and Discussions

4.1 Results Obtained from Mapping Data

The following results were obtained by mapping the various parameters collected with the shape file. From Fig. 2, it can notice that various wards in Trichy are having different population, and the population of the city varies with the slum population. Some wards with high population might have less slum population, and some wards with low population may have high slum population; for example, for the ward no. 40, the population is higher and the range is higher, whereas in terms of slum population, the ward no. 40 is having less density, and it all depends on various parameters such as

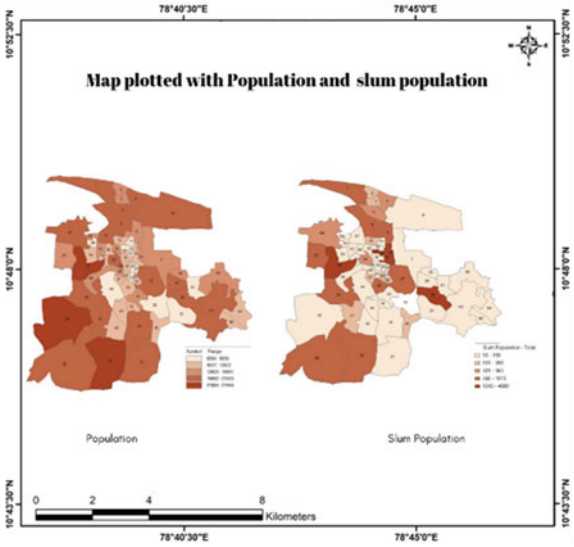

Fig. 2 Map plotted with population and slum population

adequate street lighting facilities, adequate road length, sufficient water distribution, and electricity connections.

4.2 Identified Slums and Recognized Slums

An identified slum is defined as a densely populated and poorly constructed area with at least 300 residents or 60–70 households, characterized by substandard living conditions with limited access to basic amenities such as clean water and proper sanitation. The slums are declared as recognized by the state or local government, including the housing and slum boards, and are often located in unsanitary environments. The number of recognized and identified slums in each of the city's 65 wards is depicted in Fig. 3.

4.3 Housing Conditions, Street Lights, and Street Light Availability

Figure 4 shows us the no. of kutcha housing as well as no. of pucca housing units in Trichy city. Generally, kutcha houses are made of mud and they are weak in structure, whereas pucca houses on the other hand are built of concrete and they are generally stronger than kutcha houses, and they are costly to construct, so in slums which are underdeveloped, we notice more kutcha houses than pucca houses. Slums with toilet

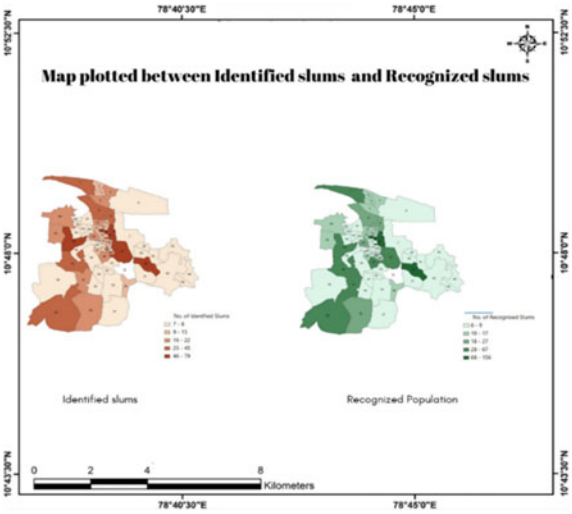

Fig. 3 Map plotted between identified slums and recognized slums

facilities are shown in Fig. 5. Figure 6 shows us the total area and number of street lights per km of the road; this data gives us the data about the lighting facilities in the night time.

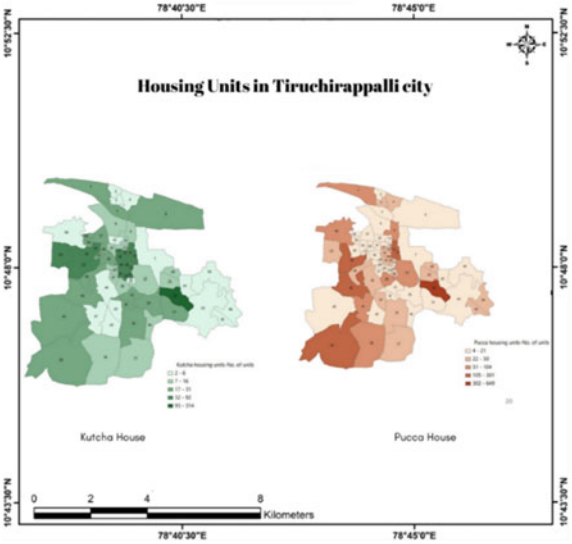

Fig. 4 Housing conditions in Tiruchirappalli city

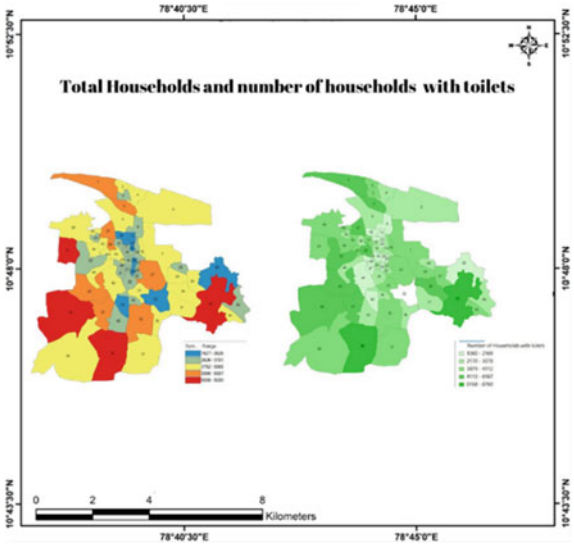

Fig. 5 Total households and number of households with toilet

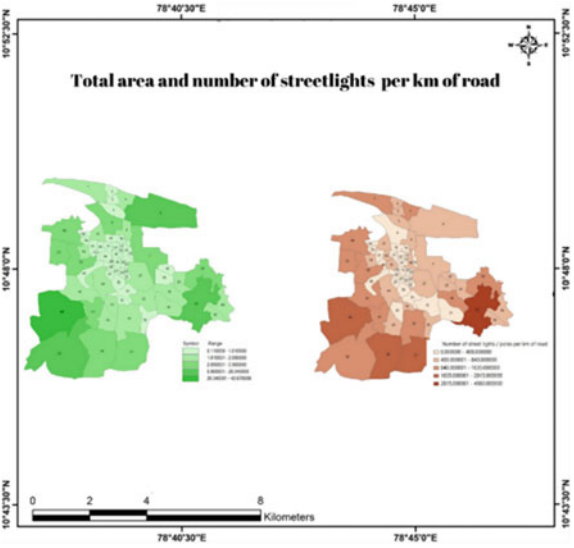

Fig. 6 Total area and number of streetlights per km of road

4.4 Slum Analysis

The data collected from field surveys and websites provides insights into the present conditions of slums in Tiruchirappalli city, including infrastructure, services, and population. UN-Habitat's criteria are used to assess slum households, distinguishing between satisfactory and below satisfactory conditions. GIS technology enables

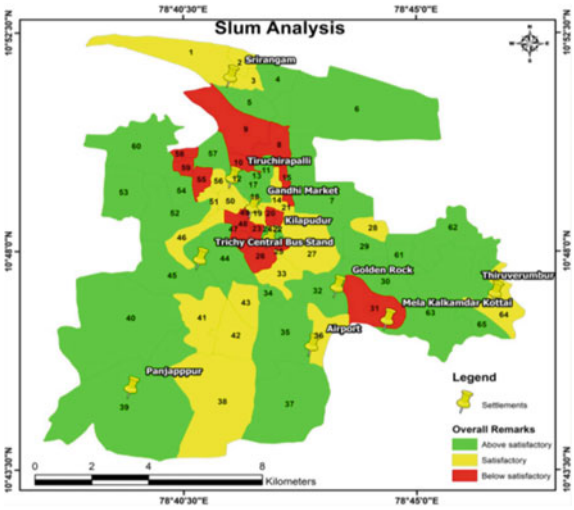

Fig. 7 Quality analysis of slums in Tiruchirappalli city

comprehensive mapping of slums, aiding in planning and resource allocation. The study categorizes slums into three groups: satisfactory, above satisfactory, and below satisfactory, with a focus on addressing the latter. Thematic maps visualize facility distribution, guiding interventions. This analysis highlights disparities and informs strategies for improving slum conditions. Efforts should be concentrated on below satisfactory wards, while progress in above satisfactory wards can serve as examples. The findings support targeted interventions and resource allocation, aiming to uplift living conditions. Overall, this analysis contributes to understanding variations in slum conditions and guides strategies to enhance living conditions in Tiruchirappalli's slums and it was shown in Fig. 7.

5 Conclusions

The study utilized GIS technology and satellite imagery to map the slums in Tiruchirappalli city and collect data on various parameters. The collected data was ranked based on threshold values, resulting in three categories: satisfactory, above satisfactory, and below satisfactory. Out of the 65 wards analyzed, 19 were classified as satisfactory, while 30 were above satisfactory, and 16 were below satisfactory. The findings provide insights for targeted interventions and resource allocation, with a focus on improving the living conditions in below satisfactory wards. The analysis also recognizes the progress made in above satisfactory wards, which can serve as examples for successful interventions. The slum mapping helps visualize the current conditions and identifies areas in need of attention and improvement. It supports quick identification and updates of features and attributes, facilitating development activities and potential relocation efforts by the government. Overall, the study guides

strategies for enhancing the quality of life in slums and addressing disparities among different wards.

References

1. UN-Habitat (2015) State of Indian cities: slums—a statistical compendium. Retrieved from https://unhabitat.org/books/state-of-indian-cities-2015/
2. Ramachandra TV, Bharath HA, Subramanian DK (2015) The unplanned expansion of cities: implications on sustainable development in the peri-urban interface. J Environ Manag 148:3–15. https://doi.org/10.1016/j.jenvman.2014.05.015
3. Chen A (2020) The pursuit of urban equity: mobilizing resources for the urban poor. Oxford University Press
4. Narain V (2015) Slums and urban development: questions on society and globalization. Routledge
5. Roy A (2005) Urban informality: toward an epistemology of planning. J Am Plann Assoc 71(2):147–158
6. Dhanabalan M (2008) GIS applications in urban planning—a case study of Cheyyur Taluk. In: International conference of the Association of Scientists and Engineers, ESSTA-2008, Satyabama University, Chennai
7. Kamal Kumar M (2014) Mapping and assessment of pochamma kunta slum using remote sensing and GIS. Int J Dev Res 4(5):1068–1080
8. GOI (Government of India), Census of India, Registrar General and Census Commissioner, Ministry of Home Affairs, Office of the Registrar General, New Delhi (2011)
9. Ishtiaque A, Mahmud MS (2011) Migration objectives and their fulfillment: a micro study of the rural–urban migrants of the slums of Dhaka City. Malays J Soc Space 7:24–29
10. Kamal Kumar M (2014) Mapping and assessment of pochamma kunta slum using remote sensing and GIS. Int J Dev Res 4(5):1068–1080
11. Sumanta Das MR (2014) Slum redevelopment strategy using GIS based multi-criteria system: a case study of Rajkot, Gujarat, India. World J Civ Eng Constr Technol 1(2):012–041
12. Desai V, Loftus A (2013) Speculating on slums: infrastructural fixes in informal housing in the global south. Antipode 45:789–808
13. McDonnell BP (1998) Principle of geographical information systems. Oxford University Press, New York, USA
14. Dubovyk O, Sliuzas R, Flacke J (2011) Spatio-temporal modelling of informal settlement development in Sancaktepe district, Istanbul, Turkey. ISPRS J Photogramm Remote Sens 66:235–246
15. TNSCB (2013) Slum free city plan of action for Tiruchirappalli Region. TNSCB, Tiruchirappalli
16. Tiwari S (2019) Mapping urban slums using geospatial technology: a review of methods and applications. ISPRS Int J Geo Inf 8(5):224
17. Gopikumar K, Sengupta A (2018) Health and well-being in India's urban slums. Oxford Research Encyclopedia of Global Public Health
18. Dhanabalan M (2018) Mapping and maintenance of slum areas using geospatial technology—a case study Indira Nagar, Ponmalai Region, Tiuchirappalli Dt., Tamil Nadu, India. Int J Emerg Sci Eng (IJESE) 5(10)

Assessment on the Impact of Land Use, Land Cover in the Upstream of the Adyar River Basin, Tamil Nadu, India

Uma Maheswari Kannapiran and Aparna S. Bhaskar

Abstract Globally, significant factors such as the economy, population growth, and climate change have resulted in dramatic changes to Earth's LULC, over the last few decades of Earth. Effective environmental management, particularly water management practises, depend on an understanding of land use and land cover (LULC) changing trends. Using multitemporal Landsat satellite imagery from 2005, 2010, 2015, and 2021, in South Asia, upstream of the Adyar River system, this study evaluated LULC changes. Divide the study area into five categories using remote sensing and geographic information systems: agricultural area, build-up land, waterbody, vegetation, and barren land. Most changes have occurred in the waterbody, built-up land, and agriculture categories. However, in 2005–2021, the change matrix table shows all LULC modifications for all LULC classes. As the study area's population, the study area has increased, so as the levels of development along with the waterbodies. Therefore, to avoid resource-use conflicts in the study area, adequate basin management is necessary, including land use planning.

Keywords LULC · Geographic information systems · Remote sensing · Landsat · DEM · Environmental

1 Introduction

The management of environmental transformations and environmental assets now includes monitoring changes in LULC [1, 2]. Large-scale changes to Earth's land surface brought about by rising human activities are having an impact on the efficiency of global systems. Humans have significantly altered LULC by using its resources for their material, cultural, and spiritual advancement. Rapid LULC changes, especially in emerging nations, have had a negative impact on water, soil, and vegetation. Moreover, there is a regional origin for the activities that result in

U. M. Kannapiran · A. S. Bhaskar (✉)
Department of Civil Engineering, Faculty of Engineering and Technology, SRM Institute of Science and Technology, Kattankulathur, Tamil Nadu 603203, India
e-mail: aparnab@srmist.edu.in

K. R. Reddy et al. (eds.), *Recent Advances in Civil Engineering*, Lecture Notes in Civil Engineering 398, https://doi.org/10.1007/978-981-99-6229-7_14

LULC changes. However, due to their speed, scope, and intensity, they have a wide range of significant global effects, particularly on environmental assets [3]. The increasing pace of growth is worrisome because it has the potential to have many consequences for ecosystems on all scales. Information gathered from LULC is used by researchers, policymakers, and planners for various purposes, including but not limited to analysing trends in expansion and spotting changes in natural assets [4]. It is crucial to categorize LULC changes when researching land dynamics. Changes in LULC are crucial in many fields and industries, including hydrology, agriculture, forestry, the environment, geology, and ecology. This has been demonstrated empirically by researchers from many different backgrounds [5–9]. The study of LULC change detection has always stimulated the interest of researchers [10–12]. Many researchers worry that if LULC were to change, it would throw ecosystems out of balance and negatively affect the environment due to human activities in advancing climate change [13–20]. Furthermore, their research supports claims that methods that emphasize evidence of the effects and rates of LULC change and the allocation of these changes across space–time should be a crucial part of current approaches for control equipment of modifications and carried out regularly [21–26].

Numerous studies have demonstrated that using spatial visuals to track changes in LULC, particularly in Asia, is an effective method. The LULC categorization is likely among the most well-known applications of geospatial technology. It has been known for a long time that the implementation of RS and GIS is crucial and extremely effective in determining changes in LULC across a variety of spatial scales. Evidence has been gleaned from data collected by remotely sensed sensors using a variety of change detection and image analysis techniques. However, GIS integrates the data obtained through RS so that users can gain a better understanding of LULC simulating. With the assistance of RS and GIS, an accurate LULC pattern detection was finally accomplished. In addition, observing alterations in LULC through the integration of satellite RS and GIS is a strategy that is both reliable and cost-effective.

2 Study Area: Upstream of the Adyar River Basin

The total area covered upstream of the Adyar sub-basin is a massive 1081.4% of a square kilometre. Only forty kilometres in length, the Adyar River is relatively short. This river starts in the Adanur tank, winds through the southern part of Chennai, and finally empties into the Bay of Bengal via Adyar creek. When it rains, the southern part of Chennai city usually gets flooded. “Fig. 1 Map showing the location of the upstream area of the Adyar River Basin” shows that the basin encompasses the latitude range of 12°44′10″ N to 13°16′40″ N and the longitude range of 79°49′10″ E to 80°10′50″ E. The lower parts of the basin are frequently flooded because of its location in a cyclone-prone coastal zone. A lack of drainage is a common issue in the delta because of its flat terrain. Another significant problem in the basin is the perennial one of the Adyar River drying up during the summer.

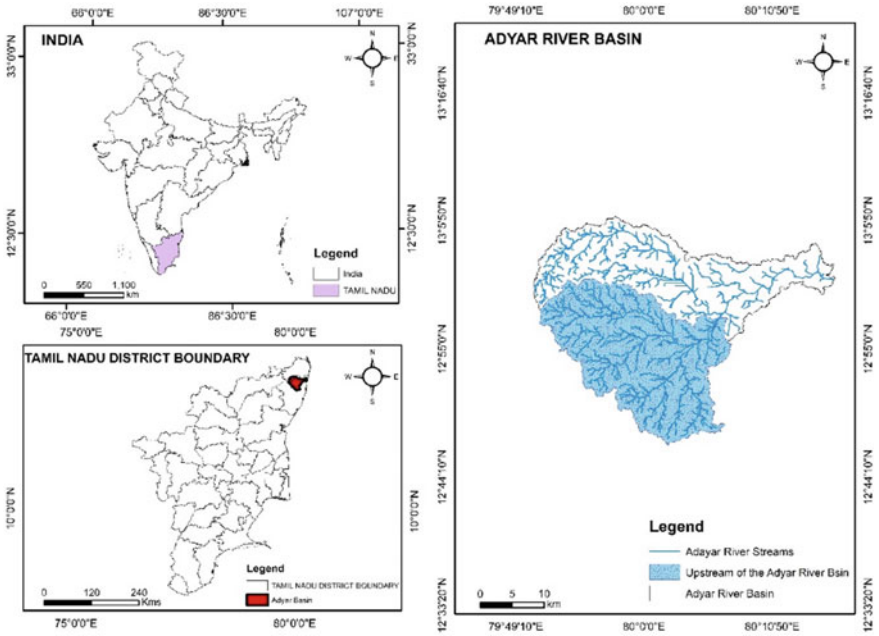

Fig. 1 Map showing the location of the upstream area of the Adyar River Basin

3 Methods and Data Acquisitions

For the years 2005, 2010, 2015, and 2021, the methodology for detecting LULC transformation has used supervised classification can be broken down into several steps:

Data acquisition: Obtain satellite images for four years from a reliable source such as Landsat 5, Landsat 7, and Landsat 8.

Image preprocessing: Preprocess the images to reduce noise, correct for atmospheric effects, and enhance the features of interest. This can involve radiometric and geometric corrections, atmospheric correction, and image fusion.

Image segmentation: Divide the images into homogeneous regions using techniques such as mean shift or watershed segmentation. This will allow for a more accurate classification of the pixels within each region.

Training data selection: Identify areas in the images representing the different land cover classes of interest. These areas will be used to train the classification algorithm. Ground truth data can be collected through field surveys or existing land use maps.

Feature extraction: Extract spectral and spatial features from the training data using image processing techniques such as principal component analysis (PCA) or texture analysis.

Classification: Apply a supervised classification algorithm to the preprocessed images using the extracted features and the training data. Popular algorithms for LULC classification include maximum likelihood, support vector machines (SVM), and random forests.

Change detection: Compare the classified images for the different years to identify alterations in land cover and use. This can be done using techniques such as image differencing or post-classification comparison.

Accuracy assessment: Evaluate the accuracy of the classification results by comparing them to ground truth data or existing land use maps. This will allow for identifying any errors or misclassifications in the classification output.

By following these steps shows in "Fig. 2 Methodology of LULC Analysis", it is possible to generate accurate and reliable information about LULC change over time using supervised classification techniques.

The DEM data from the SRTM, which has a resolution of 30 m, was used to extract the basin's topographic features. ISRO Landsat 5, 7, 8 satellite's data were used for create a LULC map used in the study; this data was obtained through the Earth

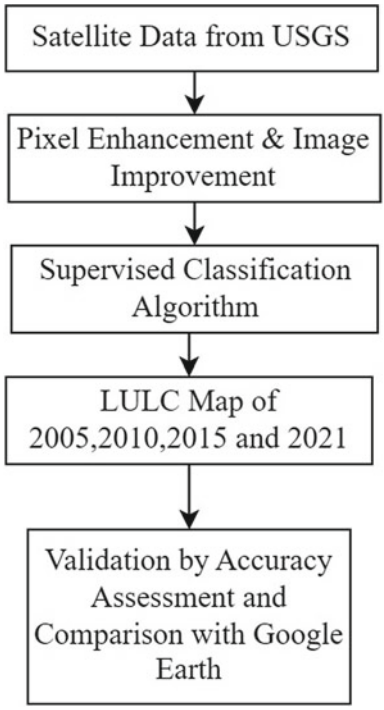

Fig. 2 Methodology of LULC analysis

Table 1 U pstream of the Adyar River Basin's LULC classifications

LULC class	2005		2010		2015		2021	
	Km^2	%	Km^2	%	Km^2	%	Km^2	%
Waterbody	7.47	1.71	22.45	5.13	14.74	3.37	4.52	1.03
Urban	12.98	2.97	36.66	8.37	55.94	12.78	83.44	19.06
Agriculture	118.56	27.08	192.80	44.04	82.57	18.86	107.04	24.45
Vegetation	143.41	32.76	54.74	12.50	82.95	18.95	111.10	25.38
Barren land	155.38	35.49	131.15	29.96	201.60	46.05	131.70	30.08

Explorer data site (https:///earthexplorer.usgs.gov/) [27, 28]. The decadal vectorized LULC maps (2005, 2010, 2015, 2021) were used to create the LULC map. In this study, the necessary input data sets were prepared using ERDAS Imagine and ArcGIS tools. Data quality and availability guided the selection of the dates, and Landsat 5, 7, 8 imagery was used to calculate the LULC change.

4 Result and Discussion

4.1 Land Use Land Cover Classification (LULC)

Waterbodies, developed land, farmland, vegetation, and barren land were the categories that were defined. To select appropriate training samples, polygons were drawn around representative locations of each LULC type. The aim of selecting spectral signatures was to minimize confusion between different land cover types. These polygons, based on satellite imagery, contained the pixels used to record the spectral signatures for the various LULC types [29]. The categories included waterbodies, developed land, farming land, vegetation, and barren land (Table 1). All misclassified pixels were found using topographic maps and high-resolution satellite images, and the visual interpretation procedure was repeated for each one of them [25, 30, 31]. Accuracy assessment is a crucial step to ensure the reliability of classification data for change detection. In order to take the confusion matrix's diagonal and other elements into account, a nonparametric Kappa test was conducted, which allowed for a more precise measurement of the classification accuracy [32].

4.2 Accuracy Assessment

The error matrix is the typical representation of the reliability of remote sensing classifications. Usually, a mix of user accuracy and producer accuracy is used to

determine accuracy. A producer's efficacy is evaluated by its classification performance on data from a training set. The percentage of correctly labelled pixels can be used as a proxy for user accuracy when compared to a predetermined threshold or standard. Kappa (K) is a statistical measure used to assess the degree to which two groups agree or disagree with one another, beyond what would be predicted by chance alone. Kappa is an estimate of the fraction of agreement after allowing for chance agreement. To determine reliability, kappa findings were calculated for a categorized map. Kappa was determined using the formula provided in Eqs. (1), (2), (3).

$$\text{Kappa} = \frac{p_o - p_e}{1 - p_e} \tag{1}$$

P_o is the proportion of agreements that have been confirmed, whereas p_e is the proportion of anticipated confirmations.

$$p_o = \sum_{i=1}^{c} p_{ij} \tag{2}$$

$$p_e = \sum_{i=1}^{c} p_i T p T_j \tag{3}$$

Equation, c denotes the overall number of raster categories, p_{iT} the total sum of all cells in the i-th row, p_{Tj} the total sum of cells in the j-th column, etc. Studies have shown the relationship between the i-th and j-th cells using a table, a special type of matrix that shows the frequent distribution of the data. This matrix's connections among its cells have been calculated, and the results. Because every cell complied with the requirements, the result is obvious.

4.3 Upstream of the Adyar basin's LULC Change Deduction

The basin was mapped in 2005, 2010, 2015, and 2021, creating a total of five classes: waterbody, built-up, agriculture, vegetation, and barren land (Error! Reference source not found. **a, b, c, d**). The Table 1 displays the total area in square kilometres of various LULC types for four different years—2005, 2010, 2015, and 2021.

Waterbody: The area of waterbodies in sq.km has decreased over time from 7.3458 in 2005 to 4.5171 in 2021. This indicates a loss of waterbodies and could be due to human activities such as damming, land use changes. The percentage decrease in waterbodies from 2005 to 2021 is about 38.4%.

Urban: The urban land area has increased significantly from 123,525 km^2 in 2005 to 83.444 km^2 in 2021. This indicates a significant increase in urbanization and could

be due to population growth, economic development, and migration. The percentage increase in urban land from 2005 to 2021 is about 576.3%.

Agriculture: Agriculture-related land use has fluctuated over time, reaching a peak of 192.798 square kilometres in 2010 and a current area of 107.037 square kilometres in 2021. This could be due to changes in farming practices, climate, or economic factors. The percentage decrease in agriculture land from 2005 to 2021 is about 9.7%.

Vegetation: The area of land covered by vegetation has also fluctuated over time, with a peak of 143.4078 km^2 in 2005 and a current area of 111.0978 km^2 in 2021. With a peak of 192.798 square kilometres in 2010 and a current area of 107.037 km^2 in 2021, the area of land used for agriculture has changed over time.

Barren land: The area of barren land has also fluctuated over time, with a peak of 201.294 km^2 in 2015 and a current area of 131.6997 km^2 in 2021. This could be due to natural disasters, land use changes, or climate factors. The percentage decrease in barren land from 2005 to 2021 is about 15.2%. Overall, "Fig. 3 A graphic depiction of how land use and cover have changed over time in the area upstream of the Adyar basin" shows that graphical representation of changes in the LULC throughout time in the upstream of the Adyar basin and Table 1 provides information about the changes in different LULC types over time, which can be useful for understanding the influence of human activities and landscape effects of environmental factors.

The accuracy of the LULC 2021 map was evaluated by selecting 95 sites at random from five different categories. The confusion error matrix was constructed after the user's accuracy, and Cohen's kappa was computed with the mapped and ground reference locations (Table 2). Significantly, the overall Kappa coefficient for the sample was 0.89, indicating an 89% accuracy in categorization (Fig. 4).

5 Conclusion

Over the past 20 years, the Adyar basin has experienced significant changes in LULC. These alterations include a decline in the number of aquatic environments, an increase in the amount of land that is urban, variations in agriculture and vegetation, and changes in land that is uncultivated. Changes in land use and dam construction are examples of human activities that, along with natural disasters and changing climate patterns, may be responsible for these changes. It is essential to understand the impact these factors an understanding of the impact that factors have had on the landscape of the Adyar basin. Then the findings of this study provide valuable insights into this subject matter.

The research results can be applied to the creation of conservation and sustainable land use regulations that give priority to the protection of waterbodies, agriculture, and vegetation while addressing the growing demand for urban land. Adopt sustainable land use policies and conservation strategies using these initiatives. In order to lessen the effects of these changes, research can be done in the future to pinpoint their underlying causes and to create more efficient land use planning and management techniques.

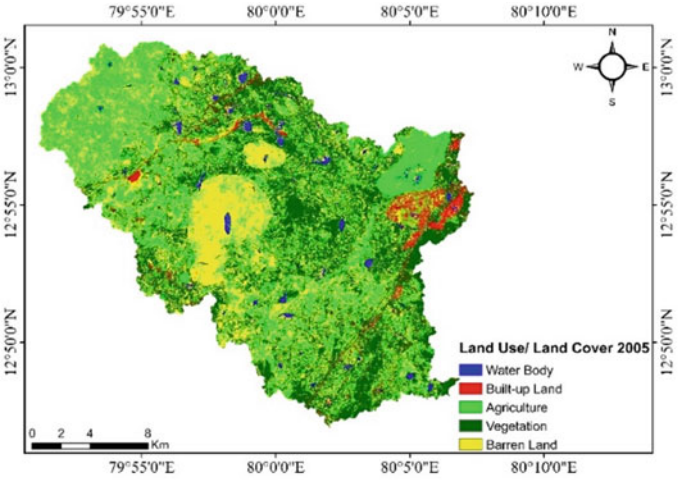

(a)

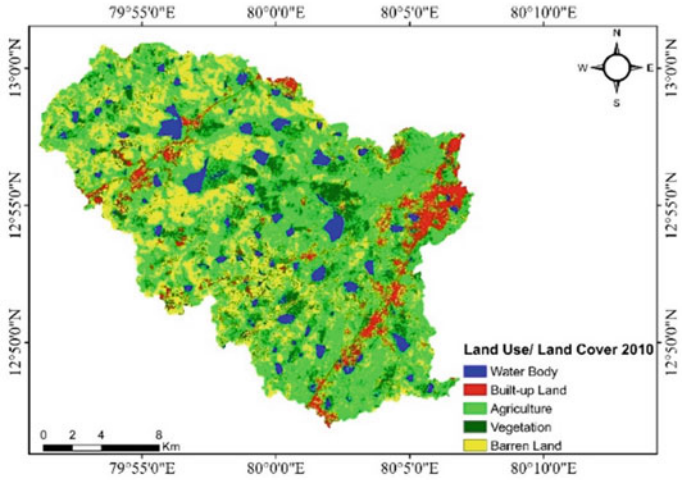

(b)

Fig. 3 **a**,**b**,**c**,**d** Changes of the LULC throughout time in a upstream of the Adyar River system **a** 2005, **b** 2010, **c** 2015, **d** 2021.

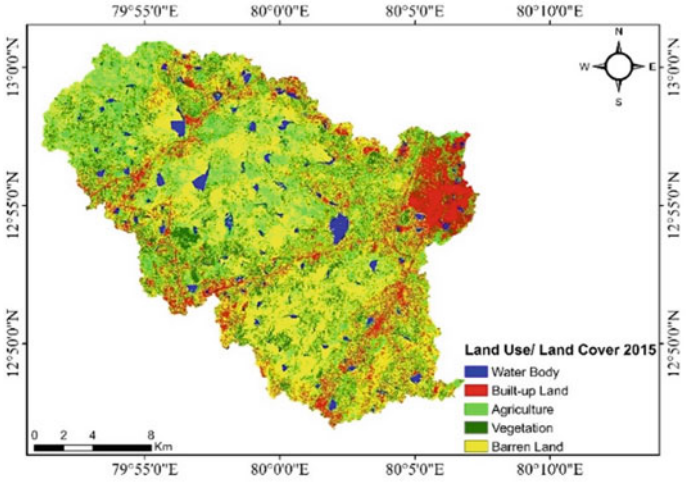

(c)

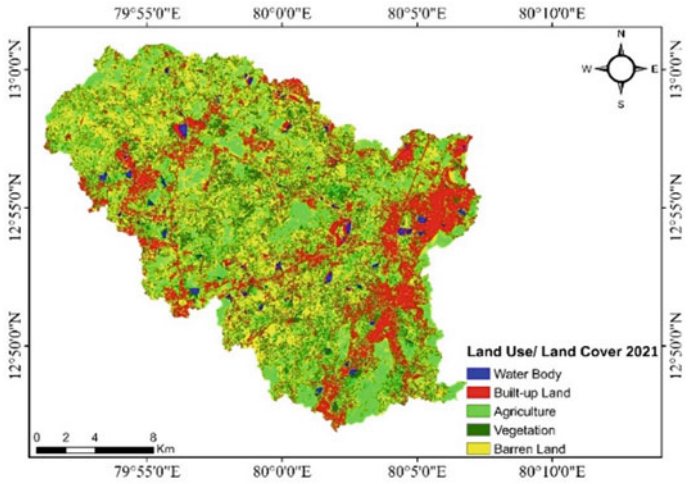

(d)

Fig. 3 (continued)

References

1. Rogan J, Chen DM (2004) Remote sensing technology for mapping and monitoring land-cover and land-use change. Prog Plann 61(4):301–325. https://doi.org/10.1016/S0305-9006(03)00066-7
2. Zhao Y, Zhang K, Fu Y, Zhang H (2012) Examining land-use/land-cover change in the lake dianchi watershed of the Yunnan-Guizhou plateau of Southwest China with remote sensing

Table 2 Analysis of the Adyar LULC map's accuracy using an error matrix

	Waterbody	Built-up	Agriculture	Vegetation	Barren Land	User
Waterbody	15	1	0	1	0	17
Built-up	1	18	0	0	1	20
Agriculture	0	0	22	1	0	23
Vegetation	1	0	1	16	0	18
Barren Land	1	0	2	0	14	17
Producer (Total)	18	19	25	18	15	95

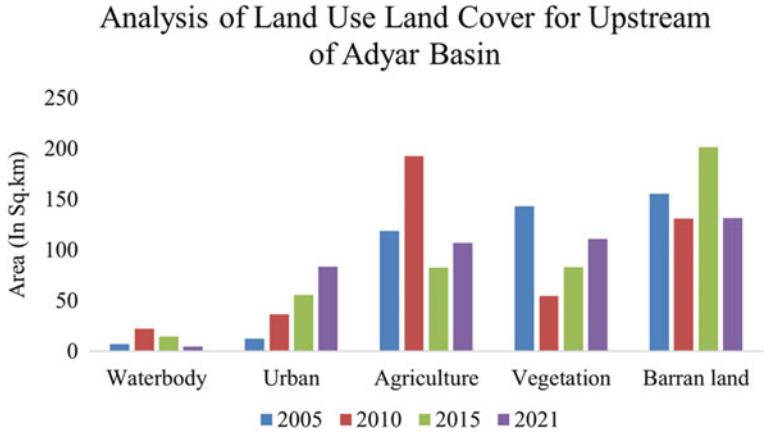

Fig. 4 A graphic depiction of how land use and cover have changed over time in the area upstream of the Adyar basin

and GIS techniques: 1974–2008. Int J Environ Res Public Health 9(11):3843–3865. https://doi.org/10.3390/IJERPH9113843

3. Hansen MC, Sohlberg R, Defries RS, Townshend JRG (2000) Global land cover classification at 1 km spatial resolution using a classification tree approach. Int J Remote Sens 21(6–7):1331–1364. https://doi.org/10.1080/014311600210209
4. Roy PS et al (2015) Development of decadal (1985–1995–2005) land use and land cover database for India. Remote Sens 7(3):2401–2430, Feb 2015. https://doi.org/10.3390/RS70302401
5. Thenkabail PS et al (2009) Irrigated area maps and statistics of India using remote sensing and national statistics. Remote Sens (Basel) 1(2):50–67. https://doi.org/10.3390/RS1020050
6. Friedl MA et al (2010) MODIS Collection 5 global land cover: Algorithm refinements and characterization of new datasets. Remote Sens Environ 114(1):168–182. https://doi.org/10.1016/J.RSE.2009.08.016
7. Akinyemi FO (2017) Land change in the central Albertine rift: Insights from analysis and mapping of land use-land cover change in north-western Rwanda. Appl Geogr 87:127–138. https://doi.org/10.1016/J.APGEOG.2017.07.016
8. Yang D, Kanae S, Oki T, Koike T, Musiake K (2003) Global potential soil erosion with reference to land use and climate changes. Hydrol Process 17(14):2913–2928. https://doi.org/10.1002/HYP.1441

9. Adnan NA, Atkinson PM (2011) Exploring the impact of climate and land use changes on streamflow trends in a monsoon catchment. Int J Climatol 31(6):815–831. https://doi.org/10.1002/JOC.2112
10. Ansari A, Golabi MH (2019) Prediction of spatial land use changes based on LCM in a GIS environment for Desert Wetlands—a case study: Meighan Wetland, Iran. Int Soil Water Conserv Res 7(1):64–70. https://doi.org/10.1016/j.iswcr.2018.10.001
11. Al-sharif AAA, Pradhan B (2014) Monitoring and predicting land use change in Tripoli Metropolitan City using an integrated Markov chain and cellular automata models in GIS. Arab J Geosci 7(10):4291–4301. https://doi.org/10.1007/s12517-013-1119-7
12. Abdi AM (2020) Land cover and land use classification performance of machine learning algorithms in a boreal landscape using Sentinel-2 data. GIsci Remote Sens 57(1):1–20. https://doi.org/10.1080/15481603.2019.1650447
13. Alam A, Bhat MS, Maheen M (2020) Using Landsat satellite data for assessing the land use and land cover change in Kashmir valley. Geo J 85(6):1529–1543. https://doi.org/10.1007/s10708-019-10037-x
14. Abijith D, Saravanan S (2022) Assessment of land use and land cover change detection and prediction using remote sensing and CA Markov in the northern coastal districts of Tamil Nadu, India. Environ Sci Pollut Res 29(57):86055–86067. https://doi.org/10.1007/S11356-021-15782-6/TABLES/6
15. Hua AK, Gani P (2023) Urban Sprawl prediction using CA-Markov Model: A case study of Melaka River Basin, Malaysia. Appl Ecol Environ Res 21(1):157–171. https://doi.org/10.15666/AEER/2101_157171
16. Pal R, Mukhopadhyay S, Chakraborty D, Suganthan PN (2023) A hybrid algorithm for urban LULC Change detection for building smart-city by using World view images. IETE J Res. https://doi.org/10.1080/03772063.2022.2163928
17. Mitra R, Das J (2023) A comparative assessment of flood susceptibility modelling of GIS-based TOPSIS, VIKOR, and EDAS techniques in the Sub-Himalayan foothills region of Eastern India. Environ Sci Pollut Res 30(6):16036–16067. https://doi.org/10.1007/S11356-022-23168-5
18. Saha P, Mitra R, Chakraborty K, Roy M (2022) Application of multi layer perceptron neural network Markov Chain model for LULC change detection in the Sub-Himalayan North Bengal. Remote Sens Appl 26:100730. https://doi.org/10.1016/J.RSASE.2022.100730
19. Luo H, Liu C, Wu C, Guo X (2018) Urban change detection based on Dempster-Shafer theory for multitemporal very high-resolution imagery. Remote Sens (Basel) 10(7). https://doi.org/10.3390/RS10070980
20. Inglada J, Vincent A, Arias M, Tardy B, Morin D, Rodes I (2017) Operational high resolution land cover map production at the Country scale using satellite image time series. Remote Sens (Basel) 9(1):95. https://doi.org/10.3390/RS9010095
21. Yan J, Wang L, Song W, Chen Y, Chen X, Deng Z (2019) A time-series classification approach based on change detection for rapid land cover mapping. ISPRS J Photogramm Remote Sens 158:249–262. https://doi.org/10.1016/J.ISPRSJPRS.2019.10.003
22. Serda M et al (2013) Synteza i aktywność biologiczna nowych analogów tiosemikarbazonowych chelatorów żelaza. Uniw śląski 7(1):343–354, 10. 2/JQUERY.MIN.JS
23. Wang J et al (2023) Remote sensing of soil degradation: progress and perspective. Int Soil Water Conser Res. https://doi.org/10.1016/J.ISWCR.2023.03.002
24. Muhammad R, Zhang W, Abbas Z, Guo F, Gwiazdzinski L (2022) Spatiotemporal change analysis and prediction of future land use and land cover changes using QGIS MOLUSCE plugin and remote sensing big data: a case study of," mdpi.com, 2022. https://doi.org/10.3390/land11030419
25. Yatoo SA, Sahu P, Kalubarme MH, Kansara BB (2022) Monitoring land use changes and its future prospects using cellular automata simulation and artificial neural network for Ahmedabad city, India. GeoJ 87(2):765–786. https://doi.org/10.1007/S10708-020-10274-5
26. Khan F, Das B, Mohammad P (2022) Urban growth modeling and prediction of land use land cover change over Nagpur City, India using cellular automata approach. pp 261–282. https://doi.org/10.1007/978-981-16-7373-3_13

27. LULC prediction: ANN-CA—Coastal Hazards and Energy System Science (CHESS) Lab. https://home.hiroshima-u.ac.jp/~leehs/?page_id=2020 (Accessed 28 Feb 2023)
28. Halder S, Das S, Basu S (2023) Use of support vector machine and cellular automata methods to evaluate impact of irrigation project on LULC. Environ Monit Assess 195(1), Jan 2023. https://doi.org/10.1007/S10661-022-10588-6
29. Chowdhury M, Hasan ME, Abdullah-Al-Mamun MM (2020) Land use/land cover change assessment of Halda watershed using remote sensing and GIS. Egypt J Remote Sens Space Sci 23(1):63–75. https://doi.org/10.1016/J.EJRS.2018.11.003
30. Hussain M, Chen D, Cheng A, Wei H, Stanley D (2013) Change detection from remotely sensed images: From pixel-based to object-based approaches. ISPRS J Photogramm Remote Sens 80:91–106. https://doi.org/10.1016/J.ISPRSJPRS.2013.03.006
31. Rahman A, Kumar S, Fazal S, Siddiqui MA (2012) Assessment of land use/land cover change in the North-West District of Delhi using remote sensing and GIS techniques. J Indian Soc Remote Sens 40(4):689–697. https://doi.org/10.1007/S12524-011-0165-4
32. Helmer EH, Brown S, Cohen WB (2000) Mapping montane tropical forest successional stage and land use with multi-date Landsat imagery. Int J Remote Sens 21(11):2163–2183. https://doi.org/10.1080/01431160050029495

Spatial Analysis of Soil Organic Carbon in the Thuckalay Block of the Kanyakumari District

A. P. Arthi and J. Satish Kumar

Abstract The soil has organic and inorganic matter, which helps the plants to grow. The main component of organic matter is soil organic carbon (SOC). SOC is studied in the Thuckalay block of the Kanyakumari district with Sentinel-2 data. The following indices, Normalized Difference Vegetation Index (NDVI), Bare Soil Index (BSI), and Soil Adjusted Vegetation Index (SAVI), are analyzed using linear regression, and R^2 values were compared. The linear regression values for NDVI are $R^2 = 0.5146$; for BSI, $R^2 = 0.7608$; and for SAVI, $R^2 = 0.7493$. Then 15 soil samples were collected, and the Walkley-Black technique was used for the analysis of soil organic carbon for validation. The relationship between SOC and BSI is high, while the relationship between SOC and NDVI is very low, and the relationship between SOC and SAVI is medium. When BSI is high, the SOC will also be increased, and vice versa, and the SOC has a low impact due to the vegetation content. Land degradation causes nutrient depletion and soil erosion which can be reduced by analyzing the relationship between LULC and land degradation. The identification of SOC helps in precision farming and good yield for agriculture. Increasing SOC levels in degraded soils helps to restore soil health, improve soil fertility, and enhance the capacity of the soil to support healthy ecosystems.

Keywords SOC · BSI · SAVI · Soil

1 Introduction

Organic and inorganic components exist in soil, and their amounts change from place to place or within the exact location [1]. The soil has organic carbon, the medium for climatic change and agricultural production. SOC is the measure of organic carbon present in the soil. SOC is arguably one of the most critical metrics of soil health due

A. P. Arthi (✉) · J. S. Kumar
Department of Civil Engineering, Faculty of Engineering and Technology, SRM Institute of Science and Technology, Kattankulathur, Tamil Nadu 603203, India
e-mail: aa8503@srmist.edu.in

K. R. Reddy et al. (eds.), *Recent Advances in Civil Engineering*, Lecture Notes in Civil Engineering 398, https://doi.org/10.1007/978-981-99-6229-7_15

to its contribution to well-functioning ecosystems [2–4] and agricultural productivity [5–8].

SOC is an essential component of healthy soil for maintaining soil fertility and providing ecosystem services. When soils are degraded, the amount of SOC in the soil is reduced, leading to decreased soil fertility, reduced soil water holding capacity, and increased susceptibility to erosion.

Land degradation refers to the loss of natural or semi-natural ecosystems caused by human activities such as deforestation, agriculture, and urbanization. These activities can lead to loss of vegetation cover, soil erosion, and reduced soil fertility. The loss of vegetation cover can lead to reduced photosynthesis, reducing the amount of carbon sequestered in the soil. A key sign of land degradation is soil erosion [9–11]. Estimates of the world's carbon stocks are the result of research on SOC dynamics over the past several decades [7, 12, 13].

The studies have also concentrated on understanding the evaluation of the effects of cultivation and land use on SOC [3, 7, 14, 15] or the complexity of SOC dynamics and climate change [16–19]. LULC refers to the human use and changes in the land, including agriculture, urbanization, deforestation, and other activities. These land use changes can cause soil degradation, leading to a decline in soil quality, reduced soil fertility, and increased soil erosion. Plot-level and landscape-scale analyses of SOC dynamics under various land use, including interactions with land degradation processes, still have gaps.

SOC is a crucial component of the carbon cycle, and at a depth of 1 m, there is still about 1500 Gt (gigatonne) of carbon in soils [13, 20]. Different conventional methods were employed for SOC monitoring but were time-consuming and expensive [21, 22]. The Walkley-Black method is used to analyze SOC using conventional methods, the best and most widely practiced method.

According to some studies, it is necessary to investigate and implement new, cutting-edge techniques for all environments and soil [23]. Remote sensing is identifying and monitoring the physical characteristics of Earth or any other planet by measuring its reflected and emitted radiation at a distance without touching the object. Remote sensing practice is effective, affordable, and environmentally sound for various soil characteristics analyses such as SOC estimation [24].

In our study, the Sentinel-2 data is used to assess the soil organic carbon using remote sensing. The Sentinel-2 data is processed, and the parameters like NDVI, BSI, and SAVI are identified. Then the fifteen soil samples were collected, and the SOC was determined using Walkley-Black method. And then, the statistical analysis uses linear regression to find the relationship between SOC, BSI, and SAVI.

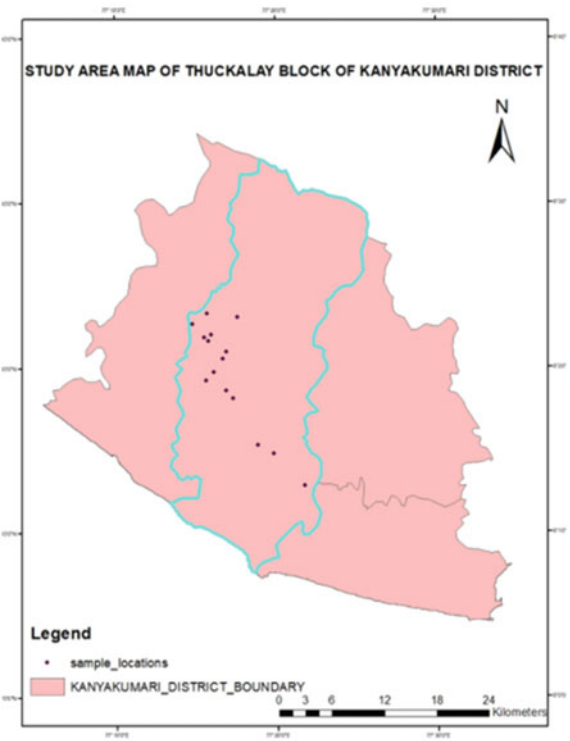

Fig. 1 Study area map of Thuckalay block of Kanyakumari district

2 Materials and Methods

2.1 Study Area Description

The selected study area is the Thuckalay block of Kanyakumari district. The headquarters of Kanyakumari district is Nagercoil. The total area of Thuckalay block is 130.33 km^2, has a population density of 1119/ km^2, and is next to Chennai. It has forest areas, paddy fields, rubber plantations, and the Western Ghats (Fig. 1).

2.2 Data

The data used for the study are soil samples and satellite images (Sentinel-2).

Table 1 Band information of Sentinel-2

Band	Description	Resolution (m)	Wavelength (nm)
B2	Blue	10	490
B3	Green	10	560
B4	Red	10	665
B5	Near-infrared	20	705

Remote Sensing Data

The Sentinel-2 data is used to analyze SOC using remote sensing. There are 13 bands in Sentinel-2, in which the bands 2 (blue), 3 (green), 4 (red), and 5 (NIR) are only used, and the band information is given below (Table 1).

Sample Collection

Fifteen samples, each 1 kg of soil, are collected using random sampling. The soil is then packed in a closed polythene bag and taken to the laboratory for analysis. Then the samples are oven dried, and 1 g of soil is passed through the mesh, and the SOC is analyzed using Walkley-Black method. Then the samples are processed using software and the Sentinel-2 data.

2.3 Methodology

The methodology of this paper is given below in Fig. 2. The data, such as satellite image (Sentinel-2) and field samples (soil), are collected alternatively. Then the satellite image is corrected, and the indices like NDVI, BSI, and SAVI are identified. Then the soil samples are taken to the laboratory, and the soil organic carbon (SOC) is determined using the Walkley-Black method. Then, the spatial analysis is done using the SOC, NDVI, BSI, and SAVI, and the relationship is determined using linear regression.

3 Indices

The indices used in this study are NDVI, BSI, and SAVI.

3.1 Normalized Difference Vegetation Index (NDVI)

Normalized Difference Vegetation Index (NDVI) measures vegetation health and density in an area. The NIR (band 5) and red (band 4) of the Sentinel-2 data are used

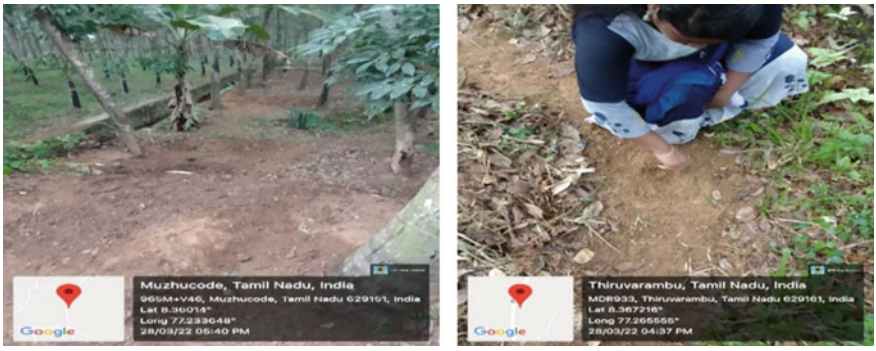

Fig. 2 Sample collection locations

to estimate Normalized Difference Vegetation Index (NDVI) values which were formulated by [25].

$$\mathbf{NDVI} = (\mathbf{NIR} - \mathbf{Red})/(\mathbf{NIR} + \mathbf{Red})$$

NDVI values vary between −1 and + 1, whereas the (+1) value indicates vegetation surfaces, and (−1) indicates areas with no vegetation.

3.2 Bare Soil Index (BSI)

BSI measures the amount of bare soil in a given area**.** The NIR (band 5), green (band 3), blue (band 2), and red (band 4) are used to identify Bare Soil Index, which was formulated by Saei Jamalabad and Abkar [26].

$$\boldsymbol{BSI} = ((\mathbf{Red} + \mathbf{SWIR}) - (\mathbf{NIR} + \mathbf{Blue}))/((\mathbf{Red} + \mathbf{SWIR}) + (\mathbf{NIR} + \mathbf{Blue}))$$

BSI values vary between −1 and + 1, whereas the (+1) value indicates areas with no vegetation, and (−1) indicates areas with vegetation.

3.3 Soil Adjusted Vegetation Index (SAVI)

Soil Adjusted Vegetation Index (SAVI) is a remote sensing technique used to measure vegetation health and density [27]. The NIR (band 5) and red (band 4) of the Sentinel-2 data are used to identify the SAVI of the region along with the correction factor of 0.5.

Table 2 Relationship values of Sentinel-2

Sl. no	Index	Relationship
1	NDVI	0.5146
2	BSI	0.7608
3	SAVI	0.7493

$$\mathbf{SAVI} = ((\mathbf{NIR} - \mathbf{RED})/(\mathbf{NIR} + \mathbf{RED} + \mathbf{L})) * (\mathbf{1} + \mathbf{L})$$

4 Results

4.1 Relationship Between SOC, BSI, and SAVI

Soil is a non-renewable resource; restoring it once degraded or washed away is challenging. Desertification of fertile land due to inadequate agriculture, deforestation, and drought is known as desertification. It is a land degradation that leads to the expansion of desert areas. The districts of Tamil Nadu most affected by desertification are Theni, Nilgiris, and Kanyakumari.

The statistical relationship between SOC, NDVI, and SAVI is given below in Table 2. The statistical relationship of Sentinel-2 data between SOC and BSI is $R^2 = 0.7606$, the relationship between SOC and NDVI is $R^2 = 0.5146$, and the relationship between SOC and SAVI is $R^2 = 0.7493$.

The relationship between SOC and NDVI is low when compared to BSI. But, when there is high vegetation, the NDVI is high, and the NDVI is low when there is a settlement or bare land, which is given in Fig. 3.

The LULC has a high impact on SOC. LULC describes the land use and land cover types in the given area. By analyzing the relationship between NDVI and LULC, the impact of land use changes in vegetation health or vegetation affecting the land use patterns can be analyzed. The decrease in NDVI values in an area recently undergoing urbanization indicates that the land use change has negatively impacted vegetation health. By correlating NDVI and LULC data, the complex interactions between land use and vegetation and more informed decisions about land management and conservation can be identified.

The statistical relationship of Sentinel-2 data between SOC and BSI is $R^2 = 0.7606$. The relationship between the SOC is low in waterbodies and high in vegetation areas. The relationship between SOC and BSI is high, and the vegetation increases as the BSI is low, and there will be high SOC in regions with high BSI values, which is given in Fig. 4. By analyzing the relationship between BSI and LULC, the impact of soil health and erosion due to land use changes or the changes in soil cover, which affects the land use patterns, can be analyzed. The increased BSI values in a recently undergoing deforestation indicate that the land use and land

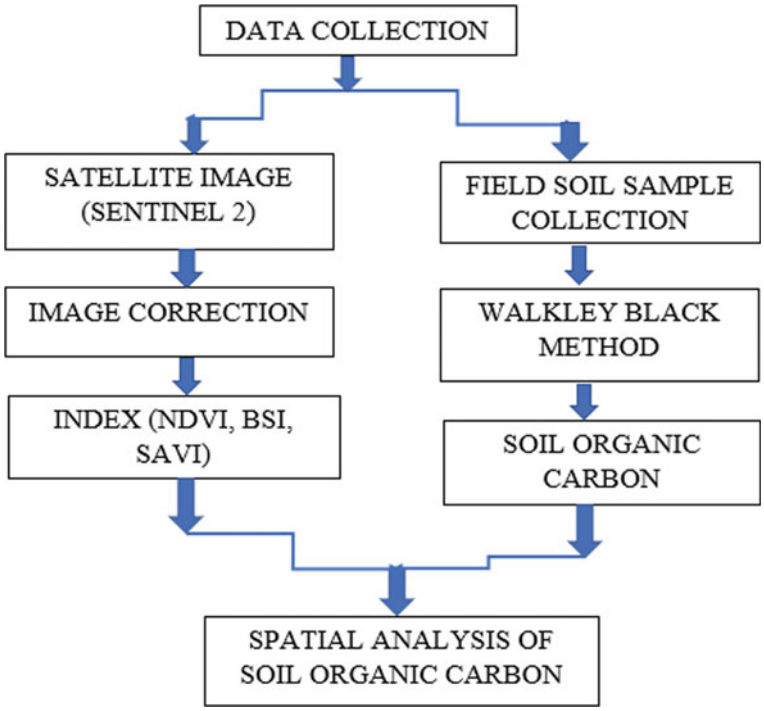

Fig. 3 Methodology

change has led to increased soil erosion and loss of soil cover. By correlating BSI and LULC data, the complex interactions between land use and soil health can be identified.

BSI monitors changes in land cover and assesses the extent of land degradation in an area. Various factors, including natural erosion and human activities such as deforestation, overgrazing, and unsustainable land use practices, can cause land degradation. As a result of land degradation, there is an increase in bare soil as vegetation cover is lost, leading to decreased soil fertility, increased soil erosion, and reduced ecosystem services. If BSI values increase over time, land degradation occurs, while a decrease in BSI values indicates that the land restoration efforts are positively impacting.

The statistical relationship of Sentinel-2 data between SOC and SAVI is $R^2 = 0.7493$. The relationship between SOC and SAVI is low when compared to BSI. So, when there is high vegetation, the SAVI is high, and the SAVI is low when there is a settlement or bare land, which is given in Fig. 5.

SAVI can be used to monitor land degradation; it is not directly related. However, SAVI is a helpful tool in identifying areas where vegetation is struggling and indicates potential land degradation. SAVI is not directly associated with SOC. Vegetation is essential in the carbon cycle, as it absorbs carbon dioxide from the atmosphere

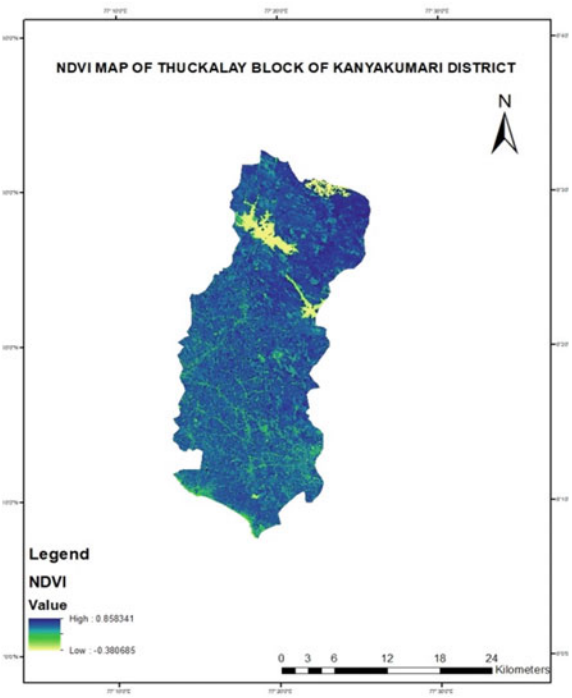

Fig. 4 NDVI map of Thuckalay block of Kanyakumari district

through photosynthesis and stores it in plant tissues and Soil. Therefore, SAVI can indirectly provide information about levels by indicating the health and density of vegetation in the given area (Fig. 6).

Therefore, SAVI, SOC, and land degradation are all related in that they are interconnected components of the larger ecosystem. By monitoring vegetation health and density using SAVI and measuring SOC levels, we can better understand the health of the ecosystem and the potential for land degradation.

The LULC has a significant impact on SOC. So, the LULC map of the area (Fig. 7) is prepared and compared. The forest area has high SOC as the vegetation is high in forest areas. When there is desertification, there will be no vegetation growth since the SOC will be very low. During erosion, the top layer of soil, which has high organic matter which is high in SOC, gets depleted so that the SOC will be very low.

Environmental factors like water availability, biodiversity, and climate change can also influence LULC. Deforestation and urbanization can also lead to decreased water availability and biodiversity loss, while changes in agricultural practices can affect greenhouse gas emissions and soil carbon storage.

By analyzing the relationship between SOC and LULC, the impact on soil health and carbon storage due to changes in land use or the changes in soil carbon affecting land use patterns are identified. The decreased SOC values in an area recently undergoing intensive agriculture indicate that the land use and change has led to a loss of soil organic matter and reduced carbon storage.

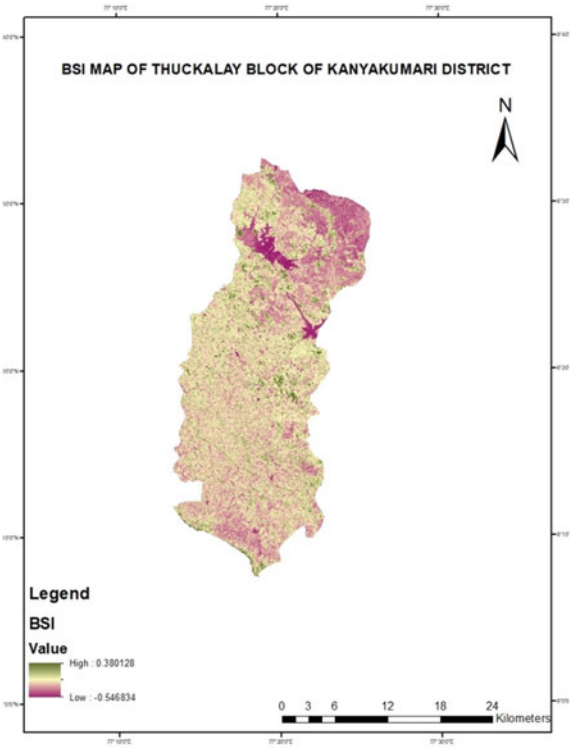

Fig. 5 BSI map of Thuckalay block of Kanyakumari district

The identification of indices like SAVI, NDVI, and BSI is used to find the SOC levels in the soil. These indices can indirectly provide information about SOC levels by indicating the health and density of vegetation in a given area. Areas with healthy and dense foliage are likely to have higher levels of SOC. By using SAVI, NDVI, and BSI to monitor vegetation health and density, we can identify areas with high levels of SOC. However, it is essential to note that while these indices can provide helpful information about SOC levels, they are not direct measures of SOC. To accurately measure SOC levels, soil samples must be collected and analyzed in a laboratory.

5 Discussion

Maximum studies that are based on the change in land use and land cover on SOC focus on the top layer of soil (0–20), which has the maximum SOC values and high microbial activity [28]. Because the LULC is also directly linked with SOC, which shows variation in SOC based on the LULC changes. Various studies also report conflicting results on the impact of LULC change on SOC [29]. Controlling natural forests and permanent grasslands to agricultural land reduces SOC content [30]

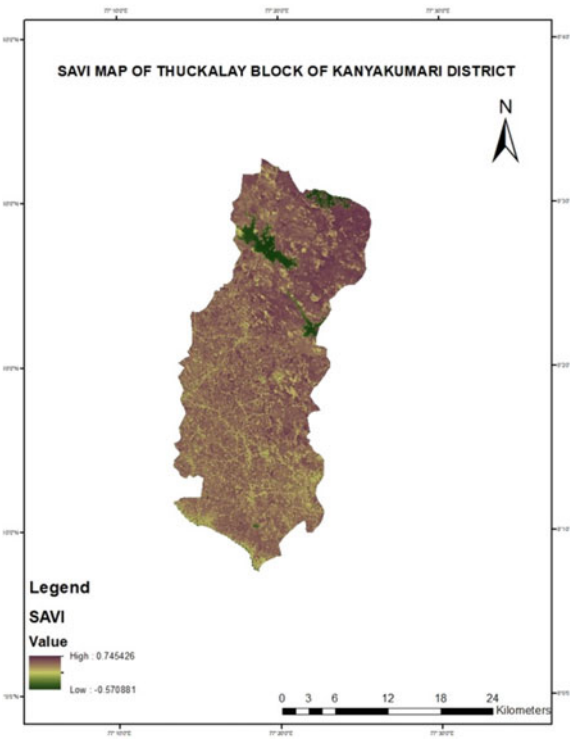

Fig. 6 SAVI map of Thuckalay block of Kanyakumari district

because the forest has high SOC resources. When converted to agricultural lands, the SOC gets depleted, showing significant changes in our study. Land use change converted from forests to grasslands or croplands leads to substantial changes in the dynamics of SOC [31], which leads to carbon loss.

Land degradation is caused by inappropriate land use practices that lead to nutrient depletion, soil erosion, and other forms of damage to soil. Land degradation is exacerbated by changes in land use, such as converting forests or grasslands into croplands, which can lead to further soil degradation. Conversely, prevent or mitigate land degradation. Therefore, understanding the relationship between LULC and land degradation is essential for developing sustainable land use practices that support healthy ecosystems and promote long-term environmental sustainability.

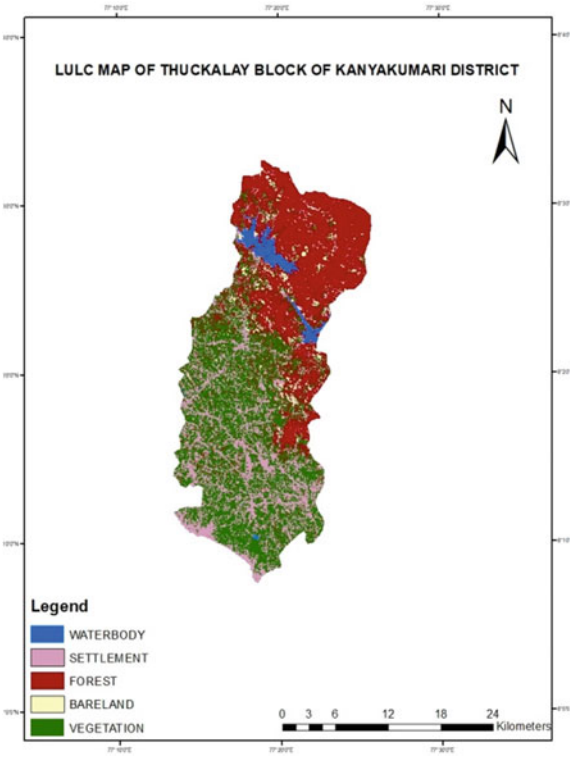

Fig. 7 LULC map of Thuckalay block of Kanyakumari district

6 Conclusion

The relationship between SOC and parameters like NDVI, BSI, and SAVI is studied using Sentinel-2 data. The NDVI is high in forest areas, whereas in agricultural fields, it is medium, and in bare soils, the SOC is low. In comparison, the BSI is high in bare soils and low in forest areas. This shows that there is a direct relationship between NDVI and SOC. When NDVI is high, the SOC is also high; when NDVI is low, the SOC is low. When BSI is low, the NDVI is also low. When SAVI is high, the NDVI is high, but the BSI is low. By understanding the relationship between BSI and land degradation, land managers can develop strategies to prevent or mitigate soil degradation and promote the restoration of a healthy ecosystem. The Sentinel-2 has higher spatial and spectral resolution than Landsat data and helps identify small-scale variations in SOC. Still, it also means that it covers a smaller area per image. The additional spectral bands in Sentinel-2 provide more information on SOC than Landsat data, especially in areas with more complex vegetation. So, Sentinel-2 data is beneficial in identifying SOC at a trim-scale level. Increasing SOC levels in degraded soils through practices such as soil conservation, agroforestry, and organic farming can help to restore soil health, improve soil fertility, and enhance the capacity of the soil to support healthy ecosystems.

References

1. Jandl et al (2014) Current status, uncertainty and future needs in soil organic carbon monitoring. Elsevier. https://doi.org/10.1016/j.scitotenv.2013.08.026
2. Lal R (2010) Beyond Copenhagen: Mitigating climate change and achieving food security through soil carbon sequestration. Food Secur 2(2):169–177. https://doi.org/10.1007/S12571-010-0060-9/TABLES/3
3. Schlesinger WHA, Jeffrey A (2000) Soil respiration and the global carbon cycle. Biogeochemistry 48:7–20
4. Verchot et al (2007) Climate change: linking adaptation and mitigation through agroforestry. Mitig Adapt Strateg Glob Chang 12(5):901–918. https://doi.org/10.1007/s11027-007-9105-6
5. Lal R (2006) Carbon management in agricultural soils. Mitig Adapt Strateg Glob Chang. https://doi.org/10.1007/s11027-006-9036-7
6. Driss H, John M, Elizabeth RP, Zarco-Tejada, Strachan PJ, Ian B (2003) Hyperspectral vegetation indices and novel algorithms for predicting green LAI of crop canopies: Modeling and validation in the context of precision agriculture. Remote Sens Environ. https://doi.org/10.1016/j.rse.2003.12.013
7. Post WM, Kwon KC (2000) Soil carbon sequestration and land-use change: processes and potential. Glob Chang Biol 6:317–328
8. Gunnar VT, Lal R, Singh BR (2005) Soil carbon sequestration in sub-Saharan Africa: a review. Land Degrad Dev 16(1):53–71, Jan 2005. https://doi.org/10.1002/LDR.644.
9. Lal R (2003) Offsetting global CO2 emissions by restoration of degraded soils and intensification of world agriculture and forestry. Land Degrad Dev 14(3):309–322. https://doi.org/10.1002/LDR.562
10. Pimentel D, Kounang N (1998) Ecology of soil erosion in ecosystems. Ecosystem
11. Vågen TGW, Leigh A (2013) Mapping of soil organic carbon stocks for spatially explicit assessments of climate change mitigation potential. Environ Res Lett 8(1):015011, Feb 20130. https://doi.org/10.1088/1748-9326/8/1/015011
12. Amundson R (2001) The carbon budget in soils. Earth Planet Sci
13. Jobbagy EGJ, Jobba J, Robert B (2000) April 2000 423 Belowground processes and global change 423 the vertical distribution of soil organic carbon and its relation to climate and vegetation. Ecol Appl 10(2):423–436
14. Guo LB, Gifford RM (2002) Soil carbon stocks and land use change: a meta analysis. Glob Chang Biol 8(4):345–360. https://doi.org/10.1046/J.1354-1013.2002.00486.X
15. Haboudane DM, Pattey JR, Zarco-Tejada E, Strachan PJ, Ian B (2004) Hyperspectral vegetation indices and novel algorithms for predicting green LAI of crop canopies: Modeling and validation in the context of precision agriculture. Remote Sens Environ. https://doi.org/10.1016/j.rse.2003.12.013.
16. Berthrong ST, Jobbagy EG, Jackson RB (2009) A global meta-analysis of soil exchangeable cations, pH, carbon, and nitrogen with afforestation. Ecol Appl 19(8):2228. https://doi.org/10.1890/08-1730.1
17. Noreen B et al. (2002) Linkages between climate change and sustainable development. Clim Policy 2:129–144, Accessed: 02 Feb 2023. [Online]. Available: www.oecd.org
18. Mark J, Tim W (2007) A framework for assessing climate change vulnerability of the Canadian forest sector. Forest Chronicle 83
19. Lal R (2004) Soil carbon sequestration to mitigate climate change. Geoderma 123(1–2):1–22. https://doi.org/10.1016/J.GEODERMA.2004.01.032
20. Kirschbaum MUF (2000) Will changes in soil organic carbon act as a positive or negative feedback on global warming? Biogeochemistry 48:21–51
21. Scharlemann JPW, Tanner EVJ, Hiederer R, Kapos V (2014) Global soil carbon: understanding and managing the largest terrestrial carbon pool. Carbon Manag 5(1):81–91. https://doi.org/10.4155/CMT.13.77/SUPPL_FILE/TCMT_A_10816421_SM0001.DOC

22. Keshavarzi A, Sarmadian F, Shiri J, Iqbal M, Tirado-Corbalá R, Omran ESE (2017) Application of ANFIS-based subtractive clustering algorithm in soil cation exchange capacity estimation using soil and remotely sensed data. Measurement 95:173–180. https://doi.org/10.1016/J.MEASUREMENT.2016.10.010
23. Jandl R et al (2013) Current status, uncertainty and future needs in soil organic carbon monitoring ☆. Sci Total Environ. https://doi.org/10.1016/j.scitotenv.2013.08.026
24. Vaudour E, Gilliot JM, Bel L, Lefevre J, Chehdi K (2016) Regional prediction of soil organic carbon content over temperate croplands using visible near-infrared airborne hyperspectral imagery and synchronous field spectra. Int J Appl Earth Obs Geoinf 49:24–38. https://doi.org/10.1016/J.JAG.2016.01.005
25. Zeng Y, Huang W, Zhan F, Zhang H, Liu H (2010) Study on the urban heat island effects and its relationship with surface biophysical characteristics using MODIS imageries. Geo-Spat Inf Sci 13(1):1–7. https://doi.org/10.1007/S11806-010-0204-2
26. Saei Jamalabad M, Abkar AA (2004) Forest canopy density monitoring, using satellite images. Int Soc Photogrammetry Remote Sens
27. Huete AR (1988) A soil-adjusted vegetation index (SAVI). Remote Sens Environ 25(3):295–309. https://doi.org/10.1016/0034-4257(88)90106-X
28. Umrit G, Ng Cheong R, Gillabel J, Merckx R (2014) Effect of conventional versus mechanized sugarcane cropping systems on soil organic carbon stocks and labile carbon pools in Mauritius as revealed by 13C natural abundance. Plant Soil 379(1–2):177–192, Jun 2014. https://doi.org/10.1007/S11104-014-2053-5/FIGURES/4
29. Jandl R et al (2014) Current status, uncertainty and future needs in soil organic carbon monitoring. Sci Total Environ 468–469:376–383. https://doi.org/10.1016/j.scitotenv.2013.08.026
30. Wei X, Shao M, Gale W, Li L (2014) Global pattern of soil carbon losses due to the conversion of forests to agricultural land. Sci Rep. https://doi.org/10.1038/srep04062
31. ShunHua Y et al (2015) The spatial variability of soil organic carbon in plain-hills transition belt and its environmental impact. China Environ Sci 35(12):3728–3736

Analytical Hierarchy Process for Land Suitability Analysis of Urban Growth in Latakia, Syria

Waseem Ahmad Ismaeel and J. Satish Kumar

Abstract Urban areas keep growing continuously, and cities expand over new land developing it into urban areas. Geographic Information Systems (GIS) were used in this study to identify suitable areas to be developed into urban areas and cities. The site suitability analysis provides an appropriate method to detect and propose the unsurpassed and most suitable sites consistent with the main criteria. Integration of Analytical Hierarchy Process (AHP) and GIS were used in this study. Therefore, the used criteria are land use, land elevation, land slope, distance from the coastline, distance from water bodies, distance from existing settlements, and road proximity. A pairwise comparison matrix for these criteria was calculated, and the weight for each was created depending on their comparative importance. The final urban suitability map was derivative according to the criteria and their weights. The findings of this paper indicate that more than half of the study area (51%) falls under high suitable areas while the unsuitable areas rate is 3.9% only and the very high suitable area rate is 2.03%. The study grants a vision of urban development planning using GIS practices and points out the substantial limitations that the study area is facing.

Keywords AHP · GIS · Suitability · Latakia

1 Introduction

The type of land uses within cities vary, no matter how small their size, the built-up area in the city is divided into several basic uses represented by the main functions that it performs in the service of its inhabitants and the inhabitants of the neighboring regions. As the population grows, there will be innovative build-up areas to respond to their multiple purposes such as residential, commercial, services, and public places. Finding proper locations for urban development represents a significant issue for developing a city [1]. However, successful planning for cities requires

W. A. Ismaeel (✉) · J. S. Kumar
Department of Civil Engineering, Faculty of Engineering and Technology, SRM Institute of Science and Technology, Kattankulathur, Tamil Nadu 603203, India
e-mail: wi7084@srmist.edu.in; waseem.ismaeel.24@gmail.com

K. R. Reddy et al. (eds.), *Recent Advances in Civil Engineering*, Lecture Notes in Civil Engineering 398, https://doi.org/10.1007/978-981-99-6229-7_16

creative thinking, analyzing of data and must take into consideration all factors and services to ensure a civilized lifestyle. Therefore, defining the most suitable locations for newly developed areas is considered one of the essential features of urban areas.

Site suitability analysis practices spatial and nonspatial data to achieve final goals [2], "Site suitability is a geospatially linked process. GIS can perform the suitability analysis using certain parameters which are related to the final purpose." [3]. GIS applications allow users to perform geospatial inquiry and edit the data to produce the results in form of maps or graphs. GIS-MCDA is one of these approaches associated with land suitability problems [4].

AHP approach was used in many applications such as most suitable areas for sustainable urban development [5, 6], land suitability analysis of urban growth and development [7–10], determining the most appropriate areas for reconstruction [11], evaluate possible locations of building sites [2], landfill site suitability for waste management [12], and site suitability for agricultural land use [13]. In this study, an AHP technique integrated with GIS was implemented to reach the most suitable site for new urban areas in Latakia, Syria.

2 Materials and Methods

2.1 Study Area

Latakia Governorate, on the eastern coast of the Mediterranean Sea, the western part of Syria, and the implementation of the country's main seaport. It is located between 35° 43′ 7" E ~ 36° 15′ 33" E longitudes and 35° 13′ 15" N ~ 35° 56′ 30" N latitudes as shown in the Fig. 1 with an overall area of 2416 km^2.

2.2 Multicriteria Evaluation (MCE) Method and Thematic Maps Preparation

MCE technique commonly used for urban studies, it starts with identifying the main factors affects the main objective, then comparing them with each other to form pair-wise matrix which leads to calculate final weights, then implementation of weighted overlay leads to find final suitability map. Figure 2 shows used methodology.

In this study seven criteria were used which are: Land Slope (LS), Land Elevation (LE), Land Use (LU), Roads Proximity (RP), Distance from water bodies (DW), Distance from Coastline (DCL), and Distance from Existing urban areas (DEU). All thematic maps were created depending on the following standardization (Table 1), "factors were weighted to state their relative influence on the suitability of urban" [14].

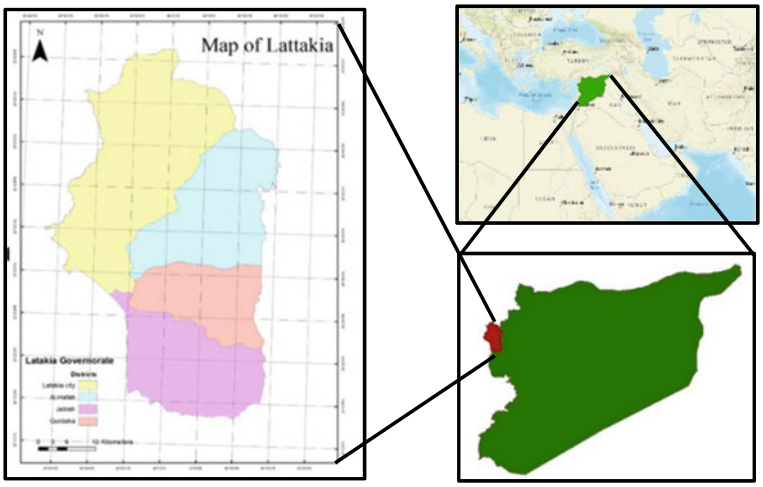

Fig. 1 Study area

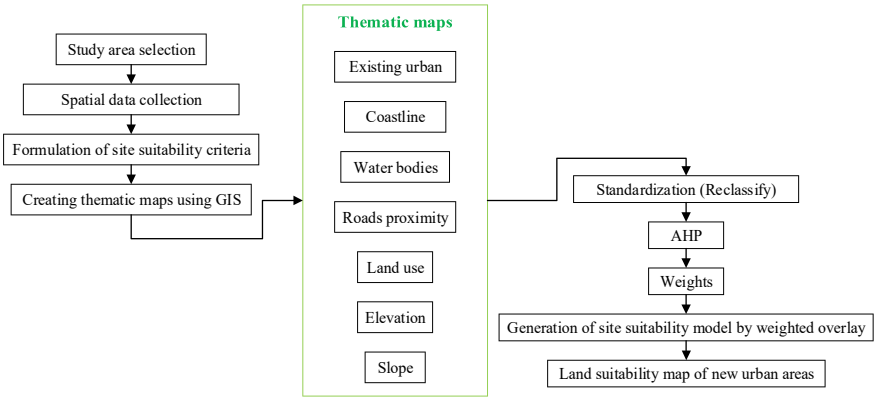

Fig. 2 Methodology of urban areas site suitability

The site suitability model demonstrated in (Fig. 3) was developed in the software environment using model builder, which allows simple creation and representation of tasks and workflow to get the final output.

2.3 Defining Criteria Weights Using AHP

In AHP there is a specific algorithm to calculate and assign final weight to each criterion, therefore a 9-point scale was applied and must comply that: aii = 1 and

Table 1 Database characteristics

Score	LS (degrees)	LE (m)	LU	RP (m)	DW (m)	DCL (m)	DEU (m)
5	0–3	0–300	Built-up	<1000	2000–6000	200–10,000	< 2500
4	3–10	300–700	Agricultural land	1000–2000	100–2000	10,000–20,000	2500–5000
3	10–15	700–1000	–	2000–3000	6000–8000	20,000–25,000	5000–10,000
2	15–20	1000–1200	Forests	3000–4000	> 8000	> 25,000	> 10,000
1	20–30	–	–	> 4000	–	–	–
Restricted	>30	1200–1544 Or ≤ 0	Water bodies	–	< 100 or > 8000	< 200	–

Fig. 3 Developed model of the site suitability for urban areas by software

aij = 1/aji, also the index Consistency Ratio (RC) which should be less than 10% [15, 16].

The calculation of criteria weights values was done by the amalgamation of priorities of AHP. Pairwise compression matrix (Table 2) was produced by comparing each criterion with all of the other criteria depending on its importance. To ensure consistency of this weights consistency ratio CR calculated using the formula [15, 16]:

$$\mathrm{CR} = \frac{\mathrm{CI}}{\mathrm{RI}} \tag{1}$$

here Random Consistency Index (RI) = 1.32 as 7 factors were used as given in Saaty's RI table; and Consistency Index (CI), calculated using formula (2) [15, 16].

Table 2 Pairwise compression matrix

	(1)	(2)	(3)	(4)	(5)	(6)	(7)	Weight
(1) LU	**1**	1/2	7	3	5	4	3	0.24904
(2) LS	2	**1**	7	3	5	5	3	0.31534
(3) LE	1/7	1/7	**1**	1/5	1/3	1/3	1/3	0.03035
(4) DEU	1/3	1/3	5	**1**	3	5	1/3	0.12619
(5) DWB	1/5	1/5	3	1/3	**1**	2	1/5	0.06001
(6) DCL	1/4	1/5	3	1/5	1/2	**1**	1/5	0.04991
(7) RP	1/3	1/3	3	3	5	5	**1**	0.16917

$$\text{CI} = \frac{(\lambda_{\max} - n)}{n-1} \quad \text{hence} : \text{CI} = \frac{(7.684 - 7)}{7-1} = 0.108 \tag{2}$$

Hence: CR = 0.108/1.32 = 0.0818 < 0.10 then it is consistent.

3 Results and Discussion

The site suitability analysis for developing new urban areas criteria that are effective as follows.

3.1 Land Slope

Although low and moderate slope values give an attractive design for urban area, high values represent a high level of steepness which is not valid for developing or building new urban. Therefore, it is important to calculate this effect as a slope value less than 10 degrees consider to be a suitable value for urban, and more than that will increase the cost of buildings [17]. "The output slope raster can be calculated as percent of slope or degree of slope" [18, 19]. So, the values between 0 and 3 degrees were classified as extremely suitable areas and between 3 to 10 degrees as high suitable. In the study area, majority of coastal and central areas have low slope degrees and this slope increases from west toward east and south-east also toward north and north-east, as shown in (Fig. 4a). Mountains located mainly in eastern side and north so that the higher slopes are located in these places, so it is unsuitable areas for new built-up.

3.2 Land Elevation

The altitude above sea level plays a major role to select and prefer one site above others due to the high costs for the high areas from one side and the disparity of weather and climate properties from another side. Elevation map (Fig. 4b) indicates that the heights are generally located in the eastern region, which is part of the western mountain chain and is called Latakia Mountains. Most of them lack to the main services because of their ruggedness and hard accessibility. As for the coastal plain and central regions, their height does not exceed 300 m, and most of them are serviced and do not need much rehabilitation.

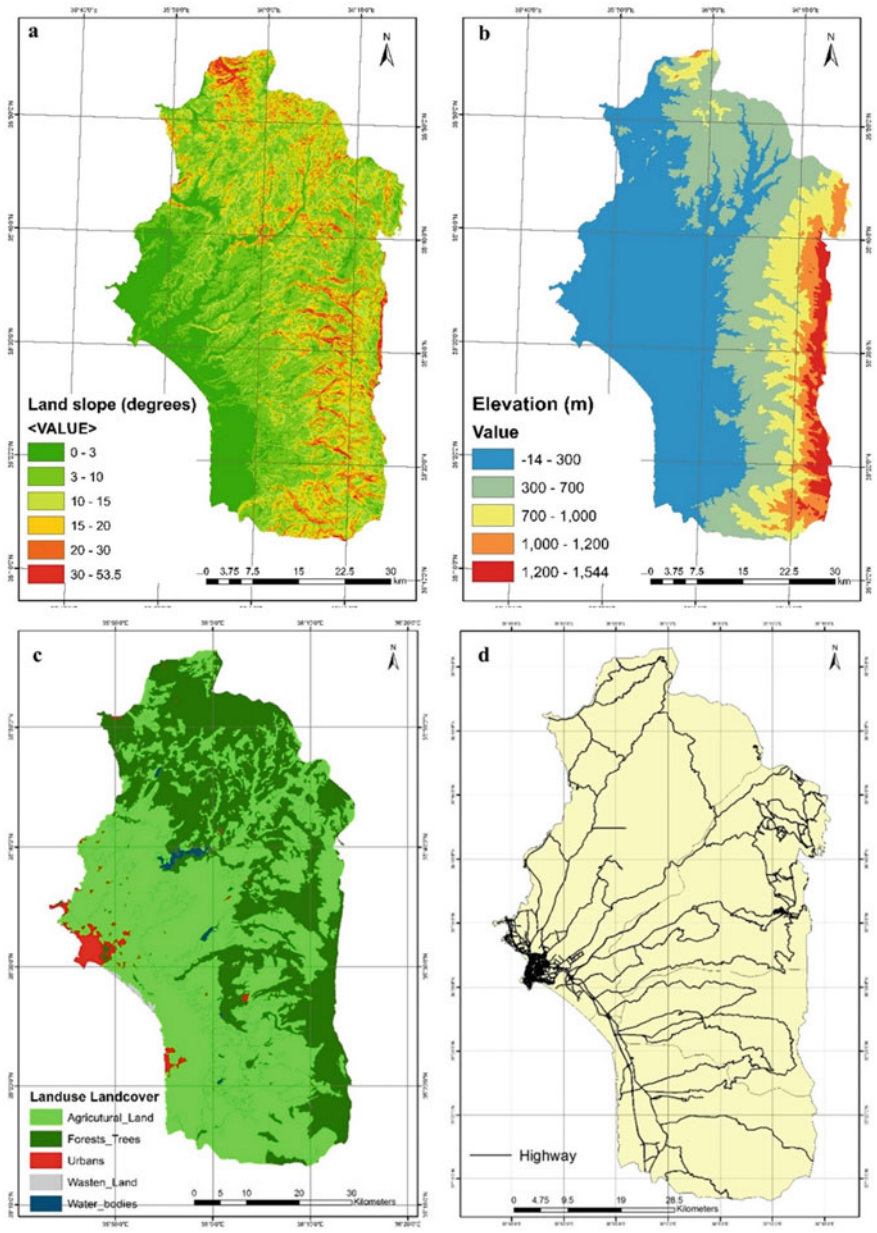

Fig. 4 **a** Slope; **b** Elevation; **c** Land use land cover; **d** Road map for study area

Table 3 Area and percentage of existing land use

Land Use	Area km^2	Percentage%
Agricultural Land	1487.87	61.59
Urbans	38.215	1.58
Waste land	6.107	0.25
Water bodies	14.079	0.58
Forests	869.954	36
Total	2416.225	100

3.3 Land Use (LU)

It contains five classes: agricultural land, forest–trees, urban, water bodies, and waste-land as presented in (Fig. 4c). The area and percentage for each class are exposed in Table 3.

3.4 Road Proximity

One of the essential components of urban area which ensure accessibility to all parts and sections of it, also this reduces the construction cost and avoids building new roads and infrastructure. Major road map is shown in (Fig. 4d). A multiple ring buffer tool was used followed by reclassify tool to generate zones according to road accessibility.

3.5 Water Bodies

Dams and lakes help in defining the suitable areas for new built-up according to the distance from them. As closest areas to them have a high probability to affect by floods and ground water issues.

3.6 Coastal Line

This feature is similar to water bodies in effect, as new urban areas should be planned away from it to protect the urban areas from floods, high waves, and other sea disasters.

3.7 Existing Settlements

Cities, towns, and villages, all have the required infrastructure and features for urban. Therefore, new and suitable areas for new settlements could use these services and infrastructure.

The final urban suitability map (Fig. 5) was derivative through the developed model in Fig. 3.

The very high suitable areas are located mainly near Latakia city and some existing urban in the middle, and north of the study area, this is due to high accessibility, road network density, and availability of services, while unsuitable areas are distributed between high mountains in the middle of study area that have step slope with very low accessibility due to lack of roads, coastal strip as a 200 m buffer was taken from coastline as a restricted area for built-up due to coastal hazards and water bodies. The outcomes of study shows that the largest area is suitable for new built-up as high suitable areas represent almost 51% (1229.254 km^2) of the total area as exposed in Table 4 and extremely or very high suitable area rate is 2.03% (49 km^2), while unsuitable areas rate is 3.9% (94.219 km^2). Moderate suitability grade areas form 39.43% (950.437 km^2) of the total area, and low suitability areas represent 3.65% (87.916 km^2).

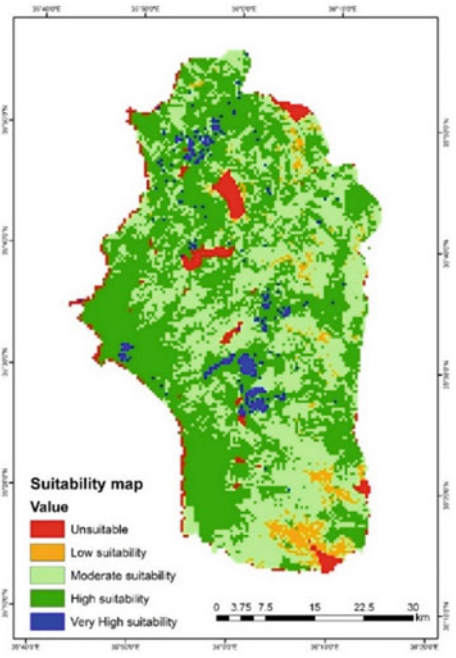

Fig. 5 Urban suitability map of Latakia governance

Table 4 Area and ratio of urban suitability classes

Suitability class	Area (km^2)	Ratio (%)
Unsuitable	94.219	3.9
Low suitability	87.916	3.65
Moderate suitability	950.537	39.43
High suitability	1229.254	50.99
Very high suitability	49	2.03

4 Conclusion

In this paper, an AHP and GIS approach to specifying land suitability for new urban regards selected criteria. The result shows that the very high suitability areas are limited to 2% of study area and spread near Latakia city, existing urban areas in the middle and north. Also, more than half (51%) of the study area is classified under high suitability which represents a secondary region to urban expansion. Moreover, unsuitable areas limited to 3.9% only, while low and moderate suitable areas form 3.65% and 39.43%, respectively. This model may be developed by using new statistical approaches to determine the pairwise matrix values depending on relationship between each tow thematic maps. so, the final consistency ratio will be refined and the final result will be more reliable.

References

1. Mukhopadhaya S (2016) GIS-based site suitability analysis case study for professional college in Dehradun. J Civ Eng Environ Technol 3:60–64
2. Al-shalabi MA, Bin MS, Bin AN, Shiriff R (2006) GIS Based Multicriteria approaches to housing site suitability assessment. XXIII FIG Congress Shaping the Change Munich, Germany, 8–13 Oct 2006, pp 1–17
3. Vanegas P, Cattrysse D, Wijffels A, Van Orshoven J (2010) Finding sites meeting compactness and on- and off-site suitability criteria in raster maps. In: 2nd international conference on advanced geographic information systems, applications, and services, GEOProcessing 2010, pp 15–20
4. Malczewski J (2006) GIS-based multicriteria decision analysis: a survey of the literature. Int J Geogr Inf Sci 20:703–726
5. Raman B, Kumar S, Roy PP, Sen D (2017) Site suitability evaluation for urban development using remote sensing, GIS and analytic hierarchy process (AHP). Adv Intell Syst Comput 459, AISC:V–VI.
6. Deliry SI, Uyguçgİl H (2020) GIS-based land suitability analysis for sustainable urban development: A Afyon Kocatepe Üniversitesi Fen ve Mühendislik Bilimleri Dergisi GIS-based land suitability analysis for sustainable urban development : a case study in Eskisehir. Turkey Sürdürüle 20:634–650
7. Aburas MM, Abdullah SHO, Ramli MF, Asha'Ari ZH (2017) Land suitability analysis of Urban Growth in Seremban Malaysia, using GIS based analytical hierarchy process. Procedia Eng 198:1128–1136

8. Youssef AM, Pradhan B, Tarabees E (2011) Integrated evaluation of urban development suitability based on remote sensing and GIS techniques: contribution from the analytic hierarchy process. Arab J Geosci 4:463–473
9. Parvez M, Islam S (2020) Sites suitability analysis of potential urban growth in Pabna municipality area in Bangladesh: AHP and geospatial approaches. J Geogr Stud 3:82–92
10. Shah Pooja B, Sheladiya Kaushik P, Patel J, Patel CR, Tailor RM (2020) Assessing land suitability for managing urban growth: an application of GIS and RS. Int Geosci Remote Sens Symp (IGARSS). 4243–4246
11. Khalil M, Satish Kumar J (2021) The use of Ahp within gis for destructed areas in Damascus, Syria. Int Arch Photogrammetry, Remote Sens Spat Inf Sci XLIII-B4–2:103–109
12. Hazarika R, Saikia A (2020) Landfill site suitability analysis using AHP for solid waste management in the Guwahati Metropolitan Area, India. Arab J Geosci 13
13. Pramanik MK (2016) Site suitability analysis for agricultural land use of Darjeeling district using AHP and GIS techniques. Model Earth Syst Environ 2:1–22
14. Masuya A (2014) Flood vulnerability and risk assessment with spatial multi-criteria evaluation. Dhaka Megacity Geospatial Perspect Urbanisation Environ Health
15. Saaty RW (1987) The analytic hierarchy process-what it is and how it is used. Math Model 9:161–176
16. Saaty TL (2007) Time dependent decision-making ; dynamic priorities in the AHP/ANP : Generalizing from points to functions and from real to complex variables 46:860–891
17. Mustafa IS, Din NM, Ismail A, Omar RC, Khalid NHN (2015) Site suitability analysis for landslide monitoring base station using GIS-based multicriteria evaluation technique. In: 2015 5th national symposium on information technology: towards new smart world, NSITNSW 1–6
18. Rawat JS (2010) Database management system for Khulgad Watershed, Kumaun Lesser Himalaya, Uttarakhand, India. Curr Sci 98:1340–1348
19. Kumar M, Shaikh VR (2013) Site suitability analysis for urban development using GIS based multicriteria evaluation technique: a case study of mussoorie municipal area, Dehradun District, Uttarakhand, India. J Indian Soc Remote Sens 41:417–424

Geospatial Analysis of Urban Sprawl Using Landsat Data in Kannur, Kerala

Sachikanta Nanda, Tejaswi Ratnakaran, M. Subbulakshmi, R. Annadurai, and Anupam Ghosh

Abstract The urban population is rising at an uncontrollable pace and it has a vital role in causing unplanned development in the fringes of the cities. This uncontrolled growth called urban sprawl causes many environmental as well as social impacts. The first step to keep the sprawl at check is to detect, map and monitor. Geospatial practices have been found to be faster and easier in these processes than the conventional methods. Kannur is an urban cluster considered as million plus UA/city, situated in the state of Kerala. This paper categorized the urban evolution using hybrid geospatial techniques over the years in the emerging metropolitan city of Kannur which is one of the oldest municipalities in India. The study has been done over three decades from 2002 to 2020 and the geographical variation analyzed to understand the urban sprawl. Land use and land cover maps of 2002, 2010 and 2020 are prepared using Landsat data and are classified into five broad categories which are urban region, water body, vegetation, agricultural land and barren land. The area covered by each class in each period is compared by calculating the area of each class. Accuracy assessment is carried out for each LULC maps. Built-up area map is prepared using NDBI and the area calculated gives an idea about how much the built-up feature has encroached on the other land features over the period nearly two decades. The study finally confirms the decline in agricultural land and vegetation on a large extent and the barren land and water body is the least affected by urbanization.

Keywords Remote sensing and GIS · Urban sprawl · MLC · NDBI

1 Introduction

As per the statistics issued by the United Nations Population Division in 2019, it is stated that the urban population all around the globe is going to increase up to 490 crores by the year 2030. There is an extraordinary expansion occurring in the urban

S. Nanda (✉) · T. Ratnakaran · M. Subbulakshmi · R. Annadurai · A. Ghosh
Department of Civil Engineering, Faculty of Engineering and Technology, SRM Institute of Science and Technology, Kattankulathur, Tamil Nadu 603023, India
e-mail: sachikan@srmist.edu.in

K. R. Reddy et al. (eds.), *Recent Advances in Civil Engineering*, Lecture Notes in Civil Engineering 398, https://doi.org/10.1007/978-981-99-6229-7_17

regions all over the world. The urban population is multiplying in such a way that it is anticipated that around 60% of the total global population will sleep in cities by 2030. It is obvious that majority of this growth is going to take place in countries like India. In India, this rapid development has caused the urban population to leap from 7.9 crores to 46 crores from 1961 to 2018. India's urban population is expected to be increased by 7.3 crores by 2021. China has the largest urban population in the world and India is in the second place. And being a fast developing and also the second largest populated country in the world, India has the urban population greater than the overall global inhabitants in the urban area (apart from China, Russia and the USA). This huge soar in the urban population and an uncontrolled, accelerated urbanization rate, have a vital role in causing this unplanned development in the peripheries of the cities, and it is recognized as urban sprawl [1]. Urban sprawl is a complicated occurrence, which has environmental, economic as well as social impacts. Due to its complexity, it is difficult to define urban sprawl [2]. Anyway, an urban sprawl can be defined as an uncontrolled and uncoordinated low-density development evolved in the peripheries of a city and is not much related to its nearby land uses. It appears in different forms such as leapfrog, isolated development, ribbon development, etc., in dispersed form of settlements and commercial buildings, along with traffic congestion [3]. Urban sprawl has too much of impact on the environment such that it has led to the leveling of agricultural lands and green spaces and filling up of water bodies causing many negative effects on the environment [4]. The transition of rural area into urban land causes a hike in impervious surfaces on land and this has led to the occurrence of urban heat island (UHI) effect [5]. The UHI could be defined as the upsurge in temperature in the urban regions in contrast to that of the nearby suburban areas. This has several negative effects on urban life, like increasing air pollution and concrete heat waves. Mapping the urban sprawl helps in various aspects like spotting the zones where environmental, land and many other natural resources are intimidated and predict the probability of patterns of sprawls and the directions which it may spread in the future. Mapping and monitoring of urban sprawl are one of the vital applications of satellite imaging. From the Landsat-MSS data of 70 m resolution and TM of 28.5 m resolution to the IRS-P6 MSS having 5.8 m high resolution, are more capable of spotting the changes in land cover more accurately [6].

In China, to compute and track the level of sprawl in cities and towns, Shannon's entropy values were calculated with the help of satellite data and geospatial technology. More scattered development was identified for the cities and towns which are having higher values of entropy. This signalizes higher rate of sprawl in those regions. In Pune, India, which is facing a high level of increase in population, this technique was wont to check the urban sprawl. The sprawl has put severe oppression on various natural resources since the area of the city has stretched to a great dimension.

In many of the developing and developed countries, numerous researches have been executed for estimating the quantity of urban sprawl. In most of the studies, the behavior of built-up features and the rise in the density of population over the spatial and temporal changes are examined. The increase in population is one of

the crucial stimulators of urban sprawl. Both spatial and statistical criteria could be used for analyzing the sprawl, such as land use, built-up feature, population, etc. Landsat images of three different periods were taken to draw out the settlement area classes in the region. The urban sprawl that occurred within a time period of 18 years was estimated based on the variation in built-up feature in the region. The urban development evidently has lots of negative effects on the surrounding ecosystems in many ways. The damaging dimensions of conurbation are pretty much severe, and in order to sustain our environment, it is necessary to restrain it [7]. In order to realize such changes which are happening to our cities, quantification of sprawl is to be carried out. Time series analysis of urbanization is to be carried out to quantify the growth occurred in different time periods. Sprawl has an intimidating effect on the environmental and natural resources [8]. In order to keep these at check and to know where and how much this sort of expansion is occurring, the initial steps to be taken are to detect, map and monitor the past and present situation of sprawl. And this way it is possible to predict the future directions.

2 Study Area

Kannur is an emerging metropolitan city in the North Malabar Zone in Kerala, India. Kannur is estimated to be the sixth largest urban agglomeration in Kerala. The Municipal Corporation of Kannur was formed in 2015 by merging Municipality of Kannur and the five nearby grama panchayats which include Pallikunnu, Puzhathi, Edakkad, Elayavoor and Chelora. Kannur is the administrative headquarters of Kannur District. The population of the corporation is estimated to be 232,486 as of 2011 census. The geographical extent of the region is 76.41 km^2 with coordinates 110 48′ 28.8″ N–110 55′ 33.6″ N and 750 20′ 2.4″ E–750 27′ 25.2″ E and its shown in Fig. 1. This city is situated on the coastline of Arabian Sea and is located at a height of 1.02 m from the mean sea level. Kannur has a humid tropical monsoon climate. The average daily maximum temperature is around 35 °C in the months of April and May. In December and January, the temperatures are low, i.e., about 20° to 24 °C. In this region heavy rainfall occurs during the southwest monsoon, from June to September. The yearly average rainfall is 3438 mm. Around 68% of this rainfall is experienced in the end of summer.

3 Materials and Methodology

The spatial input which is used is tabulated in Table 1. These data were acquired from the USGS GloVis. Apart from these, zonal boundary map of Kannur Municipal Corporation has been used. In addition, Google Earth application is also used for reference purpose.

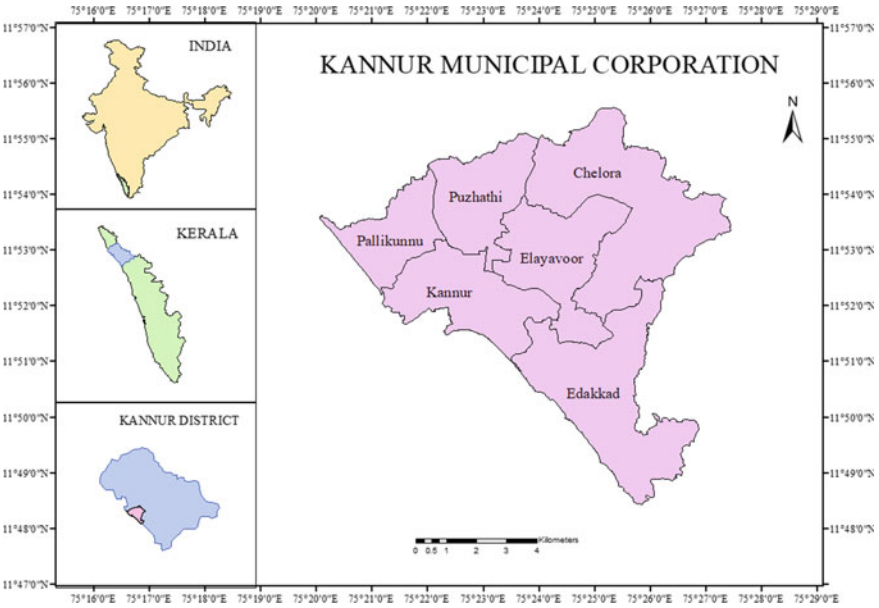

Fig. 1 Study area map of Kannur Municipal Corporation

Table 1 Specifications of the spatial data

Date	Sensor	Path/Row	Spatial resolution
08/01/2002	Landsat 7 ETM +	145/52	30 m
03/03/2010	Landsat 7 ETM +	145/52	30 m
03/02/2020	Landsat 8 OLI/TIRS	145/52	30 m

Landsat data of the years 2002, 2010 and 2020 were taken for carrying out this study. The images of around same time period (January–March) were used for the study to reduce the errors from temporal variation and ArcGIS software is used for all exercises.

The methodology adopted for the study is shown in Fig. 2. ArcGIS software (ESRI) is used to produce different thematic layers. Landsat ETM + data of 2002 and 2010 and Landsat 8 OLI/TIRS data of 2020 were made use of for preparing the land use and land cover maps of these three time periods.

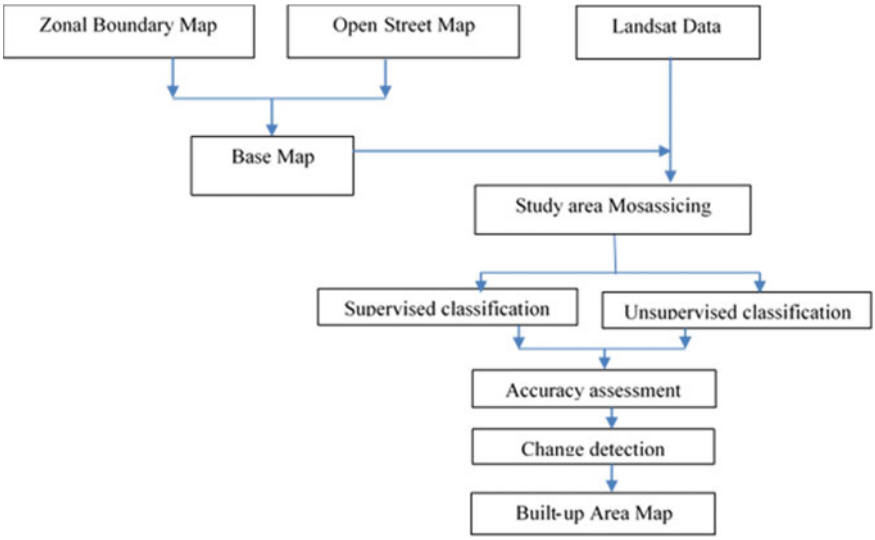

Fig. 2 Systematic diagram of the methodology

3.1 Land Use/Land Cover Classifications

Satellite images were classified using both unsupervised and supervised classification procedure [9]. Unsupervised classification was carried out by using IsoData and K—Mean methods [10]. These methods did not bring out the required results since some of the classes were mixed. The MLC scheme has been used to carry out supervised classification. Each composed image was ordered into five categories, such as water bodies, vegetation, built-up areas, barren land surfaces and fallow lands.

3.2 Accuracy Assessment

The intention of accuracy assessment is the quantitative evaluation of how effectively the pixels of different features are sampled to the actual or true land cover classes [11]. Error matrix is produced for each image using ArcMap, to evaluate the accuracy of classification. The overall percentage of accuracy of classification could be calculated from the formula,

$$\text{Percentage of accuracy} = (\text{Total true value})/(\text{Total sample value}) \quad (1)$$

3.3 Change Detection

To trace the direction of future expansion, the nature and magnitude of variation in land use and land cover is to be identified. The two different, MLC classified images are employed for the post classification to generate a change detection analysis [12]. By using the statistical tool, the table of change class can be obtained. Finally, this classification could indicate the nature and magnitude of variation.

3.4 Built-up Area Map

Built-up area map gives a transparent picture of the sprawl in a region. Built-up area of each year is to be extracted in order to quantify the growth of urban area and to identify and analyze the patterns of sprawl. The NDBI uses the NIR and SWIR wavelength to extract manufactured built-up regions.

$$\text{NDBI} = (\text{SWIR}-\text{NIR})/(\text{SWIR} + \text{NIR}) \tag{2}$$

The NDBI has proved to be useful in different studies for mapping the built-up features by using the Landsat images.

4 Results and Discussion

4.1 Land Use and Land Cover Map

Based on the supervised classification of the Landsat images, the land use and land cover was classified into five categories; urban region, water bodies, vegetation, agricultural land and barren land. Table 2 gives the area of various classes in each year. Land use land cover map for the years 2002, 2010 and 2020 was shown in Fig. 3. Statistics shows that in 2002, vegetation makes the largest land use/land cover category in Kannur. They collectively occupy an area of 50.10 km^2, representing 65.56% of the overall land cover of the area. The barren land is the least found land cover type. It occupied an area of 1.91 km^2 which represents 2.49% of the total land cover area. The agricultural land takes 14.25% of the total area.

Observations from above land use and land cover statistics show that, a significant increase is in the built-up feature class from 11.11 km^2 in 2002 to 22.01 km^2 in 2010 which implies an increase from 14.45% to 28.56% of the total area of 76.41 km^2, whereas, the vegetation decreases from 50.10 to 41.91 km^2, i.e., 65.56% to 54.84%. Also, between 2010 and 2020, built-up areas feature has the highest rate of increase from 22.01 35.10 km^2 which is from 28.80 to 45.93%, while there was loss of

Table 2 Area of land use and land cover classes of Kannur municipality

LULC classes	Area in km^2 2002	Area in km^2 2010	Area in km^2 2020
Water body	2.40	1.91	1.19
Urban region	11.11	22.01	35.10
Agricultural land	10.89	9.87	8.19
Vegetation	50.10	41.91	31.6
Barren land	1.91	0.71	0.33
Total	76.41	76.41	76.41

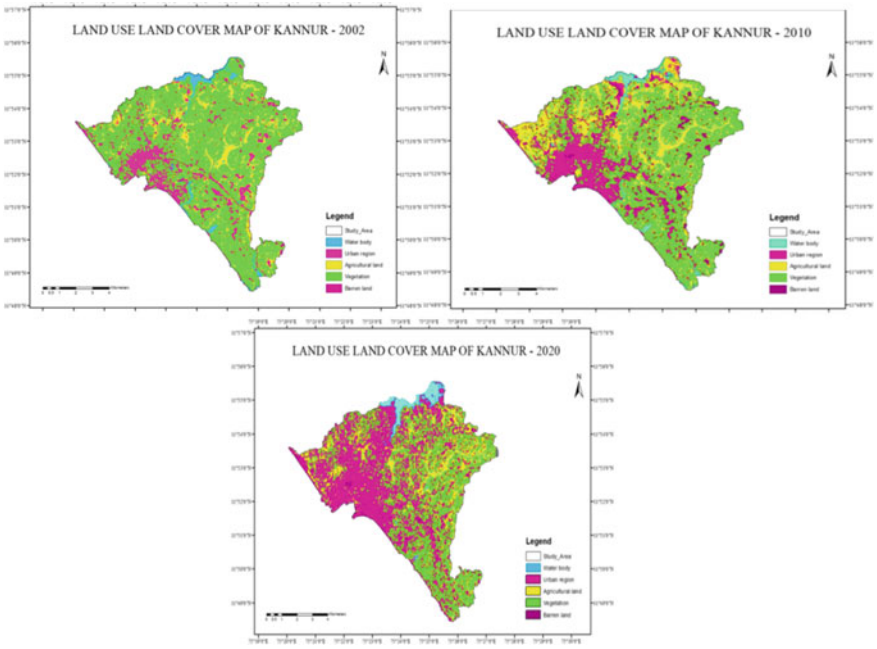

Fig. 3 Land use and land cover map of 2002, 2010 and 2020 of Kannur Municipal Corporation

vegetation, agricultural land and barren land. In 2020, most of the area is taken over by the urban development.

Figure 4 is showing the change detection in the urban region over the periods of 2002, 2010 and 2020 in one image. The urban region has increased from 11.11 to 35.10 km^2 in 18 years. Large area of vegetation, agricultural land and barren land has lost to urban development throughout this period. The study implies an exceptional amount of urban sprawl in the city since 2002 to 2020.

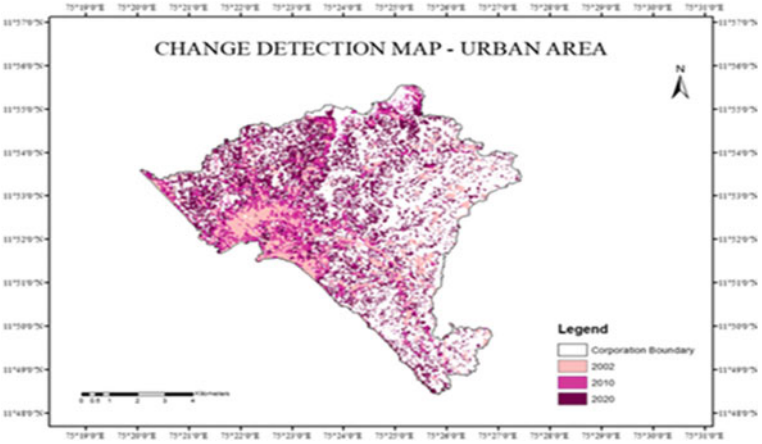

Fig. 4 Change detection in urban density of Kannur Municipal Corporation

Table 3 Accuracy of LULC classifications from the images of 2002, 2010 and 2020

LULC area in	% Accuracy
2002	93.548%
2010	82.758%
2020	90%

4.2 Accuracy Assessment

Error matrix is produced for each image using Arc Map in order to evaluate the accuracy of classification. The error matrix shows the relationship between the onsite and the classified output [13–16]. It is a square matrix consisting of rows and columns in which column shows the ground truth and row indicates to which class each image pixels are assigned. For the accuracy assessment, a total of 31 points in 2002 image, 29 points in 2010 and 30 points in 2020 image were selected from the MLC classified image.

Table 3 gives the percentage of accuracy of the LULC classification calculated from the error matrix using the percentage accuracy formula.

4.3 Change Detection in Built-up Area

Built-up area is extracted for each year using NDBI and it is given in Fig. 5. The built-up area maps of each year emphasize the successive progress of different patterns of urban growth such as linear, clustered and leap frog. In the 2002 image clustered growth is more prominent, whereas we can see a linear pattern of sprawl in the

2010 image, along with an expanded cluster in the CBD. In the 2020 image, a well-defined linear pattern could be seen along with a much broader cluster and a scattered distribution of buildings could be seen in the rural regions which are to be categorized into leap frog.

The normalized difference built-up index (NDBI) is considered as a graphical or numerical gauge that can be used to analyze the remote sensing measurements. The NDBI uses the NIR and short wave infrared bands to extract manufactured built-up areas. Calculations of NDBI for a given pixel always have values ranging from minus one (−1) to plus one (+1). It is observed that higher (0 to + 1) NDBI indicates the presence of built-up areas, while lower NDBI values correspond to other feature classes. 2002 has the lowest NDBI value, while 2020 has the highest which indicates the increase in NDBI (Table 4).

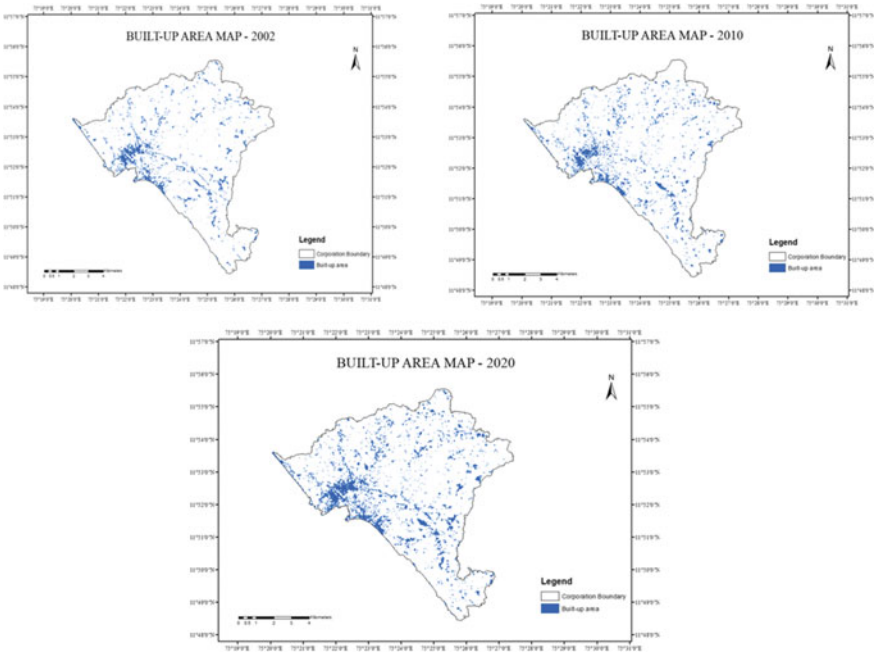

Fig. 5 Built-up area map derived from NDBI—2002, 2010 and 2020 of Kannur Municipal Corporation

Table 4 Total built-up area derived from NDBI

Land use	Coverage in km^2 2002	Coverage in km^2 2010	Coverage in km^2 2020
Total built-up area	4.923	5.142	7.351

5 Conclusion

The pattern and distributions of urban sprawl in Kannur Municipal Corporation have been investigated. In this study, the built-up area is employed as a measure of urban sprawl. Normalized difference built-up index is used for the extraction of built-up area. The built-up area changes over the years, which is brought out through geospatial techniques, has given impressive information about the type and extent of urban sprawl. This study reveals how the direction and pattern of development is occurring as the time proceeds. The results disclose the patterns of urban development occurring in the area over periods of 2002, 2010 and 2020 in the region. The major land use and land cover changes are the vegetation and agricultural land to built-up area as well as few water bodies are also converted to the built-up area.

References

1. Soni S, Birke H, Madan E, Tegegne E (2018) Assessment of urban sprawl using geospatial technology: a case study of Debre Berhan town, Ethiopia. Int J Adv Technol Eng Res
2. Thonfeld F, Steinbach S, Muro J, Kirimi F (2020) Long-term land use/Land cover change assessment of the Kilombero catchment in Tanzania using random forest classification and robust change vector analysis. Remote Sens 12:1057. https://doi.org/10.3390/Rs12071057
3. Krishnaveni KS, Anilkumar PP (2020) Managing urban sprawl using remote sensing and Gis. Int Arch Photogrammetry. Remote Sens Spat Inf Sci Xlii-3-W11:59–66. https://doi.org/10.5194/Isprs-Archives-Xlii-3-W11-59-2020
4. Kavzoglu T, Bilucan F (2022) Effects of auxiliary and ancillary data on Lulc classification in a heterogeneous environment using optimized random forest algorithm. Earth Sci Inform 1:1–21. https://doi.org/10.1007/S12145-022-00874-9/Figures/1
5. Wang SW, Munkhnasan L, Lee WK (2021) Land use and land cover change detection and prediction in Bhutan's high altitude city of Thimphu, using cellular automata and Markov chain. Environ Challenges 2:100017. https://doi.org/10.1016/J.Envc.2020.100017
6. Rahman A, Kumar S, Fazal S, Siddiqui MA (2012) Assessment of land use/Land cover change in the North-West District of Delhi using remote sensing and gis techniques. J Indian Soc Remote Sens 40:689–697. https://doi.org/10.1007/S12524-011-0165-4
7. Santra A, Mitra SS, Sinha S, Routh S (2020) Performance testing of selected spectral indices in automated extraction of impervious built-up surface features using resourcesat Liss-Iii image. Arab J Geosci 13:1–11. https://doi.org/10.1007/S12517-020-06183-Z/Figures/6
8. Alam A, Bhat MS, Maheen M (2020) Using landsat satellite data for assessing the land use and land cover change in Kashmir Valley. GeoJournal 85:1529–1543. https://doi.org/10.1007/S10708-019-10037-X/Tables/4
9. Balha A, Mallick J, Pandey S, Gupta S, Singh CK (2021) A comparative analysis of different pixel and object-based classification algorithms using multi-source high spatial resolution satellite data for lulc mapping. Earth Sci Inform 14:2231–2247. https://doi.org/10.1007/S12145-021-00685-4/Tables/7
10. Yin C, Yuan M, Lu Y, Huang Y, Liu Y (2018) Effects of urban form on the urban heat Island effect based on spatial regression model. Sci Total Environ 634:696–704. https://doi.org/10.1016/J.Scitotenv.2018.03.350
11. Bhat PA, Shafiq MU, Mir AA, Ahmed P (2017) Urban sprawl and its impact on landuse/land cover dynamics of Dehradun City, India. Int J Sustain Built Environ 6:513–521. https://doi.org/10.1016/J.Ijsbe.2017.10.003

12. Ghosh DK, Mandal ACH., Majumder R, Patra P, Bhunia GS (2018) Analysis for mapping of built-up area using remotely sensed indices—A case study of Rajarhat block in barasat sadar sub-division in West Bengal (India). J Landscape Ecol (Czech Repub) 11:67–76. https://doi.org/10.2478/Jlecol-2018-0007
13. Xu X, Cai H, Qiao Z, Wang L, Jin C, Ge Y, Wang L, Xu F (2017) Impacts of park landscape structure on thermal environment using quickbird and landsat images. Chin Geogr Sci 27:818–826. https://doi.org/10.1007/S11769-017-0910-X
14. Avdan U, Jovanovska G (2016) Algorithm for automated mapping of land surface temperature using landsat 8 satellite data. J Sens 2016:1–8. https://doi.org/10.1155/2016/1480307
15. Dadras M, Mohd Shafri HZ, Ahmad N, Pradhan B, Safarpour S (2014) Land use/cover change detection and urban sprawl analysis in Bandar Abbas City, Iran. Sci World J 2014:1–12. https://doi.org/10.1155/2014/690872
16. Bhatti SS, Tripathi NK (2014) Built-up area extraction using landsat 8 oli imagery. Gisci Remote Sens 51:445–467. https://doi.org/10.1080/15481603.2014.939539

Estimation and Monitoring on Fraction of Absorbed Photosynthetically Active Radiation (FPAR) Changes in Sathyamangalam Reserve Forest

N. Giridharan and R. Sivakumar

Abstract Forest gives a variety of goods and services to living things and encompasses 30% of the Earth's surface globally. Its growth and production are significantly affected by temperature variations leading to shedding of leaves. The fraction of photosynthetically active radiation (FPAR) is a significant index to assess live leaves for photosynthesis, which is essential for forest canopy growth. In the present research, the variations in FPAR are examined for the two years of interval period between 2016 to 2022 and estimated through high-resolution satellite data (SENTINEL 2A) for Sathyamangalam Reserve Forest. The values of FPAR were estimated with the help of the normalized difference vegetation index (NDVI) and the result was further analyzed. The importance of FPAR has been carried out to estimate the active photosynthetic radiation changes activity during pre-monsoon and post-monsoon for the years 2016, 2018, 2020 and 2022. The result shows that the changes in FPAR during pre-monsoon is about 183.30 km^2 (2016) and post-monsoon 184.71 km^2 (2016). Similarly, for the remaining years has been derived. Hence, the changes must be monitored for better sustainable growth in future development.

Keywords Forest · Remote sensing · High-resolution · Satellite data · NDVI · FPAR

1 Introduction

The amount of photosynthetically available radiation in a specific 400—700 nm spectrum that is absorbed by canopies is measured as the fraction of photosynthetically active radiation [1]. It is a vital component in numerous models, including those that analyze crop yield, ecosystem productivity, water, energy and carbon balance of vegetation and serve as the key detection index [2]. It plays a crucial role in many

N. Giridharan · R. Sivakumar (✉)
Department of Civil Engineering, College of Engineering and Technology, SRM Institute of Science and Technology, Kattankulathur, Chengalpattu, Tamil Nadu 603203, India
e-mail: sivakumr@srmist.edu.in

K. R. Reddy et al. (eds.), *Recent Advances in Civil Engineering*, Lecture Notes in Civil Engineering 398, https://doi.org/10.1007/978-981-99-6229-7_18

land surface models and acts as a clear indicator of photosynthesis in vegetation [3]. It denotes the capacity of vegetation for capturing and absorbing energy [4]. The amount of FPAR that is available to the plants are decreased by anything that blocks out sunlight, such as clouds, trees, building shade and cloud cover [5]. The global carbon cycle depends heavily on forest ecosystems, but retrieving precise forest FPAR is difficult due to complex interactions between electromagnetic radiation and forest canopies [6]. The amount of sunlight that can reach plants is filtered by air pollution or precipitation, which also has an impact on FPAR [7, 8]. It is difficult to precisely retrieve forest FPAR data, because of the complex interface of electromagnetic radiation with forest canopies [9]. In hilly terrain, additional issues appear. The majority of studies estimate forest FPAR through empirical models [10]. Regression analysis establishes simple-to-understand and computationally efficient linear or nonlinear functional relationships between field-assessed FPAR and satellite-derived vegetation indices that can be used on vast scales [11].

The two main categories of traditional methods to estimate FPAR are physical and empirical techniques. The radiative transfer model, gap relative risk, and recollisional occurrence used in physical methods to model FPAR describe how the photons interact with the canopy and soil [12]. A 3D radiative transmission model and a look-up table recovery algorithm were used to create the coarse-resolution FPAR satellite products through SENTINEL 2A satellite [13]. The clumping index and soil reflectance are the two parameters needed by physical methods for FPAR estimation at a fine resolution, but obtaining these factors can be challenging and raise the uncertainty of the FPAR estimation [14]. Empirical techniques use ground measurement data or simulations of physical models to determine the linear or nonlinear relationships between remotely sensed reflectance and FPAR [15]. They are simple and effective but have trouble to adjust different types of land cover or enormous spatial scale. Nowadays, geospatial technique becomes a crucial tool for estimating biophysical parameters which help to manage and monitor the forest ecosystem [16]. This research paper discusses about the changes in photosynthetic active radiation during pre- and post-monsoon period between 2016–2022.

2 Normalized Difference Vegetation Index

Normalized difference vegetation index (NDVI) computes vegetation by comparing the near-infrared (which vegetation strongly reflects) and red light (which vegetation absorbs) [17].

$$\text{NDVI} = \frac{(\text{Near Infra red band} - \text{Red band})}{(\text{Near Infra red band} + \text{Red band})} \tag{1}$$

Equation (1) represents the formula for NDVI. This formula generates a value that ranges from -1 to $+1$[18]. In general, NDVI is a consistent method to assess

accurate vegetation. An area has healthier vegetation if the NDVI value is high. There is no vegetation if the NDVI value is low.

3 Significance of FPAR

FPAR is the main element of solar radiation which is absorbed by plants during photosynthesis. It is a parameter used in remote sensing and in ecosystem modelling that signifies the portion of PAR observed by the plants [19]. It is commonly used in ecosystem models because it has an important influence on exchange of energy water vapour and carbon dioxide between the surface of Earth and atmosphere [20]. The amount of FPAR that plants observe is primarily influenced by temperature and precipitation [21]. It is a crucial factor in determining how much biomass is produced because vegetation growth is correlated with the rate at which vegetation detects radiant energy [22]. It is expressed as a unitless percentage of the incoming radiation that the land surface has absorbed. Based on its relationship with the NDVI Index, the FPAR Index is calculated [23]. It can be expressed in the Eq. 2 and generally applicable to South Asian nations.

$$\text{FPAR} = -c + (d * \text{NDVI}) \tag{2}$$

where the empirical coefficients c and d for the South Asian region are −0.08 and 1.075, respectively. The main objective of this study is to estimate the FPAR changes during pre-monsoon and post-monsoon period in Sathyamangalam Reserve Forest.

4 Study Area

Sathyamangalam Reserve Forest in Erode district (Fig. 1) is the study area situated in the southwest portion of the Eastern Ghats and spans 2438.62 km^2 between latitudes 11º 29’ N and 11° 43’ N and longitudes 76° 50’ E and 77° 27’ E. It is a crucial wildlife corridor linking the Western and Eastern Ghats. A vast range of ecosystems is seen from the reserve forest’s eastern to the western side. The gradient of rainfall from east to west that describes the spatial–temporal pattern is thought to be the cause for the change in vegetation. The two perennial rivers that flow through the forest area are Bhavani and Moyar. The forest is renowned for its abundance of flora and fauna, including sandalwood (Santalum album) and the Asian elephant (Elephas maximus), respectively. The study area consists of three forest divisions, namely Erode division, Sathyamangalam division and Hassanur division. Out of 2438.57 km^2, the Erode division comprises 861.4 km^2, Sathyamangalam division 981.3 km^2 and Hassanur division 595.86 km^2 in Tamil Nadu. The study area is covered by Salem division on east, Nilgiri district on northwest region, Tiger Reserve on north direction and Coimbatore district on south. The five major types of forests

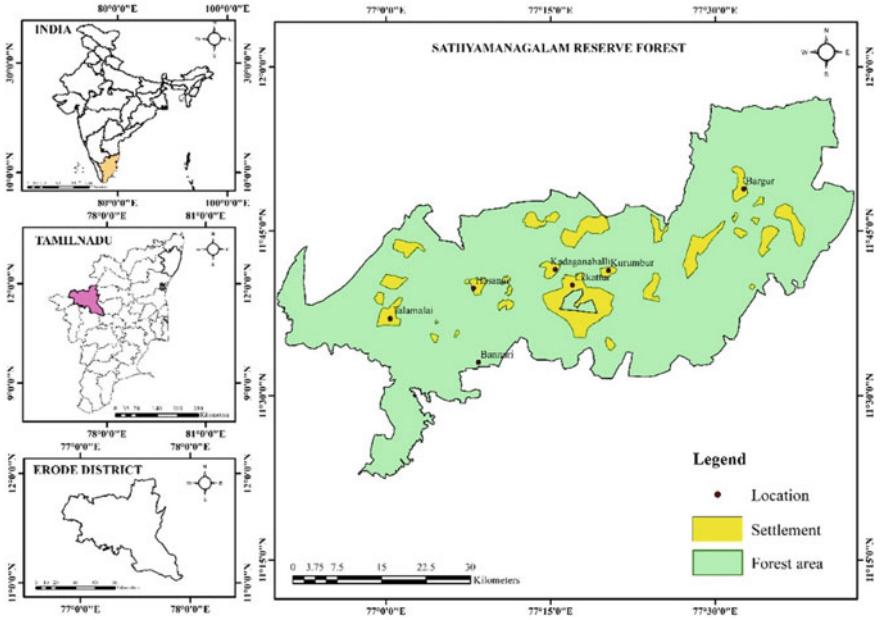

Fig. 1 Location of study area

are tropical evergreen, semi-evergreen, mixed deciduous, dry deciduous and thorn forest. Tropical dry forests comprise most of the area, including dry thorn, deciduous, semi-evergreen and savanna forest types.

5 Data Source

A European optical imaging satellite named Sentinel-2A was launched in 2015. A high-resolution multi-spectral imager with a large field of view and 13 spectral bands is carried by the satellite. It will observe on the ground to boost functions like monitoring forests, spotting the land cover changes and management of natural disasters. In order to calculate the vegetation index, the sensor specifies two bands: near-infrared (Band 8) and red (Band 4). By correlating these two bands, to derive vegetation index and then forwarded to calculate FPAR with help of it [19]. The collection of satellite data for the present study is listed in Table 1.

Table 1 Data description

Satellite image	Resolution	Date of acquisition	
		Pre-monsoon	Post-monsoon
Sentinel 2A	10 m	20-03-2016	17-12-2016
		22-03-2018	21-11-2018
		03-04-2020	15-11-2020
		14-03-2022	25-11-2022

6 Methodology

The study area was extracted from a Toposheet 1:50,000 which was acquired from the Survey of India website. The multi-spectral satellite data (SENTINEL 2A) was collected from Bhoonidhi from National Remote Sensing Centre (NRSC) website to estimate the FPAR in forest area for the years 2016, 2018, 2020 and 2022. NDVI was performed to determine the vegetation area over the study area through near-infrared and red bands. Figure 2 represents the methodology of the present study. NDVI is a simplified visual representation that can be used to assess whether an area is covered in live green vegetation through geospatial technology [24]. The thematic maps (NDVI map) were determined through QGIS platform for the year 2016, 2018, 2020 and 2022. The map displays the NDVI values between −1 and + 1[25]. The NDVI value is used to estimate the FPAR value of the area which is derived through raster calculator tool in QGIS software.

This research focuses on the FPAR to derive pixel data related to the active photosynthesis radiation, which is helpful to classify the data in the image. The variation in temporal and spatial characteristics, as well as the variation trends of FPAR in

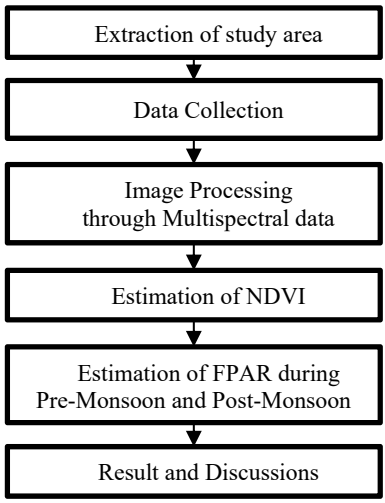

Fig. 2 Flowchart of methodology for FPAR estimation

2016, 2018, 2020 and 2022, were examined using SENTINEL 2A data products for the forest area.

7 Result and Discussion

The Figs. 3a–d and 4a–d represent FPAR maps during pre-monsoon period for the years 2016, 2018, 2020 and 2022. The result confirms that the high, moderate and low regions of FPAR that occurred during the pre-monsoon and post-monsoon periods are represented by the colours green, sandal and brown colour, respectively. The changes in photosynthetic radiation are observed in the study area which is represented in Table 2.

The result states that during post-monsoon, the photosynthetically active radiation is high when compared with pre-monsoon period due to climatic changes. The present study states that the FPAR changes in the study area is minimum to maximum at post-monsoon period when compared with pre-monsoon for the years 2016, 2018, 2020 and 2022. In 2016 and 2018, forest area shows very low FPAR (Figs. 3a, b, 4a and b). The FPAR value 0.824 was observed as high in 2020 and 0.995 in 2022 which is due to better monsoon conditions as shown in Figs. 4c and d and Table 3.

8 Result and Discussion

The changing trends of FPAR were analyzed for 2016, 2018, 2020 and 2022 for pre- and post-monsoon based on the SENTINEL 2A remote sensing data product. The FPAR index has demonstrated its ability to track changes in active photosynthesis radiation in addition to other methods. In present study, the FPAR was observed with value of 0.824 and 0.573 for pre-monsoon in 2020 and 2022, respectively; similarly, the FPAR value 0.824 and 0.995 for post-monsoon in 2020 and 2022. The reflectance of FPAR with positive higher values predicts the presence of active photosynthesis radiation. The reflectance was low with value of 0.464 and 0.499 in the year 2016 and 2018. The change in FPAR area was observed to be decreased from 8.66% (2016) to 5.97% (2018) and increased from 7.31% (2020) to 15.99% (2022), which is due to better monsoon condition. The present study recommends a special course of action to preserve the reserve forest with sustainable environment around it.

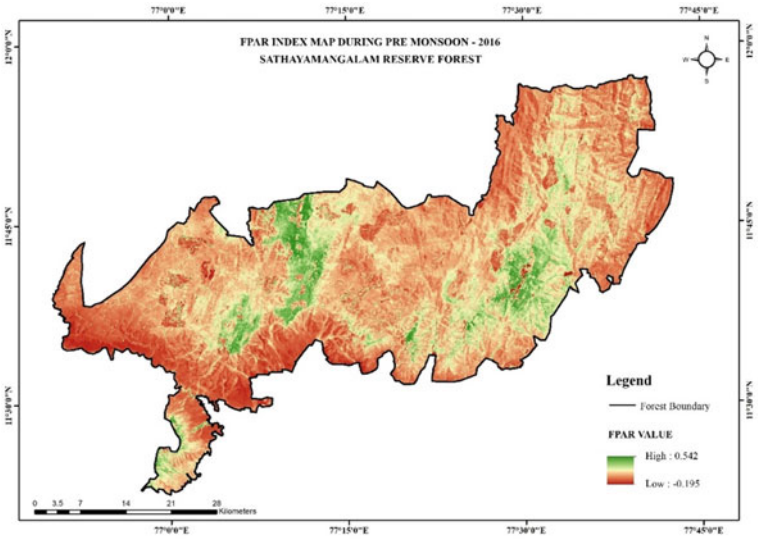

(a)

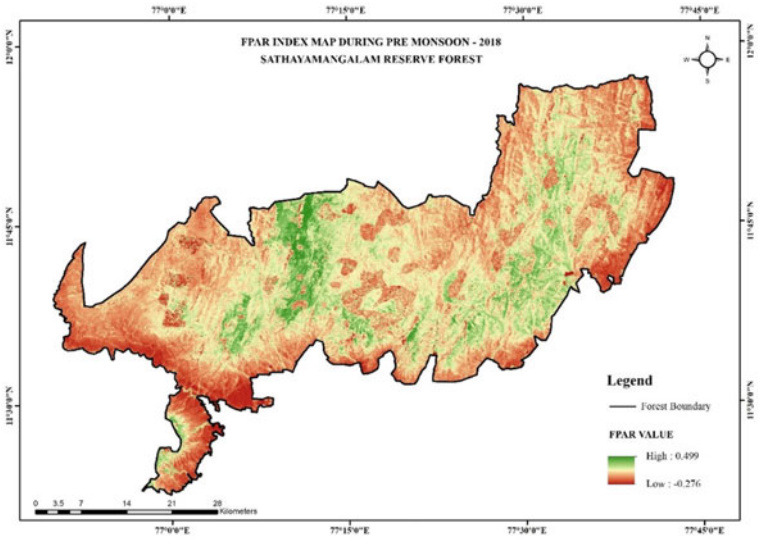

(b)

Fig. 3 **a** FPAR map during pre-monsoon for the year 2016. **b** FPAR map during pre-monsoon for the year 2018. **c** FPAR map during pre-monsoon for the year 2020. **d** FPAR map during pre-monsoon for the year 2022

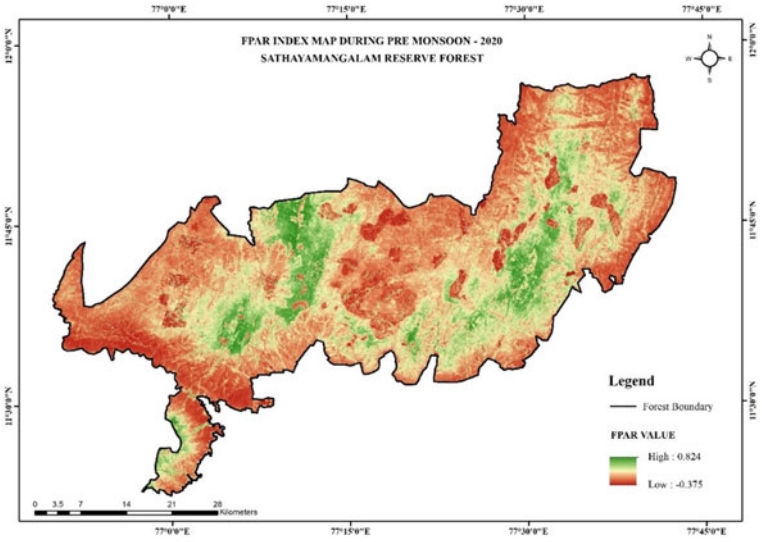

(c)

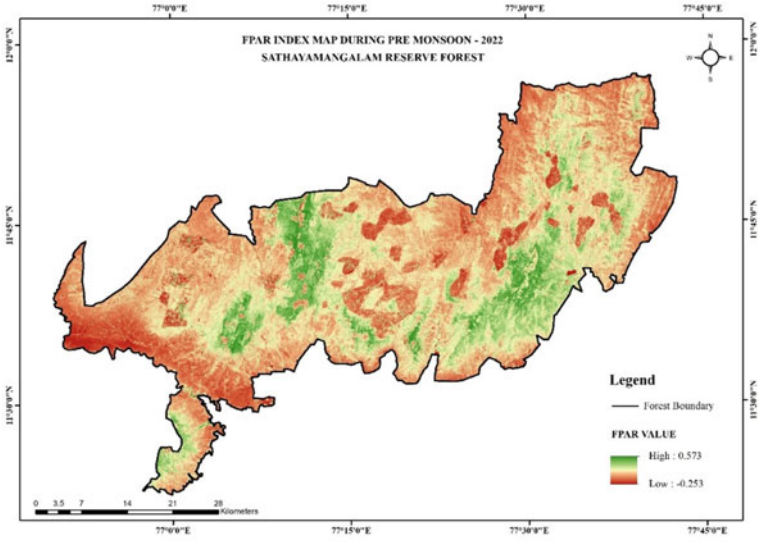

(d)

Fig. 3 (continued)

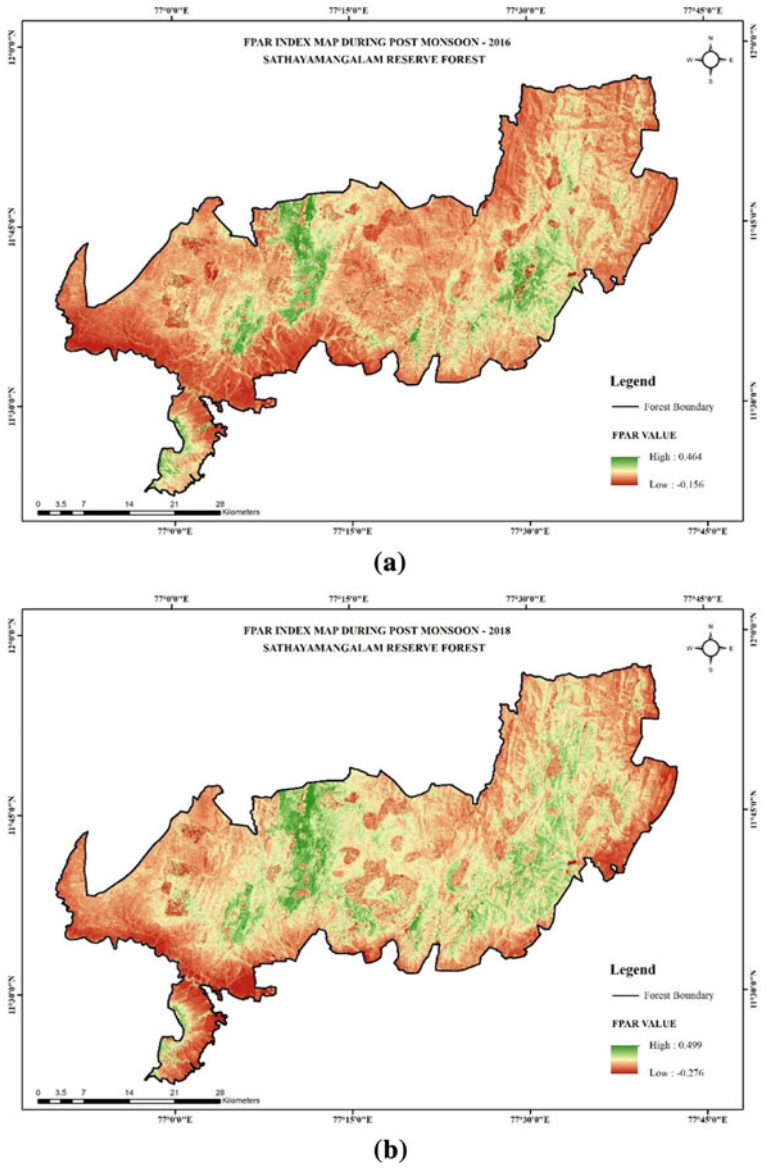

Fig. 4 **a** FPAR map during post-monsoon for the year 2016. **b** FPAR map during post-monsoon for the year 2018. **c** FPAR map during post-monsoon for the year 2020. **d** FPAR map during post-monsoon for the year 2022

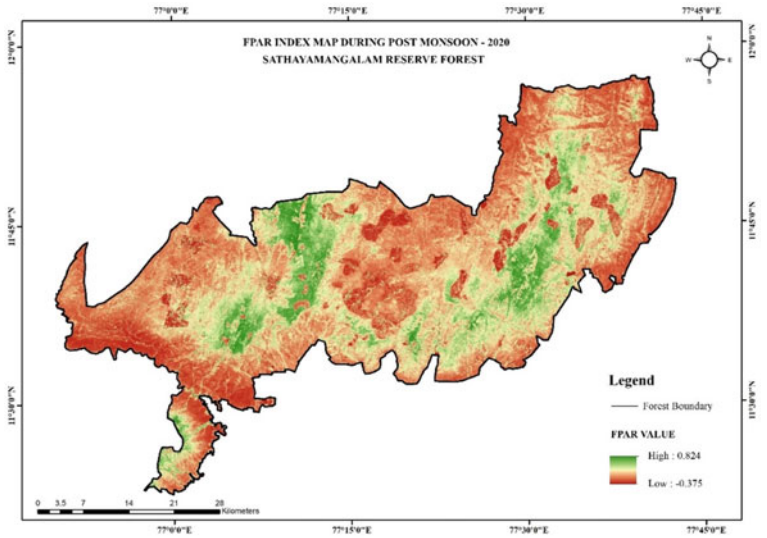

(c)

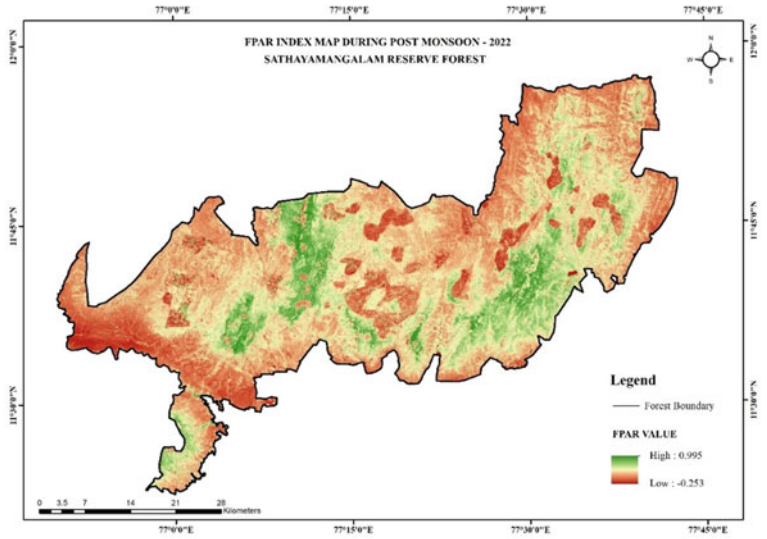

(d)

Fig. 4 (continued)

Table 2 Occurrence of FPAR area

Year	Pre-monsoon	Post-monsoon
	Area (in sq.km)	
2016	183.30	184.71
2018	156.37	180.79
2020	307.22	440.75
2022	423.57	498.18

Table 3 Occurrence of FPAR value

Year	Pre-monsoon	Post-monsoon
2016	0.542	0.464
2018	0.499	0.499
2020	0.824	0.824
2022	0.573	0.995

Acknowledgements The authors are grateful to SRM Institute of Science and Technology, Kattankulathur for providing all necessary amenities and encouragement for doing this research work.

Conflict of Interest The authors declare that there is no conflict of interest.

References

1. Yang F, Zhu Y, Zhang J, Yao Z (2012) Estimating fraction of photosynthetically active radiation of corn with vegetation indices and neural network from hyperspectral data. Chin Geogr Sci 22(1):63–74. https://doi.org/10.1007/s11769-012-0514-4
2. Zhang X, Pourreza A, Cheung KH, Zuniga-Ramirez G, Lampinen BD, Shackel KA (2021) Estimation of fractional photosynthetically active radiation from a canopy 3D model; case study: almond yield prediction. Front Plant Sci 12(August):1–19. https://doi.org/10.3389/fpls.2021.715361
3. Pandey AC et al (2023) Evaluating biochemical and biophysical characteristics of tropical deciduous forests of eastern India using remote sensing and in-situ parameter estimation. Remote Sens Appl Soc Environ 29:100909. https://doi.org/10.1016/J.RSASE.2022.100909
4. Chen Y et al (2019) Generation and evaluation of LAI and FPAR products from Himawari-8 advanced Himawari imager (AHI) data. Remote Sens 11(13). https://doi.org/10.3390/rs11131517
5. Leolini L et al. (2022) Use of remote sensing-derived fPAR data in a grapevine simulation model for estimating vine biomass accumulation and yield variability at sub-field level. Precis Agric 0123456789. https://doi.org/10.1007/s11119-022-09970-8
6. Dong T, Zhang H, Meng J, Wu B (2013) Mapping FPAR in China with modis time-series data based on the wide dynamic range vegetation index. Int Geosci Remote Sens Symp 2790–2793. https://doi.org/10.1109/IGARSS.2013.6723403
7. Yang ZI, bin Zhang T, Yi GH, Li JJ, Qin YB, Chen Y (2021) Spatio-temporal variation of fraction of photosynthetically active radiation absorbed by vegetation in the Hengduan Mountains, China. J Mt Sci 18(4):891–906. https://doi.org/10.1007/s11629-020-6465-9

8. Tan C et al (2018) Remotely assessing fraction of photosynthetically active radiation (FPAR) for wheat canopies based on hyperspectral vegetation indexes. Front Plant Sci 9(June):1–9. https://doi.org/10.3389/fpls.2018.00776
9. Chen BX, Zhang XZ, Sun YF, Wang JS, He YT (2017) Alpine grassland fPAR change over the Northern Tibetan Plateau from 2002 to 2011. Adv Clim Chang Res 8(2):108–116. https://doi.org/10.1016/j.accre.2017.05.008
10. Wang Y et al (2022) Rapid estimation of decameter FPAR from sentinel-2 Imagery on the Google Earth Engine. Forest 13(12). https://doi.org/10.3390/f13122122
11. Acosta D, Doran PT, Myers M (2020) GIS tool to predict photosynthetically active radiation in a Dry Valley. Antarct Sci 32(5):315–328. https://doi.org/10.1017/S0954102020000218
12. Shouzhen L, Huimin Y, Meng W, Xueyan S, Xuehui H, Tao L (2016) Simulation of canopy FPAR and its relation with vegetation index: a case study of evergreen coniferous forests. 4th Int Work Earth Obs Remote Sens Appl EORSA 2016 Proc 3(1):102–106. https://doi.org/10.1109/EORSA.2016.7552775
13. Myneni RB, Williams DL (1994) On the relationship between FAPAR and NDVI. Remote Sens Environ 49(3):200–211. https://doi.org/10.1016/0034-4257(94)90016-7
14. Myneni RB (1997) Estimation of global leaf area index and absorbed par using radiative transfer models. IEEE Trans Geosci Remote Sens 35(6):1380–1393. https://doi.org/10.1109/36.649788
15. Sensing R (2000) Assessment of crop productivity for major river basins in Asia Using gis and rs data. 1–6
16. K AS, Mittapalli VG, Giridhar VSS (2017) Geomatics applications for landuse land cover at micro level. Dec 2008
17. Ochi S, Shibasaki R (1999) Estimation of NPP based agricultural production For Asian countries using remote sensing data and GIS. 1994, 9–11
18. Seong NH, Jung D, Kim J, Han KS (2020) Evaluation of NDVI estimation considering atmospheric and BRDF correction through Himawari-8/AHI. Asia-Pac J Atmos Sci 56(2):265–274. https://doi.org/10.1007/s13143-019-00167-0
19. Ochi S, Shibasaki R, Murai S (2000) Assessment of primary productivity for food production in major basins of Asia Using R. S. and Gis. Int Arch Photogrammery Remote Sens XXXIII(B7):P1051–1057
20. McCree KJ (1972) Test of current definitions of photosynthetically active radiation against leaf photosynthesis data. Agric Meteorol 10(C):443–453. https://doi.org/10.1016/0002-1571(72)90045-3
21. Junges AH, Fontana DC, Lampugnani CS (2019) Relationship between the normalized difference vegetation index and leaf area in vineyards. Bragantia 78(2):297–305. https://doi.org/10.1590/1678-4499.2018168
22. Fang J, Wang ZM (2001) Forest biomass estimation at regional and global levels, with special reference to China's forest biomass. 587–592
23. Goward SN, Huemmrich KF (1992) Vegetation canopy PAR absorptance and the normalized difference vegetation index: an assessment using the SAIL model. Remote Sens Environ 39(2):119–140. https://doi.org/10.1016/0034-4257(92)90131-3
24. Giridharan N, Sivakumar R (2022) NDVI based image processing for forest change detection in Sathyamangalam reserve forest. Proc Int Conf Technol Adv Comput Sci ICTACS 2022, 731–734. https://doi.org/10.1109/ICTACS56270.2022.9988184
25. Shary PA, Sharaya LS (2014) Change in NDVI of forest ecosystems in Northern Caucasus as a function of topography and climate. Contemp Probl Ecol 7(7):855–863. https://doi.org/10.1134/S1995425514070099

Environmental Engineering

Microplastics and the Environment: A Review

Augustine Crispin and Purushothaman Parthasarathy

Abstract Microplastics are a large class of contaminants comprising a sophisticated combination of chemicals and polymers prevalent in water and sediment. Numerous aquatic environments, including microplastics have been established as critical environmental contaminants in all matrices. Although microplastic pollution is widespread in the soil, rivers, and atmosphere, these ecosystems are frequently regarded as distinct entities. Consequences of environmental microplastics engaging with biotic and abiotic elements include absorption, settling, biofouling, degradation, disintegration, and entry into the food web with a subsequent transfer throughout the food supply chain. As plastic items are used often and poorly managed, microplastics are released into the environment and are known to carry heavy metals. Absorption of heavy metal microplastics may transport toxic metals across the food web and cause ecological stress due to this large fraction of overall pollution. Toxic metals sorption on microplastics is an impulsive reaction driven by the microplastic surface. The coexistence of MPs and heavy metals poses a threat to the viability of organisms. It has recently been identified as a rising and continuing environmental calamity on a variety of substrates across the world. It is crucial to link the origin and interaction of microplastics in water and sediment with metal pollutants, focusing on toxicities and accumulation and their detrimental effects on organisms and ecosystems, to better comprehend and minimize the potential uncertainties of microplastics.

Keywords Microplastics · Toxic metals · Sediments · Aquatic environment · Environmental toxicology · Environmental hazard

A. Crispin · P. Parthasarathy (✉)
Department of Civil Engineering, Faculty of Engineering and Technology, SRM Institute of Science and Technology, Kattankulathur, Tamil Nadu 603203, India
e-mail: purushop1@srmist.edu.in

K. R. Reddy et al. (eds.), *Recent Advances in Civil Engineering*, Lecture Notes in Civil Engineering 398, https://doi.org/10.1007/978-981-99-6229-7_19

1 Introduction

Polymers are crucial in contemporary life and have benefited society in several ways. Because of the many benefits plastics provide over more conventional materials, their manufacturing and usage have increased. Enterprises and individuals are efficient materials because of their inherent qualities, low cost, and seeming ease of disposal. Plastic has several attractive traits, but it is also dangerous to life and accumulates as toxic waste in landfills and the ecosystem because of these same characteristics. There is a concern with plastic debris that requires a long remedy since it dissipates in the ecosystem exceptionally slowly. Across the globe, 90% of floating waste is made of plastic, which accounts for 60–80% of aquatic waste [1]. The portrayal that arises when one considers aquatic debris, however, consists primarily of onshore or floating materials made of plastic, including PET bottles, containers, and wrappers. Nevertheless, this is only one component of a greater whole. The ecosystem is considered far more at risk from tiny fragments of plastic that are frequently invisible to the unaided eye. Smaller pieces, or "microplastics," a recently identified and characterized environmental danger, have gotten far less attention. Numerous tiny plastic fibers and residues in the ecosystem have been collected in the depths of the oceans and geological ecosystems. According to current research and observations, the effects of microplastic pollution have been assessed throughout time. Tiny plastic waste poses a severe hazard to the ecosystem, which has progressively and frequently been brought to the attention of researchers [2–4]. Small plastics have been the focus of discussion for the past ten years, but no concrete, consistent findings have been established. Researchers are starting to identify that the slowly dissolving plastic materials may eventually threaten food networks. Tiny plastic debris is so prevalent that many remedies are required. The production, use, and recycling of polymeric products should be the main points of concern. This paper aims to discuss the recently discovered hazard that microplastics cause.

2 Literature Survey

Using the term "microplastics," articles published during the past ten years both internationally (Fig. 1) and in the Indian context (Fig. 2) were found using a literature search. Science Direct, Scopus, and Web of Science (WoS), including research publications and review articles were the search's only prominent journal database sources. According to the study, China, the U.S., and Europe were the most common reporting nations for research.

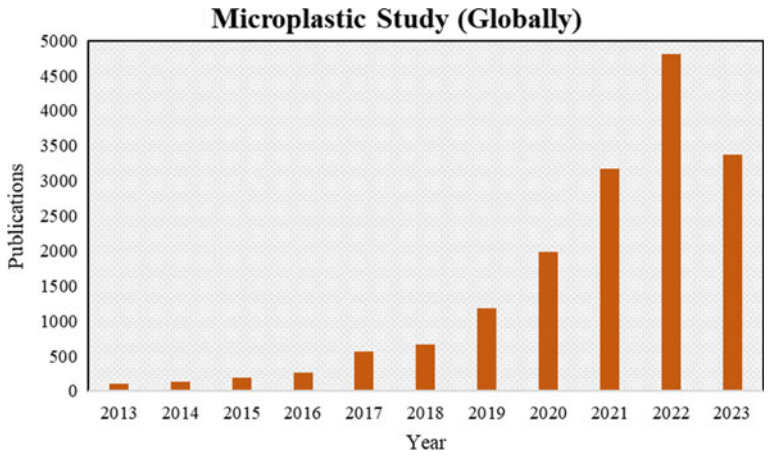

Fig. 1 Worldwide publications about microplastics from 2013 to 2023

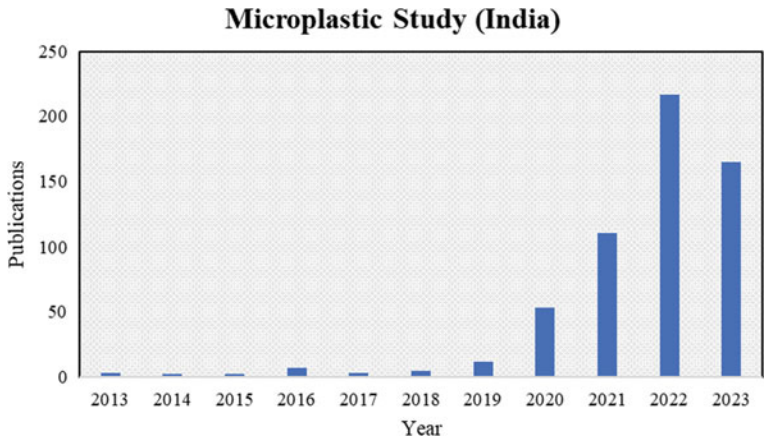

Fig. 2 Indian publications about microplastics from 2013 to 2023

3 Sources of Microplastics

Even as microscopic, primarily industrialized microparticles are present among most plastic discovered in ecosystems, these are usually fragments of significantly larger items. The US Environmental Protection Agency indicated in a study that the sources come from inefficiencies during manufacturing and transportation before the production phase [5]. The "Plastic Age" has resulted in polymers having an infinite variety of possible sizes, shapes, and colors [6]. Two sources are most likely to generate microplastics. The initial comes from tiny plastic fragments employed as abrasive scrubbers in cleaning goods, while the other refers to a cluster broken up

from bigger particles. Certain plastics cannot fragment into a small dimension as a natural functionality, so microplastics of minimal microscopic levels instead emerge from the source. The first widely acknowledged form of microplastics comes from commercial and household items [7–9]. These microplastics are more prone to be carried by sewage through wastewater treatment facilities and end up in aqueous environments. Microplastics generated due to the disintegration of more substantial plastics are referred to as having a "secondary source." Coastlines are favorable depositional environments for the dispersal of plastic fragments because most of the polymers discovered there have surface textures that have been mechanically and chemically degraded [10]. It is important to emphasize that breakdown of plastic particles is much more probable on the surface than in oceans, because radiation from the sun and mechanical degradation are least likely to emerge [11]. In the coastal ecosystem, fracturing can also be brought on by high tides and erosion by silt particles. In general, secondary microplastic formation rates rely on the properties of the plastic, the degree of aging, and the surrounding ecology [10, 12]. Soil is the primary pathway for microplastics to penetrate plant ecosystems in terrestrial habitats. The entrance of runoff from the surface and crop irrigation water, residual breakdown of farm mulch film and plastic debris, land usage of urban sewage, and the accumulation of microplastics from the surrounding environment are the primary sources of microplastics observed in ecosystems of plants [13].

4 Distribution and Accumulation of Microplastics

Microplastics have been extensively recorded in the marine ecosystem in practically every region of the open and confined seas, from densely populated beaches to uninhabited coastlines, from freshwater to deep sea sediments, and from the equator to the polar zones [14]. Lighter, dense floating plastics have the potential to sink to great depths due to biofouling when they are present in the coastal habitat, in addition to being dispersed in saltwater [15]. Subsurface currents can also carry plastics that seem to be denser than salt water [16]. Increased sea levels and changed precipitation, radiation from the sun, wind velocity, tides, and marine wave action brought on by global temperature shifts are anticipated to introduce accumulated plastic waste into the water [17]. Even though there is ample evidence of marine microplastic contamination, freshwater ecology has received less attention. Although the preponderance of ocean microplastic pollution is thought to come from land-based sources, river systems may serve as a significant route for microplastics to infiltrate the coastal environment [18]. Microplastic fibers made of nylon and polyester have also received much research. As a result of washing garments, sewage discharge may be the source of microplastic fiber in the surroundings. Plastic waste can penetrate terrestrial habitats by airborne deposition and agricultural water tainted with microplastics. Moreover, a significant source of plastic waste is the plastic mulch used in horticultural or farming areas. Furthermore, due to the increased O_2 abundance and direct solar exposure, plastic waste in land ecosystems, particularly in surface soils and sediments,

may disintegrate more quickly than in aquatic habitats [18, 19]. Microplastics are unevenly distributed in plant ecosystems primarily due to the varied absorption capacities of various flora species. There have been reports of microplastics in atmospheric dispersal and plastic trash escaping landfills as wind-blown debris [20].

5 Fate of Microplastics

Plastic's lifetime is projected to reach thousands of years, owing to its resilient qualities. As a result, it is critical to understand the long-term destiny of microplastics in the ecosystem. Research has revealed distinct tendencies in the temporal buildup of floating plastic trash across several periods, which aids interpretation [20–22]. Long-term contact exists between floating and trapped microplastic and the ground surface. The deep water might serve as a microplastic sink in the coastal ecosystem. Plastic deterioration would occur in both micro and nano disintegration. Microbes also appear to have a part in the destiny of microplastics [23]. But it is becoming abundantly evident that freshwaters and soils may operate as sinks rather than conveyors for discarded plastic, holding a significant amount of the microplastic contamination they absorb [23–25]. Farming lands may be a considerable distributor of microplastics to rivers due to using sludge as fertilizers; however, a large amount will most likely be preserved. Research on the retention of microplastics in soils discovered synthetic fibers and filaments formed from sewage sludge in treated farm soil for a minimum of fifteen years after the previous sludge treatment. This study also revealed that concentration hotspots could occur deep, with fibers discovered at depths more than 25 cm in locations with substantial downstream discharge movement through the soil [26]. Microplastic transmission by soil microbes is highly influenced by the microplastics' size and shape and the organisms' correspondence with the microplastics. When particles reach rivers, they undergo identical movement mechanisms that deploy other sediments in channels, such as silt and sand. The variability in particle behavior due to size, shape, and density demonstrates the difficulty in determining and simulating microplastic fate and movement in river systems [27]. The density and form of microplastic fragments will significantly impact their movement and persistence in sediments. Though several polymer particles possess low densities and hence float, numerous forms of polymers are denser than freshwater and, thus, naturally sink. Numerous other variables, such as wind direction and speed, vertical pollutant intensity gradient, rainfall, and temperature all impact the destiny of microplastics in ambient air conditions [28].

6 Hazard of Microplastics

Microplastics might alter sediments' physical characteristics in adequate quantities, affecting biotas. The presence of buoyant microplastics in the river may influence the dispersion of sunlight, which may be accessible to organisms and disrupt their everyday life processes. The most severe issue about microplastics in the ecosystem has always been ingestion by creatures. Microplastics have been discovered to be consumed by a diversity of species [26, 28]. Microplastics were detected in many tissues, including the gills, digestive glands, gut, and cells of the liver, according to studies on microplastic intake [29–31]. Destruction to organisms and cultures at lower trophic stages can have a blowing impact on food webs, either because of lowered communities of smaller organisms, leading to a decreased source of food, or because predators consume vast quantities of contaminated prey, focusing microplastics in their cells [32, 33]. Microplastics impact plant communities on the biomass of specific plants. Toxic compounds that are already on microplastics or have been absorbed into them would severely impact the roots of plants and the makeup of the soil's fauna and microbial life, which might further damage plant development and lower the biomass of vegetation ecosystems [34]. Microplastics may have repercussions for soil ecological processes, e.g., experimental investigations have demonstrated that microplastics affect earthworm reproduction—a crucial organism for nutrient availability and soil oxygenation [35, 36]. The harmful effects of chemicals or particulates on organisms might negatively influence agricultural output. Concerns have lately been expressed about the potential impact of extensive microplastic contamination on human health, as microplastics are highly likely to be swallowed or breathed frequently [37]. Employees in the textile industry who suffered respiratory problems after inhaling synthetic particulate matter have drawn attention to the possibility of health impacts. However, this has not yet been contrasted directly to the implications of nonpolymeric dust, such as cellulose fibers, which may be correspondingly inhaled [38, 39]. Because there is insufficient clinical data on the short- and long-term health impacts of microplastic consumption, this remains a priority research subject to be resolved.

7 Conclusions

Microplastics are found in the land, aquatic, coastal, and atmospheric ecosystems. They are readily disseminated away from their origins, can be created from more significant plastic items in the ecology, and may eventually be trapped within a specific site through absorption into soils and sediments. Instead, they may continually cycle through various settings driven by weather and currents. While particle characteristics determine behavior and destiny, biological, chemical, and physical interactions influence particle movement. Future research will need to contemplate interactions among microplastics and the habitat across a range of environmental

vectors, as well as how the destiny of microplastics may influence their ecological footprint to establish a comprehensive perspective on the causes, severity, and consequences of microplastic contamination at a more extensive network dimension.

Acknowledgements Augustine Crispin thanks the Management and Dean (CET), SRM Institute of Science and Technology, Kattankulathur, and the SRMIST Directorate of Research for their financial support in the form of a Doctoral Research Fellowship. The authors would like to express their gratitude to the SRM Institute of Science and Technology for their facilities and support.

References

1. Singh N et al. (2021) Characteristics and spatial distribution of microplastics in the lower Ganga River water and sediment. Mar Pollut Bull 163, Feb 2021. https://doi.org/10.1016/j.marpolbul.2020.111960
2. Thompson RC et al (2004) Lost at sea: where is all the plastic? Science (1979), 304(5672):838–838. [Online]. Available: www.sciencemag.org/cgi/content/full/304/5672/838/
3. Guo X, Wang J (2019) The chemical behaviors of microplastics in marine environment: a review. Mar Pollut Bull 142:1–14. Elsevier Ltd. 01 May 2019. https://doi.org/10.1016/j.marpolbul.2019.03.019
4. Chen G, Feng Q, Wang J (2020) Mini-review of microplastics in the atmosphere and their risks to humans. Sci Total Environ 703, 10 Feb 2020, Elsevier B.V. https://doi.org/10.1016/j.scitotenv.2019.135504
5. EPA (1992)
6. Moore CJ (2008) Synthetic polymers in the marine environment: a rapidly increasing, long-term threat. Environ Res 108(2):131–139. https://doi.org/10.1016/j.envres.2008.07.025
7. Teuten EL et al (2009) Transport and release of chemicals from plastics to the environment and to wildlife. Philos Trans R Soc B Biol Sci 364(1526):2027–2045. https://doi.org/10.1098/rstb.2008.0284
8. Rochman CM (2018) Microplastics research-from sink to source. Science 360(6384). Am Assoc Adv Sci 28–29. https://doi.org/10.1126/science.aar7734
9. Karbalaei S, Hanachi P, Walker TR, Cole M (2018) Occurrence, sources, human health impacts and mitigation of microplastic pollution. Environ Sci Pollut Res 25(36):36046–36063. Springer, 01 Dec 2018. https://doi.org/10.1007/s11356-018-3508-7
10. Arthur JB, Bamford H (2009) Proceedings of the international research workshop on the occurrence, effects, and fate of microplastic marine debris 2009. [Online]. Available: www.MarineDebris.noaa.gov
11. Andrady AL (2011) Microplastics in the marine environment. Mar Pollut Bull 62(8):1596–1605. https://doi.org/10.1016/j.marpolbul.2011.05.030
12. Browne MA, Dissanayake A, Galloway TS, Lowe DM, Thompson RC (2008) Ingested microscopic plastic translocates to the circulatory system of the mussel, Mytilus edulis (L.). Environ Sci Technol 42(13):5026–5031. https://doi.org/10.1021/es800249a
13. Yu ZF, Song S, Xu XL, Ma Q, Lu Y (2021) Sources, migration, accumulation and influence of microplastics in terrestrial plant communities. Environ Exp Bot 192. Elsevier B.V., 01 Dec 2021. https://doi.org/10.1016/j.envexpbot.2021.104635
14. Wang J, Tan Z, Peng J, Qiu Q, Li M (2016) The behaviors of microplastics in the marine environment. Mar Environ Res 113:7–17. Elsevier Ltd, 01 Feb 2016. https://doi.org/10.1016/j.marenvres.2015.10.014
15. Cózar A et al (2014) Plastic debris in the open ocean. Proc Natl Acad Sci U S A 111(28):10239–10244. https://doi.org/10.1073/pnas.1314705111

16. Engler RE (2012) The complex interaction between marine debris and toxic chemicals in the ocean. Environ Sci Technol 46(22):12302–12315. 20 Nov 2012. https://doi.org/10.1021/es3027105
17. Browne MA et al (2011) Accumulation of microplastic on shorelines woldwide: sources and sinks. Environ Sci Technol 45(21):9175–9179. https://doi.org/10.1021/es201811s
18. Eriksen M et al (2013) Microplastic pollution in the surface waters of the Laurentian Great Lakes. Mar Pollut Bull 77(1–2):177–182. https://doi.org/10.1016/j.marpolbul.2013.10.007
19. Rochman CM, Hentschel BT, The SJ (2014) Long-term sorption of metals is similar among plastic types: implications for plastic debris in aquatic environments. PLoS One 9(1). https://doi.org/10.1371/journal.pone.0085433
20. Dris R, Gasperi J, Saad M, Mirande C, Tassin B (2016) Synthetic fibers in atmospheric fallout: a source of microplastics in the environment? Mar Pollut Bull 104(1–2):290–293. https://doi.org/10.1016/j.marpolbul.2016.01.006
21. Wu P et al (2019) Environmental occurrences, fate, and impacts of microplastics. Ecotoxicol Environ Saf 184, 30 Nov 2019, Academic Press. https://doi.org/10.1016/j.ecoenv.2019.109612
22. Wong JKH, Lee KK, Tang KHD, Yap PS (2020) Microplastics in the freshwater and terrestrial environments: prevalence, fates, impacts and sustainable solutions. Sci Total Environ 719, 01 Jun 2020, Elsevier B.V. https://doi.org/10.1016/j.scitotenv.2020.137512
23. da Costa JP, Santos PSM, Duarte AC, Rocha-Santos T (2016) (Nano)plastics in the environment—Sources, fates and effects. Sci Total Environ 566–567. Elsevier B.V., pp. 15–26, 01 Oct 2016. https://doi.org/10.1016/j.scitotenv.2016.05.041
24. Ricciardi M, Pironti C, Motta O, Miele Y, Proto A, Montano L (2021) Microplastics in the aquatic environment: Occurrence, persistence, analysis, and human exposure. Water (Switzerland) 13(7), Apr 2021. https://doi.org/10.3390/w13070973
25. Horton AA, Walton A, Spurgeon DJ, Lahive E, Svendsen C (2017) Microplastics in freshwater and terrestrial environments: evaluating the current understanding to identify the knowledge gaps and future research priorities. Sci Total Environ 586:127–141, 15 May 2017, Elsevier B.V. https://doi.org/10.1016/j.scitotenv.2017.01.190
26. Zubris KAV, Richards BK (2005) Synthetic fibers as an indicator of land application of sludge. Environ Pollut 138(2):201–211, Nov 2005. https://doi.org/10.1016/j.envpol.2005.04.013
27. Horton AA, Dixon SJ (2018) Microplastics: an introduction to environmental transport processes. WIREs Water 5(2), Mar 2018. https://doi.org/10.1002/wat2.1268
28. Wang C, Zhao J, Xing B (2021) Environmental source, fate, and toxicity of microplastics. J Hazard Mater 407. Elsevier B.V., 05 Apr 2021. https://doi.org/10.1016/j.jhazmat.2020.124357
29. Wright SL, Thompson RC, Galloway TS (2013) The physical impacts of microplastics on marine organisms: a review. Environ Pollut (Barking, Essex : 1987), 178:483–492. https://doi.org/10.1016/j.envpol.2013.02.031
30. de Sá LC, Oliveira M, Ribeiro F, Rocha TL, Futter MN (2018) Studies of the effects of microplastics on aquatic organisms: what do we know and where should we focus our efforts in the future? Sci Total Environ 645:1029–1039, Elsevier B.V., 15 Dec 2018. https://doi.org/10.1016/j.scitotenv.2018.07.207
31. Wang HT et al (2019) Exposure to microplastics lowers arsenic accumulation and alters gut bacterial communities of earthworm Metaphire californica. Environ Pollut 251:110–116. https://doi.org/10.1016/j.envpol.2019.04.054
32. Ha J, Yeo MK (2018) The environmental effects of microplastics on aquatic ecosystems. Mol Cellular Toxicol 14(4):353–359. Springer, Berlin, 01 Oct 2018. https://doi.org/10.1007/s13273-018-0039-8
33. Li WC, Tse HF, Fok L (2016) Plastic waste in the marine environment: a review of sources, occurrence and effects. Sci Total Environ 566–567, 333–349. Elsevier B.V. 01 Oct 2016. https://doi.org/10.1016/j.scitotenv.2016.05.084
34. Qi Y et al (2020) Effects of plastic mulch film residues on wheat rhizosphere and soil properties. J Hazard Mater 387, Apr 2020. https://doi.org/10.1016/j.jhazmat.2019.121711
35. Watts AJR et al (2014) Uptake and retention of microplastics by the shore crab carcinus maenas. Environ Sci Technol 48(15):8823–8830. https://doi.org/10.1021/es501090e

36. Mattsson K, Johnson EV, Malmendal A, Linse S, Hansson LA, Cedervall T (2017) Brain damage and behavioural disorders in fish induced by plastic nanoparticles delivered through the food chain. Sci Rep 7(1). https://doi.org/10.1038/s41598-017-10813-0
37. Cox KD, Covernton GA, Davies HL, Dower JF, Juanes F, Dudas SE (2019) Human consumption of microplastics. Environ Sci Technol 53(12):7068–7074. https://doi.org/10.1021/acs.est.9b01517
38. Rillig MC, Leifheit E, Lehmann J (2021) Microplastic effects on carbon cycling processes in soils. PLoS Biology 19(3) 30 Mar 2021. https://doi.org/10.1371/JOURNAL.PBIO.3001130
39. Huerta Lwanga E et al. (2016) Microplastics in the terrestrial ecosystem: implications for lumbricus terrestris (Oligochaeta, Lumbricidae). Environ Sci Technol 50(5):2685–2691, Mar 2016. https://doi.org/10.1021/acs.est.5b05478

Microplastic Pollution Investigation for Chennai Coast

Jeeva Ra Ga and S. Ramesh

Abstract In response to a rise in the intake of abandoned garbage from plenty of resources, there is an increasing concern about the presence of microplastics, or plastic materials smaller than 5 ml, near the coastline. Microplastic trash was evaluated and divided into four distinct size categories in order to assess the amount of microplastic contamination in the seashores (25 spots) along the Tamil Nadu coast (1076 km), India. Riverine, tourists, and fisheries were employed to categorize the coastlines concerning their propensity for contamination. Microplastic was substantially more prevalent in seaside specimen collections made at higher waves when compared to lower tides. Shore's riverbanks showed a significantly greater quantity of microplastics than coastlines affected by fisheries and tourist activities. Plastic shards made up the majority of the overall trash found (47–50%), followed by line/fibres (24–27%) and foamy (10–19%) components. These three predominant kinds of microplastics observed on these coastlines are polyethylene, polypropylene, and polystyrene, according to Fourier transform infrared spectroscopy (FTIR) study. Analyses of the intestinal contents of highly significant fishes gathered from shore regions showed that 10.1% of the fishes had consumed plastic particles. The findings emphasize the need for microplastics filtering from estuaries, coastline waters, and other potential causes and suggest that microplastic build-up in the maritime ecosystem, particularly close to stream openings, because to its propensity to contaminate the marine food cycle, could pose a severe hazard.

Keywords Aquatic ecosystem · Coastline trash · Microplastic · Marine environment

J. R. Ga · S. Ramesh (✉)
Department of Civil Engineering, SRM Institute of Science and Technology, Kattankulathur, Tamilnadu 603203, India
e-mail: rameshs@srmist.edu.in

K. R. Reddy et al. (eds.), *Recent Advances in Civil Engineering*, Lecture Notes in Civil Engineering 398, https://doi.org/10.1007/978-981-99-6229-7_20

1 Introduction

Plastics are physically robust and highly resistant long-chain monomers with a greater molecular mass and lower density. Plastics are regarded as the best packing materials because they are chemically resistant, robust and flexible, generally transparent, and particularly inert to oxygen and moisture ingress.

Microplastics may be broken down further into two categories: primary plastics and secondary plastics. If a piece of plastic is smaller than 5 mm in size when it enters the environment, we call it a microplastic. To name a few examples: clothes microfibers, microbeads, and plastic pellets typically used as packing materials. Secondary microplastics are produced when bigger plastic items break down in the environment due to weathering. Fluid and drink jars, blocking nets, and polythene covers are all examples of secondary plastics.

Chennai's rivers, the Adyar and the Cooum, are the primary conduits for the particles' transport to the Indian Ocean [1].

1.1 Microplastic Definition

Microplastics are very tiny fragments of plastics that cause environmental contamination. Microplastics are not just an exact form of plastic, but some sort of hard fragment with respect to the countrywide atmospheric and oceanic organization (NOAO), USA, smaller than 5 mm in thickness.

They reach natural ecosystems in variety of ways such as cosmetics, disposals, clothing, and industrial methods. There are two classifications of microplastics, basically (Fig. 1).

Fig. 1 Presence of microplastics in beach sediments

1.2 Primary Microplastics

These are any synthetic pieces or objects that previously have a dimension of 5.0 mm before they reach the environment. Those involve fabric tiny fibres, microbeads, and pellets made of plastic. Initial microplastics are tiny particles of synthetic which be created deliberately. These are commonly used in face cleaners or cosmetics, and in air blasting [2].

1.3 Secondary Microplastics

Secondary plastics are comparatively tiny fragments of plastics that are created by decomposing larger plastic waste at ocean and on terrain [1]. A combination of corporeal biochemical, and chemphotodegradation like photodegradation induced by daylight revelation that, over time [3], decreases plastic debris structural quality to a degree so as to virtually inaudible to the bare eye.

1.4 Sources of Microplastics

Aquatic studies often establish the existence of plastic debris within the environment. This involves collecting samples of plankton, examining sandy and gritty sediments, studying feeding of vertebrates and invertebrates, and evaluating associations with environmental contaminants [4]. Through these methods, microplastics are seen to be present from numerous sources in the environment, based on 2017 IUCN.

1.5 Potential Effects on the Environment

Microplastics are already found in any aspect of the world according to a systematic analysis of empirical evidence conducted by the Empirical Advice Mechanism of the European Union in 2019. Although thumbs down proof of well-known environmental danger from tiny plastic contamination, if emission persists at its current pace, threats would certainly become common within a century. At 2008 workshop on International Research at the Tacoma University of Washington on the Existence, Consequences and further Fate of Microplastic Aquatic Debris, researchers agreed those tiny synthetic is a problem in aquatic environment.

Microplastics can cause genetic damage to marine life. Studies have shown that microplastics absorb polycyclic aromatic hydrocarbons, which causes immunotoxicity, neurotoxicity, and genotoxicity to galloprovincialis, and can cause genetic damage to mussels [5].

1.6 Study Area

Chennai Metropolitan City is situated on India's south-east coast with 56 km of coastline and is Tamil Nadu state's capital city. Chennai is India's fourth most populated metropolitan region and sixth largest city with an annual population agglomeration of over 8.6 million residents. Marina Beach is an industrial beach in the town of Chennai, in the Bay of Bengal's Indian Ocean part [6]. The Marina Beach extends for 12 km down the town's shoreline. Two rivers ramble through Chennai, halfway through the Cooum Dam, and south of the Adyar Valley. Our study was performed out in a limited area of the beach of Marina, in the estuaries of Adyar and Cooum Bay, considering further microplastics chances. Samples were obtained in Adyar and Cooum estuaries [7] (Fig. 2).

Fig. 2 Satellite image of study area from Adyar to Cooum river estuaries along Marina beach, Tamilnadu, India

1.7 Necessity for the Project

Microplastics are an increasing global and local environmental concern. Plastic is manmade and is commonly known as plastic since it "breaks down" into pieces tinier than 5 mm (microplastics).

These are frequently confused as fruit and eaten by all types of aquatic creatures, from plankton to large whales. When the toxins are swallowed, they are released into the aquatic food system where they influence the biodiversity and fish [7].

1.8 Objective of the Project

i. To summarize the source of tiny plastics present in ocean ecology.
ii. To estimate microplastic load in coastal sediments and marine water.
iii. To discuss the environmental impact of microplastics in marine environment.
iv. To prevent or control this pollution characteristics and load should be known (Figs. 3, 4 and 5).

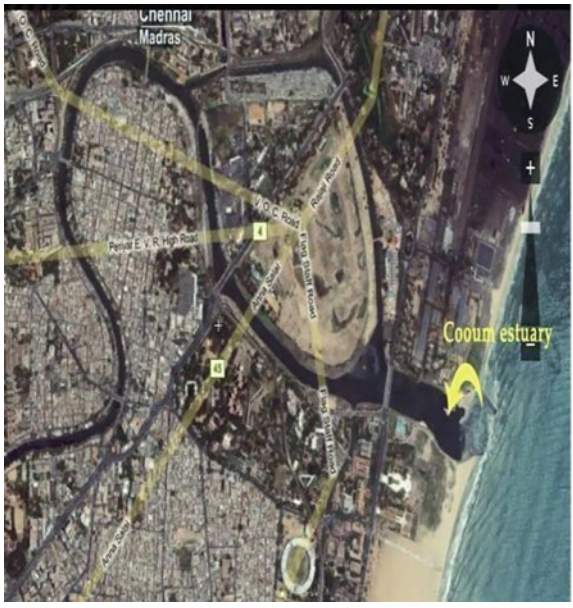

Fig. 3 Cooum estuary map

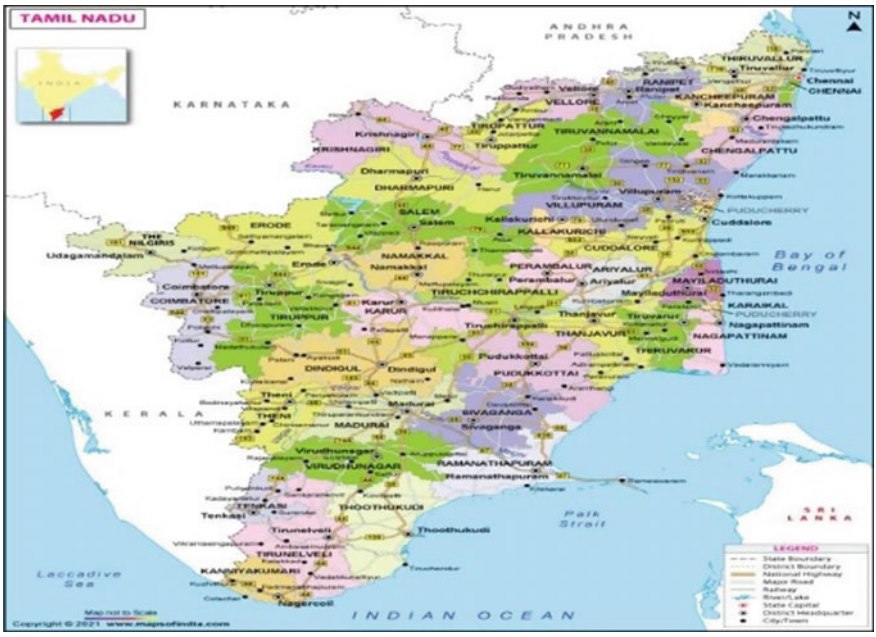

Fig. 4 Tamilnadu map

Fig. 5 India map

2 Methodology for Water Samples

2.1 General

Laboratory method used for determining the presence of plastics can be applicable for many common plastics including PE (0.00092–0.00097 kg/l), PPE (0.00097 kg/l), PVC (0.0014 kg/l), and PS (0.00105 kg/l). The microplastic size considered in this work is from 5 mm till 0.3 mm. This approach operationally describes microplastic debris as any firm substance in precise length range that is challenging to WPO, experiences flotation in a high molar salt solution, and passes successful visual examination at 40 × power under a microscope.

2.2 Sampling

Water samples are collected from the project area from different points by using centrifugal tubes of 100 ml volume, besides these bottles are also used for collecting volumes of larger quantity. Sampling of water was done for every metre distance of the previous (Fig. 6).

3 Methodology for Beach Sediments

3.1 General

This approach may be used to examine plastic debris gathered per shovel or spade in beach sand. Plastics include strong plastics, soft plastics (for example foams), prints, boards, fabrics, and papers. Sewing dry beach samples through 5 mm is to extract big macroscopic debris [6]. Figure 7 shows an inquiry of the microplastics analyses in beach sediments (Fig. 8).

4 Conclusion

The experiment was carried out in finding the microplastic load, and it was found to be feasible and low-cost method besides which it takes times [8]. The observation of the project has provided valuable insights into the presence and impact of microplastics in coastal ecosystems. The findings of this project highlight the urgent need for effective measures to address the issue of microplastic pollution and to protect marine environments.

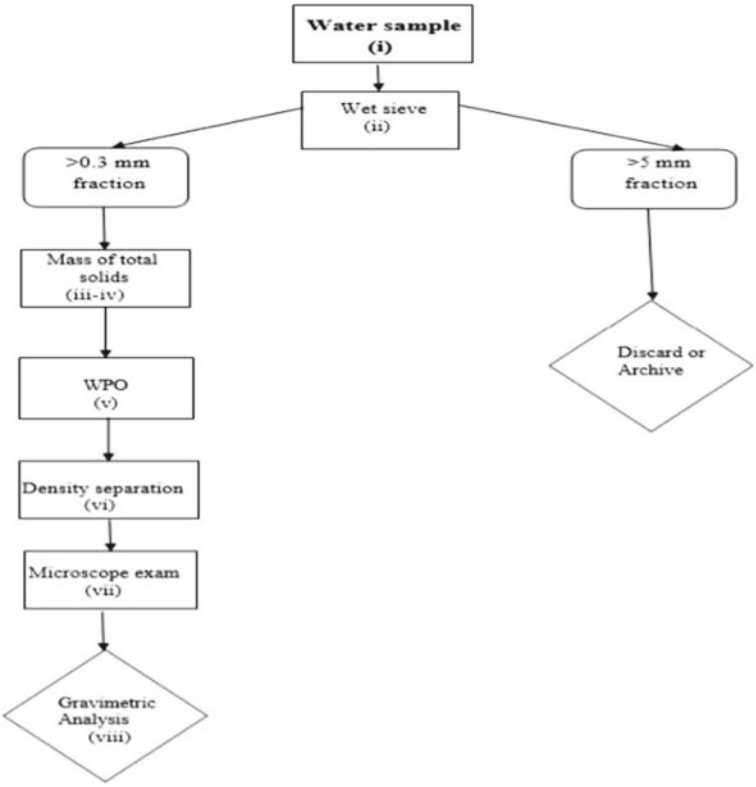

Fig. 6 Showing brief cote of the procedure carried out for laboratory testing

Through rigorous sampling and analysis, it was observed that beach sand is indeed a reservoir for microplastics, with various types and sizes of plastic particles being detected. This presence of microplastics poses a significant threat to marine life [9], as they can be ingested by organisms and enter the food chain, potentially causing long-term ecological consequences. Furthermore, the project shed light on the potential sources of microplastics in beach sand, such as urban runoff, improper waste management, and plastic debris from recreational activities. This information is crucial for designing targeted mitigation strategies and raising awareness among the public to prevent further contamination of coastal areas [10].

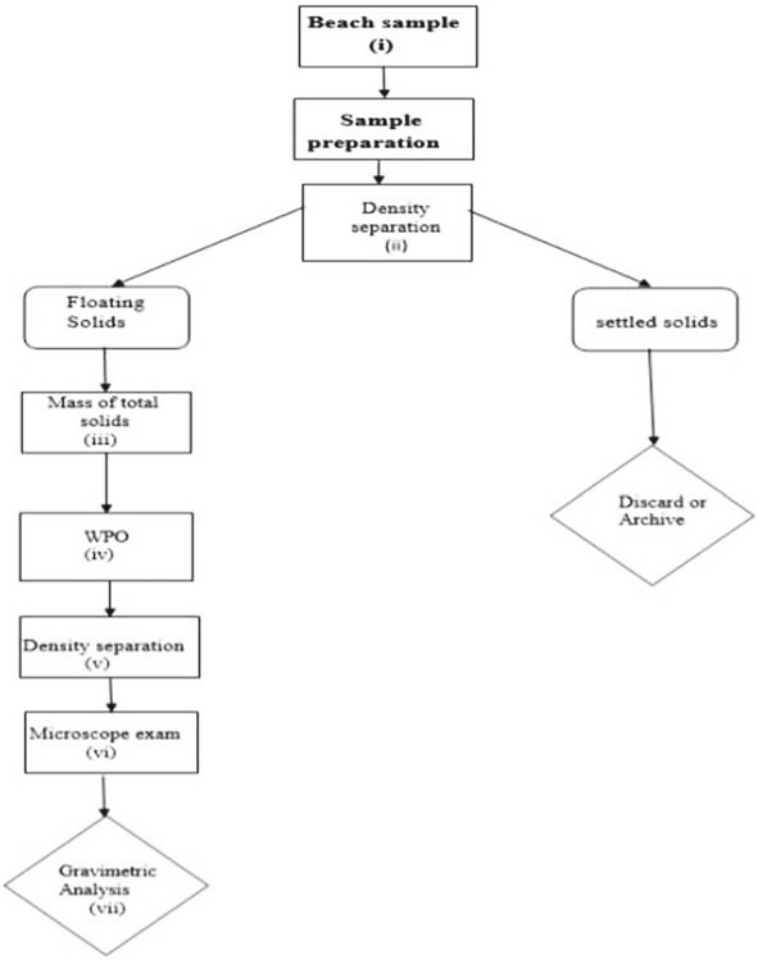

Fig. 7 Flow chart showing the laboratory procedure for beach sediment

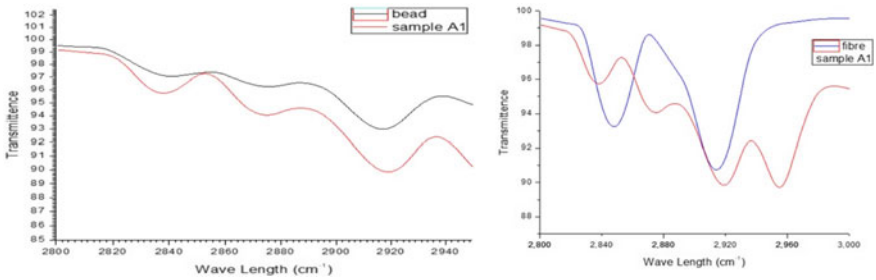

Fig. 8 Graphs showing presence of plastics in samples by transmittance values

References

1. Andrady AL (2011) Microplastics in the marine environment. Mar Pollut Bull 62:1596–1605
2. Cole M et al (2011) Microplastics as contaminants in the marineenvironment: a review. Mar Pollut Bull 62:2588–2597
3. Wang J et al (2016) The behaviors of microplastics in the marine environment. Mar Environ Res 113:7–17
4. Auta HS et al (2017) Distribution and importance of microplastics in the marine environment: a review of the sources, fate, effects, and potential solutions. Environ Int 102:165–176
5. Wrighta SL et al (2013) The physical impacts of microplastics on marine organisms. Environ Pollut 178:483–490
6. Claessensa M et al (2021) Occurrence and distribution of micro plastics in marine sediments along the Belgian coast. Mar Pollut Bull 62:2199–2204
7. Ivar do Sul JA et al (2014) The present and future of microplastic pollution in the marine environment. Environ Pollut 185:352–364
8. Coppock RL et al (2017) A small-scale, portable method for extracting microplastics from marine sediments. Environ Pollut 230:829–837
9. Ng KL, Obbard JP (2006) Prevalence of microplasticsin Singapore's coastal marine environment. Marine Pollut Bull 52:761–767
10. Ryan PG et al (2009) Monitoring the abundanceof plastic debris in themarine environment. Philos Trans R Soc B Biol Sci 364:185–215

Treatment of Wastewater with Phytoremediation Using Water Hyacinth—A Review

Niharika Bindal and S. Ramesh

Abstract The environment faces a growing threat from wastewater pollution, and traditional treatment techniques, such as chemical precipitation fail to provide long-term solutions as they merely transfer contaminants to sludge residue that ends up in landfills. However, water hyacinth, despite being a toxic species that can cause clogging in waterways, can be harnessed in line with sustainable development principles to effectively treat certain industrial wastes. Water hyacinth possesses the unique ability to naturally absorb toxic substances like lead, mercury, strontium-90, and other carcinogenic compounds, often present in concentrations thousands of times higher than those found in natural water sources. By utilizing the roots of water hyacinths, these pollutants can be effectively removed, offering a sustainable approach to wastewater treatment for both industrial and sewage water. The roots of water hyacinth create an environment conducive to the growth of aerobic bacteria, which aids in the elimination of various contaminants from water. This natural process enhances the water purification process, augmenting existing wastewater treatment procedures. Consequently, this paper provides a review of the efficacy of water hyacinths in removing pollutants from wastewater. In summary, water hyacinth demonstrates its potential as a valuable tool in wastewater treatment. Despite its invasive tendencies, when managed appropriately, water hyacinth can effectively remove pollutants from industrial and sewage water, contributing to sustainable water purification practices. This paper aims to explore and evaluate the effectiveness of water hyacinth in wastewater treatment as an eco-friendly solution for addressing the growing issue of water pollution.

Keywords Water hyacinth · Water pollution · Phytoremediation · Effluent treatment · Biological treatment

N. Bindal · S. Ramesh (✉)
Department of Civil Engineering, Faculty of Engineering and Technology, SRM Institute of Science and Technology, Kattankulathur, Tamilnadu 603203, India
e-mail: rameshs@srmist.edu.in

K. R. Reddy et al. (eds.), *Recent Advances in Civil Engineering*, Lecture Notes in Civil Engineering 398, https://doi.org/10.1007/978-981-99-6229-7_21

1 Introduction

Wastewater effluent poses a significant threat to the global ecosystem, and water pollution has become a major concern. The rate of wastewater generation has reached environmentally hazardous levels, with rapid population growth being a major contributor to this phenomenon. Consequently, pollution levels in bodies of water continue to rise [1]. A detrimental impact on aquatic life arises from the presence of excessive waste in water bodies. In recent years, numerous studies have been conducted to address water pollution and its effects on aquatic ecosystems.

One effective method for wastewater treatment involves the use of water hyacinth (*Eichhornia crassipes*), a free-floating aquatic plant. This remarkable plant possesses the unique ability to absorb nutrients and other substances from water, thereby reducing pollution levels [2]. The roots of water hyacinth play an active role in wastewater treatment, serving as the primary mechanism through which contaminants enter the plant. These roots exhibit a large surface area, enabling them to efficiently absorb and accumulate pollutants.

Conventional sewage treatment methods, such as trickling filters and activated sludge processes require substantial amounts of energy, cost, and manpower. To align with the shift toward non-conventional energy sources, it is crucial to urgently implement eco-friendly and energy-saving techniques for sewage treatment. Natural methods, which are highly cost-effective, should be prioritized in this regard [3]. Traditional wastewater treatment systems, such as the activated sludge process and trickling filters necessitate the use of energy. Furthermore, due to economic and space constraints, such treatment processes are extremely difficult to implement in rural areas. Such treatment plants also necessitate the use of skilled labor [4]. As a result, we must find a cost-effective and environmentally friendly substitute for such treatment plants [5].

Water hyacinth (*Eichhornia crassipes*) is a perennial, aquatic plant that thrives in shallow water and floats freely. It reproduces through stolons, allowing it to propagate and spread. With a height range of 100–200 mm, this plant can reach a maximum height of 1 m. Its distinguishing features include long, fluffy roots and glossy green leaves.

The flowers of water hyacinth are approximately 50 mm in diameter and display a pale violet or blue coloration. A water hyacinth plant is shown in Fig. 1. This versatile plant can thrive in both alkaline and acidic water conditions, although it demonstrates optimal growth in neutral water. Notably, studies have shown that wastewater does not have any adverse effects on the morphology of the plant [6]. This highlights its remarkable capacity for rapid and sustained growth, making it a valuable species for various applications and ecosystems.

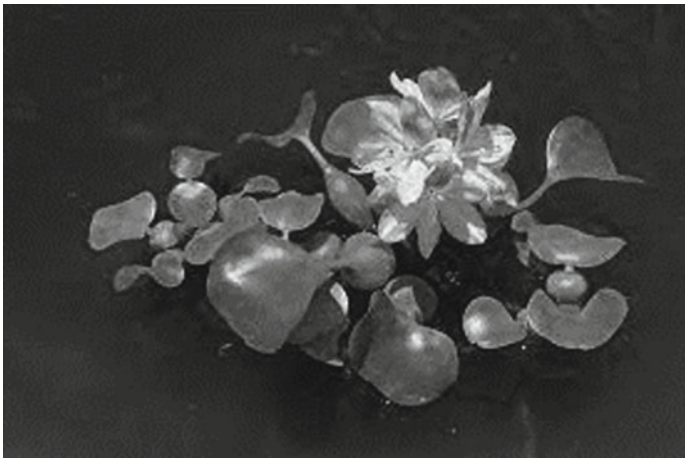

Fig. 1 Water hyacinth

An environmentally favorable element of ecological technology is its capacity for resource recovery and repurposing. For instance, in aquatic habitats, ecological food chains allow nutrients from phosphorous and nitrogenous. The utilization of wastewater components to generate usable biomass has become an important area of research and development. One promising candidate for wastewater treatment and biomass production is the water hyacinth (*Eichhornia crassipes*). This aquatic plant thrives in warm and nutrient-rich water, making it an ideal choice for wastewater treatment applications.

Water hyacinths can tolerate a wide range of hydrogen values, with the optimal growth occurring at a neutral H + ion potential. This characteristic makes them versatile in treating wastewater. The optimum water temperature for water hyacinth growth ranges from 28 to 30 °C. However, temperatures exceeding 33 °C can hinder their further development. Similarly, the ideal air temperature for their growth falls between 21–30 °C.

One remarkable feature of water hyacinths is their ability to grow in both nutrient-rich and nutrient-poor water, as well as in water contaminated with various biological and inorganic industrial effluents containing metal ions. This adaptability further enhances their potential as a wastewater treatment plant. Water hyacinths are popular and abundant free-floating plants that can quickly reproduce vegetatively and survive in harsh conditions. The highest possible reproductive rate is recorded as 54.4 g dry weight/m^2/day. During the summer season, their growth accelerates, resulting in a 15% increase in daily surface area.

Despite their benefits, water hyacinths pose significant challenges when they spread along rivers and inland canals. They can affect drainage systems, disrupt waterway traffic, and reduce agricultural output. Moreover, water hyacinths severely impact water supplies and restrict fishing activities. Their rapid expansion during

the rainy season also creates favorable breeding grounds for mosquitoes and other disease-carrying insects.

However, water hyacinths have not only been regarded as a nuisance but also as a valuable and precious raw material for handicrafts. Since the flood season in 2000, they have been exploited and utilized, leading to their recognition as a "new discovery of the twenty-first century."

In conclusion, water hyacinths offer the potential to recycle wastewater components into usable biomass while serving as a versatile and efficient wastewater treatment plant. Their ability to thrive in various conditions, coupled with their rapid growth rate, makes them a promising solution. Nonetheless, their uncontrolled spread and negative impacts on water resources and ecosystems require careful management and mitigation strategies.

This handicraft sector has helped many communities combat unemployment issues and raise farmers' incomes, which has helped fight hunger and reduce poverty. This profession's growth has improved the number of jobs and household incomes for farmers. As a result, water hyacinth is also extensively used as a source of manufacturing inputs [7–9].

The proliferation of water hyacinths in various water bodies, particularly during the rainy season, is a persistent issue. These plants exhibit extraordinary productivity, with just 10 individuals capable of generating an additional 600,000 plants over an eight-month growing season. This remarkable growth rate has earned water hyacinth the reputation of being one of the most productive photosynthetic plants globally. While this rapid expansion poses concerns in rivers, it can actually be advantageous when considering their implementation in wastewater treatment systems.

Phytoremediation, which involves utilizing plants and their inherent metabolic and hydraulic processes, provides a method to remove, degrade, or contain contaminants. Water hyacinths possess desirable characteristics that make them well-suited for integration into wastewater treatment systems. Extensive research has shown the effectiveness of water hyacinth in enhancing the quality of effluent in oxidation ponds and integrated treatment systems. Furthermore, it has the ability to absorb significant amounts of inorganic nitrogen and phosphorus present in both domestic sewage and industrial wastewater.

The roots of water hyacinth play a crucial role in the absorption of heavy metals from the water. These metals are then transported to the shoots and other tissues of the plant, resulting in their accumulation. This process highlights the potential of water hyacinths in remediation efforts targeting heavy metal contamination.

Overall, water hyacinths offer an opportunity for efficient wastewater treatment through their rapid growth, nutrient absorption capabilities, and heavy metal remediation potential. By harnessing these attributes, they can play a valuable role in improving the quality of water bodies affected by pollutants. This natural process aids in the removal and sequestration of heavy metal contaminants, contributing to the overall purification of wastewater [10]. Textile industry map of India is shown in Fig. 2.

Research Gap-A fixed mechanism and process is not given for the setup of the hyacinth treatment plant. Hyacinth has not been used to the extent that the reuse of

Fig. 2 Textile industry map

water can be done. Analysis of wastewater with different amounts of plants was not done.

2 Literature Review

Survey of the past research papers and journals have been done to understand the procedures of the work and find out what has been done. By doing these literature review, enough information was obtained to help with the project. This literature has been studied and summarized below [11].

Saravanan et al. studied the usage of water hyacinth to treat the textile effluent water. In this study textile wastewater is collected from textile industries. The samples

are collected in three fish tanks. The collected water was diluted at three different ratios and water hyacinth roots were used for phytoremediation of the chemical dye. The test was conducted for five days. Utilizing water hyacinth, study determines the decrease of chromium and iron (*Eichhornia crassipes*). Drinking water is diluted at the ratios of 35, 40, and 45% to treat wastewater. With time, it demonstrates that all of the contaminants have significantly decreased as a result [7].

Shamima Siddika et al. studied the characteristics of the raw textile effluent and then collected the sample in 4-L jars. One glass jar and one plastic jar were used. Roots of water hyacinth were used for the test. Then various tests, such as BOD, COD, DO, TSS, and pH were performed. Standard techniques and tools were used to measure the parameters. BOD, COD, TSS, TDS, pH, DO, and dye concentration. In general, DO was absent from every sample of collected wastewater. The amount of DO increased following water hyacinth treatment, as seen [8].

Kulkar et al. studied the usage of water hyacinth by using an underground trench. The underground trench was made one brick thick and lining was provided. Textile industry effluent was collected in the underground trench and plastic cover was provided. Water hyacinth is released in the trench. Then various tests like COD and heavy metals were performed as per as standard methods of APHA [9].

Nuredin Muhammed et al. studied about the adsorption capabilities of water hyacinth. Water hyacinth was collected from Lake Tana, Bahir dar, Ethiopia. Adsorption test was done by varying pH, WH dose and initial concentration of RR HE3B dye [12].

Khan et al. studied about removal of dye by water hyacinth. First several parameters, such as BOD, COD, DO, TSS, and pH were measured and then water hyacinth was used to treat the wastewater effluent. Standard techniques and tools were used to measure the parameters. A BOD incubator was used to measure BOD, a COD test kit was used to measure COD, a portable DO meter was used to measure DO, a standard thermometer was used to measure temperature, a digital PH meter was used to measure PH, a digital TDS meter was used to measure TSS, and a standard titration method was used to measure hardness. In-house testing was done on these parameters at DBL ETP [13].

Sanmuga et al. studied about the removal of dye methylene blue with the help of water hyacinth. Maximum sorption for methylene blue and Victoria blue was measured, second-order model and Lagergren's model was used [3].

3 Materials and Methodology

Water hyacinth is an aquatic vascular plant characterized by its rounded, upright, shiny green leaves, and orchid-like lavender flowers. It is a perennial plant that exhibits rapid growth and possesses a high rate of reproduction. Notably, water hyacinths thrive optimally in neutral water pH conditions, but they can tolerate pH values ranging from 4 to 10. This adaptability is significant as it indicates the potential of water hyacinths for treating diverse types of wastewater.

In the pursuit of advanced techniques for treating heavy metals in wastewater, one approach involves precipitating the metals as hydroxides using lime or caustic at a pH level where their solubility is at its lowest. However, depending on the reagent used, this process can be costly. Furthermore, the resulting precipitates still require proper disposal, often involving concentration and containment in drums for ultimate disposal or disposal in landfills. Consequently, while this method addresses the immediate concern of pollution in water, it simply transfers the issue to another environmental medium—land. Therefore, this approach cannot be considered a sustainable long-term solution to the wastewater problem [14, 15].

Domestic wastewater is created by human activities such as bathing, washing dishes, doing laundry, disposing of trash, using the toilet, and other household tasks. Even small amounts of contaminants in domestic wastewater can have a significant adverse impact on the environment. Pathogenic bacteria, contagious viruses, common household chemicals, and excessive nutrients like nitrate are often found in domestic wastewater. Therefore, effective purification of domestic wastewater is essential to mitigate these pollutants [12, 16, 17]. Water hyacinth, with its high capacity for pollutant removal, proves to be an excellent choice for treating domestic wastewater. Specific purification goals are established based on principles that support the removal of contaminants. Implementation of water hyacinth treatment significantly reduces coliform counts [18]. In recent years, artificial wetlands utilizing various types of rooted, emergent, and free-floating aquatic plants, as well as facultative ponds, have gained considerable attention for the treatment of domestic sewage.

The water hyacinth (*Eichhornia crassipes*), with its rapid growth rate and extensive root system, is particularly suitable for pollutant removal. In a water hyacinth lagoon, this free-floating species serves as a horizontal trickling filter, and the immersed roots provide physical support for the growth of biofilm bacteria. Despite global efforts, the construction of aquatic systems, including water hyacinth treatment, has not gained widespread popularity due to the significant land area and financial investment required [19, 20]. In a standard water hyacinth system, the transfer of oxygen through the floating plants results in the separation of the water column into three distinct zones: facultative, aerobic, and anaerobic. This zoning contributes to the overall effectiveness of the water hyacinth treatment process.

In summary, even the presence of small amounts of contaminants in domestic wastewater necessitates effective purification methods. Water hyacinth has proven to be a valuable option for pollutant removal, with its ability to reduce coliform counts and its suitability for treatment systems. However, the widespread adoption of water hyacinth treatment faces challenges due to land requirements and financial considerations. Understanding the zoning and oxygen transfer within water hyacinth systems enhances their efficiency in purifying domestic wastewater.

Wastewater produced by a wide range of production and processing procedures is known as industrial effluent. Industrial wastewater can contain a variety of different components, depending on the business. Along with other components like heavy metals, acids, and alkalis, organic molecules like oils, lipids, alcohols, and flavorings also interact with the water. Before being discharged to sewage treatment facilities for the general public, the environment, or internal reuse, this type of wastewater

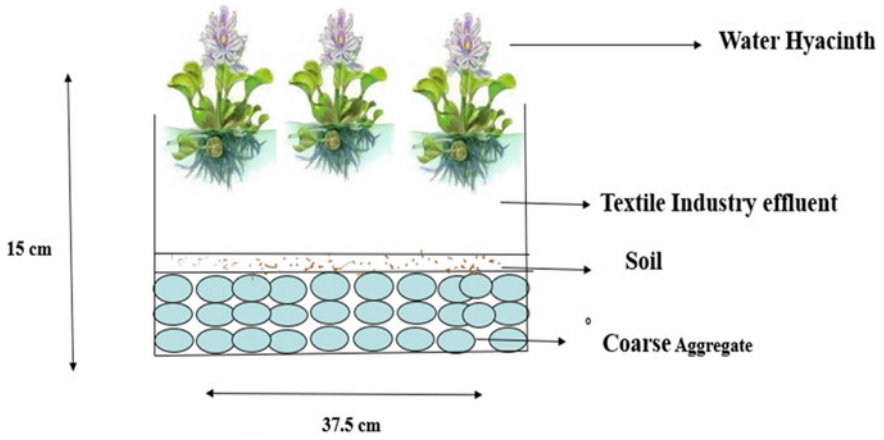

Fig. 3 Design of phytoreactor

must first undergo pretreatment. The utilization of aquatic macrophytes for phytoremediation of industrial effluent has gained popularity as an alternative to costly and energy-intensive treatment technologies [4]. Phytoremediation proves to be a viable method for treating both industrial effluent and municipal wastewater [11]. Water hyacinth, in particular, has been found to effectively treat paper mill effluent. Water hyacinth exhibits a faster growth rate in polluted wastewater and displays a high tolerance level compared with other aquatic plants [21].

Overall, the use of water hyacinth and other aquatic macrophytes in phytoremediation offers a cost-effective and environmentally friendly approach for treating industrial effluent and municipal wastewater, contributing to the restoration and preservation of water quality. Design of phytoreactor is shown in Fig. 3.

The application of traditional methods, such as heavy metal treatment by physical and chemical processes has a number of drawbacks, including many complex processes, high economic costs, and high technical requirements. Several metals have incredibly strong water hyacinth attraction and accretion capabilities [11, 18]. In a sense, a typical marshland populated by water hyacinths might serve as "nature's kidney" for effective sewage treatment, protecting the planet's priceless water resources [3]. Water hyacinth has attracted a lot of interest due to its ability to grow in highly polluted water and its propensity to absorb metal ions. Around the world, water scarcity is growing more common, and by the end of the year, it may be inescapable in many nations.

4 Results and Discussion

During the trial period, water hyacinth demonstrated notable treatment efficiencies for several heavy metals. Specifically, the efficiencies for Cd, As, Pb, Zn, and Cu were recorded as 59.4%, 60.8%, 92.4%, 60.2%, and 60.7%, respectively. These efficiencies corresponded to initial concentrations of 0.5, 0.5, 2, 5, and 5 mg/l. At the conclusion of the 30-day survey period, the water hyacinths exhibited high rates of heavy metal removal, ranging from 59 to 92% [22, 23]. Notably, after 30 days, the remaining heavy metal content in the water treated with water hyacinths significantly decreased. Only 7.65% of the initial Pb concentration (2 mg/l) remained [22, 23].

Conventional methods are not efficient for removing color from wastewater. However, phytoremediation, which involves using plants, including water hyacinth, has proven to be an effective technique for removing heavy metals and other pollutants [24]. Water hyacinth possesses dye absorption properties, along with a good growth rate and low maintenance requirements in contaminated areas. Additionally, it has the capability to eliminate harmful pathogenic bacteria [16]. In the phytoremediation process, photosynthetic activity and plant growth rate play crucial roles. To address the challenges associated with water resource usage, various sustainable techniques have been developed, and wastewater recovery and reuse have become top priorities. Anthropogenic sources, such as domestic and industrial waste are significant contributors to metal contamination in aquatic habitats [25]. Even trace amounts of heavy metals in water pose hazards. The industrial revolution has led to a dramatic increase in dangerous metal contamination in the biosphere. Aquatic plants, such as water hyacinth play a critical role in wastewater treatment as they efficiently remove various contaminants from water. Nutrient pollution and eutrophication of water bodies primarily stem from nitrogen and phosphorus.

The principles governing nutrient removal in plants, such as water hyacinths differ from those governing biological waste degradation in sewage and oil refinery effluent-holding ponds [2, 6, 10]. Nutrients enter watercourses at an alarming rate due to municipal wastewater discharges, agricultural runoff, and industrial waste disposal [20]. In another study, a facultative lagoon that incorporated water hyacinths throughout the year achieved a reduction of 70% in both total suspended solids (TSS) and five-day biological oxygen demand (BOD5). This lagoon received discharge from a primary aerated lagoon, and due to the shorter wastewater retention time (averaging only seven days), the overall BOD and TSS reductions were slightly lower compared with the first study (where the retention time was 51 days) [4]. The research suggests that shallow holding ponds require shorter holding periods than relatively deep ponds, and a series of small interconnected ponds can be more efficient than a single large pond. Water hyacinth plants have shown an increased absorption of phosphorus as the concentration of phosphorus in the water increased from 0 to 40 mg/l. The desired purity of the final sewage effluent can be controlled by adjusting the surface area of the water hyacinth, harvest rate, and retention time [26].

4.1 Limiting Growing Factor

Water hyacinths only have floats when grown in direct sunlight. Flowering is significantly delayed at either end of the spectrum (red or violet). Water hyacinths cannot tolerate cold temperatures and are susceptible to frost damage. The ideal temperature is close to 24 °C [27, 28]. Utilizing a closed/covered/controlled environment, water hyacinths culture can still prove to be an inexpensive but efficient method for waste treatment. The water hyacinth can tolerate salt water only briefly. Plants can tolerate 1000 mg/1 salinity for indefinite periods; whereas, 2000 mg/1 salinity is usually lethal after 30-day exposure periods. Plant reproduction is hampered in waters with an average dissolved oxygen concentration of 1 mg/1. When the dissolved oxygen level is 3.5–4.8 mg/1, water hyacinths grow rapidly [9]. Because reoxygenation from the surface is inhibited, the water beneath a dense mat of water hyacinths is virtually devoid of all life. Mechanical aeration, in addition to frequent harvesting, may be required to keep the pond surface aerobic when using water hyacinths for wastewater treatment [29].

5 Alternative Uses of Water Hyacinth

Water hyacinths have been studied for a variety of useful applications. Schemes for harvesting compost and soil additives, extracting chlorophyll and carotene, producing high-protein cattle feed, producing pulp, paper, and fiber, and, most importantly, providing biogas as an energy source are all included. Now, it is possible to recover valuable heavy metals by gathering, igniting, and extracting from the ash, the metals. Plant ash would have a greater metal concentration than most ores if it contained 1% by weight of a metal, which is more than the metal content found in most ores [28]. As an alternative, the harvested water hyacinths can be utilized to produce biogas, with the non-biodegradable waste being put back into the ground [18].

6 Modification of Process

Multiple researchers have explored the potential of enhancing the biosorption properties of water hyacinth and its various components through chemical modification and processing. Their findings indicate that acid/alkali-treated water hyacinth exhibits greater effectiveness in removing specific metal ions compared with untreated plant components. The effects of treating biomass with acids and alkalis have been extensively studied to investigate the biosorption of metal ions. This is attributed to the ionization of different functional groups present on the surface of the adsorbents in an aqueous solution, enabling them to participate in cation binding with the metal ions [30].

7 Conclusion

The utilization of water hyacinth in phytoremediation processes for wastewater treatment holds significant promise and merits attention as an environmentally friendly and sustainable solution. Water hyacinth's ability to rapidly absorb and remove various pollutants, including heavy metals and organic compounds, makes it a valuable asset in the purification of industrial and sewage water. By harnessing the unique characteristics of water hyacinth, such as its fast growth rate, extensive root system, and adaptability to diverse environmental conditions, effective remediation of wastewater can be achieved. The roots of water hyacinth provide an ideal habitat for aerobic bacteria, facilitating the breakdown and removal of contaminants through biological processes. Moreover, the use of water hyacinth aligns with the principles of sustainable development as it offers an alternative to traditional treatment techniques that often result in the transportation of pollutants to landfills. By utilizing water hyacinth, pollutants are naturally absorbed, preventing their release into the environment and minimizing the ecological impact.

In conclusion, the treatment of wastewater through phytoremediation using water hyacinth presents an effective, cost-efficient, and sustainable approach to addressing the issue of wastewater pollution. Further research and exploration are needed to optimize the operational parameters, assess potential ecological impacts, and develop integrated treatment systems that combine water hyacinth with complementary technologies. By harnessing the potential of water hyacinth, we can work toward a cleaner, healthier environment and secure a more sustainable future for wastewater management [31–33].

References

1. Sanmuga Priya E, Senthamil Selvan P (2017) Water hyacinth (*Eichhornia crassipes*)—an efficient and economic adsorbent for textile effluent treatment—a review. Arab J Chem 10:S3548–S3558
2. Low KS, Lee CK, Tan KK (1995) Biosorption of basic dyes by water hyacinth roots. Bioresour Technol 52(1):79–83
3. Huynh AT et al (2021) A small-scale study on removal of heavy metals from contaminated water using water hyacinth. Processes 9(10):1802
4. Dahake AS, Hedaoo MN (2008) Application of water hyacinth (*Eichhornia crassipes*) in wastewater treatment—a review. Int Res J Eng Technol 2008. Accessed 31 Jan 2023
5. Wrona Z, Buchwald W, Ganzha M, Paprzycki M, Leon F, Noor N, Pal C-V (2023) Overview of software agent platforms available in 2023. Information 14(6): 348
6. Kutty SRM, Ngatenah SNI, Isa MH, Malakahmad A (2009) Nutrients removal from municipal wastewater treatment plant effluent using Eichhornia crassipes. pp 1115–1123
7. Honlah E, Yao Segbefia A, Odame Appiah D, Mensah M, Atakora PO (2019) Effects of water hyacinth invasion on the health of the communities, and the education of children along River Tano and Abby-Tano Lagoon in Ghana. Cogent Soc Sci 5(1):1619652
8. Sutadian AD, Muttil N, Yilmaz AG, Perera BJC (2018) Development of a water quality index for rivers in West Java Province, Indonesia. Ecol Indic 85:966–982

9. Soeprobowati TR et al (2016) The water quality parameters controlling diatoms assemblage in Rawapening lake, Indonesia. Biodiversitas 17(2):657–664
10. Jayaweera MW, Kasturiarachchi JC, Kularatne RKA, Wijeyekoon SLJ (2008) Contribution of water hyacinth (*Eichhornia crassipes* (Mart.) Solms) grown under different nutrient conditions to Fe-removal mechanisms in constructed wetlands. J Environ Manage 87(3):450–460
11. Cotoruelo LM, Marqués MD, Díaz FJ, Rodríguez-Mirasol J, Rodríguez JJ, Cordero T (2010) Equilibrium and kinetic study of Congo red adsorption onto lignin-based activated carbons. Transp Porous Med 83:573–590
12. Buasri A, Chaiyut N, Tapang K, Jaroensin S, Panphrom S (2012) Biosorption of heavy metals from aqueous solutions using water hyacinth as a low cost biosorbent. Civil Environ Eng 2(2):17–24. Accessed 31 Jan 2023
13. Soeprobowati TR, Tandjung SD, SUTIKNO S, Hadisusanto S, Gell P, HADIYANTO H, Suedy SWA (2016) The water quality parameters controlling diatoms assemblage in Rawapening Lake, Indonesia. Biodiversitas J Biological Diversity 17(2)
14. Center TD, Spencer NR (2023) The phenology and growth of water hyacinth (*Eichhornia crassipes* (Mart.) Solms) in a eutrophic north-central Florida lake. Aquat Bot 10:1–32. https://doi.org/10.1016/0304-3770(81)90002-4
15. Lake V et al The growth rate and chlorophyll content of water hyacinth under different type of water sources You may also like Water hyacinth as a possible bioenergy resource: a case of The growth rate and chlorophyll content of water hyacinth under different type of water sources
16. Bhattacharya A, Kumar P (2010) Water hyacinth as a potential biofuel crop 9(1)
17. Robinson T, McMullan G, Marchant R, Nigam P (2001) Remediation of dyes in textile effluent: a critical review on current treatment technologies with a proposed alternative. Bioresour Technol 77(3):247–255
18. dos Santos AB, Cervantes FJ, van Lier JB (2007) Review paper on current technologies for decolourisation of textile wastewaters: perspectives for anaerobic biotechnology. Bioresour Technol 98(12):2369–2385
19. Soeprobowati TR (2017) Lake management: Lesson learn from rawapening lake. Adv Sci Lett 23(7):6495–6497
20. Rahim A, Soeprobowati TR (2019) Water pollution index of Batujai reservoir, Central Lombok Regency-Indonesia. J Ecol Eng 20(3):219–225
21. Chanakya HN, Borgaonkar S, Meena G, Jagadish KS (1993) Solid-phase biogas production with garbage or water hyacinth. Bioresour Technol 46(3):227–231
22. (PDF) The Growth Rate of Water Hyacinth (*Eichhornia crassipes* (Mart.) Solms) in Rawapening Lake, Central Java. https://www.researchgate.net/publication/352174689_The_Growth_Rate_of_Water_Hyacinth_Eichhornia_Crassipes_Mart_Solms_in_Rawapening_Lake_Central_Java. Accessed 11 Feb 2023
23. Prasetyo S, Anggoro S, Soeprobowati TR (2021) The growth rate of water hyacinth (*Eichhornia crassipes* (Mart.) Solms) in Rawapening Lake, Central Java. J Ecol Eng 22(6):222–231
24. Rezania S et al (2016) The efficient role of aquatic plant (water hyacinth) in treating domestic wastewater in continuous system. Int J Phytoremed 18(7):679–685
25. Prasetyo S, Anggoro S, Soeprobowati TR (2021) The growth rate of water Hyacinth (Eichhornia crassipes (Mart.) Solms) in Rawapening Lake, Central Java. J Ecol Eng 22(6)
26. Nutrient Removal by Water Hyacinths on JSTOR (2023)
27. Worqlul AW et al (2020) Spatiotemporal dynamics and environmental controlling factors of the lake tana water hyacinth in Ethiopia. Remote Sens 12(17):2706
28. Ho YS, McKay G (1998) Sorption of dye from aqueous solution by peat. Chem Eng J 70(2):115–124
29. Tolerance limits for industrial effluents discharged into inland surface water-Textile industries
30. Kriticos DJ, Brunel S (2016) Assessing and managing the current and future pest risk from water hyacinth, (*Eichhornia crassipes*), an invasive aquatic plant threatening the environment and water security. PLoS One 11(8):e0120054
31. Ingole NW, Bhole AG (2003) Removal of heavy metals from aqueous solution by water hyacinth (*Eichhornia crassipes*). J Water Supply Res Technol AQUA 52(2):119–128

32. Prasetyo S, Anggoro S, Soeprobowati TR (2021) The growth rate of water hyacinth (*Eichhornia crassipes* (Mart.) Solms) in Rawapening Lake, Central Java. J Ecol Eng 22(6):222–231
33. Jadia CD, Fulekar MH (2010) Phytoremediation of heavy metals: recent techniques. Afr J Biotechnol 8(6):921–928

An Overview of Algae-assisted Microbial Fuel Cell for the Treatment of Sugarcane Industry Effluent

S. K. Amaya, S. Dhansekar, and C. Sharan

Abstract Algae, being a photosynthetic eukaryotic organism, play a major role as oxygen producers in water bodies. Apart from that, they have the ability to absorb nutrients and convert them into biomass. Thus, considered as a favorable wastewater treatment agent. The sugarcane industry plays a vital role in the global agro-based sector, producing a significant amount of sugar annually. However, the cultivation process results in the generation of large volumes of contaminated effluent. Sugarcane industry produces more than 180 million metric tons of sugar annually on a global scale produce around 1 m^3 of contaminated effluent per ton of sugarcane processing. Incorporating algae in sugarcane industry effluent treatment using microbial fuel cell (MFC) can give highly efficient output as it contains more nutrients. In recent years, the integration of algae-assisted microbial fuel cells (AMFCs) has emerged as a promising technology for effluent treatment. This review aims to provide a comprehensive overview of the application of AMFCs in treating sugarcane industry effluent. The review examines the underlying principles of AMFCs, highlighting their ability to harness the power of microbial communities and algae for simultaneous wastewater treatment and energy generation. It presents case studies and experimental results to illustrate the performance and potential of AMFCs in removing pollutants and producing electricity from sugarcane industry effluent. And sufficient removal of pollutants such as BOD, COD, ammonia, total nitrogen, and phosphorus are identified. And power generation of AMFC is varying according to the type of wastewater, type of algal species used, as well as the conditions provided. Overall, this review sheds light on the significant role of algae-assisted microbial fuel cells in the sustainable treatment of sugarcane industry effluent, offering insights into their potential as an innovative and eco-friendly solution for the industry's wastewater management.

Keywords Algae · Sugarcane industry effluent · Biological wastewater treatment · Phycoremediation · Microbial fuel cell

S. K. Amaya · S. Dhansekar (✉) · C. Sharan
Department of Civil Engineering, Faculty of Engineering and Technology, SRM Institute of Science and Technology, Kattankulathur, Tamilnadu 603203, India
e-mail: dhanases@srmist.edu.in

K. R. Reddy et al. (eds.), *Recent Advances in Civil Engineering*, Lecture Notes in Civil Engineering 398, https://doi.org/10.1007/978-981-99-6229-7_22

1 Introduction

Industrialization plays vital role for development of any country in the world. Due to industrialization, urbanization, and population explosion, fresh water utilization and wastewater production is unavoidable. Even though water consumption depends upon the technological processes inside the plant, sugar industry is one of the top water user and wastewater generator. Almost every division of sugarcane industry like processing plant, boilers, mill house, cooling towers, etc., makes use of huge amount of water which results in generation of wastewater [1]. It has become a practice that sugar industry is discharging of its effluent into surrounding terrestrial and aquatic systems. Approximately 1 m^3 of water is required for processing 1 ton of sugarcane. So minimum 0.8 m^3 of wastewater may be generated. This effluent consists of organic and inorganic pollutants. While other industries are adopting new process technologies and developments, sugarcane industry has been following the same processes for almost past 50 years, which results in serious environmental pollution [2]. In the socioeconomic and agricultural status of a country, sugar industry plays a major role [3]. Due to lack of environmentally friendly technologies, sugarcane industry will lead to water pollution as well as reduction in environmental quality. The discharge of untreated or not properly treated effluent into the surrounding will create water pollution, soil pollution, and will have a negative impact on fish, crops, and human health. Effect of sugarcane industry effluent on soil includes change in physio-chemical properties of soil, effect on microflora, change in cellulase, enzyme activity in soil, etc. [2]. That of water includes surface and ground water pollution.

Sugarcane is a tall perennial grass that belongs to *Saccharum* genus and it comprises of 10 different species. Sugar was produced from sugarcane plant after first century AD in India. By the end of medieval period, as sugar is known worldwide, it became expensive and considered as a "fine spice". But later on, from about sixteenth century due to technological improvements and new world sources of raw material, it turned into a much cheaper commodity. In 1939, global sugar production is estimated to have been 35 million tons. But due to the outbreak of World War 2, output declined to 28 million tons. The world production rose from just below 86.64 million tons in 1974–1975 to over 181.1 million metric tons in 2021–2022 [4].

Worldwide total sugar production has been changing up and down throughout the decade due to climate change, demand, and other several independent reasons. One of the main crops used to generate foreign exchange in India is sugarcane, which plays a significant role as a cash crop there. The sugar industry operates only for a maximum of 5–6 months out of the year. Even though it is possible to create sugar from sugar beets, corn, and other fruits and vegetables, sugarcane is the primary raw material used in the production of sugar due to its high amount of sucrose concentration. Worldwide, about 80% of sugar comes from sugarcane, whereas the rest is derived from sugar beets. 70% of sugarcane contains water, 10–15% sucrose, 14% fiber, and 2–3% of soluble impurities. Production of sugar involves two major processes. They are, conversion of sugarcane to raw sugar and processing of raw sugar into refined sugar [5].

Among the wide varieties of sugarcane, *Saccharum officinarum* has high sugar content. Collection of raw material is a major step in sugar production as percentage of sugar plays a major role in quantity of sugar produced and thereby the economy of production. Cleaning of sugarcane, crushing and extraction of sugar juice is done at the stage of milling. In some countries extraction is done using diffusion process as it can give high rate of extraction with reduced energy consumption and low operation and maintenance cost. The juice is heated and filtered during the process of clarification along with sulfitation and carbonation. There are 732 installed sugar industries in India with an annual output of approximately worth Rs. 80,000 crores. It is identified that sugarcane industry effluent contains miscellaneous qualities such as high BOD, COD, grease, dissolved solids, etc. Higher BOD level can lead to eutrophication or leachate formation with time as well as it will eventually affect human body through food chain [1].

Microalgae have a great deal of potential as a biological phytoremediation agent that could be used to remediate wastewater as well as produce energy and third-generation biofuel. The cost of water treatment is influenced by the capacity of microalgae to treat various water sources, which varies due to various water properties. Microalgae play a significant role in supplying the world's energy needs and serve as the primary raw material for sustainable goods. The advantage of algal treatment of wastewater over traditional wastewater treatment is the cost-effectiveness of the operation, which benefits developing nations. For instance, the expense associated with mechanical aeration can be reduced by using the O_2 produced during the photosynthetic activity of microalgae. Due to their adaptability to a variety of environmental conditions, simplicity in structure and growth requirements, and capacity to produce a wide range of end products, microalgae have been used in several applications around the world. In reality, microalgae may remove undesired nutrients from polluted water bodies, which serve as a growth source for microalgae while providing a promising number of important end products. This involves utilizing the plentiful nitrogen and phosphate found in wastewaters for growth [6].

2 Materials and Methodology

2.1 Bioremediation

Bioremediation is the process of using biological agents to restore natural resources. These bioremediation techniques use bacteria (anaerobic, aerobic-activated sludge, fermentation) and other microbes (fungi in composting), plants (phytoremediation), and algae (phycoremediation). Due to organisms' intrinsic ability to absorb, collect, and breakdown prevalent and emerging pollutants, using biological assets to clean up contaminated settings has risen in favor. As it seeks to be affordable, scalable, sustainable, and eco-friendly, bioremediation may offer significant advantages over traditional physicochemical treatment methods [7].

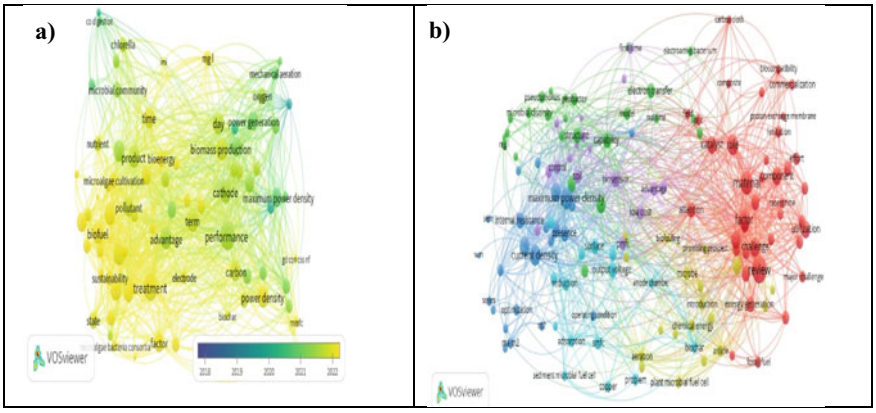

Fig. 1 **a** Bibliometric analysis based on recent five-year data; **b** Systematic review based on key words

2.1.1 Phycoremediation

Strategies for phycoremediation, a type of bioremediation, take into account the potential for using a variety of algae to remove dangerous chemicals. The term phycoremediation is often referred to as "use of algae to treat wastes or wastewaters". The algae have the ability to reduce carbon emissions when paired with the production of biofuel and integrated with waste treatment [8].

2.2 Different Types of Wastewater Treatment Using Different Algae

Bibliometric analysis based on last five- year data and systematic review based on key words are shown in Fig. 1a and b respectively.

2.3 Sugarcane Industry Wastewater

The sugar factory produces wastewater that is extremely variable in both quality and quantity by using freshwater in various sugar production units. Due to the complicated nature of the wastes produced and the limited technology to remove all contaminants at once, inappropriate management of industrial wastewater is one of the most serious environmental issues facing emerging countries.

Hence, using wastewater from the sugar industry directly to irrigate crops without sufficient treatment and dilution severely reduces the growth of seedlings and germination of seeds.

Table 1 Observed values of untreated effluent from sugarcane industry and general standards of discharge

Parameters	Unit	Observed values of untreated effluent from sugarcane industry	General standards of discharge as per Environmental Protection Act (1986)
pH	–	5.5–8.0	5.5–9.0
BOD_3	mg/L	500–1000	30
COD	mg/L	1500–2500	250
TSS	mg/L	100–400	100
TDS	mg/L	1000–2500	–
Sulfate	mg/L	750–800	–
Color	–	Light brown	All efforts should be made to remove color and unpleasant odor as far as practicable
Temperature	°C	30–40	Shall not exceed 5 °C above the receiving water temperature
Chloride	mg/L	180–210	< 250
oil and grease	mg/L	16–20	10

Observed values of untreated effluent from sugarcane industry and general standards of discharge as per Environmental Protection Act (1986) [9] are given in Table 1.

3 Microbial Fuel Cell

Microbial fuel cell is an advanced waste to energy technology that is used in effluent treatment plants recently. Implementation of microbial fuel cell (MFC) in treatment process will help in removing pollutants as well as generating electricity at the same time. Microbial fuel cell is a bio-electrochemical process in which electricity is generated by electrons derived from biochemical reaction. The removal rates obtained with the aid of MFC technology are equivalent to those obtained with industrial wastewater treatment systems, especially without significant energy consumptions. Microbial fuel cell approximately removes 90% of COD and BOD, and compared with other biological processes it releases 50–90% lesser sludge [10]. During late twentieth century, MFCs are first proposed in wastewater treatment. Enhanced productivity in this technology is achieved since then by continuous development [11, 12]. Major benefits of MFCs are it produces electricity by utilizing chemical energy from waste water, works at room temperature, reduced sludge production, and environmentally friendly [13, 14].

The increasing uses of microbial fuel cell technology have surpassed bioelectricity generation capability, and today, more attention is being paid to remediate effluents

generated from different sources [15]. A typical MFC consists of two half cells anode and cathode which may or may not be separated by an ion exchange membrane [15, 16]. Hydrogen ion thus produced will pass to cathodic chamber via ion exchange membrane, whereas the electron will pass to other half cell via wire connecting both the chambers [17, 18]. Bioelectricity is produced as a result of this flow of electrons across the outer circuit. Oxygen will combine with hydrogen ion and electron to produce water in cathodic chamber [19, 20]. A typical MFC is depicted in Fig. 1.

3.1 Types of MFC in Wastewater Treatment and Its Efficiency in Earlier Studies

There are different types of MFC designs existing, which are single-chambered MFC, double-chambered MFC, stacked MFC, and up-flow MFC. Single-chambered MFC and double-chambered MFC are most commonly used. Anode and cathode are both contained in the same chamber of a single-chambered MFC. The anode is positioned either far or close to the cathode and is separated by PEM. Schematic design of single-chambered MFC and double-chambered MFC is shown in Fig. 2a and b, respectively.

Microorganism used in conventional MFC is bacteria. In recent years, algae got significant interest in implementing them in wastewater treatment. Algae is a photosynthetic eukaryotic organism that includes in kingdom Protista, which lacks various structures that characterizes land plants such as leaf, root, stem, etc. It is predominantly seen in waterbodies. As algae have the ability to absorb nutrients and convert them into biomass, it is considered as a favorable wastewater treatment agent.

The reason behind use of algae in wastewater treatment is, algae utilizes organic and inorganic pollutants, nitrogen (N), phosphorus (P) present in wastewater for their growth and in the meantime, wastewater will have significant reduction in concentration of pollutants.

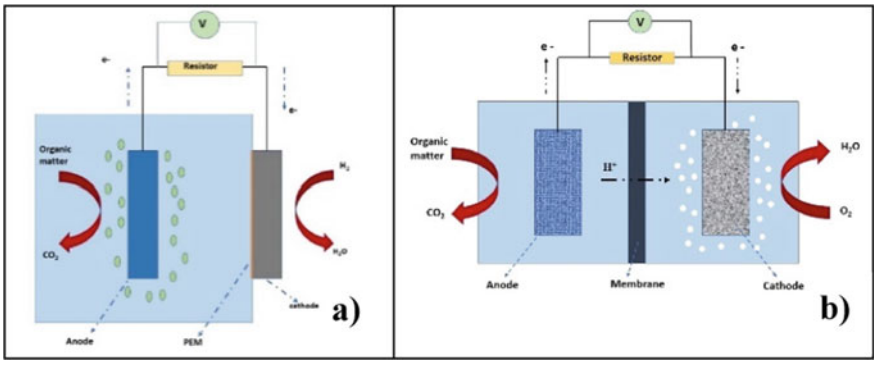

Fig. 2 **a** Single-chambered MFC. **b** Double-chambered MFC

Thus, instead of conventional MFC using bacteria, algae-assisted MFC cell will have more efficiency as well as sustainability.

3.2 Algae-assisted MFC

Low-power densities at large reactor capacities are a significant disadvantage of employing bacterial species to produce electricity. Combining MFCs with algae-assisted cathodes (AFCs) to treat wastewater and generate energy in order to avoid the scale-up problems caused by employing simply bacteria is a recent advancement in MFC. Microalgae operate as biocatalysts inside the cathode chamber, giving high-power densities at small reactor volumes, similar to bacterial MFCs, however these systems are still ineffective at providing commercially viable power densities at larger volumes [21].

Algae can be used at the cathode chamber of a dual-chambered MFC in place of energy-intensive passive aeration. Algal biomass can be employed inside the anode chamber after pretreatment since it is high in carbs, lipids, and vitamins. Instead of bacteria, by using photosynthetic organisms like algae in the cathode, we can obtain biomass, dissolved oxygen, and electron acceptors from photosynthesis to aid in the reduction of electrons at the cathode. Microalgae may thrive in less-than-ideal settings and can store huge amounts of proteins, lipids, and carbohydrates.

Based on the literature that is currently available, *Chlorella vulgaris, Spirulina, and Scenedesmus* are chosen for the current study since they are commonly utilized for wastewater treatment. Bolds Basal Media (BBM) is used for mass-culturing algae. In earlier studies, utilizing Chlorella vulgaris in the cathodic chamber resulted in a higher power density that was six times greater than the power generated without the use of algae and it was found that utilizing algae rather than bacteria increased the removal of organic material by up to. Earlier studies using algae-assisted microbial fuel cell is given in Table 2.

4 Conclusion

The potential for bioelectricity generation has been eclipsed by the increasing applications of microbial fuel cell technology, and now treatment of effluents from other sources is receiving more attention. By analyzing the different initial characteristics, it is concluded that introduction of algae for treatment will be more efficient in primary treated sugarcane industry effluent. Removal efficiency of several pollutants can be analyzed by comparing the characteristics of effluent after treatment with initial characteristics. While designing and fabricating, there are several aspects to be considered which will give future generations a plentiful, environmentally friendly, and effective source for producing bioelectricity. The only way MFCs can be commercialized is if the price is reduced. Therefore, it is necessary to create

Table 2 Earlier studies using algae-assisted microbial fuel cell

Type of algae	Specification of MFC	Type of wastewater	% Removal/power generation	Reference
Chlorella vulgaris	Anode: Activated sludge Cathode: *C. vulgaris*	Activated sludge from conventional domestic wastewater treatment plant	70% ($NH4^+$ removal), 75% (COD removal), and 26% (PO4 3—removal	[22]
Chlorella vulgaris	Photosynthetic microalgae microbial fuel cell (PMMFC)	Municipal wastewater	COD removal of 5.47%	[23]
Scenedesmus obliquus	Two identical chamber of an H-type MFCs	Municipal wastewater	Maximum power density—153 mW/m^2	[24]
Spirulina platensis	A photosynthetic microbial fuel cell using a graphite carbon cloth as the cathode and a gilding gold mesh as the anode	Synthetic wastewater	Power density—10 mW/m^2	[25]

MFCs for upcoming generations using products that are both affordable and of high quality. Adopting algae-assisted MFC in other type of industries has future scope and economical design and fabrication of microbial fuel cell chamber setup is identified as limitation which has a higher future scope of study.

Acknowledgements We would like to express our heartfelt thanks to the Head, Department of Civil Engineering, SRMIST and Environmental Engineering Laboratory, Department of Civil Engineering SRMIST for providing us with the opportunity to carry out this work.

References

1. Kushwaha JP (2015) A review on sugar industry wastewater: sources, treatment technologies, and reuse. Desalin Water Treat 53:309–318. https://doi.org/10.1080/19443994.2013.838526
2. Nagaraju M, Narasimha G, Rangaswamy V (2009) Impact of sugar industry effluents on soil cellulase activity. Int Biodeterior Biodegr 63:1088–1092. https://doi.org/10.1016/j.ibiod.2009.09.006
3. Moraes MAFD, Oliveira FCR, Diaz-Chavez RA (2015) Socio-economic impacts of Brazilian sugarcane industry. Environ Dev 16:31–43. https://doi.org/10.1016/j.envdev.2015.06.010
4. Jasmin Nivetha B, Bhakyalakshmi SV, Dinesh Kumar S, Santhanam P, Vijayalakshmi D, Divya M, Krishnaveni N (2019) Utilization of sugarcane industry effluent for high value biomass and photosynthetic pigments production of *Chlorella vulgaris* (PSBDU06). Bioresour Technol Rep. 7:100260. https://doi.org/10.1016/j.biteb.2019.100260
5. Ranjan P, Singh S, Muteen A, Biswas MK, Vidyarthi AK (2021) Environmental reforms in sugar industries of India: an appraisal. Environ Challenges 4. https://doi.org/10.1016/j.envc.2021.100159

6. Dhanasekar S, Sathyanathan R (2023) Bioenergy potential of *Chlorella vulgaris* under the influence of different light conditions in a bubble column photobioreactor. Global J Environ Sci Manage 9:36. https://doi.org/10.22035/gjesm.2023.04
7. Anusha Gowri RV, Dhanasekar S, Sathyanathan R (2022) Comparison of nutrient removal efficiency, growth characteristic and biomass cultivation of two microalgal strains provided with optimal conditions in agricultural wastewater. In: Loon LY, Subramaniyan M, Gunasekaran K (eds) Advances in construction management. Lecture notes in civil engineering, vol 191. Springer, Singapore. https://doi.org/10.1007/978-981-16-5839-6_25
8. Sevugamoorthy D, Rangarajan S (2023) Comparative analysis of biodegradation and characterization study on agal-assisted wastewater treatment in a bubble column photobioreactor. Environ Challenges 10:100659. https://doi.org/10.1016/j.envc.2022.100659
9. GeneralStandards
10. Du Z, Li H, Gu T (2007) A state of the art review on microbial fuel cells: a promising technology for wastewater treatment and bioenergy. https://doi.org/10.1016/j.biotechadv.2007.05.004
11. Adeleye S, Okorondu S (2015) Bioelectricity from students' hostel waste water using microbial fuel cell. Int J Biol Chem Sci 9:1038. https://doi.org/10.4314/ijbcs.v9i2.39
12. Siegert M, Sonawane JM, Ezugwu CI, Prasad R (2019) Economic assessment of nanomaterials in bio-electrical water treatment. In: Nanotechnology in the life sciences. Springer Science and Business Media B.V., pp 1–23. https://doi.org/10.1007/978-3-030-02381-2_1
13. Gude VG (2016) Wastewater treatment in microbial fuel cells—an overview. https://doi.org/10.1016/j.jclepro.2016.02.022
14. Angosto JM, Fernández-López JA, Godínez C (2015) Brewery and liquid manure wastewaters as potential feedstocks for microbial fuel cells: a performance study. Environ Technol 36:68–78. https://doi.org/10.1080/09593330.2014.937769
15. Kumar SS, Kumar V, Malyan SK, Sharma J, Mathimani T, Maskarenj MS, Ghosh PC, Pugazhendhi A (2019) Microbial fuel cells (MFCs) for bioelectrochemical treatment of different wastewater streams. Fuel 254. https://doi.org/10.1016/j.fuel.2019.05.109
16. Kumar SS, Basu S, Gupta S, Sharma J, Bishnoi NR (2019) Bioelectricity generation using sulphate-reducing bacteria as anodic and microalgae as cathodic biocatalysts. Biofuels 10:81–86. https://doi.org/10.1080/17597269.2018.1426161
17. Lin CW, Wu CH, Chiu YH, Tsai SL (2014) Effects of different mediators on electricity generation and microbial structure of a toluene powered microbial fuel cell. Fuel 125:30–35. https://doi.org/10.1016/j.fuel.2014.02.018
18. Kondaveeti S, Lee J, Kakarla R, Kim HS, Min B (2014) Low-cost separators for enhanced power production and field application of microbial fuel cells (MFCs). Electrochim Acta 132:434–440. https://doi.org/10.1016/j.electacta.2014.03.046
19. Kouam Ida T, Mandal B (2022) Microbial fuel cell design, application and performance: a review. Mater Today Proc. https://doi.org/10.1016/j.matpr.2022.10.131
20. Mathuriya AS (2016) Novel microbial fuel cell design to operate with different wastewaters simultaneously. J Environ Sci 42:105–111. https://doi.org/10.1016/j.jes.2015.06.014
21. Sivakumar P, Ilango K, Praveena N, Sircar A, Balasubramanian R, Sakthisaravanan A, Kannan R (2018) Algal fuel cell. In: Microalgal biotechnology. InTech. https://doi.org/10.5772/intechopen.74285
22. Gonzalez Del Campo A, Perez JF, Cañizares P, Rodrigo MA, Fernandez FJ, Lobato J (2015) Characterization of light/dark cycle and long-term performance test in a photosynthetic microbial fuel cell. Fuel 140:209–216. https://doi.org/10.1016/j.fuel.2014.09.087
23. Bazdar E, Roshandel R, Yaghmaei S, Mardanpour MM (2018) The effect of different light intensities and light/dark regimes on the performance of photosynthetic microalgae microbial fuel cell. Bioresour Technol 261:350–360. https://doi.org/10.1016/j.biortech.2018.04.026
24. Kakarla R, Min B (2014) Photoautotrophic microalgae *Scenedesmus obliquus* attached on a cathode as oxygen producers for microbial fuel cell (MFC) operation. Int J Hydrogen Energy 39:10275–10283. https://doi.org/10.1016/j.ijhydene.2014.04.158
25. Lin CC, Wei CH, Chen CI, Shieh CJ, Liu YC (2013) Characteristics of the photosynthesis microbial fuel cell with a *Spirulina platensis* biofilm. Bioresour Technol 135:640–643. https://doi.org/10.1016/j.biortech.2012.09.138

A Review of the Pre-treatments that Are Used in Membrane Distillation

V. M. V. Sai Krishna and K. Prasanna

Abstract Membrane distillation (MD), a new thermal-based membrane technique, can filter wastewater and high-salt brines. Low electrical energy usage, the removal of non-volatile solutes, and ambient operating pressures are a few advantages of MD versus pressure-driven processes. Unfortunately, issues with membrane fouling and pore wetting are still preventing its widespread industrial adoption. Effective pre-treatment and cleaning methods are essential to manage this issue, much like with other membrane processes. These issues receive little attention in the MD literature, despite their significance in providing a stable and reliable water treatment process. Despite their significance in maintaining a steady and dependable water treatment process, this is the case. This is demonstrated by the fact that, despite the vast and expanding body of literature on MD, a thorough examination of membrane cleaning and pre-treatment is still lacking. An extensive description of pre-treatment procedures for a variety of MD applications is provided in this paper. In order to help researchers in this sector create membrane distillation technology for broader commercial applicability, future research directions are also highlighted.

Keywords Adsorption · Coagulation–flocculation · Membrane distillation · Oxidation · Pre-treatment

1 Introduction

Membrane distillation (MD), which purifies high-salinity water streams to produce freshwater, has garnered attention recently. In the MD process, a membrane-based vapour-driven thermal desalination technology, only vapour molecules can pass through the porous and hydrophobic membrane. The four main designs are DCMD, AGMD, VMD, and SGMD [1]. The membrane directly contacts both hot and cold

V. M. V. S. Krishna · K. Prasanna (✉)
Department of Civil Engineering, College of Engineering and Technology, SRM Institute of Science and Technology, Kattankulathur, Tamilnadu 603203, India
e-mail: prasannk@srmist.edu.in

K. R. Reddy et al. (eds.), *Recent Advances in Civil Engineering*, Lecture Notes in Civil Engineering 398, https://doi.org/10.1007/978-981-99-6229-7_23

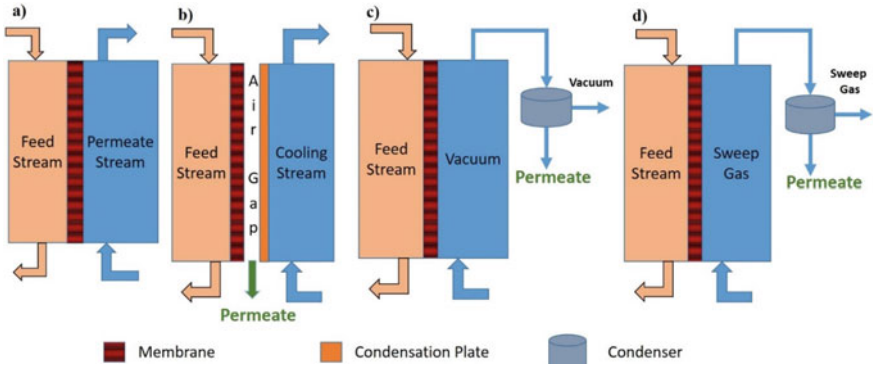

Fig. 1 Different variations in MD: **a** DCMD, **b** AGMD, **c** VMD and **d** SGMD

streams in the direct contact MD (DCMD) design depicted in Fig. 1. It loses the most heat due to membrane thermal conduction.

An AGMD has stagnant air between the membrane and the condensing surface. This layer is cooled by a cold stream. This air layer's insulation and mass-transfer barrier minimise heat loss and permeate flux. Vacuuming the membrane permeate side lowers VMD pressure. Evaporation reduces heat loss. The Hoover pump and condenser add complexity and electricity. The membrane's invading sides force gas to sweep peripherally. Final SGMD stage: The vapour from this gas condenses outside the system.

When correctly operated with small pores, MD separates non-volatile components 99.9% efficiently, separating salts, heavy metals, dyes, and other impurities. This is because few pollutants can pass through the condensate's tiny pores. MD works on saltwater [2], mining effluent [3], textile wastewater [4], produced water [5], and other wastewater [6, 7].

Processing parameters eliminate unstable feed items and change settings. MD eliminates ammonia from biofuel ethanol, water, and agricultural effluent [8, 9]. MD may operate at higher salinities than pressure-driven processes like reverse osmosis because vapour pressure is less sensitive to feed concentration. A crystalliser unit helps MCr recover resources and discharge no liquid [10, 11].

Membrane cleaning and pre-treatment have received less attention than other MD plant operations, despite the many benefits outlined above and substantial research into the MD process. Clean the membrane surface of cake debris and pore-deficiency chemicals to maintain performance. Cake fouling and pore-deficiency chemicals hinder membrane function. Pre-treatment and cleaning prevent fouling buildup. Foulant molecules clog pores in compulsion-forced membrane processes, raising permeate resistance. Fouling of MD was usually wet by less than 90%. The debris layer may lower the liquid-vapour interface temperature, decreasing vapour mobility [12].

The scientific community should study the most important membrane distillation cleaning and pre-treatment techniques. This study evaluates current MD pre-treatment technologies and recommends feed solutions and application-specific approaches. After that, we build super hydrophobic and omniphobic membranes with "self-cleaning" properties like the Padma leaf and study the research's physical cleaning mechanisms.

This work offers academic and industrial researchers a pre-treatment technique that can assist in the commercialisation of MD in a number of different applications.

2 Pre-treatments

MD may benefit from pre-treatment. Oils, surfactants, humic compounds, and their mixtures in feed water make MD moist easily. Pre-treatment is another solution. Figure 2 illustrates MD pre-treatment methods.

This figure argues for reverse osmosis-based saltwater desalination [13]. This shows how much better reverse osmosis is and how straightforward MD is for this application.

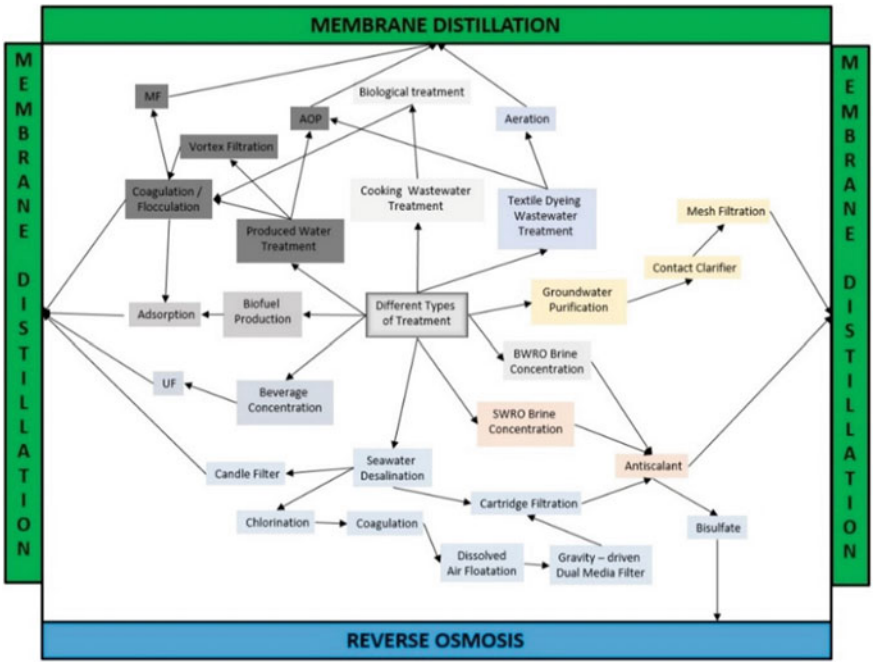

Fig. 2 Illustration compares MD pre-treatments to reverse osmosis for saltwater desalination applications [13–26]

3 Adsorption

Membrane processes commonly use high-surface-area adsorption pre-treatment. Water can be cleaned via adsorption. High-performance materials like graphene, zeolites, metal organic frameworks, AC, etc. are being developed for this cost-effective treatment. Despite its efficacy, its use as the first MD treatment is restricted. Zhang et al. [16] precipitately softened shale oil and gas production water with anhydrous aluminium sulphate (15 ppm, pH 10) and walnut shell adsorption and filtration. Anhydrous aluminium sulphate softened. Aluminium salt, not ferric, prevented silica scaling. Walnut shells removed 95% of water contaminants, including benzene, toluene, ethylbenzene, and xylenes (BTEX), after reducing feed turbidity by 94%. The MD's permeate met regulatory standards, water recovery was 80%, and brine TDS was 180,000 mg/L.

Zhang et al. [14] used AC or Amberlite IRA67 with VMD. This concentrated and detoxified biofuel contains lignocellulosic hydrolyzates. Adsorption increases acetic acid elimination, which limits fermentation and membrane distillation. The combined technique produced ten times more ethanol than the untreated fermentation process. Pre-treatment can recover more than water.

4 Coagulation-Flocculation

Coagulation and flocculation remove suspended particles and colloids from water. Pressure-driven wastewater treatment improves membrane distillation fouling. Li et al. treated biologically treated coking wastewater with MD, PACl, and PAM coagulants [19]. 175 and 2 mg/L of PACl and PAM were excellent. PACl increased rejection and flux during tests, despite MD's excellent raw water purification. Pre-treated groundwater prevented $CaCO_3$ scaling [22]. Contact clarifiers eliminated pollutants by coagulating and softening raw water with $FeSO_4{\cdot}7H_2O$ and $Ca(OH)_2$. Scalants were not entirely removed from the water, leaving membrane deposits of silicon dioxide, magnesium, calcium, iron, and titanium (Fig. 3).

Membrane fouling drastically reduced flux after several hundred hours of MD operation with a high water recovery ratio. Chemicals aggravated this. Occasionally washing with 5% HCl restored module efficiency, but subsequent runs rewetted faster. Pre-filter mesh hindered membrane scaling with heterogeneous nucleation.

Cho et al. [17] compared FMX vortex filtration (FMX-B) with flocculation-sedimentation (FS) and FSMF for pre-treating shale gas wastewater with a TDS of more than 120,000 mg/L. By eliminating phenolic and fluvic acid-like substances from the feed, all pre-treatment methods reduced organic fouling in MD treatment. FSMF treatment reduced flow at higher temperatures, while organic fouling was stronger with previous techniques.

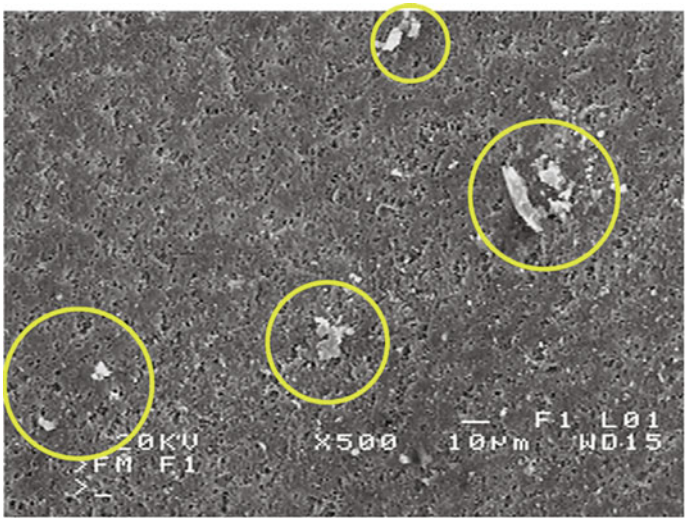

Fig. 3 SEM images of a membrane surface following a 75-h MD procedure. The feed is river water that has been processed in an accelerator, and debris from scale are highlighted in yellow [22]

5 Foam Fractionation

Compressed air eliminates surfactants in foam fractionation. A long-term pilot investigation showed this approach treated real textile wastewater [20]. Over 65 days, only the untreated feed caused moisture. Caustic membrane cleaning restored a periodic flux reduction from 5 $LM^{-2}H^{-1}$ (LMH) to 2 LMH to 4 LMH. After three months, ammonium was found in permeate, even though its electrical conductivity dropped to 204 μS/cm. The pre-treatment methods worked. Its use in MD pre-treatment is limited [27].

6 Advanced Oxidation Processes

AOP membrane distillation applications are restricted yet fascinating. Ricceri et al. [18] desalinated water with Fenton oxidation pre-treatment. The permeate tank's TOC increased with paraffin and VOCs, but flux and conductivity did not. Before pre-treatment, permeate conductivity is enhanced because SDS wets PTFE membrane pores before [4]. SDS inhibited water recovery after acidifying feed water to pH 3. $FeSO_4$ (19 mM) and H_2O_2 (32 mM) enhanced water recovery. SDS recovered 40% pre-wetting. Pre-treatment prevents instant moisture. Membrane scaling restricted recovery to 60–70% without SDS. Permeate TOC was considerably lower than in the no-pre-treatment scenario, indicating organic molecules were broken down. Fenton oxidation and MD can treat generated water without surfactants.

Shin et al. [28] employed electrochemical oxidation and membrane distillation to break down organic components in water and generate thermal driving force via ohmic heating. Combining the two techniques achieved this. BDD anodes and Ti cathodes have potentials ranging from − 1.25 to 2.3 V. $^{\cdot}OH$, $SO_3^{\cdot -}$, and persulfate ions efficiently degraded several organic components. Even with 0.4 mM SDS in the water, they maintained steady fluxes and low permeate conductivity, showing this method is more successful than Fenton oxidation.

Yatmaz et al. [21] photocatalysed azo dyes with ZnO and TiO_2 catalysts with UVA or UVC light before membrane distillation. Not fouling prevention, the study improved MD COD elimination. After photocatalytic oxidation, MD separation improved efficiency. AOPs reduce fouling, increase rejection, and handle complex water types in small membrane distillation systems that need research.

7 Pre-filtration

Water treatment often begins with cartridge filters, microfiltration, ultrafiltration, or nanofiltration. It size-fractionates feed water components and stabilises treatment [29] it provides. Quist-Jensen et al. [23] added UF and DCMD to concentrated orange juice. UF eliminated suspended particles and turbidity, and DCMD drained water to concentrate the juice. During the 40-h test, flux averaged 0.6 LMH. Low-temperature operation (24 ± 1 °C) retains juice flavour and lowers fluxes, 24 ± 1 °C distilled.

Pre-filtration before the MD module crystallises brines and other high-inorganic fluids [30], it froze. MD modules enhance thermal and water recovery. Multiple-feed recirculation performed this. One ship pilot desalinated saltwater with a candle filter before vacuum membrane distillation. Desalination works. Waste heat from the vessel's engine rejected 99.99% of the salt for five months [26]. Membrane distillation needs less pre-treatment than RO [13].

8 Scale Inhibitors

Many industries use antiscalants to avoid membrane scaling. Dissolved ions adsorb onto crystals or nuclei. This prevents crystals from precipitating. Time-dependent methods may not eradicate crystal formation. Instead, membrane separation will lengthen the induction time [31]. Rejected RO brine retains them because they are cheaper than acids. Antiscalants help MD, but if they form compounds with iron, they can promote organic fouling antiscalants to still help MD [32].

Martinetti et al. [24] used Pre-treat Plus 0400 and Y2K to decrease scaling in MD and FO brackish water desalination brine concentration operations. San Diego-based King Lee Technologies sells scale inhibitors. Concentration factor 2 reduced flow rapidly and sustainably. Scale inhibitor-free: Flow decreased sooner at 1–8 ppm scale inhibitor doses. Membrane silica gel caused this. After this, the flow revived on

its own, and when a scale inhibitor concentration of 4 ppm was employed, the flux continued to be stable up to a concentration factor of 4, after which it declined again. Scientists hypothesised that silica gels would harden and could be removed from the membrane surface, restoring flow. Cleaning PTFE and PP membranes using 0.029 M Na_2EDTA and 0.058 M NaOH almost restored flux. Membrane crystal nucleation sites speed flux decline after cleaning membrane crystals.

Polyphosphate antiscalant inhibited MD-induced $CaCO_3$ crystallites [33]. MD uses HCO_3^- water. The membrane developed a thin amorphous layer (Fig. 4). In pilot-scale desalination studies utilising commercial vacuum multi-effect MD modules, the biodegradable antiscalant carboxyline CMI from Cosun Biobased products in the Netherlands was successful [25]. Only 20–50 μm cartridge filtering was pre-treated. Fed Beach: 2 g/L citric acid eliminated pre-antiscalant scale and largely restored performance. The second antiscalant prevented scaling (36 m^3 distillate). Water complexes cause organic fouling, although MD antiscalants prevent scaling. Water complexes contain foul organics. When compared to capacitive deionization, ultrafiltration, and nanofiltration, antiscalants as a single pre-treatment for MD-concentrated saltwater RO brine produced the least expensive water and the least expensive option [15].

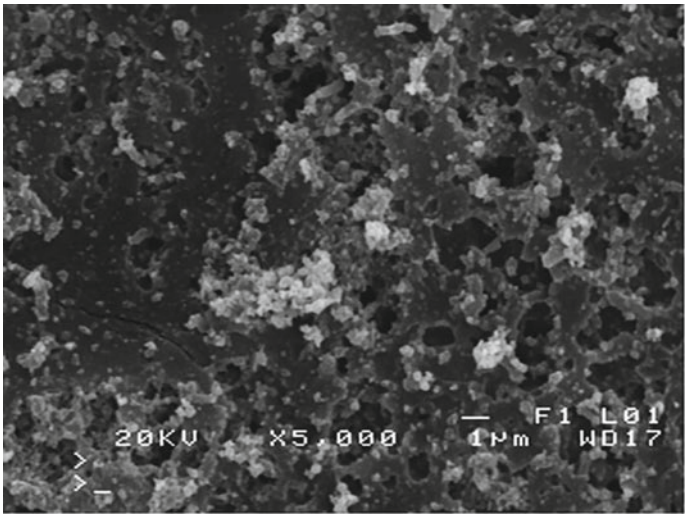

Fig. 4 SEM images of the membrane surface after 30 h of MD water desalination indicate a deposit. HCO_3^- enriched tap water (4.5 mmol/L). Antiscalant: 8 mg/L $(NaPO_3)n$ [33]

9 Conclusions and Future Outlook

This study discusses recent Maryland water reclamation pre-treatment approaches, and Table 1 lists their restrictions. Pre-treatment methods can manage and lessen its consequences.

Hydrophobic membrane-organic molecule interactions induce MD organic fouling. Hydrophobic side chains link organic molecules. NaOH removes organic molecules to restore membrane function. Due to irreversible fouling, which affects MD more than RO and FO, this cleaning process may lose efficiency. Coagulation-flocculation, foam fractionation, adsorption, advanced oxidation, and pre-filtration prevent organic fouling and improve outcomes. Few MD studies have examined these techniques. Pressure-driven membrane separation is affordable. Proven approaches: Unlike pressure-driven applications, MD procedures require one pre-treatment. Despite fouling, MD may be cheaper, simpler, and better for the environment than

Table 1 Providing an overview of the various pre-treatments included in this review

	Achieve by	Limitations	References
Pre-treatments	Adsorption [34]	• Produces waste sludge that must be discarded • Additional stages of separation, such as filtration, sedimentation, or centrifugation can be required to achieve a successful solid–liquid separation • Exorbitant price for adsorbents	[35]
	Coagulation-flocculation [36]	• Sludge development • An increase in price due to coagulant chemicals • Coagulants for fresh and marine habitats	[37]
	Foam fractionation [38, 39]	• Limited selectivity for proteins and anionic surfactants	[39, 40]
	Advanced oxidation process [41–43]	• Extra electricity consumption • Generates by-products which need to be safely disposed of • Further study is necessary	[44]
	Pre-filtration [45]	Extra membrane expense	[46]
	The use of scale inhibitors [47–49]	• Need for environmentally safe antiscalants • Microbe growth can be sped up by antiscalants that include phosphorus	[50, 51]

pressure-driven applications. MD is better for treating produced water and wastewater, manufacturing food and drinks, treating agricultural water, and other high-organic load applications because it controls organic matter and biofouling. This enhances its use. Thus, fouling-mitigation measures must be effective and affordable.

References

1. Choudhury MR, Anwar N, Jassby D, Rahaman MS (2019) Fouling and wetting in the membrane distillation driven wastewater reclamation process—a review. Adv Colloid Interface Sci 269:370–399. https://doi.org/10.1016/j.cis.2019.04.008
2. Al-Obaidani S, Curcio E, Macedonio F, Di Profio G, Al-Hinai H, Drioli E (2008) Potential of membrane distillation in seawater desalination: thermal efficiency, sensitivity study and cost estimation. J Memb Sci 323(1):85–98. https://doi.org/10.1016/j.memsci.2008.06.006
3. Sivakumar M, Ramezanianpour M, O'Halloran G (2013) Mine water treatment using a vacuum membrane distillation system. APCBEE Proc 5:157–162. https://doi.org/10.1016/j.apcbee.2013.05.028
4. Leaper S, Abdel-Karim A, Gad-Allah TA, Gorgojo P (2019) Air-gap membrane distillation as a one-step process for textile wastewater treatment. Chem Eng J 360:1330–1340. https://doi.org/10.1016/j.cej.2018.10.209
5. Alkhudhiri A, Darwish N, Hilal N (2013) Produced water treatment: application of air gap membrane distillation. Desalination 309:46–51. https://doi.org/10.1016/j.desal.2012.09.017
6. Quist-Jensen CA, Ali A, Mondal S, Macedonio F, Drioli E (2016) A study of membrane distillation and crystallization for lithium recovery from high-concentrated aqueous solutions. J Memb Sci 505:167–173. https://doi.org/10.1016/j.memsci.2016.01.033
7. Alves VD, Coelhoso IM (2006) Orange juice concentration by osmotic evaporation and membrane distillation: a comparative study. J Food Eng 74(1):125–133. https://doi.org/10.1016/j.jfoodeng.2005.02.019
8. Zarebska A, Nieto DR, Christensen KV, Norddahl B (2014) Ammonia recovery from agricultural wastes by membrane distillation: fouling characterization and mechanism. Water Res 56:1–10. https://doi.org/10.1016/j.watres.2014.02.037
9. Shirazi MMA, Kargari A, Tabatabaei M (2015) Sweeping gas membrane distillation (SGMD) as an alternative for integration of bioethanol processing: study on a commercial membrane and operating parameters. Chem Eng Commun 202(4):457–466. https://doi.org/10.1080/00986445.2013.848805
10. Drioli E, Di Profio G, Curcio E (2012) Progress in membrane crystallization. Curr Opin Chem Eng 1(2):178–182. https://doi.org/10.1016/j.coche.2012.03.005
11. Osman A, Leaper S, Sreepal V, Gorgojo P, Stitt H, Shokri N (2019) Dynamics of salt precipitation on graphene oxide membranes. Cryst Growth Des 19(1):498–505. https://doi.org/10.1021/acs.cgd.8b01597
12. Gryta M (2008) Fouling in direct contact membrane distillation process. J Memb Sci 325(1):383–394. https://doi.org/10.1016/j.memsci.2008.08.001
13. Badruzzaman M, Voutchkov N, Weinrich L, Jacangelo JG (2019) Selection of pretreatment technologies for seawater reverse osmosis plants: a review. Desalination 449(May 2018):78–91. https://doi.org/10.1016/j.desal.2018.10.006
14. Zhang Y, Li M, Wang Y, Ji X, Zhang L, Hou L (2015) Simultaneous concentration and detoxification of lignocellulosic hydrolyzates by vacuum membrane distillation coupled with adsorption. Bioresour Technol 197:276–283. https://doi.org/10.1016/j.biortech.2015.08.097
15. Bindels M, Carvalho J, Gonzalez CB, Brand N, Nelemans B (2020) Techno-economic assessment of seawater reverse osmosis (SWRO) brine treatment with air gap membrane distillation (AGMD). Desalination 489(October 2019):114532. https://doi.org/10.1016/j.desal.2020.114532

16. Zhang Z, Du X, Carlson KH, Robbins CA, Tong T (2019) Effective treatment of shale oil and gas produced water by membrane distillation coupled with precipitative softening and walnut shell filtration. Desalination 454(December 2018):82–90. https://doi.org/10.1016/j.desal.2018.12.011
17. Cho H, Choi Y, Lee S (2018) Effect of pretreatment and operating conditions on the performance of membrane distillation for the treatment of shale gas wastewater. Desalination 437(March):195–209. https://doi.org/10.1016/j.desal.2018.03.009
18. Ricceri F et al (2019) Desalination of produced water by membrane distillation: effect of the feed components and of a pre-treatment by Fenton oxidation. Sci Rep 9(1):1–12. https://doi.org/10.1038/s41598-019-51167-z
19. Li J, Wu J, Sun H, Cheng F, Liu Y (2016) Advanced treatment of biologically treated coking wastewater by membrane distillation coupled with pre-coagulation. Desalination 380:43–51. https://doi.org/10.1016/j.desal.2015.11.020
20. Dow N et al (2017) Demonstration of membrane distillation on textile waste water assessment of long term performance, membrane cleaning and waste heat integration. Environ Sci Water Res Technol 3(3):433–449. https://doi.org/10.1039/c6ew00290k
21. Yatmaz HC, Dizge N, Kurt MS (2017) Combination of photocatalytic and membrane distillation hybrid processes for reactive dyes treatment. Environ Technol 38(21):2743–2751. https://doi.org/10.1080/09593330.2016.1276222
22. Gryta M (2008) Chemical pretreatment of feed water for membrane distillation. Chem Pap 62(1):100–105. https://doi.org/10.2478/s11696-007-0085-5
23. Quist-Jensen CA et al (2016) Direct contact membrane distillation for the concentration of clarified orange juice. J Food Eng 187:37–43. https://doi.org/10.1016/j.jfoodeng.2016.04.021
24. Martinetti CR, Childress AE, Cath TY (2009) High recovery of concentrated RO brines using forward osmosis and membrane distillation. J Memb Sci 331(1–2):31–39. https://doi.org/10.1016/j.memsci.2009.01.003
25. Andrés-Mañas JA, Ruiz-Aguirre A, Acién FG, Zaragoza G (2018) Assessment of a pilot system for seawater desalination based on vacuum multi-effect membrane distillation with enhanced heat recovery. Desalination 443(May):110–121. https://doi.org/10.1016/j.desal.2018.05.025
26. Xu Y, Zhu BK, Xu YY (2006) Pilot test of vacuum membrane distillation for seawater desalination on a ship. Desalination 189(1–3 SPEC. ISS.):165–169. https://doi.org/10.1016/j.desal.2005.06.024
27. Palmer M, Hatley H (2018) The role of surfactants in wastewater treatment: impact, removal and future techniques: a critical review. Water Res 147:60–72. https://doi.org/10.1016/j.watres.2018.09.039
28. Shin YU, Yun ET, Kim J, Lee H, Hong S, Lee J (2020) Electrochemical oxidation-membrane distillation hybrid process: utilizing electric resistance heating for distillation and membrane defouling through thermal activation of anodically formed persulfate. Environ Sci Technol 54(3):1867–1877. https://doi.org/10.1021/acs.est.9b05141
29. Van Der Bruggen B (2013) Integrated membrane separation processes for recycling of valuable wastewater streams: nanofiltration, membrane distillation, and membrane crystallizers revisited. Ind Eng Chem Res 52(31):10335–10341. https://doi.org/10.1021/ie302880a
30. Gryta M (2009) Scaling diminution by heterogeneous crystallization in a filtration element integrated with membrane distillation module. Polish J Chem Technol 11(2):60–65. https://doi.org/10.2478/v10026-009-0026-x
31. Gloede M, Melin T (2006) Potentials and limitations of molecular modelling approaches for scaling and scale inhibiting mechanisms. Desalination 199(1–3):26–28. https://doi.org/10.1016/j.desal.2006.03.012
32. Sweity A, Ronen Z, Herzberg M (2014) Induced organic fouling with antiscalants in seawater desalination. Desalination 352:158–165. https://doi.org/10.1016/j.desal.2014.08.018
33. Gryta M (2012) Polyphosphates used for membrane scaling inhibition during water desalination by membrane distillation. Desalination 285:170–176. https://doi.org/10.1016/j.desal.2011.09.051

34. Woo YC et al (2018) Hierarchical composite membranes with robust omniphobic surface using layer-by-layer assembly technique. Environ Sci Technol 52(4):2186–2196. https://doi.org/10.1021/acs.est.7b05450
35. Bogler A, Bar-Zeev E (2018) Membrane distillation biofouling: impact of feedwater temperature on biofilm characteristics and membrane performance. Environ Sci Technol 52(17):10019–10029. https://doi.org/10.1021/acs.est.8b02744
36. Yao M et al (2020) A review of membrane wettability for the treatment of saline water deploying membrane distillation. Desalination 479(October 2019):114312. https://doi.org/10.1016/j.desal.2020.114312
37. Hooshangi S, Bentley WE (2008) From unicellular properties to multicellular behavior: bacteria quorum sensing circuitry and applications. Curr Opin Biotechnol 19(6):550–555. https://doi.org/10.1016/j.copbio.2008.10.007
38. Gryta M (2005) Long-term performance of membrane distillation process. J Memb Sci 265(1–2):153–159. https://doi.org/10.1016/j.memsci.2005.04.049
39. Tijing LD, Woo YC, Choi JS, Lee S, Kim SH, Shon HK (2015) Fouling and its control in membrane distillation—a review. J Memb Sci 475:215–244. https://doi.org/10.1016/j.memsci.2014.09.042
40. Zodrow KR, Bar-Zeev E, Giannetto MJ, Elimelech M (2014) Biofouling and microbial communities in membrane distillation and reverse osmosis. Environ Sci Technol 48(22):13155–13164. https://doi.org/10.1021/es503051t
41. Skuse C, Gallego-Schmid A, Azapagic A, Gorgojo P (2021) Can emerging membrane-based desalination technologies replace reverse osmosis? Desalination 500(October 2020):114844. https://doi.org/10.1016/j.desal.2020.114844
42. Goh S et al (2013) Impact of a biofouling layer on the vapor pressure driving force and performance of a membrane distillation process. J Memb Sci 438:140–152. https://doi.org/10.1016/j.memsci.2013.03.023
43. Antony A, Low JH, Gray S, Childress AE, Le-Clech P, Leslie G (2011) Scale formation and control in high pressure membrane water treatment systems: a review. J Memb Sci 383(1–2):1–16. https://doi.org/10.1016/j.memsci.2011.08.054
44. Jiang L, Chen L, Zhu L (2020) Fouling process of membrane distillation for seawater desalination: an especial focus on the thermal-effect and concentrating-effect during biofouling. Desalination 485(December 2019):114457. https://doi.org/10.1016/j.desal.2020.114457
45. Gryta M (2008) Alkaline scaling in the membrane distillation process. Desalination 228(1–3):128–134. https://doi.org/10.1016/j.desal.2007.10.004
46. Yang Y, Bogler A, Ronen Z, Oron G, Herzberg M, Bernstein R (2020) Initial deposition and pioneering colonization on polymeric membranes of anaerobes isolated from an anaerobic membrane bioreactor (AnMBR). Environ Sci Technol 54(9):5832–5842. https://doi.org/10.1021/acs.est.9b06763
47. Gryta M (2010) Desalination of thermally softened water by membrane distillation process. Desalination 257(1–3):30–35. https://doi.org/10.1016/j.desal.2010.03.012
48. Gryta M (2020) Separation of saline oily wastewater by membrane distillation. Chem Pap 74(7):2277–2286. https://doi.org/10.1007/s11696-020-01071-y
49. Gryta M (2018) The effect of unfavourable process conditions on the water desalination by membrane distillation. Desalin Water Treat 128(June):1–10. https://doi.org/10.5004/dwt.2018.22568
50. Jiang L, Chen L, Zhu L (2019) Electrically conductive membranes for anti-biofouling in membrane distillation with two novel operation modes: capacitor mode and resistor mode. Water Res 161:297–307. https://doi.org/10.1016/j.watres.2019.06.015
51. Sabri S et al (2019) Antibacterial properties of polysulfone membranes blended with Arabic gum. Membranes 9(2):1–16. https://doi.org/10.3390/membranes9020029

Prioritization of the Sub-watersheds Through Morphometric Analysis in the Chinar Watershed

M. Subbulakshmi and Sachikanta Nanda

Abstract Morphometric parameters of a watershed encompass a range of measurable features and characteristics that play a vital role in understanding its hydrological behavior and guiding water resource management decisions. An attempt has been made to categorize the sub-watersheds through morphology of the Chinnar basin on the flood. Based on topography basin is divided into 29 sub-watersheds. Stream order, stream number, stream length, basin length, stream length ratio, mean stream length, bifurcation ratio, drainage area, perimeter, drainage density, stream frequency, texture ratio, elongation ratio, circularity ratio, form factor, compactness ratio, length of overland flow, ruggedness number, time of concentration, relief, relief ratio, relative relief, slope, infiltration number were evaluated for Chinnar. The highest and lowest elevations are 886 m and 50 m. Prioritization is done by the compound factor method. The sub-watershed is classified to the following categories of flood: very high, high, moderate, low, and very low. Sub-watershed 4,11,17,24 are very high-risk classes for flood and sub-watersheds 8,13,14 are very low-risk classes.

Keywords Morphometric analysis · Watershed prioritization · Flood · Linear · Aerial · Relief

1 Introduction

A watershed is a hydrologic division of an area that drains into the same outlet. The development plan should be prepared for watersheds instead of an administrative boundary. Flood and drought are extreme hydrological disasters that control entire watershed [1]. Both disasters are influenced by geomorphology (streams, slope, infiltration number, basin shape, length), climate (temperature, wind, humidity), and meteorology parameters (precipitation, cyclone, lightning). Humans have less control over climate and meteorological parameters. Studying the geomorphology

M. Subbulakshmi · S. Nanda (✉)
Department of Civil Engineering, Faculty of Engineering and Technology, SRM Institute of Science and Technology, Kattankulathur, Tamil Nadu 603203, India
e-mail: sachikan@srmist.edu.in

K. R. Reddy et al. (eds.), *Recent Advances in Civil Engineering*, Lecture Notes in Civil Engineering 398, https://doi.org/10.1007/978-981-99-6229-7_24

of a watershed gives the knowledge of the hydrologic response of that watershed, which helps to develop a structural or non-structural plan for integrated management [2, 3]. Morphometric parameters help understand about the watershed. Linear, aerial, and relief aspects of morphometric parameters helped understand watersheds. Geological structure affects both the surface water and ground water. Identification of flood risk areas is most important for prevention and mitigation measures [4–6]. The morphometric properties of the sub-watersheds are used in this study to prioritize them.

2 Study Area

From Nagoor Forest, the Chinnar River flowed into the Vellar River at Pilanthurai in the Cuddalore district. Chinnar is a significant tributary of the river Vellar. Chinnar lies between 11.18°–11.39°N and 78.66°–79.18°″E, as shown in Fig. 1. The geographical area of the lower Vellar basin is 657.9 km^2. The Chinnar sub-basin has a typical climate. Chinnar benefits from the North East monsoon primarily and slightly during the summer. The annual average weighted rainfall of the sub-basin is 973.79 mm. The climate is mainly tropical, with temperatures between 28–38 °C. The soil types in this watershed are met by a combination of Incept sol, Alf soil, and Vitriol. Incept sol is the more prominent type with relative humidity between 70–80% and temperatures between 28–38 °C, the climate is primarily tropical. Paddy, sugarcane, maize, cotton, groundnut, sorghum, and pulses are significant crops grown in the sub-basin. Most farmers go for double or triple-crop cultivation. Paddy–sugarcane–paddy, paddy–Paddy (or) paddy–maize (or) paddy–groundnut. Chinnar watershed was divided into 29 sub-watersheds and it's shown in Fig. 2. The sub-watershed number is given based on area. The sub-watershed, which has the lowest area, is named as SW 1, the second lowest sub-watershed as SW 2, and so on.

3 Data Collection

Morphometric characteristics are categorized into three aspects (linear, aerial, and relief) for hydrological studies. DEM was downloaded from the USGS website and was further processed to delineate sub-watersheds and create a stream order map. The morphometric parameters are computed using the formulae of Horton, Strahler, Schumm, Miller, and Gravelius [7–9]. Figure 3 illustrates the streams of Chinnar watershed.

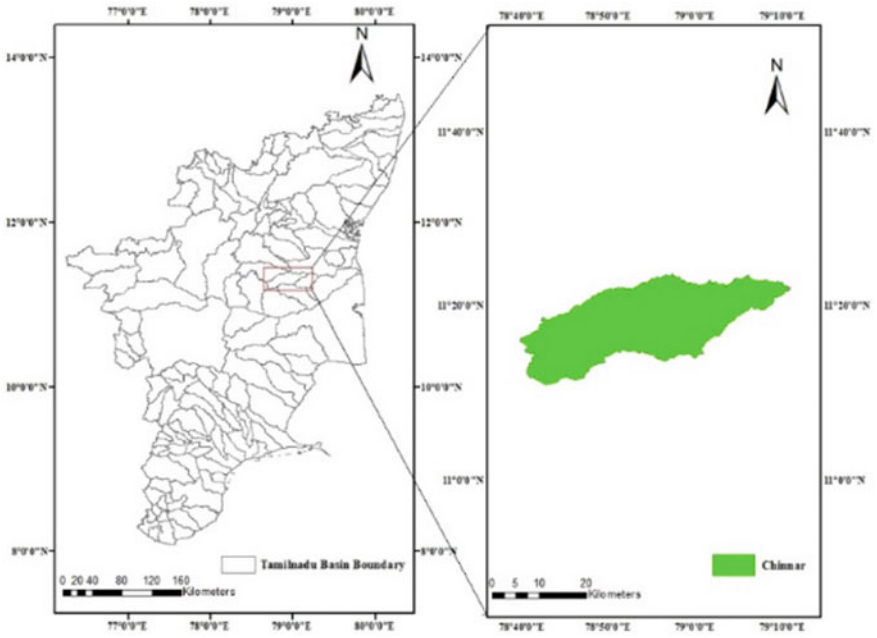

Fig. 1 Geographical map of the study area

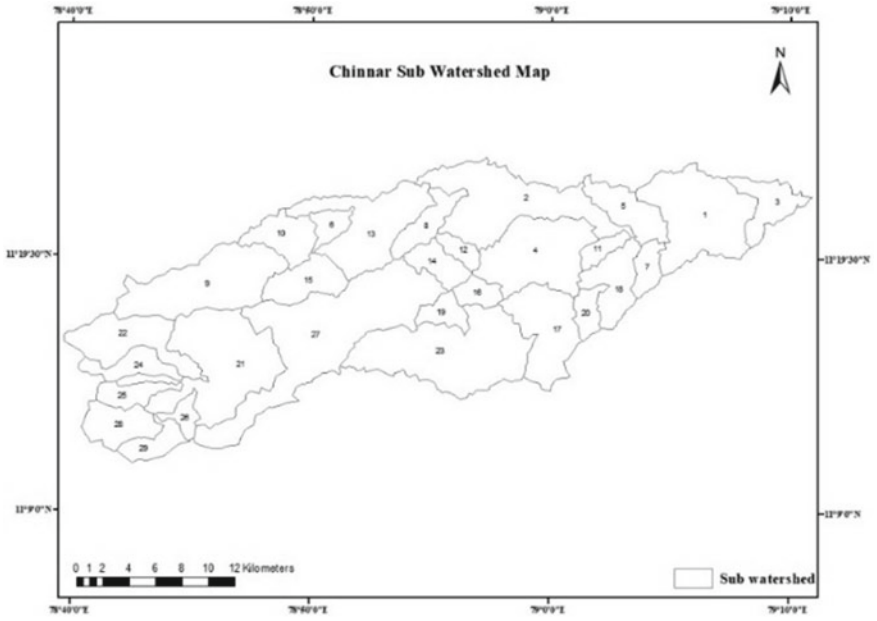

Fig. 2 Sub-watershed map of Chinnar watershed

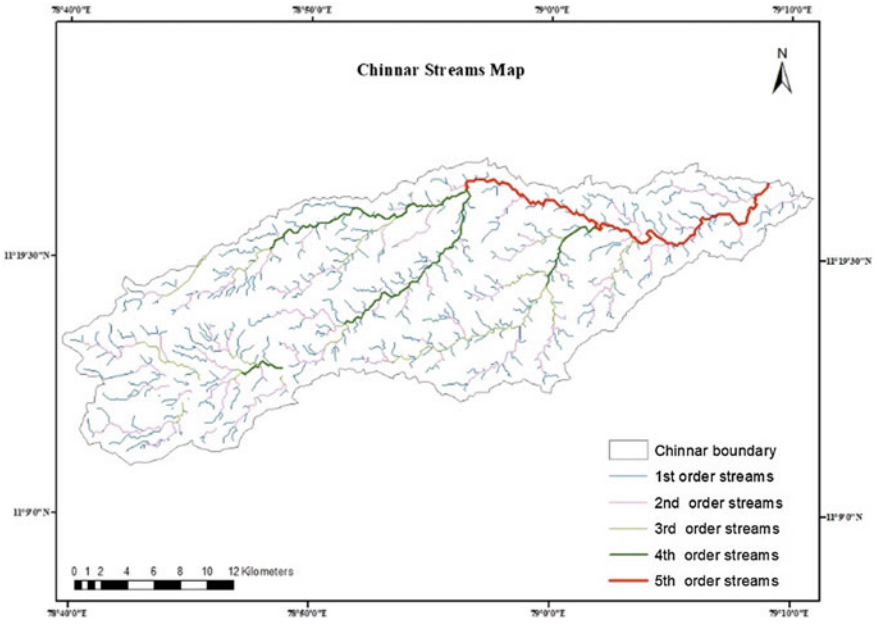

Fig. 3 Chinnar watershed stream map

4 Results and Discussion

Using remote sensing DEM data, basin area, perimeter, length, orders of streams, numbers of streams, length of streams and relief data were measured. From that information, morphometric parameters were derived and it is discussed below.

4.1 Stream Order

Stream order is a system for classifying streams and rivers based on their relative position in a drainage network [10]. The Chinnar River is a fifth-order Hortonian stream.

4.2 Drainage Density (Dd)

By dividing the total length of streams in an area by the area itself, the drainage density of that area is determined [11]. Dd has influence in drainage texture. The

drainage density of complete Chinnar sub-watersheds is lesser than 2, indicating a very coarse drainage texture.

4.3 Bifurcation Ratio (Rb)

The branching structure of a stream network is quantified using the bifurcation ratio [12]. In Chinnar, sub-watersheds have Rb values that range from 0 (SW 4) to 6.1 (SW 17). SW 1,2,3,4,5,6,7,8,9,10,12,14,12,15,16,19,20,25,26,27,28,29 is having Rb values less than or equal to 3, which indicates that this watershed has lineament density. SW 11,13,17,18,21,22,23,24 is having high Rb values (more than 3) which are high lineament density.

4.4 Stream Frequency (Fs)

Fs is determined by ratio of the total number of streams to the area (Fs) [11]. High-stream frequency leads to high drainage density and vice versa. 0.57 (SW 3) is the least Fs and 1.97 (SW 1) is the highest frequency in Chinnar sub-watershed.

4.5 Drainage Texture (Rt)

The drainage texture is characterized by shape and size of streams, and it can be used to describe the overall structure of a stream network. All Chinnar sub-basins are of very coarse drainage texture.

4.6 Circularity Ratio (Rc)

Rc is derived by dividing the basin's area by a circle's area that has the same perimeter as the basin. It varies from zero to one, where one means circular basin, zero means elongated or irregular basin [13]. 17 sub-watersheds have Rc range between 0.4–0.64 which shows that drainage system is structurally controlled.

4.7 Elongation Ratio (Re)

A higher elongation ratio indicates a more elongated, or stretched out, drainage network, while a lower ratio indicates a more compact network [12]. Sub-watersheds

20–29 have less than 0.7 elongation ratio which means elongated. Sub-watersheds 1–19 have elongation ratio greater than 0.7 which means less elongated.

4.8 Form Factor (Rf)

The area of a watershed divided by the area of a circle with the same perimeter is referred to as the form factor (Rf), which is a measurement of a watershed's shape [11]. A value of 1 for the form factor indicates a circular shape, while a value less than 1 indicates a more elongated or irregular shape. Sub-watersheds in Chinnar have Ff value between 0.3–0.47 which indicate moderately elongated.

4.9 Length of Overland Flow (Lo)

Lo is a measure of the distance that rain drop travels over the land of a watershed to enter a channel [11]. The lowest length of overland flow in Chinnar sub-watershed is 0.37 (SW 18) and highest Lo 0.58 (SW 8).

4.10 Relief (H)

Relief (H) is a measurement of the difference in elevation between its maximum and minimum points [12]. Chinnar basin relief is varying between 20–786.

4.11 Ruggedness Number (Rn)

H and Dd combine to produce Rn [14]. Sub-watershed 14 has lowest Rn and sub-watershed 20 has high Rn.

4.12 Infiltration Number (Ni)

The infiltration rate, also known as the infiltration number, is a measure of the rate at which water enters the soil. In Chinnar sub-basin, infiltration number varies between 0.58–2.32.

Table 1 Details of prioritization class

Range	Class number	Prioritization class
72–101.4	1	Very low
101.8–131.5	2	Low
131.6–161.3	3	Medium
161.4–191.1	4	High
191.2–221	5	Very high

4.13 Relief Ratio (Rr)

The relief ratio is calculated as the ratio of the distance between the maximum and minimum points' elevation deviation [12]. 14 sub-watersheds have low relief ratio (17.7–46.41), 6 sub-watersheds have moderate relief ratio (52.2–231.23), and remaining 9 sub-watersheds have high relief ratio (365.95–835.51).

4.14 Prioritization based on Compound Factor

Bifurcation ratio, drainage density, stream frequency, drainage texture, circularity ratio, form factor, ruggedness number, infiltration number, and relief ratio have direct relationship with flood [15–17]. Elongation ratio and length of overland flow have inverse relationship with flood. Assigned lower value to rank 1 and second lowest to rank 2 and so on for directly related parameter and vice versa for inversely related parameters. Compound parameter is calculated by adding all the ranks. The compound parameter varies between 72–221. It's grouped into five groups as given in Table 1. Table 2 and Fig. 4 shows Chinnar sub-watersheds prioritization.

Table 2 Details of Chinnar sub-watershed prioritization by compound factor analysis

Sub-watershed	A	P	Mean Rb	Dd	Fs	Rt	Rc	Re	Lo	Rn	Rr	Ni	Compound parameter	Class
1	5.08	12.95	20	9	29	12	9	29	9	19	20	28	184	4
2	5.23	10.91	21	8	20	9	26	28	8	2	13	16	151	3
3	5.25	11.52	13	18	1	1	21	27	18	5	16	2	122	2
4	6.09	12.64	1	28	28	16	19	26	28	9	12	29	196	5
5	6.50	11.33	3	14	26	17	29	25	14	10	15	25	178	4
6	6.61	12.92	5	15	10	5	22	24	15	11	14	9	130	2
7	7.20	13.46	6	25	6	4	23	23	25	18	19	10	159	3
8	7.26	12.89	7	1	5	6	25	22	1	7	17	4	95	1
9	8.40	16.54	9	5	2	2	10	21	5	24	28	1	107	2
10	8.67	16.54	2	13	24	14	14	20	13	22	26	24	172	4
11	10.01	15.56	25	22	27	18	24	19	22	3	8	27	195	5
12	10.50	20.11	11	7	9	7	7	18	7	26	29	7	128	2
13	11.35	19.98	26	3	4	3	8	17	3	4	11	3	82	1
14	13.86	23.49	16	2	13	10	5	16	2	1	1	6	72	1
15	14.52	19.67	17	11	8	11	17	15	11	12	9	8	119	2
16	14.68	17.75	4	23	3	8	28	14	23	23	25	5	156	3
17	15.67	18.78	29	17	25	23	27	13	17	21	23	26	221	5
18	15.82	22.42	23	29	14	15	13	12	29	6	3	22	166	4
19	17.13	23.53	8	16	23	20	11	11	16	14	10	23	152	3
20	25.28	31.52	15	24	7	13	6	10	24	29	27	11	166	4
21	29.21	28.03	27	4	21	24	16	9	4	8	4	13	130	2
22	36.79	40.57	22	20	17	22	4	8	20	15	6	19	153	3
23	39.27	31.86	24	12	22	28	20	7	12	17	7	20	169	4
24	45.03	35.55	28	26	15	26	15	6	26	28	24	18	212	5
25	45.37	34.62	18	19	12	25	18	5	19	13	2	12	143	3
26	49.62	54.04	12	10	16	21	1	4	10	16	5	15	110	2
27	56.18	57.10	14	27	11	19	2	3	27	27	22	17	169	4
28	59.78	43.93	10	6	18	29	12	2	6	20	18	14	135	3
29	81.56	67.31	19	21	19	27	3	1	21	25	21	21	178	4

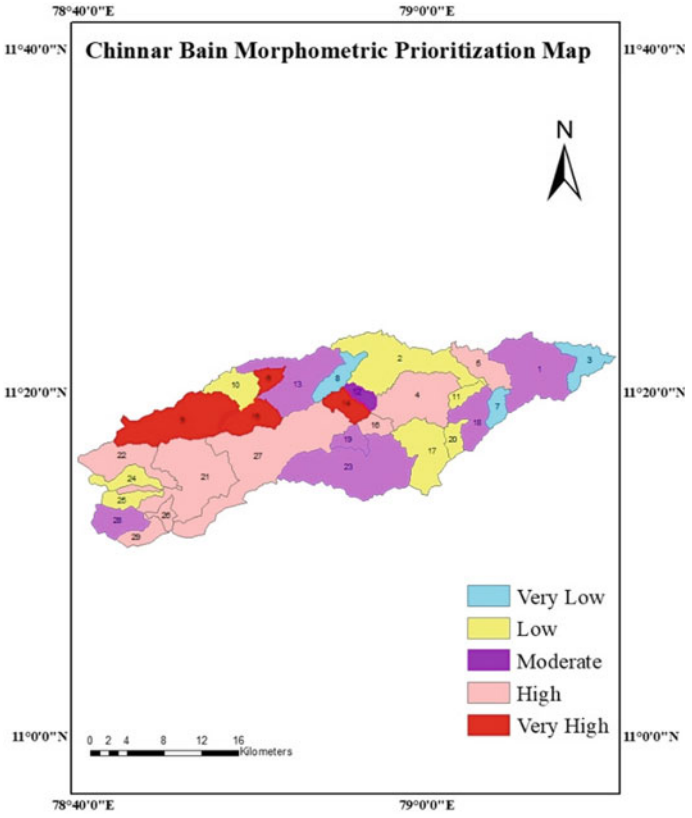

Fig. 4 Prioritization map of Chinnar sub-watershed

5 Conclusion

From the bifurcation ratio, number 19 sub-watersheds are flat basins, and ten are mountainous basins. Most sub-watersheds are semi-circular in shape and have moderate relief. From the observation, the basin is not controlled by geological structures. Based on compound parameters, sub-watersheds are grouped into five classes. The details of each classes corresponding sub-watershed and the total number of the watershed in that class were tabulated in Table 3. Sub-watersheds 1,5,10,18,20,23,27,29 are at high risk and sub-watersheds 4,11,7,24 are at very high risk of flood, so the conservation measures should concentrate on this area. This paper only deals with morphometric characteristics, not climate and soil parameters.

Table 3 Number of sub-watersheds in each class

Class	Sub-watersheds	No. of sub-watersheds
Very low	8,13,14	3
Low	3,6,9,12,15,21,26	7
Medium	2,7,16,19,22,25,28	7
High	1,5,10,18,20,23,27,29	8
Very high	4,11,17,24	4

References

1. Waiyasusri K, Chotpantarat S (2020) Watershed prioritization of Kaeng Lawa sub-watershed, Khon Kaen Province using the morphometric and land-use analysis: a case study of heavy flooding caused by tropical storm Podul. Water 12:1570. https://doi.org/10.3390/W12061570
2. Sreedevi PD, Subrahmanyam K, Ahmed S (2005) The significance of morphometric analysis for obtaining groundwater potential zones in a structurally controlled terrain. Environ Geol 47:412–420. https://doi.org/10.1007/S00254-004-1166-1/FIGURES/5
3. Odiji CA, Aderoju OM, Eta JB, Shehu I, Mai-Bukar A, Onuoha H (2021) Morphometric analysis and prioritization of upper Benue River watershed, Northern Nigeria. Appl Water Sci 11:1–28. https://doi.org/10.1007/S13201-021-01364-X/FIGURES/11
4. Ghasemlounia R, Utlu M (2021) Flood prioritization of basins based on geomorphometric properties using principal component analysis, morphometric analysis and Redvan's priority methods: a case study of Harşit River basin. J Hydrol 603:127061. https://doi.org/10.1016/J.JHYDROL.2021.127061
5. Utlu M, Ghasemlounia R (2021) Flood prioritization watersheds of the Aras River, based on geomorphometric properties: case study Iğdır Province. J Geomorphol Res 21–40. https://doi.org/10.46453/JADER.781152
6. Obeidat M, Awawdeh M, Al-Hantouli F (2021) Morphometric analysis and prioritisation of watersheds for flood risk management in Wadi Easal Basin (WEB), Jordan, using geospatial technologies. J Flood Risk Manag. 14:e12711. https://doi.org/10.1111/JFR3.12711
7. Selvan MT, Ahmad S, Tamil Selvan M, Rashid SM (2011) Analysis of the geomorphometric parameters in high altitude glacierised terrain using SRTM DEM data in Central Himalaya, India. 1(1)
8. Thakkar AK, Dhiman SD (2007) Morphometric analysis and prioritization of miniwatersheds in Mohr watershed, Gujarat using remote sensing and GIS techniques. J Indian Soc Remote Sens 35:313–321. https://doi.org/10.1007/BF02990787/METRICS
9. Mundetia N, Sharma D, Dubey SK (2018) Morphometric assessment and sub-watershed prioritization of Khari River basin in semi-arid region of Rajasthan, India. Arab J Geosci 11:1–18. https://doi.org/10.1007/S12517-018-3819-5/FIGURES/6
10. Richard H (1995) Horton, R.E. 1945: Erosional development of streams and their drainage basins: hydrophysical approach to quantitative morphology. Bulletin of the Geological Society of America 56, 2 75–370. Prog Phys Geogr 19:533–554. https://doi.org/10.1177/030913339501900406/ASSET/030913339501900406.FP.PNG_V03
11. Horton RE (1932) Drainage-basin characteristics. EOS Trans Am Geophys Union 13:350–361. https://doi.org/10.1029/TR013I001P00350
12. Schumm SA (1956) Evolution of drainage systems and slopes in badlands of Perth Amboy. Bull Geol Soc Am 67:597–646
13. Miller VC (1957) A quantitative geomorphic study of drainage basin characteristics in the clinch Mountain Area, Virginia and Tennessee. V. C. Miller. J Geol 65:112–113. https://doi.org/10.1086/626413
14. Arthur SN (1952) Dynamic basis of geomorphology geology. Geol Soc Am Bull 63:923–938

15. Shaikh M, Yadav S, Manekar V (2022) Application of the compound factor for runoff potential in sub-watersheds prioritisation based on quantitative morphometric analysis. J Geol Soc India 98:687–695. https://doi.org/10.1007/S12594-022-2045-7/METRICS
16. Meraj G, Romshoo SA, Yousuf AR, Altaf S, Altaf F (2015) Assessing the influence of watershed characteristics on the flood vulnerability of Jhelum basin in Kashmir Himalaya. Nat Hazards 77:153–175. https://doi.org/10.1007/S11069-015-1605-1/FIGURES/6
17. Mathew A, Shekar PR (2023) Flood prioritization of basins based on geomorphometric properties using morphometric analysis and principal component analysis: a case study of the Maner River Basin, pp 323–353. https://doi.org/10.1007/978-981-19-7100-6_18

Municipal Engineering

Factors Influencing the Density and Compressive Strength of Foam Concrete: An Examination

Y. Sivananda Reddy, S. Anandh, and S. Sindhu Nachiar

Abstract Foam concrete (FC) is one among the lightweight concrete, which is usually considered for its low strength and therefore it is majorly used as a filling material. Regardless, it is observed that there is a growing interest in FC to use in various building elements such as floors, walls, slab, etc. The study aims to develop FC as a structural material. A 1600 kg/m^3 density is fixed for the design mix and overall, seventeen mix ratios were designed, cast and tested for compression, splitting tensile and flexural strength. The mixes were designed by varying the materials such as foam volume (FV) of 12–1%, coarse aggregate 10–50%, water cement ratio 0.27–0.40% and cement-sand ratio of 1:1, 1:1.5, and 1:2. The experimental values shows that with the increase in FV, there is a drop in FC density and it is also observed that density is directly proportional to mechanical properties. Therefore, the maximum strength is achieved at 1% FV with the density of 1753 kg/m^3 and the respective compressive strength of 25.6 N/mm^2.

Keywords Foam concrete · Foam volume · Physical properties · Mechanical properties · Density

1 Introduction

Lightweight, durable, user-friendly, cost-effective, and environmentally friendly concrete is seen as the future of the concrete industry. As a result, extensive research is being conducted on the behaviour of lightweight concrete in structural applications. One such material is foam concrete (FC), which possesses the desired characteristics such as self-flowing properties, enhanced thermal conductivity, superb resistance to freeze–thaw cycles, and reduced aggregate usage [1–3]. FC has many advantages, such as self-flowing properties, superior thermal conductivity, excellent freeze–thaw resistance, and reduced aggregate usage. Maintaining the density is a critical role,

Y. S. Reddy · S. Anandh (✉) · S. Sindhu Nachiar
Department of Civil Engineering, Faculty of Engineering and Technology, SRM Institute of Science and Technology, Kattankulathur, Tamil Nadu 603203, India
e-mail: anandhs@srmist.edu.in

K. R. Reddy et al. (eds.), *Recent Advances in Civil Engineering*, Lecture Notes in Civil Engineering 398, https://doi.org/10.1007/978-981-99-6229-7_25

while in production of FC, therefore a proper foam dosage should be maintained to achieve, it is suggested that with appropriate foam dosage a density of FC ranges between 400–1800 kg/m^3 [4].

Cement, sand, foam, and water are commonly used to make FC, cement and sand and water is mixed to foam slurry material and artificial porous foam is mixed with slurry in a concrete mixer to create a cohesive composition [5–9]. The artificial porous foam is generated using a solution made up of water and foaming solution, and then it is introduced into a foaming machine along with compressed air, which causes the solution to bubble up. The foaming agent used has the capability to produce durable air bubbles that can endure the physical and chemical processes involved in concrete production [10]. Due to its recent evolution, FC is used in various projects around the world in recent time [10–12].

As the low strength to weight ratio it is discovered that FC is mostly used as non-structural element. However, the use of coarse aggregate in conjunction with the foaming agent, on the other hand, may result in the formation of FC suitable for structural purposes. Current research intends to optimise the volume of coarse aggregate to produce FC for structural applications and then evaluate its physical and mechanical properties. The ultimate objective is to create a lightweight structural concrete.

2 Experimental Programme

In the present work, foam concrete (FC) was prepared by carefully combining cement, fine, coarse aggregate water, and foam. FC was cast and tested for three mechanical property tests.

The mix design and proportions were calculated using a formula developed by the University of Dundee [13]. The density of FC was determined by the sum of the weight of materials like cement, aggregate, and water. The density of 1600 kg/m^3 and water as 180 L were selected to make the concrete suitable for use as a structural element [14, 15].

For the mix ratios without coarse aggregate the mix design was calculated using the following equation:

$$D = C + F + W \tag{1}$$

where

C:Cement (kg/m^3)
F:Fine aggregate (kg/m^3)
W:Water (litres)
D:Design density (kg/m^3).

$$1600 = C + F + W \tag{2}$$

$$1600 = C + F + 180 \tag{3}$$

$$C : F = 1 : 1 \tag{4}$$

$$1600 - 180 = C + F \tag{5}$$

$$1420 = C + F \tag{6}$$

Therefore,
C710 kg/m^3
F710 kg/m^3
W180 l
For the mix ratio with coarse aggregate, the equation is taken as follows:

$$D = C + A + W \tag{7}$$

where A = aggregate (fine + coarse).

2.1 Preparation of FC

Preparation process of FC is relatively straightforward and involves several key steps. As per codal provision, a performing method is adopted to produce FC [16]. To begin, a pre-made foam is created by pumping a diluted foam solution (1 part foam solution to 20 parts water) into a foam machine along with compressed air. This foam is then combined with cement, water, and fine aggregate in a large mixing vessel to form a slurry. The mixture should be thoroughly stirred to ensure homogeneity. In some cases, a densifier material like fly ash or silica fume, will increase the durability and strength when added to the mixture. Once the mixture has been prepared, it can be poured into moulds or laid on the ground and compacted using a tamping machine. After casting, the FC should be cured for at least 24–48 h to allow the chemical reactions to take place and the strength of the concrete to develop. Finally, if desired, the surface of the FC can be finished by trowelling or by applying a layer of conventional concrete. It is important to follow the manufacturer's recommendations and to perform appropriate tests to ensure the desired properties are achieved [17–19]. The preparation process of FC is shown in Fig. 1.

Fig. 1 Flowchart of foam concrete production

2.2 Physical Properties of Raw Materials

The components used to make FC are listed in Table 1 with their respective physical characteristics. The study utilised ordinary Portland Cement (OPC) 53-grade, which met the standards set by [20]. The fine aggregate of 4.75 mm size is used in the study and sourced from Zone II, as specified by [21]. According to [22], coarse aggregate of 6.3 mm was also utilised, in accordance with the criteria indicated in [23]. In accordance with [24] the study used portable water. The protein-based foaming agent was mixed with 1 part of foam solution and 40 parts of water, as per [16] through a trial-and-error method to create the foam (Table 2).

3 Analysis and Interpretation of Findings

3.1 Influence of Water-Solids Ratio on Consistency of FC

The consistency of FC can be significantly influenced by the water-solids ratio. Generally, increasing the water-solids ratio will result in a more fluid mixture and a wetter consistency. This can make the FC easier to pour and work with, but it may also lead to a lower strength and durability. The impact of the w/c ratio on the consistency of FC is shown in Fig. 2.

The flow values for various w/c ratios are depicted in Fig. 2. It can be inferred from the graph that a w/c ratio of 0.3–0.4% yields a consistency of 140–145% for

Table 1 Mix proportions for FC

Batches	Mix No's	Mix Ratio	C (kg/m^3)	FA (kg/m^3)	CA (kg/m^3)	w/c (%)	FV (%)	Admixture	Design Density (kg/m^3)
B1	M1	C: FA 1:1	625	710	0	00.29	12	Adam Plast—1%	1600
	M2	C: FA 1:1.5	500	852	0	00.36	12		1600
	M3	C: FA 1:2	416	946	0	00.43	12		1600
B2	M4	C: FA 1:1	667	710	0	00.27	6		1600
	M5	C: FA 1:1.5	533	852	0	00.34	6		1600
	M6	C: FA 1:2	445	946	0	00.4	6		1600
B3	M7	C: FA 1:1	667	355	355	00.27	6		1600
	M8	C: FA 1:1.5	533	426	426	00.34	6		1600
	M9	C: FA 1:2	445	473	473	00.4	6		1600
B4	M10	C: A 1:1.5	533	426	426	00.33	6		1600
	M11		533	511	340	00.33	6		1600
	M12		533	596	255	00.33	6		1600
	M13		533	682	170	00.33	6		1600
	M14		533	766	85.2	00.33	6		1600
B5	M15		551	426	426	00.33	3	Sika 903—3%	1600
B6	M16		557	426	426	00.32	2		1600
B7	M17		562	426	426	00.32	1		1600

C cement, *FV* foam volume, *FA* fine aggregate, *w/c* water-to-cement ratio, *CA* coarse aggregate

12% FV, 129–139% for 6% FV, and 122–98% for 3, 2, and 1% FV. Hence, reducing the FV in concrete can result in a decrease in flow value.

3.2 Influence of Water-Solids Ratio on Density of FC

The fresh mix was used to determine the wet density of the FC, while the cured and dried samples were used to find the dry density of the FC. Figure 3 shows the values for dry and wet density, respectively. Figure 4 depicts the factor for water solid

Table 2 Constituent material physical properties

Properties	Constituent materials			
	Cement	Fine aggregate	Coarse aggregate	Foaming agent
Specific gravity	3.12	2.81	2.84	–
Fineness modulus (%)	2.18	3.32	4.29	–
Consistency (%)	32	–	–	–
Soundness (mm)	2	–	–	–
Initial setting time (min)	44	–	–	–
Impact resistance (%)	–	–	18.22	–
Shape	–	Granular	Granular and sub angular	–
Bulking (%)	–	31	–	–
aggregate zone	–	Zone II	–	–
Flakiness index (%)	–	–	13	–
Crushing strength (%)	–	–	12.73	–
Final setting time (min)	429	–	–	–
pH	–	–	–	6.5–8.5
Kinematic viscosity (mm^2/s)	–	–	–	11
Abrasion value (%)	–	–	11.7	–

ratio on FC density. The dry density is increased from 1534 to 1759 kg/m^3 when the FV was decreased from 12 to 1%. Lower water-to-cement ratio FC revealed interconnecting pores. This outcome shows the fact that a lower water-to-cement ratio would lead to greater tiny particles and high surface area, ultimately small pore walls and more connection between the pores [25]. It is also apparent that all the mixes had a density ratio of 1, indicating that they all achieved a lightweight density.

3.3 Influence of Density on Compressive Strength of FC

The results shows the relationship between the density and compressive strength of foam concrete. As illustrated in Fig. 5, the compressive strength of FC increases with density. This is because denser concrete often has fewer voids or pores, which can weaken the substance by serving as locations for fracture initiation and propagation under compressive pressures. Mixture 17, for example, had a compressive strength of 25.6 N/mm^2 and a density of 1753 kg/m^3, but mixture 1 had a density of 1534 kg/

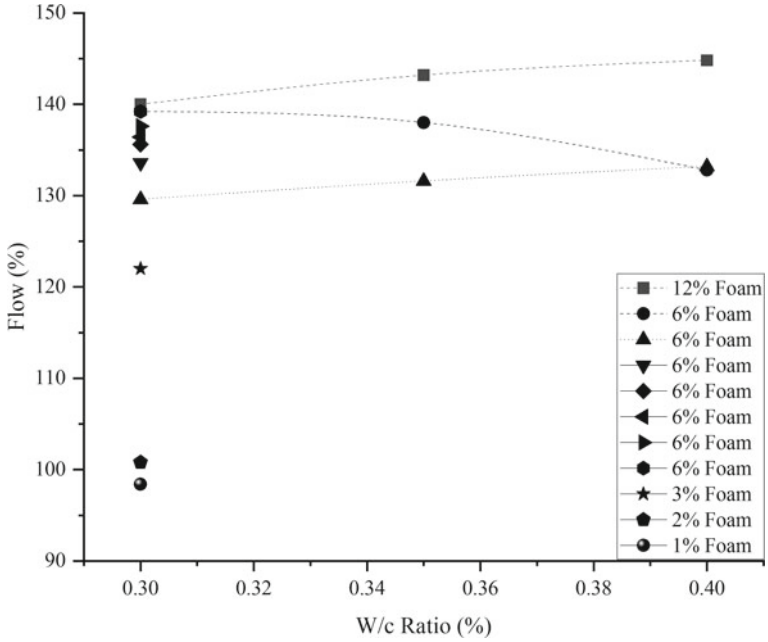

Fig. 2 Variation of consistency with w/c ratio and foam volume

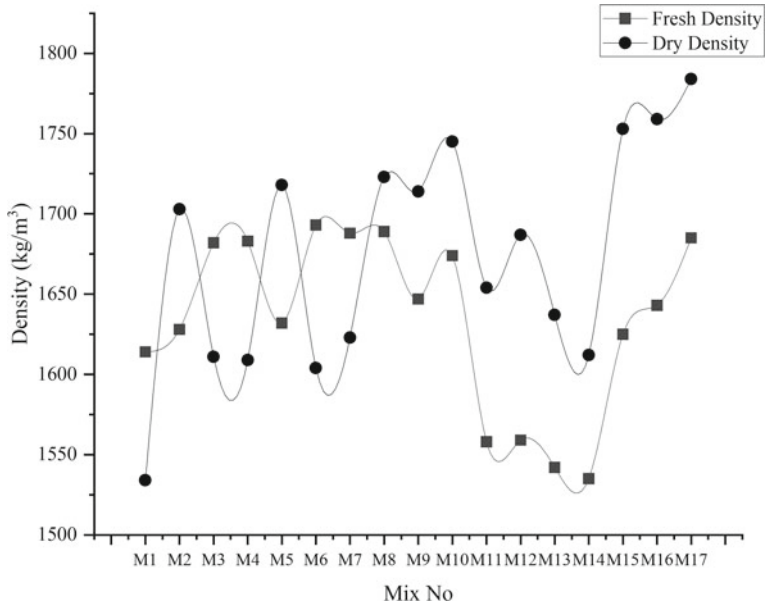

Fig. 3 Foam concrete dry and wet density relationship

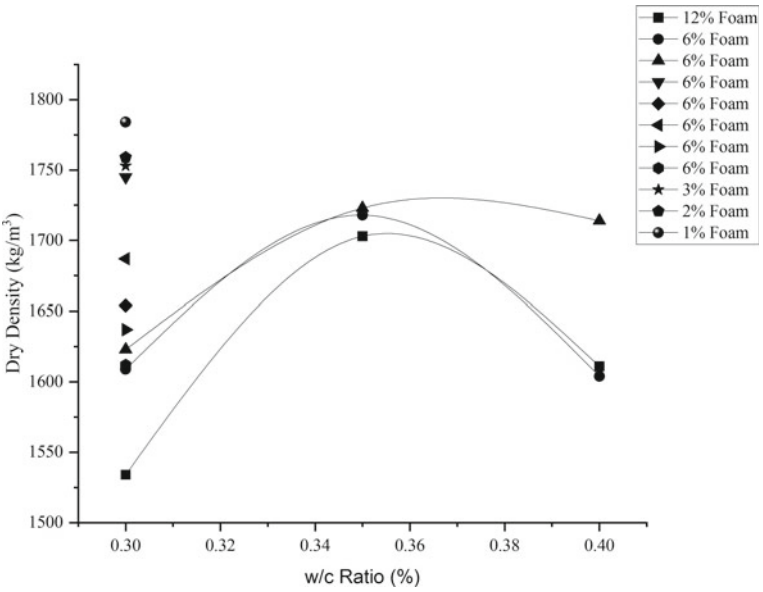

Fig. 4 Foam concrete dry density, w/c ratio, and foam volume relationship

m^3 and a compressive strength of just 5.7 N/mm^2. The foam concrete density plays the major role in the compressive strength.

3.4 Influence of Foam Volume on Compressive Strength of FC

The current study evaluates 17 different mixes, calculated using varying FV of 12, 6, 3, 2, and 1% as shown in Fig. 6. From the graph, the use of foam dose has a direct impact on compressive strength. A lower FV resulted in higher compressive strength of 5.7 N/mm^2, with 1% foam exhibiting the highest compressive strength of 25.6 N/mm^2, which is 127% higher compared with 12% foam volume. Therefore, it can be said that reduction in FV leads to increase in compressive strength.

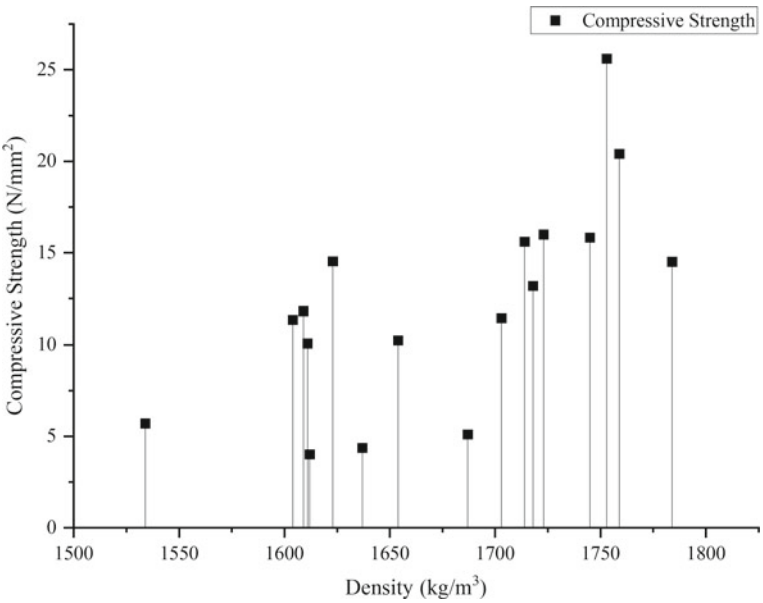

Fig. 5 Variation of compressive strength with density in FC

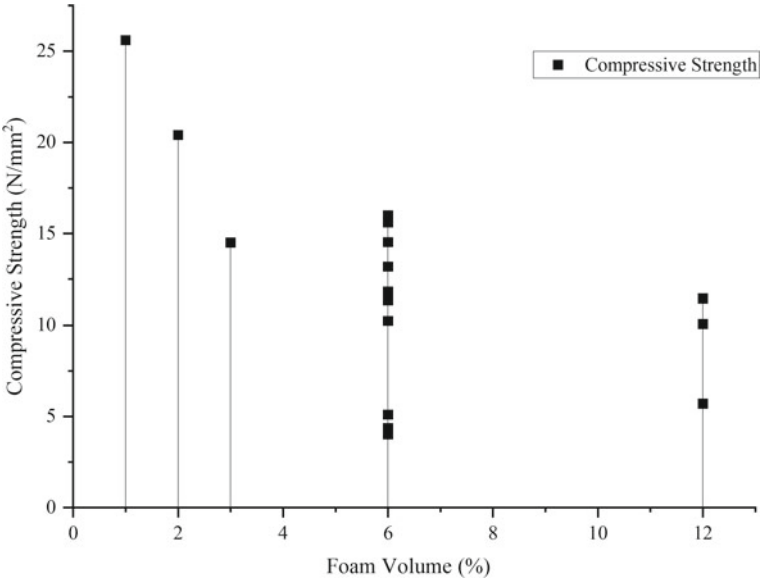

Fig. 6 Foam volume variation with respect to compressive strength

4 Conclusion

The experiment explored the effect of numerous parameters, such as water-solids ratio, density, coarse aggregate, and FV on consistency, compressive strength, and split tensile strength of FC.

- The increasing water-solids ratio led to a more fluid mixture and wetter consistency, but also reduced strength and durability. The concrete mixes that were made using 1% foam had a significantly lower flow value compared with the concrete mix prepared with 12% foam content. Specifically, the flow value of the 1% was found to have 34.89% lower than the mixture with 12% FV.
- Coarse aggregate improves the mechanical properties for FC, but the size and shape of the aggregate should be carefully controlled and ensured that the resulting mixture has the desired properties. Coarse aggregate with 426 kg/m^3 showed better performance in mechanical properties when compared with others.
- As density increased, compressive strength increased due to fewer voids or pores weakening the material. The density of FC specimen varies from 1534 to 1784 kg/m^3 where lower density showed a lower compressive strength and higher density showed higher compressive strength of 25.6 N/mm^2, which is 127% higher compared with the mix with lower density.
- Compressive strength is influenced by coarse aggregate, density, and FV. Increasing density and reducing FV can result in an increase in compressive strength, while adding coarse aggregate can also improve compressive strength.
- The use of 12% foam in FC is not recommended because it increases flow value and reduces the mechanical properties.
- There is a complex interplay between the different factors affecting FC properties, and careful testing and experimentation may be required to determine the optimal mix for a given application.

References

1. Bhandari PS, Tajne KM (2014) Cellular lightweight concrete using fly ash 3:17635–17638. https://doi.org/10.15680/IJIRSET.2014.0311076
2. Trivedi Manoj S, Patel Harsh M (2015) An experimental work on cellular light-weight concrete. Int J Adv Eng Res Dev 2:313–319. https://doi.org/10.21090/ijaerd.020352
3. Nambiar EKK, Ramamurthy K (2006) Influence of filler type on the properties of foam concrete 28:475–480. https://doi.org/10.1016/j.cemconcomp.2005.12.001
4. Roslan AF, Awang H, Mydin MAO (2013) Effects of various additives on drying shrinkage, compressive and flexural strength of lightweight foamed concrete (LFC). Adv Mater Res 626:594–604. https://doi.org/10.4028/www.scientific.net/AMR.626.594
5. Jiang J, Lu Z, Niu Y, Li J, Zhang Y (2016) Study on the preparation and properties of high-porosity foamed concretes based on ordinary Portland cement. Mater Des 92:949–959. https://doi.org/10.1016/j.matdes.2015.12.068

6. Hashim M, Tantray M (2021) Comparative study on the performance of protein and synthetic-based foaming agents used in foamed concrete. Case Stud Constr Mater 14:e00524. https://doi.org/10.1016/j.cscm.2021.e00524
7. Raj A, Sathyan D, Mini KM (2019) Physical and functional characteristics of foam concrete: a review. Constr Build Mater 221:787–799. https://doi.org/10.1016/j.conbuildmat.2019.06.052
8. Bagheri A, Samea SA (2018) Parameters influencing the stability of foamed concrete. J Mater Civ Eng 30:04018091. https://doi.org/10.1061/(asce)mt.1943-5533.0002290
9. Gökçe HS, Hatungimana D, Ramyar K (2019) Effect of fly ash and silica fume on hardened properties of foam concrete. Constr Build Mater 194:1–11. https://doi.org/10.1016/j.conbuildmat.2018.11.036
10. Kumar NV, Arunkumar C, Senthil SS (2018) Science direct experimental study on mechanical and thermal behavior of foamed concrete. Mater Today Proc 5:8753–8760. https://doi.org/10.1016/j.matpr.2017.12.302
11. Zhang H, Qi X, Wan L, Zuo Z, Ge Z, Wu J, Song X (2020) Properties of silt-based foamed concrete: a type of material for use in backfill behind an abutment. Constr Build Mater 261:119966. https://doi.org/10.1016/J.CONBUILDMAT.2020.119966
12. Falliano D, De Domenico D, Ricciardi G, Gugliandolo E (2018) Experimental investigation on the compressive strength of foamed concrete: effect of curing conditions, cement type, foaming agent and dry density. Constr Build Mater 165:735–749. https://doi.org/10.1016/j.conbuildmat.2017.12.241
13. Jones MR, McCarthy A (2005) Preliminary views on the potential of foamed concrete as a structural material. Mag Concr Res 57:21–31. https://doi.org/10.1680/macr.2005.57.1.21
14. Sabaa B, Ravindrarajah RS (1997) Engineering properties of lightweight concrete containing crushed expanded polystyrene waste. Proceedings of the symposium MM: advances in materials for cementitious composites, pp 1–3
15. Suraneni P, Bran Anleu PC, Flatt RJ (2016) Factors affecting the strength of structural lightweight aggregate concrete with and without fibers in the 1200–1600 Kg/m^3 density range. Mater Struct Constr 49:677–688. https://doi.org/10.1617/s11527-015-0529-2
16. IS 2185 (2008) Concrete masonry units, part 4: preformed foam cellular concrete blocks
17. Harith IK (2018) Study on polyurethane foamed concrete for use in structural applications. Case Stud Constr Mater 8:79–86. https://doi.org/10.1016/j.cscm.2017.11.005
18. Pan Z, Hiromi F, Tionghuan W (2007) Preparation of high performance foamed concrete from cement. Sand Mineral Admixt 1881:295–298. https://doi.org/10.1007/s11595-005-2295-4
19. De Rose L (1999) The influence of the mix design on the properties of micro-cellular concrete. In: Specialist techniques and materials for concrete construction, pp 185–197
20. IS 12269 (2013) Ordinary Portland cement, 53 grade - specification
21. IS 383 (2016) I. Coarse and fine aggregate for concrete - specification
22. BIS (Bureau of Indian Standards) (2016) Coarse and fine aggregate for concrete-specification IS 383:2016. BIS, New Delhi, pp 1–21
23. IS 2386 (1963) Part III method of test for aggregate for concrete. Part III—specific gravity, density, voids, absorption and bulking. Bur Indian Stand New Delhi (Reaffirmed 2002)
24. IS 456 (2000) Plain concrete and reinforced. Bur Indian Stand Delhi, pp 1–114
25. Liu Z, Zhao K, Hu C, Tang Y (2016) Effect of water-cement ratio on pore structure and strength of foam concrete. Adv Mater Sci Eng. https://doi.org/10.1155/2016/9520294

Investigation on Possible use of Industrial Waste as Partial Replacement of Cement in Concrete

Senthil kumar Ganapathy, Sujitha Ravi, and Chidambaranathan Subramanian

Abstract Concrete is a common traditional material used by the construction industry. Depending on the demand, concrete grades like M10, M20, M30, M40, M50, M60, and M70 were commonly used in building construction. Concrete of a higher grade requires cement with good quality characteristics. Cement production generates a significant quantity of carbon emissions. By replacing some of the virgin cement with pozzolanic materials or industrial wastes, it is possible to reduce CO_2 emissions. A variety of industrial wastes, including tannery waste, paper pulp, and electroplating waste, were utilized in the current experiment. An analysis of the waste materials is carried out for determining its fundamental qualities. M20 concrete grade was used for the present study and concrete cubes with standard dimensions of 150 $\times$ 150 $\times$ 150 mm were made using cement, and cubes were also made using the industrial waste as partial replacement for cement. The cubes were evaluated on 7, 14, and 28th days for its compressive strength and tensile strength. The outcome of the study reflects electroplating sludge (also known as chrome waste) had a higher compressive strength and tensile strength when compared to paper pulp and tannery waste.

Keywords Concrete · Compressive strength test · Electroplating waste · Paper pulp · Tannery waste · Tensile strength test

S. Ganapathy (✉) · S. Ravi
Environmental Engineering Laboratory, Annamalai University, Chidambaram, India
e-mail: cdm.gsk@gmail.com

S. Ravi
e-mail: sujitharavi215@gmail.com

C. Subramanian
Manufacturing Engineering, Annamalai University, Chidambaram, India
e-mail: s_cdm@yahoo.com

K. R. Reddy et al. (eds.), *Recent Advances in Civil Engineering*, Lecture Notes in Civil Engineering 398, https://doi.org/10.1007/978-981-99-6229-7_26

1 Introduction

Current global population growth has had the greatest impact on sustainable development. Building our communities in a way that allows people to combine peacefully without depleting all our resources is essential. Depleting the natural resources has an impact on the environment. It is commonly recognized that concrete plays a significant role in the development of contemporary infrastructure, industrialization, and urbanization to accommodate the expanding human population. The most needed and popular construction material is concrete [1]; due to the enormous strain on demand for construction materials in the construction sector, renewable resources like stream rock and sand are being exploited [2]. Cement, sand, and blue metal make up conventional concrete, and the impact of aggregates on the physical properties of the concrete plays an important role in determining its strength [3]. On the other hand, the high output of industrial waste or by-products is one of the primary challenges that the construction industry and other industries are currently facing. By using these materials in place of cement in concrete, it is simple to deal with the growth of landfills and dust in the environment generated by demolition of age old structures. and in the disposal of industrial waste [4–6]. Increasing the production efficiency and reducing the impact on men and material, the Circular Economy model and the concept of Cleaner Production are introduced but met with formidable challenges. For replacing the naturally occurring materials that are used in concrete, sustainable substitutes must be found. It is become increasingly difficult to recycle industrial waste and in the future, waste recycling and recovery programms may necessitate replacing some natural resources, notably those used in the construction sector [7]. The production of concrete for contemporary infrastructure now uses ordinary Portland cement (OPC), the second-most consumed material after water. Since only the production of OPC accounts for around 7% of the daily CO_2 emissions into the atmosphere, the rate of global warming is increasing. OPC clinker burning (at a temperature of about 14,000 °C) is not just responsible for CO_2 emissions. Overall, scientists, engineers, and everyone else involved in this issue would have a unique responsibility and alternative approach to take. Cement can partially be replaced by industrial waste which helps in reductioniefort ce of CO_2 emission. In the present study industrial waste is used to partially replace the cement using industrial wastes like sludge from tanneries (TS), paper pulp (PP), and waste from electroplating (ETP). As an alternative to landfill disposal, the use of waste paper pulp residuals in concrete compositions was examined [8]. In the raw, dry paper sludge, the main components are silica, calcium oxide, alumina, and magnesium oxide. There is a lot of potential for pollution that the tanning industry could create [9]. Raw skin or hide is converted into leather during the tannery process, which is subsequently used to make a range of items. Tanning is the first step in the process that gives the leather its stability. About 80–90% of tanneries employ chromium (III) salts, notably chromium sulfate, in their tanning processes [10–13]. Chromium salt-tanned hides exhibit superior mechanical resistance, exceptional dying adaptability,

and hydrothermal resistance when compared to hides treated with plant-based chemicals [14–16]. Furthermore, the high rate of penetration into the interfibrillar regions of the skin by chromium salts leads to a decrease in production time and enhanced process control [17, 18]. The use of ETP sludge to partially substitute building materials is becoming more and more widespread. The comprehensive investigation of the use of hazardous wastes and by-products as an additional green concrete component resulted in the finding that the strength of concrete and other properties is not significantly impacted by the partial replacement of solid hazardous wastes with conventional building materials like gravel, sand, blue metal, etc. The study also considered the usage of ETP waste as a potential building material [19]. Most of the dust and particulate metallic, ceramic, or organic substances produced during the mechanical pre-treatment and finishing of manufactured parts make up the solid waste produced during electroplating processes. Washing operations and the sludge from wastewater treatment systems are two additional sources of waste, both of which have high levels of heavy metals [20, 21]. The removal of trash from the cement matrix is one method employed in the building sector. This approach has been used to remediate several industrial pollutants, particularly those with high concentrations of heavy metals [7, 19, 21–23].

2 Materials and Methods

2.1 Study Area

APHA standard methods for examining water and waste water is used [24], in characteristic investigation of waste and experimental investigations are carried out at the Advanced Environmental Engineering laboratory of the Department of Civil Engineering, Annamalai University. The physical characteristics like, slump test, sieve analysis, and specific gravity of freshly hardened concrete compressive strength test, split tensile strength test, are carried out at the structural Engineering laboratory.

2.2 Aggregate Used

The equivalent of 85% of the volume of mass concrete and 55% of the volume of mortar, respectively, are made up of aggregate. Aggregate in concrete can only be larger than 15 mm in size and contains a size of 4.75 mm or smaller in mortar. Course aggregate ranging between 4.75 and 80 mm in size are used for the grade M20 as per IS 383:1970 [25]. **Fine aggregate** are passing through 4.75 mm to 150 microns. **Water** makes the chemical reaction with cement, and a crucial component of concrete. The quantity and quality of water contributes to the cement gel that provides strength.

The cement used in all mixtures was 53-grade Portland pozzolanic cement (PPC), which corresponds to IS 1489-1991 PPC [26].

2.3 Test / Analysis of Samples

2.3.1 Water Extraction

A modified standard test technique as mentioned (ASTM D3987 - 2006) [27] for shake extraction of solid waste with water was used to prepare the water extracts. Decantation, pressure filtration, or centrifugation were used to remove the surface water, which was then stored at 4°C for further examination of parameters such pH, EC, TDS, chloride, sulfate, sodium, calcium, potassium, magnesium, and lithium.

2.3.2 Acid Digestion

Metals must be dissolved from solid samples for examination through acid digestion. As suggested by NEPM (1999) [28], acid digests of solid waste samples obtained from process industry were prepared . Boiling aqua regia (3:1) was used to remove the metals from the samples to determine their total metal content. Using an Atomic Absorption Spectro Photometer, the acid digests were examined for the presence of heavy metals such as iron, zinc, copper, cadmium, nickel, and lead.

2.3.3 Specific Gravity

Concrete mix designs are calculated using specific gravity. Regarding the workability measurements, specific gravity is also required for determining the compacting factor.

2.3.4 Sieve Analysis

Sieve analysis can be performed on all granular material, down to a minimum size, depending on the exact technique. This includes sands, crushed rock, clays, granite, feldspars, coal, soil, a wide variety of manufactured powders, grain, and seeds. Given that it is simple to recognize, it is most likely the method of particle size that is most widely used.

2.3.5 Slump Test

The workability of fresh concrete is evaluated empirically using the concrete slump test. The consistency of the concrete in that batch is measured with increased accuracy. This test is carried out to evaluate the consistency of recently constructed concrete.

2.3.6 Compression Strength Test

The most frequent test performed on hardened concrete is the compression test. The compression test is typically performed between 7 and 28 days. The load must be delivered gradually and without shock, increasing by around 140 kg/cm/min, until the specimen loses its capacity to withstand the increased load and no more load can be sustained.

2.3.7 Split Tensile Strength Test

One of the fundamental and significant characteristics of concrete is its tensile strength. When a bigger load cannot be sustained, the load is delivered to the specimen lifted constantly without shock at a rate to produce a split tensile stress of around 1.4–2.1 N/mm^2/min known as the failure load, is applied.

3 Results and Discussion

3.1 Slump Test

It is essential to investigate the consistency of concrete and slump due to the partial replacement of industrial waste to concrete. Slump tests were performed in the laboratory using standard procedure, for M20 concrete as per IS 1199:1959 [29] with water cement ratio (w/c) ranging between 0.45 and 0.80. As a standardized measure 4500 g of fine aggregate, 5000 g of coarse aggregate, and 2400 g of cement were taken for slump test. To this mixture, 600 g of waste (20%) collected from various industries was added and tested. It can be observed that the true slump of concrete with 20% partial replacement of paper pulp waste occurs in between a water–cement ratio of 0.55–0.70, and beyond this, the slump of shear and collapse occur. Similarly, in the case of chrome waste from tanning a water–cement ratio of 0.50–0.55 true slump, and beyond this, the slump collapsed.

3.2 Physical–Chemical Characteristics

The water extract and acid digest of waste samples were subjected to experimental analysis, and the result was given based on the physico–chemical analysis; it is observed that the the lime waste obtained from the tanning process is having a pH of 11.65 and a higher concentration of TDS 17,550 mg/l, chlorides 8200 mg/l, sodium 21,705 mg/l. The chrome waste obtained from the leather industry is having a TDS of 20,150 mg/l, calcium of 8210 mg/l, and sodium of 38,030 mg/l. The hypo-sludge obtained from the paper industry is having a pH of 7.27 with a TDS of 4 mg/l and less concentration of sulfate, calcium, and sodium. Since water is an important ingredient of the concrete which is responsible for chemical reactions with cement, the quantity and quality of water are very important. The water which is fit for drinking is considered to be fit for concrete making or should satisfy the requirements as per IS 456 - 2000 [30].

3.3 Sieve Analysis

All the waste materials collected from the respective industry are dried, powered and mixed well to remove the air lumps. On the dried waste samples, sieve analysis was performed and the results are given in Fig. 1. From Fig. 1 it is observed the chrome waste, tannery waste, and paper pulp gradually increased from the lower sieve size to the higher sieve number.

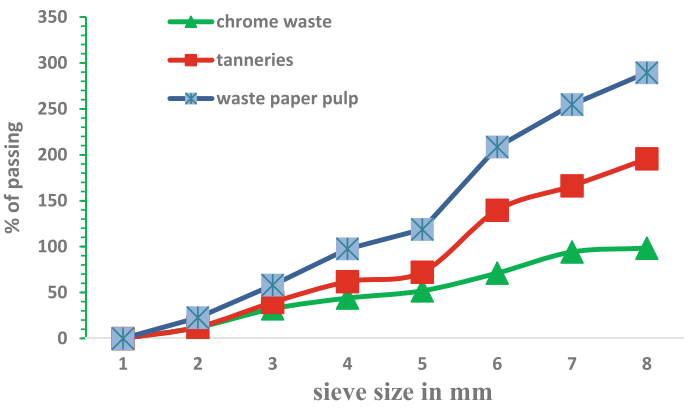

Fig. 1 Sieve size in mm for wastes

3.4 Mix Design

The mix design and strength of concrete are not an easy task—on account of the varying properties of constituent materials. Hence, properties of constituent material are essential, and thus, it becomes complex. The chrome and recycled paper and pulp waste were identified as partial replacements for cement in concrete as per IS 10262:1981 [31]. For making M20 concrete cubes, 20% of waste paper pulp (0.78 kg) was first replaced with cement and 20% of electroplating chrome was replaced (0.78 kg) for the second case, and for the third case, 20% tannery waste (0.78 kg) was added to the cement. The concrete cubes (M20-16 numbers) were casted as per the combinations of ingredients.

3.5 Compression Strength Test

The compressive strength test was conducted on M20 grade concrete cubes of size 150 mm × 150 mm × 150 mm as per IS 516:1959 [32]. Specimens with Portland pozzolanic cement were replaced with 20% of industrial wastes, and about 16 cubes were casted. The cubes were made manually during casting, and the molds were removed after 24h. Cubes underwent curing and tested for 7, 14, and 28 days. A 200-ton capacity-calibrated compression testing machine was used to assess the specimens' compressive strength after curing. It is observed from Table 1 that the concrete cubes tested on the 7th day without replacement of waste (control) give a compressive strength of 12 N/mm^2. During the test on the 7th day, the concrete cubes added with 20% replacement of paper pulp gives a compressive strength of 4.88 N/mm^2. Figure 3 shows the compressive strength test value with a curing period of 7, 14, and 28 days respectively. The cubes with 20% partial replacement of tannery waste in cement have a compressive strength of 6.22 N/mm^2. These values obtained for 20% replacement of electroplating waste gives the compressive strength 8 N/mm^2. The 14th and 28th days of compressive values are found to be higher at 11.55 and 14.22 N/mm^2. Table 1 gives the results of compressive strength test and the tensile strength test of the specimen cubes and Figure 2 shows the compressive strength testing machine.

3.6 Split Tensile Strength Test

The splitting tensile strength test was conducted on M20 grade concrete cubes of size 150 mm × 150 mm × 150 mm. Specimens with Portland pozzolanic cement were replaced with 20% of industrial wastes, and about 16 cubes were cast. During casting, the cubes were manually compacted and the molds were removed after 24 h; then, they were subjected to curing for 7, 14, and 28 days. After curing, the specimens

Table 1 Test on concrete cubes on 7th, 14th, and 28th days

Replacement level	7 days		14 days		28 days	
	Compressive strength (N/mm^2)	Tensile strength (N/mm^2)	Compressive strength (N/mm^2)	Tensile strength (N/mm^2)	Compressive strength (N/mm^2)	Tensile strength (N/mm^2)
Concrete cube without replacement	12	1.62	20	2.31	26.67	2.78
20% by paper pulp	4.88	0.70	7.11	1.20	9.33	1.20
20% by tannery waste	6.22	1.20	8.44	2.08	11.11	1.85
20% by electroplating waste	8	2.08	11.55	2.78	14.22	3.01

Fig. 2 Compression testing machine

were tested for split tensile strength. The split tensile strength is obtained by dividing 0.52 times of maximum load at which the specimen fails to the area of the specimen. It is observed from the tables that the concrete cubes tested on the 7th day without replacement of waste gives a tensile strength of 1.62 N/mm^2. During the test on the 7th day, the concrete cubes added with 20% replacement of paper pulp give 0.70 N/mm^2, and as shown in Fig. 4. The cubes with 20% replacement of tannery waste and

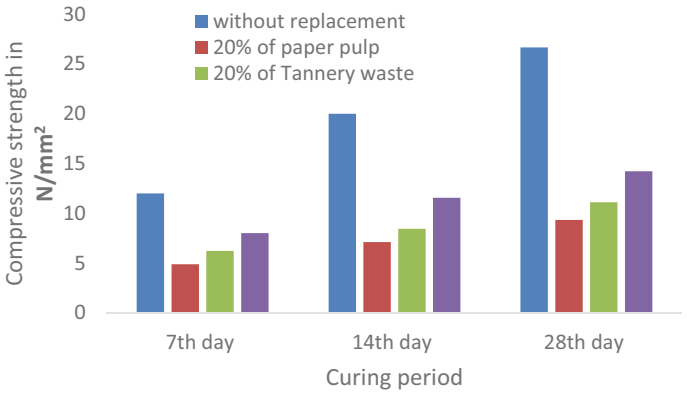

Fig. 3 Compressive strength in N/mm^2

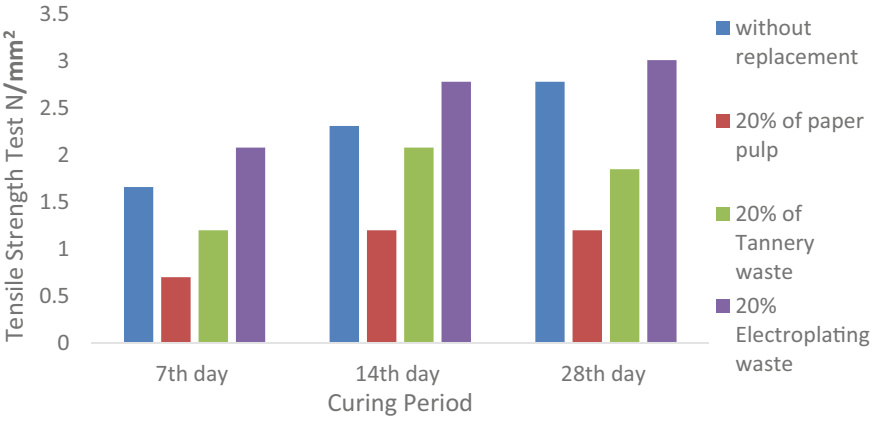

Fig. 4 Tensile strength in N/mm^2

20% replacement electroplating waste have the tensile strength of 1.20 N/mm^2 and 2.08 N/mm^2, respectively.

4 Conclusions

Industrial wastes investigated in the present study revealed the fact that the waste investigated offers immense scope for possible partial replacement of cement in concrete, and this measure will largely help in reducing the need for virgin material required for making cement. The application of waste in making concrete helps in

reducing the waste entering the landfills. The waste samples collected from paper mill, electroplating waste (chrome waste), and tannery waste are characterized.

- The chrome waste, tannery waste, and paper pulp waste used for the present were characterized for their physicochemical parameters, such as pH, EC, TDS, chloride, sulfate, and nitrate, found that the parameters tested are acceptable for use as a partial replacement for cement in concrete making. The waste opted for the study exhibits less toxicity.
- When electroplating waste was added to concrete at a 20% concentration, the concrete's compressive strength increased to 8 N/mm^2 and its tensile strength to 2.08 N/mm^2 on the seventh day. It was also tested for 14 and 28 days.
- When compared to paper pulp waste and tannery waste, the quality of electroplating waste added to the concrete produces the better results in terms of compressive and tensile strength in 20% of replacement. Compressive strength and tensile strength were measured at 14.22 N/mm^2 and 3.01 N/mm^2, respectively, on the 28th day.
- As a result, it is concluded that less hazardous industrial waste can used to partially replace cement in the manufacturing of concrete because concrete with a higher concentration of hazardous materials may not perform well.
- Depending on circumstances and the type of work, the waste utilized as a partial replacement for cement in concrete can be used for both structural and non-structural applications. Further research into the potential use of waste in the manufacturing of concrete is required in order to evaluate the large-scale utilization of waste material for concrete making. Concrete can be made more regular from industrial waste, which can lower disposal costs and promote sustainable growth.

Acknowledgements The Department of Civil Engineering at Annamalai University has provided the authors with laboratory support as well as other infrastructure facilities, for which the authors would like to express their heartfelt gratitude.

References

1. Kaish ABMA, Odimegwu TC, Zakaria I, Abood MM (2021) Effects of different industrial waste materials as partial replacement of fine aggregate on strength and microstructure properties of concrete. J Build Eng 35:102092. https://doi.org/10.1016/j.jobe.2020.102092
2. Singh S, Siddique R (2016) Effect of coal bottom ash as partial replacement of sand on workability and strength properties of concrete. J Clean Prod 112(1):620–630. https://doi.org/10.1016/j.jclepro.2015.08.001
3. Aggarwal Y, Siddique R (2014) Microstructure, and properties of concrete using bottom ash and waste foundry sand as partial replacement of fine aggregates. Constr Build Mater 54:210–223. https://doi.org/10.1016/j.conbuildmat.2013.12.051
4. Boukhelkhal A, Azzouz L, Belaïdi ASE, Benabed B (2016) Effects of marble powder as a partial replacement of cement on some engineering properties of self-compacting concrete. J Adhes Sci Technol 30:2405–2419. https://doi.org/10.1080/01694243.2016.1184402

5. Singh M, Srivastava A, Bhunia D (2017) An investigation on the effect of partial replacement of cement by waste marble slurry. Constr Build Mater 134:471–488. https://doi.org/10.1016/j.conbuildmat.2016.12.155
6. Pal S, Singh A, Pramanik T, Kumar S, Kisku N (2016) Effects of partial replacement of cement with marble dust powder on properties of concrete. Int J Innov Res Sci Technol 3:41–45. https://doi.org/10.17577/IJERTV3IS030812
7. John UE, Jeferson I, Boardman DI, Ghataora GS, Hills CD (2011) Leaching evaluation of cement stabilization/solidification treated kaolin clay. Eng Geol 123(4):315–323. https://doi.org/10.1016/j.enggeo.2011.09.004
8. Mohammed BS, Fang OC (2011) Mechanical and durability properties of concretes containing paper mill residuals and fly ash. Constr Build Mater 25:717–725. https://doi.org/10.1016/j.conbuildmat.2010.07.015
9. Vegas I, Urreta J, Frías M, García R (2009) Freeze-thaw resistance of blended cement containing calcined paper sludge. Constr Build Mater 23(8). https://doi.org/10.1016/j.conbuildmat.2009.02.034
10. Houshyar Z, Khoshfetrat AB, Fatehifar E (2012) Influence of ozonization process on characteristics of pre-alkalized tannery effluents. Chem Eng J 191:59–65. https://doi.org/10.1016/j.cej.2012.02.053
11. Kiliç E, Puig R, Baquero G, Font J, Çolak S, Gürler D (2011) Environmental optimization of chromium recovery from tannery sludge using a life cycle assessment approach. J Hazard Mater 192:393–401. https://doi.org/10.1016/j.jhazmat.2011.05.040
12. Shakir L, Ejaz S, Ashraf M, Qureshi NA, Anjum AA, Iltaj I, Javeed A (2012) Ecotoxicological risks associated with tannery effluent wastewater. Environ Toxicol Phar 34:180–191. https://doi.org/10.1016/j.etap.2012.03.002
13. Torras J, Buj I, Rovira M, de Pablo J (2012) Chromium recovery from exhausted baths generated in plating processes and its reuse in the tanning industry. J Hazard Mater 209–210:343–347. https://doi.org/10.1016/j.jhazmat.2012.01.036
14. Krishnamoorthy G, Sadulla S, Sehgal PK, Mandal AB (2012) Green chemistry approaches the leather tanning process for making chrome-free leather with unnatural amino acids. J Hazard Mater 215–216, 173–182. https://doi.org/10.1016/j.jhazmat.2012.02.046
15. Nashy ESHA, Al-Ashkar E, Moez AA (2012) Optical and spectroscopic studies on tannery wastes as a possible source of organic semiconductors. Spectrochim Acta A 86:33–38. https://doi.org/10.1016/j.saa.2011.09.052
16. Sundarapandiyan S, Brutto PE, Siddhartha G, Ramesh R, Ramanaiah B, Saravanan P, Mandal AB (2011) Enhancement of chromium uptake in tanning using oxazolidine. J Hazard Mater 190:802–809. https://doi.org/10.1016/j.jhazmat.2011.03.117.
17. Basegio T, Beck Leão AP, Bernardes AM, Bergmann CP (2009) Vitrification: an alternative to minimize the environmental impact caused by leather industry wastes. J Hazard Mater 165:604–611. https://doi.org/10.1016/j.jhazmat.2008.10.045
18. Cassano A, Drioli E, Molinari R, Bertolutti C (1996) Quality improvement of recycled chromium in the tanning operation by membrane processes. Desalination 108:193–203. https://doi.org/10.1016/S0011-9164(97)00027-1
19. Chaudhari R, Malviya R (2006) Factors affecting hazardous waste solidification/stabilization: a review. J Hazard Mater 137(1):267–276. https://doi.org/10.1016/j.jhazmat.2006.01.065
20. Chen Y, Ko M, Lai Y, Chang J (2011) Hydration and leaching characteristics of cement paste made from electroplating sludges. Waste Manag 31(6):1257–1363. https://doi.org/10.12989/aer.2014.3.4.337
21. Shopia AC, Swaminathan K (2005) Assessment of the mechanical stability and chemical leachability of immobilized electroplating waste. Chemosphere 58(1):75–82. https://doi.org/10.1016/j.chemosphere.2004.09.006
22. Asavapisit S, Avapisit S, Chotkland D (2004) Solidification of electroplating sludge using alkali-activated pulverized fuel ash as cementitious binder. Cement Concrete Resour 34(2):349. https://doi.org/10.1016/j.cemconres.2003.08.012

23. Gollmann MA, Silva MM, Masuero AB, Santos JHZ (2010) Stabilization and solidification of Pb in cement matrices. J Hazard Mater 179(1–3):507–514. https://doi.org/10.1016/j.jhazmat.2010.03.032
24. APHA (2017) Standard methods for the examination of wastewater 20th edition by American Public Health Association. American Water Works Association, Water Environment Federation
25. IS 383:1970 Specifications for course and fine aggregates from natural sources for concrete. Bureau of Indian Standards, New Delhi. https://www.iitk.ac.in/ce/test/IS-codes/is.383.1970.pdf
26. IS 1489-1 (1991): Specification for portland pozzolana cement, Part 1: Fly ash based. [CED 2: Cement and Concrete]. https://law.resource.org/pub/in/bis/S03/is.1489.1.1991.pdf
27. ASTM D 3987:2006 Standard test method for shake extraction of solid waste with water. https://www.document-center.com/standards/show/ASTM-D3987/history/2006%20EDITION
28. NEPM (1999) National environment protection (assessment of site contamination) measure. https://www.legislation.gov.au/Details/F2013C00288
29. IS 1199:1959 Methods of sampling and analysis of concrete. Bureau of Indian Standards, New Delhi. https://www.iitk.ac.in/ce/test/IS-codes/is.1199.1959.pdf
30. IS 456:2000 Code of practice for plain and reinforced concrete. Bureau of Indian Standards, New Delhi. https://www.academia.edu/6262807/IS_456_2000
31. IS 10262 1981 IS method of mix design. Bureau of Indian Standards, New Delhi. https://www.ijsr.net/archive/v8i1/ART20194592.pdf
32. IS 516-1959 Methods of tests for the strength of concrete. Bureau of Indian Standards, New Delhi. https://www.iitk.ac.in/ce/test/IS-codes/is.516.1959.pdf

A Study on the Mechanical Properties of the Brick with PCB Powder

M. VishnuPriyan and R. Anna Durai

Abstract The rapid pace of technological development and progress has decreased the valuable lifetime of electronic devices. This process generates a lot of Printed Circuit Board (PCB) waste that can be recycled to replacement for fine natural aggregates. This investigation aims to evaluate concretes containing PCB powder as fine aggregates The testing of physical and mechanical properties is performed. This study utilized a PCB powder as an acceptable aggregate replacement (5–30% by volume) in brick. The results show that replacing PCB powder with fine aggregates enhances the mechanical strength of brick. The results indicated that up to 25% replacement of PCB powder yielded better results. Linear Regression (LR) and Artificial Neural Networking (ANN) models have been developed for forecasting purposes in this study. In paraments, cement, fine aggregate, and PCB powder are used with compressive strength as the goal. Linear Regression (LR) and Artificial Neural Networking (ANN) were utilized to compare and optimize properties. At the end of the study, it was determined that both models produced the best results, but the ANN findings of predicting concrete strength were superior. Regarding its ability to predict strength, the LR model performs better than the ANN model.

Keywords PCB powder · Artificial Neural Networks (ANNs) · Linear Regression (LR) · Concrete Brick

1 Introduction

Bricks have a long history of widespread use as a building material due to their durability, versatility, and appealing appearance [1, 2]. They have various applications in the construction industry, including building walls and foundations and creating decorative features such as arches and columns. The increasing demand for

M. VishnuPriyan (✉) · R. A. Durai
Department of Civil Engineering, Faculty of Engineering and Technology, SRM Institute of Science and Technology, Kattankulathur, Tamil Nadu 603203, India
e-mail: vm3188@srmist.edu.in

K. R. Reddy et al. (eds.), *Recent Advances in Civil Engineering*, Lecture Notes in Civil Engineering 398, https://doi.org/10.1007/978-981-99-6229-7_27

new buildings, homes, and infrastructure creates a need for bricks in the construction industry. Bricks are needed because of this demand. Bricks will likely play a significant role in meeting the demand for new construction projects as the global population grows [3, 4]. This is because there is an increasing need to accommodate this growth, which results in an increasing need for new construction projects.

Nevertheless, the most recent expansion in the construction industry can be attributed mainly to the rising demand for and production of concrete, which has been a significant contributor to the deterioration of the environment. It is imperative that the environmental impact of the materials used in construction can be considered, and sustainable alternatives should be searched for whenever possible. As a result, there has been a rise in the search for alternative materials and methods to manufacture bricks with enhanced environmental performance. Polychlorinated biphenyl (PCB) powder, a hazardous waste material that is commonly found in electrical equipment, is one example [5–8]. By incorporating PCB powder into brick production, this waste material can not only be recycled, but its mechanical properties may also be enhanced [9–14]. This article examines the effects of incorporating PCB powder into brick production and optimizing the mechanical properties of the resulting bricks. The study will evaluate the compressive strength, water absorption, and durability of bricks containing varying concentrations of PCB powder. This research may lead to the development of a sustainable, cost-effective method for producing high-performance bricks while reducing the environmental impact on waste materials.

Multiple Linear Regression (MLR) and Artificial Neural Networks (ANNs) are popular computational tools used to study building materials. The compressive strength of concrete can be predicted using ANN models and a wide range of inputs. As an alternative, Multiple Linear Regression (MLR) is a linear regression-based statistical technique for examining the association between multiple variables. The application of artificial intelligence (AI) methods to studying building materials has recently been highlighted in the academic literature. Both Artificial Neural Networks (ANNs) and Multiple Linear Regression (MLRs) have been used to predict concrete's compressive strength. Predictions of concrete compressive strength using ANN models have been studied extensively, with promising results. In recent years, research has focused on using artificial intelligence techniques like ANN and MLR to predict concrete's compressive strength and using PCB powder as a sustainable alternative to conventional fine aggregates in concrete production [5].

This study's findings will help develop more environmentally friendly and sustainable building materials, reduce electronic waste generation, and promote using waste materials in construction. This study aims to predict the compressive strength of the resulting concrete using both ANN and MLR models and to examine the viability of using PCB powder as a partial replacement for fine aggregates in concrete production. In this study, we will evaluate the concrete's mechanical properties and how well the ANN and MLR models predicted its compressive strength. Furthermore, comparing the ANN and MLR models can provide useful insights into the efficacy of various predictive models for compressive strength in concrete. Overall, this

study has important implications for the construction industry and environmental sustainability.

2 Material and Methods

Cement, fine aggregate, water, and PCB powder are used in this experiment. Fine aggregate was replaced with PCB powder at various percentages (0, 5, 10, 15, 20, 25, and 30%) and ordinary Portland cement (OPC) as the binder. Mix the proportion of PCB powder brick 1:6 as per IS 6042.1969. To conduct compressive strength tests, 230 mm × 110 mm × 70 mm brick specimens were cast. A curing tank was used to age the specimens for 28 days. A compression testing machine was used to determine the materials' compressive strengths. The different mix combinations used for the experimental investigation are shown in Table 1.

2.1 ANN

The acronym ANN denotes an Artificial Neural Network. This computational system operates in parallel and is specifically engineered to replicate the human brain's cognitive processes for information processing and analysis. Using data derived from previous experiences, it is possible to construct models, classify information, recognize patterns, and make predictions about a diverse array of issues. Artificial Neural Networks are computational models that mimic how the human brain learns and makes predictions using data [15, 16]. In general, an Artificial Neural Network (ANN) comprises an initial layer for input, one or more hidden intermediate layers, and a final layer for output. The neural network comprises interconnected processing units, with multiple tiers of neurons linked to each other through weighted connections. Compressive strength predictions of concrete have seen widespread use of ANN models, with studies reporting high accuracy levels. This study considers a single concealed layer for the ANN architecture. Therefore, a four-layer network is

Table 1 Mix combination

MIX ID	Cement	Fine aggregate	PCB powder
PCB0	100	100	0
PCB5	100	95	5
PCB10	100	90	10
PCB 15	100	85	15
PCB 20	100	80	20
PCB 25	100	75	25
PCB 30	100	70	30

employed. The first and second layers consist of four input and seven hidden neurons, respectively. The third layer consists of the mechanical properties of the PCB powder brick's compressive strength and density as the output layer [17, 18]. The power of ANN lies in its capacity to learn and adapt to situations where the relationships between variables are highly nuanced and nonlinear. However, ANN training takes time and resources and many data.

2.2 MLR

Multiple Linear Regression (MLR) is a statistical method that uses linear regression to find a correlation between two variables [19–21]. Compared to ANN, MLR requires less computing power and is easier to implement. The compressive strength of concrete can be predicted with some precision using MLR, as it establishes a linear relationship between the relevant variables. MLR's strength lies in the fact that it is straightforward to understand. However, MLR can only model linear relationships between variables, so it may not apply to model complex nonlinear relationships. The present study employs regression analysis to examine the relationship between the percentage of PCB powder replacement for fine aggregate and the compressive strength of brick after 28 days. The statistical significance of a model term was determined based on the magnitude of its *p*-value. The coefficient of determination (R2) is calculated to determine the correlation level between the brick's compressive strength. The determination of the peak compressive strength and the percentage of PCB powder is achieved by utilizing the fitted line plot equation after 28 days.

3 Results and Discussion

The current study shows that compressive strength was significantly affected when fine aggregate was partially replaced with PCB powder in concrete bricks. According to the results shown in Fig. 1, the best compressive strength was achieved when PCB powder replaced fine aggregate at a rate of 20%. When mixed with PCB powder, concrete bricks' compressive strength increased to a certain percentage but then dropped. PCB powders lower specific gravity and poor water absorption capacity compared to fine aggregate explain this phenomenon. Because of this, the concrete's bricks' compressive strength decreases as the percentage of replacement increases.

From Fig. 1, it is clear that the percentage of replacement PCB powder increases the strength and density of the concrete brick decrease. The study's results correspond to those above 25% of PCB powder replacement of fine aggregate which yields the lowest compressive strength (2.9 N/mm^2) and density (1.99 kg/m^3). Reducing waste and conserving natural resources, using PCB powder as a partial replacement for fine aggregate can also help to lessen the construction industry's environmental impact.

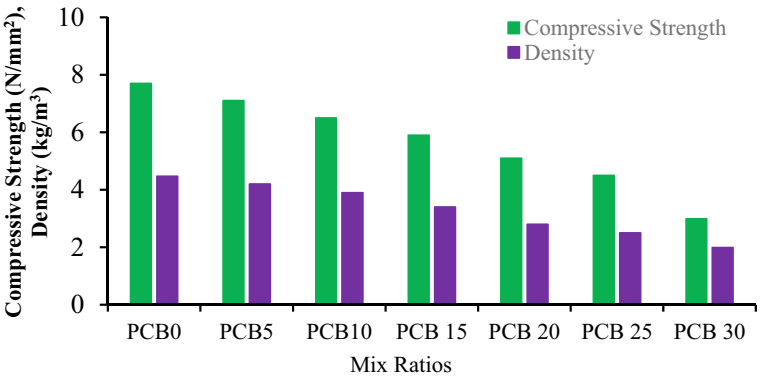

Fig. 1 Compressive strength and density

Table 2 Compressive strength and density of PCB powder concrete brick

Mix ID	Cement	Fine aggregate	PCB powder	Compressive strength (N/mm^2)	Density (kg/m^3)
PCB0	100	100	0	7.7	4.47
PCB5	100	95	5	7.1	4.2
PCB10	100	90	10	6.5	3.9
PCB15	100	85	15	5.9	3.4
PCB20	100	80	20	5.1	2.8
PCB25	100	75	25	4.5	2.5
PCB30	100	70	30	2.99	1.99

Further, Artificial Neural Network (ANN) and Multiple Linear Regression (MLR) models were developed to predict the compressive strength of concrete with PCB powder as a partial replacement for fine aggregate. The experimental results of compressive strength tests are shown in Table 2, which were used to train and validate the models.

3.1 MLR Analysis

Using Multiple Linear Regression (MLR) analysis, this study investigated the impact of replacing fine aggregate with PCB powder on concrete brick's compressive strength and density. R-square values of 98.6 and 98.9 for compressive strength and density indicate a strong correlation between the predictor variables (i.e., PCB powder replacement percentage and fine aggregate) and the response variables (i.e., compressive strength and density). According to Fig. 2 the high R-square values, the MLR model provides a satisfactory fit to the data, explaining 98.6% and 98.9% of the

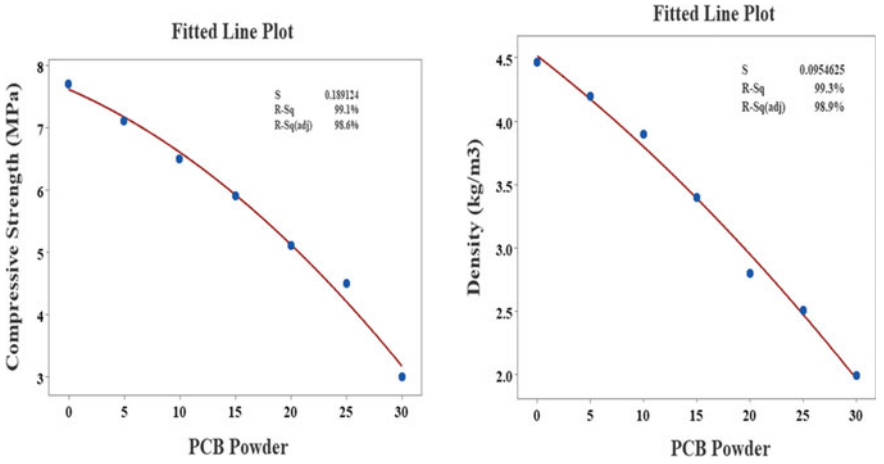

Fig. 2 MLR regression for compressive strength and density

variance in compressive strength and density, respectively. Based on these results, the percentage of PCB powder replacement and the amount of fine aggregate are significant predictors of concrete brick's compressive strength and density. Adjustments to these variables can be used to anticipate adjustments to the properties of the concrete Eqs. 1 and 2 Regression equation for compressive strength and density of the Concrete Brick.

The regression equation is

$$\text{Compressive strength (MPa)} = 7.611 - 0.07736\ \text{PCB Powder} - 0.002357\ \text{PCB Powder}^2, \quad (1)$$

$$\text{Density}\left(\text{kg/m}^3\right) = 4.519 - 0.06529\ \text{PCB Powder} - 0.000667\ \text{PCB Powder}^2. \quad (2)$$

3.2 ANN Analysis

Using Artificial Neural Network (ANN) analysis, the effect of replacing PCB powder with fine aggregate on concrete's compressive strength and density was investigated. A high degree of correlation was found in our analysis between the input variables (i.e., percentage of PCB powder replacement and amount of fine aggregate) and the output variables (compressive strength and density) (i.e., compressive strength and density). Figure 3 shows the neural diagram used for ANN analysis.

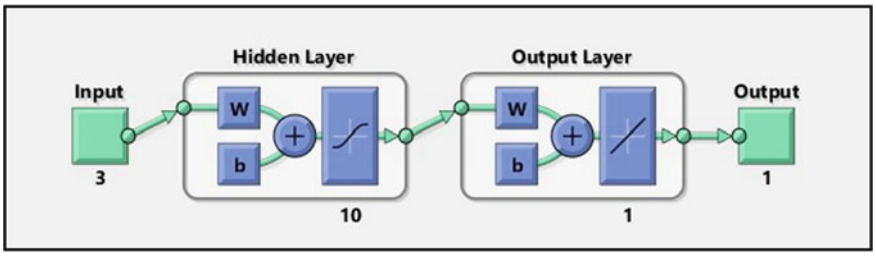

Fig. 3 ANN model in software

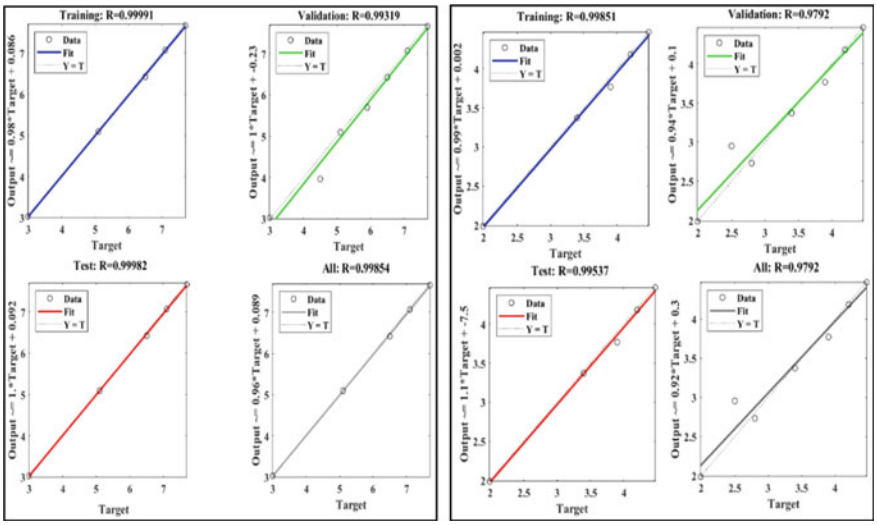

Fig. 4 ANN regression plots for compressive strength and density

ANN regression plots for the compressive strength and density of the PCB powder bricks are shown in Fig. 4. The performance plot shows that the ANN model performed very well in predicting compressive strength, with the lowest error occurring at the three epochs from Fig. 5. It took the model fewer iterations to reach an acceptable level of accuracy for density 4 Epochs Fig. 6, with the minimum error reached by the third iteration.

3.3 Discussion of Comparing Results of MLR and ANN

This study analyzes the impact of using s as fine aggregate instead of traditional aggregate on the compressive strength and density of concrete using Multiple Linear Regression (MLR) and Artificial Neural Network (ANN) methods. While both

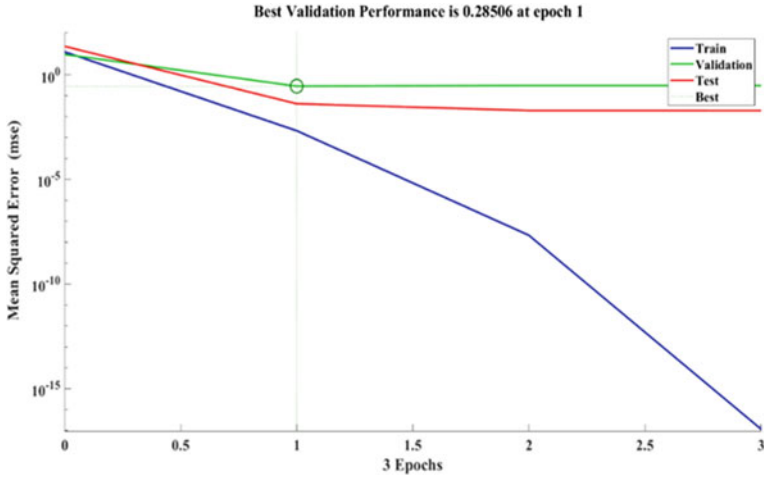

Fig. 5 Performance plots for compressive strength of the concrete brick

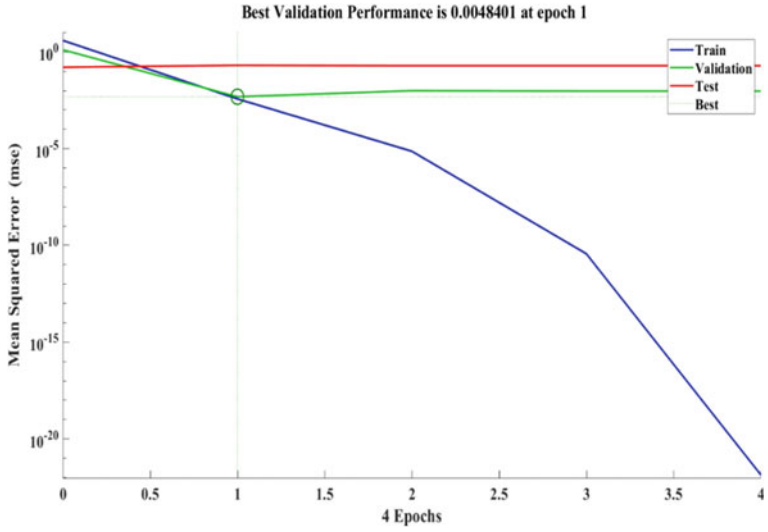

Fig. 6 Performance plots for density of the concrete brick

methods were successful in their predictions of concrete properties, there were noticeable distinctions between them. Compressive strength R-squared values of 98.67% and density R-squared values of 98.61% were obtained from an MLR analysis. The R-square values for the ANN model were 0.99854 for compressive strength and 0.9792 for density, respectively. The ANN model's performance plot also revealed that in contrast to compressive strength, a lower number of epochs were needed to

reach an acceptable level of accuracy for density. MLR and ANN models successfully predicted concrete properties as a function of PCB powder replacement and fine aggregate content. The ANN model was significantly more accurate than the MLR model when predicting compressive strength.

The analysis of nonlinear systems benefits significantly from the ANN model's ability to predict intricate relationships between input and output variables. MLR models, on the other hand, work best with linear systems that have a straightforward relationship between their input and output variables.

4 Conclusion

This research shows that compressive strength and density can be significantly altered when fine aggregate is partially replaced with PCB powder in concrete bricks.

- Compressive strength was decreased as the percentage of fine aggregate replacement by PCB powder increased. According to the study, beyond 25% replacement of PCB powder replacement was not recommended because of the poor strength of the brick compared to all the other mixes. Reducing waste and conserving natural resources, using PCB powder as a partial replacement for fine aggregate can also help to reduce the construction industry's environmental impact.
- R correlation coefficients for compressive strength and density of PCB powder brick were calculated using ANN analysis to be 0.99991, 0.99319, 0.99982, 0.99854, 0.99851, 0.9792, 0.99537, and 0.9792, respectively. The ANN model was appropriate because all models' correlation coefficient is close to 1.
- R-square values for compressive strength and density of brick were calculated using MLR analysis to be 98.6% and 98.9%, respectively. Because the correlation is close to 100% for all models, the MLR model was appropriate.
- In addition, Artificial Neural Network (ANN) and Multiple Linear Regression (MLR) models were created to predict the compressive strength and density of the brick with PCB powder as a partial replacement for fine aggregate. Regarding predicting brick properties, both the ANN and MLR models were entirely accurate; however, the ANN model was more accurate when estimating concrete bricks' compressive strength.
- The study demonstrates the promise of ANN modeling for predicting brick properties. It offers essential insights into using PCB powder as a partial replacement for fine aggregate in brick.

More studies can be done to perfect the application of such methods to analyze green concrete or brick ingredients.

Acknowledgements The authors acknowledge the Department of Civil Engineering, SRM Institute of Science and Technology, for providing study facilities.

References

1. Brahmacharimayum M, Shijagurumayum C, Suresh T (2021) E-waste in concrete—a review. J Civil Eng Environ Technol 6(6):384–387. Accessed: 21 Dec 2021. [Online]. Available: http://www.krishisanskriti.org/Publication.html
2. Jagarapu DCK, Sri Hari M, Goud MS, Eluru A (2020) Alternative coarse aggregate in concrete: a review. Int J Emerg Technol Eng Res (IJETER) 8
3. Ali B, Qureshi LA, Shah SHA, Rehman SU, Hussain I, Iqbal M (2020) A step towards durable, ductile and sustainable concrete: simultaneous incorporation of recycled aggregates, glass fiber and fly ash. Constr Build Mater 251:118980. https://doi.org/10.1016/J.CONBUILDMAT.2020.118980
4. Paruthi S, Husain A, Alam P, Khan AH, Hasan MA, Magbool HM (2022) A review on material mix proportion and strength influence parameters of geopolymer concrete: application of ANN model for GPC strength prediction. Constr Build Mater 356:129253. https://doi.org/10.1016/j.conbuildmat.2022.129253
5. Marimuthu V, Ramasamy A (2023) Investigation of the mechanical properties of M40-grade concrete with PCB fiber from recycled electronic waste. J Hazard Toxic Radioact Waste 27(1):4022034. https://doi.org/10.1061/(ASCE)HZ.2153-5515.0000725
6. Colledani M, Copani G, Rosa P (2014) Zero waste PCBs: a new integrated solution for key-metals recovery from PCBs. In: SUM 2014—2nd symposium on urban mining, May 2014, pp 19–21
7. Mishra SM, Trivedi MK (2021) Utilisation of PCB and cost-reduction of concrete. Int J Appl Eng Res 13:11461–11465. Accessed: 21 Dec 2021. [Online]. Available: http://www.ripublication.com
8. Pothinathan SKM, Kumar P, Arunachelam N, Gnanaraj SC (2021) Effect of PCB as partial replacement of fine aggregate and coarse aggregate in concrete. Mater Today Proc. https://doi.org/10.1016/J.MATPR.2021.09.363
9. Sua-iam G, Chatveera B (2021) A study on workability and mechanical properties of eco-sustainable self-compacting concrete incorporating PCB waste and fly ash. J Clean Prod 329:129523. https://doi.org/10.1016/J.JCLEPRO.2021.129523
10. Luhar S, Luhar I (2019) Potential application of E-wastes in construction industry: a review. Constr Build Mater 203:222–240. https://doi.org/10.1016/J.CONBUILDMAT.2019.01.080
11. Muthupriya P, Kumar BV Experimental investigation on concrete with E-waste—a way to minimise solid waste deposition. https://doi.org/10.46488/NEPT.2021.v20i03.026
12. Kumar A, Holuszko M, Espinosa DCR (2017) E-waste: an overview on generation, collection, legislation and recycling practices. Resour Conserv Recycl 122:32–42. https://doi.org/10.1016/J.RESCONREC.2017.01.018
13. Rashad AM (2014) Recycled waste glass as fine aggregate replacement in cementitious materials based on Portland cement. Constr Build Mater 72:340–357. https://doi.org/10.1016/J.CONBUILDMAT.2014.08.092
14. Ling T-C, Poon C-S (2014) Use of recycled CRT funnel glass as fine aggregate in dry-mixed concrete paving blocks. J Clean Prod 68:209–215. https://doi.org/10.1016/j.jclepro.2013.12.084
15. Vishnupriyan M, Annadurai R (2023) A study on the macro-properties of PCB fibre-reinforced concrete from recycled electronic waste and validation of results using RSM and ANN. Asian J Civil Eng 1:1–14. https://doi.org/10.1007/S42107-023-00595-4
16. Nakkeeran G, Krishnaraj L (2023) Prediction of cement mortar strength by replacement of hydrated lime using RSM and ANN. Asian J Civil Eng. https://doi.org/10.1007/S42107-023-00577-6
17. Marimuthu V, Annadurai R (2022) Experimental investigation on the mechanical properties of printed circuit board (PCBs) fibre reinforced concrete. In: Proceedings of international conference on novel innovations and sustainable development in civil engineering

18. Vishnupriyan M, Annadurai R (2023) Investigation of the effect of substituting conventional fine aggregate with PCB powder on concrete strength using artificial neural network. Asian J Civil Eng 1:1–9. https://doi.org/10.1007/S42107-023-00700-7
19. Yan F, Li Q, Fu X, Kong T, Mi S, Zhang YC (2023) Quality prediction of friction stir welded joint based on multiple regression: entropy generation analysis. Int J Adv Manuf Technol 1–21. https://doi.org/10.1007/S00170-023-10979-0/FIGURES/18
20. Kim J-S, Kim YS (2023) Development of a long-term repair allowance estimation model for apartments based on multiple regression analysis in Korea. Sustainability 15(5):4357. https://doi.org/10.3390/SU15054357
21. Hong Y, Cao C (2023) Institutional investors' distraction and executive compensation stickiness based on multiple regression analysis. J Risk Finan Manage 16(2):120. https://doi.org/10.3390/JRFM16020120

Experimental Investigation on E-waste as a Partial Replacement to Fine Aggregate in M50 Grade Concrete

A. Siranjeevinathan, N. Ganapathy Ramasamy, S. Prakash Chandar, and R. Kaviraja

Abstract Electronic items that are unwanted, outdated, or expired are referred to as "E-waste" or "E-waste." They also include materials and chemicals like lead, cadmium, mercury, and beryllium, as well as polymers like polychlorinated biphenyls, polyvinyl chloride, and polystyrene. E-waste presents serious risks to the environment and to people's health. Current procedures concentrate on processing and classifying e-waste carefully in an effort to lessen negative environmental effects and contaminants. E-waste can be used in place of traditional fine aggregate in concrete as a viable solution to the environmental damage E-waste causes. The purpose of this study is to examine the mechanical characteristics of M50 concrete with partial fine aggregate substitution utilizing e-waste and assess its potential to reduce environmental harm. E-waste is replaced with fine aggregate in volumes of 10, 20, and 30%. The specimens of concrete were specifically tested for compressive strength, split tensile strength, and flexural strength. The results obtained from this research demonstrate the significance of e-waste utilization in concrete production. A 10% replacement of e-waste yielded optimum outcomes, showcasing notable improvements in the mechanical properties when compared to the control concrete. The compressive strength exhibited a remarkable increase of 10.24%, while the split tensile strength and flexural strength showed enhancements of 8.93% and 5.36%, respectively. These findings affirm that e-waste can be effectively employed as a substitute material for fine aggregate in concrete. This study proposes a workable option for minimizing the environmental effect of e-waste by integrating e-waste into the manufacturing of concrete, which supports sustainable waste management methods. The research's conclusions highlight how useful E-waste may be as a resource by highlighting how it can be recycled in the desired form while causing the least amount of environmental damage. Implementing e-waste as a substitute material in concrete can enhance its structural performance and simultaneously address the pressing issue of e-waste management.

Keywords E-waste · Fine aggregate · Mechanical properties

A. Siranjeevinathan · N. Ganapathy Ramasamy (✉) · S. P. Chandar · R. Kaviraja
Department of Civil Engineering, Faculty of Engineering and Technology, SRM Institute of Science and Technology, Kattankulathur, Tamil Nadu 603203, India
e-mail: ganapatn@srmist.edu.in

K. R. Reddy et al. (eds.), *Recent Advances in Civil Engineering*, Lecture Notes in Civil Engineering 398, https://doi.org/10.1007/978-981-99-6229-7_28

1 Introduction

The most common building construction material used worldwide is concrete [1]. Indian environmental and public health concerns over electronic trash are getting more and more serious. The greatest issue facing the globe today is the lack of natural resources and waste management. In comparison to other techniques, recycling electrical trash is expensive economically [2]. With an annual production of roughly 2 million tonnes of E-waste and an undisclosed importation from other countries, India is the "Third biggest electronic rubbish producer in the world. The estimated weight of the waste produced by the main cities, including Mumbai, New Delhi, Bangalore, and Chennai, is 10,000 tonnes, 9,000 tonnes, 8,000 tonnes, and 6,000 tonnes, respectively. Yet, only 4% of it is recycled from these sources [3]." Sometimes referred to as "e-waste," electrical equipment that is nearing the completion of its "useful life," common electronic devices include televisions, desktop computers, tape recorders, music players, printers, and fax equipment [4]. Most of these things are recyclable, repairable, or reusable [5].

Electrical boards, chips, and other electronic trash pose a serious threat to both the environment and public health [6, 7]. Due to their independent behaviour and lack of affiliation with any official group, it is nearly impossible to enforce e-waste standards. The building sector is now experiencing a number of crises, and one of them is the lack of natural resources [2]. There may be long-lasting, irreversible effects from the emission of harmful chemicals linked to inadequate e-waste recycling. Human health is harmed by the lead in e-waste in various ways, including renal and nervous system damage. The handling and management of E-plastic trash have grown to be a major global challenge.

Waste glass powder (WGP) and waste electronic plastic (WEP) are found to be easily accessible due to their vast manufacture with a single use approach [8]. All of the electrical devices' printed circuit boards (PCBs) are crushed and turned into ash, which is used to substitute fine aggregate to a certain extent [6, 7, 9, 10]. The PCB's silicon (Si) content enables it to satisfy the criteria as effectively as fine aggregate. One of the popular practises in our environmentally concerned era is recycling [11]. Printed circuit board (PCB) powder is typically made from fibreglass-reinforced epoxy resin. It possesses high mechanical strength, excellent electrical insulation properties and is resistant to heat, chemicals, and moisture, making it an ideal material for manufacturing durable and reliable PCBs.

The selection of M50 grade concrete for the experimental investigation is based on the need for high strength and durability in construction applications. M50 grade concrete is known for its ability to withstand heavy loads and harsh environmental conditions, making it suitable for demanding structural projects. Using an experimental approach, this study's goal is to substitute some of the fine aggregate in M50 grade concrete with E-waste using super plasticizer, 53-grade cement, and M-sand at a percentage of 0, 10, 20, and 30% [12]. Results of tests done on the Day 3, Day 7, and Day 28 of curing are compared in relation to strengths which include flexural,

tensile, and compression. The purpose of the experiment is the fine aggregate was attempted to be replaced in part with non-biodegradable E-waste components [13].

E-waste plastics have a very low biodegradability and are produced in vast quantities, making their disposal a significant issue [14]. The disposal of significant amounts of waste can be solved economically and technically by using E-waste [15]. E-waste disposal practises not only damage the land but also affect the qualities of groundwater, making it impossible to use water for any alternative uses use cases [16].

2 Materials Used

In this experiment OPC 53 was used in accordance with IS 12269-1987 [17]. The mix proportion of concrete is made using IS: 10262-2019 [18]. The fineness of cement was utilized in accordance with IS 460 (Parts 1 and 3) [19, 20]. OPC offers systems with a lot of power and stability given to its excellent crystalline structure and good particle size distribution. Sieve analysis is performed for the aggregates [21]. As fine aggregates, river sand is often employed in the building sector. However, because of the scarcity and expense, manufactured sand is used [22, 23]. By conducting testing in accordance with IS: 2386 (Part 3): 1963 [24], the characteristics of M-sand were estimated. About 20 mm aggregate is used in this experiment. The results are displayed in Table 1. The results demonstrate that Zone II of IS:383-2016 is met by M-sand. The IS:2386 (Part 3):1963 was used to determine the characteristics of coarse aggregate. When cement and water mix together to make concrete, an important role of the chemical reaction is carried out by water. Toxins, salts, bases, and other contaminants should not have been present in the water, which was utilized in accordance with IS 456-2000 [25]. The water–cement ratio is 0.34. This water helps in the chemical reaction of bacteria with the atmosphere and is used to make mortar [26]. A highly pozzolanic substance called silica fume, the industry's by-product, is used to enhance concrete's mechanical properties [27]. For superior engineering qualities, silica fume makes a great additive for concrete [28]. It will improve resistance to attack by sulphate and acidic fluids and increase strength. In order to produce flowing, self-levelling, self-compacting, high strength, and high-performance concrete, superplasticizer is used in this process [29]. High-range water reducers, commonly known as superplasticizers (SPs), are additives used to produce concrete with a high strength. It is possible to make concrete using around 15% less water than is generally used mainly to substances known as plasticizers. Naphthalene-based Conplast SP430 is a blend of certain components. The water content of the concrete performs better because it disperses the fine particles in the mix. In this research, printed circuit boards (PCBs) have been crushed and used in this experiment as a substitute for fine aggregate in certain cases and it is added in various amounts like 10%. Sieve analysis test was done for E-waste. Figures 1 and 2 represent the PCB board and crushed PCB powder. The results of preliminary tests for the materials are shown in Table 1.

Table 1 Preliminary tests for the materials

Description	Obtained result
Fineness of cement	4%
Specific gravity of cement	3.13
Specific gravity of fine aggregate	2.76
Specific gravity of coarse aggregate	2.93
Sieve analysis of fine aggregate	3.42 (Zone II)
Sieve analysis of coarse aggregate	7.71
Specific gravity of fine aggregate (E-waste)	2.87
Sieve analysis of fine aggregate (E-waste)	3.23 (Zone I)

Fig. 1 PCB board

Fig. 2 Crushed PCB powder

Table 2 Compressive strength

Days	Partial replacement of E-waste			
	0% (N/mm^2)	10% (N/mm^2)	20% (N/mm^2)	30% (N/mm^2)
3rd	25.84	26.97	23.1	20.82
7th	40.8	43.61	35.6	33.93
28th	60.72	66.94	54.93	52.48

3 Experimental Study

The following shows the experimental investigation done in this study.

3.1 Compressive Strength of Concrete

The capacity of a material to bear a load is known as its compressive strength. On the prepared specimens of size 150 mm × 150 mm × 150 mm, compressive test was conducted. The test was done for 3, 7 and 28 days, respectively. Totally nine number of specimens are made for each. The specimens' target compressive strength of M50 grade concrete was achieved in the 28th day. The outcomes can be seen in Table 2 and Fig. 3 shows the comparison between the control concrete and different percentages of E-waste concrete.

The compressive strength result shows that using 10% partially replaced E-waste increases the strength up to 10.24% when compared to control concrete. Similar research found that the compressive strength is optimum at 10% of E-waste partially replaced to coarse aggregate in M20 grade concrete by Manjunath 2016 [11].

3.2 Split Tensile Strength

Tensile strength is one of concrete's fundamental properties. Since structural stresses can cause the material to split under tension. Concrete's tensile strength is significantly less than its compressive strength. According to some estimates, concrete's tensile strength is equal to 8–12% of its compressive strength, roughly. On the 150 mm × 300 mm prepared specimens, the split tensile test was carried out. The outcomes can be seen in Table 3, and Fig. 4 shows the comparison between the control concrete and different percentages of E-waste concrete.

The split tensile result shows that using 10% partially replaced E-waste increases the strength up to 8.93% when compared to control concrete. Similar research found that the split tensile strength is optimum at 10% of E-waste partially replaced to coarse aggregate in M20 grade concrete by Manjunath 2016 [11].

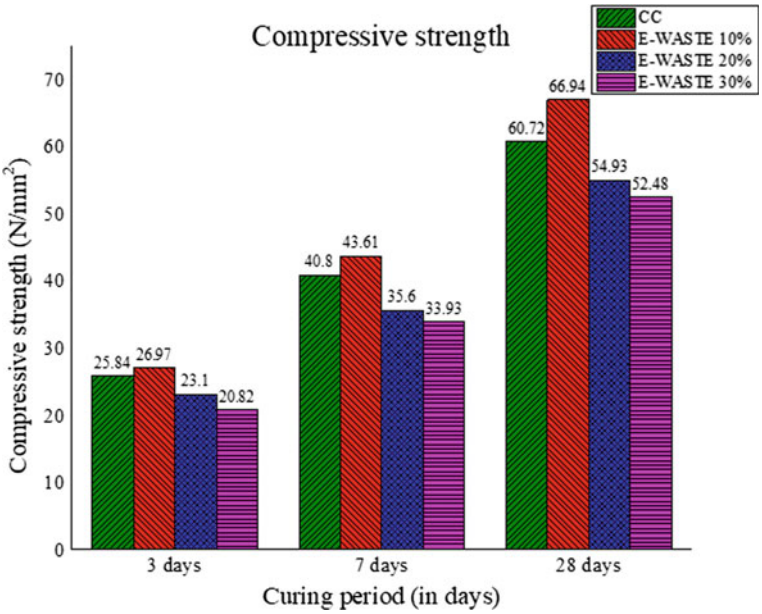

Fig. 3 Comparative study of compressive strength for CC and different percentages of E-waste

Table 3 Split tensile strength

Days	Partial replacement of E-waste			
	0% (N/mm^2)	10% (N/mm^2)	20% (N/mm^2)	30% (N/mm^2)
3rd	2.95	3.17	2.54	2.21
7th	3.58	3.96	2.96	2.65
28th	5.82	6.34	5.17	4.93

3.3 Flexural Strength

Flexural strength refers to a composites or materials capacity to withstand bending deflection when force is applied to the structure. The capability of a material to withstand bending loads is known as flexural strength that are applied perpendicular to its longitudinal axis. It measures how effectively an unreinforced concrete slab or beam can withstand failure due to bending. According to some estimates, concrete's flexural strength is equal to 10–20% of its compressive strength, roughly. The specimen size is 100 mm × 100 mm × 500 mm. The flexural strength values are shown in Table 4 and Fig. 5, comparing the control concrete and different percentages of E-waste concrete.

The flexural strength result shows that using 10% partially replaced E-waste increases the strength up to 5.36% when compared to control concrete. Similar

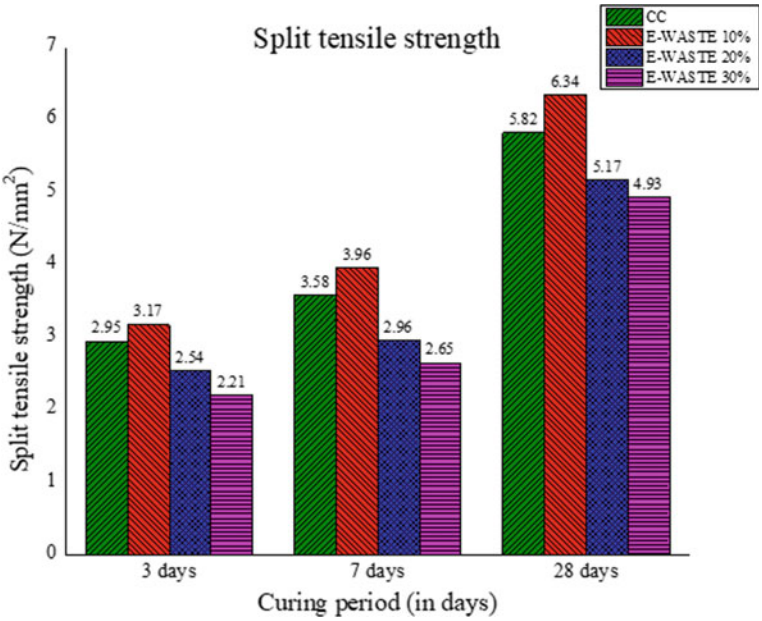

Fig. 4 Comparative study of split tensile strength for CC and different percentages of E-waste

Table 4 Flexural strength

Days	Partial replacement of E-waste			
	0% (N/mm^2)	10% (N/mm^2)	20% (N/mm^2)	30% (N/mm^2)
3rd	3.83	4.01	3.36	2.63
7th	6.12	6.41	5.47	4.31
28th	9.33	9.83	8.16	6.33

research found that the flexural strength is optimum at 10% of E-waste partially replaced to coarse aggregate in M20 grade concrete by Manjunath 2016 [11].

3.4 Regression Analysis

The relationship between the compressive strength (x-axis) and split tensile strength (y-axis) is evaluated using a simple linear regression model. The mechanical properties of various percentages of E-waste have been analyzed and the equation $y = 0.0988x - 0.243$ was formulated from the analysis, Fig. 6. The equation's R^2 value is 0.99, which denotes 99% accuracy rate.

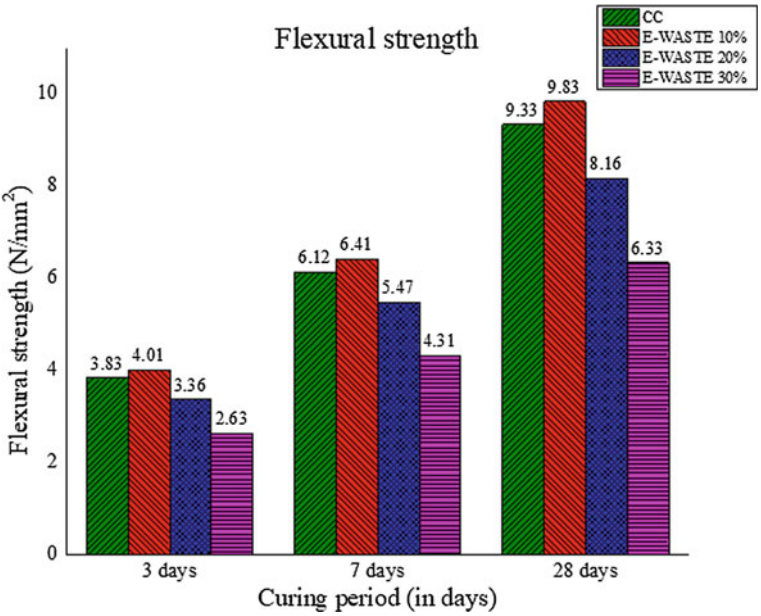

Fig. 5 Comparative study of flexural strength for CC and different percentages of E-waste

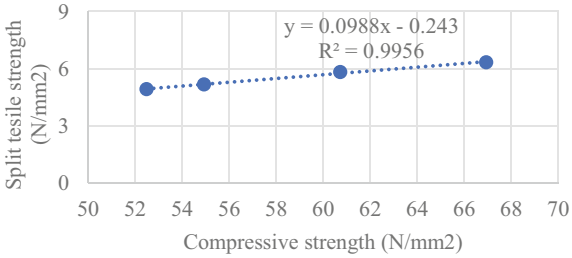

Fig. 6 Regression analysis of compressive strength versus split tensile strength

Similarly, the relationship between the compressive strength (x-axis) and flexural strength (y-axis) is evaluated using a simple linear regression model. The mechanical properties of various percentages of E-waste have been analyzed and the equation $y = 0.2198x - 4.5018$ was formulated from the analysis, (Fig. 7). The equation's R^2 value is 0.83, which denotes 83% accuracy rate.

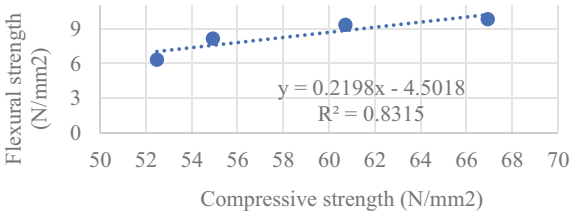

Fig. 7 Regression analysis of compressive strength versus flexural strength

4 Conclusion

Based on the findings of this project, it can be concluded that the partial replacement of fine aggregate with E-waste in concrete has a significant impact on its mechanical properties.

(1) The investigation focused on M50 grade concrete and evaluated the compressive strength, split tensile strength, and flexural strength at 3, 7, and 28 days.
(2) The results indicate that a 10% partial replacement of E-waste with fine aggregate yielded the most favourable outcome in terms of compressive strength compared to the split tensile and flexural strength.
(3) The concrete with 10% E-waste replacement exhibited an increase in compressive strength by 10.24%, split tensile strength by 8.93%, and flexural strength by 5.36% when compared to the control concrete.
(4) However, it is important to note that as the percentage of E-waste replacement increased to 20 and 30%, there was a decrease in the concrete's strength. This decrease suggests that higher levels of E-waste replacement are not suitable for achieving desirable mechanical properties in concrete.
(5) The linear regression models demonstrate a significant correlation between split tensile strength and compressive strength. The first model achieves a higher accuracy rate of 99%, indicating a stronger relationship between the variables. The second model, with an accuracy rate of 83%, still provides a reasonably good estimation of split tensile strength based on compressive strength.
(6) In summary, the research demonstrates that a 10% partial replacement of fine aggregate with E-waste can enhance the mechanical properties of concrete, particularly its compressive strength.
(7) Further studies could explore optimization strategies for incorporating E-waste in concrete mixes to maximize its benefits while ensuring the overall strength and durability of the resulting structures.

References

1. Ullah Z, Qureshi MI, Ahmad A, Khan SU, Javaid MF (2021) An experimental study on the mechanical and durability properties assessment of E-waste concrete. J Build Eng 38. https://doi.org/10.1016/j.jobe.2021.102177

2. Bharani S, Rameshkumar G, Manikandan J, Balayogi T, Gokul M, Bhuvanesh DC (2020) Experimental investigation on partial replacement of steel slag and E-waste as fine and coarse aggregate. Mater Today Proc 3534–3537. https://doi.org/10.1016/j.matpr.2020.09.419
3. Pandiyarajan M, Manikandan M, Prakash A (2017) Experimental study on e-waste concrete and comparing with conventional concrete. Ind Pollut Control 33(S3):1490–1495. https://doi.org/10.13140/RG.2.2.11666.58562
4. Pratheba S, Rajeswari M, Johnpaul V, Balasundaram N, Lingeshwaran N, Kumar V (2021) Experimental investigation on environmental utilization of e-Waste management. Mater Today Proc 5479–5482. https://doi.org/10.1016/j.matpr.2021.07.471
5. Arivalagan S (2020) Experimental study on the properties of green concrete by replacement of e-plastic waste as aggregate. Procedia Comput Sci 985–990. https://doi.org/10.1016/j.procs.2020.05.145
6. Needhidasan S, Sai P (2020) Demonstration on the limited substitution of coarse aggregate with the E-waste plastics in high strength concrete. Mater Today Proc 1004–1009. https://doi.org/10.1016/j.matpr.2019.11.255
7. Ganesh S, Danish P, Bhat KA (2020) Utilization of waste printed circuit board powder in concrete over conventional concrete. Mater Today Proc 745–749. https://doi.org/10.1016/j.matpr.2020.11.161
8. Balasubramanian B, Gopala Krishna GVT, Saraswathy V, Srinivasan K (2021) Experimental investigation on concrete partially replaced with waste glass powder and waste E-plastic. Constr Build Mater 278. https://doi.org/10.1016/j.conbuildmat.2021.122400
9. Santhanam N, Anbuarasu G (2020) Experimental study on high strength concrete (M60) with reused E-waste plastics. Mater Today Proc 919–925. https://doi.org/10.1016/j.matpr.2019.11.107
10. Mary Treasa Shinu NM, Needhidasan S (2020) An experimental study of replacing conventional coarse aggregate with E-waste plastic for M40 grade concrete using river sand. Mater Today Proc 633–638. https://doi.org/10.1016/j.matpr.2019.09.033
11. Manjunath BTA (2016) Partial replacement of E-plastic waste as coarse-aggregate in concrete. Procedia Environ Sci 35:731–739. https://doi.org/10.1016/j.proenv.2016.07.079
12. Needhidasan S, Ramesh B, Joshua Richard Prabu S (2020) Experimental study on use of E-waste plastics as coarse aggregate in concrete with manufactured sand. Mater Today Proc 715–721. https://doi.org/10.1016/j.matpr.2019.10.006
13. Arora A, Urmil D, Dave V (2013) Utilization of e-waste and plastic bottle waste in concrete. [Online]. Available: www.giapjournals.com/ijsrtm/
14. Nwaubani SO, Parsons LA (2021) Properties, durability and microstructure of concrete incorporating waste electrical and electronic plastics as partial replacement for aggregates in concrete. Case Stud Constr Mater 15. https://doi.org/10.1016/j.cscm.2021.e00731
15. Santhanam N, Ramesh B, Pohsnem FK (2020) Concrete blend with E-waste plastic for sustainable future. Mater Today Proc 959–965. https://doi.org/10.1016/j.matpr.2019.11.204
16. Hamsavathi K, Prakash KS, Kavimani V (2020) Green high strength concrete containing recycled Cathode Ray Tube Panel Plastics (E-waste) as coarse aggregate in concrete beams for structural applications. J Build Eng 30. https://doi.org/10.1016/j.jobe.2020.101192
17. B. of Indian Standards IS 12269 (1987): 53 grade ordinary Portland cement
18. I. Standard IS 10262 (2019): Concrete mix proportioning-guidelines (second revision). [Online]. Available: www.standardsbis.in
19. B. of Indian Standards IS 460-1 (1985): Test sieves: Part-I wire cloth test sieves
20. B. of Indian Standards IS 460-3 (1985): Test sieves: Part-III methods of examination of apertures of test sieves
21. Ahirwar S, Malviya P, Patidar V, Singh VK (2016) An experimental study on concrete by using e-waste as partial replacement for course aggregate. [Online]. Available: www.ijste.org
22. Suleman S, Needhidasan S (2020) Utilization of manufactured sand as fine aggregates in electronic plastic waste concrete of M30 mix. Mater Today Proc 1192–1197. https://doi.org/10.1016/j.matpr.2020.08.043

23. Rajkumar R, Ganesh VN, Mahesh SR, Vishnuvardhan K (2020) Performance evaluation of E-waste and Jute Fibre reinforced concrete through partial replacement of Coarse Aggregates. Mater Today Proc 6242–6246. https://doi.org/10.1016/j.matpr.2020.10.689
24. B. of Indian Standards IS 2386-3 (1963): Methods of test for aggregates for concrete, Part 3: Specific gravity, density, voids, absorption and bulking
25. B. of Indian Standards IS 456 (2000): Plain and reinforced concrete—code of practice
26. De la Colina Martínez AL (2019) Recycled polycarbonate from electronic waste and its use in concrete: effect of irradiation. Constr Build Mater 201:778–785. https://doi.org/10.1016/j.conbuildmat.2018.12.147
27. B. of Indian Standards IS 5816 (1999): Method of test splitting tensile strength of concrete
28. Bulut HA, Şahin R (2017) A study on mechanical properties of polymer concrete containing electronic plastic waste. Compos Struct 178:50–62. https://doi.org/10.1016/j.compstruct.2017.06.058
29. Shetty Be MS Concrete technology theory and practice (An ISO 9001: 2000 Company)

Study the Effects of Rice Husk on Geochemical Properties of Soil and Its Growth Promotions

Sampathkumar Velusamy, Manoj Shanmugamoorthy, Raja Kanagaraju, K. S. Navaneethan, N. Jothilakshmi, Umabharathi Chandrasekar, Vishwa Kumar, and Syed Mohamed Ibrahim Khutpudeen

Abstract The fertility of the soil is decreasing day by day. Because of that, the crop yield has decreased. To improve soil fertility more fertilizers are required. But the chemical fertilizers are costly and also harmful to the environment. So that an alternate way for chemical fertilizers are to be identified. Our study is focused on the improvement of soil fertility with the help of rice husk and *Bacillus* spp. The soil samples were collected and tested in the laboratory to find out the soil fertility. Two different seeds (Fenugreek, Greengram) were taken to analyze the soil fertility. The three different types of samples like tap water, treated water, and controlled water were used. The analysis of plant growth was carried out with application of the three samples. The plant growth in terms of no. of leaves; stem size and root length is analyzed. The estimation of carbohydrate, protein, and chlorophyll content of the plant samples were discussed in this study. In this study we use growth assay, height assay techniques to find out the plant growth. And also various tests like carbohydrate test, protein test, and chlorophyll tests are conducted to find out plant nutrition content in order to find out the soil fertility level. The result was interpreted with the help of graphs. Our study has revealed that application of rice husk in soil can alter plant growth and nutrition. Compared to the normal tap water our control, treated sample shows better shoot, root length. The carbohydrate, protein, and chlorophyll values of the control, treated sample show better results.

Keywords *Bacillus* spp. · Carbohydrate · protein test · Geochemical properties · Plant growth techniques · Rice husk · Soil fertility

S. Velusamy · M. Shanmugamoorthy · K. S. Navaneethan · N. Jothilakshmi · U. Chandrasekar (✉) · V. Kumar · S. M. I. Khutpudeen
Department of Civil Engineering, Kongu Engineering College, Perundurai 638060, India
e-mail: umabarathichandrasekar@gmail.com

R. Kanagaraju
Department of Civil Engineering, Sona College of Technology, Salem 636005, India

K. R. Reddy et al. (eds.), *Recent Advances in Civil Engineering*, Lecture Notes in Civil Engineering 398, https://doi.org/10.1007/978-981-99-6229-7_29

1 Introduction

A significant global issue is the deterioration of agricultural land and the rise in the production of agricultural waste. This is particularly true in Asia, where grain production continues to be a key economic driver and a major source of income for many people [1]. Since the demand for agricultural products in Asia is anticipated to increase as a result of the region's rapid population expansion and growing economic development, researchers are working to create novel solutions to these problems [2]. To combat soil nutrient problems, agriculture depends on inorganic fertilizers, however this has long-term effects. This is due to the fact that frequent, imbalanced fertilizer application results in the mineralization of organic matter, a reduction in soil carbon stores, an increase in soil acidity, and a reduction in soil nutrition [9].

The soil is the most vital component of our environment. Chemical and physical properties are the two types of soil properties [1]. The components of the soil determine its properties. The most serious problem today is soil infertility. As a result, crop yield is continuously decreasing. The nitrogen, potassium, and phosphorus content in the soil determine its fertility. Fertility of the soil must be increased to increase plant yield. We need a huge amount of chemical fertilizers, and that are bad for the soil, to get there. Another method for increasing soil fertility is to keep soil microorganisms alive. Microbes growth, on the other hand, is not simple. It requires a typical environment to grow. According to research, rice husk is the perfect medium for microbes. The husk, which is abundant, is a waste material of the rice mill [2].

1.1 Problem Identification

1.1.1 Soil Fertility Decline

Soil fertility diminishes when nutrients are added to the soil in higher quantities than they are taken out by agricultural crops, and at this point, the soil's reserves of nutrients are used up until they are no longer sufficient to meet the needs of the crop. Plant output and growth are consequently slowed down [7].

1.1.2 Causes of Soil Fertility

The two main reasons for agricultural waste removal and insufficient fertilizer use are what reduce soil fertility. The following factors contribute to soil erosion and continuous cultivation [4].

- Climate
- Soil types
- Improper cropping systems
- Continuous cropping systems.

1.2 Rice Husk—Agro Waste

The majority of the milled husk used in paddy processing boilers, which employ direct combustion and gasification to produce power, is used in India, the country with the biggest rice production worldwide [5]. This RHA poses a serious hazard to the ecology because of how the earth has been damaged and the area where it has been put. When using this RHA for industrial applications, several disposal methods are being taken into account. In countries where rice is grown, the rice plant's husk is a common form of agricultural waste. Worldwide, over 580 million tons of rice are produced each year, and both rice consumption and world population are increasing [3]. Due to its weak cellulose and other sugar content, feeding rice husk to cattle is frequently not advised.

1.3 Burning of Rice Husk

The enormous amount of rice husks that are discarded every day causes problems for farmers and agriculturalists all around the world. While the husks were being buried, the rest of their crops could not grow, and burning the husks led to a more significant ecological problem. The predicament for local species is made worse by the burning of husks since the fires quickly spread, destroying the ecosystem, and putting nearby residents in danger [8].

Burning agricultural waste is a problem because it causes air pollution, which includes the release of soot, elemental C, black carbon, aerosols, particles, toxic gasses, CO, NO, and hazardous gasses in small quantities [10]. Detrimental effects on health Nutrient loss, including nutrient cycling disruption, almost complete loss of C and N, 25% loss of P, 20% loss of K, and 50% loss of S. Soil erosion and runoff have increased. Reduction in the amount of soil-based organic carbon and energy-dense wastes, which has a negative impact on the soil's quality [6].

Fertilizer use results in infertility of the soil. The growth of microorganisms that are necessary for plant growth cannot occur in infertile soil. On the other hand, rice husk is a type of agricultural waste that is produced in greater quantities globally. The proper disposal of waste is very difficult. The ability of rice husk to retain moisture, which is essential for the growth of microbes. So, the material selected for the growth of microorganisms is rice husk. The physio-chemical characteristics of the soil are enhanced by those microbes to promote plant growth.

Table 1 Properties of rice husk

Properties	Values
Moisture	8.7%
Specific gravity	2.1
Ash	23.85%
Volatile matter	54.10%
Fixed carbon	13.35%

1.4 Objectives of This Study

- To cultivate *Bacillus* spp., using rice husk as the best source.
- Application of different growth hormone samples on various soil to check growth variability.
- To improve the soil fertility and growing.

2 Materials and Methodology

2.1 Materials

2.1.1 Rice Husk

One of the most common agricultural wastes in Vellakovil, in the Tiruppur district, is rice husk. This rice husk serves as a substrate for the growth of microorganisms. The position of the waste collection is 10.946190°N (latitude) and 77.712914°N (longitude) (longitude). The rice husk was dried in order to make it a suitable growing medium. The best growing medium is rice husk since it offers superior environmental conditions (Table 1).

2.1.2 Soil

The earth has a variety of soil kinds. However, we decided to explore red soil. Because red soil typically fosters the growth of green grains (Table 2).

2.1.3 Seeds

From nearby organic stores, three distinct types of seeds green gram, paddy, and fenugreek are gathered. The harvested seeds ought to be of high quality. 4.1.4 *Bacillus* spp.

Table 2 Properties of red soil

Physio-chemical properties	Values
pH	5.46
Specific gravity	2.4
Sand	60.7%
Silt	13.8%
Clay	25.5%
Ca	4.36 cmol/kg
Mg	0.84 cmol/kg
Na	0.21 cmol/kg

2.1.4 *Bacillus* spp.

Bacillus spp. are the microorganisms used in this study. It is grown using rice husk as the growing media. It supports the cycle of soil nourishment. Bacillus species need the right conditions to grow.

2.2 Chemicals Used

See Tables 3 and 4.

2.3 Preparation Media

- 20 ml of distilled water is used to create 0.5 g of Luria Bertani broth.

Table 3 Luria bertani broth

Composition	mg/L
Casein enzymic hydrolysate	10
Yeast extract	5
Sodium chloride	10

Table 4 Production media

Composition	mg/L
Casein enzymic hydrolysate	10
Yeast extract	5
Sodium chloride	10
Rice husk	2

- After making the broth, it was autoclaved for 15 min at 121 °C and 15 LBS.
- *Bacillus* spp. was added to the broth from the agar plate after sterilization, and the broth was then incubated for 24 h at 37 °C in the incubator.

2.4 Production Media

- After preparation, sterilization was completed at 121 °C and 15 LBS for 15 min in the autoclave.
- In the laminar air flow chamber, the media were separated in equal amounts.
- LB broth is created with 10% of rice husk for 40 ml.

2.5 Bacterial Inoculation

- The production media was inoculated with *Bacillus* spp., designated as the treated sample, and then incubated at 37 °C for 24 h.
- Another medium was kept as a control sample.

2.6 Seed Sowing

- Green gram and fenugreek seeds were used, and after being well rinsed with water, they were placed on a paper towel and sealed inside a zip-top bag for two days to sprout.
- The soil is watered down and sprouting seed is added before the containers are filled.
- After two days, controlled, treated, and tap water was supplied to the plants at one-day intervals for four days.
- After eight days, the plant growth was noticed in terms of the quantity of leaves, the size of the stems, and the length of the roots.

2.7 Estimation of Protein

The protein was estimated for three samples by the Lowry method [12].

2.8 Estimation of Carbohydrate

The carbohydrate was estimated by the anthrone method [13].

Table 5 Solvents (UV)

	Acetone	Methanol
Control	0.401	0.580
Tap water	0.489	0.587
Treated	0.463	0.601

Table 6 Plant growth results

Sample	No of leaves	Shoot size (cm)	Root length (cm)
Tap water	2	10.5	1.5
Control	5	14.5	2
Treated	5	15.4	3.3

2.9 Estimation of Chlorophyll

The chlorophyll content was estimated by spectrometer test [11] (Table 5).

3 Experimental Results and Discussion

3.1 Plant Growth Analysis Results Are Tabulated Below

Table 6 displays the results of an investigation of the plant growth of three separate tap water samples: control and treated. The number of leaves, shoot length, and root length were measured as part of the growth analysis. According to the results, the treated sample had more shoot length (15.4 cm), root length (3.3 cm), and leaf count than the control and tap water samples.

3.2 Carbohydrate Estimation Results Are Tabulated Below

The estimated carbohydrates are displayed in Fig. 1. The OD value is shown on the *Y* axis, and the *X* axis displays the carbohydrate concentration in μg. The relevant carbohydrate value is shown for each OD value. The final graph demonstrates that the concentration of carbohydrates in tap water is 20 μg, in control water is 40 μg, and in treated water is 60 μg.

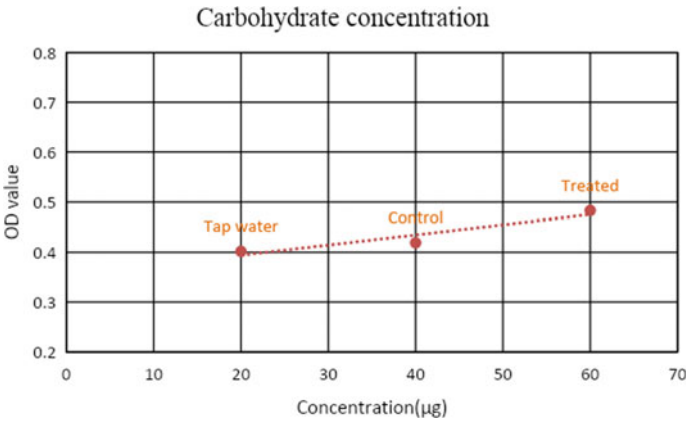

Fig. 1 Estimation of carbohydrate

3.3 Protein Estimation Results Are Tabulated Below

The estimated proteins are displayed in Fig. 2. The OD value is shown on the *Y* axis, and the *X* axis displays the protein concentration in µg. The relevant protein value is shown for each OD value. The final graph demonstrates that the concentration of protein in tap water is 20 µg, in the treated sample it is 40 µg, and in the control sample it is 60 µg.

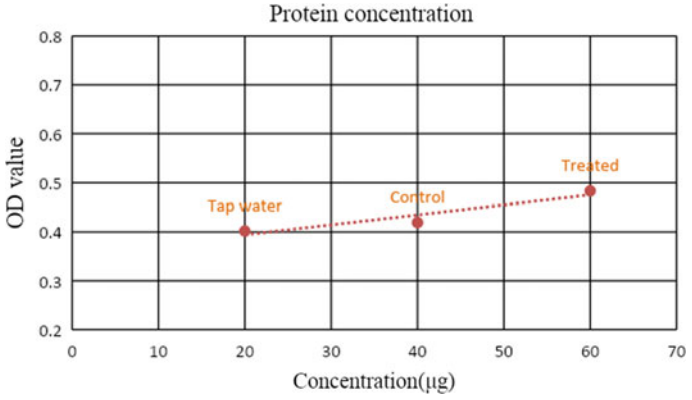

Fig. 2 Estimation of protein

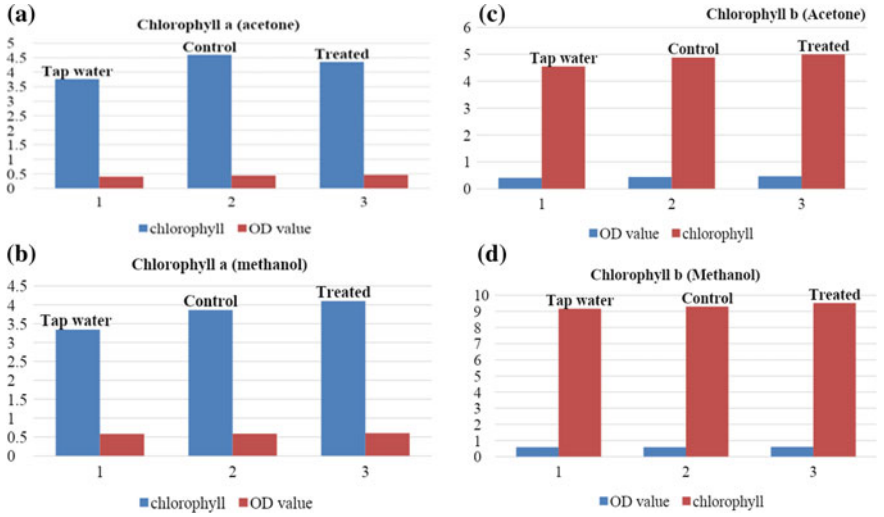

Fig. 3 **a** Chlorophyll a (acetone). **b** Chlorophyll a (methanol). **c** Chlorophyll b (acetone). **d** Chlorophyll b (methanol)

3.4 Chlorophyll a Estimation Result is Tabulated Below

Figure 3a shows the chlorophyll for acetone solution. The bar graph shows the OD value of three samples and corresponding chlorophyll content in the sample. The chlorophyll a for tap water (3.76 mg/L), control (4.6 mg/L), and treated (4.35 mg/L).

Figure 3b shows the chlorophyll for methanol solution. The bar graph shows the OD value of three samples and corresponding chlorophyll content in the sample. The chlorophyll a for tap water (3.34 mg/L), control (3.86 mg/L), and treated (4.1 mg/L).

Chlorophyll b estimation results are tabulated below.

Figure 3c shows the chlorophyll b for acetone solution. The bar graph shows the OD value of three samples and corresponding chlorophyll content in the sample. The chlorophyll a for tap water (4.55 mg/L), control (4.88 mg/L), and treated (5 mg/L).

Figure 3d shows the chlorophyll b for methanol solution. The bar graph shows the OD value of three samples and corresponding chlorophyll a content in the sample. The chlorophyll a for tap water (9.3 mg/L), control (9.17 mg/L), and treated (9.52 mg/L).

4 Discussion

It was determined how rice husk affected the soil's geochemical characteristics. In terms of plant growth, carbohydrate content, protein content, and chlorophyll content, treated and controlled samples perform better than tap water. RH has the potential to change the physico-chemical characteristics of soil due to its distinct physical qualities and nutritional content. It hasn't yet been thoroughly discussed how rice husk affects the characteristics of the soil. Further research is being done to determine the association between rice husk and soil characteristics.

5 Conclusion

- In comparison to tap water, the control, and treated samples exhibit better plant growth.
- Our control treated sample displays better shoot and root length when compared to the regular tap water.
- The treated sample's carbohydrate value is 60 g, compared to 40 g for the control. Protein content of the treated sample is 40 g, compared to 60 g for the control sample. The acetone-treated control samples' chlorophyll b levels are 4.5 mg/L. And it is 9 mg/L for methanol. The variations in physico-chemical qualities are what cause these variations in carbohydrate, protein, and chlorophyll values.
- This work can be done with addition of other acceptable organic wastes including maize cobs, wheat husk, and other crop residues may be employed for environmentally friendly agriculture.

References

1. Hossain A, Krupnik TJ, Timsina J, Mahboob MG, Chaki AK, Farooq M, Bhatt R, Fahad S, Hasanuzzaman M (2020) Agricultural land degradation: processes and problems undermining future food security. Environment, climate, plant and vegetation growth. Springer International Publishing, Cham, pp 17–61
2. Obi FO, Ugwuishiwu BO, Nwakaire JN (2016) Agricultural waste concept, generation, utilization and management. Niger J Technol 35(4):957–964
3. Ajala AS, Gana A (2015) Analysis of challenges facing rice processing in Nigeria. J Food Process
4. Ibrahim S, Mumtaz E (2014) Application of agro-waste products as organic and value added bio fertilizer for improving plant growth. J Pharm Clin Sci 8:35–41
5. Kumar S, Sangwan P, Dhankhar RMV, Bidra S (2013) Utilization of rice husk and their ash: a review. Res J Chem Env Sci 1(5):126–129
6. Daily G (2020) What are ecosystem services? In: Global environmental challenges for the twenty-first century. Resources, consumption and sustainable solutions, pp 227–231
7. Havlin JL (2020) Soil: fertility and nutrient management. In: Landscape and land capacity, pp 251–265

8. Mulder K (ed) (2017) Sustainable development for engineers: a handbook and resource guide. Routledge
9. Srinivasarao C, Kundu S, Lakshmi CS, Rani YS, Nataraj KC, Gangaiah B, Laxmi MJ, Babu MVS, Rani U, Nagalakshmi S, Manasa R (2019) Soil health issues for sustainability of South Asian agriculture. EC Agric 6(5):310–326
10. Manisalidis I, Stavropoulou E, Stavropoulos A, Bezirtzoglou E (2020) Environmental and health impacts of air pollution: a review. Frontiers Public Health 14
11. Wellburn AR (1994) The spectral determination of chlorophylls a and b, as well as total carotenoids, using various solvents with spectrophotometers of different resolution. J Plant Physiol 144:307–313
12. Lowry OH, Rosebrough NJ, Farr AL, Randall RJ (1951) Protein measurement with the Folin phenol reagent. J Biol Chem 193:265–275
13. Plummer DT (1990) An introduction to practical biochemistry, 3rd ed., p 179

Comparative Study on Stabilisation of Bentonite Clay Using Municipal Incinerated Bottom Ash and Fly Ash

K. Raja, V. Sampathkumar, S. Anandaraj, S. Hariswaran, G. Dheeran Amarapathi, and B. Srisaran

Abstract The major destructions in Civil Engineering structures are due to the expansive soils. To prevent severe effects on infrastructural elements like roads, buildings, dams, embankments, etc., expansive soil is stabilised. A sustainable approach of stabilising expansive soil especially bentonite clay using Municipal Incinerated Bottom Ash (MIBA) and fly ash from the municipal incinerator plant has been presented in this study work. The laboratory investigations are carried out to determine the geotechnical characteristics of stabilised soil through its index and engineering properties. Further, the results are compared for MIBA and fly ash treated soil which concludes that bentonite treated with fly ash at 30% performs better with higher stress values. The maximum stress value is obtained for bentonite with 30% MIBA (270.74 kPa) at a curing phase of 14 days. On the accumulation of further percentage, the stress values are decreasing. In case of fly ash, the results are observed to be increasing with increasing days of curing, and the extreme stress value is found for bentonite with 30% fly ash (311.24 kPa) at a curing period of 14 days.

Keywords Bentonite · Bottom ash · Expansive soil · Fly ash · Stabilisation

K. Raja (✉)
Department of Civil Engineering, Sona College of Technology, Salem 636005, India
e-mail: krajakec@gmail.com

V. Sampathkumar · G. D. Amarapathi · B. Srisaran
Department of Civil Engineering, Kongu Engineering College, Erode 638060, India

S. Anandaraj
Department of Civil Engineering, KPR Institute of Engineering and Technology, Coimbatore, India

S. Hariswaran
Department of Civil Engineering, Sri Venkateswara College of Engineering, Sriperumbudur 602117, India

K. R. Reddy et al. (eds.), *Recent Advances in Civil Engineering*, Lecture Notes in Civil Engineering 398, https://doi.org/10.1007/978-981-99-6229-7_30

1 Introduction

In India, the expansive soils occur prominently in Maharashtra, Madhya Pradesh, Andhra Pradesh, Gujarat, Orissa and along the river valleys of Tapti, Krishna, Narmada and Godavari which have the capacity to swell and shrink corresponding to various moisture contents. These expansive soils produce a great threat to the society in various aspects in the construction field. Thus, it is very important to arrive at a solution by stabilising these expansive soils. The term "stabilisation of soil" refers to a variety of techniques used to change the soil characteristics and enhance its engineering performance [1]. The three stabilising techniques are physical, chemical and polymer techniques. Among these three, the polymer method of stabilisation has numerous significant advantages over the other two methods. Unlike chemical remedies, these polymers are affordable and substantially less harmful to the environment. On the other hand, because of quick industrialisation of our nation and growing population, huge volume of waste is being produced, and this is increasing day by day. It is more expensive both in terms of cost to use the landfill and for additional pre-treatment for waste. Municipal solid waste burning is a treatment option that is gaining in importance because it not only entails recovering energy from the garbage during combustion but also causes a significant decrease in the amount of waste. Thus, taking sustainability into consideration the bottom ash and fly ash gathered from the incinerator plant can be used to strengthen the expansive soil. A by-product of combustion coal in thermal power plants is bottom ash. Related to fly ash, which has an excessive shear strength and a low compressibility, bottom ash particles are coarser [2]. Sharma et al. [3] have made a study on the use of a 6:12:18 combination of fly ash, gypsum and blast furnace slag to stabilise expansive soil and concluded from UCC test result as the strength increased by 300% and also there was decrease in the swelling pressure. Cokca et al. [4] made use of 25% of Class-C fly ash constituting 18.98% of CaO and carried out the research work. The treated specimen with 20% of fly ash when tested shows the swelling pressure 75% reduction after 7 days of cure and 79% reduction after 28 days of curing, respectively. Murmu et al. [5] have studied the effectiveness of using the geopolymer made of alkali-activated fly ash and the expansive soil exhibits significant increase in the strength as a result of unconfined compression test. The study also concluded that the swell pressure and shrinkage gets decreased. The results were found to depend on the size of particles and the fly ash volume and also the ratio of alkaline solution which includes NaOH and Na_2SiO_3. Lynn et al. [6] conducted a detailed study on the characteristics of bottom ash from municipal incinerators and this research concludes that the main oxides in Municipal Incinerated Bottom Ash (MIBA) are SiO_2, CaO and Al_2O_3 [7]. In an investigation into the stabilisation and crystallisation of a solid municipal waste combustion residue utilising fly ash-based geopolymers, it was found that fly ash including heavy metals like Pb, Cd, Cr, or Zn could be solidified using this technique. Chindaprasirt et al. [8] carried out a comparison of the features of bottom ash and fly ash geopolymers. Municipal solid waste incineration (MSWI) is the process of minimising the amount of garbage generated by properly utilising the thermal

processes of melting, combustion and other reactions. Electricity can be produced using incineration heat. Air pollution will however result from faulty incineration conditions control [9]. From this research, it has been estimated that the addition of NaOH with these additives influences their characteristics. Thus, the challenging soil in the current investigation, an expansive soil considered for effectiveness of stabilisation using Municipal Incinerated Bottom Ash and the results are compared with the effectiveness of stabilisation using fly ash.

2 Materials and Methodology

2.1 Description

Tests were performed on the bentonite clay, municipally burned bottom ash, and fly ash after the samples were collected. Specific gravity, Atterberg Limits, Differential Free Swell Test, Compaction Characteristics and Unconfined Compressive Strength are among them.

2.2 Collection of Bottom Ash and Fly Ash

Erode District produces about 310 Tonnes of MSW of which about 100 Tonnes are non-recyclable wastes. Erode district has three Operational Incineration Plants. About 150 kg of municipal burnt bottom ash and 200 kg of fly ash is produced every day. Municipal burnt bottom ash and fly ash are collected from the municipal incinerator plant situated at Erode. The process of collecting the municipal burnt bottom ash and fly ash is pictorially represented in Fig. 1a–c.

3 Experimental Results and Discussions

The basic index properties of the bentonite clay, MIBA and fly ash are experimentally investigated and are verified with the IS 2720 codes. The outcomes obtained are exposed in Table 1.

The liquid limit of the clay is evaluated as 252.6% which indicates that the clay is highly compressible. The plasticity index is obtained as 200.1% for the clay which reveals that the plasticity of clay as high plasticity as per [10]. One can determine the free swell index of clay from the divergent free swell test as 192.3% from which it is clear that the bentonite sample has high swelling property as per [11].

Fig. 1 **a** Pre-processing in 120 mm sieve. **b** Heap formation. **c** Processing of the municipal solid waste in the municipal incinerator plant

Table 1 Properties of the sample

Properties	Values	Remarks
Specific gravity for bentonite clay	2.51	
Specific gravity for MIBA	2.7	
Specific gravity for fly ash	2.63	
Liquid limit of clay [9]	252.60%	
Plastic limit of clay [9]	52.50%	
Flow index of clay	50	
Plasticity index of clay [9]	200.10%	Highly plastic
Free swell Index of clay [11]	192.30%	High swelling
Specific gravity for bentonite clay	2.51	

3.1 Standard Proctor Test

The optimal moisture content (OMC) and maximum dry density (MDD) were found experimentally using the conventional Proctor compaction test. The experiment is carried out using a Proctor mould with a 944-cc capacity, 10.2 cm for the internal diameter and 11.6 cm for the height. With the 2.5 kg hammer dropping through, the clay is deposited in the Proctor mould and compacted in three levels with 25 blows each [12]. It emphasises how a soil's dry density for a specific compactive effort

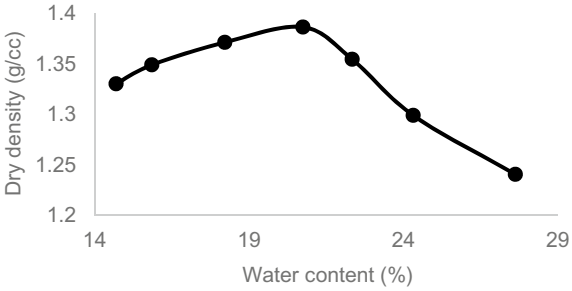

Fig. 2 Proctor curve for bentonite clay

Table 2 OMC and MDD

Sample	OMC %	MDD (kN/m^3)
Bentonite	20.74	1.38
Bentonite with 10% MIBA	22.34	1.47
Bentonite with 20% MIBA	24.49	1.48
Bentonite with 30% MIBA	26.53	1.482
Bentonite with 40% MIBA	29.91	1.46
Bentonite with 10% fly ash	25.78	1.33
Bentonite with 20% fly ash	27.24	1.34
Bentonite with 30% fly ash	29.92	1.39
Bentonite with 40% fly ash	27.64	1.38

depends on the amount of water present in the soil at the stage of soil compaction [13]. The bentonite soil and the Proctor curve are shown in Fig. 2.

From Fig. 2, it is estimated that the OMC is 20.74% and MDD is 1.38 kN/m^3. The test was also done for the bentonite soil treated with 10, 20, 30, and 40% of MIBA and fly ash. The optimum moisture content and the maximum dry density relations as per the [14] were obtained from the graph, and the resulting values are illustrated in Table 2. From Table 2, it is observed that the OMC and MDD of bentonite clay increase with the percentage increment of MIBA, whereas in case of addition of fly ash, it increases up to 30% addition and decreases further. The highest MDD is obtained for 30% MIBA addition (1.482 kN/m^3) and for 30% addition of fly ash (1.39 kN/m^3).

3.2 Unconfined Compression Test

The unconfined compressive strength characteristics of clay soil "Qu" were found experimentally by conducting unconfined compression strength test. A cylindrical soil sample is prepared for the test by trimming it such that the ends are comparatively smooth and the length-to-diameter proportion is in the range of two. The

metal loading frame is loaded, then the soil sample is set on it [15]. The unconfined compression test was performed for the bentonite clay, MIBA treated bentonite and fly ash preserved bentonite each at its optimum moisture content.

The resulting stress–strain graphs obtained from the UCC test with the samples having undergone curing at the time periods of 0 days (i.e. without curing), 3 days, 7 days and 14 days are shown in Figs. 3, 4, 5, 6, 7, 8, 9, 10 and 11.

From Fig. 3, 4, 5, 6, 7, 8, 9, 10 and 11, it can be observed that stress values in all the cases increases for the increased days of curing. For virgin bentonite clay, the highest stress value is 146.3 kPa for 14 days of curing. The maximum values are reached in case of addition of 30% MIBA for MIBA treated bentonite and 30% fly ash for fly ash treated bentonite. In case of bentonite treated with 30% MIBA, the highest stress value is 270.74 kPa for 14 days of curing, and for 30% fly ash treated bentonite, the peak value recorded is 311.2 kPa for 14 days of curing. On the addition of further percentage, the stress values are decreased. On comparing those values bentonite treated with 30% fly ash shows the highest value 311.2 kPa for a curing phase of 14 days. The determined stress values of all the samples are specified in Table 3.

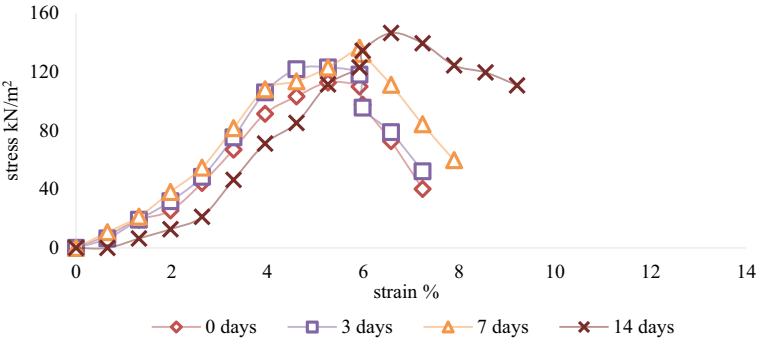

Fig. 3 Stress–strain curve of bentonite with curing period of 0, 3, 7 and 14 days

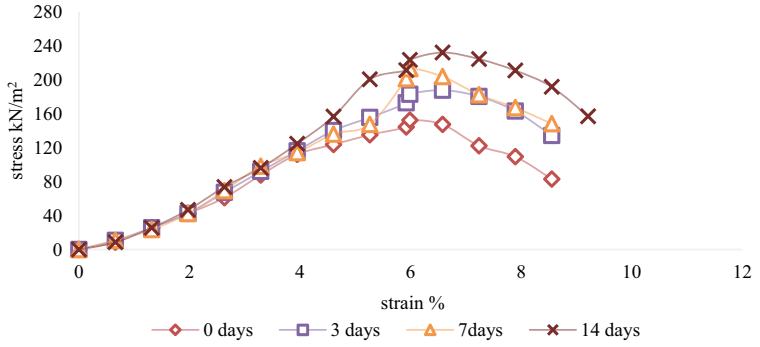

Fig. 4 Stress–strain curve of bentonite with 10% MIBA with 0, 3, 7 and 14 days of curing

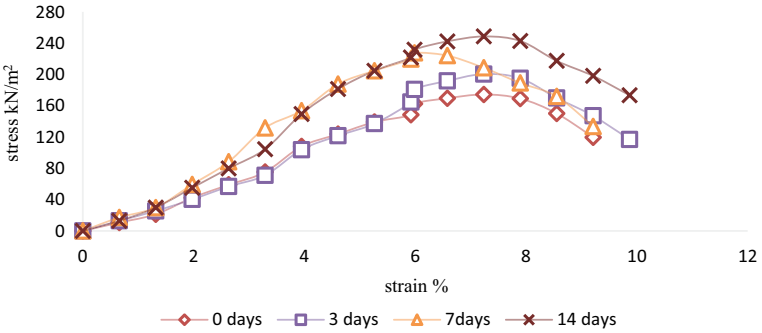

Fig. 5 Stress–strain curve of bentonite with 20% MIBA with 0, 3, 7 and 14 days of curing

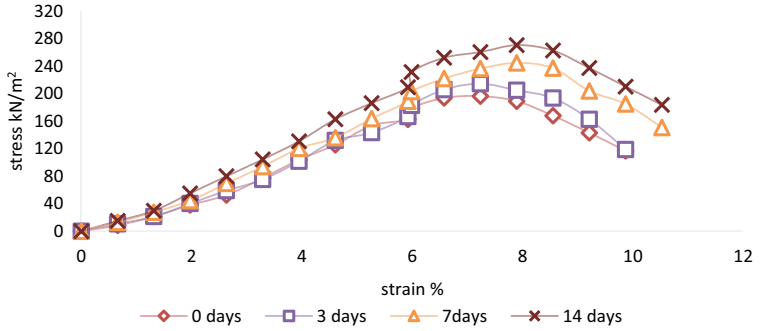

Fig. 6 Stress–strain curve of bentonite with 30% MIBA with 0, 3, 7 and 14 days of curing

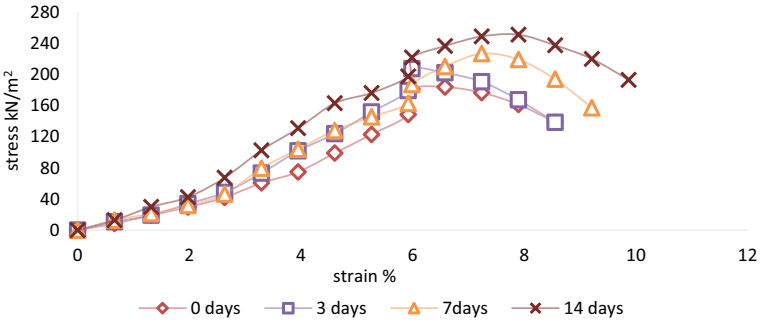

Fig. 7 Stress–strain curve of bentonite with 40% MIBA with 0, 3, 7 and 14 days of curing

However, from Table 3, it can be observed that the stress values of the virgin bentonite clay for curing period of 0 days, 3 days, 7 days and 14 days are lower compared to the values obtained for MIBA treated and fly ash treated samples. The maximum stress value is obtained for bentonite with 30% MIBA (270.74 kPa) at a

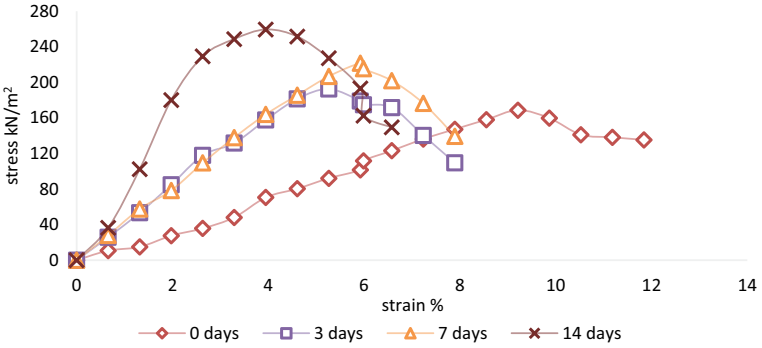

Fig. 8 Stress–strain curve of bentonite with 10% fly ash with 0, 3, 7 and 14 days of curing

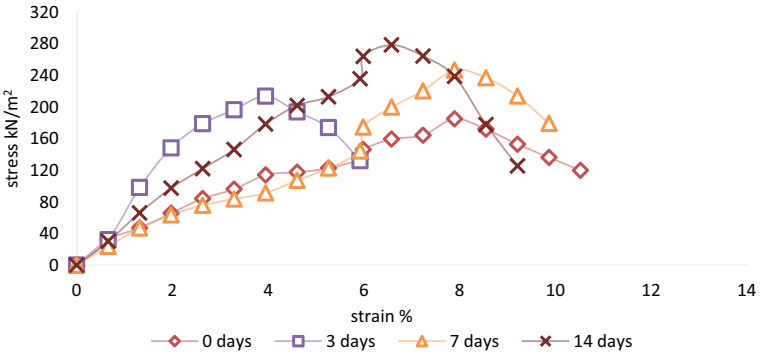

Fig. 9 Stress–strain curve of bentonite with 20% fly ash with 0, 3, 7 and 14 days of curing

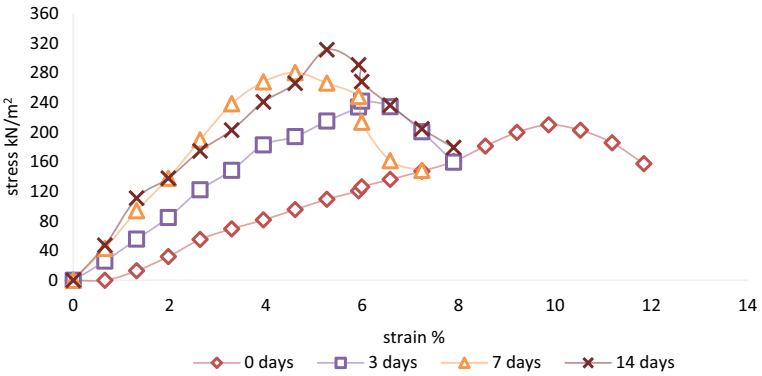

Fig. 10 Stress–strain curve of bentonite with 30% fly ash with 0, 3, 7 and 14 days of curing

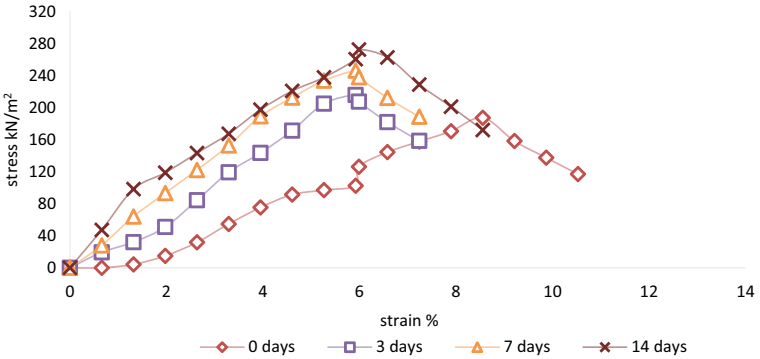

Fig. 11 Stress–strain curve of bentonite with 40% fly ash with 0, 3, 7 and 14 days of curing

Table 3 UCC results summary

Sample	Unconfined compressive strength (kPa)			
	0 days curing	3 days curing	7 days curing	14 days curing
Bentonite	112.62	122.86	136.24	146.3
Bentonite with 10% MIBA	152.4	187.78	213.36	232.21
Bentonite with 20% MIBA	174.43	200.5	227.58	248.61
Bentonite with 30% MIBA	196.49	214.53	244.86	270.74
Bentonite with 40% MIBA	183.74	207.26	226.56	250.83
Bentonite with 10% fly ash	168.76	192.48	221.64	259.51
Bentonite with 20% fly ash	185.14	213.83	246.85	278.65
Bentonite with 30% fly ash	209.97	241.8	280.41	311.24
Bentonite with 40% fly ash	187.13	215.54	246.64	272.28

curing phase of 14 days [16, 17]. On the accumulation of further percentage, the stress values are decreasing. In case of fly ash, the results are observed to be increasing with increasing days of curing and the extreme stress value is found for bentonite with 30% fly ash (311.24 kPa) at a curing period of 14 days. This may be due to the inappropriate percentage of addition of the additives with the expansive clay.

4 Conclusion

- The bentonite clay when treated with MIBA and fly ash shows better UCS values with increased days of curing. The highest UCS value is obtained when MIBA is added to the bentonite clay, when it is added in the percentage of 30%.

- The highest UCS value is obtained when fly ash is added to the bentonite clay, when it is added in the percentage of 30%. Comparing the UCS results obtained it is observed that bentonite clay has better values in case of bentonite clay with 30% fly ash is more desirable with high stress values.
- The present research has attempted only on the addition of MIBA and fly ash as stabilising agents.
- This work can be extended by the addition of some alkali-activated geopolymers, and the results can be studied for the effectiveness of utilising the alkali-activated MIBA and fly ash as a stabilising substance for the porous soil.

References

1. Selvam VS, Sivaraja M, Raja K, Navaneethan KS, Amarapathi GD (2016) Minimisation of subgrade thickness using natural and synthetic additives in roads. IOSR J Mech Civil Eng (IOSR-JMCE) 13:66–72
2. Manikandan AT, Ibrahim Y, Dheebikhaa B, Raja K (2017) A study on effect of bottom ash and coconut shell powder on the properties of clay soil. Int Res J Eng Technol 4(2):550–553
3. Sharma VB, Reddy AR, Sastry SS (1992) Some studies on utilizing agro-industrial wastes in soil stabilization. In: Proceedings of national conference on CBMIW, pp 34–42
4. Cokca E, Yazici V, Ozaydin V (2009) Stabilization of expansive clays using granulated blast furnace slag (GBFS) and GBFS-cement. Geotech Geol Eng 27(4):489
5. Murmu AL, Jain A, Patel A (2019) Mechanical properties of alkali activated fly ash geopolymer stabilized expansive clay. KSCE J Civ Eng 23(9):3875–3888
6. Lynn CJ, Ghataora GS, Obe RKD (2017) Municipal incinerated bottom ash (MIBA) characteristics and potentialor use in road pavements. Int J Pavement Res Technol 10(2):185–201
7. Galiano YL, Pereira CF, Vale J (2011) Stabilization/solidification of a municipal solid waste incineration residue using fly ash-based geopolymers. J Hazard Mater 185(1):373–381
8. Chindaprasirt P, Jaturapitakkul C, Chalee W, Rattanasak U (2009) Comparative study on the characteristics of flyash and bottom ash geopolymers. Waste Manage 29(2):539–543
9. Beylot A, Villeneuve J (2013) Environmental impacts of residual municipal solid waste incineration: a comparison of 110 French incinerators using a life cycle approach. Waste Manage 33(12):2781–2788
10. IS: 2720 (part 5) (1985) Determination of liquid limit, plastic limit and shrinkage limit. Bureau of Indian Standards
11. IS: 2720 (part XL) (1977) Determination of free swell index. Bureau of Indian Standards
12. IS: 2720 (part 8) (1980) Determination of water content-dry density relation using standard compaction. Bureau of Indian Standards
13. Selvam VS, Sivaraja M, Raja K, Amarapathi GD (2018) Behavioral study of soft clay reinforced with randomly distributed polyester fibers. Int J Civil Eng Technol (IJCIET) 9(5):135–143
14. Raja K, Dheeran Amarapathi G, Santhosh Kumaar K (2020) Spatial analysis of geotechnical characteristics of soils in Perundurai. Int J Sci Technol Res 9(02):3415–3425
15. Selvam VS, Sivaraja M, Raja K, Amarapathi GDD (2018) Behavior of strip footing in soft clay stabilized with various additives. Int J Civil Eng Technol (IJCIET) 9(6):152–161
16. Lynn CJ, Ghataora GS, Obe RKD (2017) Municipal incinerated bottom ash (MIBA) characteristics and potential for use in road pavements. Int J Pavement Res Technol 10(2):185–201
17. Mohamedzein YEA, Al-Aghbari MY, Taha RA (2003) Stabilization of desert sands using municipal solid waste incinerator ash. Geotech Geol Eng 24:1767–1780

Experimental Study on Impact of Al_2O_3 and High Alumina Cement in Heat-Resistant Floor Tiles

Ye Min Paing, Balasubramanian Murugesan, and Monisha Ravi

Abstract In Asian nations, heat-resistant tiles are crucial, which obviously raises the demand for natural resources. A significant supply of raw materials must be obtained in order to meet the rising demand. Generally, raw resources may be sourced from international and domestic regions. Finding a sustainable source of raw materials is essential to prevent production interruptions in the tile sector. The primary goal of this study is to identify the characteristics of the materials used to make tiles, assess the effects of Al_2O_3 and high alumina cement exposure on cementitious floor tiles, and determine the strength and durability qualities of tiles by combining copper powder with the raw materials. In this paper, three types of samples of tiles (250 mm × 250 mm × 12 mm) were manufactured from extracted aluminum oxide. To determine the materials' utility as raw material in the ceramic industry, properties of tiles such as water absorption capacity and rupture modulus of the materials were compared with standard conventional tile. In addition to copper powder and alumina, the proposed new heat resistance technique would make it possible to effectively use additional waste products that are rich in alumina and conduct a cost analysis to check the financial feasibility.

Keywords Heat-resistant tiles · Floor tiles · Copper powder · Thermal comfort tile · Alumina cement

1 Introduction

In order to meet demand, ceramic tile, one of the most often used building materials, has been widely developed in India, where new development may total 2 billion square meters annually. Many raw materials are needed to make ceramic tiles; for example, a recent study found that 20 kg of raw materials was needed to make 1 m^2 of ceramic tile. Hence, there would be a conspicuous demand for raw resources. It

Y. M. Paing · B. Murugesan (✉) · M. Ravi
Department of Civil Engineering, Faculty of Engineering and Technology, SRM Institute of Science and Technology, Kattankulathur, Tamil Nadu 603203, India
e-mail: balasubm1@srmist.edu.in

K. R. Reddy et al. (eds.), *Recent Advances in Civil Engineering*, Lecture Notes in Civil Engineering 398, https://doi.org/10.1007/978-981-99-6229-7_31

is vital to look for alternative raw materials with high availability given the dearth of high-quality raw resources and the rising expense of doing business. Given that it accounts for 30% of industrial employment in India and 10.4% of the country's GDP, the construction industry has a significant positive impact on both society and the economy [1–3]. However, the building industry is also regarded as the largest energy consumer in India, accounting for approximately 40% of all energy use and producing nearly 36% of all greenhouse gas (GHG) emissions. Together with pollutants, the built environment also stores much material in its structures [4]. There are growing concerns about and orientations toward more sustainable construction processes, with a focus on resource usage efficiency and the use of more environmentally friendly materials that have a lower environmental impact throughout their entire life cycle, as a result of the significant environmental effects of the construction industry [5, 6, 22]. Inorganic, nonmetallic resources, such as minerals and rocks make up the ceramic materials that are customarily employed in the construction industry. Its primary distinguishing feature is that they are made from a natural blend of raw materials, including silica, at least one argillaceous mineral, and typically alkaline oxides. However, the final ceramic goods may differ depending on the mixture in a number of ways, including porosity, color, and the presence of enamel [7, 8].

In addition to the advantages for the ceramic industry, a side benefit from the waste organic matter content and accompanying energy qualities is possible. However, the typical ceramic tile is a member of the Al_2O_3 ternary system, with the raw material mixture's CaO level being less than 3 weight percent and Al_2O_3 content ranging from 15 to 25 weight percent. This makes it necessary to expand the standard ceramic preparation area. Hence, the application of an alumina-rich ceramic system to produce high-quality ceramic tiles for use in unique settings is the driving force behind the current work. The fabrication of ceramic tiles employing high alumina cement and Al_2O_3 as the raw material in combination with conventional raw materials was proposed in this study as a unique alumina-rich ceramic system [9]. Comprehensive research was done on the macroscopic characteristics of water absorption capacity, bulk density, rupture modulus, and microstructure. The suggested novel ceramic method would establish the groundwork for the use of other alumina-rich waste in addition to realizing the efficient exploitation of Al_2O_3, which is high in alumina. This examination examines the suitability of tile ash as a partial replacement for clay and cement [10–12]. Important findings were obtained after a thorough investigation and comparison of the strength and structural performance of these concrete mixtures with corresponding conventional tiles.

2 Literature Survey

2.1 A. Olgun et al.

Fly ash from thermal power plants was utilized to create materials for glass, glass–ceramic, and ceramics without the use of any additives. The glass sample was found to be in the amorphous phase using x-ray diffraction (XRD) investigation. The glass ceramic sample had an augite phase, whereas the ceramic samples contained enstatite and multiple phases. SEM studies showed that small crystallites diffused equally in the microstructure of the glass–ceramic sample while elongated crystals formed in the ceramic samples. The resulting sample density values are equivalent to those of commercially available tile samples of glass, glass–ceramic, and ceramic materials [13].

2.2 Mohammad A. Alim et al.

Solar cell integration into architectural components, like roof tiles is becoming more and more popular. Unfortunately, the conversion efficiency of photovoltaic cells is temperature-dependent, and it will decline at high temperatures. In this work, the performance of mortar roof tiles with embedded solar cells and safety glass is studied. To control the temperature of the solar cells, a phase change material (PCM) was added to the mortar of the roof tiles at a concentration of 3 weight percent. To ascertain the financial viability and assess the effect of the PCM on solar-to-electrical power generation for solar roof tiles, a life cycle cost study is conducted. During winter days, it has been found that solar roof tiles with PCM produce electrical energy that is roughly 4.1% more than their counterparts without PCM, whereas on six summer days, the improvement is between 2.2–4.3%.

2.3 Nor Baizura Hamid et al.

This research was done to see whether waste materials may be used in place of raw resources while making tiles. We can determine the material's physical and mechanical properties based on seven different types of tests, including those for combustion shrinkage, water absorption, density, porosity, tensile strength, and compression, using a four-stage process of identification, inspection, qualification, and inclusion to locate sources in books and journals. With a lower water absorption rate ranging from 0.5 to 0.15% for the water absorption test, the electric furnace has the lowest water absorption percentage result for tiles made from alternative materials. Overall, depending on the results of standard testing, it can make tiles that are up to the requirements that have been established [14].

2.4 Mohd Amirhafizan Bin Husin et al.

In this study, samples are made in a unique design with dimensions of 50 mm in length, 10 mm in breadth, and 5 mm in thickness. There are three different size categories for this wood dust: small, medium, and giant. A compression machine with a pressure of 9.80665 N was used to create the sample. After the mechanical characteristics of the sample were determined, the pressure and hardness tests produced favorable results.

3 Literature Summary

This literature survey concludes that tiles are made up of waste materials, fly ashes, and PCM materials to improve the durability, strength, and performance of floor tiles and the thermal properties, which improve the sustainable development of raw materials in the tile manufacturing process. The aesthetics and comfort of a building can both be enhanced by floor treatments. Tile is one of the finishes that is frequently utilized in industry. To create light tiles with a low water absorption percentage and durability, this finish can be applied as an exterior layer to both walls and floors. This study was carried out to examine the use of waste materials as replacement materials in the production of tiles as a means of resolving this issue.

4 Materials

4.1 Al_2O_3

Among the variety of technical ceramics, alumina is one of the most commonly utilized and economically advantageous materials. The easily available and fairly priced raw ingredients used to manufacture this high-performance technical grade ceramic lead to fabricated alumina shapes that offer good value for the money. Given its excellent combination of characteristics and competitive pricing, fine grain technical grade alumina's wide range of applications should not come as a surprise. The shape, size, physical, and chemical properties of the materials perfectly match those of the conventional tile-making process.

4.2 High Alumina Cement

High alumina cement gains strength quickly. After 24 h, approximately 80% of the maximum strength develops, and even after just 8 h, it is strong enough to remove

the formwork. Strength grows quickly because of its quick hydration. Furthermore, it has many calories [15].

4.3 Copper

For the reaction of oxygen with copper powder, cuprous oxide (Cu_2O), cupric oxide (CuO), and cuprous sulfide (Cu_2S) are produced as powders. The goods are used in antifouling paints, reagents in chemical reactions, catalysts in the manufacturing of silicone compounds, nonferrous melt hydrogen degassing in foundries, antifouling coating in tiles to introduce antibacterial tiles, and antifouling coating in silicone compounds [16].

5 Experimented Programmed

The experimental investigation of tiles uses the following materials to introduce novel tiles in sustainable technologies. High alumina cement (HAC) of 35 grade with a specific gravity of 3.10 and a bulk density of 3.03 g/cc was employed in this investigation. According to the production of tiles, marble and black chips are essential, but they differ in the ratio for a suitable replacement percentage. Table 1 gives the tile mix proportions of tiles during casting.

From Table 1, the materials are batched and cast into different types of samples accordingly. The tile size was 250 mm × 250 mm × 12 mm with different material compositions. The optimum ratio of mix design is 1:2. Figure 1 shows the casting proof of the tiles in the manufacturing plant. Step-by-step steps are followed in tile casting: Step 1, batching of materials; Step 2, mixing of the materials and preparation of clay; Step 3, molding and vibrating; and Step 4, demolding and drying.

6 Results

6.1 Mechanical Properties

Bulk Density The density of each material was examined based on the density of the separate materials and its influence on the bulk density of the final product as a tile after tile casting and curing. The densities of Al_2O_3, high alumina cement, and copper are 2700 kg/m^3, 800 kg/m^3, and 8830 kg/m^3, respectively. Influencing these materials in heat-resistant tiles, the overall bulk density is evaluated as per IS 3630 [17].

Table 1 Types of tile samples ratio details

Name of the sample	Materials required	Grams per tile
Conventional tile	White cement	420
	Admixture	420
	Marble chips	800
	Black chips (8 mm)	800
Heat-resistant tile 1	Al_2O_3	420
	Marble chips	800
	Black chips (8 mm)	800
	Copper	10
Heat-resistant tile 2	White cement	420
	Al_2O_3	420
	Marble chips	800
	Black chips (8 mm)	800
Heat-resistant tile 3	High alumina cement	420
	White cement	420
	Marble chips	800
	Black chips (8 mm)	800
	Copper	10

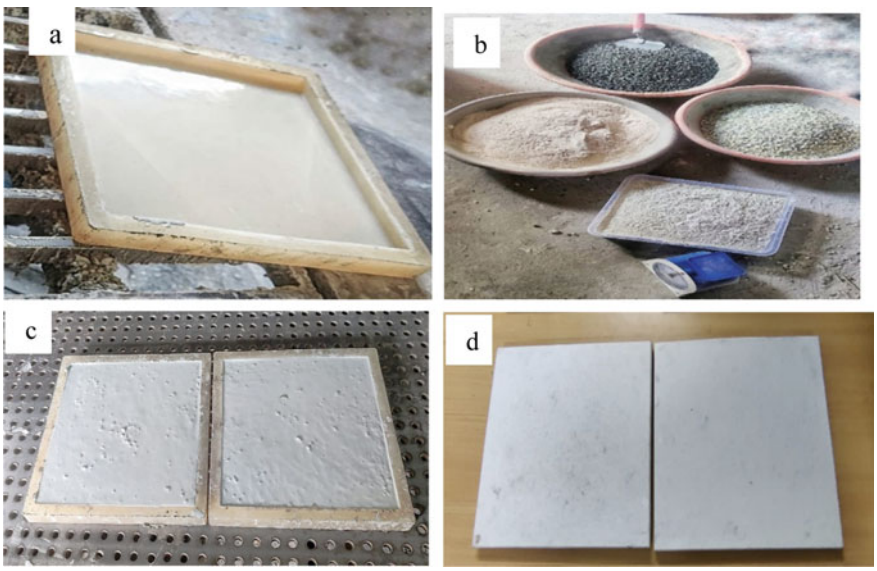

Fig. 1 Shows the experimental proof of tile manufacturing **a** Tile mold, **b** Batching of materials, **c** Casted tiles, **d** Demolded tiles

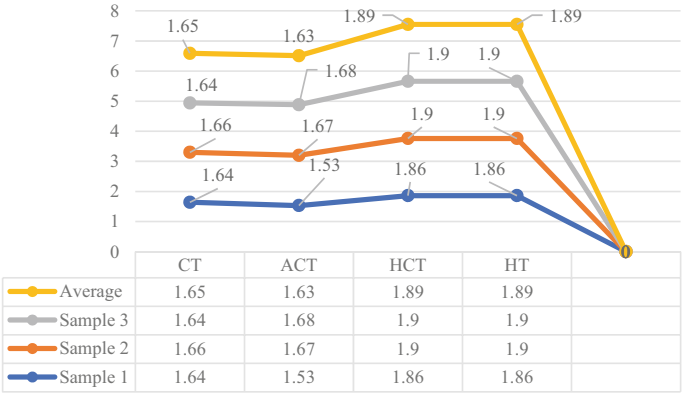

	CT	ACT	HCT	HT
Average	1.65	1.63	1.89	1.89
Sample 3	1.64	1.68	1.9	1.9
Sample 2	1.66	1.67	1.9	1.9
Sample 1	1.64	1.53	1.86	1.86

Fig. 2 Shows the density of the tiles with different ratios

In high alumina cement and copper-based tiles, the maximum density is 1.89 kg/m^3, which is comparatively higher than that of conventional tiles, as shown in Fig. 2. The density of the HAC is lower than that of the conventional and Al_2O_3, even though it increases the bulk density of the heat-resistant tiles.

Modulus of Rupture By measuring the fundamental parameters that influence a specimen's behavior under compressive loads, compression testing can be used to determine how a product responds when it is compressed by loading [18]. The modulus of the rupture test is calculated using a universal testing machine with the point loading condition shown in Fig. 3a, b. The tests are conducted with convention tiles and aluminum copper tile (ACT), high alumina copper tile (HCT), and high alumina cement tile (HT). The maximum wet transverse strength reaches 21.1 N/mm^2 in HCT samples on the 28th day and next 19.69 N/mm^2 observed in aluminum oxide tiles. The performance of the newly replaced hybrid tiles attains the best values compared with conventional tiles. The experimental results are plotted in Fig. 4. The materials in the interlocking mechanism of tiles are an essential reason to improve the strength. The chemical phases of the materials are using X-ray diffractive analysis of the composite materials used in heat-resistant tiles [21].

Water Absorption The samples were weighed after they had dried completely (dry mass) according to the ISO 10545 (Part 1) process, and then they were submerged in boiling water for two hours. The ceramic pieces are then left submerged in water for 4 h (water immersion time) to cool naturally after the heating device has been turned off. Following this step, a damp cloth is used to eliminate any remaining moisture from the sample surfaces, and their mass is then measured once more (wet mass) [19]. The absorption rate of the tile varies by 2–6% from the conventional tiles. The absorption of the different samples is indicated in Fig. 5. The bonding nature of the material composition in the transition process of tiles reduces the water absorption rate in tiles. Compared with the conventional tiles, the Al_2O_3 and copper components have pores that affect the water absorption in the hardened stages. High alumina

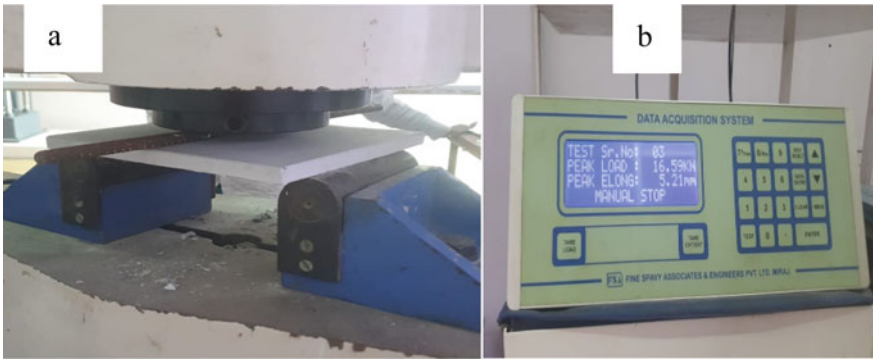

Fig. 3 Shows the experimental test procedure of tiles during modulus of rupture **a** Apply breaking load, **b** Digital display of load

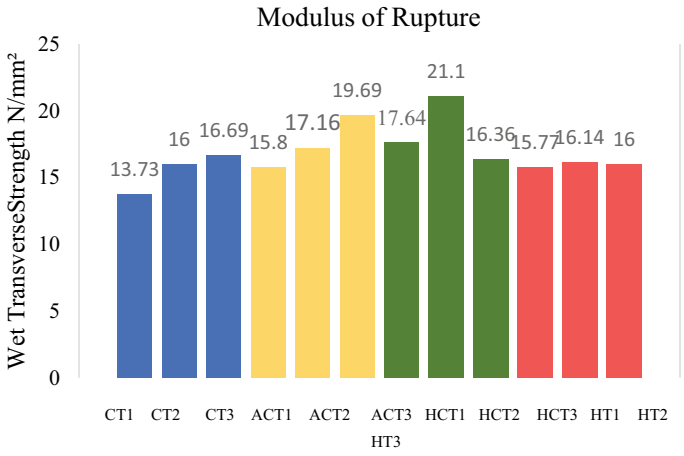

Fig. 4 Shows the test results of modulus of rupture

cement reaches the best performance, but internal pores cause slight increases in the absorption rate.

6.2 XRD Analysis

The findings of comparing the XRD patterns on the four chosen HCT, ACT, HT, and CT tiles at both the edges and core of each tile revealed only minor variations in the formed phases for the edges and cores [20]. The XRD patterns for the tested specimens' edge and center are depicted in Fig. 6a–d, respectively. This shows that the temperature throughout the kiln was consistent during the firing treatment stage. In

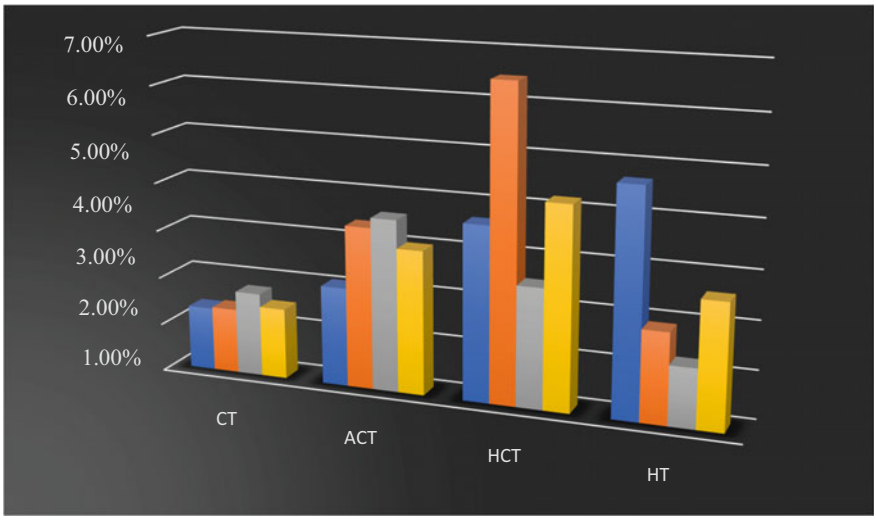

Fig. 5 Shows the water absorption rate of the tiles

this study, XRD analyses showed that the main phases in the glassy phase of the four tile types were quartz (SiO_2), mullite ($3Al_2O_32SiO_2$), and albite ($NaAlSi_3O_8$). The internal phases show the purity of the substances in the tile stages. The materials have low thermal conductivity and low carbon emissions compared with the conventional manufacturing process. Copper is highly heat resistant in nature, and it is also an antibacterial component that improves tiles in thermal aspects.

6.3 Cost Analysis

With regard to the restrictions on cost optimization, the ideal ratio of Al_2O_3 and copper in ceramic tiles to achieve the lowest cost was 40% Al_2O_3 and 40% HAC of trash ceramic tiles. The best among the top four tiles that are estimated and shown in Fig. 7 was determined to be this combination, which resulted in an INR price of 45–60rs. When comparing the experimental results, the same combination was seen to achieve the lowest cost with economic and ecological benefits.

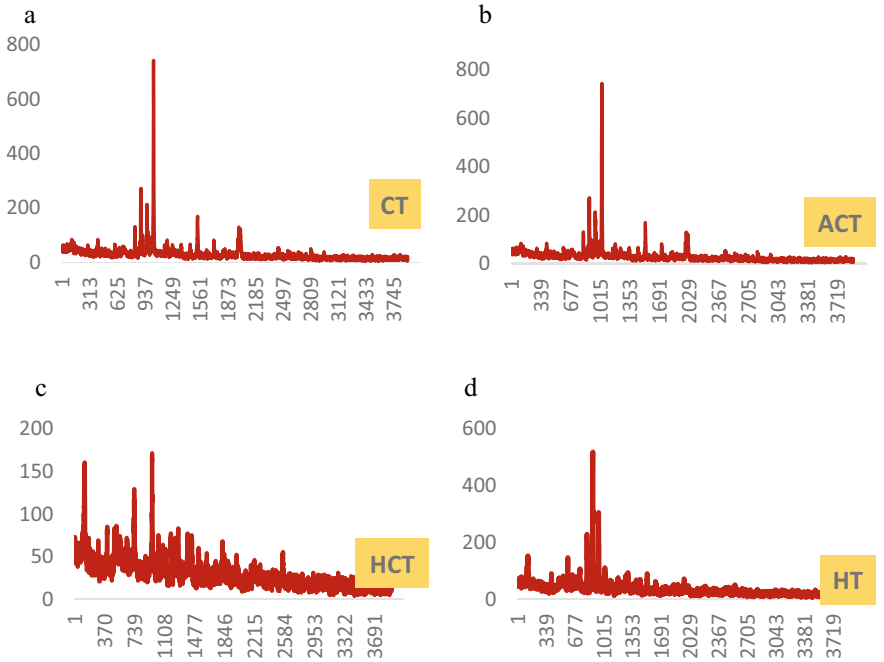

Fig. 6 XRD results **a** XRD range of conventional, **b** XRD range of Al_2O_3, **c** XRD range of HAC and copper tile, **d** XRD range of HAC and cement tile

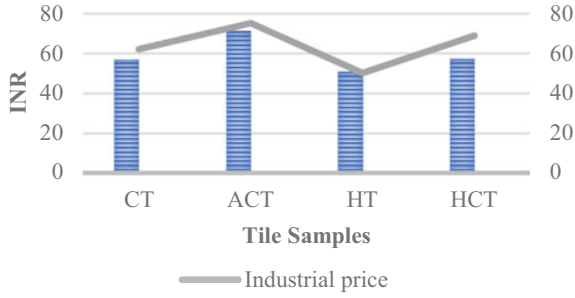

Fig. 7 Different tile sample cost variation statistical analysis

7 Conclusion

In this article, the findings of a study on the potential reuse of Al_2O_3, high alumina cement, and copper as replacement components in the production of ceramic tiles are discussed.

1. To evaluate the quality of the experimental analysis, physical–mechanical tests were conducted on all four combination tiles, and a comparison with products that have been on the market for a long time was made.

2. The obtained results were extremely encouraging, spurring further study for the study to be expanded with low emission that has comparable textural and compositional characteristics.
3. The tiles are economically suitable for all clients with perfect satisfaction of the product.

References

1. El Nouhy HA (2013) Assessment of some locally produced Egyptian ceramic wall tiles. HBRC J 9(3):201–209. https://doi.org/10.1016/j.hbrcj.2013.08.001
2. Yibing T (2020) Technical analysis of water absorption rate of ceramic tiles. E3S Web Conf 185:1–3. https://doi.org/10.1051/e3sconf/202018504039
3. Anderson CE, Morris BL (1992) The ballistic performance of confined Al_2O_3 ceramic tiles. Int J Impact Eng 12(2):167–187. https://doi.org/10.1016/0734-743X(92)90395-A
4. Alim MA, Tao Z, Abden MJ, Rahman A, Samali B (2020) Improving performance of solar roof tiles by incorporating phase change material. Sol Energ 207:1308–1320. https://doi.org/10.1016/j.solener.2020.07.053
5. Erol M, Küçükbayrak S, Ersoy-Meriçboyu A (2008) Comparison of the properties of glass, glass-ceramic and ceramic materials produced from coal fly ash. J Hazard Mater 153(1–2):418–425. https://doi.org/10.1016/j.jhazmat.2007.08.071
6. Ji R, Zhang Z, Yan C, Zhu M, Li Z (2016) Preparation of novel ceramic tiles with high Al_2O_3 content derived from coal fly ash. Constr Build Mater 114:888–895. https://doi.org/10.1016/j.conbuildmat.2016.04.014
7. Niranjan T, Jose Ravindraraj B (2018) Experimental research of heat resistant weathering tiles. Int J Civ Eng Technol 9(4):1600–1605
8. Amin SK, Abdel Hamid EM, El-Sherbiny SA, Sibak HA, Abadir MF (2018) The use of sewage sludge in the production of ceramic floor tiles. HBRC J 14(3):309–315. https://doi.org/10.1016/j.hbrcj.2017.02.002
9. Inberg A, Ashkenazi D, Feldman Y, Dvir O, Cvikel D (2020) A tale of two tiles: characterization of floor tiles from the nineteenth-century Akko tower Shipwreck (Israel). Coatings 10(11):1–23. https://doi.org/10.3390/coatings10111091
10. Belfiore CM, Amato C, Pezzino A, Viccaro M (2020) An end of waste alternative for volcanic ash: a resource in the manufacture of ceramic tiles. Constr Build Mater 263:120118. https://doi.org/10.1016/j.conbuildmat.2020.120118
11. Cokca E, Yilmaz Z (2004) Use of rubber and bentonite added fly ash as a liner material. Waste Manag 24(2):153–164. https://doi.org/10.1016/j.wasman.2003.10.004
12. Ozturk ZB, Gultekin EE (2015) Preparation of ceramic wall tiling derived from blast furnace slag. Ceram Int 41(9):12020–12026. https://doi.org/10.1016/j.ceramint.2015.06.014
13. Olgun A, Erdogan Y, Ayhan Y, Zeybek B (2005) Development of ceramic tiles from coal fly ash and tincal ore waste. Ceram Int 31(1):153–158. https://doi.org/10.1016/j.ceramint.2004.04.007
14. Hamid NB et al (2021) A review: potential of waste materials in tiles production. Multidiscip Appl Res Innov 2(1):91–102. [Online]. Available: https://doi.org/10.30880/mari.2021.02.01.008
15. Ozturk ZB, Yildiz B (2016) Effect of alumina characteristics and concentration on thermal behavior, phase evolution, and aesthetic properties of tile glaze coatings. Glas Phys Chem 42(3):257–262. https://doi.org/10.1134/S1087659616030196
16. Patel P, Gupta P, Sujata KM, Garg Solanki R (2023) Structural and optical properties of copper selenide nanolayered tiles. Mater Proc. https://doi.org/10.1016/j.matpr.2022.12.220

17. B. of Indian Standards (2006) IS 13630-1 to 15 (2006): Ceramic tiles—methods of test, sampling and basis for acceptance
18. Dondi M (2007) Mechanical and tribological properties of ceramic tiles: a reappraisal, November 2007
19. Vieira AW et al (2017) Comparison of methods for determining the water absorption of glazed porcelain stoneware ceramic tiles. Mater Res 20(Table 1):644–650. https://doi.org/10.1590/1980-5373-mr-2017-0089
20. Science M (1975) The conversion of high alumina cement/concrete the conversion reaction in high alumina cement/concrete samples is examined by scanning electron microscopy and differential thermal analysis. The transformation, which involves the dissolution of pla, vol 23, pp 43–53
21. Prashanth R, Selvan SS (2019) Experimental investigation on durability. RJC 12(2):685–690
22. Guru Kumar MS, Balasubramanian M (2020) Application of FGC blocks for sustainable. Mater Sci Eng 912:062057, 1–8

A Review on Banana Fiber Reinforced Concrete

K. Pushpa, S. Jayakumar, and N. Pannirselvam

Abstract Sustainability and usage of Eco-friendly material in the field of construction is the need of the hour. Concrete, the most widely used material is poor in ductility and is prone to crack formation due to tensile stress and shrinkage. Fiber Reinforced Concrete (FRC), can reduce this disadvantage of concrete. Both natural and synthetic fibers are used in FRC. Banana fiber (BF), when added in small quantities is found to decrease the crack spalling, improve impact resistance, toughness of hardened concrete, and decrease permeability, and bleeding in concrete. High water absorption and less workability are the disadvantages of BF. In this paper, an effort is made to review the investigations done so far on BF to study the physical, chemical, durability properties and treatments of BF so as to be used as reinforcement in concrete.

Keywords Banana fiber · Chemical treatment · Compressive strength · Fiber reinforced concrete · Microstructure · Natural fiber

1 Introduction

Banana Fiber Reinforced Concrete is a type of concrete that incorporates banana fibers as a reinforcement material. The fibers are extracted from the stem of the banana plant and then processed for use in concrete production. BFRC offers several advantages over traditional concrete, such as improved tensile strength, ductility, and crack resistance.

K. Pushpa
Civil Engineering, Women's Polytechnic College, Puducherry, India

S. Jayakumar
Civil Engineering, SMVEC, Puducherry, India

N. Pannirselvam (✉)
Department of Civil Engineering, Faculty of Engineering and Technology, SRM Institute of Science and Technology, Kattankulathur, Tamil Nadu 603203, India
e-mail: pannirsn@srmist.edu.in

K. R. Reddy et al. (eds.), *Recent Advances in Civil Engineering*, Lecture Notes in Civil Engineering 398, https://doi.org/10.1007/978-981-99-6229-7_32

1.1 Advantage of Banana Fiber

Low density, adequate stiffness, mechanical qualities, high disposability, and renewability are only a few of the significant benefits of natural fibers. Additionally, they are biodegradable and recyclable [5]. Banana fiber is a natural fiber that can be found in the pseudo stem of the Musaceae family's banana plant. Stems of banana plant are agro waste, those are cut and thrown after harvest of fruit in landfills or burnt, both causing environmental issues. The natural additive banana fibers (BFs) add additional qualities to regular cement concrete [2]. BF provides resilience to abruptly applied stresses, restricts shrinkage cracking, reduces permeability, and eventually lessens water bleeding [1]. BF enhances the flexibility to resist cracking and spalling of concrete [1, 2, 21]. Mechanical and ecological properties are good in banana fiber. It is also easily available and eco-friendly. Adding banana fiber to concrete will increase the strength and workability of concrete and also reduces the cracks into the structures. It gives environmentally friendly solution to support sustainable construction [10]. BF decreases the workability of concrete mix, due to high water absorption property of untreated BF. Leading to tangling or balling of fibers, this can be overcome by using super plasticizers [2].

1.2 Banana Fiber Extraction

The pseudo stems of the banana plant are used to harvest banana fiber. The mechanical decorticator, also known as a fiber extracting machine, receives longitudinal slices cut from stems. It is made up of a beater and two feed rollers. Between the squeezing roller and the scrapper roller, the slices are supplied to the beater. Fibers are removed from the pulp and then air dried in the shade [3, 5]. In water retting technique of fiber extraction, freshly cut banana stems are submerged in water for six weeks. They are then taken out of the water, slackened, cleaned, dried in the sun, and combed. Cutting devices are used to separate the fibers [9].

1.3 Characteristics of BF

Mouli et al. [1], Attia et al. [3], Pannirselvam et al. [4], Mugume [6], Jagadeesh et al. [9], Kumar et al. [11] have given the physical, chemical, and mechanical characteristics of BF (Table 1).

Table 1 Mechanical, physical, and chemical composition of BFs [1, 3]

Properties	Values for BFs	References
Mechanical properties		
Tensile strength (MPa)	56	[1, 4, 11, 20]
Young's modulus (MPa)	3.5	[1, 4, 11, 20]
Elongation at break (%)	2.60	[1, 4, 11, 20]
L/D ratio	150	[3]
Physical properties		
Density (Kg/m^3)	1350	[1, 3, 4, 11, 20]
Moisture content (%)	10	[3]
Width or diameter (μm)	80–250	[3]
Chemical composition (%)		
Cellulose	63.2	[3]
Hemicellulose	18.6	[3]
Lignin	5.10	[3]

1.4 Chemical Treatment for BF

Natural fibers have tendency to absorb more water when added in concrete mix, thereby reducing both the workability of fresh mix and the strength of hardened concrete. Alkali treatment of BF using sodium hydroxide solution (NAOH) is considered to be a more effective chemical treatment method. Alkali treatment increases the roughness of fiber surface thereby making it more reactive and binding [2, 3, 11]. In alkali treatment, BFs are cleaned well and soaked in NaOH solution for two hours at room temperature. They are washed again in clean water tank till un-reacted alkalis are removed. BFs are then filtered, rinsed in running water, and dried for 24 h at 80 °C in an oven [2, 11].

Kumar et al. [11] studied the effects of chemically treated BF in concrete. BFs were treated with 1, 2, 3, and 6% weight/volume concentrations of NaOH. The sample to alkali ratio for treatment was 1:30. Results revealed that treating banana fiber by 3% improved compressive strength by 10–15% and reduced the moisture content of banana fiber.

1.5 Treatment with Sodium Silicate

Sodium silicate is found as a crystalline solid or white powder. It accelerates setting process of concrete, improves water proofing and durability of concrete. But adding sodium silicate in concrete leads to a reduction in its compressive strength. This disadvantage can be overcome by addition of silica fume [10].

Table 2 Effect of addition of sodium silicate in concrete strength [10]

S. No	% of banana fiber	% of sodium silicate	Slump (mm)	Compressive strength (N/mm^2)	Flexural strength (N/mm^2)	Split tensile strength (N/mm^2)
1	0	0	25	30.22	4.80	3.96
2	3	3	30	20.44	4.40	4.42
3	3	4	34	27.56	5.20	4.52
4	3	5	41	35.11	6.00	5.09

John et al. [10] investigated the effect of sodium silicate treatment on BF. BF of 40 mm length with a constant proportion of 3% volume fraction was treated with 3, 4, and 5% sodium silicate. Concrete of the M25 grade and regular Portland cement of grade 53 were used. Their research findings are listed in Table 2. Results show that adding sodium silicate and banana fiber has increased the mechanical properties of concrete compared to normal concrete.

2 Mixing Procedure

Concrete was mixed according to ACI guidelines (ACI211.1-91 2002, ACI 544.1R-96 2002) which included introducing aggregates, sand and cement into the mixer and then dry mixing for 1.5 min. The mixing water, which contained a super plasticizer admixture, was added to the ingredients, and blended for another 2 min. Finally, the BFs were manually dispersed throughout the mixture and mixing was continued to ensure total homogeneity [3, 6, 8].

3 Water Absorption

Untreated BF absorb more water, reducing workability of concrete [2, 3, 17]. BFs length and volume fractions (VFs) and their effects on the mechanical, physical properties of concrete were studied by Attia et al. [3]. The authors carried out test using BF samples with fiber lengths of 12, 25 and 35 mm and VF of 0, 0.5, 1.0, and 1.5% in concrete mixes. They observed that water absorption increased gradually up to 44.8%, 39.42%, and 32.05%, respectively, compared to the reference concrete. The fiber length has an influence on absorption, which decreases as the length of the fiber increases.

3.1 Workability

Workability decreases with increase in BF ratio [3, 6, 16, 17]. Abrar [17] evaluated the workability property of Plain Concrete (PC) with Banana Fiber Reinforced Concrete (BFRC) using 50 mm long BF of 2.5% VF and observed that addition of BF reduced the workability of BFRC by 75% as compared to PC. Attia et al. [3] in his experimental studies observed that when fibers were added, the slump value decreased and when long fibers were used compared to short ones with the same amount of fiber, the slump value increased. The results exhibited a significant influence of fiber length on workability, which improved as fiber length increased. At 0.5% BFs, increasing the fiber length from 12 to 35 mm increased the slump value by up to 14.65%. The slump values for fiber with lengths of 12 mm, 25 mm, and 35 mm, was 11.76 mm, 12.03 mm, and 13.37 mm, respectively, when using BFs by 1.5%. Workability can be enhanced by prewetting the BF in water, including additional water during mixing or by using water reducing super plasticizers [2, 3].

3.2 Unit Weight Properties

Attia et al. [3] observed that increasing BFs reduces the unit weight of concrete in general regardless of fiber length. The reason for this is that BFs have a lower specific gravity than other concrete constituents. In comparison to samples with 12, 25, and 35 mm fibers, those with 35 mm fibers length and volume fraction of 1.5% had the minimum density with 2415 kg/m^3.

3.3 Bond Stress

Depending on the length and VFs of fibers, Attia et al. [3] observed the increase in bond stress to be between 4.9 and 11.2% with different length from 12 to 35 mm. The BFs sample with 35 mm length and 1.5% VFs showed the highest value by 6.75 MPa. Bond stress can be seen to improve by increasing the fiber length.

4 Microstructure Analysis/SEM Analysis

Scanning Electron Microscope (SEM) analysis of concrete with BF helps to increase our understanding about Interfacial Transition Zones (ITZs), the morphology of concrete. Attia et al. [3] employed specimens with a diameter of 5–10 mm that were removed from cubes. By increasing cohesiveness between the BFs and the matrix and minimizing the size of ITZ, the addition of fiber helped to build the

microstructure of concrete. As a result, the matrix's porosity was also decreased by filling its pores, which led to the development of the composite's mechanical properties [3, 6]. Rodgers B. Mugume investigated that adding 1% of banana fibers to BFRC improved its microstructure. He recommends using short fibers compared to long fibers.

5 Strength Properties

5.1 Compressive Strength

Mouli et al. [1] investigated on compressive strength of BF concrete. The authors varied the combinations of Metakaolin from 0 to 30% by weight of cement and BF of Volume Fraction (VF) from 0 to 6% for a M30 grade concrete with 40 mm long BF. He has reported that 15 + 3% combination of Metakaolin and BF showed the maximum increment of compressive strength 44.92 and 41.54% for 7 days and 28 days.

The strength of BF of length 50 mm and VF 0, 0.5, 1, and 1.5% were examined by Mir Firasath Ali et al. Concrete reinforced with banana fibers has the highest compressive strength at 0.5% fiber content for a 50 mm long fiber. The concrete's compressive strength at 0.5% fiber content is 58.5 N/mm^2, which is 18.18% more compared to the concrete's strength at 0% fiber content used as a reference.

Pannirselvam et al. studied the effect on mechanical properties by using the combination of nano silica (NS) and banana fibers (BF) using 40 mm BF. BF replacement from 1 to 5% by volume and NS replacing cement by 0, 2, 2.5, 3, 3.5, 4, and 4.5% by weight. Beyond 3% of NS+BF, there has been a gradual decline in the compressive strength of concrete. For 3 + 3%, 7 and 28 days strength increased by 35.2 and 41.25%.

According to Mugume et al. [6], at lower fiber levels up to 0.25%, fiber length had no markable effect on compressive strength, but at larger dosages above 0.25%, shorter fibers were more effective.

The characteristics of 40 mm long BF with VFs of 1, 2, 3, 4, 5, and 6% were examined by Chandramouli et al. In comparison to reference concrete at 28 and 90 days, he claimed that adding 3% banana fiber improved its strength by up to 35.04% and 40.83%, respectively. For a 56-day curing period, the Banana Fiber Reinforced Concrete's compressive strength increased by 34.62% in comparison to unreinforced concrete.

Tirkey et al. [13] used ratio of BF 0, 0.5, 1%, and found the compressive strength with fiber content 0.5% is higher than that of 1%.

With fiber lengths of 20 mm and usual curing times of 7 and 28, Kesavraman [16] tested with BF of VF at 0, 0.5, 1.5, and 2%. Results show an increase in strength upto 0.5% and decline beyond it.

5.2 Split Tensile Strength

For the 15 + 3% combination of Metakaolin and BF, Mouli et al. [1] showed maximal increases in split tensile strength of 50.16% and 43.39% for 7 days and 28 days, respectively.

The strength of BF of length 50 mm and VF 0, 0.5, 1, and 1.5% were examined by Mir Firasath Ali et al. split tensile strength at 0.5% fiber content was found to be 4.65 N/mm^2, which is 9.1% greater to control concrete.

According to Pannirselvam et al. [4], the split tensile strength of concrete significantly increased up to a 3 + 3% combination of nano silica and BF and gradually reduced after that point. The maximum split tensile strength increase, at 3 + 3%, is 26.9% for 7 days and 43.03% for 28 days. For a low fiber dosages of up to 1%, Mugume et al. [6] found that an increase in fiber content had a favorable impact on the tensile strength of concrete. Similarly longer fibers were found to be more effective than shorter ones at lower fiber levels of up to 1%.

Khaskheli et al. [7], used banana fiber with an aspect ratio (AR) of 150 and 200 to concrete at 0.5, 1, and 1.5% and reported that 1.5% banana fiber and AR-150 is more effective.

According to Chandramouli et al. [12], the addition of banana fiber to concrete resulted in a gradual rise in tensile strength up to 4% and a gradual decrease in tensile strength after that point. With the addition of 4% banana fiber, there was an increase of 47.39, 46.91, and 46.14% at 28, 56, and 90 days of curing.

Kesavraman [16] observed that split tensile strength was highest at 0.5% VF of BF for 20 mm long fiber.

5.3 Flexural Strength

Mir Firasath Ali et al. studied the strength of BF of length 50 mm and VF 0, 0.5, 1, and 1.5% and found that 0.5% VF gave maximum flexural strength of 6.3 N/mm^2, which is 16.64% greater than the control concrete.

According to Mugume et al. [6], effect of short fiber at lower fiber dose had a minimal effect on the flexural strength of concrete.

According to Kesavraman [16], fiber content of 0.5% gave maximum flexure strength 17.64% higher than control concrete.

5.4 Crack Resistance

The addition of BFs increased the concrete specimens' crack resistance to a higher extent, and the specimens remained attached to one another even after failing under pressure, making it a non-brittle failure [1–3, 8, 21].

5.5 Pulse Velocity Test

As per IS 516 (Part 5-sect1) Ultra-Sonic Pulse Velocity test is one of the non-destructive testing methods of concrete. It is used to assess the quality and integrity of a concrete by measuring the speed of an ultra-sonic wave passing through the specimen. Higher value of pulse velocity indicates that the elastic modulus, density and integrity of the concrete are high. Pannirselvam et al. [4] have studied the combined effect of adding nano silica and BF on the properties of hardened concrete. Nano silica is used as partial replacement of cement by 0, 2, 2.5, 3, 3.5, 4, and 4.5% by weight and BF by volume substitution from 1 to 6%. Author has demonstrated that the value of pulse velocity test showed the maximum increment of 4587 m/s at 3 + 3% addition of nano silica and banana fibers. The authors used banana fibers having 40 mm length.

5.6 Toughness Index

According to Afraz et al. [8], the maximum load value and rupture modulus of BFRC are 39% lower than those of PC. However, BFRC out performs PC in terms of overall energy absorption and hardness index by 404% and 580%, respectively. BF fibers have good bridging properties and binding with concrete matrix. BFRC can withstand high impact loads due to its toughness index [8].

5.7 Impact Strength

Kesavraman [16] observed that impact strength of BF increases with increase in fiber length and fiber content. He studied on BF of length 20 mm and VF from 0 to 2%. The fiber addition results in cracks that are more closely spaced, and because the cracks' widths are smaller, more energy may be absorbed. At 2% fiber content, the energy required to form crack was 56.7 J/mm, which is 36.9% higher than control concrete. The overall length of the crack is also noted, along with the specimen's impact strength. It has been discovered that as the fiber content rises, so does the lateral length of the crack. This demonstrates how adding banana fibers to concrete prevents cracks formation.

6 Results and Discussion

From the investigations carried out on the physical properties of BF by various authors, it is observed that water absorption is more in untreated BF and it can be reduced by alkali treatment using NaOH and sodium silicate treatment [2, 3, 10, 11, 17]. Absorption decreased with increase in fiber length and bond strength gets enhanced with increase in fiber length [3]. Workability and unit weight of concrete reduced with increase in BF ratio [3, 6, 16, 17]. Workability can be improved by prewetting of BF in water, including additional water during mixing or by using water reducing super plasticizers [2, 3]. SEM analysis of Banana Fiber Reinforced Concrete BFRC, shows improvement in microstructure and reduction in porosity on addition of BF in concrete [3, 6].

As far as mechanical properties of BF are considered, experimental works done on BFRC proves that addition of BF to concrete has increased the compressive strength, split tensile strength and flexural strength of concrete [1–3, 6, 16]. Investigation on the combined effect of adding nano silica (NS) and BF reported increase in mechanical properties of hardened concrete [4]. Shorter fibers were observed to perform better than longer ones at higher dosages more than 0.25% [3]. Addition of metakaolin, fly ash, silica fumes with BF has improved the strength of BFRC [1, 4]. Maximum load value and modulus of rupture of BFRC were lower but total energy absorption and toughness index of BFRC is higher than that of plain concrete [6, 8]. Impact strength of BFRC increased with increase in fiber length and fiber content [16]. Cracking resistance of concrete improved to a greater extent with addition of BFs. Specimens were intact with each other even after the failure of specimen under loading thus making it a non-brittle failure [1, 3, 8, 16, 21].

7 Conclusion

From the above investigations and results of experimental works carried on with Banana Fiber Reinforced Concrete, it can be reported that:

1. Banana fiber, an agro waste can be utilized as sustainable natural fiber in Fiber Reinforced Concrete.
2. BF has high water absorption properties, which can be reduced by prewetting of BF, Alkali treatment using NaOH, and treatment using sodium silicate.
3. Workability of concrete reduces with an increase in BF ratio. Workability can be improved by using water reducing super plasticizers.
4. Additions of metakaolin, silica gel, fly ash, nanofibers are found to enhance the properties of BFRC.
5. Compression, tension, and flexural property have increased by the addition of BF.
6. Higher values of impact resistance, crack resistance, toughness index, and energy absorption make BFRC more suitable for buildings prone to impact loads.

7. Though BF is easily available, economical and sustainable, strength gain due to BF in concrete is less when compared to synthetic fibers like steel fibers, polypropylene, and glass fibers.

References

1. Chandra Mouli K, Pannirselvam N, Vijaya Kumar D, Valeswara Rao S, Mouli KC, Anitha V, Rao SV (2019) Strength studies on banana fiber concrete with metakaolin. Int J Civil Eng Technol 10(2):684–689
2. Firasath Ali M, Haseeb Ali S, Tanveer Ahmed M, Khaja Patel S, Wahib Ali M (2020) Study on strength parameters of concrete by adding banana fibers. Int Res J Eng Technol
3. Attia MM, Al Sayed AAKA, Tayeh BA, Shawky SMM (2022) Banana agriculture waste as eco-friendly material in fiber-reinforced concrete: an experimental study. Adv Concr Constr 14(5):355–368. https://doi.org/10.12989/acc.2022.14.5.355
4. Narayanan P, Mouli CK, Kumar VD (2018) Pulse velocity test on banana fiber concrete with nano silica. Article Int J Civil Eng Technol 9(11):2853–2858
5. Mukhopadhyay S, Fangueiro R, Arpaç Y, Şenturk U Banana fibers-variability and fracture behaviour. http://www.jeffjournal.org
6. Mugume RB, Karubanga A, Kyakula M (2021) Impact of addition of banana fibers at varying fiber length and content on mechanical and microstructural properties of concrete. Adv Civil Eng 2021. https://doi.org/10.1155/2021/9422352
7. Ali Khaskheli A, Ahmed Memon F, Hussain Tunio A, Ali Abro N, Hussain Tunio M, Mehran C Effect of banana fibers as a reinforcement material on hardened properties of concrete. Int Res J Modernization Eng 787
8. Afraz A, Ali M (2021) Effect of banana fiber on flexural properties of fiber reinforced concrete for sustainable construction. Eng Proc 12(1). https://doi.org/10.3390/engproc2021012063
9. (2015) Characterisation of banana fiber—a review. J Environ Nanotechnol 4(2):23–26. https://doi.org/10.13074/jent.2015.06.152154
10. John A, Sunil A, Jose B, George J, Nija SM (2021) Effect of sodium silicate on properties of banana fiber reinforced concrete. Int Res J Eng Technol
11. Kumar SS, Akash BM, Kabilan M, Karna H, Navaneethan S (2019) An experimental study and behaviour of banana fiber in concrete. http://www.ijser.org
12. Narayanan P (2019) Experimental investigation on banana fiber reinforced concrete with conventional concrete Fiber Reinforced Polymer View project. Int J Rec Technol Eng (7). https://www.researchgate.net/publication/333134461
13. Tirkey N, Ramesh GB Experimental study on the banana fiber reinforced concrete. http://www.acadpubl.eu/hub/
14. Subagyo A, Chafidz A (n.d.) Banana pseudo-stem fiber: preparation, characteristics, and applications. www.intechopen.com
15. Abrar M, Ali M (2021) Bleeding in banana, rice-husk and yarn fiber reinforced concrete and its effect on compressive strength of FRCs. https://www.researchgate.net/publication/362305944
16. Kesavraman S (2017) Studies on metakaolin based banana fiber reinforced concrete. Int J Civil Eng Technol 8(1)
17. Abrar M (n.d.) Workability of banana fibers reinforced concrete for easy pouring. https://www.researchgate.net/publication/354858425
18. Awwad E, Mabsout M, Hamad B, Khatib H (2011) Preliminary studies on the use of natural fibers in sustainable concrete. Leban Sci J 12(1). http://proquest.umi.com
19. Jordan W, Chester P (2017) Improving the properties of banana fiber reinforced polymeric composites by treating the fibers. Procedia Eng 200:283–289. https://doi.org/10.1016/j.proeng.2017.07.040

20. Mouli KC, Anitha V, Sree J, Chaitanya N (2018) Comparative study of banana fiber reinforced concrete with normal concrete. http://www.internationaljouralssrg.org
21. Elbehiry A, Elnawawy O, Kassem M, Zaher A, Mostafa M (2021) FEM evaluation of reinforced concrete beams by hybrid and banana fiber bars (BFB). Case Stud Constr Mater 14. https://doi.org/10.1016/j.cscm.2020.e00479
22. Khalifa M, Chappar SS (2014) Experimental investigation of tensile properties of banana reinforced epoxy composites. Int J Sci Res. www.ijsr.net
23. Ikechukwu Anowai S, Fredrick Job O (2017) Durability properties of banana fiber reinforced fly ash concrete. Int Res J Eng Technol
24. Shyamala G, Rajesh Kumar K, Olalusi OB (2020) Impacts of nonconventional construction materials on concrete strength development: case studies. SN Appl Sci 2(11). Springer Nature. https://doi.org/10.1007/s42452-020-03687-x
25. Abrar M, Karachi P, Ali M (n.d.) Damping of hybrid natural fiber reinforced concrete. https://www.researchgate.net/publication/361264772

Assessment of Volatile Organic Compound Emission from Municipal Solid Waste Disposal Sites (A Case Study of Perungudi, Chennai, Tamil Nadu, India)

Durgadevagi Shanmugavel

Abstract Air pollution is one of the major environmental concerns in India due open disposal and burning of municipal solid waste (MSW). Improper solid waste management is the major threat to ecological integrity and human well-being. Air pollution was assessed on the basis of determination of volatile organic compound (VOCs) concentrations, which were emitted from interior materials. In the present study area Perungudi, dumping of MSW has been continuing for decades. The qualitative and quantitative analysis of VOCs emitting from the MSW disposal site is presented in this paper. The samples were collected from three locations based on three different categories such as fresh waste, 80–100 days waste, and above 120 days waste. The VOCs sample was analysed using the gas chromatography–mass spectrometry (GC–MS). GC–MS analysis result shows that the fresh waste consists of trichloroethylene, chloro benzene, N-butyl benzene Tricholorofluoro methane, and benzene, whereas the aged waste consists of sec butyl benzene, o-xylenes, ethyl benzene, toluene M&P-xylenes, and T-butyl benzene in higher rate; this leads to serious health issues for the people living in the area and hence it should be given importance. The dispersion pattern of VOCs is also identified and the map showing the dispersion is presented.

Keywords VOCs · Odour measurements · MSW · GC–MS

1 Introduction

Scientifically speaking, odour is "a sensation resulting from the reception of stimulus by the olfactory sensory system," which translates to "the perception of smell." Odour is caused by inhaling volatile organic or inorganic compounds found in the

D. Shanmugavel (✉)
Department of Civil Engineering, SRM Institute of Science and Technology, Kattankulathur, Tamil Nadu, India
e-mail: durgades@srmist.edu.in

K. R. Reddy et al. (eds.), *Recent Advances in Civil Engineering*, Lecture Notes in Civil Engineering 398, https://doi.org/10.1007/978-981-99-6229-7_33

air. Population growth, industry, and urbanisation have all contributed to the problem of unpleasant odours. Offensive odours are often the result of urbanisation without adequate sanitary infrastructure. Industrial processes that produce unpleasant odours have increased as industrialisation has spread. The most difficult aspect of dealing with air pollution is odour. Odour pollution is unique from typical air pollutants but shares some properties with noise pollution. Offending odours have the same disruptive effect on humans as loud noises. Scent has a few distinct features, one of which is that it is more likely to elicit a complaint if it is unfamiliar rather than a recognised scent. When an odour is consistently strong, people get numb to it; it is only when the strength shifts that they take note. The perception of a distinct fragrance may not be affected by olfactory fatigue, but the perception of a comparable odour will be hindered. One's opinion on a smell might swing dramatically depending on whether or not they have positive or negative memories connected to it. Animals generally have a better sense of smell than humans do. When two smells of the same intensity, they can blend into one another and become unrecognisable. Scents drift in the wind. A long-distance nose is a real talent. Substances with the same or different chemical composition may have the same or similar smell. A mixture of two or more odoriferous compounds may neutralise the odour of one another, or the odour of one substance may be masked by the odour of the other. The presence of a strong odour masks the odour of a weaker one.

1.1 Odour Classification

There are a variety of ways to categorise smells. But thus far, no one-of-a-kind or completely suitable plan has arisen. Seven major scents were identified in a study of 600 chemical substances; these included camphor, musk, flowery, peppermint, ether, pungent, and rotten. Later research revealed that this figure could shift depending on the assessor's familiarity with the scent, the nature of the product or service being evaluated, and other factors. While the American Society for Testing and Materials (ASTM) contains a thorough list of 830 smell descriptors, the atlas of smell character profiles only includes 146 CPCB [6].

1.2 Effects of Odour

Odours are significant even at low doses because of the stress they cause psychologically rather than physically. Bad smells can make you feel sick to your stomach, which can lead to dehydration, difficulty in breathing, nausea, vomiting, and mental disruption. Detrimental effects on personal and communal pride, interpersonal interactions, the willingness to commit capital, social standing, and economic growth might result from persistent exposure to disagreeable scents. It's important to note that high concentrations of some noxious odorants (like H_2S) might be harmful. As

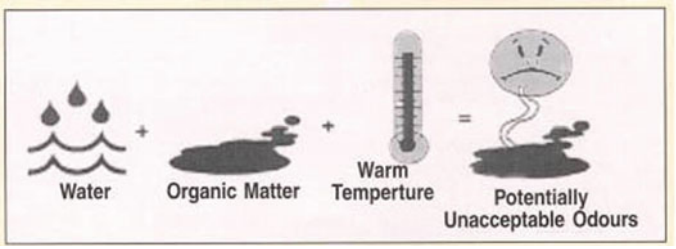

Fig. 1 Conditions for potential foul odour. *Source* CPCB

a result of these issues, market and rental property prices, tax revenues, wages, and sales could all drop.

1.3 Sources of Odour

Hydrogen sulphide (which has a rotten egg aroma) and ammonia (which has a strong, pungent odour) are two of the most often observed odour-causing chemicals. Aside from sulphur dioxide and mercaptans, other prevalent odorants include phenols, certain petroleum hydrocarbons, and the byproduct of the breakdown of proteins (particularly those of animal origin). The anaerobic breakdown of rotting meat, manure, feed, or sullage is the source of the most repulsive odours. For instance, there are more than 168 different odour-producing chemicals responsible for the smell of manure from animals. As seen in Fig. 1, anaerobic decomposition and the subsequent formation of bad odours are facilitated by elevated temperatures.

1.4 Study Area Description

Chennai is one of India's four major cities, having a population of over five million. The problem of solid waste management in Chennai has been growing at an alarming rate as a result of urbanisation, population growth, and shifts in lifestyle and consumption habits. The majority of Chennai's MSW is dumped in open pits at two large landfills: Perungudi in the south and Kodungaiyur in the north.

Urbanisation has caused significant shifts in the pattern of land use in the Chennai metropolitan area. Site coordinates (12°, 57 min, 22 s): 80°, 14 min, 21 s east. The landfill is low-lying and poorly drained, with large swaths of marshy terrain that remain permanently wet and are flooded yearly. Alluvial sediments of recent age were observed to have a total thickness of 6.0–7.5 m in the uppermost silty clays and sandy clays. It reaches from the northern Pallikaranai wetland to the southern Sholinganallur. It's an eastern coastline. From 3 to 12 m deep, the sand ranges from fine to medium grains. Section 2.1 (Fig. 3) displays a map of the research region.

Since 1987, the dump has been serving the community. There are currently around 3500 t/day of municipal solid waste produced in the city. The present daily trash disposal rate at the Perungudi site is at about 1750 tonnes. About 73 ha have been designated as disposal sites. At the landfill, the water table is roughly 2 m below the surface. Chennai's municipal solid waste (MSW) consists of primarily residential garbage (68%), followed by commercial waste (16%), institutional waste (14%), and then industrial waste (2%). The majority of the municipal solid waste (MSW) in Chennai is made up of organic materials (32.3%), while inert materials (34.7%), such as stones and glass make up the rest [8]. Food wastes account for 8% of the total garbage at the Perungudi dumpsite, while green waste makes up 32.20%, timber (wood) accounts for 6.99%, consumable plastic accounts for 5.86%, industrial plastic accounts for 1.80%, steel and material accounts for 0.13%, textiles and paper account for 3.14%, and inert materials account for 33.98% and 1.45%, respectively. The trash has a calorific value of 4565 kJ/kg and a moisture content of 27.60 [8]; its organic content is 46.06%; its carbon content is 21.53%; its nitrogen content is 0.73%; and its phosphorous content is 0.63%. Seven of the Corporation of Chennai's (COC) fifteen zones (divisions 9–15) send their municipal solid waste (MSW) to the Perungudi (PDG) landfill. Kodungaiyur (KDG) receives the municipal solid waste from the other five zones. Figure 2 displays the COC map with the various zones labelled.

2 Materials and Methods

Both instrumental approaches (using tools like a gas chromatograph to calculate the ppm concentration of odorous gases) and olfactory sensory methods (relying on people's innate abilities to detect odours) have been used in odour measurements conducted by Iwasaki [9].

The A.S.T.M. syringe method was frequently used to measure smell concentration in Japan until 1975, as described by Iwasaki [9]. Taking readings at the smelly origins was a breeze with a syringe.

The vapour phase control of odours can be managed in a number of ways, as reported by Riva's [2] research. Oxidation can occur chemically or thermally.

Di Francesco et al. [3] looked into the methods used to evaluate the population's exposure to odorous emissions, sometimes to confirm the veracity of people's complaints and other times, proactively, to prevent them. By using gas chromatography and mass spectrometry (GC/MS), researchers were able to determine which chemicals were present in the air and how much of each was there. This method is laborious and costly, and it yields limited insight into how people perceive the world. Only in cases where potentially harmful compounds are present will GC/MS be used. The perception threshold, the intensity of the scent sensation, and the hedonic tone can all be ascertained with the help of olfactometric methods, which are described in detail in a number of guidelines.

Measurements of CH_4, CO_2, and N_2O emissions were taken in December 2003 and September 2004 at the KDG and PGD landfills in Chennai, as reported by

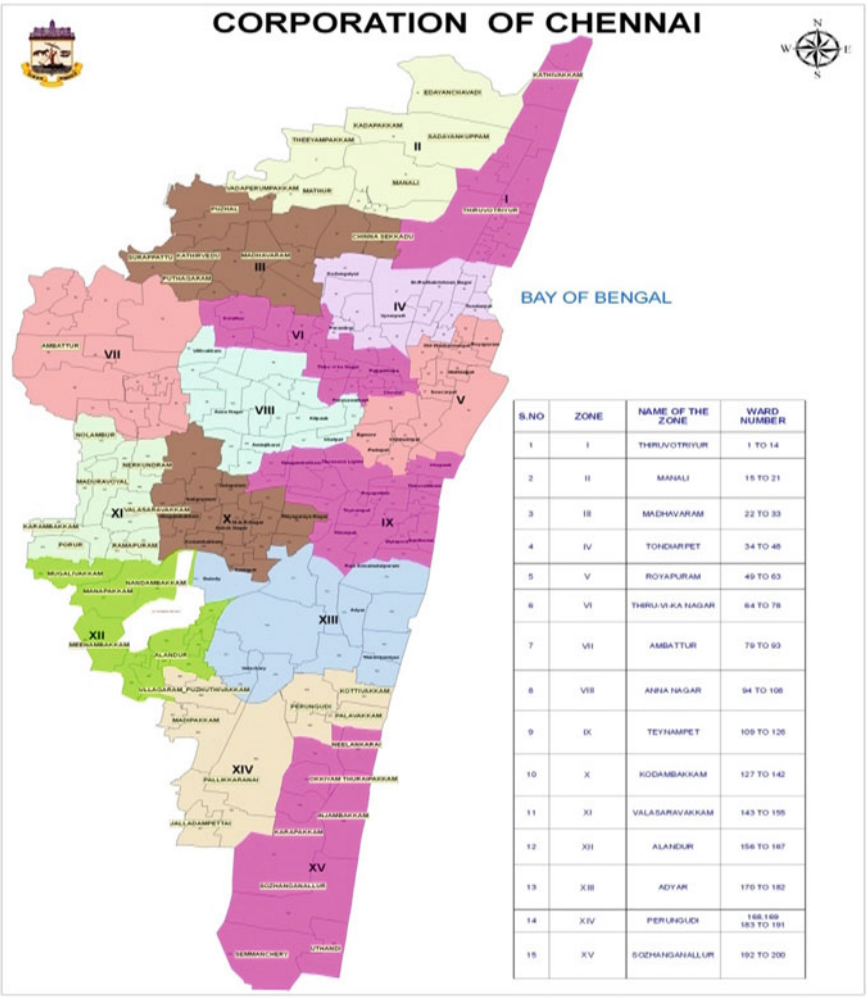

S.NO	ZONE	NAME OF THE ZONE	WARD NUMBER
1	I	THIRUVOTRIYUR	1 TO 14
2	II	MANALI	15 TO 21
3	III	MADHAVARAM	22 TO 33
4	IV	TONDIARPET	34 TO 48
5	V	ROYAPURAM	49 TO 63
6	VI	THIRU-VI-KA NAGAR	64 TO 78
7	VII	AMBATTUR	79 TO 93
8	VIII	ANNA NAGAR	94 TO 108
9	IX	TEYNAMPET	109 TO 126
10	X	KODAMBAKKAM	127 TO 142
11	XI	VALASARAVAKKAM	143 TO 155
12	XII	ALANDUR	156 TO 167
13	XIII	ADYAR	170 TO 182
14	XIV	PERUNGUDI	168,169 183 TO 191
15	XV	SOZHANGANALLUR	192 TO 200

Fig. 2 Zone map of Corporation of Chennai. *Source* Corporation of Chennai

Jha et al. [1]. The MSW surface layer age (2–4 years) and the MSW deposition height (5–15 feet) at the landfill's core and periphery informed the selection of sampling locations. Gases were sampled using a chamber method. Every 15 min for 45 min, 50 cc syringes were used to collect gas samples from each location. The researchers also took note of the ambient and MSW temperatures at each location. Dry weight percentages were calculated from MSW soil samples. Samples of gas were run through a gas chromatograph (SRI, USA, Model 8610 C) equipped with a flame ionisation detector and a methaniser to determine the concentrations of carbon monoxide and methane. The GC-electron capture detector was used to determine the levels of N_2O present. Calibration gas standards of CH_4 (5.63 ppmv), CO_2 (500

Fig. 3 Area map with sampling location

ppmv), and N_2O (0.31 ppmv) were employed in sample analysis. Annual emissions were determined by multiplying the emission fluxes of these gases by the landfill area.

The methane samples taken from three Delhi landfill sites in December 2008 and June 2009 were analysed by Rawat et al. [5]. The gas chromatography flame ionisation detector (FID) was used to evaluate these samples. Both the air temperature and the temperature of the landfill were tracked constantly. Porapak Q column of gas chromatograph (GC) FID was used to evaluate the gas samples. A thermometer that had previously been calibrated was used to take readings from the ground and the air.

2.1 Sampling Station

Taking into account the local weather, researchers collect air samples to analyse for the presence and concentration of volatile organic compounds (VOCs) throughout time and space. The samples were taken from three distinct locations throughout the disposal site. The samples were transported straight to the lab for further examination after collection (Fig. 3).

2.2 Sample Collection

Air samples will be taken near the solid waste dumping yard at varying distances to measure the concentration of odour-causing substances, as odours are always present in the surrounding air. The ADT Sampling Probe will be connected to a BDX II Abatement Air Sampler pump to draw in ambient air containing the odour-causing chemicals at a rate of 0.5–3.0 LPM. The BDX II Abatement Air Sampler is

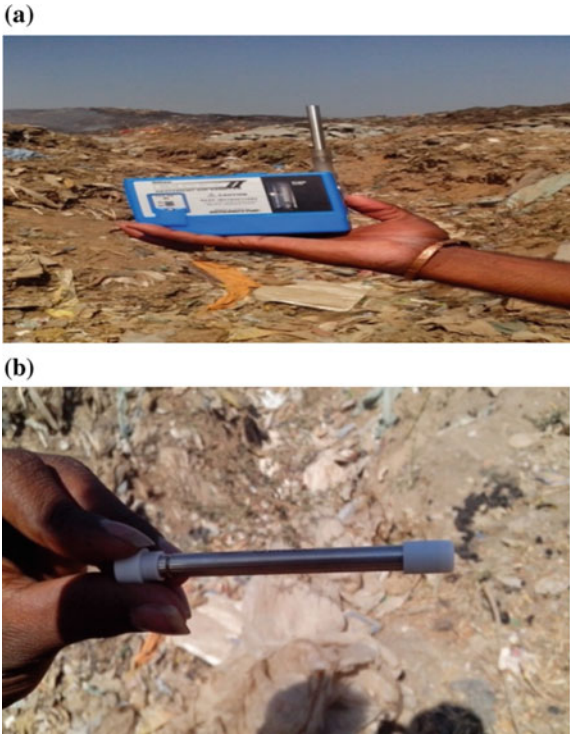

Fig. 4 **a** BDX II Abatement Air Sampler. **b** ADT Probe

a convenient tool that allows for on-the-go modification of the electronic flow rate. It runs on a battery that can be recharged. In order to gather samples of VOCs, an ADT Probe was used, which is compatible with either electronically marked or untagged tubes measuring 9.1 cm. After sampling, the tube's opening will be securely closed off and labelled with the location, date, and time of the collection. The concentration of the scent will be determined by sending this sampling tube to a lab (Fig. 4).

2.3 Instruments Used in Measuring VOCs Odour

A gas chromatograph (GC) is used to measure VOCs odour. Agilent 6890 N series GC (gas chromatograph system) with single flame ionisation detector (FID) column was used to find the VOCs concentrations. Single 100 psi EPC split-less injection ports are used for injecting the sample in the particular temperature. Auto sampler 6890 Control Electronics, 6890 Injector, Pentium Computer and 17 inch flat panel monitor are part of the GC.

3 Results and Discussion

Air samples are collected using ADT probes at the three sampling locations shown in Fig. 3. The samples collected are from three different locations in the solid waste dumping yard. The obtained ambient air from the dumping yard was analysed, for various VOCs compounds. Depending upon the solid waste and their duration of age, VOCs concentrations and compounds are shown in Figs. 5, 6, and 7.

The VOCs odour dispersion pattern is presented in Fig. 8. The dispersion contour refers to the concentration levels of VOCs.

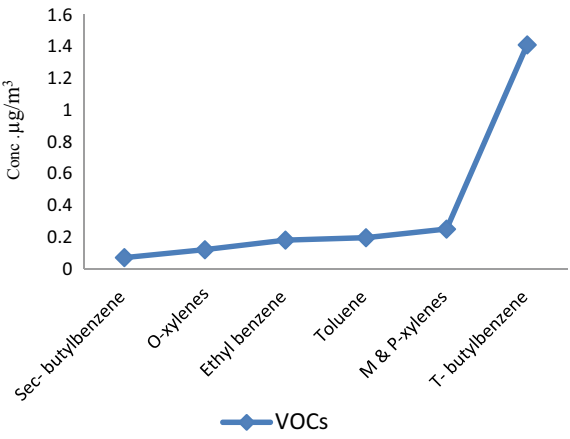

Fig. 5 Age of waste (120 days-above) at Station-1

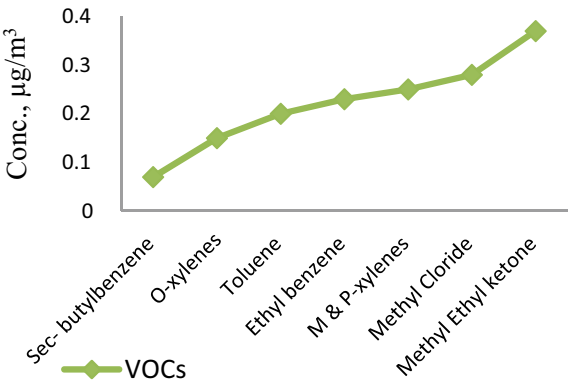

Fig. 6 Age of waste (80–100 days) at Station-2

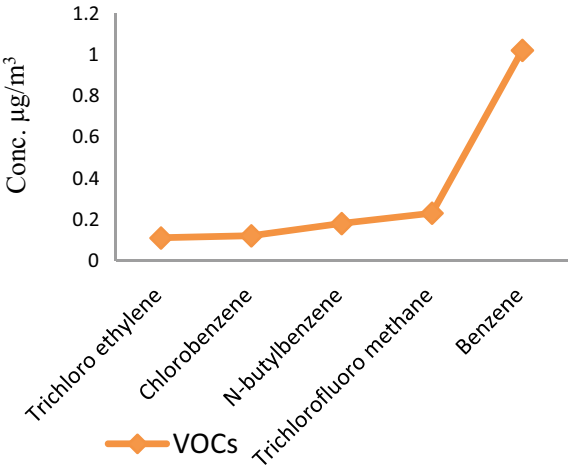

Fig. 7 Age of waste (fresh waste) Station-3

Fig. 8 Odour iso-concentration curves

4 Conclusion

VOCs odour concentration was measured by collecting samples at three different sampling locations selected at the Perungudi Municipal Solid Waste dumping yard. The following VOCs are to identify in the analysis carried out in GC–MS 6280N.

Three different dumps having different ages of the dump were selected for sampling. The sampling maximum VOCs concentration (T-butyl benzene) was recorded in the 120 days old dumping yard and value is 1.41 $\mu g/m^3$. The minimum VOCs concentration of 0.07 $\mu g/m^3$ was recorded in the sample collected at age 80–100 days dump (Sec-butyl benzene). The dispersion patterns of the VOCs odour concentration are also presented, it shows that the odour is carried towards to the downwind.

References

1. Jha AK, Sharma C (2007) Greenhouse gas emissions from MSW management in Indian mega-cities. Chemosphere
2. Riva G (1999) Sewage and wastewater odour control. Spartan Environmental Technologies
3. Di Francesco F, Lazzerini B (2000) An electronic nose for odour annoyance assessment. Atmos Environ, 24th July
4. Bortone I, Carrillo S et al (2012) Mitigation of the odorous impact of a waste landfill located in a highly urbanized area. Ital Assoc Chem Eng
5. Rawat M, Ramanathan AL (2011) Assessment of methane flux from MSW landfill areas of Delhi, India. J Environ Prot 399–407
6. Mauskar JM (2008) Guidelines on odour pollution and its control. Central Pollution Control Board (CPCB), May
7. Metcalf & Eddy (2003) Wastewater engineering, treatment and reuse, 4th ed., pp 72–74
8. Vasanthi P, Kaliappan S, Srinivasaraghavan R (2007) Impact of poor solid waste management on ground water. Environ Monit Assess 143(1–3):227–238
9. Iwasaki Y (1975) Practical problems of odour measurements and odour control

Predicting the Compressive Strength of Concrete Containing Fly Ash Cenosphere Using ANN Approach

M. Kowsalya, S. Sindhu Nachiar, and S. Anandh

Abstract The rising solid waste produced by industries is a major problem in different countries. Fly ash cenosphere (FAC) is a by-product of thermal power plants, which can partially replace fine aggregate in concrete. A reliable model for predicting concrete strength can save time, effort, and money. The present investigation implemented an artificial neural network (ANN) to predict the compressive strength of concrete that incorporates fine aggregate replacement with FAC. This research endeavors to predict the compressive strength of concrete that incorporates FAC at different levels of replacement, specifically at 7, 14, and 28 days. The utilization of the ANN methodology is employed to analyze and model three distinct variables, namely the fine aggregate content, the percentage of FAC ranging from 0 to 100%, and the water-to-cement (w/c) ratio. As an outcome, it is observed that FAC concrete is strongly influenced by cement content, % of FAC, and w/c ratio. Experimental data are highly correlated with ANN models as well. ANNs, however, demonstrate a higher degree of accuracy than other models. The results also signify that the ANN approach for concrete compressive strength prediction is solitary of the utmost best-fit method.

Keywords Fly ash cenosphere · Waste materials · Artificial neural network (ANN) approach · Fine aggregate replacement · Concrete compressive strength · Mechanical properties

1 Introduction

Due to the extensive expansion of industries, enormous quantities of waste are being produced along with the materials that are being manufactured. Utilizing waste is thought to be crucial for sustainability in the construction industry [1]. Non-biodegradable waste elements used in concrete can mitigate some of the unavoidable

M. Kowsalya · S. Sindhu Nachiar (✉) · S. Anandh
Department of Civil Engineering, Faculty of Engineering and Technology, SRM Institute of Science and Technology, Tamil Nadu, Kattankulathur 603203, India
e-mail: sindhus@srmist.edu.in

K. R. Reddy et al. (eds.), *Recent Advances in Civil Engineering*, Lecture Notes in Civil Engineering 398, https://doi.org/10.1007/978-981-99-6229-7_34

side effects of garbage collection and landfilling. Numerous initiatives have been launched in the building industry to move toward a more environmentally friendly model. Reducing the amount of hazardous waste sent to landfills and the amount of raw materials has needed to produce concrete by incorporating waste products into the mixtures. In order to create more environmentally friendly products, the concrete industry has widely utilized a wide range of by-product and waste materials as partly or complete replacements for the concrete components. Different types of sustainable concretes include those that contain recycled aggregate [2], waste foundry sand [3] and ceramic, tire rubber [4]. Fly ash cenosphere (FAC) is a waste product of the thermal power plant industry in which cenosphere of high-quality alumina silica sand with specific sizes ranging from 100 to 500 m is used in the construction process [5]. Approximately 500 MT [6] of fly ash is wasted from thermal plants worldwide each year. The wasted fly ash contains a significant amount of waste cenosphere, which is a big concern in terms of waste management. The processing technique of FAC from fly ash makes an detrimental effect of introducing in concrete. The use of FAC as a material replacement for natural sand and M sand is found to be beneficial to the construction industry's sustainability as a new approach. Before being extensively used as a novel material, the concrete industry examines the necessity of mechanical properties of FAC. The mechanical characteristics of concrete are subjected to influence from a range of extrinsic factors, encompassing the mechanical attributes of the aggregate component, as well as the binder type, admixture impact, volume and weight replacement level, water–cement ratio, etc.; it is important to consider these factors in adding to the properties of the conventional elements of the concrete. For concrete containing FAC, it is important to develop reliable artificial neural network (ANN) models. This should be done while considering all potentially significant factors. Recent studies have used extrapolation techniques, regression analysis, compressible packing models, artificial neural networks (ANNs), genetic algorithms, fuzzy logic theorem to forecast the compressive strength of concrete [7]. Golafshani et al. [8] constructed models to predict fly ash compressive strength in normal concrete and blast furnace slag in high-performance concrete. And ANN was used for this purpose to study the compressive strength of Waste Foundry Sand (WFS). Golafshani et al. [9] used MOMVO model and algorithm to investigate precision of the model incorporating ANN. Prasad et al. [10] used ANN model to predict the 28-day compressive strength self-compacting and high-performance concrete using high volume fly ash. Various literatures have been studied the concrete properties discovering the practice of ANN to predict through different algorithms. Although there are multiple methodologies available, it appears that ANNs are the most effective and relevant due to their ability to acquire knowledge from input–output relationships in multifaceted problematic areas. The ANN is a suitable instrument for the cartography of diverse characteristics of concrete, encompassing but not restricted to slump, filling capacity, segregation, and tensile strength. It can also be used for different types of concrete, such as self-compacting, high strength, high-performance, and lightweight concretes. While there have been many studies on the application of ANNs, there is a lack of literature available for predicting the compressive strength of concrete when fine aggregate replacement is done using FAC. Therefore, the present study

offers a novel method of predicting the compressive strength of fly ash cenosphere, an eco-friendly concrete using ANN.

2 Materials and Methodology

As a binding substance, ordinary Portland cement (OPC) was used. M sand is adopted as fine aggregate with a size range of 75 m–4.75 mm. The fly ash cenosphere (FAC), a partial replacement for fine aggregate, was gathered from thermal power plants. M sand and FAC had fineness moduli of 3.32 and 1.97, respectively. In this study, 10–12 mm crushed stone was used as a typical coarse aggregate. FAC aggregate was used in place of fine natural aggregate in various ratios, including 0%, 5%, 15%, 20%, 25%, 30%, 35%, 35%, 40%, 45%, 50%, 75%, and 100%. The mix ratio of the concrete mix adopted is 1:1.95:1.96. The water–cement ratio throughout the experiment is 0.5. All alterations in this study were carried out using the percentage volume fraction. The cylindrical molds used for pouring the concrete specimens had a diameter of 100 mm. To complete the concrete casting, a tamping rod was utilized to apply 25 blows to each of the two layers. The concrete samples were subjected to ambient conditions for a duration of 24 h to achieve dryness and then immersed in fresh water and left to undergo the curing process for durations of 7, 14, and 28 days. A set of 108 concrete specimens were cast to determine the mean compressive strength of concrete at different curing intervals. A minimum of three specimens was utilized to represent each mix proportion. The compressive strength test was performed as per the guidelines outlined in IS 516:2018 [11]. Table 1 represents the experimental data adopted for the ANN model.

3 Developing ANN Model

The artificial neural network (ANN) exists as an analogous system for computing human brain to emulate the cognitive processes for analyzing and processing data. The collection of data from experimental investigations is used to model, categorize, recognize, and predict issues. The interconnected layers of artificial neural network structures, comprising of input, hidden, and output layers, are effectively utilized using regression problems. The artificial neural network (ANN) comprises hidden and output layers, each containing central units known as artificial neurons. These neurons perform two significant mathematical computations. To compute an artificial neuron, the first step is to calculate the net value. This is done by summing the subjective inputs established from the preceding neurons. In mathematical computation, the second stage involves applying an activation function to the net value. This results in an activated value that is then transmitted to the next neurons in the subsequent layer. In addition, it is noted that there exist bias nodes within both the input and hidden layers that establish connections with all nodes in their respective subsequent

Table 1 Experimental results of fly ash cenosphere concrete

Identification	Description (kg/m^3)				Compressive strength (N/mm^2)		
	OPC	M Sand	FAC	CA	7 days	14 days	28 days
F0	430	838.72	0	845.05	23.03	29.97	38.40
F5	430	796.78	11.55	845.05	17.67	24.30	27.50
F10	430	754.85	23.11	845.05	18.60	25.70	29.60
F15	430	712.91	34.66	845.05	20.60	25.90	30.00
F20	430	670.98	46.21	845.05	21.13	26.13	31.13
F25	430	629.04	57.76	845.05	21.20	27.57	32.67
F30	430	587.1	69.32	845.05	22.73	29.37	33.40
F35	430	545.17	80.87	845.05	23.20	29.10	32.90
F40	430	503.23	92.42	845.05	21.47	24.50	28.47
F45	430	461.3	103.97	845.05	20.77	22.30	26.50
F50	430	419.36	115.97	845.05	18.63	20.83	24.10
F75	430	209.68	173.29	845.05	13.67	15.53	18.10
F100	430	0	231.05	845.05	10.93	12.67	14.10

layers. This study involved using the Neural Network Toolbox to create the neural network models using MATLAB software. The network consists of one input data and one output data consisting of 78 datasets. The input layer of the ANN model used 15 hidden neurons as shown in Fig. 1. The input output fitting issue is solved using a two-layer feedforward neural network and a neural network fitting app. It is designed to assist with various aspects of neural network development, including data selection, network construction, training, and performance evaluation. It utilizes regression analysis and mean square error to achieve accurate results.

When the statistics were tallied, about 70% were used for training, 15% for testing, and 15% for validation. In order to train the network, it is first exposed to training data, and then its parameters are adjusted based on the network's error. Levenberg–Marquardt backpropagation training was used to train the artificial neural network (ANN) model. To find the best fit or the least amount of error, nonlinear least squares problems are typically solved using the Levenberg–Marquardt (LM) algorithm. The

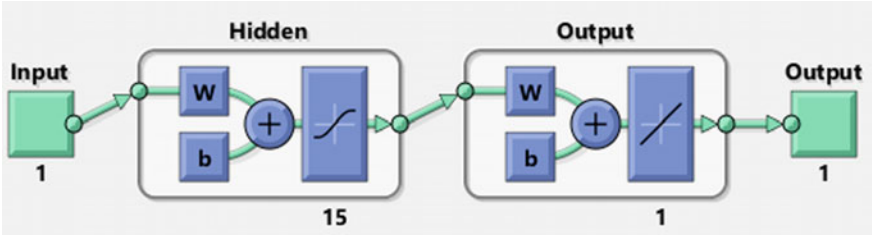

Fig. 1 ANN model

Table 2 Characteristics of ANN model

Parameters	Description
Input layer—neurons	1
Output layer—neurons	1
Hidden layers	15
Training algorithm	Levenberg–Marquardt back propagation
Activations function—hidden layer	Sigmoid
Activations function—output layer	Linear

backpropagation training algorithm is a commonly utilized method for training artificial neural networks (ANNs). This algorithm is preferred for engineering problems due to its numerous advantages, making it an ideal choice for training deep neural networks. The technology provides several benefits, including efficient computation, gradient-based optimization, universal approximation, error attribution, and adaptability to various research developments. Table 2 presents a summary of the various ANN features employed in the model.

4 Results and Discussions

This section discusses the compressive strength that was experimentally determined and interpreted in the ANN model for predicting it. Figure 2 illustrates the comparison between the network's outputs and their corresponding target values across the training, validation, and test datasets. For a perfect fit, the network outputs and targets must be equal and lie on a 45° line. The compressive strength accuracy performance indicators (R) on 7th, 14th, and 28th days of testing were found to be 0.998, 0.999, and 0.996. Furthermore, highest R value obtained in training dataset indicates an excellent fit for all datasets of compressive strength measured on the 7th, 14th, and 28th days. From the findings, model has a sufficient precision and trained adequately.

The performance plot of ANN for 7th, 14th, and 28th days is represented in Fig. 3. From this figure, there is conclusive evidence that the gradient is leveling off as a result of these studies when the epoch equals 3 on the 7th day, epoch equals 1 on 14th day, and epoch equals 5 in 28th day of compressive strength of concrete. The findings indicate that this investigation's ANN model, which employed 15 hidden layers, could predict concrete's compressive strength more accurately and with higher reliability than almost all other investigations.

Different performance parameters, such as coefficient of determination (R^2), mean square error (MSE), root mean squared error (RMSE), and the mean absolute error (MAE), were used to evaluate the efficiency of the developed models.

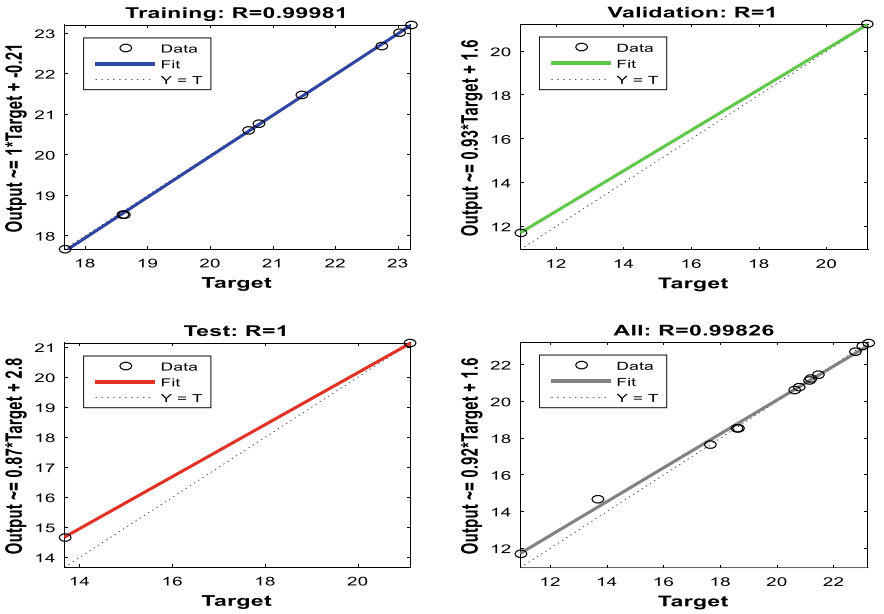

Fig. 2 Regression analysis of ANN

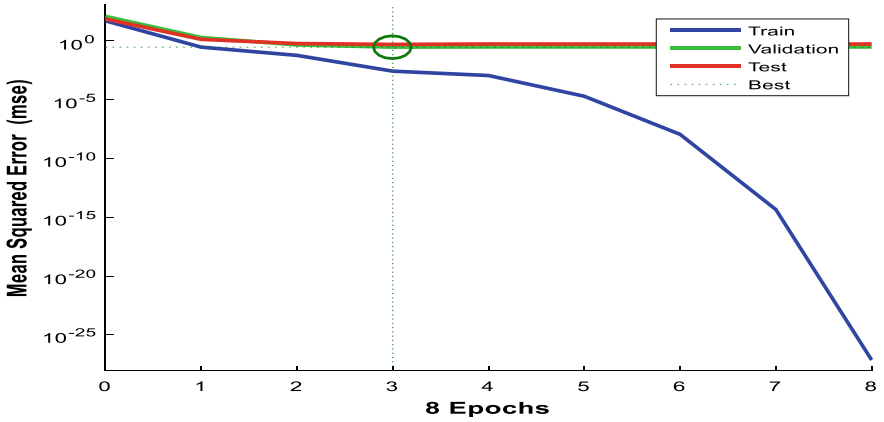

Fig. 3 Performance of ANN

$$R^2 = \frac{\sum_{i=1}^{n}\left(f_{\mathrm{Exp},i} - \overline{F}_{\mathrm{Exp}}\right)\left(f_{\mathrm{ANN},i} - \overline{F}_{\mathrm{ANN}}\right)}{\sqrt{\sum_{i=1}^{n}\left(f_{\mathrm{Exp},i} - \overline{F}_{\mathrm{Exp}}\right)^2\left(f_{\mathrm{ANN},i} - \overline{F}_{\mathrm{ANN}}\right)^2}}, \tag{1}$$

$$\mathrm{MSE} = \frac{1}{n}\sum_{i=1}^{n}\left(f_{\mathrm{ANN},i} - \overline{F}_{\mathrm{Exp},i}\right)^2, \tag{2}$$

Table 3 Performance analysis for model accuracy

Indicators	R^2	MSE	RMSE	MAE
ANN model	0.99	1.54	3.81	2.42

$$\text{RMSE} = \sqrt{\frac{1}{n}\sum_{i=1}^{n}\left(f_{\text{ANN},i} - f_{\text{Exp},i}\right)^2}, \tag{3}$$

$$\text{MAE} = \frac{1}{n}\sum_{i=1}^{n}\left|f_{\text{ANN},i} - f_{\text{Exp},i}\right|. \tag{4}$$

The coefficient of determination (R^2) quantifies the extent of variance observed in the output variable of a regression model which can be attributed to the input variables. The metric offers an assessment of the degree of conformity between the model and the data, with a numerical scale that spans from 0 to 1. A greater R^2 value denotes an improved goodness of fit. To evaluate the quality of a model's predictions, root mean squared error (RMSE) metric is used; less RMSE values indicate higher performance. Mean absolute error (MAE) provides a straightforward measure of the model's prediction error, without considering the direction of the errors. Mean squared error (MSE): MSE measures the average of the squared differences between the predicted and actual values. The performance indicators for precise compressive strength are presented in Table 3.

The R^2 of the ANN model is found to be 0.99 offering a degree of accuracy of good fit model. Similar observation has been encountered by various researchers like Lin et al. [7], Golafshani et al. [8], and Khan et al. [12] indicating the ANN prediction with a R^2 value in the range of 0.99–1 indicting the best fit of model with accuracy. Similarly, the MSE value obtained from ANN is 1.54, whereas the RMSE is 3.81. The values suggest that the disparity between the predicted when compared to experimental is constrained. The MAE value suggests that the disparity between the experimental compressive strength and the predicted data is indicating the minimal error on an average of 2.42.

5 Conclusions

This research focused on predicting the compressive strength of fly ash cenosphere concretes by MATLAB software interpreting an artificial neural network concept. The learning methods, architecture, and feedforward and backpropagation techniques for determining the compressive strength of concrete at 7, 14, and 28 days of the curing period were obtained from experimental work. This work yields significant inferences, which include:

- The variables such as concrete age, cement content, admixture range, and water–cement ratio and other various other parameters are introduced in the ANN model to predict the compressive strength of the concrete containing fly ash cenosphere as fine aggregate. The results exhibited that the effective approach in ANN is using multilayer feedforward techniques.
- Compressive strength precision performance indicators (R) are found to be $\geq$ 0.99 with the epoch range of 3–5. Small discrepancies between experimental and predicted values can be seen in model errors calculated from R^2 and RMSE.
- The aforementioned findings indicate that the viable option for predicting the compressive strength of fly ash cenosphere concrete can be done by ANN.

References

1. Safiuddin M, Jumaat MZ, Salam MA, Islam MS, Hashim R (2010) Utilization of solid wastes in construction materials. Int J Phys Sci 5:1952–1963
2. Ghosn S, Cherkawi N, Hamad B (2020) Studies on hemp and recycled aggregate concrete. Int J Concr Struct Mater. https://doi.org/10.1186/s40069-020-00429-6
3. Martins MAB, Barros RM, Silva G, Santos IFS (2019) Study on waste foundry exhaust sand, WFES, as a partial substitute of fine aggregates in conventional concrete. Sustain Cities Soc 45:187–196. https://doi.org/10.1016/j.scs.2018.11.017
4. Tamayo-García B, Albareda-Valls A, Rivera-Rogel A, Cornado C (2019) Mechanical characterization of a new architectural concrete with glass-recycled aggregate. Buildings 9:145. https://doi.org/10.3390/BUILDINGS9060145
5. Ray S, Haque M, Ahmed T, Nahin TT (2021) Comparison of artificial neural network (ANN) and response surface methodology (RSM) in predicting the compressive and splitting tensile strength of concrete prepared with glass waste and Tin (Sn) can fiber. J King Saud Univ Eng Sci. https://doi.org/10.1016/j.jksues.2021.03.006
6. Ranjbar N, Kuenzel C (2017) Cenospheres: a review. Fuel 207:1–12. https://doi.org/10.1016/j.fuel.2017.06.059
7. Lin CJ, Wu NJ (2021) An ANN model for predicting the compressive strength of concrete. Appl Sci. https://doi.org/10.3390/app11093798
8. Golafshani EM, Behnood A, Arashpour M (2020) Predicting the compressive strength of normal and high-performance concretes using ANN and ANFIS hybridized with grey wolf optimizer. Constr Build Mater 232:117266. https://doi.org/10.1016/j.conbuildmat.2019.117266
9. Golafshani EM, Behnood A (2021) Predicting the mechanical properties of sustainable concrete containing waste foundry sand using multi-objective ANN approach. Constr Build Mater 291:123314. https://doi.org/10.1016/j.conbuildmat.2021.123314
10. Prasad BKR, Eskandari H, Reddy BVV (2009) Prediction of compressive strength of SCC and HPC with high volume fly ash using ANN. Constr Build Mater 23:117–128. https://doi.org/10.1016/j.conbuildmat.2008.01.014
11. Bureau of Indian Standards (2018) Method of tests for strength of concrete, IS 516:2018. BIS, New Delhi
12. Khan MS, Abbas H (2015) Effect of elevated temperature on the behavior of high volume fly ash concrete. KSCE J Civ Eng 19:1825–1831. https://doi.org/10.1007/s12205-014-1092-z

Prediction of Mechanical Properties of the Cement Brick with Bio-aggregate

G. Nakkeeran and L. Krishnaraj

Abstract Agricultural-industrial activity leads to an abundance of waste generation and disposal, which is a desirable source for replacing fine aggregates. These compounds are known as bio-aggregates. For this research, 10–40% by volume of fine aggregate was replaced with raw rice husk in bricks. Physical and mechanical properties test was conducted. In this study, linear regression (LR) and artificial neural networking (ANN) model has been developed for prediction. The input parameters consist of cement, fine aggregate, and raw rice husk, with the output parameter being the target compressive strength. MLR and ANN were utilized to predict and compare properties. The study's conclusion was that both models were highly accurate, but that the ANN results were better at forecasting concrete strength. The MLR model is greater than the ANN model when it discusses predicting strength.

Keywords Raw rice husk · Artificial neural networks (ANN) · Multiple linear regression (MLR) · Concrete brick

1 Introduction

The use of sustainable materials in the construction industry has become a crucial aspect of modern-day engineering. Concrete is the most widely used building material used construction material globally due to its strength, durability, and versatility [1]. However, the production of concrete has significant environmental impacts because of the high energy usage and carbon footprint associated with its production [2, 3]. Furthermore, environmental issues, including soil erosion, loss of wildlife habitat, and water pollution have resulted from the overexploitation of natural resources like fine aggregates [4]. The use of sustainable and eco-friendly materials in concrete production has, therefore, gained attention in recent years.

G. Nakkeeran · L. Krishnaraj (✉)
Department of Civil Engineering, Faculty of Engineering and Technology, SRM Institute of Science and Technology, Tamil Nadu, Kattankulathur 603203, India
e-mail: krishnal@srmist.edu.in

K. R. Reddy et al. (eds.), *Recent Advances in Civil Engineering*, Lecture Notes in Civil Engineering 398, https://doi.org/10.1007/978-981-99-6229-7_35

Waste is rice husk material produced during the milling of rice and is a potential candidate for replacing fine aggregates in concrete production. Rice husk is an abundant material in many parts of the world and has several properties that make it a promising alternative to traditional fine aggregates in concrete [5]. For instance, rice husk is lightweight, has high silica content, and is cost-effective. The addition of rice husk as a supplement to fine aggregates in concrete production can help reduce waste and promote sustainable and eco-friendly construction practices [6].

ANN and MLR are computational tools that have gained popularity in the field of construction materials research. ANN models have been successfully used in predicting the properties of concrete based on various parameters. Alternatively, MLR is a statistical method that uses linear regression [7, 8].

Recent literature has highlighted the use of artificial intelligence (AI) techniques in the field of construction materials research. ANN and MLR are two commonly used AI techniques that have been applied in the prediction of compressive strength in concrete. Several studies have been predicting the compressive strength of concrete, and these studies have reported high accuracy levels [9]. Recent literature highlights the potential of AI techniques such as ANN and MLR in predicting the compressive strength of concrete and the potential of rice husk as a sustainable alternative to traditional fine aggregates in concrete [10].

The persistence of this study is to forecast the compressive strength of the resulting material using both ANN and MLR models, and to examine the feasibility of using rice husk as an alternative material for fine particles in brick manufacture. The mechanical properties will be studied, and the performance of the ANN and MLR models for forecasting compressive strength will be compared. In addition to reducing trash produced by the rice sector, the findings of this study will also encourage the use of waste materials in building projects. Additionally, the comparison of the ANN and MLR models can provide valuable insights into the effectiveness of different predictive models for compressive strength in concrete. Overall, this research has significant implications for the construction industry and environmental sustainability.

2 Experimental Methods and Materials

The materials used in this study include cement, fine aggregate, water, and rice husk. OPC cement was used as the binder, and FA was replaced with rice husk at varying percentages (0%, 10%, 20%, 30%, and 40%). Figure 1 shows a methodology of this study.

In Table 1 show, design mix of concrete was carried out. The mix proportions for each mix were calculated based on the weight of cement used. Preparation of specimens of cubes of 100 × 100 × 100 mm were cast, respectively, in Fig. 2. The specimens cured for 28 days in a curing tank. A universal testing machine was used to conduct the compressive strength tests.

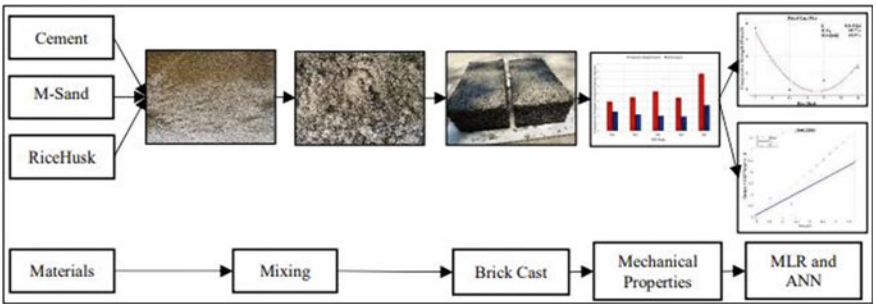

Fig. 1 Methodology

Table 1 MIX combination

MIX ID	Cement	Fine aggregate	Rice husk
RH1	100	90	10
RH2	100	80	20
RH3	100	70	30
RH4	100	60	40
RH0	100	100	0

(a) MIX combination of materials (b) Mixed raw materials with water (c) Raw Rice Husk Concrete Brick

Fig. 2 Casting of raw rice husk concrete brick

2.1 ANN

ANN is a computational model that simulates the functioning of a human brain to learn and make predictions from a dataset. Numerous studies have demonstrated that ANN models are highly accurate at strength of concrete in predicting. The advantage of ANN is its ability to learn and adapt to complex nonlinear relationships between variables. However, ANN requires a large dataset for training and can be time-consuming and computationally intensive [11–14]. ANN structure of this study is shown in Fig. 3.

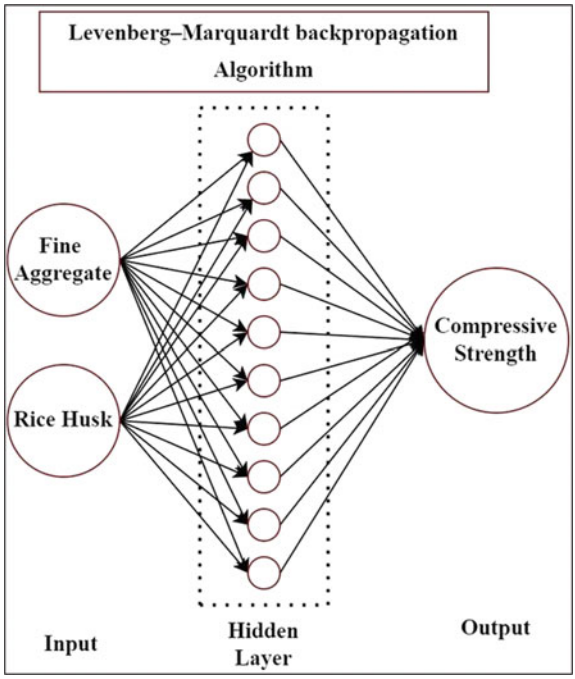

Fig. 3 ANN structure

2.2 MLR

MLR is a mathematical approach that establishes the connection between dependent and independent variables using linear regression. MLR is a simpler and less computationally intensive technique compared with ANN. MLR establishes a linear relationship between variables and can be used with reasonable precision to predict the compressive strength of concrete. The advantage of MLR is its simplicity and ease of interpretation. However, MLR is limited to linear relationships between variables and may not be suitable for modeling complex nonlinear relationships [15].

3 Results and Discussion

According to the results of the current investigation, the compressive strength of concrete brick specimens was drastically altered when fine aggregate was partially replaced with rice husk. Figure 4 shows that the best compressive strength was attained when fine aggregate was replaced with rice husk at a rate of 30%. Up to a specific amount of rice husk replacement, the compressive strength of the concrete bricks increased, but then dropped. Rice husk's lower specific gravity and higher water-absorption capacity compared with fine aggregate explain these phenomena.

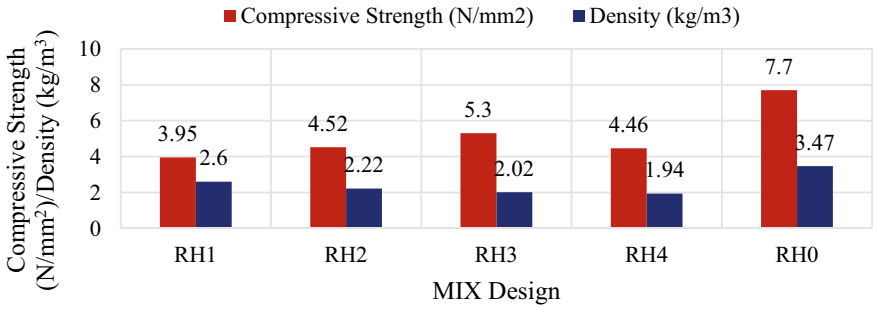

Fig. 4 Compressive strength and density

Therefore, the concrete's compressive strength diminishes as the replacement percentage rises.

The results obtained in the study are in agreement with studies that reported an optimum replacement percentage of fine aggregate with rice husk for 30% maximum compressive strength 5.3 N/mm^2 and density is 2.02 kg/m^3. Using rice husk as a partial replacement for fine aggregate can also reduce the environmental impact of the construction industry by minimizing waste and conserving natural resources.

Moreover, the study developed ANN and MLR models to predict the compressive strength of concrete containing rice husk as a partial replacement for fine aggregate. The models were trained and evaluated using experimental results from compressive strength tests.

3.1 MLR Analysis

This study investigated the effect of replacing rice husk with fine aggregate on the compressive strength and density of concrete using multiple linear regression (MLR) analysis. In Fig. 5, analysis resulted in an R-square value of 89.67 for compressive strength and 99.61 for density, indicating a strong correlation between the predictor variables (i.e., rice husk replacement percentage and fine aggregate) and the response variables (i.e., compressive strength and density).

The regression equation is

$$\text{Compressive Strength } \left(\text{N/mm}^2\right) = 7.495 - 0.4061\,\text{RH} + 0.01132\,\text{RH}^2 \quad (1)$$

$$\text{Density}\left(\text{kg/m}^3\right) = 3.455 - 0.09755\,\text{RH} + 0.001675\,\text{RH}^2 \quad (2)$$

The high R^2 values suggest that the MLR model is a good fit for the data, and the model can explain 89.67% and 99.61% of the variability in compressive strength and

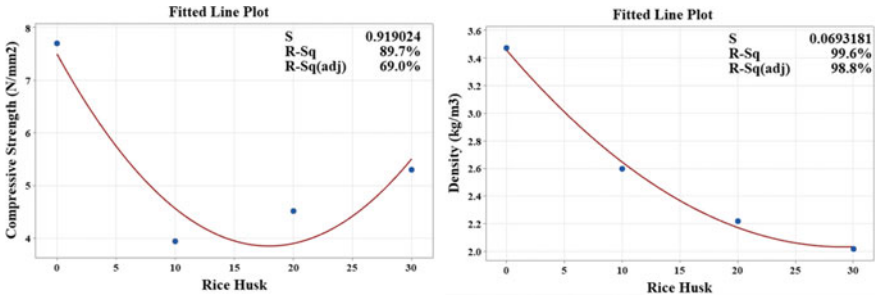

Fig. 5 MLR fitted line plot

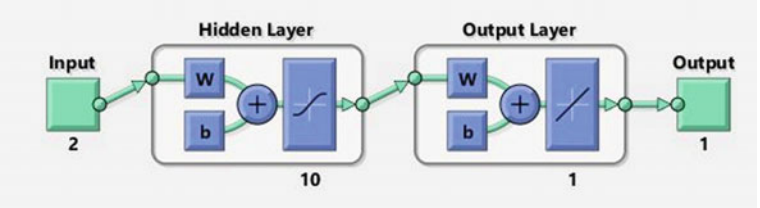

Fig. 6 ANN model in software

density, respectively. This finding implies that the percentage of rice husk replacement and the amount of fine aggregate are significant predictors of compressive strength and density in concrete, and changes in these variables can be used to anticipate changes in the properties of concrete.

3.2 ANN Analysis

This study investigated the effect of replacing rice husk with fine aggregate on the compressive strength and density of concrete using ANN analysis shown in Fig. 6. In Fig. 7, analysis resulted in an R^2 value of 95.99% for compressive strength and 85.917% for density, indicating a strong correlation between the input variables and the output variables.

3.3 Discussion of Compared Results of MLR and ANN

Both MLR and ANN analysis were used in this study to investigate the effect of replacing rice husk with fine aggregate on the compressive strength and density of concrete. While both techniques were able to forecast the attributes of concrete

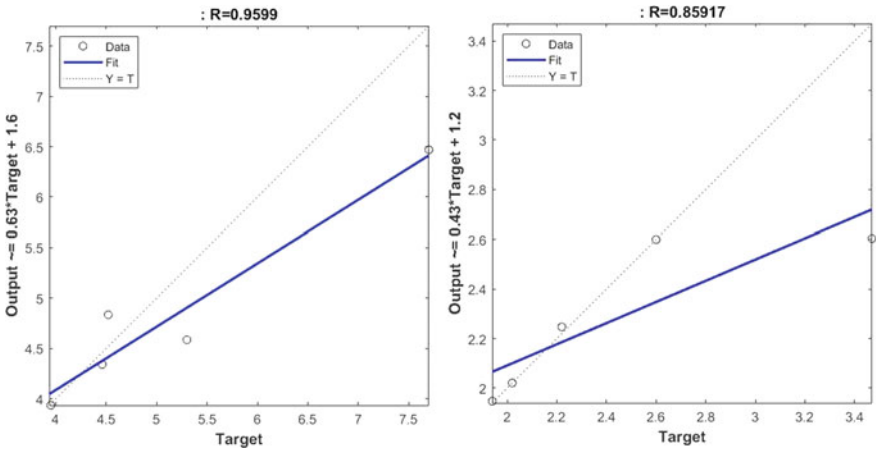

Fig. 7 ANN plots

accurately, there were some notable differences between the results obtained from the two methods. MLR analysis resulted in high R^2 values of 89.67% for compressive strength and 99.61% for density. In contrast, the ANN model achieved even higher R^2 values of 95.99% for compressive strength and 85.917% for density. Additionally, the performance plot of the ANN model showed that it required fewer epochs to achieve an acceptable level of accuracy for density compared with compressive strength. Finally, both MLR and ANN models were able to effectively predict the properties of concrete based on the percentage of rice husk replacement and the amount of fine aggregate. However, the ANN model performed better MLR model regarding precision, especially for predicting compressive strength.

The ANN model is a powerful tool for predicting complex relationships between input and output variables, making it particularly well-suited for the analysis of nonlinear systems. On the other hand, in the case of linear systems with correlated input and output variables, MLR models are more appropriate.

4 Conclusion

This research shows that compressive strength and density can be drastically altered when fine aggregate is partially replaced with rice husk in concrete bricks.

- The results showed that a 30% replacement of fine aggregate with rice husk resulted in the highest compressive strength. The use of rice husk as a partial replacement for fine aggregate can help reduce the environmental impact of the construction sector by conserving resources and reusing waste products.

- The compressive strength and density of concrete using rice husk as a partial replacement for fine aggregate were also predicted using artificial neural networks and multi-layer perceptrons.
- While both methods were successful in predicting concrete attributes, the ANN model outperformed the MLR model, particularly in predicting compressive strength. The work demonstrates the ability of ANN modeling for predicting the characteristics of concrete and offers valuable insights into the usage of rice husk as a partial replacement for fine aggregate in concrete.

There is room for more study into the best ways to apply these methods to the examination of green concrete ingredients.

References

1. Amantino GM, Hasparyk NP, Tiecher F, Toledo Filho RD (2022) Assessment of bio-aggregate concretes' properties with rice residue. J Build Eng 52:104348. https://doi.org/10.1016/J.JOBE.2022.104348
2. Krishnaraj L, Ravichandran PT (2019) Investigation on grinding impact of fly ash particles and its characterization analysis in cement mortar composites. Ain Shams Eng J 10(2):267–274. https://doi.org/10.1016/J.ASEJ.2019.02.001
3. Krishnaraj L, Niranjan R, Kumar GP, Kumar RS (2020) Numerical and experimental investigation on mechanical and thermal behaviour of brick masonry: an efficient consumption of ultrafine fly ash. Constr Build Mater 253:119232. https://doi.org/10.1016/J.CONBUILDMAT.2020.119232
4. Nakkeeran G, Krishnaraj L (2023) Developing lightweight concrete bricks by replacing fine aggregate with vermiculite: a regression analysis prediction approach. Asian J Civil Eng 1:1–9. https://doi.org/10.1007/S42107-023-00586-5
5. Khan R, Jabbar A, Ahmad I, Khan W, Khan AN, Mirza J (2012) Reduction in environmental problems using rice-husk ash in concrete. Constr Build Mater 30:360–365. https://doi.org/10.1016/J.CONBUILDMAT.2011.11.028
6. Ganasen N, Bahrami A, Loganathan K (2023) A scientometric analysis review on agricultural wastes used as building materials. Buildings 13(2):426. https://doi.org/10.3390/BUILDINGS13020426
7. Kavya BR, Sureshchandra HS, Prashantha SJ, Shrikanth AS (2022) Prediction of mechanical properties of glass and basalt fiber reinforced concrete using ANN. Asian J Civil Eng 23(3):877–886. https://doi.org/10.1007/s42107-022-00460-w
8. Nakkeeran G, Krishnaraj L (2023) Prediction of cement mortar strength by replacement of hydrated lime using RSM and ANN. Asian Journal of Civil Engineering 1:1–10. https://doi.org/10.1007/S42107-023-00577-6/TABLES/5
9. Vishnupriyan M, Annadurai R (2023) A study on the macro-properties of PCB fiber-reinforced concrete from recycled electronic waste and validation of results using RSM and ANN. Asian J Civ Eng 1:1–14. https://doi.org/10.1007/S42107-023-00595-4/FIGURES/22
10. Kumar GP, Thirumurugan V, Satyanarayanan KS (2023) Artificial neural network prediction of window openings and positions in reinforced concrete infilled frames with pneumatic interface. Asian J Civil Eng 1:1–11. https://doi.org/10.1007/S42107-023-00611-7
11. Moradi MJ, Khaleghi M, Salimi J, Farhangi V, Ramezanianpour AM (2021) Predicting the compressive strength of concrete containing metakaolin with different properties using ANN. Measurement 183:109790. https://doi.org/10.1016/J.MEASUREMENT.2021.109790

12. Pattanayak S, Loha C, Hauchhum L, Sailo L (2021) Application of MLP-ANN models for estimating the higher heating value of bamboo biomass. Convers Biorefin 11(6):2499–2508. https://doi.org/10.1007/S13399-020-00685-2/TABLES/4
13. Boumaaza M, Belaadi A, Bourchak M, Jawaid M, Hamid S (2022) Comparative study of flexural properties prediction of *Washingtonia filifera* rachis biochar bio-mortar by ANN and RSM models. Constr Build Mater 318:125985. https://doi.org/10.1016/J.CONBUILDMAT.2021.125985
14. Golafshani EM, Behnood A, Arashpour M (2020) Predicting the compressive strength of normal and high-performance concretes using ANN and ANFIS hybridized with grey wolf optimizer. Constr Build Mater 232:117266. https://doi.org/10.1016/J.CONBUILDMAT.2019.117266
15. Adesanya E, Aladejare A, Adediran A, Lawal A, Illikainen M (2021) Predicting shrinkage of alkali-activated blast furnace-fly ash mortars using artificial neural network (ANN). Cem Concr Compos 124:104265. https://doi.org/10.1016/J.CEMCONCOMP.2021.104265

Hydraulics and Water Power Engineering

A Wastewater Reclamation Using Soil Aquifer Treatment (SAT) Technology to Enhance Groundwater Recharge

L. Chandrakanthamma and K. Prasanna

Abstract Soil aquifer treatment (SAT) is a water purification technique that involves a combination of physical, chemical, and biological processes (American Public Health Association (APHA) in Standard Methods for The Examination of Water and Wastewater. American Public Health Association, Washington, DC, 1998) to improve the quality of wastewater effluent as it seeps through layers of soil. This technology is particularly useful in developing countries like India due to its affordability and ease of operation, as it does not require specialized expertise from wastewater treatment plant operators. SAT (Bahgat et al. in Water Res 33:1949–1955, 1999) is a dependable method that consistently produces high-quality treated wastewater that meets accepted standards. Furthermore, it provides supplementary treatment for primary, secondary, and tertiary effluents from wastewater treatment plants (Arye et al. in Chemosphere 82(2):244–252, 2011). The utilization of wastewater effluent for soil aquifer treatment (SAT) (Bahgat et al. in Water Res 33:1949–1955, 1999) has emerged as a promising solution to address water scarcity in arid and semi-arid regions. However, further investigations are necessary to evaluate the impact of various factors on SAT performance, including organic micro pollutants, pathogens, nutrients, organic matter, suspended solids, rate of hydraulic loading, type of soil, temperature changes, redox conditions, pre-treatment of wastewater, biological activity, and wetting and drying cycles. This research involves analyzing data from laboratory-scale soil columns, horizontal subsurface flow constructed wetlands, and on-site soil analyses. By obtaining a comprehensive understanding of SAT performance, treated municipal wastewater can be considered a feasible option for providing water to communities in such areas. In the present study, the

The original version of the chapter has been revised: The affiliations of the first and second author have been updated. A correction to this chapter can be found at https://doi.org/10.1007/978-981-99-6229-7_61

L. Chandrakanthamma · K. Prasanna
Department of Civil Engineering, Easwari Engineering College, Ramapuram, Chennai, India

K. Prasanna (✉)
Department of Civil Engineering, Faculty of Engineering and Technology, SRM Institute of Science and Technology, Kattankulathur, Tamil Nadu 603203, India
e-mail: prasannk@srmist.edu.in

K. R. Reddy et al. (eds.), *Recent Advances in Civil Engineering*, Lecture Notes in Civil Engineering 398, https://doi.org/10.1007/978-981-99-6229-7_36

water from STP is filtered through a medium of sand and Biochar. The filtered water is checked for its characteristics, before recharging the ground water.

Keywords Leachate · Alum coagulation · Floc · Phyto-remediation · Hydraulic loading rate (HLR) · Biological activity

1 Introduction

In present scenario of water scarcity everywhere, with the SAT technology if ground water is recharged, sufficient water will be available to meet the needs of human kind. Life is dependent on the availability of fresh water (Table 1), but the world is currently encountering a widespread issue of ensuring a consistent and safe water supply for its inhabitants. This challenge arises from various factors, such as population expansion, climate change, and pollution of freshwater sources. Currently, about one-third of the global population (2.5 billion individuals) resides in regions where water scarcity is a pressing concern, according to the United Nations.

The disposal of untreated wastewater and improperly treated water into bodies of water and land is becoming a widespread issue globally, more specifically in developing countries [1] due to reasons like population growth, urbanization, and inadequate investment in (conventional) wastewater treatment plants [2]. Furthermore, the majority of current wastewater treatment plants are outdated and over whelmed, intended to serve only a small percentage of the population they are meant to serve. This issue is exacerbated by rising water scarcity and competition for water resources across various sectors. To address the problem of surface water pollution and achieve efficient water resource management [3] through water reuse, it is necessary to establish and implement various treatment technologies [3] with low energy consumption and a minimal chemical footprint. One possible solution is to plan for the use of effluents in soil aquifer treatment (SAT) [4] to treat wastewater effluents for subsequent reuse.

Table 1 As per recent studies, the global water distribution (*Source* Internet)

S. No.	Source	Availability (%)
1	Salt water	97.5
2	Fresh water	2.5
3	Glaciers, permanent snow cover	68.9
4	Fresh groundwater	29.9
5	Fresh water lakes an river storages	0.3
6	Others	0.9

1.1 Feasibility Analysis and Design of SAT System

After identifying SAT as a potential solution, to achieve the established goals, it is important to conduct a comprehensive feasibility analysis that considers various factors like legal, economical, technical, institutional, social, and environmental aspects [5]. Once all the requirements in these areas are met, the preliminary design can then be developed.

The factors to consider in the design of SAT systems [4]:

(i) The pre-treatment requirements must be considered, including the level of wastewater treatment necessary and any additional treatment required for successful operation of the system.
(ii) The rate of infiltration, measured in hydraulic loading, should be determined based on the characteristics of the soil and the amount of water that can be effectively absorbed.
(iii) The amount of land required should take into account wet and dry cycles to ensure that the system can function effectively throughout the year.
(iv) The number of wells required and their production capacity must be determined based on the expected water demand and the characteristics of the groundwater resources in the area.
(v) The spacing between wells should be optimized to maximize the water recovery while minimizing the potential for contamination.
(vi) The distance between the wells and the infiltration pond or injection well must be carefully considered to ensure that the water is effectively treated and can be safely injected or infiltrated into the ground.
(vii) The pumping rate should be optimized to ensure that groundwater flow and velocity are not disrupted, which could impact the quality of the water recovered.
(viii) The percentage of native groundwater present in the reclaimed water must be monitored to ensure that the quality of the water meets regulatory standards.
(ix) The quality of water obtained from the SAT system must be regularly monitored to ensure that it meets the required standards for its intended use.
(x) Any post-treatment requirements, operation and maintenance requirements, and monitoring protocols must be established to ensure the long-term viability and success of the system.

The initial stage in assessing the possibility and creating designs for Subsurface Absorption Technology (SAT) systems is choosing a suitable site with hydrogeological conditions that are appropriate. To do this, a comprehensive site investigation must be conducted, including various tests such as boreholes, infiltration tests, test pits, groundwater wells, and soil and groundwater quality sample analyses.

1.2 Selection of Site and Soil Requirements

The selection of site is a critical factor for the successful implementation of a soil aquifer treatment (SAT) system. Several key factors should be considered during site evaluation and selection, including the depth of the soil, permeability, depth to groundwater, and aquifer thickness (i.e., depth from the water table to the bedrock [1]). These factors play a crucial role in determining the effectiveness of the SAT system in treating wastewater and preventing contamination of groundwater resources. Therefore, careful consideration of these factors is essential when selecting a site for a SAT system.

The use of effluent [6] for soil aquifer treatment (SAT) is a potential solution to alleviate water scarcity in arid and semi-arid regions. However, further research is required to assess the impact of various factors on SAT performance, such [7] as organic micropollutants, pathogens, nutrients, organic matter, suspended solids, rate of hydraulic loading, type of soil, different temperature fluctuations, redox conditions, wastewater pre-treatment, biological activity, and wetting and drying cycles. This study involves analyzing data from laboratory-scale soil columns, horizontal subsurface flow constructed wetlands, and on-site soil analyses. A comprehensive understanding of SAT performance will enable treated municipal wastewater to be considered a viable option for supplying water to communities in the area of Ramapuram, Chennai.

2 Materials and Methods

2.1 Treatment Methods

In order to investigate multiple parameters using SAT, there are two systems followed, one is a specialized soil-column system (as shown in Fig. 1) that mimics aquifer conditions using three columns, each measuring 55 cm in length and 10 cm in inner diameter. The columns, made of acrylic, will be capped with rubber gaskets at the top and bottom. A screen will be positioned at the base of each column to provide support for a layer of 2.5 cm of sand, followed by a depth of 2.5 cm of gravel, and 50 cm of soil.

Second one is tank model of 10 m*3 m with various details as given below also in progress to check various parameters along with vertical columns (Fig. 2).

Before starting the experiments, the soil columns and the horizontal tanks are to be biologically prepared by infiltration of feed water for 6 months.

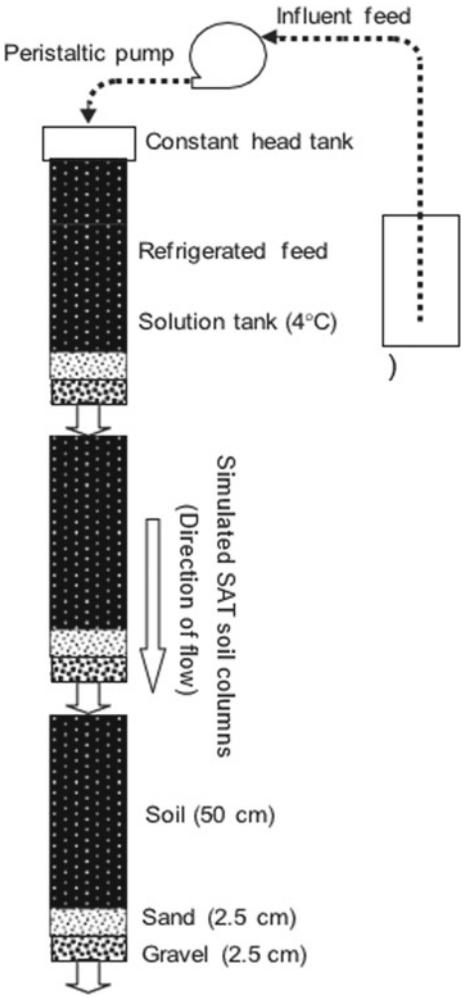

Fig. 1 Laboratory model soil aquifer treatment system (*Source* Water Research [4])

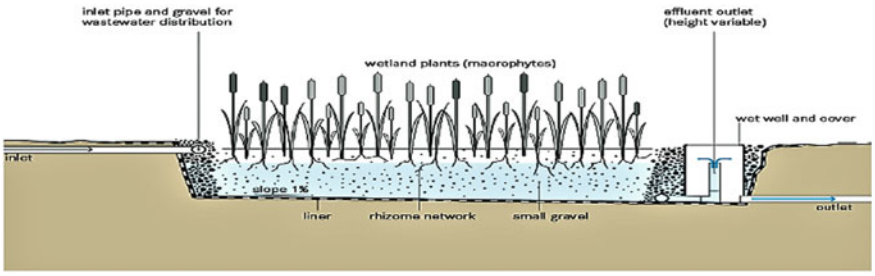

Fig. 2 Diagram of the horizontal subsurface flow constructed wetland [1] (*Source* http://www.mdpi.com/journal/water)

Table 2 Various soil tests were conducted before applying the methods mentioned above to know the soil characteristics

S. No.	Parameter	Value
1	Specific gravity of soil	2.6
2	Sieve analysis of soil	
	(i) % of gravel (> 4.75 mm)	1.4%
	(ii) % of coarse sand (4.75–2.00 mm)	0.1%
	(iii) % of medium sand (2.00–0.425 mm)	78%
	(iv) % of fine sand (0.425–0.075 mm)	6.5%
	(v) Fineness modulus	0.418
	(vi) Uniformity coefficient Cu	4.454
3	Liquid limit of the soil	35.67%
4	Plastic limit of the soil	23.3%
5	Density of soil	1.43 gm/cc
6	Coefficient of permeability of the soil	0.015 cm/s
7	pH of soil	8
8	Water quality data for the STTP	
	pH	7.5
	COD	52 mg/l
	Nitrate	4.3 mg/l

3 Results and Discussions

Various tests were conducted to find the soil characteristics (the preliminary tests done are field based and further work will be carried under controlled conditions).

Knowing the parameters of the reference sample, further tests will be conducted on the water filtered through the test columns which are provided with a bioindicator and a check well. Preliminary tests are conducted to know the soil structure.

References

1. Kivaisi AK (2001) The potential for constructed wetlands for wastewater treatment and reuse in developing countries: a review. Ecol Eng 16:545–560
2. Jenssen PD, Siegrist RL (1990) Technology assessment of wastewater treatment by soil infiltration systems. Water Sci Technol 22(3/4):83–93
3. Altmann J, Rehfeld D, Träder K, Sperlich A, Jekel M (2016) Combination of granular activated carbon adsorption and deep-bed filtration as a single advanced wastewater treatment step for organic micropollutant and phosphorus removal. Water Res 92:131–139
4. Bouwer H (1985) Renovation of wastewater with rapid infiltration land treatment system. In: Asano T (ed) Artificial recharge of groundwater. Butterworth, Boston, pp 249–282
5. Roberts PV, McCarty PL (1978) Direct injection of reclaimed water into the aquifer. J Environ Eng Div Am Soc Civ Eng 104(5):933–949

6. Idelovitch E et al (1983) Behavior of Organics during Soil-Aquifer Treatment (SAT). Scientific Report for First Research Year1982, Joint German-Israeli Research Program, Tahal Publication No. 04/83/12 (1983)
7. Benstoem F, Nahrstedt A, Boehler M, Knopp G, Montag D, Siegrist H, Pinnekamp J (2017) Performance of granular activated carbon to remove micropollutants from municipal wastewater—a meta-analysis of pilot- and large-scale studies. Chemosphere 185:105–118
8. American Public Health Association (APHA) (1998) Standard methods for the examination of water and wastewater. American Public Health Association, Washington, DC
9. Bahgat M, Dewedar MA, Zayed A (1999) Sand-Filters used for wastewater treatment: build up and distribution of microorganisms. Water Res 33:1949–1955
10. Carlson RR et al (1982) Rapid-infiltration treatment of primary and secondary effluents. J Water Pollut Control Fed 54:270
11. Ak M, Gunduz O (2013) Comparison of organic matter removal from synthetic and real wastewater in a laboratory-scale soil aquifer treatment system. Water Air Soil Pollut 224(3):1–16
12. Arye G, Dror I, Berkowitz B (2011) Fate and transport of carbamazepine in soil aquifer treatment (SAT) infiltration basin soils. Chemosphere 82(2):244–252
13. Cha W, Kim J, Choi H (2006) Evaluation of steel slag for organic and inorganic removals in soil aquifer treatment. Water Res 40(5):1034–1042
15. Arye G, Dror I, Berkowitz B (2011) Fate and transport of carbamazepine in soil aquifer treatment (SAT) infiltration basin soils. Chemosphere 82(2):244–252
16. Aiken GL, McKnight DM, Thorn KA, Thurman EM (1992) Isolation of hydrophilic organic acids from water using nonionic macroporous resins. Org Geochem 18(4):567–573
17. Chellam S, Krasner SW (2001) Disinfection byproduct relationships and speciation in chlorinated nanofiltered waters. Environ Sci Technol 35(19):3988–3999
18. Drewes JE, Fox P (1999) Fate of nature organic matter (NOM) during groundwater recharge using reclaimed water. Water Sci Technol 40(9):241–249
19. Kanokkantapong V, Marhaba T, Pavasant P, Panyapinyopol B (2006) Characterization of haloacetic acid precursors in source water. J Environ Manage 80(3):214–221
20. Quanrud DM, Hafer J, Karpiscak MM, Zhang J, Lansey KE, Arnold RG (2003) Fate of organics during soil-aquifer treatment: sustainability of removals in the field. Water Res 37(14):3401–3411
21. Rauch T, Drewes JE (2004) Assessing the removal potential of soil aquifer treatment systems for bulk organic matter. Water Sci Technol 50(2):245–253
22. Westerhoff P, Pinney M (2000) Dissolved organic carbon transformations during laboratory-scale groundwater recharge using lagoon-treated wastewater. Waste Manage 20(1):75–83
23. Rajeshkumar V, Chandrakanthamma L, SenthilKumar M, Gokulan R (2023) Enhancement of adsorption efficiency by surface modified avocado seed for xylene removal. Global NEST J 25(3):130–138
24. Jothilakshmi M, Chandrakanthamma L, Dhayachandhran KS, Mohan A (2019) Flood control and water management at basin level—at Orathur of Kanchipuram district. Int J Eng Adv Technol 8(6 Special Issue 3):1418–1421

Industrial Wastewater Treatment Using Nano Material as an Adsorbent: An Investigation

N. Singh, J. S. Sudarsan, K. Prasanna, S. Mohanakrishna, and S. Nithiyanantham

Abstract Pollution caused by dangerous substances, including heavy metals, is currently one of the most significant ecological concerns and public health issues. The removal of these materials from soil and water poses a significant decontamination challenge. The pollution of environment due to improper disposal of wastewater without treatment caused different types of pollution and it also affects the functioning of the ecosystem. The discharge from numerous industrial procedures, such as electroplating and tannery operations, a range of chemical contain, such as alkaline and acidic cleaners, electro-cleaners, and pickling solutions. The removal of metal ions can be treated by unit operation or unit process technique of wastewater treatment, sulfide precipitation, ion exchange, and evaporation are found to be effectively for most of the effluent treatment. Existing wastewater treatment techniques involve more time, cost and coagulants etc., these are becoming redundant nowadays due to several reasons. Adsorption techniques are commonly employed for treating industrial wastewater, particularly aqueous streams. This study aimed to evaluate the efficacy of a Nano adsorbent in removing metal ions from industrial effluents. The nanoparticles are used, such as zero valent iron, titanium dioxide, and magnetite, as medium which decreases has become more prevalent due to their low operating and maintenance costs. Additionally, their obtainability, potency, and has sustain to degrade pollutants have result in their increasing usage. The study seeks to investigate the effectiveness of the Nano adsorbent in treating various industrial effluents

N. Singh
Ministry of Environment, Forest and Climate Change, New Delhi 110003, India

J. S. Sudarsan (✉)
School of Energy and Environment, NICMAR University (National Institute of Construction Management and Research (NICMAR)), Balewadi, Pune 411045, India
e-mail: sudarsanjss@gmail.com

K. Prasanna · S. Mohanakrishna
Department of Civil Engineering, Faculty of Engineering and Technology, SRM Institute of Science and Technology, Kattankulathur, Tamil Nadu 603203, India

S. Nithiyanantham
Post Graduate and Research Department of Physics (Applied Energy Resources/Bio-Physics Divisions), Thiru. Vi. Kalyanasundaram Govt Arts and Science College (Affiliated to Bharathidasan University, Tiruchirapalli), Thiruvarur, Tamil Nadu 610003, India

K. R. Reddy et al. (eds.), *Recent Advances in Civil Engineering*, Lecture Notes in Civil Engineering 398, https://doi.org/10.1007/978-981-99-6229-7_37

with varying wastewater concentrations. Using different kinds of Nano adsorbent in several trails it was observed that these Nano adsorbents are effectively functioning in the removal of heavy metal compounds, like lead and chromium. Based on study it was clear from the SEM analysis, the heterogeneous nature of Nano adsorbent gives good adsorption of Cr by porosity of surface texture. The Nano adsorbent in the form of titanium dioxide was found to be potency in removing the heavy metal compounds from the industrial discharge as it has an potency of 89–97%. Based on the several trails it was evident that the Nano adsorbent found to be effective in treatment of heavy metals from the industrial effluent.

Keywords Adsorption · Nano adsorbent · Industrial effluent · Heavy metal · SEM analysis

1 Introduction

In recent years, water pollution is the major concern because the water is a main resource of all living beings [1–3]. Many industries of various sectors (textile, pharma, leather, and sewage) produce wastewater contains the mixture of organic contaminants mainly heavy metal ions which causes disease when it is reused without appropriate purification. Heavy metal contamination in air, water, and soil due to anthropogenic sources is a global issue. They can enter the food chain and this ultimately causes significant bioaccumulation. This has instigated the mandatory control of the concentration of metals in the effluents to be discharged into the water bodies [4]. Extended exposure to lead (Pb) can result in acute or chronic damage to the human nervous system [5]. It has been linked to renal issues, and high levels of exposure can lead to obstructive lung disease, kidney failure, lung cancer, liver damage, and gastric damage [6–8]. Chromium (Cr) is used in the pigments and metal alloys for the paints, cements, and other materials [9]. Exposure to low levels of chromium can irritate the skin and lead to ulceration, while prolonged exposure can result in liver and kidney damage [10].

2 Material and Methods

Samples from the tannery and electroplating industries were collected from the equalization tank and preserved at 4 °C [4, 11]. Their general characteristics as per the World Bank Group Report (WBGR) are given in Tables 1 and 2. And the list of parameters and their respective methods are given in Table 2. The characteristics of the water samples were tested [12]. The three nanoparticles were prepared in the laboratory. Then each of the three nanoparticles was separately introduced in the diluted sample and it's analyzed [11, 12]. Analysis was carried out and checked the reduction in effluent characteristics. The performance of each of the nanoparticles

Table 1 General characteristics of effluents [13]

S. No.	Parameters	Effluent characteristics	
		Tannery	Electroplating
1	pH	6.1	3.2
2	BOD (mg/l)	1110	34
3	COD (mg/l)	4117	7.26
4	TSS (mg/l)	1420	23
5	TDS (mg/l)	7668	78,000

Table 2 List of parameters and respective methods

S. No.	Parameters	Methods
1	pH	Electrometric
2	Oil and grease	Separating funnel
3	TDS	Potentiometric
4	TSS	Dry method
5	Chloride	Argentometric
6	Sulfide	Iodometric
7	COD	Closed reflux
8	BOD	Winkler

in varying concentrations (between 30 and 100 ppm) of effluents was analyzed and tabulated. The dilution was done in order to check the impact of nanoparticles on heavy metals at lower concentrations. These results for lower concentrations as the removal efficiency is much higher than normal methods. The performances of the three nanoparticles on removal of the various effluents were tabulated and discussed graphically with their relative merits/demerits.

2.1 Analytical and Characterization Technique

The wastewater parameters were evaluated using the standard methods specified in the APHA manual [10, 11]. While the conc. of the heavy metals in the effluent determined by digesting and diluting the samples before analyzing the metal content through atomic absorption spectroscopy. (Atomic Absorption Spectrometer—AAS4141 Electronic Corporation of India Ltd, Hyderabad). Air acetone was the flame used and hollow cathode lamp of the corresponding was the response time source [12].

2.2 Sample Preparation Method

The industrial effluent of the sample tested using low concentration sample. Specifically, the concentration of the sample are prepared at 30, 50, 70, and 100 ppm, using the synthetic wastewater and the actual industrial effluents [9].

2.3 Zero Valent Iron Nanoparticle

The synthesis of the iron nanoparticles was performed by the method described by mixing the two equal volumes of 0.94 M $NaBH_4$ 0.18 M $FeCl_3$ and stirring at 400 rotations per minute. The black precipitate of iron nanoparticles was then cultivated using vacuum filtration through 0.2-micron filter paper. The synthesized iron particles were subsequently washed multiple times with deionized water, following this scheme.

2.4 Magnetite Nanoparticle

For synthesizing this magnetic nanoparticle Ferric chloride hydraxate, ferrous chloride tetrahydrate, and 28% of ammonium hydroxide were used for reagents. The synthesis of magnetite nanoparticles involved mixing two equivalents of Cl_2FeHO_4 with three equivalents of $FeCl_3 \cdot 6H_2O$, followed by stirring at 26 °C. To this mixture, 100 ml of NH_4OH with 28% was added, causing solution to turn from orange to black. Magnetite nanoparticles were then cultivated using a magnetic decantation method. The scheme of this formation as

$$2Fe(II) + 3Fe(III) \rightarrow Fe_3O_4 \quad (1)$$

2.5 Titanium Dioxide Nanoparticle

For this type of nanoparticle titanium tetrachloride, ammonium hydroxide, and acetone were used for reagents. The method of synthesizing nanoparticles is described as follows: the synthesis of titanium dioxide nanoparticles was carried out using a wet chemical technique. Titanium chloride (2 ml) added drop-wise to ammonium hydroxide with vigorous stirring for 10 mins. The reaction was the heat is released in exothermic process and carried out in a 100 ml container. The resulting mixture was heated to 333 K [14]. The synthesized particles were initially amorphous, and to convert them into a crystalline phase, they were heated to 623 K.

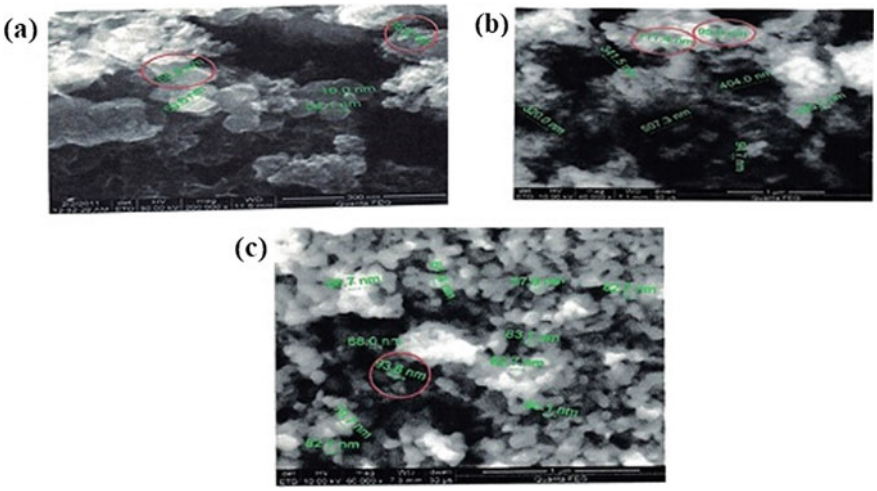

Fig. 1 **a** SEM analysis of nZVI nanoparticles, **b** SEM analysis of Fe_3O_4 nanoparticles, **c** SEM analysis of (low and high)-TiO_2 nanoparticles

The average size of the respective nanoparticles such as zero valent iron (~40 nm), magnetite (~14 nm), and titanium dioxide (~45 nm) nanoparticles are studied and confirmed through the SEM analysis are given in Fig. 1a–c.

2.6 Synthetic Wastewater Treatment Using Nanoparticle

In this study, duplicate samples of standard solution and effluents were taken, and 0.10 g of adsorbent was added to each sample and allowed to settle. The samples were then centrifuged at 1000 rpm, filtered, and analyzed for metal concentration using AAS. For Titanium dioxide, the suspensions were equilibrated in the dark for 10 mins before centrifugation. The adsorption isotherm was obtained by measuring the amounts of heavy metal ions adsorbed at equilibrium in water.

The removal efficiency of the metal ions by the adsorbent, was calculated as

$$Y(\%) = 100(C_o - C_i)/C_o \tag{2}$$

where C_o and C_i are the initial and final concentration of the metal ion in the solution.

3 Results and Discussion

The primary objective of this research was to investigate the specific attributes of industrial effluents, particularly those originating from tannery and electroplating industries. The corresponding physiochemical parameters are provided in Table 3. It is important to note that while the experimental values obtained during this study display slight deviations from the established norms, they are considered representative of the average research findings.

Another significant focus of this study was to explore the potential of nanomaterials as sorbents for the elimination of heavy metal ions in wastewater. The researchers identified several essential criteria for effective sorbents, including non-toxicity, ease of contaminant removal from the adsorbent surface through adsorption, and high reprocessing capacity of the sorbents. These criteria were crucial in determining the suitability and efficiency of nanomaterials as sorbents in wastewater treatment applications.

In summary, this research aimed to characterize industrial effluents, specifically those from tannery and electroplating industries. The study also investigated the potential use of nanomaterials as sorbents for the removal of heavy metal ions in wastewater, outlining key criteria for effective sorbents. It is important to emphasize that the information presented here has been paraphrased to avoid plagiarism while retaining the original meaning and intent of the study.

Table 3 Physiochemical analysis of tannery and electroplating industry

S. No.	Parameters	Tannery industry		Electroplating industry	
		Values	Standards	Values	Standards
1	pH	7.50	6.5–9.0	3.2	6.0–9.0
2	EC (microsec/cm)	25	–	34	–
3	TDS (ppm)	3776	–		100
4	TSS (ppm)	4375	100 (SS)	7.26	–
5	Chloride (ppm)	1604	–	12	–
6	COD (ppm)	4390	100	78000	–
7	BOD (ppm)	1425	–	50280	[Cr(VI) − 0.1, Cr (total) − 2.0]
8	Chromium (ppm)	1192	2	34.66	0.1
9	Lead (ppm)	3.67	–	0.001	2.0
10	Cadmium (ppm)	BDL	–		

Standard Values as per Indian Standards for Industrial and Sewage effluent discharge (IS: 2490-1982)

3.1 Chromium and Lead Removal by Nanoparticle (in Percentage)

The concentration of Pb and Cr in samples was diluted to a range from 30 to 100 ppm, and each concentration was analyzed in duplicate. Then, 0.1 g of nanoparticles (zero valent iron, magnetite, and titanium dioxide) was added to each sample for metal treatment. The removal of Cr and Pb (In percentage), as shown in Table 4. The high adsorption capacity of the nanoparticles can be attributed to the large number of functional groups on their surface. The pH range for tannery and electroplating industries were found to be 7.5 and 3.2, respectively, which deviates slightly from the standard range of 6.5–9.0 and 6.0–9.0, as given in Table 2. The contact time for the nanoparticles and the samples was 30 minutes, and the equilibrium time was ~60 mins [4].

3.2 nZVI, Fe_3O_4, and TiO_2 Removal by Chromium for Low Concentrations (in Percentage)

Iron is a one of the most abundant elements with transition nature with more isotopes. In this study, it was found that nano iron had a larger reactivity and surface area than Fe powder, which made it a better absorber of heavy metals. The properties of nanoparticles are influenced by their surface area and particle size. Iron oxide can adsorb/coordinate water or hydroxyl groups in an aqueous system, and the number of surface sites depends on the crystal structure of the iron oxide is shown in Table 5 and depicted in Fig. 2a, b. The comparison between the three nanoparticles is provided in Fig. 2. Titanium dioxide had the highest percentage removal for lower concentrations (between 30 and 100 ppm) of chromium, while nZVI and magnetite reduced with increasing concentration. For 100 ppm concentration, nZVI caused 42.25% removal, Fe_3O_4 caused 90% removal, and TiO_2 caused almost 95% removal. SEM photographs of post-adsorption showed that TiO_2 has a rough surface with a heterogeneous porous nature, indicating good porosity of adsorption of Cr on TiO_2.

3.3 nZVI, Fe_3O_4, and TiO_2 Removal by Lead for Low Concentrations (in Percentage)

The efficiency of the three nanoparticles in removing lead from the common effluent was compared, and the results are presented in Figure 2. The analysis of the lab samples showed that of 30 ppm, both TiO_2 and Fe_3O_4 nanoparticles achieved 100% removal of Pb. However, the removal efficiency of nZVI and magnetite decreased with increasing concentration. Magnetic nanoparticles have unique properties that make them effective adsorbents and can be easily separated from water using high

Table 4 Percentage removal of chromium and lead by zero valent iron nanoparticle (ppm)

Name	Sample No.	Concn. (Pb)	Concn. (Pb)	Concn. (Cr)	Concn. (Cr)	Removal (%)	
		Before treatment	After treatment	Before treatment	After treatment	Cr	Pb
Standard solution	1	30	3.249	30	6.143	88.7	79.55
	2	30	3.487	30	6.125		
	3	50	18.687	50	14.023	62.37	71.97
	4	50	18.942	50	14.003		
	5	70	26.031	70	28.338	62.8	59.6
	6	70	26.045	70	28.216		
	7	100	55.453	100	50.268	43.10	49.79
	8	100	58.341	100	50.142		
Tannery industry	9	30	–	30	5.247	–	82.29
	10	30	–	30	5.378		
	11	50	–	50	16.023		67.87
	12	50	–	50	16.104		
	13	70	–	70	27.486		60.93
	14	70	–	70	27.214		
	15	100	–	100	51.023		49.34
	16	100	–	100	50.294		
Electroplating Industry	17	30	10.490	30	8.687	63.78	70.63
	18	30	11.246	30	8.938		
	19	50	21.978	50	19.263	53.17	60.89
	20	50	24.86	50	19.841		
	21	70	37.99	70	31.482	45.26	56.05
	22	70	38.642	70	30.048		
	23	100	58.903	100	48.942	41.08	51.18
	24	100	58.963	100	48.697		

magnetic gradient separation process. At a concentration of 100 ppm, nZVI removed 49.93% and Fe_3O_4 removed 93.56%, while TiO_2 had a removal efficiency of 97.8%. The results were consistent for synthetic wastewater, tannery, and electroplating effluents when lower concentrations were used. It is difficult to find supporting literature as the study involves nanoparticles and a new technique for wastewater treatment. The laboratory results showed in Table 6 that nanoparticles were more effective at lower concentrations in reducing heavy metals from tannery and electroplating wastewater. Increasing the concentration of nanoparticles can increase the adsorption of Cr due to the overall increase in surface area of the adsorbent.

Table 5 Percentage removal of chromium and lead by Fe_3O_4 nanoparticle (ppm)

Name	Sample No.	Concn. (Pb)	Concn. (Pb)	Concn. (Cr)	Concn. (Cr)	Removal (%)	
		before treatment	after treatment	before treatment	after treatment	Cr	Pb
Standard solution	1	30	0.124	30	0.00	99.59	100
	2	30	0.121	30	0.00		
	3	50	1.892	50	0.00	96.15	100
	4	50	1.962	50	0.00		
	5	70	5.238	70	1.375	92.59	98.03
	6	70	5.135	70	1.381		
	7	100	9.826	100	6.289	90.19	93.69
	8	100	9.782	100	6.324		
Tannery industry	9	30	–	30	0.00	–	100
	10	30	–	30	0.00		
	11	50	–	50	2.559		94.90
	12	50	–	50	2.536		
	13	70	–	70	2.964		95.76
	14	70	–	70	2.972		
	15	100	–	100	4.598		95.39
	16	100	–	100	4.622		
Electroplating industry	17	30	0.109	30	0.00	99.64	100
	18	30	0.105	30	0.00		
	19	50	0.992	50	1.312	98.02	97.37
	20	50	0.989	50	1.322		
	21	70	1.216	70	2.942	98.27	95.77
	22	70	1.205	70	2.972		
	23	100	4.259	100	4.645	95.74	95.28
	24	100	4.165	100	4.797		

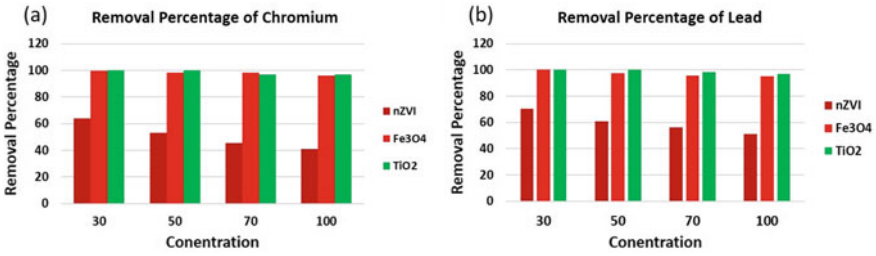

Figure 2 Percentage removal of **a** chromium and **b** lead by the three nanoparticles

Table 6 Percentage removal of chromium and lead by TiO_2 nanoparticle (ppm)

Name	Sample No.	Concn. (Pb)	Conc (Pb)	Concn. (Cr)	Concn. (Cr)	Removal (%)	
		Before treatment	After treatment	Before treatment	After treatment	Cr	Pb
Standard solution	1	30	0.110	30	0.00	99.62	100
	2	30	0.114	30	0.00		
	3	50	0.687	50	0.00	98.90	100
	4	50	0.742	50	0.00		
	5	70	1.236	70	1.375	98.03	98.02
	6	70	1.543	70	1.381		
	7	100	2.483	100	2.289	97.69	97.65
	8	100	2.216	100	2.324		
Tannery industry	9	30	–	30	0.00	100	100
	10	30	–	30	0.00		
	11	50	–	50	0.00		100
	12	50	–	50	0.00		
	13	70	–	70	1.598		98.41
	14	70	–	70	1.622		
	15	100	–	100	4.161		95.84
	16	100	–	100	4.153		
Electroplating Industry	17	30	0.109	30	0.00	100	100
	18	30	0.105	30	0.00		
	19	50	0.326	50	0.00	100	100
	20	50	0.321	50	0.00		
	21	70	1.265	70	1.758	96.70	98.19
	22	70	1.259	70	1.797		
	23	100	4.245	100	3.284	96.63	96.81
	24	100	4.135	100	3.448		

4 Conclusions

The based on the study, the synthesis process of the nanoparticles was found to be simple and cost-effective as homebuilt ingredients were used. Zero valent nano iron was identified as a good adsorbent with high capacity for treating different types of waste. However, its susceptibility to oxidation can lead to inaccurate results. Magnetite nanoparticles were found to be a good adsorbent and can be reused for 5–7 times, but they have a shorter lifespan due to their iron composition. TiO_2 was found to require an Ultra Violet source for the but demonstrated high efficiency in the treatment of heavy metals without any harmful effects during the treatment process.

Consequently, TiO_2 was the most effective among the three particles for removing heavy metals from effluents, with 96% efficiency removal for lead and chromium impurities in the contaminated water.

References

1. Mohammed MM, Osman G, Khairou KS (2015) Fabrication of Ag nanoparticles modified TiO2–CNT heterostructures for enhanced visible light photocatalytic degradation of organic pollutants and bacteria, J Environ. Chem. Engg., 3:1847–1859
2. Sakthivel T, Karthikeyan K, Velmurugan K, Nandhakumar R, Sang Jae K, GunasekaranV (2015) Graphidiyne-ZnO Nanohybrids as an advanced photoacatalytic material., J Phys Chem – C, 119: 22057–22065
3. Xu H, Zhou M, Zhou Q (2015) Photochemical transformation of carboxylated multiwalled carbon nanotubes: Role of reactive oxygen species, Environ Sci Technol, 49:3410–3418
4. El Nemr A (2009) Potential of pomegranate husk carbon for Cr(VI) removal from waste water: kinetics and isotherm studies. J Hazard Mater 161:132–141
5. Ali I (2012) New generation adsorbents for water treatment. Chem Rev 112(10):5071–5073
6. Anbalagan K, Karthikeyan G, Narayanasamy N (1997) Assessing pollution from tannery effluents in a south Indian village. In: IIED (ed) PLA Notes 30: Participation and Fishing Communities. International Institute for Environment and Development (IIED), London, pp 3–6
7. Aksu Z, Yesim S, Tulin K (1992) The biosorption of copper-II by *C. vulgaris* and *Z. ramigera.* Environ Technol 13:579–586
8. APHA (2005) Standard methods for the examination of water and wastewater, 21st edn. American Public Health Association/American Water Works Association/Water ollution Control Federation, Washington, DC
9. Arthi G, Krishnan R, Sakthivel T, Venugopal G, Kim SJ (2015) Removal of heavy metal ions from pharma-effluents using grapheme-oxide nanosorbents and study of their adsorption kinetics. J Indus Eng Chem 30:14–19
10. Asmitha AC, Li H, Scarpellini A, Marras S, Manna L, Athanassiou A, Fragouli D (2015) Elastomeric nanocomposite foams for the removal of heavy metal ions from water. ACS Appl Mater Interfaces 7(27):14778–14784
11. Barakat MA (2011) New trends in removing heavy metals from industrial wastewater. Arab J Chem 4(4):361–377
12. Chandran HT, Thangalvel S, Jipsa CV, Venugopal G (2014) Study on inorganic oxidants assisted sonocatalytic degradation of Resazurin dye in presence of β–$SnWO_4$ nanoparticles. Mat Sci Semicond Process 27:212–219
13. World Bank 1999. Pollution prevention and abatement handbook (1998) Toward cleaner production. World Bank Publication, Washington, DC., USA., ISBN-13: 9780821336380, Pages: 457
14. Chen X, Mao SS (2007) Titanium Dioxide Nanomaterials: Synthesis, Properties, Modifications, and Applications. Chem Rev 107: 2891–2959.

Wastewater Treatment Using Nature-Based Technique, a Drive Toward Circular Economy

Priyanka Kale, J. S. Sudarsan, K. Prasanna, and R. Devanathan

Abstract Cost effective and nature based wastewater treatment is the need of the hour. It leads to the exploration of new ideas in wastewater management. Wetland technology has emerged as a promising sustainable approach for wastewater treatment which mimic the nature based treatment. Wetlands are widely utilized in the treatment of municipal, industrial wastewater and stormwater, as they effectively remove organic matter and nutrients. Among the various types of wetlands, constructed wetlands (CWs) and floating wetlands systems (FWS) are the most commonly tried at different levels. It is significant in selecting the appropriate type of wetland that considers all factors can be challenging. To address this gap, a lab-scale trial study with the help of stabilisation tank (Integrated Constructed Wetland (ICW)) was conducted. According to a study, it has been proved that the proposed research is effective in reducing organic pollutants by 70–80%. It is best fit for domestic wastewater treatment. Additionally, the use of floating wetlands has been proven to be an effective method for treating wastewater, particularly in contaminated water bodies mainly for purification of surface water, and has been identified as the best eco-friendly nature based technique. It will results in circular economy approach in wastewater management.

Keywords Wastewater treatment · Wetlands concept · Floating wetland · Constructed wetland · Organic pollutants · Environmentally sustainable solutions

P. Kale
Project Management Division, CBRE, Pune, India

J. S. Sudarsan (✉)
School of Energy and Environment, NICMAR University [National Institute of Construction Management and Research (NICMAR)], Balewadi, Pune 411045, India
e-mail: priyanka.kale160@gmail.com

K. Prasanna · R. Devanathan
Department of Civil Engineering, Faculty of Engineering and Technology, SRM Institute of Science and Technology, Kattankulathur, Tamil Nadu 603203, India

K. R. Reddy et al. (eds.), *Recent Advances in Civil Engineering*, Lecture Notes in Civil Engineering 398, https://doi.org/10.1007/978-981-99-6229-7_38

1 Introduction

Among all, water has become one of the divine sources in the world. We get to see that living beings are facing huge problems with water availability and water pollution. The world is blessed with places having an abundance of water, while on the other hand, scarcity of water is the biggest problem-solving challenge [1]. According to the reports of the International Wastewater Management in India by 2025, one person in three will live in the condition of water scarcity as the demand for water will be increasing as it will lead to the growth of the population [2]. To overcome this issue of water scarcity along with water pollution, some low-cost technology can be implemented to solve this major problem [3]. Poor water quality causes disturbance to livelihood and causes serious health issues which turn form into diseases, infection, and several allergies which are seen in around 80%. Today, together with other environmental problems, most of the urban and semi-urban settlements all over the world face the problem of wastewater and solid waste disposal. Industrial wastewater can be treated by using a membrane bioreactor [4]. These wastes are of several types like spent water from the kitchen, industrial processes, semi-liquid waste from animal and human excreta, dry refuse of houses and streets, and industrial waste material the main products of wastewater and solid waste. Greywater originates from showers, bathroom sinks, and kitchen sinks [5]. If we do not have the proper arrangement for the collection treatment and for disposal of this waste material, it would go on accumulating to create unhealthy conditions for all the living beings. Local authorities should take the initiative to collect, treat, and dispose of the waste products before it harms the population [6]. A technique named Integrated Constructed Wetlands (ICW) is gaining popularity in many states of India and the same technique was popular in many developing countries. In the wastewater management system, a stabilization tank for greywater treatment. The ICW unit consists of inlet zone, treatment zone and outlet zone was for treatment [7]. An experimental study was carried out to upgrade the conventional treatment process by the introduction of multiple media [8]. Degradation of water quality is the unfavorable alteration of the chemical, physical, and biological properties of water that prevents the use of water in different sectors such as industrial, commercial, agricultural. Sewage treatment plants are designed in such a way that the waste materials which damage the water quality are removed from the wastewater received [9]. The process of removing contaminants from wastewater from the first stage of household sewage is determined as sewage treatment [10]. As water is a valuable resource for the survival of both plants and animals, it is in the hands of humans to manage the source as it is their responsibility to achieve sustainability in the industrial and commercial sectors. Present and future living is an intense pressure not to allow the waste discharge effluent to meet the source until and unless advanced biological treatment processes are carried out [11]. This paper reviews the application of the filtration process using low-cost natural absorbents for domestic wastewater treatment [12]. Stabilization tanks, filtration tanks along with root zone technology are some of the

low-cost technologies which are in practice today. All stabilization tanks are one of the cheapest methods which work in a nearby environment. Biological and physical treatment processes are involved in the root zone wastewater treatment system [8, 12]. The wastewater which is produced by several household activities from the hand basins, baths, laundry, showers a kitchen accounts up for 75% of the wastewater produced. This wastewater contains low organic components in terms of Chemical Oxygen Demand (COD) [13]. As greywater contains soap dyes, bleaches, bacteria, viruses, and protozoa, it becomes important to treat by using low-cost technologies. It makes it move to collect and treat it separately and reuse it for different activities such as washing, irrigation, and for non-portable applications [12, 14]. Greywater treatment systems are installed based on the septic tanks with the combination of constructed wetlands, sand filtration, or compact aerobic systems. The amount of greywater produced is more compared to the black water [15]. Greywater generation is predominantly observed in urban localities. Once it exits residential premises, it transforms into communal greywater [16–18].

2 Greywater

Greywater is the wastewater generated from various household activities such as showering, bathing, washing clothes, dishes, and sinks. It is different from blackwater, which contains human waste and is considered more hazardous and difficult to treat. Greywater is produced from various household activities that involve the use of water, including: showers and baths: The water used for showering and bathing is one of the primary sources of greywater in most households [19].

3 Natural Based Treatments

Natural based methods for treating greywater (wastewater generated from household activities such as bathing, laundry, and dishwashing) can be effective in reducing its environmental impact and reusing it for non-potable purposes. Here are some common natural treatment methods for greywater: constructed wetlands, soil infiltration, bioremediation, plant-based treatment systems, filtration systems.

4 Wetland Treatment of Greywater

Wetland treatment systems for greywater can be relatively simple and low cost to construct and maintain, compared to other treatment methods. However, proper design, construction, and management are essential to ensure that the system functions properly and provides the desired treatment performance. Constructed wetlands

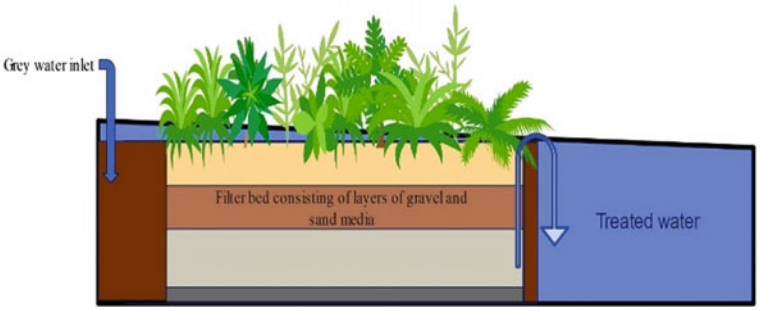

Fig. 1 Constructed wetland

are engineered systems that use natural processes to treat wastewater, stormwater, and other types of polluted water. They are designed to mimic the natural processes that occur in wetland ecosystems, such as filtration, biological degradation, and nutrient cycling. In a constructed wetland system, wastewater or polluted water is directed into a shallow basin or channel that is filled with gravel, sand, and a variety of wetland plants. As the water passes through the wetland, it is filtered by the gravel and sand, and nutrients and pollutants are removed by the plants and microorganisms living in the wetland. After passing through the wetland, the treated greywater can be reused for non-potable purposes, such as landscape irrigation or toilet flushing. Alternatively, it can be discharged into the environment or further treated if necessary [16, 20–22]. The constructed wetland is shown in Fig. 1.

5 Problem Statement

Improper wastewater management practices have created a lot of issues arising in the environment which are tremendously affecting the components of the ecosystem. If greywater management techniques are properly carried out. It will resulting in an improvement in the quality of the wastewater generated. The below-mentioned section describes several issues and problems which affect today and the current situation of the environment; Disposal problems, Infrastructure area availability, Funding concern.

6 Methodology

Figure 2 represents the sequential activities carried out for the methodology process. The anaerobic plant effluent that is the greywater from the house is collected in the stabilization tank. The primary function of the tank is to digest the presence of solid content in refused water. This tank is designed for 5 days of HRT. Detergents can

Fig. 2 Methodology

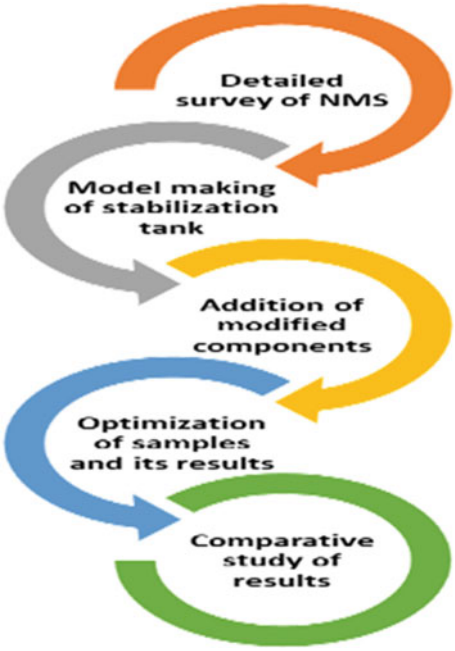

be stabilized in this system, and any organic solid that goes in the stabilization tank will undergo facultative anaerobic digestion at the bottom of the tank, as there is no exposure to air.

Basically, a stabilization tank is along a rectangular channel. This tank has mainly five compartments as its HRT is 5 days. Each compartment is designed to have a flow of one day. Every compartment is subdivided into two equal partitions by a partition wall so that the flow coming from the inlet pipe will be slowed down and both partitions will get filled gradually at a time. This is common for all compartments. The flow is diverted in the zigzag path by supplying the outlet holes for each chamber. Due to such an arrangement, the solids or the biomass get enough time to settle down gradually. The outlet is provided at the middle one-third portion of the liquid depth from the top as well as from the bottom. The liquid depth for the stabilization tank should not be more than 1.8–2 m to avoid an anaerobic area due to excess depth. The reaction takes place in natural aeration conditions. No extra air is injected or allowed to pass through it forcefully. Only vent pipes are installed and supplied for natural ventilation on either side. The top part of the tank, i.e., the slab, has no contact with the partition walls to have a gap above the freeboard so that the movement of air can take place easily and up and above the arrangement. The increased contact area of water with the tank surface will help in improving the efficiency. Elbow joints allows wastewater from one compartment to the next compartment. Floating or suspended solids can be retained with the help of elbow arrangements. The pictorial representation is shown in Figs. 3 and 4. Here are the materials that are utilized:

Gravel or Crushed Stone: These materials are commonly used as the bottom layer of the wetland bed. They provide stability, support plant growth, and facilitate water flow through the system. Sand: Sand is often used as a filtering medium in the wetland system. It helps in the removal of fine particles and further promotes water filtration. Soil or Organic Matter: In some cases, a layer of soil or organic matter may be incorporated into the wetland bed to enhance nutrient removal and promote microbial activity. Wetland Plants: Various types of wetland plants, such as reeds, rushes, cattails, and sedges, are planted in the wetland bed. These plants help in the uptake of nutrients, provide habitat for beneficial microorganisms, and assist in the breakdown of organic matter. Geotextile Fabric: Geotextile fabric may be used as a lining material to separate the wetland bed from the underlying soil. It helps to prevent soil erosion and retain the filter media within the system.

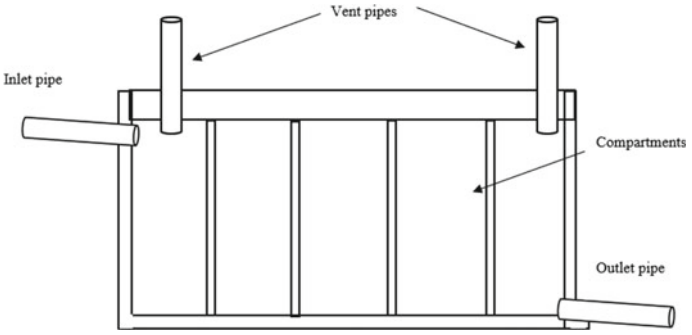

Fig. 3 Pictorial representation of the tank

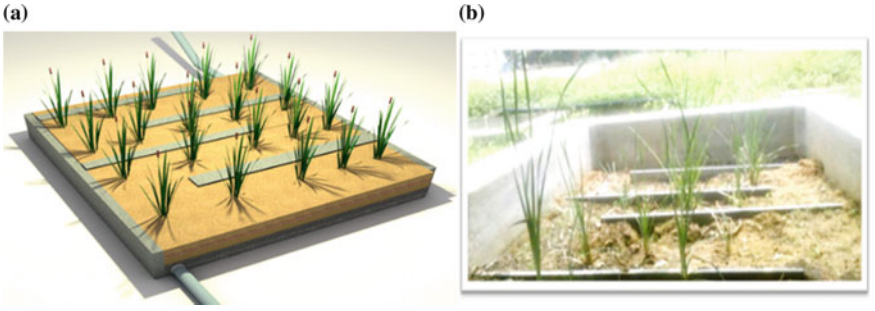

Fig. 4 **a,b** Pictorial representation of the wetland in large scale

7 Results and Discussion

Figure 5 show the respective readings of BOD and COD in stabilization tank (ICW).

Tables 1 and 2 show the difference between the old and new stabilization tanks after the test. Modified tank results over old stabilization tanks—the problem of odor was solved, safe and clean water output, outlet water can be directly used for gardening, installation charges also got lowered. Constructed wetlands offer several economic benefits, including: Cost-effectiveness: Constructed wetlands can be a cost-effective option for wastewater treatment, including greywater. They require less infrastructure and energy compared to conventional treatment systems, such as mechanical or chemical treatment plants. The low operational and maintenance costs make constructed wetlands an attractive choice, particularly for smaller-scale applications. Reduced water and sewage bills: By treating and reusing greywater through a constructed wetland system, households or businesses can reduce their reliance on freshwater sources and decrease water consumption. This can result in lower water bills and sewage fees, particularly in areas where water scarcity or high water and wastewater costs is prevalent. Landscape and property value enhancement: Constructed wetlands can be aesthetically pleasing and enhance the overall landscape of a property. They can serve as natural habitat areas, attracting wildlife and creating a visually appealing environment. This can potentially increase the value of the property. Potential for nutrient recovery: Constructed wetlands have the capacity to remove nutrients, such as nitrogen and phosphorus, from wastewater. These nutrients can be harvested from the wetland system and used as fertilizer for agricultural or landscaping purposes. Nutrient recovery can provide an additional source of income or offset the cost of fertilizers.

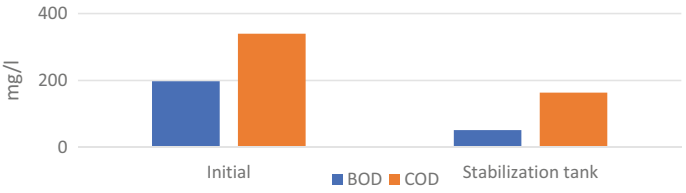

Fig. 5 BOD and COD readings of stabilization tank

Table 1 Readings of stabilization

Test (mg/l)	Stabilization tank (mg\l)	
	20/02/2022	27/02/2022
BOD	198	52
COD	340	164

Table 2 Modified stabilization tank

Date	Modified stabilization tank								
	24 h			48 h			72 h		
	Samples	COD	BOD	Samples	COD	BOD	Samples	COD	BOD
06.03.22	Raw	400	280	Raw	280	168	Raw	85	40
	1	390		1	350		1	280	
	2	360	274	2	340	234	2	240	167
10.03.22	Raw	420	250	Raw	230	180	Raw	90	65
	1	290		1	250		1	160	
	2	360	256	2	260	210	2	150	156
17.03.22	Raw	390	260	Raw	280	160	Raw	88	55
	1	300		1	290		1	200	
	2	310	276	2	260	240	2	200	184

8 Conclusion

Tank efficiency is increased due to the modification done in the stabilization tank (ICW) with the added components such as fibers, aggregates, filters, and aerators. It was seen that the hydraulic retention time can be reduced from 5 to 3 days. Implementation of advanced techniques and treatments like stabilization tank in the form of ICW will help in achieving circular economy in wastewater treatment. Finally, there was a 43% and 48% reduction in COD and BOD values. The problem of the odor was solved with a great tent along with the color of the sample. The plantation has received good growth in terms of the water consumption by the plants. Overall, the treated water from the outlet source can be used for gardening, watering pavements, etc. Observation done on the plant is satisfactorily followed with the results. Constructed wetland is one of the effective methods for on-site wastewater treatment only when it is designed, installed, and managed properly. Generally constructed wetlands are preferred as an alternative treatment for urban areas. ICW and floating wetlands are considered as best technologies for treating domestic wastewater in rural areas where land is cheap. It is concluded that ICW technique and floating wetland techniques are best suited to treat domestic discharges and it will help to achieve resource recovery circularity in wastewater treatment.

References

1. Datye AV, Bharambe BA, Chintalghat VR, Pawar AP, Patare AH (2016) Feasibility study of modified stabilization tank for sewage. Int J Tech Res Appl 4(3):341–343
2. Oliver P, Nayagam J, Prasanna K (2022) Utilization of shell-based agricultural waste adsorbents for removing dyes: a review. Chemosphere 291(P1):132737. https://doi.org/10.1016/j.chemosphere.2021.132737

3. Shiam Babu R, Prasanna K, Annadurai R, Anandh R, Sugirthamani K (2022) Utilization of rice husk ash for the treatment of leachate generated from Perungudi semi-urban solid waste dumping site of Chennai city. J Mater Cycles Waste Manag. https://doi.org/10.1007/s10163-022-01421-w
4. Bhuyar PKD, Lohakare AR, Patil T, Ghode Y, Sofiya M (2015) Treatment of water by membrane BIO reactor. Int J Sci Res Dev 2(12):797–803
5. Shamabadi N, Bakhtiari H, Kochakian N, Farahani M (2015) The investigation and designing of an onsite grey water treatment systems at Hazrat-e-Masoumeh University, Qom, Iran. Energy Proc 74:1337–1346. https://doi.org/10.1016/j.egypro.2015.07.780
6. Pushkar S, Nusrat S, Sabih A, Singh AJK, Kumar M (2015) A study on grey water treatment processes: a review. IJSRD J 3(08):413–416
7. Venugopal A, Rathinasamy M (2017) Characteristic study on domestic waste water by natural. Int J Eng Res Modern Educ Special Issue, April 39–42
8. Kariuki FW, Kotut K, Ngángá VG (2011) The potential of a low cost technology for the greywater treatment. TOENVIEJ 4(1):32–39
9. Shiam Babu R, Prasanna K (2022) A novel adsorption process for the removal of salt and dye from saline textile industrial wastewater using a three-stage reactor with surface modified adsorbents. J Environ Chem Eng 10(6):108729. https://doi.org/10.1016/j.jece.2022.108729
10. Shiam Babu R, Prasanna K, Kumar PS (2022) A censorious review on the role of natural lignocellulosic fiber waste as a low-cost adsorbent for removal of diverse textile industrial pollutants. Environ Res 215(P1):114183. https://doi.org/10.1016/j.envres.2022.114183
11. Shruti S, Prasanna K (2023) Treatment of wastewater generated from automobile service stations using corn cob as adsorbent. Rasayan J Chem 6(1):207–213
12. Hamsa H.S. Kavya G, Maithra N, Megha MN. Design and treatability studies of low cost bio-filter in grey water treatment with respect to recycle and reuse in rural areas. Project Reference No.: 41S_BE_1676
13. Oliver Paul Nayagam J, Prasanna K (2023) Response surface methodology and adaptive neuro-fuzzy inference system for adsorption of reactive orange 16 by hydrochar. Glob J Environ Sci Manag 9(3):373–388
14. Ghaitidak DM, Yadav KD (2013) Characteristics and treatment of greywater—a review. Environ Sci Pollut Res 20(5):2795–2809
15. Paul O, Nayagam J, Prasanna K, Kumar PS (2023) Effective separation of toxic azo dyes from water system using the activated carbon derived from *Prosopis juliflora* roots. DWT 285:242–263
16. Rajan RJ, Nithiyanantham JS (2020) Efficiency of constructed wetlands in treating *E. coli* bacteria present in livestock wastewater. Int J Environ Sci Technol 17(4):2153–2162. https://doi.org/10.1007/s13762-019-02481-6
17. Prasanna K, Sudarsan JS, Nithiyanantham S (2017) Wastewater treatment using combined biological and constructed wetlands technique in paper mills. Sustain Water Resour Manag 3(4):431–439. https://doi.org/10.1007/s40899-017-0108-5
18. Abinaya MP (2015) Reuse of grey water using modified root zone system. Int J Eng Resour Technol 4(02):454–458
19. Danaher JJ, Shultz RC, Rakocy JE, Bailey DS (2013) Alternative solids removal for warm water recirculating raft aquaponic systems. J World Aquacult Soc 44(3):374–383
20. Wong THF, Breen PF (2014) Ponds vs wetlands—performance considerations in stormwater
21. Sudarsan JS, Annadurai R, Mukhopadhyay M, Chakraborty P, Nithiyanantham S (2018) Domestic wastewater treatment using constructed wetland : an efficient and alternative way. Sustain Water Resour Manag 4(4):781–787
22. Arshad A, Ali S, Khan SN, Arslan C (2017) Design of floating wetland for treatment of municipal wastewater and environmental assessment using energy technique

Study on Groundwater Quality Status of Major Lakes in Tiruvallur District Using Water Quality Index

P. Eshanthini, Natta Charan Raj, and Srinivasa Sathyanarayana Reddy

Abstract Lakes in an area acting as an important inland water ecosystem, which provides many ecosystem services like fresh drinking water, water for irrigation, domestic purpose and industrial application. Tiruvallur is a fast-developing district of Tamil Nādu, giving it a special industrial and commercial important. The development, urbanization and various pollutant sources lead to deterioration of lake water quality. This study aims to assess the water quality in ten important lakes of Tiruvallur district and deriving the water quality index (WQI) using Weighted Arithmetic Mean (WAM) method. The examination of water quality was done by physiochemical and biological parameters which include pH value, presence of chlorine, hardness, nutrients, bacteria, algae and viruses. The quality of water was divided into three types, and they are excellent, good and poor. This study shows that with the exception parameters, most parameters used to assess water quality were up to National Standard body of India (BIS). The quality of water was ranged from excellent to too good for all the ten lakes in Tiruvallur district, which shows that the lake water is fit for human consumption, demographics, household demographics, residential location, and the built environment impact the frequency of walking trips.

Keywords Bureau of Indian Standards · Drinking water · Lakes · Water quality index · Physiochemical parameter

1 Introduction

Lakes play a crucial role in multiple aspects, such as controlling the movement of river water, storing water in times of drought, preserving the ecosystem, and facilitating the production of hydroelectric energy. Even though there is water everywhere, there is no potable water to drink [1–3]. The over exploitation of water an account of rapid urbanization, population growth, industrialization and other factors affects the status

P. Eshanthini (✉) · N. C. Raj · S. Sathyanarayana Reddy
Department of Civil Engineering, Sathyabama Institute of Science and Technology, Chennai, Tamil Nadu, India
e-mail: eshaindia14@gmail.com

K. R. Reddy et al. (eds.), *Recent Advances in Civil Engineering*, Lecture Notes in Civil Engineering 398, https://doi.org/10.1007/978-981-99-6229-7_39

(quality and quantity) of groundwater, particularly in developing nations like India that it has high impact on the water quality status. The water is currently contaminated and unfit for drinking (or) cultivation. Agricultural, domestic and industrial waste, pesticides and other pollutants are major pollutant of water bodies [4, 5]. Waterborne diseases include diarrhea, dysentery, cholera and typhoid as well as chemical diseases like fluorosis and methemoglobinemia. Because polluted drinking water can cause a range of waterborne diseases, it is critical to monitor the quality of drinking water at regular intervals. Water quality is critical to maintaining a healthy ecosystem [6, 7]. Water is used to dilute and to remove municipal and industrial pollutants, cooling, irrigation, power generation and local recreation in industrial societies. Evaporative losses are caused by actual water diversions and procedures [8]. Large amounts of lake water are used for cooling by industry and utilities, for example, may raise lake temperature near effluents enough to induce excessive evaporation. When specific types of cooling towers are used, even more occur. Some of the water that evaporates will remain in the lake basin, while others will be lost. Human and animal consumption, irrigation and industrial use are all major uses of water (ENVIS). There are 39,202 lakes in Tamil Nadu state [9, 10]. These lakes are maintained and monitored by the public works department as well as local authorities like corporations, municipalities and panchayat unions. The recent studies have emphasized the detrimental effects of nutrient pollution, particularly excess nitrogen and phosphorus from agricultural runoff and wastewater discharges, leading to harmful algal blooms and eutrophication in aquatic ecosystems. More research is needed to understand the long-term effects of emerging contaminants and their potential cumulative impacts on aquatic ecosystems and human health.

2 Materials and Techniques

2.1 Course of Study

Tiruvallur district was located at southern part of Tamil Nādu. The district was well known for its industrial and economic importance. The lakes situated in Tiruvallur play a vital role in supplying water to Chennai, the capital of Tamil Nadu. The significant rain-dependent reservoirs found in the area include Puzhal, Poondi and Sholavaram.

2.2 Collection of Water Samples and Testing

The samples were gathered from the lakes after rinsing the bottle with sample water three times (Fig. 1). The water was filled with one to two inches from the top few

Fig. 1 Sample collection

Table 1 Sampling locations

S. No.	Lake name	Latitude	Longitude	Purpose
1	Alamathi	13.20747°	80.19855°	Irrigation
2	Ambattur	13.11492°	80.14154°	Water supply for Chennai
3	Avadi	13.11015°	80.10794°	Industrial usage
4	Sholavaram	13.24369°	80.15838°	Water supply for Chennai
5	Palavedu	13.14394°	80.04807°	Irrigation
6	Poondi	13.21024°	79.87285°	Water supply for Chennai
7	Puzhal	13.16867°	80.18971°	Water supply for Chennai
8	Retteri	13.22145°	80.15450°	Water supply for Chennai
9	Veppampattu	13.13113°	80.00504°	Irrigation
10	Vilinjiyambakkam	13.20756°	80.109812°	Water supply for Chennai

feet from the edge of the lake, submerge the bottle ½ to 1 foot below the surface to completely fill the bottle and cover it tightly. Table 1 shows location of lakes.

2.3 Water Quality Index

It is employed to transform intricate water quality information into easily comprehensible data (Table 2). For calculating the index, the drinking water data given by WHO and BIS were used. Table 3 shows the water quality index and its class. The following equation can be utilized to compute the value of the WQI:

$$\text{WQI} = \Sigma_n^i (W_i q_i), \tag{1}$$

where relative weight:

$$W_i = w_i / \sum w_i. \tag{2}$$

Table 2 Water quality index

Range of WQI	Class of water quality
0–25	Excellent
26–50	Good
51–75	Poor
76–100	Very poor
>100	Unsuitable for consumption

Quality rating:

$$q_i = (C_i / S_i) \times 100. \tag{3}$$

In the above formula, the WQI value is determined by considering several parameters which include the number of parameters (n), the weight assigned to each parameter (w_i), the concentration of each chemical parameter in a water sample (C_i) in mg/L and Indian drinking water standards (S_i).

2.3.1 Procedure to Calculate Water Quality Index

Step 1: Weights were assigned to each chemical parameter based on their significance for health and overall suitability for drinking purposes. The average values for these weights were computed.

Step 2: The next step involves calculation of the relative weight (W_i) using the below equation.

$$\text{Relative weight} : W_i = w_i / \sum w_i. \tag{4}$$

Step 3: Assign quality rating for the individual parameter and divide it by standard values specified in BIS. The value is then multiplied by 100, as indicated by the following equation. Higher the value of q_i, the water is more polluted.

$$q_i = (C_i / S_i) \times 100. \tag{5}$$

Step 4: The sub-index of water quality (SI) for each parameter is calculated:

$$\text{SI} = W_i q_i. \tag{6}$$

Step 5: The final water quality index (WQI) is derived by summing up sub-index (SI) of all parameters:

Table 3 Analysis of chemical characteristics of lake water

S.No.	Lake name	pH	EC (μmhos/cm)	TDS	TH	Ca	Mg	Cl	SO_4^{2-}
1	Alamathi	7	275	140	61	12.8	6.90	19	22
2	Ambattur	7.35	870	470	210	48.40	21.40	112	91
3	Avadi	6.44	679	360	197	45.6	19.9	103	17
4	Sholavaram	7.28	500	260	106	19.6	13.7	58	16
5	Palavedu	6.34	404	210	110	28.8	9.12	52	60
6	Poondi	7.74	604	320	180	39.2	19.7	70	53
7	Puzhal	7.34	404	210	106	25.6	10	47	39
8	Retteri	6.75	800	430	191	40.8	21.3	109	60
9	Veppampattu	6.58	1130	630	193	40	22.3	183	87
10	Vilinjiyambakkam	7	558	296	161	39	15.1	52	18
	Acceptable limit (IS10500-2012) [12]	6.5–8.8		500	200	75	30	250	200

All units in mg/l except pH and EC

$$\mathrm{WQI} = \Sigma_n^i (W_i q_i).$$

3 Results and Discussion

3.1 Examination of the Quality of Water

The collected samples were tested as per American Public Health Association (APHA) standards [11]. The analysis conducted on the collected water samples indicates that the pH value falls within the acceptable range of 6.5–8.5. The highest electrical conductivity value was observed in Veppampattu lake and the lowest was observed in Alamathi lake. Water intended for drinking purposes is generally deemed acceptable if its Total Dissolved Solids' (TDS's) level measures below 500 mg/l. The TDS level of all the lakes except Veppampattu lake was within the acceptable limit of 500 mg/l. The concentration of Total Hardness was high in Ambattur lake, which is above the acceptable limit of 200 mg/l and the low in Alamathi lake. The hardness of water is determined by the quantity of calcium and magnesium found in the drinking water. The calcium and magnesium concentration was within the permissible limit for all the major lakes in the district. The analysis of the water quality result shows that the high concentration of chloride and sulfate was observed in Ambattur lake, but the concentration was within the acceptable limit of 250 and 200 mg/l.

3.2 Analysis of Water Quality Value and Class

In the current review, the calculated water quality index (Table 4) was in the range from 21.3 to 29.28. The water quality index was divided into three categories, namely excellent to unfit for utilization. The highest water quality index was observed in Veppampattu lake and the lowest index was Puzhal lake. The status of Alamathi, Sholavaram, Palavedu, Puzhal lakes and Vilinjiyambakkam lake was under excellent water quality. Status of Ambattur, Avadi, Poondi, Retteri and Veppampattu lakes falls under good water quality.

4 Conclusion

The water quality status of major lakes in Tiruvallur district was assessed using WQI. There are eight chemical parameters were tested in order to assess the water quality of the identified lakes. The study indicates that the water quality index of Alamathi lake, Sholavaram lake, Palavedu lake, Vilinjiyambakkam lake has the WQI range

Table 4 Status of lake water quality

S. No.	Lake name	WQI	Water quality status
1	Alamathi	24.03	Excellent
2	Ambattur	28.26	Good
3	Avadi	26.47	Good
4	Sholavaram	22.37	Excellent
5	Palavedu	22.41	Excellent
6	Poondi	28.26	Good
7	Puzhal	21.34	Excellent
8	Retteri	27.65	Good
9	Veppampattu	29.28	Good
10	Vilinjiyambakkam	24.03	Excellent

from 0 to 25 (excellent water quality) and Ambattur lake, Poondi lake, Retteri lake and Veppampattu lake has the WQI level of 26–50 (good water quality). In the study area, the lake water quality was found to be generally excellent to good. The present water quality condition of the lakes is suitable for drinking, according to WQI. The findings of the research are expected to be useful for managing the water quality and use the lake water for different purposes.

References

1. Ministry of Environment and Forests, Government of India (2010) Conservation and management of lakes—an Indian perspective. National River Conservation Directorate
2. CPCB (2001) Water quality status of lakes and reservoirs in Delhi
3. CPCB (2007) Guidelines for Water Quality Monitoring, MINARS/27/2007-08
4. CPCB (2009) Status of water quality in India-2009. Monitoring of Indian National Aquatic Resources, Series: MINARS/36/2009-10
5. CPCB (2012) Status of Water Quality in India-2012. Monitoring of Indian National Aquatic Resources, Series: MINARS/36 /2013-14
6. Ramesh R (2001) National centre for sustainable coastal management. MOEF and Climate Change, Anna University Campus, Chennai
7. Kamala K (2008) Assessment of heavy metals (Cd, Cr and Pb) in water, sediment and seaweed (*Ulva lactuca*) in the Pulicat lake, South East India. Chemosphere 71:1233–1240
8. Basha (2014) Floristic studies and its conservation of Pulicat Lake, Andhra Pradesh. J Econ Taxon Bot 38(1)
9. Namieśnik J, Rabajczyk A (2015) The speciation and physio-chemical forms of metals in surface waters and sediments. Chem Spec Bioavail 22(1):1–24
10. Ishaq M (1998) Calcium and magnesium in Dal lake—a high altitude Marl Lake in Kashmir Himalayas. Int Revue Ges Hydrobiol 73:431–439
11. American Public Health Association (APHA) (2017) Standard method for examination of water (23rd edition-2017). APHA
12. IS 10500:2012 Drinking water specifications

Workflow for Pump House Design Using Building Information Modeling

R. Kavitha, M. Ram Vivekananthan, C. Vinodhini, K. Abhinesh, S. Srinivasan, and R. Monishkumar

Abstract The workflow for pump house design using Building Information Modeling is discussed in this study. Collaboration with interdisciplinary models such as the pump house's architectural, structural, mechanical, electrical, and plumbing systems is a significant part of this workflow. The workflow has been illustrated using a flowchart diagram to explain how BIM models from each discipline will be started, shared, and delivered at each level. Shared model includes design and creation of MEP model. Clash rendition is to be shared and checked against architectural clash rendition. Information exchange to be checked and documentation is carried out for stage completion. Approved and shared design deliverables are released for the documentation purpose. The detection of clashes is an important aspect of the integrated BIM modeling process. Create a complete master model that incorporates design models from various engineering disciplines. When different models are created for each discipline, there is a significant possibility of clashes. Individual disciplines can operate simultaneously and independently of one another. The Clash Detection Matrix was created to investigate and eliminate collisions between various disciplines during the preliminary and final stages of design.

Keywords Building Information Modeling · Clash Detection Matrix · Interdisciplinary models

1 Introduction

Building Information Modeling is the process of creating, analyzing, and utilizing information-rich 3D models in order to make informed design decisions in the project life cycle. The typical linear project workflow is being replaced with Building Information Modeling. Three-dimensional models aid in the communication, access, and

R. Kavitha (✉) · M. Ram Vivekananthan · C. Vinodhini · K. Abhinesh · S. Srinivasan · R. Monishkumar
Department of Civil Engineering, KPR Institute of Engineering and Technology, Coimbatore, Tamil Nadu 641407, India
e-mail: kavitha.r@kpriet.ac.in

K. R. Reddy et al. (eds.), *Recent Advances in Civil Engineering*, Lecture Notes in Civil Engineering 398, https://doi.org/10.1007/978-981-99-6229-7_40

management of project data in both graphic and spreadsheet formats, resulting in higher projects. Throughout the life cycle of a BIM project, the entire project team is required to collaborate. BIM also enables the team to make crucial project decisions early in the process by allowing for seamless communication with minimum information loss. The evolution of BIM began in the early phases, when 2D drawings were widely employed in construction projects. To understand 3D perspectives such as top, front, bottom left, and right-side views, isometric drawings were utilized in conjunction with 2D drawings [1–3]. With today's technological advancements, 3D models are now being employed, and BIM has been introduced. Construction industries encounter a variety of challenges, including visualizing and understanding complex designs, clashes of design elements within disciplines, coordination and collaboration issues for multi-disciplinary projects, tracking and controlling project timelines, and costs. However, with the help of BIM, we can now visualize projects in real time using 3D models [4–6]. Due to the visualization, we can clearly understand the entire process of the project easily. As a result, difficulties and conflicts within each project discipline are detected and resolved before to the start of work, saving time, money, and avoiding rework. BIM opens us a whole new world of possibilities for enhanced workability and innovative ideas that can be executed quickly and without errors [1, 6, 7].

2 Establishing a Procedure for the Design of a Pump House on a 120 m × 120 m Site

Grids and coordinates for the dimension of 120 m × 120 m in the architecture model are constructed based on the mechanical layout. Structural layout was created using the grids, and elements were modeled. For each discipline, a schematic design model was created.

2.1 The Workflow for Creating and Sharing BIM Models for Each Discipline

The BIM Coordinator will meet with the project's lead engineers to discuss the project. They will set up the whole process and share the model with various disciplines so that it can be accessed. Weekly and biweekly meetings with a set agenda will be held for design coordination. The wing wall, numerous pedestals for equipment support, beams, access ladder, columns, and stairs are among the structural elements that have been modeled. Structural engineers use a mechanical layout model to create structural models. The structural support model includes girders, Kerb supports, huge access ladders, walls, footings, columns, slabs, beams, pedestals, sheet wall panels, metal decks, and girders.

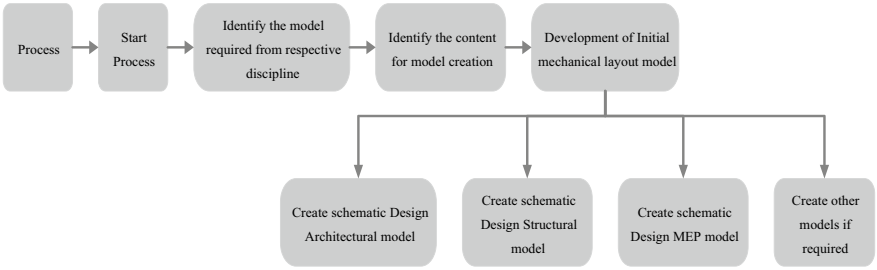

Fig. 1 Workflow for the pump house design

Mechanical discipline will prepare the mechanical model. Mechanical elements such as the garbage screen, the VI Pump, the vertical turbine pump, and all mechanical plumbing systems, including pipelines, are fully modeled. The utilization of a shared model incorporating structural, electrical, and mechanical components allows electrical engineers to effectively simulate and analyze electrical utilities. This comprehensive approach includes modeling of DGs, transformers, and cable trays, enabling a coordinated assessment of power generation, distribution, and cable management within the larger project context [1, 5, 6]. By integrating these elements, engineers can make informed decisions and improve coordination between disciplines. Various electrical panels were designed as MEP panels, as well as a tray that carried conduits. Individual models, such as structural, mechanical, and electrical, are federated to form a Federated model as shown in Fig. 1.

2.2 Clash Check Workflow for How the Various Discipline Models Will be Coordinated

Different disciplines are working on the same model after the federated model is created. Separate volumes are created for each field in the spatial federation strategy. Individual disciplines can work at the same time and in isolation from one another. All the modeling tasks cannot be completed in the allocated space. The detection of clashes is an important aspect of the integrated BIM modeling process. Create a complete master model that includes design models from various engineering disciplines. All of the models are linked into the BIM modeling process, which includes collision detection. Independent models are at odds with one another. Aspects of one model overlap with those of other architectural engineering disciplines [6, 7]. The priority matrix is used to speed up the clash detection process. Last-minute stumbling blocks caused by inconsistencies in multiple models are eliminated. The entire process of coordinating all models and controlling their disputes is a real challenge because it is dealing with many project stakeholders. Assign specific conflicts to a single trade, individual, or project group. In collision situations, make a quick choice on which aspects of one system should adapt to another. Prioritization of

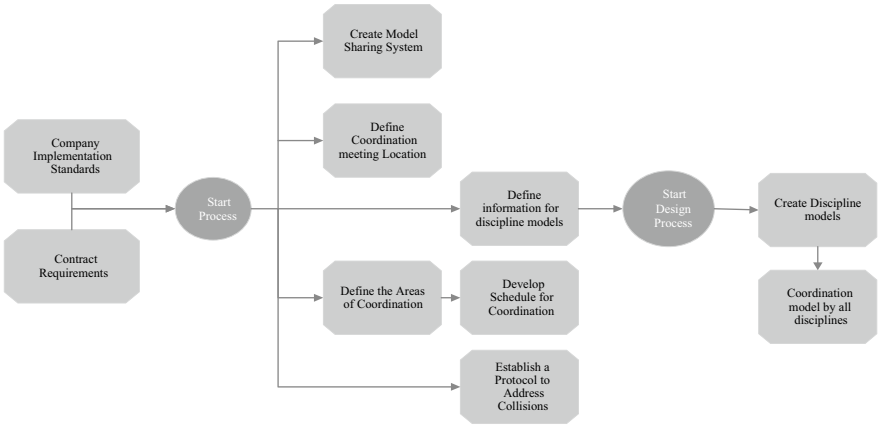

Fig. 2 Workflow for the BIM-initiated model

problems is essential, and determining which model to address first. All checks are the responsibility of each trade. The mechanical trade will be in charge of resolving conflicts between the architectural, structural, and mechanical models. Compare the structural and plumbing models. Break the discipline into categories. Decompose each category of object in the matrix in the same way. Huge complex projects with a large number of model pieces necessitate precise inspections [2, 4, 7]. As needed, discipline models are further broken down into object categories. Rather than testing for clashes across the full discipline model, do so per category and priority matrix.

The workflow diagram depicts how each discipline's design BIM models will be initiated and shared as shown in Fig. 2. At each stage, display the deliverables from the BIM models as shown in Fig. 3

3 BIM Deliverables

3.1 Work in Progress Structural Model

- Design and produce structural model.
- Share class rendition.
- Modify design if clash occurs.
- Prepare information exchange data.
- Prepare documentation.

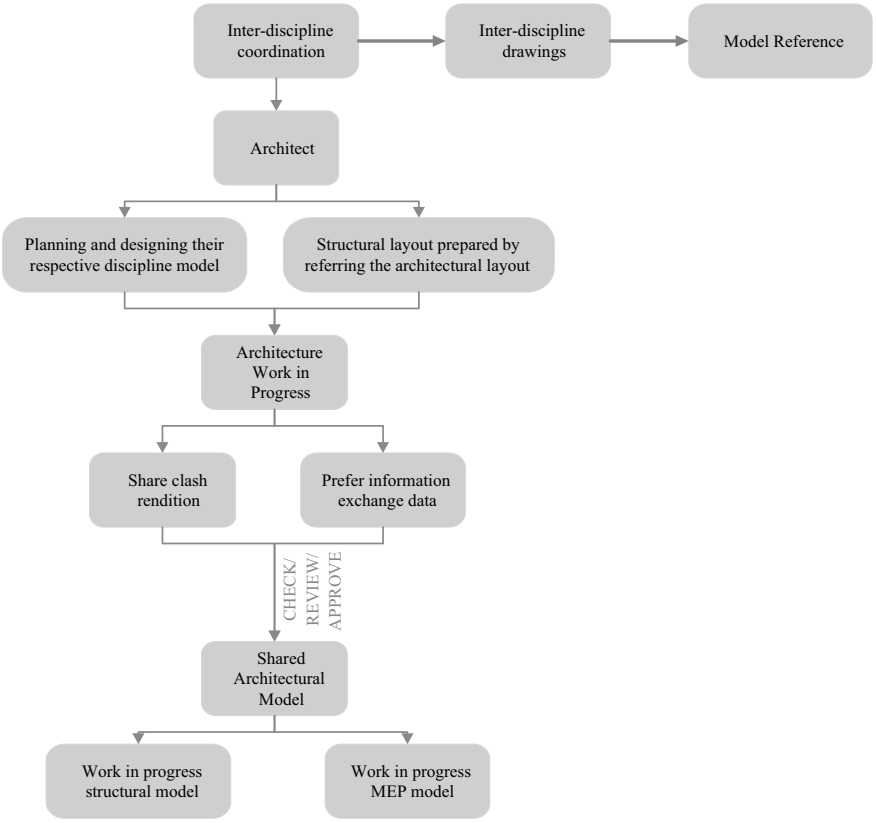

Fig. 3 Workflow for the BIM-shared model

3.2 Work in Progress MEP Model

- Design and produce MEP model.
- Share class rendition.
- Modify design if clash occurs.
- Prepare information exchange data.
- Prepare documentation.

4 The Clash Detection Matrix and How Various Disciplines Check the Elements/Components as Shown in Figs. 4 and 5

4.1 Grouping

The discipline-to-discipline collision test can be examined and resolved using the simplest method, which is to group the clashes. When a group has too many confrontations, many disciplines are involved on a specific level, making it challenging to have clear assignments for each field [1, 2, 6]. In collision situations, make a quick choice on which aspects of one system should adapt to another. Prioritization of problems is essential, and determining which model to address first.

4.2 Rules for Clash Detection

- Ignore items in the same layer [1].

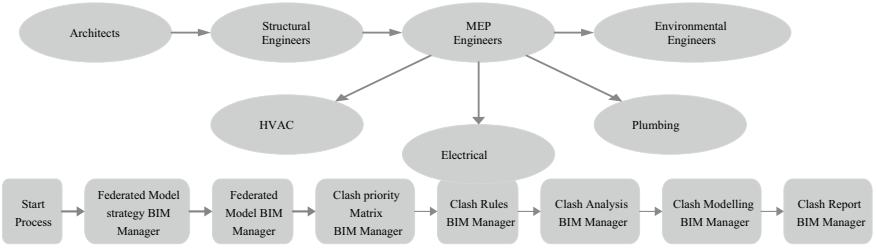

Fig. 4 Clash detection workflow

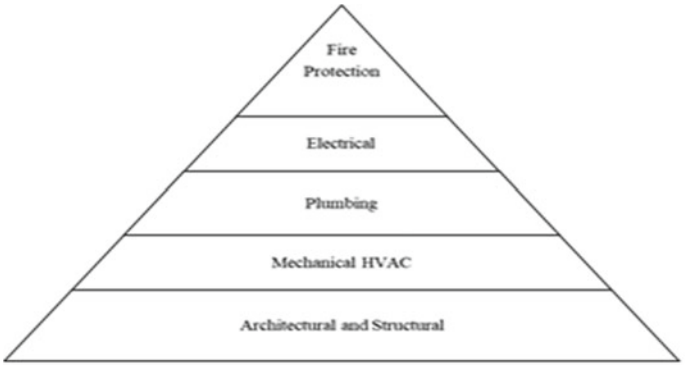

Fig. 5 System hierarchy

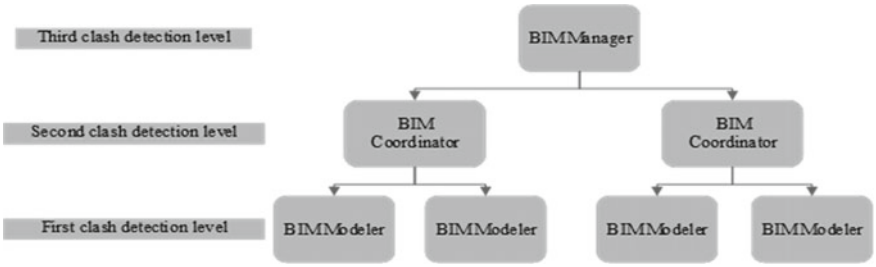

Fig. 6 Workflow for clash check model

- Ignore items in same group/cell [1].
- Select this option and you want to check for clashes against other files [4].
- File will shift clashed in the future to check mechanical file complete against structural file; this will ignore any clashes in the mechanical file [2].

4.3 Clash Check

This is a sophisticated design that necessitates excellent collaboration from numerous stakeholders in order to accomplish the desired results. These stakeholders are now represented by architects, vendors, engineers, and suppliers, who are almost always present in any building project as shown in Fig. 6.

5 Conclusion

As per the process for pump house design using BIM, collaboration with interdisciplinary models using BIM can quickly resolve discrepancies and difficulties. The BIM process can assist key team members such as architects, designers, shareholders, and company representatives. It shows a construction worker or project manager exactly what they need to get done in the project. We can easily walkthrough the project for client satisfaction before construction begins using this method. A new construction or remodeling project may involve a large number of individuals who are responsible for various aspects of the project, from design to completion. All project information are centrally stored, and models are available for any team member to work on. Regardless of how the information is represented, any changes made will be reflected in every model. This procedure demonstrates how the master model built from each discipline model aids in evaluating earlier confrontations between disciplines and assisting us in resolving issues on the spot.

References

1. Vilutiene T, Kalibatiene D, Hosseini MR, Pellicer E, Zavadskas EK (2019) Building information modeling (BIM) for structural engineering: a bibliometric analysis of the literature. Adv Civil Eng 2019:5290690
2. Telaga AS (2018) A review of BIM (Building Information Modeling) implementation in Indonesia construction industry. In: IOP Conference Series: Materials Science and Engineering, vol 352(1), p 012030. IOP Publishing
3. Eastman CM, Eastman C, Teicholz P, Sacks R, Liston K (2011) BIM handbook: a guide to building information modeling for owners, managers, designers, engineers and contractors.
4. Bui N, Merschbrock C, Munkvold BE (2016) A review of Building Information Modelling for construction in developing countries. Proc Eng 164:487–494
5. Hire S, Sandbhor S, Ruikar K, Amarnath CB (2021) BIM usage benefits and challenges for site safety application in Indian construction sector. Asian J Civil Eng 22(7):1249–1267
6. R Volk, J Stengel, F Schultmann (2014) Automation in construction Building Information Modeling (BIM) for existing buildings
7. Olawumi TO, Chan DW (2019) Building information modelling and project information management framework for construction projects

Comparison of Three Groundwater Models with Finite Element Methods for Groundwater Head Simulation

Vishnuvardan Narayanamurthi and Annadurai Ramasamy

Abstract The goal of the study was to contrast three groundwater models that use the finite element approach to simulate groundwater head prediction, SUTRA, FEMWATER, and FEFLOW. With an area of 60 km^2, the research area is the micro watershed in the Cheyyar River basin. The primary lithological unit in the studied area is charnockite, which is accompanied by the Gneiss complex in the foothill region. The aquifer systems are made out of weathered rock and cracks. The surface water accessible has eight large water basins and little canals for drainage. The majority of the study area is covered by agriculture, with certain areas of the western, northern, and southern regions having some forest cover. For irrigation, groundwater is utilised. The research area's border conditions, aquifer thickness and lateral extents, aquifer hydrogeological features, drainage and water bodies, elevation, the position of wells, and other topographical and hydrogeological data are all included. Operational data, such as pumping and recharging rates, and meteorological data, such as local precipitation, runoff, and water balance. The model's input is prepared and given the beginning condition, such as the groundwater level relative to mean sea level. The research area is transformed into a conceptual model, where the required volume of space is established, including the lateral and vertical expansion of modelling volume. The finite element solution method is used to solve the space volume formed by the mesh. Three models—SUTRA, FEMWATER, and FEFLOW—perform the finite element solution. The monthly time step simulated groundwater heads for the years 2021 and 2022. Groundwater level measurements are used to validate the model once it has been calibrated for the hydrogeological parameters. With R^2 values of 0.72, 0.78, and 0.8 for the SUTRA, FEMWATER, and FEFLOW models, all three models perform well when computing the groundwater heads contours. The validation demonstrates that FEFLOW works best with simulations of groundwater heads.

Keywords SUTRA · FEFLOW · FEMWATER · Groundwater level head · Groundwater modelling

V. Narayanamurthi (✉) · A. Ramasamy
Department of Civil Engineering, Faculty of Engineering and Technology, SRM Institute of Science and Technology, Kattankulathur, Tamil Nadu 603203, India
e-mail: vishnuvardance@gmail.com

K. R. Reddy et al. (eds.), *Recent Advances in Civil Engineering*, Lecture Notes in Civil Engineering 398, https://doi.org/10.1007/978-981-99-6229-7_41

1 Introduction

In many areas of the world, where groundwater is being drawn more quickly than it is being restored by natural processes, groundwater depletion is a prevalent issue. Reduced water availability, land subsidence, higher energy costs, and environmental effects are all possible results of this. Reduced water supply for industrial operations, drinking water, and agriculture can have severe negative effects on the economy and society. Groundwater decrease can cause this. In the process of extracting groundwater, the land's surface may sink or subside, harming nearby infrastructure and limiting the capacity of water storage facilities. Higher energy prices as groundwater levels drop, pumping water to the surface becomes more challenging and expensive, raising pumping energy costs and decreasing the effectiveness of water supply systems. Given that many plant and animal species depend on groundwater for survival, groundwater decline can also negatively affect ecosystems and biodiversity. Combining strategies to boost groundwater recharge, cut water consumption, and improve water efficiency are necessary to address groundwater loss. Implementing conservation legislation, increasing water reuse, strengthening natural groundwater recharge through land-use modifications, and enhancing irrigation methods are a few examples of these actions. Effective groundwater management laws and policies are also necessary to guarantee the long-term stewardship and preservation of this priceless resource [1, 2].

Using the finite element approach, numerical models for groundwater flow and transport are frequently created (FEM). The behaviour of groundwater flow and transport is described by partial differential equations (PDEs), which are solved numerically using this method. FEM can represent uneven geometries and different material characteristics, making it particularly helpful for modelling complicated geological settings. FEFLOW [3, 4], FEMWATER [5, 6], and SUTRA [7, 8] are a few software solutions for numerical models using the finite element approach. With its ability to simulate groundwater flow, solute transport, and heat transfer in both 2D and 3D, FEFLOW is a popular groundwater modelling programme. It is renowned for its capacity to manage intricate geological conditions and material qualities, and it offers a user-friendly interface. The U.S. Geological Survey (USGS) created FEMWATER, a groundwater modelling programme that use the finite element approach to simulate groundwater flow in both 2D and 3D. It may be downloaded for free and is intended to address a variety of groundwater issues. The USGS created the groundwater modelling programme SUTRA (Saturated–Unsaturated Transport), which can simulate groundwater flow and solute transport in both saturated and unsaturated zones. It is frequently utilised in the environmental and hydrogeology disciplines and is created to solve challenging issues with variably saturated flow. The finite element approach, which enables the depiction of intricate geometries and diverse material characteristics, is utilised by all three software programmes. Additionally, they provide a selection of tools for model calibration, visualisation, and result analysis. The choice of software is based on the particular

requirements of the modelling project, the user's expertise and experience with the programme, as well as the strengths and drawbacks of each software package [9].

There is very rare studies in comparing the existing software for certain problem of groundwater. The existing models FEMWATER and FEFLOW are commercial software developed by Groundwater modelling software (GMS) and Danish Hydraulic Institute (DHI), whereas SUTRA is an opensource software developed by United States Geological Survey (USGS). Thus, in this study the three software using finite element methods are compared for the accurate prediction groundwater level head.

2 Study Area

The study region has four micro-watersheds totalling 60 km^2. The region's groundwater potential is moderate, and the category for groundwater development is overexploited. The region is located between 12.573949 and 12.634600 degrees East longitude and latitude of 79.060752 to 79.195235 degrees North. It is a part of the Cheyyar River Basin. Elevation ranges from 900 to 162 m above sea level. The region has tropical climate conditions and is semi-arid. Monsoon seasons bring rain, with 90% of it falling in the northeast and the rest in the southwest. A total of 40,000 people live in the 9 communities that make up the study area. The primary industry is agriculture. Land-use depicts the western hilly region as having 20% woodland, 8% water bodies, 10% wasteland/barren land, 0.5% built-up lands, and the remainder being an agricultural and plantation region. In this location, 98% of irrigation is provided by groundwater. The principal aquifer systems are composed of weathered charnockite and a little amount of gneiss near the foothills, while fractured/joined charnockite and gneiss serve as secondary aquifer systems. The study area is given in Fig. 1.

3 Data and Methodology

Groundwater head simulation is the process of using computer models to simulate the behaviour of groundwater levels in an aquifer over time. The simulation is usually based on the principles of groundwater flow and mass balance, and involves the solution of mathematical equations that describe the movement of water in the subsurface. The simulation process typically involves the following steps, Developing a conceptual model, Collecting data, Defining boundary conditions, Running the simulation, and Calibrating the model. Hydrogeological data are collected from Vertical Electrical Sounding method, Aquifer properties are calculated using Pumping test, recharge values are calculated from infiltration test. In this study the step 3 is common for all the models. Numerical models FEFLOW, FEMWATER, and SUTRA is introduced in step four. Calibration is not carried out to compare the models with same

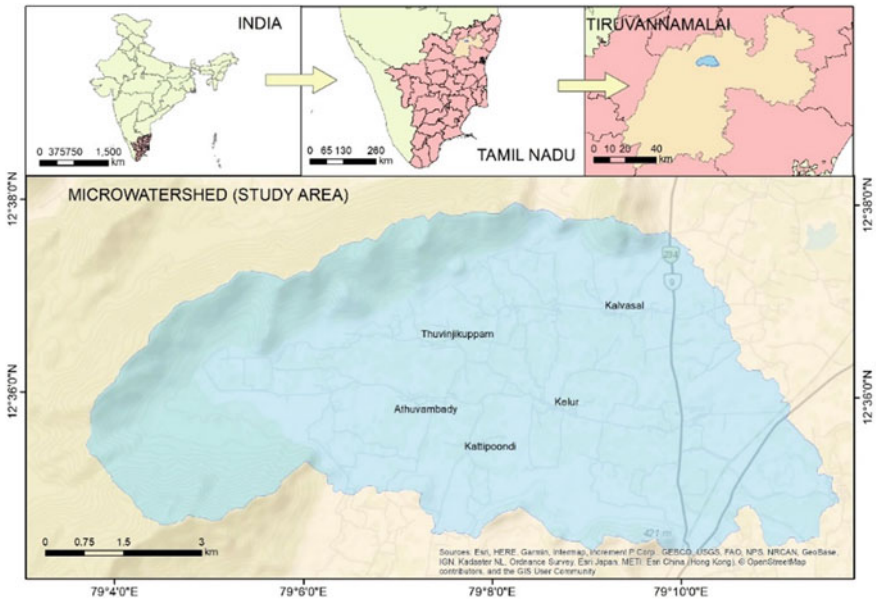

Fig. 1 Study area index map

parameter values. Only validation is carried out between observed and simulated groundwater head. The flow chart of the methodology is given in Fig. 2.

4 Results and Discussions

Subsurface profile indicates there is two aquifer system weathered charnockite and fractured charnockite. The thickness of aquifer 1 varies with 10–40 m and aquifer 2 varies with 5–80 m. the weathered and fractured aquifer is deep at the path of drainage which seem to be fault line along the western direction. Five points are considered for pumping test to find the aquifer hydraulic properties. 15 h of pumping is carried out in each points. The pumping test reviles the hydraulic conductivity varies between 2–6 m/d for aquifer system 1 and 5–12 m/d for aquifer system 2. Also, the storitivity is 0.004 and 0.0005 for system 1 and 2. For recharge value the infiltration test is carried out at various points of soil profile and water bodies. The result shows the barren or waste land have infiltration capacity of 0.5 m/d and in agricultural fields have 0.3 m/d and under water bodies with 0.4 m/d. The average rainfall in the study area is 989 mm. Spatial distribution is uniform throughout the area. Also, the pumping data are collected field wise where 98% of extracted water is used for irrigation. Pumping ranges between 2000 and 5000 l/d. 20 observation wells are used of which the monthly groundwater level is recorded from October

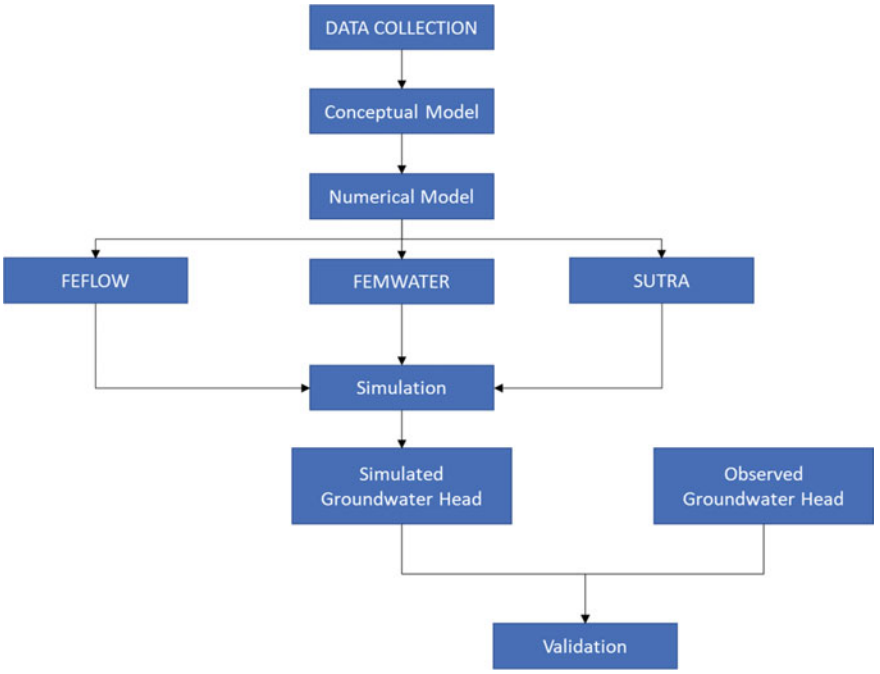

Fig. 2 Methodology of the study

2020 to September 2021 which is used for validation. The model simulation output from SUTRA, FEMWATER, and FEFLOW is computed and compared the results of 20 groundwater observation data. All the models performed well with certain uncertainties. The uncertainty is due to lack of high-resolution data. The R^2 value of SUTRA model is arrived as 0.72 (Fig. 3) which indicated the model is well developed and can perform in these conditions. Similarly, the R^2 value of FEMWATER and FEFLOW is 0.78 (Fig. 4) and 0.9 (Fig. 5) indicating much better than the SUTRA model. The algorithm and the degree of approximation of the numerical method is good in these two models. Also, the FEFLOW have a hybrid algorithm by combining stochastic and probabilistic which increases the accuracy.

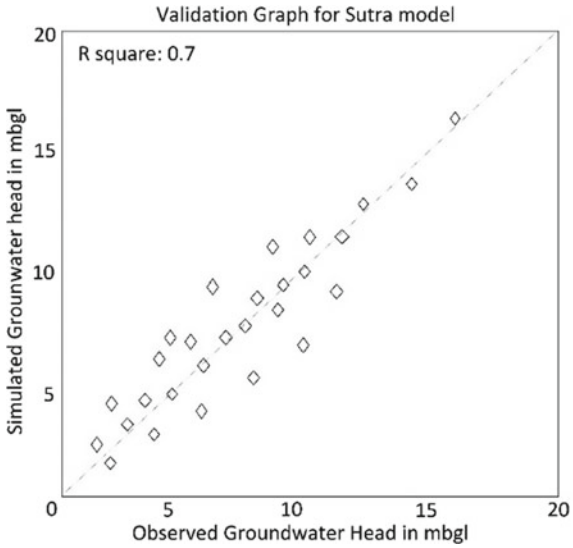

Fig. 3 Validation plot of SUTRA model

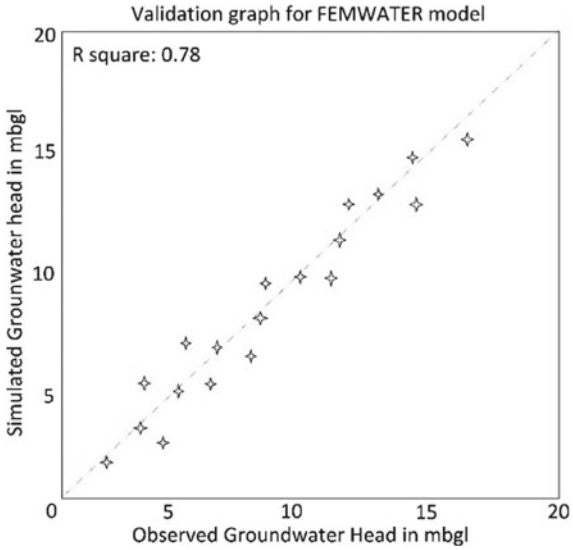

Fig. 4 Validation plot of FEMWATER model

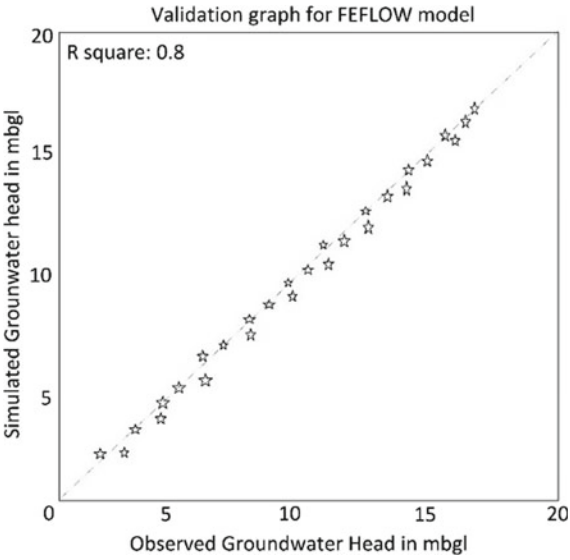

Fig. 5 Validation plot of FEFLOW model

5 Conclusion

The study aims to get adopt the best software for groundwater head prediction and simulation. The data required for the modelling are topographical, hydrological, hydrogeological, and meteorological. These data are obtained and processed as per the format for the respective software. Groundwater head is simulated for the duration of one year in daily time step. The aquifer geometry and hydraulic properties are obtained from VES and pumping test. Recharge and pumping data are acquired in the field for duration of one year. Conceptual model is developed indicating all the factors influencing the groundwater head change. Finite element mesh is generated and used in three software to simulate the groundwater head without calibration. The SUTRA model performed the least with R^2 of 0.72, FEMWATER with pure finite element method have 0.78, and hybrid model FEFLOW have 0.8. Thus, it is concluded that the FEFLOW performs well under the given condition to simulate the groundwater level head.

Acknowledgements The authors acknowledge the department of Civil Engineering, SRM Institute of Science and Technology for providing facilities for conducting the study. Also thank DHI for providing support on running FEFLOW model.

References

1. Gaur S, Johannet A, Graillot D, Omar PJ (2021) Modeling of groundwater level using artificial neural network algorithm and WA-SVR model. In: Groundwater resources development and planning in the semi-arid region, pp 129–150. https://doi.org/10.1007/978-3-030-68124-1_7
2. Gebere A, Kawo NS, Karuppannan S, Hordofa AT, Paron P (2021) Numerical modeling of groundwater flow system in the Modjo River catchment, Central Ethiopia. Model Earth Syst Environ 7:2501–2515. https://doi.org/10.1007/S40808-020-01040-0
3. Berehanu B, Ayenew T, Azagegn T, Berehanu B, Ayenew T, Azagegn T (2017) Challenges of groundwater flow model calibration using MODFLOW in Ethiopia: with particular emphasis to the Upper Awash River Basin. J Geosci Environ Prot 5:50–66. https://doi.org/10.4236/GEP.2017.53005
4. Mabrouk M, Jonoski A, Oude Essink GHP, Uhlenbrook S (2019) Assessing the fresh–saline groundwater distribution in the Nile delta aquifer using a 3D variable-density groundwater flow model. Mdpi.Com. https://doi.org/10.3390/w11091946
5. Serrano R, Guadagnini L, Riva M, Giudici M (2014) Impact of two geostatistical hydro-facies simulation strategies on head statistics under non-uniform groundwater flow. J Hydrol (Amst). https://www.sciencedirect.com/science/article/pii/S0022169413008251. Accessed 2 Mar 2023
6. Nourani V, Mousavi S (2016) Spatiotemporal groundwater level modeling using hybrid artificial intelligence-meshless method. J Hydrol (Amst). https://www.sciencedirect.com/science/article/pii/S0022169416300646. Accessed 2 Mar 2023
7. Rezaei M, Mousavi SF, Moridi A, Eshaghi Gordji M, Karami H (2021) A new hybrid framework based on integration of optimization algorithms and numerical method for estimating monthly groundwater level. Arab J Geosci 14. https://doi.org/10.1007/S12517-021-07349-Z
8. Jiao JJ, Tang Z (1999) An analytical solution of groundwater response to tidal fluctuation in a leaky confined aquifer. Water Resour Res 35:747–751. https://doi.org/10.1029/1998WR900075
9. Zhou Y, Li W (2011) A review of regional groundwater flow modeling. Geosci Front. https://www.sciencedirect.com/science/article/pii/S167498711100020X. Accessed 2 Mar 2023

Analysis and Design of Water Distribution Network for the Potheri Village, Chengalpattu District, Tamil Nadu, India

Praveen Kumar, Sathyanathan Rangarajan, Ashish Chauhan, and Ashwini Chauhan

Abstract In many developing countries, including India, water distribution systems are often plagued by inadequate and poor design, operation and maintenance issues, and economic stress. This results in a substandard quality and insufficient quantity of water reaching consumers. One of the major problems with intermittent water supply systems is that the leaks in the pipeline allow contaminants to seep into the pipeline during non-supply hours due to the vacuum that is developed inside the pipeline. A solution to this issue is to implement a continuous pressurized water supply system. This study aims to analyse the current public water distribution system of Potheri village in Chengalpattu district of Tamil Nadu, India, and to design a new and improved system using the open-source software EPANET. The study will adhere to the updated government guidelines outlined in the Atal Mission for Rejuvenation and Urban Transformation (AMRUT) 2.0 initiative (CPHEEO. Guidelines for planning, design, and implementation of 24 × 7 water supply [1]), by CPHEEO, Ministry of Housing and Urban Affairs—Government of India. The water distribution system of Potheri includes 214 High-Density Polyethylene (HDPE) pipes of diameter 150 mm having Hazen–Williams constant 140, 191 junctions, and 4 overhead tanks from which water is distributed to the whole network. Various types of scenarios were simulated like blockage of pipe, failure of the overhead tank, etc. Hydraulic analysis performed with EPANET will allow a thorough assessment of the system's performance under various operating conditions and enable the optimization of the network design for greater efficiency and reliability. The 24 × 7 water supply system brings numerous benefits to communities, such as consistent access to clean water, active leak detection, and repair, and reduced waterborne diseases and infant mortality rates. The newly developed system also conserves water resources

P. Kumar · S. Rangarajan (✉) · A. Chauhan · A. Chauhan
Department of Civil Engineering, Faculty of Engineering and Technology, SRM Institute of Science and Technology, Kattankulathur, Tamil Nadu 603203, India
e-mail: sathyanr5@srmist.edu.in

P. Kumar
e-mail: pk4445@srmist.edu.in

K. R. Reddy et al. (eds.), *Recent Advances in Civil Engineering*, Lecture Notes in Civil Engineering 398, https://doi.org/10.1007/978-981-99-6229-7_42

and reduces overall consumption by eliminating the need for water storage during non-supply hours.

Keywords EPANET · Hydraulic modelling · Network analysis · Water distribution network

1 Introduction

Water is a critical element for the survival of all living beings and it serves a multitude of purposes, ranging from household use, and irrigation to industrial processes. To meet the ever-growing demand for water, it is imperative to have an efficient and effective water distribution network. However, in many developing countries, the water supply system is plagued by several shortcomings, such as outdated and poorly designed systems, operational and maintenance problems, and financial limitations. This results in water reaching the end-users with insufficient quantity and low quality. The Government of India has been working towards enhancing the water supply system for decades, with its roots dating back to the "Environmental Hygiene Committee Report" of 1949. The report aimed to provide a continuous 24 × 7 water supply and demonstrated its feasibility in the city of Lucknow. The initiative aimed to educate the community about the importance of continuous water supply and to encourage them to adopt the same, ultimately leading to reduced water consumption.

Guidelines for Planning, Design, and Implementation of 24 × 7 Water Supply Systems, was recently released in December 2021 by the Central Public Health and Environmental Engineering Organization, which operates under the Ministry of Housing and Urban Affairs of the Government of India. This comprehensive guideline document provides valuable insights and recommendations for the development and implementation of sustainable water supply systems. The guidelines are based on the AMRUT 2.0 initiative, which aims to enhance the urban infrastructure and services in India.

In this study, a comprehensive analysis of the current water distribution network is carried out using the EPANET [2] software. EPANET is a highly regarded tool that enables the examination of water distribution systems [3], including the flow of water through pipes, the performance of pumps, and the head loss and pressure in the network. It is used for designing, modelling, and simulating water distribution systems and calculates important water quality parameters such as the age of water, mixing and concentration of contaminants. This software allows for the examination of water quality changes resulting from different operational scenarios and provides valuable information for informed decision-making. This can assist in identifying problems and improving the efficiency of the water distribution system. EPANET is utilized by water utility companies, consulting engineers, and researchers worldwide, making it a widely accepted and reliable tool in the industry.

1.1 Objective

The objective of this study is to conduct a comprehensive analysis of the current intermittent water distribution system in Potheri village. This system, which provides water to the residents of the village on a schedule that alternates between periods of availability and unavailability, has become increasingly problematic in recent years. Issues with the system include contamination of seepage into the pipeline, uneven distribution, and wastage of treated water, which have had a negative impact on the quality of life for the residents.

To address these challenges, a design was carried out to implement a new and improved water distribution system that provides a continuous supply of water to the residents of the village. This new system will take into account the specific needs and requirements of the residents, as well as the topographical features of the area. The goal is to create a water distribution system that is sustainable, efficient, and effective, and that will provide the residents of Potheri with a reliable source of clean and safe drinking water.

The design of this new system will be based on the latest guideline 'AMRUT 2.0' [1] from the Government of India. By conducting this study, the goal is to provide the residents of Potheri with a water distribution system that is designed to meet their needs and improve their quality of life and provide a model for other communities facing similar challenges (Fig. 1).

1.2 Study Area

Potheri is a thriving village located in the southern suburbs of Chennai Metropolitan city, with a land area of 2 km^2. It is part of Maraimalai Nagar municipality in Chengalpattu district of Tamil Nadu, India, and falls under the Chennai Metropolitan Area. Located approximately 40 km from the city of Chennai and 20 km from Chennai Airport, Potheri is well-connected to Chennai via the Chennai Suburban Railway Network and National Highway NH-45. The primary source of education in Potheri is provided by SRM Institute of Science and Technology and Valliammai Engineering College, and as a result, the population of Potheri is primarily comprised of students from these institutions.

Fig. 1 Map of Potheri village [4]

2 Methodology

2.1 Levelling Work for Nodal Elevation

The process of levelling work is an integral aspect of surveying, as it provides crucial information about the topographical features of a particular area. The process of levelling with the dumpy level is a multi-step process, which involves taking precise measurements at each node and then reducing the data to obtain the reduced levels. These reduced levels are then used to determine the elevation of each node with accuracy, typically to within 5 mm. In this particular case, the levelling work was carried out using dumpy level instrument in the study area where longitudinal length of the road is 976 m, while the transverse length is 593 m. The dumpy level is a versatile and precise instrument that is particularly useful in determining the relative

heights of different points on a surface. The calculation method that was employed was the Height of Instrument method [5], from the calculation the highest elevation obtained was 52.415 m while the lowest elevation was 49.855 m.

2.2 Population Forecasting

Population forecasting is a critical component of water distribution network planning and management. Accurate forecasting of population growth and demographics is essential in ensuring that the water supply infrastructure is able to meet the demands of a growing population. Without proper forecasting, the water distribution network can become quickly overwhelmed, leading to water shortages, low water pressure, and potentially, water contamination.

By forecasting population growth and demographics, informed decisions can be made on the expansion and improvement of the water supply infrastructure, ensuring that there is enough capacity to meet the demands of a growing population, now and in the future.

There are various methods to forecast population, Incremental increase method which is a modified form of the arithmetical increase method was used as it is suitable for an average size town under normal condition where the growth rate is found to be in increasing order (Tables 1 and 2).

$$Pn = P + nI + n((n+1))/2$$

where

P Present population

Table 1 Existing population of study area

Year	Population
2001	3697
2011	10,311
2021	14,682

Table 2 Projected population of the study area in next 50 years

Year	Population
2031	20,175
2041	25,667
2051	31,160
2061	36,652
2071	42,145

Design population (in 2071) = 42,145

I Average increase per decade
r Incremental increase
n Number of decades.

2.3 Water Demand Calculation

In the process of designing a water supply system, it is crucial to accurately predict the water demand [2] in the region which depends on the design population so that the necessary infrastructure can be put in place to meet the water demands of the population. The calculation of the water supply requirements is a critical aspect of this process and is done by taking into account various factors, including the standards specified by the Indian Standards (IS 1172-1971) and the guidelines laid out in the Atal Mission for Rejuvenation and Urban Transformation (AMRUT) 2.0, which is a comprehensive policy framework developed by the Central Public Health and Environmental Engineering Organization, under the Ministry of Housing and Urban Affairs, Government of India.

For population ranges between 10,000 and 50,000, the water demand ranges between 100 and 125 l/c/d [6, 7]. In this case, it has been decided to adopt a water demand rate of 125 l/c/d [8], which is an appropriate level to meet the needs of the design population of 42,145. This decision was based on a comprehensive assessment of the population's needs and the water resources available, taking into account the local climate, water quality, and other relevant factors. By adopting this water demand rate, the water supply system can be designed to ensure that adequate water resources are available to meet the needs of the population, now and in the future.

3 Hydraulic Modelling and Simulation

3.1 Digitization of Data

Creation of a pipeline network is a complex and technical process that requires data of topographical and geographical features of the area in which the pipeline is to be constructed. To achieve this, a range of tools and techniques are employed, including the use of Global Positioning System (GPS) devices, levelling equipment, and specialized software. The GPS device is used to determine the longitude and latitude of the pipeline route, while the levelling equipment is used to determine the elevation of each node along the route. The information obtained from these two sources is then used to create a precise and accurate representation of the pipeline route, including the exact location and elevation of each point along the way.

The design and analysis of a water distribution network were carried out utilizing the EPANET software, with the objective of ensuring that adequate water pressure and flow were available to meet the demands of the designated area. The method of

distribution employed in the network is the combined gravity system. This approach involves first pumping water from underground and surface sources to overhead water tanks using centrifugal pumps and then utilizing gravity to transfer the water to the main pipe.

3.2 Existing Network Layout with Intermittent Pattern

The current water supply system in the study area operates on an intermittent schedule. Residents in the area are provided with access to water only during two periods of the day: 4–7 a.m. in the morning, and 4–7 p.m. in the evening. The rest of the day, the water supply is shut off.

Figure 2 shows the pipeline network study area, a complex and extensive system, consisting of 214 High-Density Polyethylene (HDPE) pipes, 191 junctions, and 4 overhead storage tanks.

3.3 Various Scenarios

The water distribution infrastructure plays a crucial role in today's society. It is a system that provides water to various residential, commercial, and industrial areas, ensuring access to this essential resource. Despite its importance, the water distribution infrastructure is not invincible. Over the course of its lifetime, it is susceptible to various unexpected events, such as human error, and mechanical failures, that can disrupt the smooth flow of water. These incidents can lead to water shortages, low water pressure, water contamination, or even complete stoppage of supply. It is therefore very important to design the distribution system such that it can operate in different unexpected conditions while ensuring that the supplied water remains safe and reliable.

3.3.1 *24 × 7 Supply Pattern*

The implementation of a continuous supply system has proven to be a solution to the challenges faced by residents in performing their daily essential tasks such as cooking, cleaning, and maintaining personal hygiene. These tasks require a constant and steady supply of fresh water, which can be provided by a continuous supply system.

The pattern of tank operation, as depicted in Fig. 3, is designed to guarantee a continuous water supply in accordance with the demand. The demand pattern is characterized by two peaks at 7:00 a.m. and 11:00 a.m., respectively. This can be attributed to the fact that the majority of the population in the study area consists of students from SRM Institute of Science and Technology. The institute classes

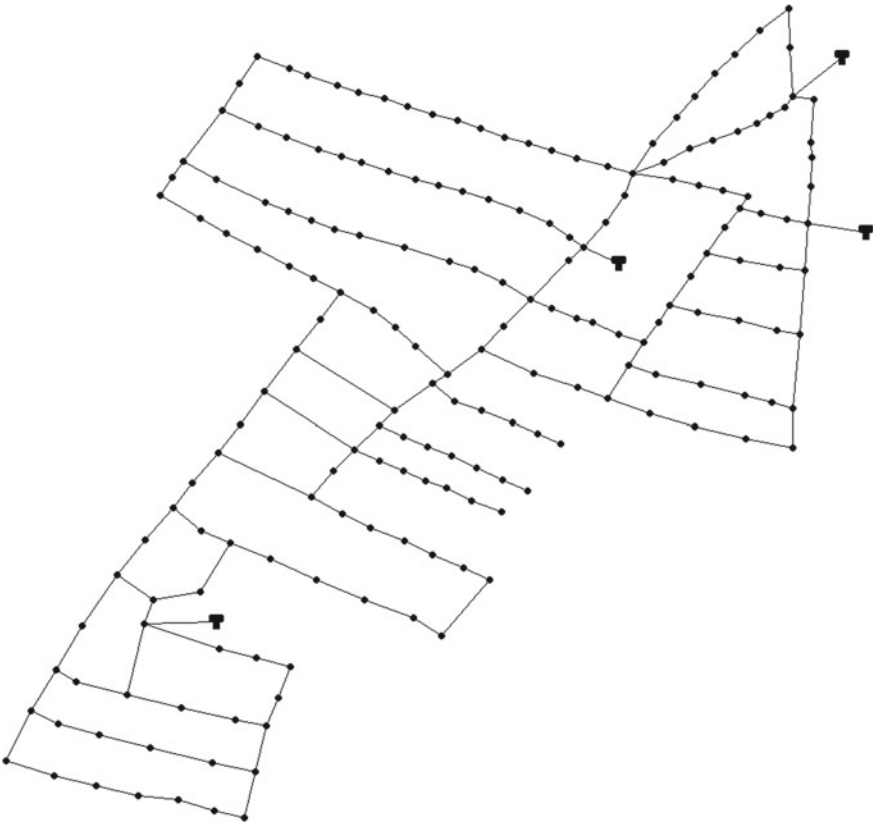

Fig. 2 Pipe network

are divided into two slots: the first slot runs from 8:00 a.m. to 12:30 p.m., while the second slot is held from 12:45 to 5:00 p.m. Additionally, the constant pressure exerted by the system helps to prevent the seepage of contamination and the active detection of leaks. The continuous supply system also improves the overall service level, increases the life of the pipeline network, and reduces water wastage. By eliminating the need for water storage during non-supply hours, this system reduces overall water consumption, contributing to water conservation efforts.

3.3.2 Stopping Supply from Tanks Due to Maintenance

One of the scenarios used in evaluating the efficiency of the water distribution infrastructure involves a temporary interruption of supply from two of the four overhead tanks. The objective of this scenario is to assess how the system operates when it is relying solely on the remaining two tanks. The results of this simulation are critical in determining the resilience of the water distribution system and the ability

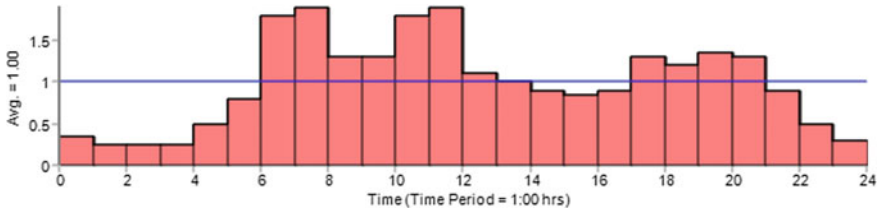

Fig. 3 Demand pattern for continuous supply

Table 3 Status of overhead tanks in each case

Overhead tank	Case 1	Case 2	Case 3
1	Open	Open	Closed
2	Open	Open	Closed
3	Open	Closed	Open
4	Open	Closed	Open

of the remaining tanks to provide adequate water supply to the entire network. This scenario provides valuable insights into the capability of the water distribution infrastructure to respond to unexpected events, such as tank failures or maintenance work, and ensures that the system can continue to provide a reliable water supply even in adverse circumstances (Table 3).

4 Result and Discussion

During the simulation, changes in selected parameters such as flow, velocity, head, and water pressure at various nodes were monitored and recorded on an hourly basis. Data obtained from the simulation revealed that the water demand during peak hours was 6686.85 LPM, while the demand during non-peak hours was 879.86 LPM. Additionally, a decrease in pressure head was observed at the peak hour as compared to the non-peak hours across all nodes. During the peak demand hours, the highest pressure recorded was 14.98 m and the lowest pressure was 12.34 m. These values were found to be within the expected range of 12–17 m for buildings with 2–3 floors. This indicates that the water distribution system was operating within the desired parameters.

In situations where only half of the available overhead tanks are functioning, the highest pressure reading was 13.41 m and the lowest pressure reading was 8.26 m. These pressure levels are deemed adequate to effectively distribute water to the designated network without encountering any significant problems.

The results of these simulations provide valuable insights into the strengths and weaknesses of the water distribution infrastructure and can facilitate future improvements to ensure a more reliable water supply for all.

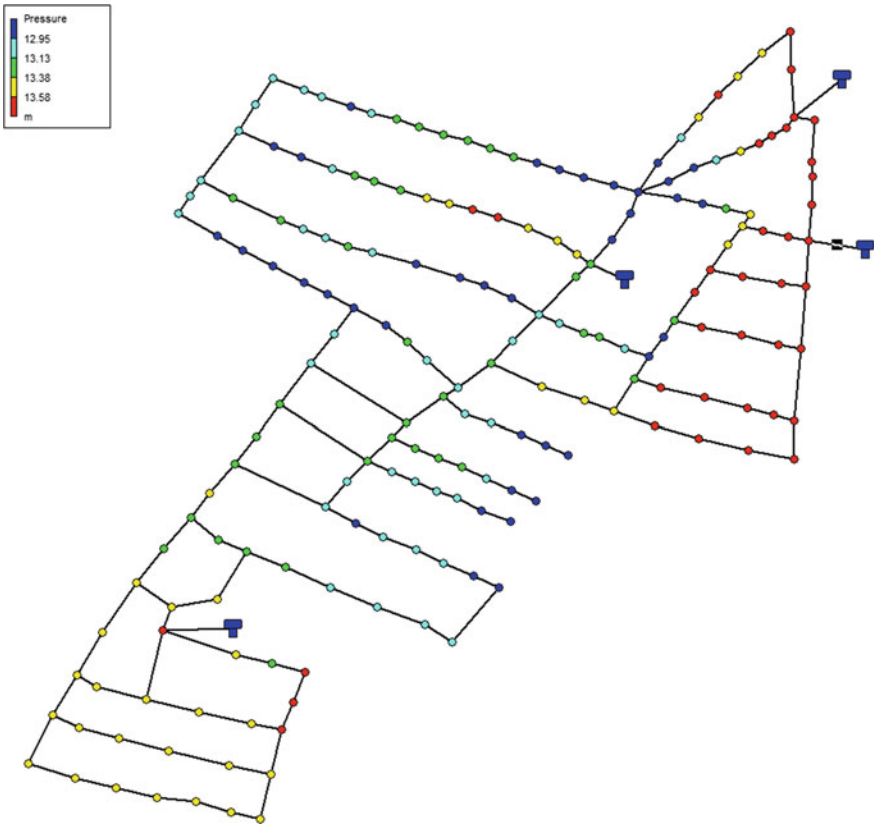

Fig. 4 Pressure of nodal pressure during peak demand hour

4.1 Pressure and Velocity at Peak Demand

Figure 4 is a representation of the pressure at each node in the system. This visual aid helps to understand the distribution of pressure along the pipeline and identify any potential problem areas. The data analysis revealed that the highest recorded pressure was 14.98 m, while the lowest pressure was recorded at 12.34 m.

4.2 Effect of Partial Supply of Water from Tanks

In the first case, all four tanks were functioning and supplying water as normal. However, in the second case, two of the tanks ceased operation. The following case, the remaining two tanks also stopped functioning, and the two tanks from the previous case resumed operation. As a result, the maximum velocity in the second and third

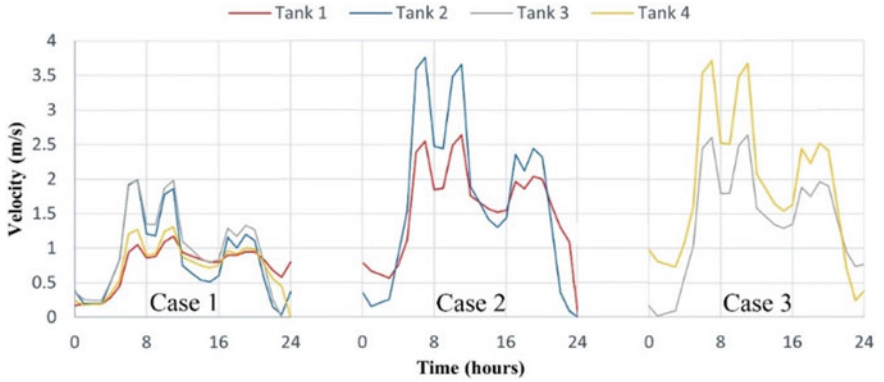

Fig. 5 Velocity of water overhead tank in each case

cases was almost double that of the first case, the same can be observed from Fig. 5, due to the decreased number of functioning tanks and the increased workload placed on the remaining two tanks.

5 Conclusion

The primary objective of this study was to conduct an in-depth analysis of the water distribution network in Potheri village, identifying the underlying problems related to the current intermittent supply system. The objective was to convert the existing system into a 24 × 7 water supply system. The analysis revealed that the pressures at all the junctions in the network were found to be higher than 8 m and the velocity in all the pipes was in the range of 0.16–2.1 m/s, which is sufficient to cater to the water requirement of the entire study area.

One of the critical issues that were encountered during the distribution system was the presence of dead-ends. These dead-ends resulted in low velocity and pressure, which can cause water to become stagnant, this challenge posed a significant threat to the efficient functioning of the system. One possible solution to this problem was to loop the pipes in the network, this would have increased the velocity and pressure, thereby reducing the chances of water stagnation. However, the site conditions were not favourable for implementing this solution, which made it challenging to address the issue effectively.

Despite this constraint, the study managed to overcome the hydraulic challenges to a considerable extent. Based on the findings of the study, it can be concluded that the pressure levels at all junctions and the flow velocity in all pipes are sufficient to cater to the water demands of the entire study area. Therefore, it can be inferred that the newly designed water distribution network has the potential to deliver a continuous

supply of clean water to the residents of Potheri village, ensuring improved health and hygiene standards.

Acknowledgements The author of this study would like to express his gratitude to SRM Institute of Science and Technology for their unwavering support and for granting access to laboratory equipment, which greatly contributed to the successful completion of the work. It is with deep appreciation that the author acknowledges the invaluable contribution made by these entities. Furthermore, the author extends his sincere thanks to his family and friends, who provided constant encouragement and support throughout the study.

References

1. CPHEEO. Guidelines for planning, design, and implementation of 24 × 7 water supply
2. Athulya T, Ullas AK (2020) Design of water distribution network using EPANET software. Int Res J Eng Technol 7:1774–1778
3. Rossman LA, Woo H, Tryby M, Shang F et al (2020) EPANET 2.2 user manual
4. Google Maps. https://www.google.com/maps
5. Sathyanathan R, Hasan M, Deeptha VT (2016) Water distribution network design for SRM university using EPANET. Asian J Appl Sci 4:669–679
6. SP 35 (1987) Handbook on water supply and drainage
7. IS 2065 (1983) Code of practice for water supply in buildings
8. IS:1172 (1993) Code of basic requirements for water supply, drainage and sanitation

A Study on Determination of Crop Water Requirement and Irrigation Scheduling for Sathyamurthi Project (Poondi)

R. Santhosh Ram and Durgadevagi Shanmugavel

Abstract In India agriculture is the mainly uses the water, so that well planned usage of water in agriculture is very much important. Nowadays in India severe shortage of water is developing and hence becoming scarcity of water for agriculture. The main motive of the project is to conserve water with the help of software that determines all the needs for the crop to grow. The initial site information such as soil details, cultivation area, and water resources are collected. Additionally, a survey is made to get the exact information on cultivated crops. With the data obtained using the software's namely CROPWAT and CLIMWAT, the geographical details can be estimated. A station is chosen, and the rainfall data is obtained. Referring to the values obtained from the station, the values are then inputted into the CLIMWAT software. This provides the data regarding the climate and the site's rainfall. We now move to the crop details and other parameters required with the climate and rainfall details being done. As we have already visited the site, the soil samples were collected prior. Sieve analysis and jar tests were conducted to determine the soil type and texture. After the determination of soil, the soil type is selected in the CROPWAT model, and then the soil data is inputted. The crops mainly grown in that surroundings were obtained by the survey made, and now this data is inputted into the CROPWAT software. This extracts the details of the crop needs, such as the water required, the soil needed, and the time to sow and harvest. The water source nearby the selected site is the Poondi reservoir, and the water requirement data is inputted, and the water/irrigation details are obtained. With this data, we know at what interval, when, and how much water is needed for the crop to grow. Thus, with this information obtained, the excessive use of water can be regulated, and water can be conserved. This is an excellent source of knowledge for anyone new to agriculture.

Keywords CROPWAT · CLIMWAT · Poondi reservoir

R. Santhosh Ram · D. Shanmugavel (✉)
Department of Civil Engineering, Faculty of Engineering and Technology, SRM Institute of Science and Technology, Kattankulathur, Tamil Nadu 603203, India
e-mail: durgades@srmist.edu.in

K. R. Reddy et al. (eds.), *Recent Advances in Civil Engineering*, Lecture Notes in Civil Engineering 398, https://doi.org/10.1007/978-981-99-6229-7_43

1 Introduction

India comes under countries which faces serious water scarcity. Agriculture being the back bone of Indian economy and the country depends on agriculture which comprises around (81%) there is a huge demand for water in the agricultural sector. For Indian agriculture it is very important to have a better understanding of the complicated interactions between crops cultivation, climate, and water [1–3]. Food waste has become a habit for the people which has put a strain on the economy and also damages our environment. Emissions of green-house gas increases due to the food waste which will contributes the change in climate so it is essential to stop food loss and food waste. Food loss means the portion of food we lost during harvest, till the retail level. Food waste means the part of the food that was wasted by the retail level or consumer [4]. To find the root causes for this problem we clearly distinct the two problems, a problem for everyone from the farmers or the producers to shop-owners and customers who can help till end. An essential thing to produce the crops are food and water [6]. Hence, from [7, 8] using the 2-model software's such as CLIMWAT and CROPWAT in the project we made an attempt to calculate the crop water requirements of main crops in various agro-ecological zones. CROPWAT is to calculate the irrigation scheduling, crop water requirements and irrigation supply to different types of crops. CLIMWAT gives to the stations at its database, monthly mean values for long-term based on to Penman–Monteith method: monthly total and effective rainfall, mean daily minimum temperature, mean daily maximum temperature, mean sunshine hours or solar radiation, mean relative humidity, mean wind speed [9].

The main objective of this project was, managing crops efficiently according to the different conditions of weather, temperature, and rainfall. This project is also done to find out water required for crops in different seasons in a particular location. Effective water management means reducing wastage of water by calculating the water necessary to the particular purpose and the water that was used for that purpose. Water conservation is different from that of water efficiency. Water efficiency mainly focuses on reducing waste but not on restricting usage, and also, we will get a particular data of the exact water we required and monthly, daily, dates of climate for that crop. This gives bright future to the agriculture and also very useful for the growing up farmers. The procedure of determining the amount of water required by the crops is critical. Farmers will save a lot of money, effort, and, most critically, water resources by using this strategy. This water resource appears to be depleting with each passing year; therefore, we can add the exact amount of water required by estimating how much water is required over the period of crop growth. This also aids in the maintenance of a healthy soil moisture level that is rich in nutrients (Fig. 1).

Fig. 1 Poondi map and dam

2 Experimental Investigation

2.1 Collection of Soil Sample

During the visit of the site, the soil samples were collected. The soil sample was then tested to determine the soil's type and texture. Once these values are determined, the type of soil is selected from the list of available soils present in the CROPWAT model software. An approximate amount of at least 6 kg of soil was collected.

2.2 Sieve Analysis

The first test that is done to determine the type and grade of soil is sieve analysis. The sieve analysis is an analytical or scientific method of determining the particle size distribution of the material. This technique involves stacking of different sizes of sieves where the biggest sieve size is placed at, and the finest sieve size is placed at the bottom. They are stacked below in a decreasing order of size. When the material is placed on the top sieve and sifted, the discrete particles are collected in each sieve after rigorous shaking and finally passes through the finest sieve. The sieves sizes that were used for the experiment are 300-micron, 600 μ, 150 μ, 1.18 mm, 4.75 mm, 2.36 mm, and pan.

2.3 Soil Pyramid Jar Test

After determining the type of soil, we need to find out the texture of soil in order input it into the CROPWAT software. This test is done to find out the texture of the

soil sample that was collected from the field. To begin, an empty glass jar is required for this experiment. The next step is to add a soil sample to 1/3 of the jar. Pour the vacant space in the jar with water, leaving a thin gap at the top for air. The jar is then aggressively shaken until all of the soil and water are thoroughly combined. Then carefully lay the jar on the tray. Set a timer for 1 min to see the sand layer form, which will be visible at the bottom of the jar due to it being the heavier particles. Then after an hour, we can observe the formation of the silt layer. After 24 h, we can observe the formation of the clay texture layer too. By measuring the relative distance of these texture layers, we can find out the % sand, silt, and clay, and using these values, we can input them into the soil pyramid chart to find out the texture of the soil (Table 1; Fig. 2).

Table 1 Particle size distribution

S. No.	Sieve size	Material retained (g)	Percentage retains (%)	Cumulative percentage retain (%)	Cumulative passing (%)
1	4.75 mm	0	0	0	100
2	2.36 mm	180	9.18	9.18	90.82
3	1.18 mm	276	14.08	23.26	76.74
4	600 µ	230	11.76	35.02	64.98
5	300 µ	600	30.61	65.63	34.37
6	150 µ	498	40	91.03	8.97
7	Pan	176	8.97	100	0
		= 1960 g	= 100%		

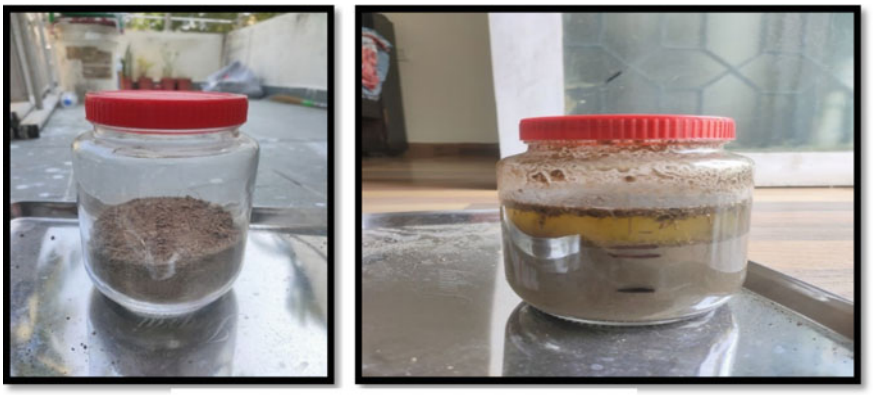

Fig. 2 Pyramid jar test

Fig. 3 Visit of farm lands

2.4 Questionnaire Survey

The survey was conducted amongst the workers on the field. The collected data gave out information on the exact area of land used for cultivation, the types of crops grown there, the soil samples, information regarding the water source, fertilizers used, and many other general details on the field of farming. According to the survey, the most common crops being cultivated are rice and tomato, but tomato in lesser quantity (Fig. 3).

3 Analytical Investigation

3.1 Climatic and Rainfall Details

Poondi is located in Tamil Nadu's Tiruvallur district. The Poondi lake, also known as the Sathyamoorthi Sagar reservoir, is an important water source for Chennai. Poondi's climatic characteristics are primarily tropical, with brutal summers with extremely high temperatures and considerable rainfall in the winter. The climatic data like humidity, wind speed, sun hours, maximum temperature, and minimum temperature, has been obtained by the Model Software known as CLIMWAT. This is a model software developed by FAO which is helpful in obtaining the climatic and weather details of a particular area. CLIMWAT contains the databases of all the available weather or meteorological stations for various countries. Firstly, the country is selected, and within the country, we have to select the station of the site location or at least the station closest to the site location. By selecting the MET-station, a weather file is created, and then we are supposed to save the file in a folder. While selecting the weather/Et_0 option in the CROPWAT software, we can open up

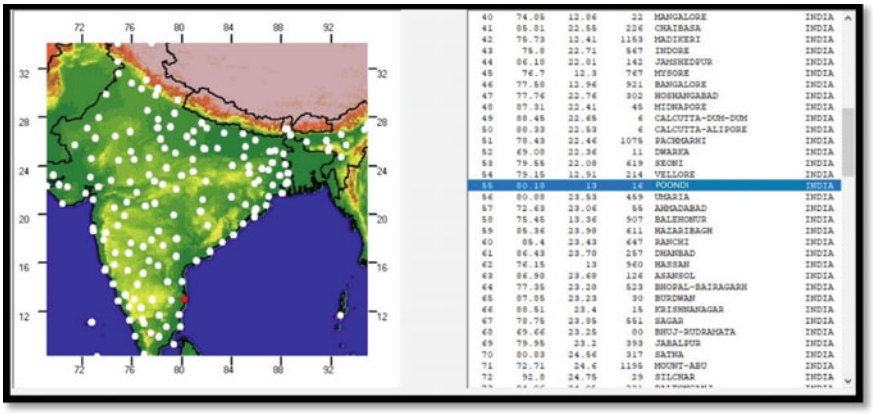

Fig. 4 CLIMWAT station selection

a weather detail file instead of manually entering the data into the table. The weather data automatically loads up after clicking on the MET-station details file (Fig. 4).

3.2 Selection of Soil in CROPWAT

After determining the type and texture of soil with the help of these experiments, then the soil type is selected in the model software. In the image above shows the properties of sandy loam soil. These values are already inputted as they are default values FAO.ORG recommends for this type of soil. They are pre calculated (Fig. 5).

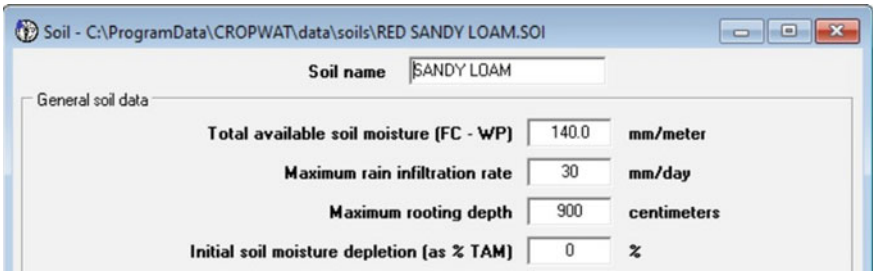

Fig. 5 Soil properties

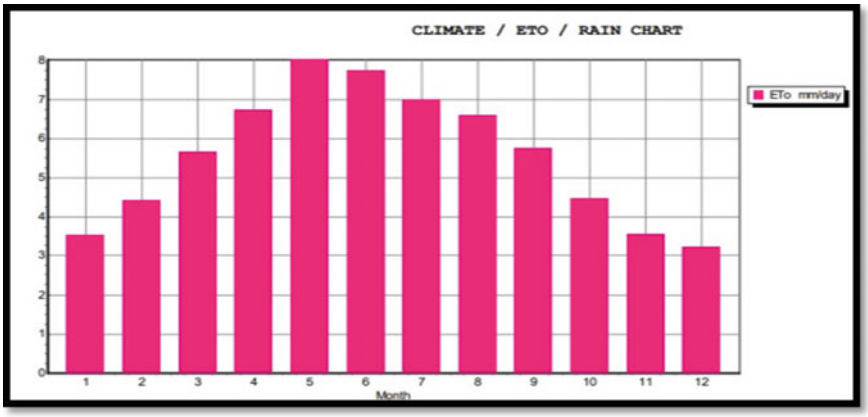

Fig. 6 ETO graph

4 Results and Discussion

4.1 ETO (Evapotranspiration)

From Fig. 6 and Table 2, the minimum ETO is 3.22 mm/day for the month of December and 8.03 mm/day for the month of May. The overall avg. ETO is 5.56 mm/day. This indicates that the evapotranspiration process takes place rigorously at the month of May due to the extreme heat conditions at that time.

4.2 Rainfall Report

Table 3 shows the rainfall data Poondi and also the effective rainfall too. From the table above we can observe that effective maximum rainfall is 95.5 mm can observe at the month of October and effective minimum rainfall is 4.0 mm can be observed in the month of February (Fig. 7).

4.3 Sieve Analysis

The graph for particle or sieve size (X-axis) versus % finer (Y-axis) is plotted using Microsoft excel and the curve is shown. The values of D10, D30, and D60 are 0.12, 0.28, and 0.51 (Fig. 8).

The uniformity coefficient (C_u) can be found using the formula

Table 2 ETO table

Country: India		Station: POONDI					
Altitude: 16 m		Latitude: 13.20° N			Longitude: 79.88° E		
Month	Max temp. (°C)	Min temp. (°C)	Humidity (%)	Wind (km/day)	Sun (h)	Rad (MJ/m^2/day)	ETO (mm/day)
Jan	18.3	28.7	75	147	7.0	17.0	3.52
Feb	18.9	31.4	69	164	8	19.8	4.42
Mar	21.6	34.5	66	216	8.8	22.5	5.66
Apr	25.3	36.8	65	268	9.5	24.2	6.73
May	27.5	38.5	56	285	10.9	26.0	8.03
June	27.3	36.3	56	285	11.2	26.1	7.76
July	26.5	34.9	59	242	10.8	25.6	7.00
Aug	25.8	33.9	64	242	10.5	25.4	6.59
Sep	25.1	33.2	70	190	9.9	24.2	5.78
Oct	23.6	31.2	78	147	8.2	20.4	4.48
Nov	21.6	28.9	81	147	6.8	17.0	3.55
Dec	19.8	27.8	78	147	6.2	15.5	3.22
Average	23.4	33.0	68	207	9.0	22.0	5.56

Table 3 Effective rainfall table

	Rain (mm)	Effective rain (mm)
January	16.0	8.0
February	8.0	4.0
March	10.0	5.0
April	16.0	8.0
May	48.0	24.0
June	82.0	41.0
July	91.0	45.5
August	114.0	57.0
September	119.0	59.5
October	191.0	95.5
November	182.0	91.0
December	90.0	45.0
Total	**967.0**	**483.5**

$$C_{\mathrm{u}} = D_{60}/D_{10}, \quad C_{\mathrm{u}} = 0.51/0.12, \quad C_{\mathrm{u}} = 4.25.$$

We can find by using coefficient of curvature (C_{c}):

$$C_{\mathrm{c}} = (D_{30})^2/D_{60} * D_{10}$$

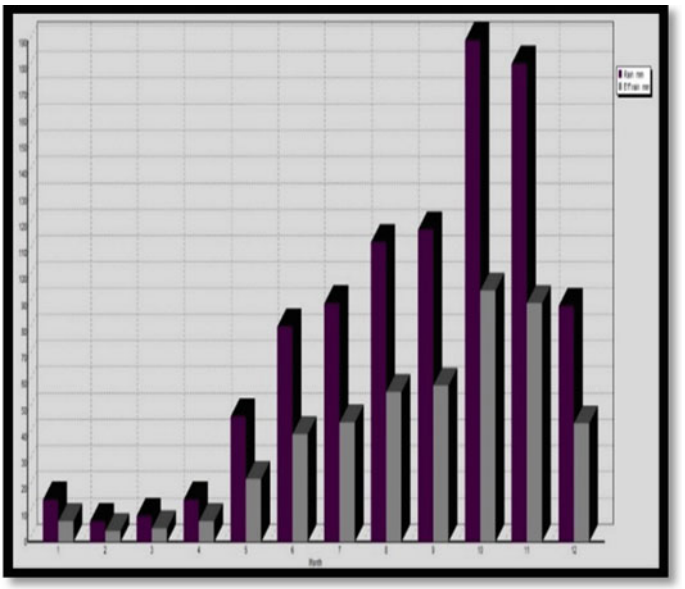

Fig. 7 Rainfall chart

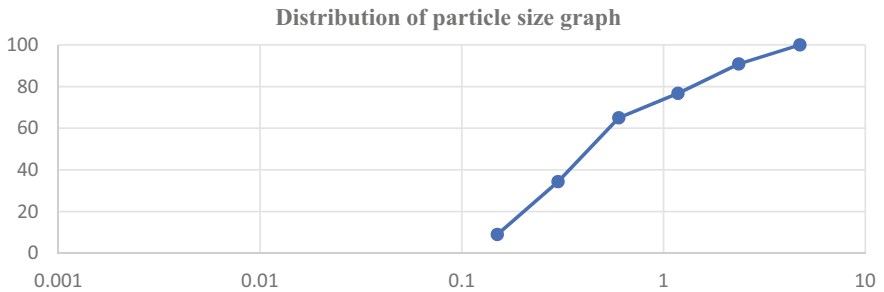

Fig. 8 Sieve analysis of soil

$$C_c = (0.28)^2/(0.51 * 0.12)$$
$$C_c = 1.28$$

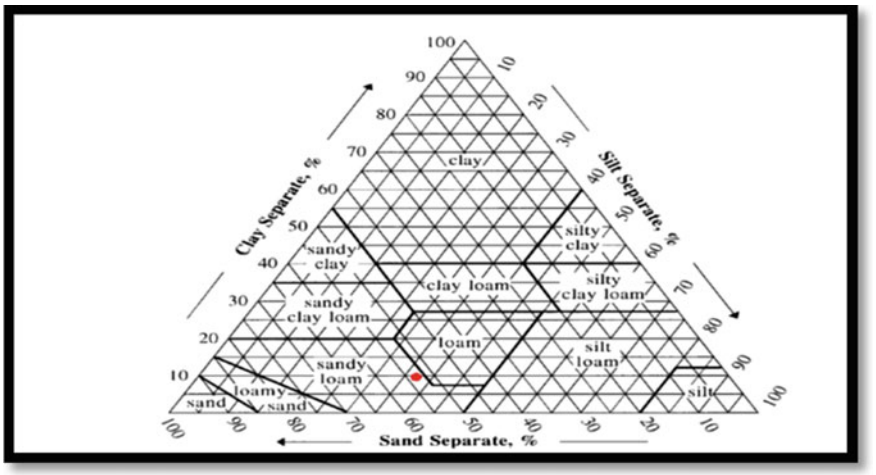

Fig. 9 Soil pyramid graph

4.4 Soil Pyramid Graph

Since the uniformity coefficient of soil is 4.25 and coefficient of curvature is 1.28, we can infer that soil is a "well graded type of soil" because the C_u value lies between 4 and 6 and C_c value lies between 1 and 3. From the curve of graph, we can also confirm that soil lies in the range of sand gravel soil.

Distance of sand layer = 30 mm, Distance of silt layer = 20 mm, Distance of clay layer = 5 mm, Total soil layer = 55 mm, Percentage of sand = 30/55 * 100 = 54.54%, Percentage of silt = 20/55 * 100 = 36.36%, Percentage of clay = 5/55 * 100 = 9.09%. With these values we are entering into the USDA online soil texture calculator (Fig. 9).

4.5 Selection of Crops

From the questionnaire survey, the most commonly crops grown are rice and tomato (Figs. 10 and 11).

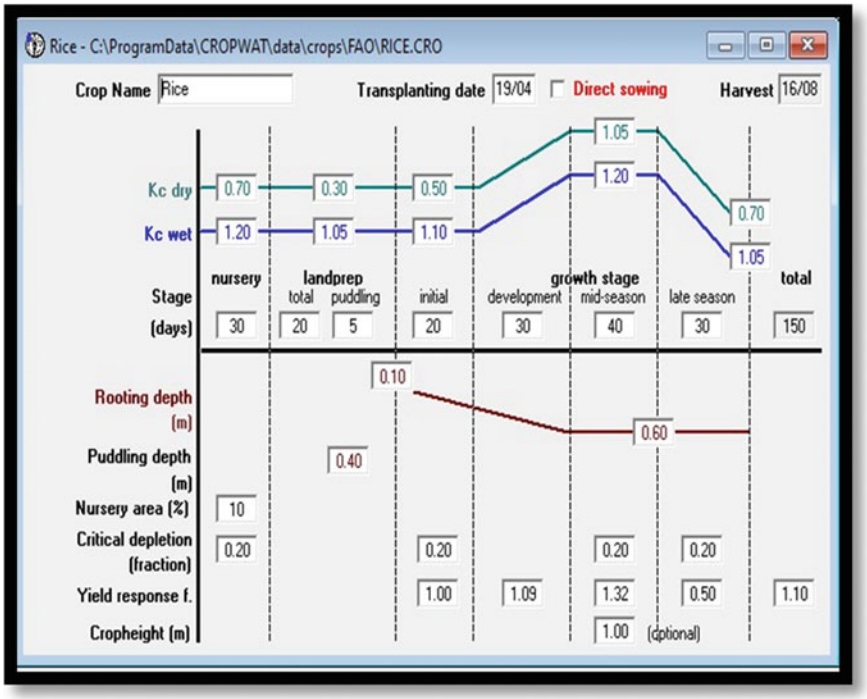

Fig. 10 Rice crop details

4.6 Cropwater Requirement

Results show that for rice, crop evapotranspiration (ETc) varied from 0.68 to 6.83 mm the total crop evapotranspiration is 1157.9 mm and the water required for crop differs from 0.7 to 31.3 mm the total irrigation requirement is 1300.2 mm for rice (Table 4).

Results show that for tomato, crop evapotranspiration (ETc) varied from 4.02 to 8.26 mm the total crop evapotranspiration is 941.9 mm and the crop water requirement varied from 8.1 to 68.1 mm the total irrigation requirement is 751.8 mm for tomato (Table 5; Fig. 12).

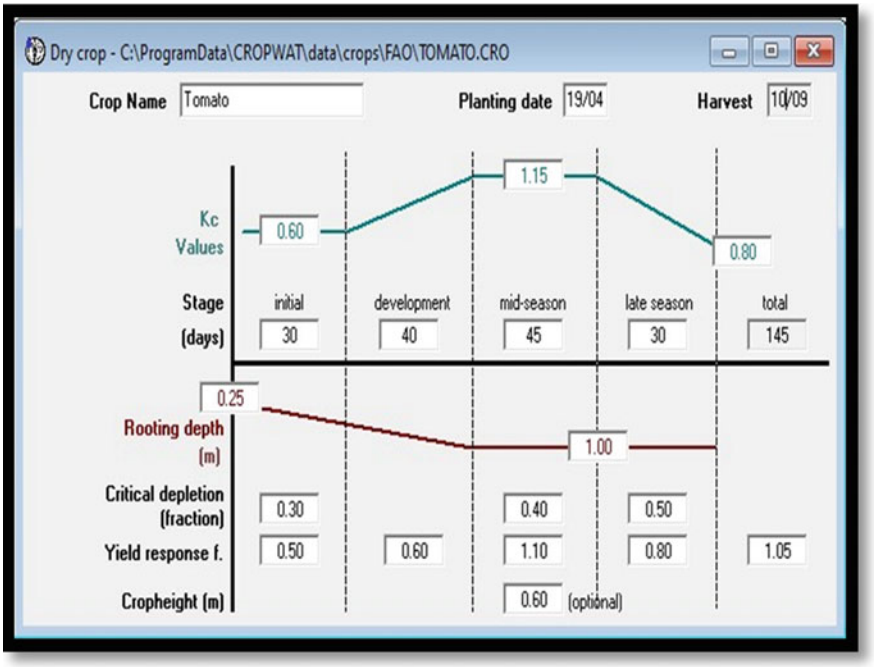

Fig. 11 Tomato crop details

4.7 Irrigation Scheduling

From the above graph, rice uses a lot more quantity of water than tomato. But the actual water needed by the crop is quite similar, but the gross irrigation value differs because when the rice is planted, the agricultural land must be prepared correctly. The water is mixed with nutrients to enrich the soil and the water is also used for the puddling process as well (Fig. 13).

Table 4 Rice CWR

ETO station: POONDI		Crop: Rice					
Rain station: POONDI		Planting date:19.04.2022					
Month	Decade	Stage	Kc (coeff)	ETc (m/day)	ETc (mm/dec)	Eff. rain (mm/dec)	Irr. req. (nun/dec)
Mar	2	Nurs	1.2	0.68	7	2	0.7
Mar	3	Nurs/LPr	1.18	1.76	193	2	78.2
Apr	1	Nurs/LPr	1.06	6.79	67.9	1.9	126
Apr	2	Init	1.07	7.2	72.2	2.1	239.8
Apr	3	Init	1.1	7.88	78.8	4	74.8
May	1	Deve	1.1	8.44	84.4	6.2	782
May	2	Deve	1.12	9.12	91.2	80	83.2
May	3	Deve	1.15	9.2	101.4	99	91.5
June	1	Mid	1.18	9.26	92.6	12.1	80.5
June	2	Mid	1.19	9.2	92	14.2	77.8
June	3	Mid	1.19	8.9	890	14.5	74.5
July	1	Mid	1.19	8.6	so	14.5	71.6
July	2	Late	1.18	8.28	82.8	14.9	68
July	3	Late	1.14	7.81	85.9	16.2	69.6
Aug	1	Late	1.08	7.26	72.6	18	54.7
Aug	2	Late	1.04	6.83	41	11.6	31.3
					1157.9	150.4	1300.2

4.8 Crop Scheme

It is a strategy in which crops are cultivated on specific farm plots for a certain length of time to maximize agricultural yields while preserving soil fertility. As a result, the most lucrative use of resources, such as land, labor, capital, and management, is linked to a cropping design. Table 6 shows the scheme result obtained for both rice and tomato crop.

Table 5 Tomato CWR

ETO station: POONDI		Crop: Tomato					
Rain station: POONDI		Planting date: 19.04.2022					
Month	Decade	Stage	Kc (coeff)	ETc (m/day)	ETc (mm/dec)	Eff. rain (mm/dec)	Irr. req. (nun/dec)
Apr	2	Init	0.6	4.04	8.1	0.4	8.1
Apr	3	Init	60	4.3	43	4	39
May	1	Init	0.6	4.6	46	6.2	39.8
May	2	Deve	0.6	4.91	49.1	8	41.1
May	3	Deve	0.71	565	62.2	9.9	52.3
June	1	Deve	0.84	6.63	66.3	12.1	54.2
June	2	Deve	0.98	7.58	75.8	14.2	61.6
June	3	Mid	1.1	8.26	82.6	14.5	68.1
July	1	Mid	1.13	8.19	81.9	14.5	67.4
July	2	Mid	1.13	7.91	79.1	14.9	64.2
July	3	Mid	1.13	7.75	85.2	18.2	69
Aug	1	Mid	1.13	7.59	75.9	18	57.9
Aug	2	Late	1.07	7.08	70.8	19.4	51.4
Aug	3	Late	0.5	6	66	19.5	46.5
Sep	1	Late	0.82	4.99	49.9	18.5	31.3
					941.9	190.5	751.8

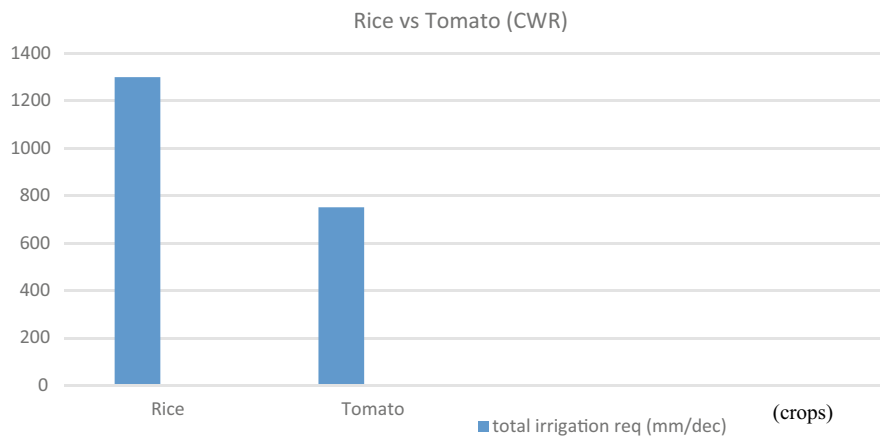

Fig. 12 Rice versus tomato

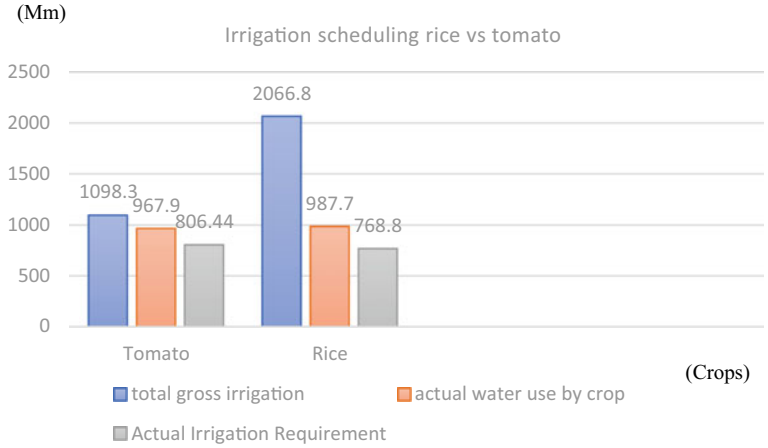

Fig. 13 Irrigation scheduling

Table 6 Crop scheme

ETO station: POONDI	Cropping pattern: Intercropping											
Rain station: POONDI												
Precipitation deficit	Months											
	Jan	Feb	Mar	Apr	May	June	July	Aug	Sep	Oct	Nov	Dec
1. Rice	0.0	0.0	78.9	440.5	252.9	232.7	209.1	85.9	0.0	0.0	0.0	0.0
2. Tomato	0.0	0.0	0.0	47.0	133.2	183.8	200.6	155.8	31.3	0.0	0.0	0.0
Net scheme irrigation required												
In mm/day	0.0	0.0	2.4	14.0	8.0	7.7	6.7	2.9	0.1	0.0	0.0	0.0
In mm/month	0.0	0.0	75.0	420.9	246.9	230.3	208.7	89.4	1.6	0.0	0.0	0.0
In l/s/h	0.00	0.00	0.28	1.62	0.92	0.89	0.78	0.33	0.01	0.00	0.00	0.00
Irrigated area (% of total area)	0.0	1.0	2.0	3.0	4.0	5.0	6.0	7.0	8.0	9.0	10.0	11.0
Irrigation required for actual area (in l/s/h)	0.00	0.00	0.29	1.62	0.92	0.89	0.78	0.33	0.12	0.00	0.00	0.00

5 Conclusion

To conclude, the climatic data was verified successfully using CLIMWAT and then it was verified using the CROPWAT. The total avg. ETO was found to be 5.56 mm/day. The rainfall data is also verified and inputted into the CROPWAT software. The

annual effective rainfall is found to be 483.5 mm. After the testing of the soil sample which was collected from the site, the soil falls under the under category of well graded soil and texture of the soil is confirmed as sandy loam type of soil. From the questionnaire survey, the crops that are selected for the project is rice and tomato as they are the most commonly grown crops in that region. The initial planting date for both rice and tomato are as 19-04-2022.The crop water requirement (CWR) for the rice crop is computed as 1300.2 mm/dec, whereas for tomato it is found to be 751.8 mm/dec. The total gross irrigation for rice is very high when it is compared to tomato. The total gross irrigation for tomato is 1098.3 and 2066.8 mm for rice. The cropping pattern is selected and the scheming is also computed automatically with the help of the CROPWAT software.

References

1. Mammen G, Joseph EJ (2015) Crop water requirement using FAO-CROPWAT and assessment of water resource for sustainable water resources. Elsevier
2. Onyancha DM, Gachene C (2017, Sept) CROPWAT model based estimation of the crop water requirement of major crops in Machakos county. Res J
3. Bouraima AK, Weihua Z (2015, Apr) Irrigation water requirement of rice using CROPWAT model in Northern Benin. IJABE
4. Ruswandi D, Perwitsari SDN (2019, Aug) Crop water requirement analysis using CROPWAT 8.0 in maize intercropping with rice and soybean. Res Gate
5. Halimi AH, Tefera AH (2019, Feb) Application of CROPWAT model for estimation of irrigation scheduling of Tomato in changing climate of Eastern Europe. SSRG-IJAES
6. Mehanuddinh H, Nikitha GR (2018, Apr) Study of water requirement of selected crops and irrigation scheduling using CROPWAT 8.0. IJIRSET
7. Diro SB, Zeleke KT (2009, Dec) Evaluation of the FAO CROPWAT model for deficit-irrigation scheduling for onion crop in a semiarid region of Ethiopia. Res Gen J Appl Hortic
8. Poornima, Ayyanagowdar MS, Polisgowadar BS (2019, Nov) Estimation of crop water requirement and irrigation scheduling of baby corn using CROPWAT model. Phyto J
9. Reddy M, Ganachari A (2020) Estimating reference evapotranspiration using CROPWAT model at Raichur region Karnataka

Highways and Transportation Engineering

Laboratory Performance Evaluation of Copper Slag in Semi-dense Bituminous Concrete

C. Sreejith, R. Jino, and K. Athiappan

Abstract In this research, the use the industrial waste, copper slag as the fine aggregate in the asphalt mix that has the properties similar to the natural sand having more toughness than the any other fine aggregate that can resist the wear and tear due to rubbing action of wheel on road surface. In this research, an attempt finds the possible use of copper slag by improving the engineering properties of asphalt mixes. The benefits of addition of copper slag as dosage 0–100% with increment of 10% by volume of aggregate on volumetric properties such as air voids, voids in mineral aggregate, and voids filled with bitumen and physical properties such as stability, flow, in asphalt mixes were investigated. The copper slag dosage of 30% dosage by volume of aggregate with an optimum bitumen content of 4.8% by weight of mix showed optimum performance.

Keywords Copper slag · Asphalt · Volumetric parameters · Physical properties

1 Introduction

In order to attain the economic and social development in the country, the transportation plays the key role for the movement of raw materials, finished goods and all necessary amenities, such as agricultural and dairy products, coal for the production of electricity, and medical facilities, which fulfill the human needs [1]. Due to rapid road infrastructure development in the developing countries such as India, there is huge demand on the natural resources such as broken stones obtained from the natural rocks, leads to natural resources in extinct. Thus the researchers or focused on using the alternative material obtained from the industries, such as flash, steel slag, blast furnace slag, and copper slag, which are in need to get disposed safely thus helps in

C. Sreejith (✉) · R. Jino
Department of Civil Engineering, Vels Institute of Science, Technology & Advanced Studies, Pallavaram, Chennai 600117, India
e-mail: sreejithchandran5512@gmail.com

K. Athiappan
Department of Civil Engineering, Thiagarajar College of Engineering, Madurai, India

K. R. Reddy et al. (eds.), *Recent Advances in Civil Engineering*, Lecture Notes in Civil Engineering 398, https://doi.org/10.1007/978-981-99-6229-7_44

safe disposal of the industrial waste and protecting the available natural resources facilitating the sustainable infrastructure development [2]. The blast furnace slag, Mill tailings and the construction waste used in the base and sub-base found act as the bulk filler with improvement in the strength when compared to the conventional material [3]. It is observed that the inclusion of metallic slag such as the steel slag, and non-ferrous slag does not affecting the volumetric and physical properties and found improving the skid resistance property to a greater extent leads to provide safer roads, thus it was found to be suitable for the asphalt mix [4]. The cement kiln dusts obtained from the cement industry are suitable for filler in the asphalt mix and effective for stabilization of the base material used in the road construction [5]. The other waste, such as marble waste, the worn out tires, glass waste, blast furnace slag, and china clay waste, are found to be suitable for the asphalt mixes [6]. It was absorbed that the inclusion of the fly ash as the filler in the asphalt mix found behave inferior and consumes more bitumen content when compared to the conventional mix and also consumes more bitumen content but satisfies the minimum requirement hence the fly ash utilized in the low volume roads after further intense research [7]. In the asphalt mixture for the stable packing of the coarse aggregate, fine aggregate and the bitumen, the filler material property used was dominant for the performance of the mix [8]. In order to achieve the maximum cohesion in the asphalt mixture, the maximum filler contribution in the asphalt mix needed [9]. The researchers found out that the physical properties such as fatigue life, indirect tensile strength and stiffness were increased in the mastic asphalt while using the following industrial waste such as the ceramic dust, steel slag, fly ash as the filler material [10]. The inclusion of steel slag in the asphalt mix found to increase the rutting and skid resistance. The only drawback identified was consuming little higher asphalt compared to the conventional mix [11]. The physical properties such as particle size distribution and fineness modulus, of the copper slag resembles with the conventional fine aggregate used in the highway construction. However, the other improved physical properties such as greater hardness, higher specific gravity, and less water absorption when compared to the convention fine aggregate [12–15]. From the above literature survey it was found out that the inclusion of copper slag in the asphalt mix (Semi-Dense Bituminous Concrete) was not investigated for possible usage in the highway construction. Hence, this research focused on using the copper slag as filler in the asphalt mixture.

2 Methodology

In this research paper, methodology involves the physical properties of bitumen, copper slag, and broken stones evaluated in the laboratory. The conventional Marshall specimen prepared and the optimum bitumen content determined. In the third stage the Marshall specimen prepared by incorporating the copper slag is replace the filler by 10% to the 100% with 10% increment and the corresponding volumetric and physical properties are determined and compared with the convention asphalt mixture

and other mechanical properties such as fatigue life and indirect tensile strength ratio are determined.

3 Materials and Methods

The bitumen VG30 confirming to the MORTH specification utilized. The coarse aggregate consist of crushed rock, crushed gravel, or other hard material retained on 2.36 mm sieve. It was clean, hard, and durable and cubical shape, free from dust and soft organic and other deleterious substances. In order to achieve the required gradation for the semi-dense bituminous mix, three different size of 12 mm, 10 mm, and filler (less than 6.3 mm) individually graded and combined together with 12 mm (20%), 10 mm (22%), and filler size less than 6.3% (58%).

For the formulation and assessment of asphalt mixture, the Marshall experiment is a straightforward and reasonably priced standardized laboratory experiment that utilized throughout the globe. During this research, stability, flow value, unit weight, air voids, voids in aggregate particles, and voids filled with asphalt are indeed the main criteria that utilized to assess the various mixtures at various asphalt percentages. The ideal asphalt percentage was chosen to achieve the highest levels of stability, particle density, and average permissible values for % air voids. As the ideal asphalt percentage, the mean of such three criteria binder content is chosen. Each Marshall criterion for the mixtures at optimum asphalt examined in relation to the corresponding information provided in MORTH (2013) [16]. Overall the bitumen content 4.8% by weight of mix satisfy all the requirement specified by the Morth shown in Table 1.

Table 1 MoRTH requirements for semi-dense bituminous concrete (SDBC)

S. No.	Characteristics	Recommended value
1	Air voids (V_a)	3–5%
2	Stability	$\leq$ 8.2 KN
3	Flow value	2–4 mm
4	V_{ma} (%)	13–17
5	V_{fb} (%)	65–75

4 Replacement of Filler by the Copper Slag

4.1 Optimum Bitumen Content (With Copper Slag)

In this research, conventional asphalt mix contained 58% of filler material size less than 6.3 mm size is replaced by the copper slag from 10 to 100% with an increment of 10% by keeping optimum bitumen as 4.8% by weight of mix obtained from the conventional mix as constant. Thereafter the volumetric properties and mechanical properties investigated to identify the appropriate percentage of copper slag to be replaced.

From the Fig. 1a, observed that, with the increase in copper slag content the air voids get decreased due to the low absorption of bitumen by copper slag, between the copper percentage 10% to 40% replaced by filler material of conventional mix, which satisfy the Morth requirement. From the Fig. 1b, observed that, with the increase in copper slag content the voids in mineral aggregate get decreased due to the low absorption of bitumen by copper slag leads to presence of excess bitumen in the mix, between the copper percentage 10% to 60 replaced by filler material of conventional mix, which satisfy the Morth requirement. From the Fig. 1c, observed that, with the increase in copper slag content, the voids filled with bitumen get decreased due to the low absorption of bitumen by copper slag leads to presence of excess bitumen in the mix, between the copper percentage 10% to 40% replaced by filler material of conventional mix, which satisfy the Morth requirement. From the Fig. 1d, observed that, with the increase in copper slag content 10–100% the stability obtained is greater than the minimum requirement specified by the MoRTH due to better interlocking and sufficient bitumen content due to the low absorption of bitumen by copper slag leads to presence of excess bitumen in the mix. From the Fig. 1e, observed that, with the increase in copper slag content, the flow value get increased, the copper percentage 10–50% replaced by filler material of mix, which satisfy the Morth requirement.

4.2 Fatigue Life and Indirect Tensile Strength Ratio

In order to access the fatigue life of the asphalt mix, the four point bending test was conducted confirming to EN 12697-24. The fatigue test set-up shown in Fig. 2. From Fig. 3, observed that, with replacement of copper slag from 10 to 40% by filler material shows increase in fatigue life, beyond that trend of decrease in fatigue life observed. Similarly to access the indirect tensile strength ratio, the indirect tensile strength for dry and wet sample determined confirming to the code EN 12697-23. The testing temperature adopted according to the standard was 25 °C. The specimen geometry adopted according to the standard 150 mm diameter and 60 mm height. From the Fig. 4, observed that, with replacement of fine aggregate from 10 to 30% by copper slag increase in ITS ratio, beyond that, the ITS ratio tends to decrease. From the Fig. 5, observed that, there is a strong linear relationship between the stability and

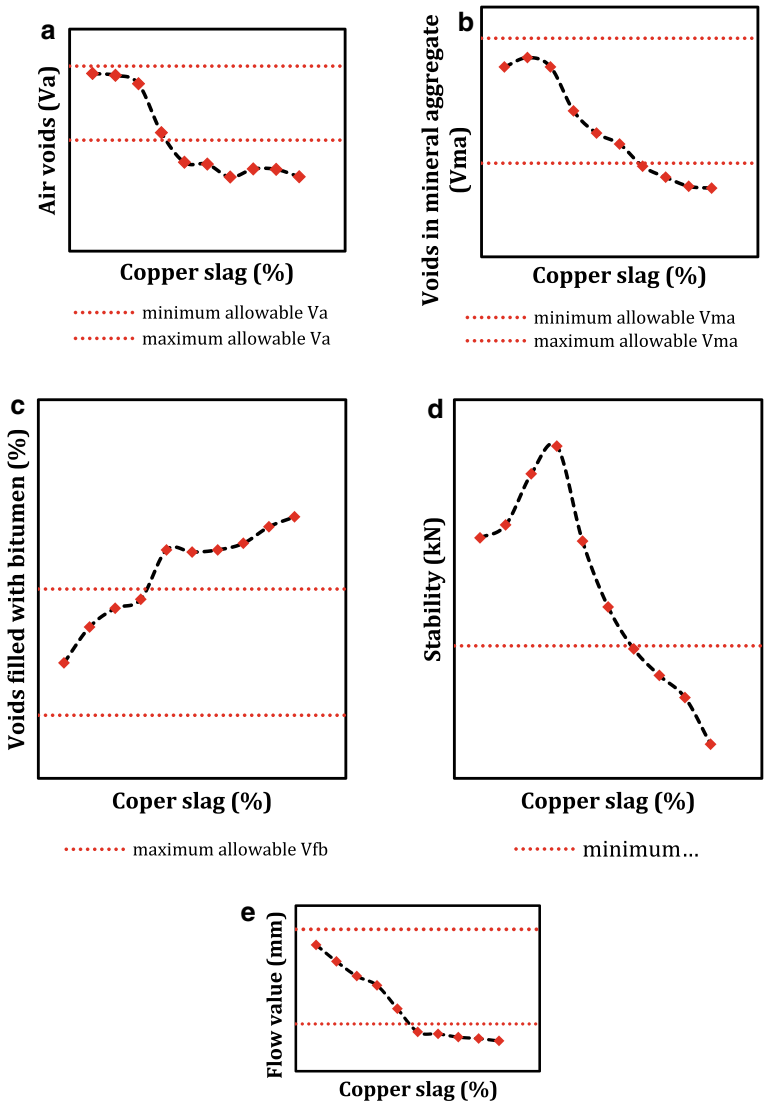

Fig. 1 **a** Variation of air voids with fine aggregate replaced by copper slag. **b** Variation of voids in mineral aggregate with fine aggregate replaced by copper slag. **c** Variation of voids filled with bitumen with fine aggregate replaced by copper slag. **d** Variation stability with fine aggregate replaced by copper slag. **e** Variation flow with fine aggregate replaced by value with copper slag

fatigue life. From Fig. 6, observed that there is a strong linear relationship between the stability and indirect tensile strength ratio (Fig. 6, Table 2).

Fig. 2 Fatigue test set-up

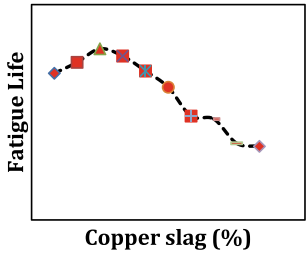

Fig. 3 Variation of fatigue life

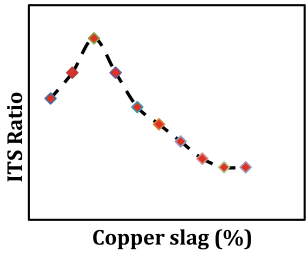

Fig. 4 Variation of ITS ratio with

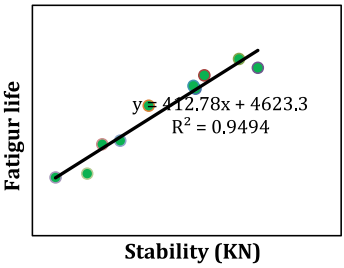

Fig. 5 Relation between Fatigue life and stability

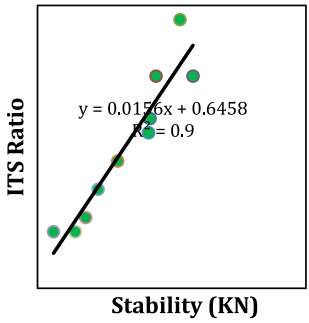

Fig. 6 Relation between ITS and stability

Table 2 Volumetric and mechanical properties of the asphalt mix with replacement of copper slag as fine aggregate

Copper slag%	G_{mb}	G_{sb}	G_{mm}	V_a (%)	V_{ma} (%)	V_{fb} (%)	Flow (mm)	Stability (kN)	Fatigue life	Indirect tensile strength
10	2.38	2.7	2.5	4.8	16.08	69.15	3.67	11.62	9450	0.82
20	2.4	2.7	2.5	4.75	16.38	71.99	3.32	12.03	9858	0.85
30	2.38	2.7	2.5	4.52	16.08	73.47	3.01	13.65	10,360	0.89
40	2.42	2.7	2.5	3.2	14.67	74.19	2.813	14.53	10,091	0.85
50	2.44	2.7	2.5	2.4	13.96	78.1	2.32	11.52	9536	0.81
60	2.45	2.7	2.5	2.35	13.61	77.93	1.83	9.43	8930	0.79
70	2.47	2.7	2.5	2	12.9	78.1	1.79	8.1	7860	0.77
80	2.48	2.7	2.5	2.22	12.55	78.62	1.72	7.26	7750	0.75
90	2.46	2.7	2.5	2.21	12.26	79.93	1.69	6.56	6850	0.74
100	2.49	2.7	2.5	2.01	12.2	80.72	1.64	5.08	6735	0.74

5 Conclusion

From the overall research, the following conclusion are drawn for the replacement of filler by the copper slag are given below.

- The optimum bitumen content for the conventional mix found to be 4.8% by the weight of asphalt mix.
- The optimum replacement of conventional filler by the copper slag was found to be 40% without compromising the volumetric and the mechanical properties of the asphalt mix.
- It observed, that there is strong relation between the stability and the fatigue life, stability and indirect tensile strength ratio.

References

1. Jayashree B, Santhanu S, Kalaiarasan B (2016) Utilization of copper slag in bituminous mix 188–202
2. Sen T, Mishra U (2010) Usage of industrial waste products in village road construction 1(2):122–126
3. Mroueh UM, Wahlström M (2002) By-products and recycled materials in earth construction in Finland—an assessment of applicability. Resour Conserv Recycl 35:117–129
4. Javed S, Lovell CW, Wood LE (1994) Waste foundry sand in asphalt concrete, vol 1437. Transportation Research Record, TRB, National Research Council, Washington, D.C., pp 27–34
5. Hawkins GJ, Bhatty JI, O'Hare AT (2003) Cement kiln dust production, management and disposal, vol 2737. Portland Cement Association, PCA, R&D
6. Nunes MCM, Bridges MG, Dawson AR (1996) Assessment of secondary materials for pavement construction: technical and environmental aspects. Waste Manage 16(1–3):87–96
7. Kar D, Panda M, Giri JP (2014) Influence of fly-ash as a filler in bituminous mixes. ARPN J Eng Appl Sci 9(6):895–900
8. Zulkati A, Diew WY, Delai DS (2011) Effects of fillers on properties of asphalt-concrete mixture. J Transp Eng ASCE 138(7):902–910
9. Kandhal PS, Lynn CY, Parker F (1998) Characterization tests for mineral fillers related to performance of asphalt paving mixtures. J Transp Res Board 1638(1):101–110
10. Muniandy R, Aburkaba E (2011) The effect of type and particle size of industrial wastes filler on Indirect tensile stiffness and fatigue performance of stone mastic asphalt mixtures. Aust J Basic Appl Sci 5(11):297–308
11. Noureldin A, McDaniel RS (1990) Evaluation of surface mixtures of steel slag and asphalt. Transp Res Rec 1269
12. Jayashree B, Santhanu S, Kalaiarasan B (2016) Utilization of copper slag in bituminous mix
13. ASTM D 1559 (1989) Test method for resistance of plastic flow of bituminous mixtures using Marshall Apparatus. American Society for Testing and Materials
14. Philadelphia, USA. ASTM D 6931 (2012) Indirect tensile (IDT) strength for bituminous mixtures. American Society for Testing and Materials, Philadelphia, USA
15. IS: 73 (2006) Paving bitumen-specification, 2nd revision. Bureau of Indian Standards, New Delhi, India
16. Ministry of Road Transport & Highways (MoRTH), Government of India (2013) Annual report 2017–18, New Delhi

Study on Pedestrian Crossing Behaviour at Uncontrolled Intersection

C. S. Surya and S. Archana

Abstract Pedestrians one of the vulnerable road users, have become more susceptible to traffic crashes with the rapid growth of motor vehicles in India. Identifying the uncontrolled intersections having more pedestrian accidents which play a key role in developing efficient and effective strategies to assess pedestrian safety. The study discusses pedestrian crossing behaviour at uncontrolled intersections. It includes a collection of primary data and secondary data. Primary data includes road geometric data and traffic volume count. Secondary data includes the pedestrian accident data from 1st January 2018 to 30th October 2022 from the District Crime Record Bureau (DCRB) of Thrissur City. From the pedestrian accident data of Thrissur district, Kunnamkulam intersection was selected as study area. Analysis was done on the influence of pedestrian attributes like age, gender and crossing patterns in pedestrian accidents. Most of the pedestrian crossing patterns are identified as one step and perpendicular crossing. Variations in crossing time, waiting time, and crossing speed were analysed for each age group and gender.

Keywords Pedestrian accidents · Crossing speed · Crossing time · Waiting time · Crossing pattern

1 Introduction

The road users consist of vehicles and pedestrians. Walk mode is an important part of individual trips made by every citizen. For those who commute by public transport facility, the first and end parts of the journey take place by walk mode. Road accidents usually include pedestrians. According to the Ministry of Traffic Transport and Highways (MORTH) 2021, there have been 412,432 documented road accidents nationwide, resulting in 153,972 fatalities and 384,448 injuries. The latest National Crime Records Bureau (NCRB) also shows that fatalities of pedestrians stood at

C. S. Surya · S. Archana (✉)
Jyothi Engineering College, Thrissur, India
e-mail: archanas@jecc.ac.in

K. R. Reddy et al. (eds.), *Recent Advances in Civil Engineering*, Lecture Notes in Civil Engineering 398, https://doi.org/10.1007/978-981-99-6229-7_45

18,900 in 2021, with the share of pedestrians in overall road deaths also continuously increasing. Uncontrolled intersections are those where no extreme traffic control measures have been implemented. The safety of the pedestrians who cross the locations depends on the behaviour of the pedestrians. Age and gender are two demographic factors that have an impact on pedestrian behaviour when crossing the roadway.

1.1 Background

Srikanth et al. [1] selected uncontrolled intersections for their study. The videographic survey is used to extract pedestrian characteristics including age, gender, the way they cross, speed, crossing time, waiting time, etc. Various combinations of the features of the vehicle and the pedestrian are taken into account during the analysis of the extracted data. A male pedestrian crosses the road more quickly than female pedestrians. Pedestrian carrying baggage spends more time compared with a pedestrian carrying without baggage.

Ravishankar and Nair [2] investigates pedestrian safety at unsignalized and midblock intersection. From the video, they were able to obtain the following information: crossing duration, speed, stages of crossing, interruptions when they cross, and the kinds of vehicles in which pedestrians accept the gap. For various age and gender groups, the propensity to exhibit rolling gap behaviour was noted, and then evaluated to assess the risk involved with these kinds of crossings. The importance of this study for pedestrians at these uncontrolled intersection should aid in planning safe pedestrian facilities. It was found that pedestrian acceptance of gaps and behaviour when crossing roads is significantly influenced by the size of the vehicle. When crossing unsignalized intersections, men pedestrians faces more risks than female pedestrians.

Dadhich et al. [3] examined pedestrian crossing behaviour to provide suitable pedestrian facilities. Age, gender, carrying luggage, and other pedestrian factors all had an impact, which was examined. They examined that how much percentage of pedestrians using oblique and perpendicular crossings. Analyses are done on pedestrian average crossing speed, waiting time and crossing time based on age and gender crossing time were determined. Male pedestrians crossed at a rate of 1.287m/s and female pedestrians at 1.219m/s. Regarding the gaps in traffic flow that pedestrians allow, pedestrian safety was also examined.

Jain et al. [4] analysed pedestrian safety about safety gaps and margins that pedestrians accepted in the flow of traffic. According to the investigation of gap acceptance and safety margins, most pedestrians had safety margins of 1 to 4s, and they accept gaps between 2 to 6s. Fewer persons cross the road in two stages and a greater proportion crosses in a perpendicular direction.

Govinda et al. [5] investigated the key variables influencing pedestrian road crossing behaviour under mixed traffic conditions. The analysis of the pedestrian crossing speeds at two uncontrolled intersections and two midblock locations aimed

to identify the main influences on the speed of pedestrian crossings. There is a noticeable variation in crossing rates between the intersection and midblock locations, according to the findings of an ANOVA test on crossing speeds.

1.2 Objectives

- To identify the most pedestrian accident intersection in Thrissur city
- To study the pedestrian crossing behaviour at the intersection

2 Data Collection

The pedestrian accident data of Thrissur city from 2018–2022 are collected from DCRB. Identified the uncontrolled intersection based on the pedestrian accident data. Figure 1 shows the selected uncontrolled intersection, Kunnamkulam.

Primary data includes road geometric data and volume count. Road geometric data were collected from Kunnamkulam Junction through a site visit. Road geometric data includes drainage type and its condition, shoulder type and its condition, carriageway details and footpath details are collected. Traffic volume count was taken by videographic survey. Peak period (5–6 p.m.) survey was conducted at the Kunnamkulam intersection. Vehicular and pedestrian counts as shown in Fig. 2.

Fig. 1 Kunnamkulam intersection

Fig. 2 Volume count

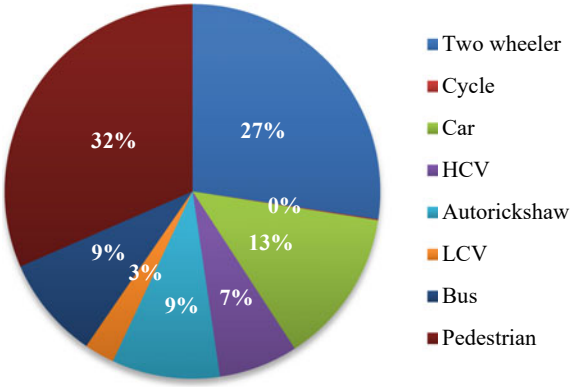

3 Pedestrian Crossing Behaviour

Various elements relating to pedestrian characteristics, pedestrian movements, traffic issues, road conditions, and environmental factors frequently influence the way pedestrians cross roads. This was analysed to access the safety of pedestrians. Both traffic volume and pedestrian volume were extracted from the videographic survey. Pedestrian crossing time, waiting time and crossing speed were determined based on the gender and age of the pedestrians by visual appearance. Genderwise analysis as shown in Fig. 3.

3.1 Crossing Pattern

One step or two steps, perpendicular or oblique are used to categorize crossing patterns. The crossing pattern identified at this intersection is one step. Percentage of pedestrians crossing the intersection in perpendicular and oblique patterns as shown in Fig. 4. The gender wise and age wise analyses were carried out to determine the percentage of pedestrians crossing the road in oblique pattern (Figs. 5 and 6).

Fig. 3 Genderwise analysis

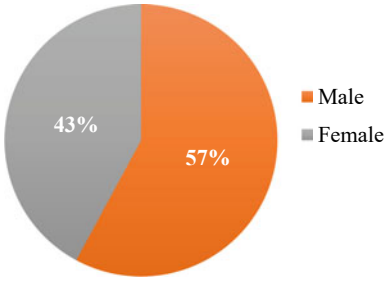

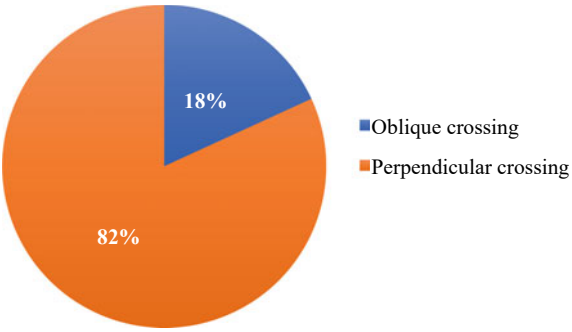

Fig. 4 Crossing pattern analysis

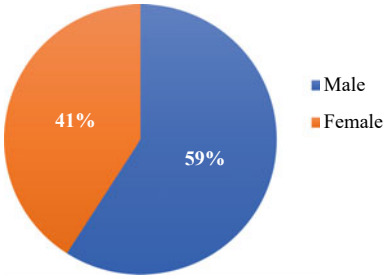

Fig. 5 Oblique crossing gender wise

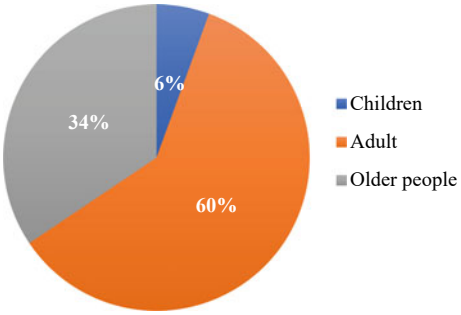

Fig. 6 Oblique crossing age wise

3.2 Waiting Time and Crossing Time

Categorize the age of pedestrians into three groups: Children (below 18 years), Adults (18–49 years), and Older people (above 50 years). Crossing time and waiting time vary based on the gender and age of pedestrians. Variations in crossing and waiting time as shown in Tables 1, 2, 3, 4 and Fig. 7.

Table 1 Waiting time and crossing time according to gender (perpendicular)

Location	Male		Female	
Kunnamkulam	Waiting time (s)	Crossing time (s)	Waiting time (s)	Crossing time (s)
	3.03	9.61	4.39	9.43

Table 2 Waiting time and crossing time with respect to age (perpendicular)

Location	Children		Adult		Older people	
Kunnamkulam	Waiting time (s)	Crossing time (s)	Waiting time (s)	Crossing time (s)	Waiting time (s)	Crossing time (s)
	4.15	9.04	3.35	8.64	5.16	9.97

Table 3 Waiting time and crossing time for oblique crossing (gender)

Location	Male		Female	
Kunnamkulam	Waiting time (s)	Crossing time (s)	Waiting time (s)	Crossing time (s)
	1.34	10.47	3.05	10.85

Table 4 Waiting time and crossing time for oblique crossing (age)

Location	Children		Adult		Older people	
Kunnamkulam	Waiting time (s)	Crossing time (s)	Waiting time (s)	Crossing time (s)	Waiting time (s)	Crossing time (s)
	5.11	10.92	1.75	10.10	2.05	11.49

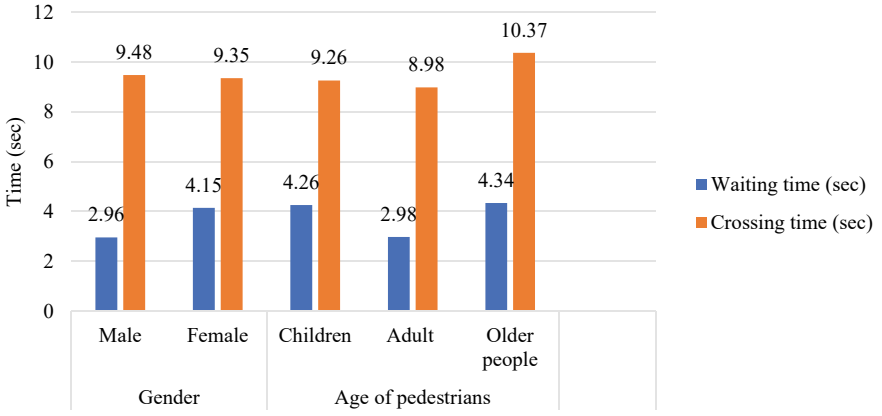

Fig.7 Variation in waiting and crossing time (overall)

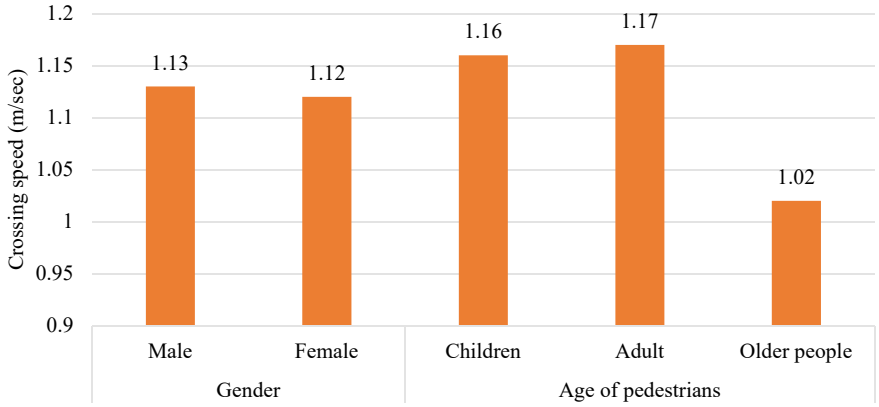

Fig.8 Variation in average crossing speed based on gender and age of pedestrians

3.3 Crossing Speed

The pedestrian crossing speed is determined from the value of pedestrian crossing time observed from the video. The speed of pedestrians is estimated using previously noted data and the value of road width sections. Pedestrian personal characteristics including age and gender are taken into account while determining the variation in speed. The average crossing speed of pedestrians is based on age and gender as shown in Fig. 8.

4 Findings

- 82% of pedestrians cross the road perpendicularly and remaining 18% of pedestrians follows an oblique pattern. 43% of female cross the road in an oblique pattern and 57% of adults were crosses the road in an oblique pattern.
- Waiting time of male and female pedestrians varies between 1 to 4.5s and crossing time varies between 9 to 11s. The waiting time of adults are found to be 2.98s, which is lower compared to childrens and older people.
- Crossing time of older people is more, found to be 10.37s. The crossing time of adults and childrens are found to be 8.98 and 9.26s.
- For an oblique crossing, the waiting time for males are found to be 1.34s and for females are found to be 3.05 s. The crossing time of male and female pedestrians are varying between 10.47 to10.85s.
- For an oblique crossing, the waiting time of older people is found to be 2.05 s and for adult and older people, it is calculated as 1.75 and 5.11 s. The crossing time of older people is 11.49s.

- The calculated average pedestrian crossing speed is 1.125 m/s. Males crosses the road at a speed of 1.13m/s, whereas females crosses at 1.12 m/s.
- The average crossing speed of childrens and adults were 1.16 and 1.17m/s. Older people crosses at a rate of 1.02 m/s.

5 Conclusion

Perpendicular and one step crossings are the two crossing patterns adopted by more pedestrians and very few pedestrians are crosses in two stages. Waiting time, crossing time, and crossing speed are varying with the gender and age of pedestrians. Waiting times for childrens and older people are more compared to adults. An adult requires less time to cross the road. Female pedestrians require less time to cross the road and the crossing speed of males is more for gender wise analysis. Pedestrians using mobile phones and carrying luggage while crossing is not considered in this study. The analysis of pedestrian crossing behaviour is a key aspect of deciding ways to ensure that pedestrians are safe on the roadways. The waiting time of pedestrians can help to determine whether the pedestrian facility are required or not in that location.

Acknowledgements I am grateful to my mentor, Ms. Archana S., and, Dr. Vincy Verghese, HoD, Department of Civil Engineering, Jyothi Engineering College, Thrissur for their excellent support throughout this project.

References

1. Srikanth S, Ballari SO, Shree Raksha UM et al (2020) Road crossing behaviour of pedestrians at uncontrolled intersections. Int J Future Gener Commun Network 13(3):2990–300
2. Ravishankar KVR, Nair PM (2018) Pedestrian risk analysis at uncontrolled midblock and unsignalised intersections. J Traffic Transp Eng (English edn) 5(2):137–147
3. Dadhich PN, Sharma V, Bhardwaj V et al (2016) Analysis of pedestrian behaviour in urban areas. Int J Eng Res Technol (IJERT) 4(23):1–5
4. Jain A, Gupta A, Rastogi R (2014) Pedestrian crossing behaviour análysis at intersections. Int J Traffic Transp Eng 4(1):103–116
5. Govinda L, Abhigna D, Nair PM et al (2020) Comparative study of pedestrian crossing behaviour at uncontrolled intersection and midblock locations. Transp Res Procedia 48:698–706

Road Crashes on National Highway-48 in Maharashtra: Inspection and Interpretation

Krantikumar V. Mhetre and Aruna D. Thube

Abstract The present study inspects the crash records for the period of 5 years from 2016 to 2020 on a 265 km highway section of NH-48 passing through Maharashtra state in India. The crash records are inspected and interpreted under the various categories like type of collision, type of injury, violation of rules, type of lane, type of road curve, type of junction, and climatic condition. The inspection revealed that 36.43% (588) of crashes have resulted from Head-on-collision, 22.37% (361) from Rear-end-collision, 16.79% (271) in deaths, 46.34% (748) in grievous injury, 36.06% (582) in minor injury, 42.99% (694) from vehicle out of control, 26.70% (431) from overspending, 97.03% (1566) on 2-lanes, 94.55% (1526) on straight roads, 98.70% (1593) on T-junction, 62.33% (1006) in fine climate condition, and 11.214% (181) in cloudy climate condition. In addition to these, there are 25.65% (414) of crashes which are not identified or recorded under the type of collision. There are only 0.806% (13) crashes which resulted in no injury, which calls for serious attention to the road safety issues of this highway section. Overall, as per the interpretation of the results, it is concluded that these interpretations are useful in deciding and implementing the road safety policies on this highway section to reduce the severity levels of the road crashes.

Keywords Road crashes · Inspection · National highway · Maharashtra

1 Introduction

Road crashes results from a variety of the factors belonging to the road geometry, road traffic, vehicle condition, human fault, etc. These factors include a vast variety of sub-factors and therefore the road crash analysis becomes a complex phenomenon to arrive at a single point solution. In terms of highest deaths in road crashes, India stood at the 1st position in the world [3]. There are 412,432 road crashes in India

K. V. Mhetre (✉) · A. D. Thube
Civil Engineering Department, COEP Tech University (Formerly College of Engineering Pune), Pune, Maharashtra, India
e-mail: kvm18.civil@coeptech.ac.in

K. R. Reddy et al. (eds.), *Recent Advances in Civil Engineering*, Lecture Notes in Civil Engineering 398, https://doi.org/10.1007/978-981-99-6229-7_46

having 153,972 deaths and 384,448 injuries. There has been an increase of 12.6% in case of road crashes, 16.9% in case of deaths, and 10.39% in case of injuries as compared to the year 2020 [4].

In order to achieve the road safety, the public involvement is a vital component in addition to the various engineering strategies [2]. A study on NH-45 in Tamil Nadu, India revealed that the major causes of road crashes in case of heavy vehicles are head-on and rear-end collisions [9]. There are various studies based on statistical analysis of road crashes on the highways based on the severity [10]. In majority of the cases, the maximum crashes result on the rural highways and therefore it is necessary to have the immediate response facilities to the road crashes and public awareness in case of rural road crashes [7].

A study on NH-1 in India revealed that the major causes of road crashes are overspeeding of heavy vehicles, and crashes occurring in day are more than crashes occurring in night [1]. To achieve the rod safety worldwide, the issues of road safety in under-developed and developing countries must be handled at priority, as the majority of road crashes are seen in under-developed and developing countries [12]. The road crashes distribution is dependent on the time, month, age, gender, and India is about to report more than 250 thousand deaths per year till 2025 [11]. Road crash records in Indian scenario are studied and a lot of recommendations based on the analysis are available [6]. Recently, the road crash record in Pakistan is also being studied and recommendations are given to reduce road crashes [8]. Sustainable Development Goals 3.6 targets for road safety can be achieved by 2030, but the fatality rate will decrease not more than 0.002% per 1000 people in Indian scenario [5]. Therefore, the road safety issues calls for the immediate attention of the researchers from various field for their contribution.

2 Methodology

The inspection and interpretation of crash records of NH-48 is done by using the methodology as shown in Fig. 1. A highway section approximately around 265 km of NH-48 is chosen for the study [13]. The crash records available with the National Highways Authority of India are collected. The inspection of the crash records includes 7 major classifications of the crash record like type of collision, type of injury, violation of rules, type of lane, type of road curve, type of junction, and climatic condition. These classifications include further sub-classifications individually. After this, the interpretation of the inspected crash records is presented with the conclusions.

Fig. 1 Study methodology

3 Results and Discussion

The crash records inspected based on the type of collision, like head-on-collision, rear-end-collision, etc., are shown in Fig. 2. There are 8 major types of collision identified and the crash records are categorized accordingly. The highest recorded types of collision are head-on-collision with 588 (36.43%) crashes, rear-end-collision with 361 (22.37%) crashes, and 414 (25.65%) crashes which are marked not identified or not recorded.

The crash records inspected based on the type of injury, like death, minor injury, no injury, etc., are shown in Fig. 3. There are 4 major types of injury identified and the crash records are categorized accordingly. The highest recorded types of injury are grievous injury with 748 (46.34%) crashes, minor injury with 582 (36.06%) crashes, and 271 (16.79%) crashes resulted in death.

The crash records inspected based on the reasons, like overspeeding, drink-and-drive, etc., are shown in Fig. 4. There are 6 major reasons identified and the crash records are categorized accordingly. The highest recorded reasons are vehicle out of control with 694 (42.99%) crashes, overspeeding with 431 (26.70%) crashes.

The crash records inspected based on the type of lane, like 2-lane, 1-lane, etc., are shown in Fig. 5. There are 4 major types of lanes identified and the crash records are categorized accordingly. The highest recorded types of lanes are 2-lane with 1566 (97.03%) crashes.

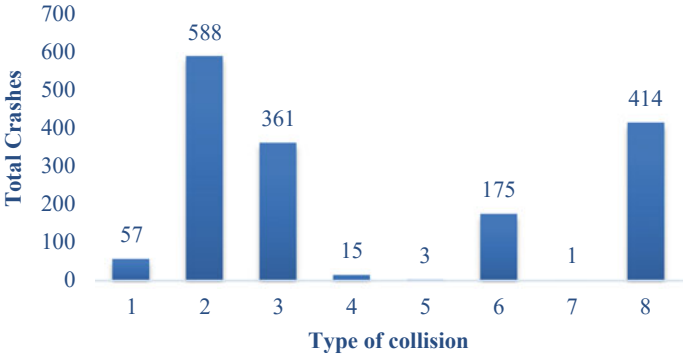

Fig. 2 Inspection based on type of collision

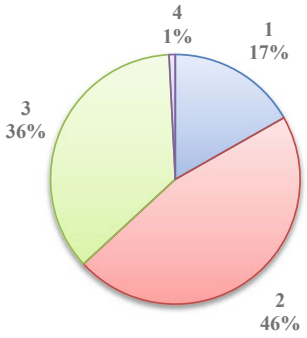

Fig. 3 Inspection based on type of injury

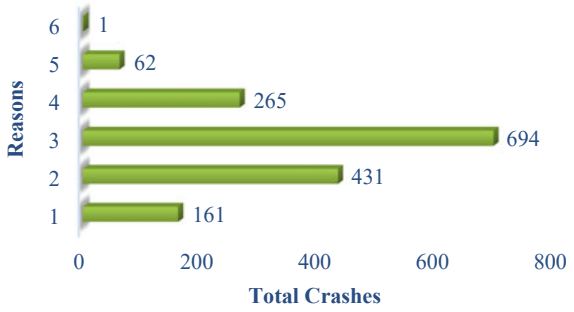

Fig. 4 Inspection based on reasons

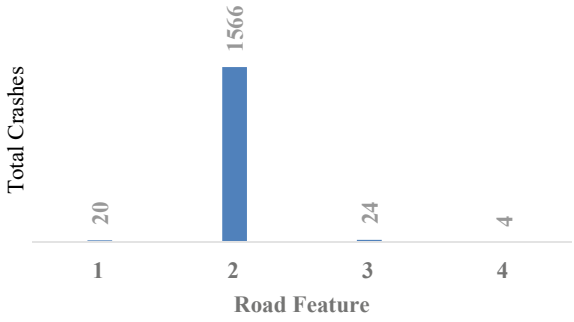

Fig. 5 Inspection based on type of lane

The crash records inspected based on the type of road curve, like slight curve, straight, sharp curve, etc., are shown in Fig. 6. There are 8 major types of road curves identified and the crash records are categorized accordingly. The highest recorded types of road curve are straight roads with 1526 (94.55%) crashes.

The crash records inspected based on the type of road junction, like Y-junction, T-junction, etc., are shown in Fig. 7. There are 9 major types of road junction identified and the crash records are categorized accordingly. The highest recorded type of road junction is T-junction with 1593 (98.70%) crashes.

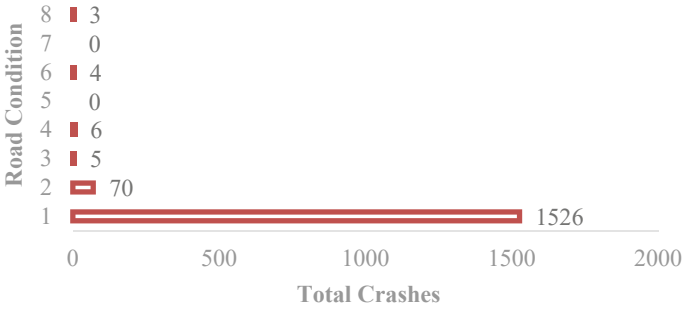

Fig. 6 Inspection based on type of road curve

Fig. 7 Inspection based on type of road junction

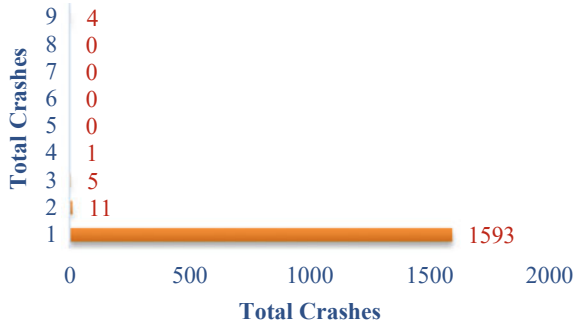

The crash records inspected based on the climatic condition, like light rain, fine, cloudy etc., are shown in Fig. 8. There are 12 major climatic conditions identified and the crash records are categorized accordingly. The highest recorded climatic conditions are fine with 1006 (62.33%) crashes, cloudy with 181 (11.214%) crashes, and 180 (11.152%) crashes occurred in light rain.

4 Conclusions

The study reveals some interesting conclusions based on the inspection and interpretation of the crash records available for the period of 5 years. The inspection revealed that 36.43% of crashes (588) have resulted from Head-on-collision, 22.37% (361) from Rear-end-collision, 16.79% (271) in deaths, 46.34% (748) in grievous injury, 36.06% (582) in minor injury, 42.99% (694) from vehicle out of control, 26.70% (431) from overspending, 97.03% (1566) on 2-lanes, 94.55% (1526) on straight roads, 98.70% (1593) on T-junction, 62.33% (1006) in fine climate condition, and 11.214% (181) in cloudy climate condition. In addition to these, there are 25.65% (414) of crashes which are not identified or recorded under the type of collision.

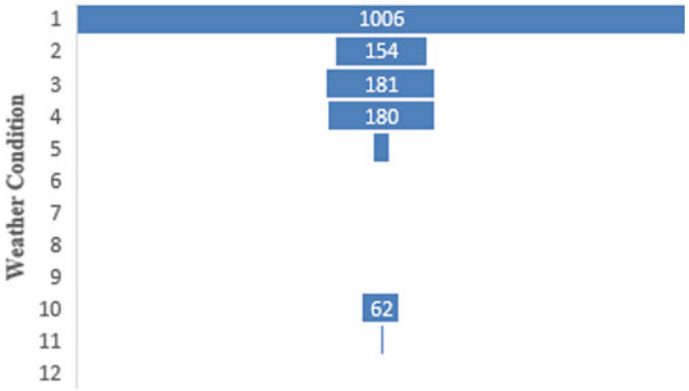

Fig. 8 Inspection based on climatic condition

There are only 0.806% (13) crashes which resulted in no injury, which calls for serious attention to the road safety issues of this highway section. Overall, as per the interpretation of the results, it is concluded that these interpretations are useful in deciding and implementing the road safety policies on this highway section to reduce the severity levels of the road crashes.

Acknowledgements The authors wish to thank the Civil Engineering Department, COEP TECH University (Formerly College of Engineering Pune) for giving the opportunity to do research in road safety. Also, extremely grateful to National Highways Authority of India for providing data used in this study.

References

1. Gourav G, Sachdeva S (2016) Analysing of Road Accidents on NH-1 between RD 98 km to 148 km. J Perspect Sci 08:392–394. https://doi.org/10.1016/j.pisc.2016.04.086
2. Landge V, Jain SS, Parida M (2005) Community participation for road safety in India. Proc Inst Civ Eng Municipal Eng 158(01):45–51. https://doi.org/10.1680/muen.2005.158.1.45
3. Ministry of Road Transport & Highways (2019) Road accidents in India-2019. Government of India, pp 15–25
4. Ministry of Road Transport & Highways (2021) Road accidents in India-2019. Government of India, pp 11–19
5. Mohan D, Jha A, Chauhan S (2021) Future of road safety and SDG 3.6 goals in six Indian cities. J IATSS Res 45:12–18. https://doi.org/10.1016/j.iatssr.2021.01.004
6. Pandey S, Pandey I (2018) Towards safety of road users. J Indian Highways 46(05):33–38
7. Ponnaluri R (2012) Road traffic crashes and risk groups in India: analysis, interpretations, and prevention strategies. J IATSS Res 35(02):104–110. https://doi.org/10.1016/j.iatssr.2011.09.002
8. Rabbani M, Musarat M, Alaloul W, Maqsoom A, Bukhari H, Waqas R (2021) Road traffic accident data analysis and its visualization. Civ Eng Architect 9(5):1603–1614. https://doi.org/10.13189/cea.2021.090530

9. Rajaraman R, Hassan A, Padmanaban J (2009) Analysis of road traffic accidents on NH 45 (Kanchipuram district). SAE technical paper, 2009-28-0056, pp 1–10. https://doi.org/10.4271/2009-28-0056
10. Savolainen P, Mannering F, Lord D, Quddus M (2011) The statistical analysis of highway crash injury severities: a review and assessment of methodological alternatives. J Accid Anal Prev 43(05):1666–1676. https://doi.org/10.1016/j.aap.2011.03.025
11. Singh S (2017) Road traffic accidents in India: issues and challenges. Transp Res Procedia 25:4708–4719. https://doi.org/10.1016/j.trpro.2017.05.484
12. Wegman F (2017) The future of road safety: a worldwide perspective. J IATSS Res 40:66–71. https://doi.org/10.1016/j.iatssr.2016.05.003
13. WIKIPEDIA [online] 25/01/2020. https://en.wikipedia.org/wiki/National_Highway_48_(India)

Walkable Neighbourhoods: Empirical Analysis of Factors Influencing Pedestrian Behaviour

Ali Shkera and Vaishali Patankar

Abstract In pedestrian travel behaviour modelling, the variable that represents the number of walking trips must be carefully considered when there is a high number of zero values. This study employs Zero-inflated Poisson regression to account for these excess zeros when analysing the frequency of walking trips. Using data from the 2013 Greater Mumbai region activity travel diary survey, census data, and an accessibility index (walk score), the paper estimates Poisson models at the individual level for the frequency of walking trips for commuting and non-commuting purposes on a single travel day. The results indicate that pedestrian socio-demographics (such as age, workplace schedule, public transportation usage, type of residence, and household income) and characteristics of the built environment (such as population density and accessibility index) have an impact on walking behaviour for both commuting and non-commuting purposes. These pedestrian travel behaviour models can be used for evaluating public health and sustainability policy and planning.

Keywords Walking frequency · Transport policies · Ordered response model

1 Introduction

The pedestrian travel behavioural modelling framework provides insights into understanding the factors which are effective in encouraging walking and evaluates pedestrian-oriented infrastructure and urban design alternatives. Such modelling frameworks have substantial implications in terms of their applicability to represent pedestrian travel behaviour, their use for the integrated land use and transportation planning requirements and address current transportation planning needs for environmental sustainability, economic viability, and public health. Pedestrian travel behaviour focuses on providing a conceptual empirical modelling framework to analyse the factors affecting walkable neighbourhoods. It guides frame policies

A. Shkera (✉) · V. Patankar
Department of Civil Engineering, Institute of Technical Education and Research, Siksha 'O' Anusandhan (Deemed to be University), Bhubaneswar, Odisha 751030, India
e-mail: engalishkera@gmail.com

K. R. Reddy et al. (eds.), *Recent Advances in Civil Engineering*, Lecture Notes in Civil Engineering 398, https://doi.org/10.1007/978-981-99-6229-7_47

for environmentally friendly, energy-saving, socially inclusive sustainable urban transportation and higher quality of life.

2 Previous Research

Pedestrian travel behaviour is characterized by a multitude of factors that determines the walking decision-making process. These factors decide the walkability of a walkable neighbourhood for sustainable urbanization by addressing the economic, social and environmental components of sustainability. The relationship between walkable neighbourhoods with the sustainability components is summarized below.

Walkable neighbourhoods create wealth by enhancing proximity [1, 2]. Walkable neighbourhoods provide a quality of life conducive to retaining corporations and people [3]. Cities with housing price gains have good walkability [4]. Dense, walkable cities make people productive by bringing them together and saving their time wasted in traffic [5]. In this way, walkable neighbourhoods address economic sustainability.

The inactivity-inducing convenience of the automotive lifestyle and automotive landscape has contributed to obesity and its related illnesses [6]. Toxic vehicle exhaust and traffic exposure cause health problems such as reduced lung function, asthma and heart attacks, high blood pressure, and lower frustration tolerance [7]. Violent speed has led to shorter lives for the current generation of youth [5]. Longer commutes report lower satisfaction with life and affect relationships, social life, community, and civic engagement [8]. In contrast, walkable neighbourhoods are accessible, and safer, have fewer traffic crashes and crime, a lower proportion of obese people, greater civic participation, promote social life, promote healthier and more livable communities, promote an active lifestyle, check pollution, promote the well-being of the residents, and provides better quality of life and lifestyle choices [1]. In this way, walkable neighbourhoods address social sustainability.

Theoretical perspectives provide a framework for identifying the different elements of walkable neighbourhoods that promote sustainable urbanization. Walkable neighbourhoods take into account accessibility, a sense of community and health. They have various economic, social and environmental aspects of sustainability that affect the walkability of the neighbourhood. This research aims to explore the different factors that influence pedestrian travel choices and encourage walking as a way of achieving walkable neighbourhoods as a model of sustainable urbanization.

3 Methodology and Data Source

An empirical approach identifies measurable attributes for research and intervention. In this study, the built environment and the socio-demographics variables are tested following an empirical approach to characterize the walkability of urban neighbourhoods which will address the three components of sustainability.

Survey data included the 2010 Greater Mumbai Region Activity Travel Survey. The study area was representative of high-density urban and suburban development. The survey instrument and sampling method are described elsewhere [9]. The survey data file provides information on demographics, household characteristics and travel activity episodes from 126 households for fifteen days. This analysis concentrates on a weekday because the sample did not reveal any difference in daily per-person trip frequency and activity sequences among the weekdays from the fifteen-day survey data as suggested earlier.

The final dataset comprises 347 observations from individual members of 126 households. The sample encompasses a total of 898 walk trips, which have been classified into two categories: home-based and non-home-based trips. The analysis concentrates on home-based trips to scrutinize the impact of the neighbouring built environment variables. Home-based walk trips have been further subdivided into work-related (commuting) and non-work-related (non-commuting) activities. Of the 898 weekday walk trips, 350 (38.98%) are home-based work-related (HBW), 342 (38.08%) are home-based non-work-related (HBO), 182 (20.27%) are non-home-based work-related (NHBW), and 24 (2.67%) are non-home-based non-work-related (NHBO) walk trips. Work-related walk trips constitute the largest proportion of weekday walk trips.

The data was systematically organized on an individual basis, resulting in the creation of separate data sets. These data sets were meticulously structured to facilitate the calculation of weekday home-based work (HBW) and home-based other (HBO) pedestrian trip frequencies, which serve as the dependent variables. In order to simplify the distribution of the dependent variable pertaining to pedestrian trip frequency generation, the number of categories was reduced. This decision was influenced by the significantly low percentage of individuals engaging in more than four walk trips. Consequently, individuals with more than four walk trips were classified within the four walk trips category. Thus, a total of five pedestrian trip frequency alternatives, ranging from zero to four walk trips, were specified for the two MMR data sets focusing on weekday walk trips.

For each observation, a total of 22 potential explanatory variables were gathered. There are 20 socio-economic indicators (personal and household characteristics) and two built environment variables (neighbourhood characteristics). The built environment variable on the walk score is used as a pedestrian accessibility index for the study region based on the geolocation of the home. Walk score is calculated for the study region using a GIS-based publicly available WalkScore™ website that measures neighbourhood walkability based on proximity to 13 amenity categories [10].

4 Modal Structure

The dependent variable on the number of walk trips in a given day is a count variable that takes on discrete values (0, 1, 2, …). This section presents the Poisson model structure to describe the endogenous discrete variable on the walk frequency models. The dependent variable is assumed to have a Poisson distribution conditional upon the quantitative or qualitative exogenous variables. The probability mass function for the Poisson distribution is given as follows:

$$P(Y = y|\mu) = \frac{\mu^y}{y!}\mathrm{e}^{-\mu}$$

For the count variable Y, the "the number of walk trips in a day", the Poisson distribution would provide the probability of 0, 1, 2, … walk trips, given the mean μ of the distribution. The dependent variable, which follows a Poisson distribution with parameter μ, is controlled by independent variables which can be depicted using the natural log (ln) link function as follows:

$$\ln(\hat{\mu}) = b_0 + b_1 X_1 + b_2 X_2 + \cdots + b_p X_p$$

Thus, μ is an exponential function of the covariates that are conditional on the covariates for each case as follows:

$$\hat{\mu} = \mathrm{e}^{b_0 + \sum b_k X_k}$$

The estimates of the parameters $B = (b_1, b_2, \ldots, b_k)$ are found by maximizing the likelihood [11].

5 Results

5.1 Estimation Results for Walking Frequency

The estimation of weekday pedestrian trip frequency, specifically home-based work (HBW) and home-based non-work (HBO) trips, was conducted using Poisson models. The maximum simulated likelihood method, implemented in LIMDEP version 9 [12], was employed for all estimations. The final model specification was determined based on the statistical significance of variables, taking into account both intuitive reasoning and previous theoretical and empirical studies. Despite their limited statistical significance, certain variables of interest were included in the final model's prediction to gain insights into their impact as policy variables. Empirical results depicting the frequency of walking for commuting (HBW) and non-commuting (HBO) purposes are presented in Table 1. A positive coefficient within

Table 1 Ordered response model of frequency of walking for commuting

Variable	Commuting (HBW)		Non-commuting (HBO)	
	Coefficient	*t*-Statistic	Coefficient	*t*-Statistic
Constant	0.7497	1.47	− 0.28413	− 0.49
Age	− 0.03652***	− 7.23	0.02213***	5.87
Gender (male)	0.18381	1.54	− 0.1408	− 1.15
Education	0.07933	0.48	− 0.22884	− 1.38
Commute mode (public)	0.27207**	2.14	− 0.43518***	− 3.24
Work place timings	0.47552***	3.05	− 0.61934***	− 3.66
Chawl	0.33934**	2.29	0.29979*	1.88
Rented	− 0.47874**	− 2.56	0.17669	1.03
Government quarter	− 0.04403	− 0.16	0.61070**	2.28
Students	0.15706**	2.19	− 0.04791	− 0.64
Vehicles ownership	− 0.39408***	− 3.89	− 0.0578	− 0.63
House hold income level	− 0.02281	− 0.49	− 0.05969	− 1.33
Population density 9K	− 0.53122	− 1.26	− 0.42067	− 1.09
Population density 12K	0.46336	1.30	− 0.51074	− 0.98
Population density 15K	0.00924	0.04	− 0.06756	− 0.26
Population density 20K	0.05222	0.25	0.08273	0.40
Population density 45K	− 0.20955	− 0.46	− 0.43228	− 0.99
Walk score	0.00025	0.04	0.00178	0.25
LL (β)	− 374798		− 401386	
LL (c)	− 459038		− 462234	
LRI ($\rho 2$)	0.184		0.132	

* p < 0.05; ** p < 0.01; *** p < 0.001

each model signifies that the corresponding factor is associated with a higher number of trips.

5.2 Effect of Pedestrians' Household Demographics

People living in Chawls walk more for work and non-work purposes [13]. The location of the Chawls provides easy access through walk mode to everyday amenities. Living in a rented quarter increases the tendency to walk more for non-commuting purposes and walk less for commuting. Mixed land use near the rented quarters provides an opportunity for making frequent walk trips for non-work purposes. However, the residents in rented housing facilities have poor walking accessibility for commuting purposes. Staying in government accommodation is associated with an increase in the walk for non-commuting trip purposes. This may be a result of better

walking infrastructure and mixed land use near such housing facilities. However, government accommodation doesn't facilitate walking for work purposes. The presence of more students in the household is linked with an increase in walking for work as well as for non-work purposes. Higher vehicle ownership and household income are linked with a decrease in walking for work as well as non-work purposes [14].

5.3 Effects of Individual Demographics of Pedestrians

The effects of Individual Demographics of pedestrians show that older individuals tend to walk more for non-commute purposes, probably because they have more leisure time after retirement compared to younger workers, and potentially spend time on recreational pursuits. The male pedestrian is more likely to walk for work purposes than the female pedestrian. This result is expected because of the low labour force participation rate for women as depicted in the employment rate information of the study region. However, non-commute walking frequency is found to be more among female pedestrians, possibly because of their higher participation levels in social activities and managing household chores.

The results inform a higher walking proclivity among commuter pedestrians who holds a graduate degree or higher education. The accessible work opportunities facilitate commuting and walking for highly educated individuals. This may also be an indication of lower-income levels among individuals possessing higher education, who then cannot afford to commute by car. However, higher education was negatively associated with non-commuting walking. It might be a result of poor walking accessibility for non-commuting purposes.

The use of public transport is highly correlated with walking for work purposes [15, 16]. This is quite intuitive as the region has good transit accessibility within walking distance. However, using public transport is negatively associated with walking for non-work purposes. This may be for cultural reasons or convenience.

A fixed work schedule has a positive impact on walking for commuting purposes. A possible reason for this is the proximity and preference for a workplace with a fixed work schedule. However, a fixed work schedule has a negative impact on non-work walking because such a schedule gives freedom to use other modes of transportation for non-work purposes in a city which takes more time to travel by personal mode of transportation otherwise. This difference in fixed and flexible schedule workers is also observed [17].

5.4 Effect of Location on Pedestrians' Households

Medium-density neighbourhood (population density in the range of 9K–45K) facilitates commute and non-commute walk trips. The built environment variable on population density indicates that very low (in the range of 9K or below) and very

high-density levels (in the range of 45K or above) are not conducive for walking. A higher walk score is associated with a decrease in home-based work walk trips. This shows a lack of walking opportunities for work purposes near the household with a higher walk score. Empirical results on walk score indicate that there are considerable opportunities for walking for home-based non-work trip purposes which shows an increase in home-based non-work walk trips, thus, informing policy decisions.

6 Summary of the Results and Conclusion

This study explores how various factors influence walking frequency and pedestrian behaviour in walkable neighbourhoods as a way to address transportation problems in urban areas. Based on a sample of residents in Mumbai, it identifies the characteristics of walkers and non-walkers and suggests how to promote walking among different groups. The main findings are that walking is common for both commute and non-commute purposes, but it varies by housing type, income level, age, gender, and location. The study recommends further research on other aspects of pedestrian behaviour, such as attitudes, preferences, perceptions, weather, household interactions, and trip chaining. It also implies that policies that support walkable neighbourhoods can enhance sustainable urbanization by integrating transportation and land use planning.

References

1. Albert Tsai T-I (2014) Strategies of building a stronger sense of community for sustainable neighborhoods: comparing neighborhood accessibility with community empowerment programs. Sustainability 6:2766–2785. https://doi.org/10.3390/su6052766
2. Foraster M, Basagaña X, Aguilera I, Rivera M, Agis D, Bouso L, Deltell A, Marrugat J, Ramos R, Sunyer J, Vila J, Elosua R, Künzli N (2014) Association of long-term exposure to traffic-related air pollution with blood pressure and hypertension in an adult population-based cohort in Spain (the REGICOR study). Repository UPF Educ 122:404–411. https://doi.org/10.1289/ehp.1306497
3. Credit K, Mack E (2019) Place-making and performance: the impact of walkable built environments on business performance in Phoenix and Boston. Environ Plan B Urban Anal City Sci 46:264–285. https://doi.org/10.1177/2399808317710466
4. Kim EJ, Kim H (2020) Neighborhood walkability and housing prices: a correlation study. Sustainability (Switzerland) 12. https://doi.org/10.3390/su12020593
5. Speck J (2012) Walkable city: how downtown can save America, one step at a time. Farrar, Straus and Giroux
6. Leinberger C (2010) The option of urbanism: investing in a new American dream. https://books.google.com/books?hl=en&lr=&id=vn1aEQDnvIEC&oi=fnd&pg=PR3&dq=The+Option+of+Urbanism:+Investing+in+a+New+American+Dream&ots=xGtjnVTYPd&sig=kwlGgUhXrVngDTYhUmPLjKEk-i8. Accessed 24 May 2021
7. Bowatte G, Lodge CJ, Knibbs LD, Erbas B, Perret JL, Jalaludin B, Morgan GG, Bui DS, Giles GG, Hamilton GS, Wood-Baker R, Thomas P, Thompson BR, Matheson MC, Abramson MJ,

Walters EH, Dharmage SC (2018) Traffic related air pollution and development and persistence of asthma and low lung function. Environ Int 113:170–176. https://doi.org/10.1016/j.envint.2018.01.028
8. Putnam RD (2000) Bowling alone: the collapse and revival of American community. In: Proceedings of the 2000 ACM conference on computer supported cooperative work—CSCW'00. ACM Press, New York, p 357. https://doi.org/10.1145/358916.361990
9. Subbarao S (2013) Activity-based travel demand analysis for a mega city in a developing country
10. Walk score methodology (n.d.). https://www.walkscore.com/methodology.shtml. Accessed 29 May 2021
11. Greene WH (2003) Econometric analysis. Prentice Hall
12. Greene W (2002) LIMDEP version 8.0: econometric modeling guide
13. Sanyal T (2018) The chawls and slums of Mumbai. https://deepblue.lib.umich.edu/handle/2027.42/143823. Accessed 23 May 2021
14. Seong E, Lee N, Choi C (2021) Relationship between land use mix and walking choice in high-density cities: a review of walking in Seoul, South Korea. Sustainability 13:810. https://search.proquest.com/openview/0de12c15f2e79b373ac1194c94f44298/1?pq-origsite=gscholar&cbl=2032327. Accessed 23 May 2021
15. Edwards RD (2008) Public transit, obesity, and medical costs: assessing the magnitudes. Prev Med (Baltim) 46:14–21. https://doi.org/10.1016/j.ypmed.2007.10.004
16. Rissel C, Curac N, Greenaway M, Bauman A (2012) Physical activity associated with public transport use—a review and modelling of potential benefits. Int J Environ Res Public Health 9:2454–2478. https://doi.org/10.3390/ijerph9072454
17. Hatamzadeh Y, Habibian M, Khodaii A (2017) Walking and jobs: a comparative analysis to explore factors influencing flexible and fixed schedule workers, a case study of Rasht, Iran. Sustain Cities Soc 31:74–82. https://doi.org/10.1016/j.scs.2017.02.012

Resource and Safety Management

Development of Interdependent Resource Management System for Construction Project Using Genetic Algorithm

S. Gopinath and T. C. Natesh

Abstract Resource allocation is a critical process to use the resources in the construction projects effectively. Time and cost constraints restrict the function of optimal resource allocation. This study was performed by integrating the resource leveling and resource-constrained scheduling concepts to obtain the optimal solution. An evolutionary-based genetic algorithm optimization approach was adopted since resource allocation belongs to the nonpolynomial combinatorial problem. Case study results indicate that the proposed method allows the user to reduce the resource demand variation with the least extension in the project duration. This paper shows that better results were obtained by interdependent resource management compared to other methods. The proposed approach is expected to help the significant stakeholders to perform effective resource allocation.

Keywords Resource leveling · Resource-constrained scheduling · Construction projects · Genetic algorithm

1 Introduction

Construction projects consist of various activities which involve complex problems with considerable amount of resource requirements to complete the project within a given time duration. In every construction, project scheduling of each activity requires specific duration of time to complete task by using various resources like materials, manpower, and machinery which is assigned to carry out task in the project [1]. Construction resource management involves the planning, scheduling, and assigning resources to activities which are performed interdependent to each other to meet project ultimate goal. Project scheduling should be done in accordance with usage of limited resource availability in efficient way; on the other hand, we must also consider difficulties, uncertainties, and risks by having constraints like resource

S. Gopinath (✉) · T. C. Natesh
Department of Civil Engineering, Faculty of Engineering and Technology, SRM Institute of Science and Technology, Kattankulathur, Tamil Nadu 603203, India
e-mail: gopinats@srmist.edu.in

K. R. Reddy et al. (eds.), *Recent Advances in Civil Engineering*, Lecture Notes in Civil Engineering 398, https://doi.org/10.1007/978-981-99-6229-7_48

limitation and duration-constrained projects. While considering resource management, unlimited number of resources are available, but in real-time project, there are only limited resources can perform. To overcome these conflicts, both resource-constrained scheduling and resource leveling problems are implemented using interdependent resource management system. In dealing with resource management problems, we may concentrate on two types of problems which are resource leveling and resource-constrained scheduling used for allocating resources like manpower, material, and machineries, carried out to assign the activities in a scheduling process of the project [2]. Scheduling of activities is the most important job to be done in construction project management. Resource availability and allocation will affect entire scheduling in real project due to limited resources, and optimizing the resource utilization is crucial. In general, resource scheduling is an important aspect of the planning and management activity in project scheduling [3]. Minimizing undesirable fluctuation in resource utilization is not that easy to perform, which are inefficient and costly to implement in real project. This can be done by resource leveling and resource-constrained scheduling techniques used for scheduling activities. This is mainly focusing on interdependent of resource management system in the construction project.

1.1 Resource Leveling Problem

The resource leveling problems (RLPs) is a common resource scheduling issue that arises in real-time projects with constrained resources [4]. In resource leveling, considerable attempt is to minimize the peaks and valleys of resource usage by adjust start and finish dates of activities considering resource constraints to minimize the variation in resource demands. Fluctuation in resource histogram usage profile shows that inefficiency of resource allocation which results in addition cost in the overall project [5]. In this method, levels of resources are considerably fixed, and on the other hand, the duration of the project is fixed and the resources are leveled using only by the availability of free float or free slack. In real-time projects, the number of activities is more that we cannot shift manually [6]. Resource leveling has that availability of resource limitation by means of minimizing the peaks in daily usage of resource profile and finds the required resources in minimum amount to be performed during each activity to complete the project in given time duration. Resource leveling problems (RLPs) are such kind of combinatorial and optimization problems with possible solutions. Therefore, solving RLP using analytical methods cannot give us optimal solutions, also using heuristic methods to solve such kind of problems will not give better solutions. This limitation of analytical and simple heuristic methods is good to have meta-heuristic approach like genetic algorithm used in this paper. This could really help in maximization and minimization problem to control resource usage profile in the construction project.

1.2 Resource-Constrained Project Scheduling Problem

The project management problem is defined as determining the time required to finish a project activities in order to meet a specific goal. It was considered in early research on project scheduling that a project's activities are represented solely by the implementation of time duration. As a result, methods such as the program evaluation and review technique (PERT) and the critical path method (CPM) that take precedence relationships between project activities into consideration have been proposed [7]. However, considering of precedence relationship as independent likes to be wrong assumption, which is having some constraints and the major limitations of the project to be considered, is resource constraints. In real-time problem, which is considerably maintained as a standard problem for scheduling activities due to some factors like limited availability of resources, addition cost for overall project, time consideration and workers health reasons, etc., to be taken into account in the resource-constrained project scheduling problem (RCPSP). The basic assumption of RCPSP is that the duration of a project may get extended due to the constraints of limited resource availability in real-time projects [8]. This problems can resolved by considering the extension of project duration done by finding the schedule duration is shortest with limited resource availability. This kind of combinatorial problems which apply selected rules on characteristics of activities like 'minimum float values' to compete for available resources. According to their priority level with minimum slack value, it should be critical activities, and other activities can be shifted or even delayed. Another rule 'shortest duration' can used in the scheduling process, which starts from project state date and finding eligible activities in respect of precedence network logics and resolving over allocation of resources by set of heuristic rules. This process where all the activities are planned without exceeding the resource constraints and logical connection but it will results in increasing cost of total project duration which is exceed the duration scheduled by CPM [9]. Heuristic methods are easy to applicable, simple to use, and easily adopted to work in computer language. They are easy to manageable in real-time projects and can be solved by meta-heuristic approach using genetic algorithm.

1.3 Genetic Algorithm

Resource leveling and resource-constrained scheduling optimization have proven difficult for individual simultaneous optimization. Given the improved meta- heuristics described in this research, the goal can be reformulated in a heuristic way as the finding for a better-optimal set of activity imports that reduce the duration of total project while simultaneously minimizing the appropriate moments of particular resources under resource constrained [10]. This aims to directly minimize the total project cost, which cannot be done using mathematical approaching methods, schedule with efficient resource utilization, and also avoids daily resource fluctuation

will reduce the project duration. To deal with multiobjectives, search optimization technique is used which is based on solving the optimization problem using artificial intelligence like genetic algorithm (GA). This method of approach has been successfully adopted for solving engineering problems in an effective means of finding near-optimum results in a large complex problem that we are facing in this paper. Genetic algorithm is used in optimization procedures for search algorithm based on the concept of natural selection and natural genetics. GA improves a fitness through natural evolution and performs random search for obtaining the optimal solution; it required representation form of optimization problem to get possible solutions. This could be obtained in the string form termed as chromosomes which is pack of genes to form a structure of string. The fitness of each gene is evaluating by its fitness objective function they combine to enhance 'survival of fittest' and the natural process for better string structure to produce an offspring by exchange information which are calculated and can be retained only if they are having higher fitness value than the other genes in the population. Generally, this procedure is carried out for more number of offspring until an optimal gene is obtained. Each genes is undergone process of during implementation of genetic algorithm technique in five major steps: (1) creating gene structure (string); (2) define objective fitness function to evaluate gene; (3) creating an initial set of population randomly; (4) generate an offspring and function using operators; and (5) coding the procedure in a computer language.

2 Methodology

This project shows the methodology and the flow of work adopted in the development of model using GA using Python and integrates resource leveling and resource-constrained scheduling model as mentioned in Fig. 1. Initial phase of work flow is followed by literature study and finding research gap to develop a resource leveling model using genetic algorithm in Python language. Research papers were collected from different database for resource leveling, and genetic algorithm was performed together and solving real-time project data. While considering resource management, unlimited number of resources are available but in real-time project, there are only limited resources can be performed. The availability and allocation of resources will have an impact on the overall schedule in real project due to limited resources, optimizing the resource utilization is crucial. Minimizing undesirable fluctuation in resource utilization is not that easy to perform. Undesirable fluctuation in resource is inefficient and costly to implement in real-time project.

Performing resource leveling and resource-constrained scheduling model in an initial stage of project scheduling leads to the deviation in resource profile utilization and may get delay in completion of the project duration. Avoid deviation by considering reduction of resource demand variation and extension of duration during the progress in project using interdependent resource management system for optimal solution.

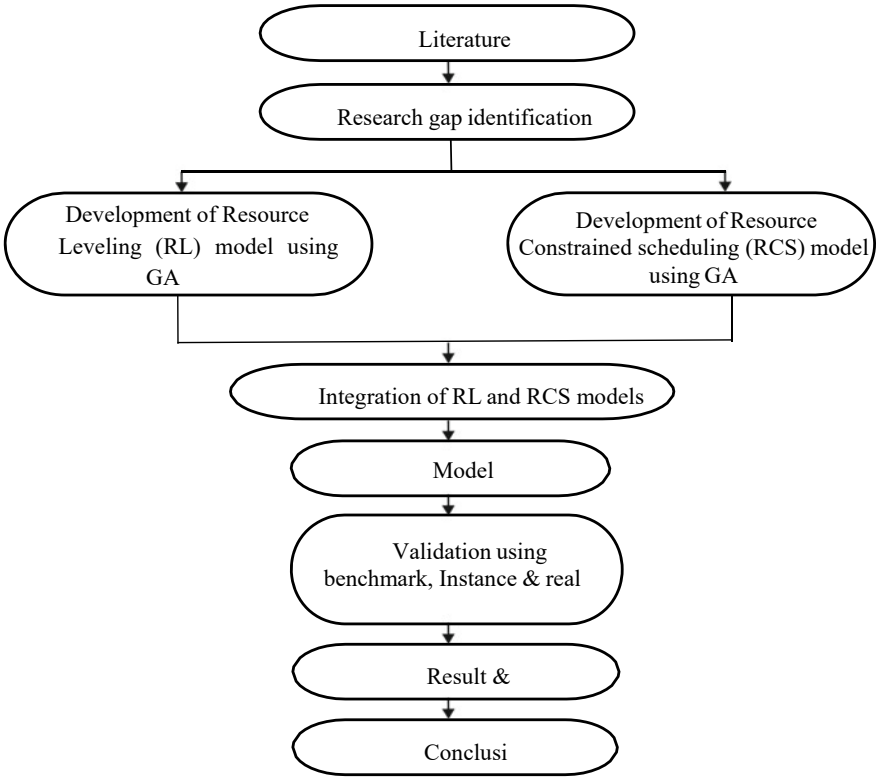

Fig. 1 Methodology flow diagram

3 Interdependent Resource Management

Resource scheduling can be done by delaying activities or splitting them by considering total float values or total slack. So that the resources are assigned to those tasks which are no longer overloaded within a given time duration of the project. Resource leveling and scheduling are performed for given sample data collected from literature having five activities on road pavement which containing description with immediate predecessor activity, duration, resources, and float values are shown in Table 1.

3.1 Resource Scheduling Technique

Based on the given data, resource leveling is performed by using Microsoft Project Software critical path method was calculated, and then critical activities and noncritical activities and float days were calculated. This technique consists of the following step:

Table 1 Sample data

S. No.	Activity name	Duration	Predecessor	T.F.	Resource
1	A	3		0	5
2	B	2	A	1	6
3	C	3	A	0	4
4	D	1	A	2	4
5	E	2	B, C	0	6

- Collection of data should be implemented in MSP software and calculate the amount of work to be done.
- Allocating the duration (days) for each activities which comprises the total duration of the project.
- Allocation of resources (labors) for each activities by considering immediate predecessor activity in the given sample data for the project.
- Calculating critical activities, noncritical activities, and float days by using Microsoft project software.
- Calculation of daily resource requirement is needed to find out the resources are allocated within the limit and does not exceed the total project duration.
- Implementing the acquired data from MSP to MS Excel to plot histogram for identification of any peaks and valleys in resource usage profile.
- By performing resource leveling using genetic algorithm optimization technique in Python programming language to acquire optimal solution.
- Finally, resource usage profile for the given data after resource leveling is done.

3.2 Genetic Algorithm Optimization

A genetic algorithm is a random heuristic approach for solving the optimization problem and requires a representation scheme to encode feasible solutions. GA technique was implemented using the following steps to perform resource leveling:

- Usually, it is complete in the form that string represented is called chromosomes, and each chromosomes is a combination of set of genes.
- Each gene represents one member (one solution) which is greater than one another.
- Fitness function is determined by evaluating its performance.
- To enhance 'survival of fittest' the natural process, where the best genes produce offspring by exchange information.
- That are estimated and retained only when they are adequate in the population than others.
- This procedure continues for huge number of offspring generations until a best gene (best solution) is arrived at some point.
- Population corresponds to the set of random candidate solution which is representing in the form of chromosomes.

- Each gene corresponds to the value for each variable of the problem defined.
- Genetic representation of solution using fitness function to generate new solution by using different operators in genetic algorithm.

1. Selection operator—roulette wheel selection is used for selecting parent chromosomes for initial population.
2. Crossover operator—single-point crossover is used to exchanging the genes of both parent chromosomes to generate new population.
3. Mutation operator—creates diversity by randomly changing genes of the chromosomes, probability of mutation is 0.01
4. Elitism—initializing the population and evaluating new generation of chromosomes by carrying best individuals.

4 Results and Discussion

The resource leveling technique using genetic algorithm helps to reduce the resource demand variation in utilization of resource profile histogram, by leveling uneven deviations in resource requirements using available resources.

4.1 Discussion

Resources usage profile shows that histogram for that given activities in the project using available resource demand to complete the project with in a given time duration. In this project, five activities were taken into consideration with resource utilization, and each activity is having their own time duration to complete their task; total duration taken to complete all activities takes 8 days. Each days having different resource usage profile initially before leveling in Figs. 2 and 3 shows resource histogram before leveling.

Activity	Before leveling-Duration (days)							
	1	2	3	4	5	6	7	8
A	5	5	5					
B(1)				6	6			
C				4	4	4		
D(2)				4				
E							6	6
Total	5	5	5	14	10	4	6	6
date	12-Mar	13-Mar	14-Mar	15-Mar	16-Mar	17-Mar	18-Mar	19-Mar

Fig. 2 Resource allocation before leveling

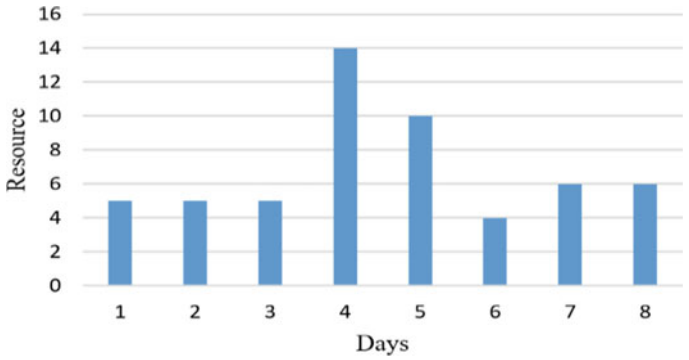

Fig. 3 Resource histogram before leveling

After getting values for each activities from the Fig. 2 and assigning their resources mentioned in y-axis to the required duration in days mentioned in x-axis, resource profile histogram for resource usage of each activities calculated as sum of total resources in each days was shown in Fig. 3. The initial stage of resource leveling model helps to minimize uneven fluctuation in resource usage profile histogram using genetic algorithm in python language. Noncritical activities are identified and resources are shifted with the available total float days, to acquire better solution shown in resource usage histogram shown in Fig. 5.

4.2 Results and Discussion

The proposed resource leveling technique shows that various trails were performed until the better result obtained. In this project, resource histogram shows better result after running code again, and again repeatedly shows best fitness value as 363 in *y*-axis and number of generations 100 which is represented in *x*-axis with a graphical result were shown in Fig. 4.

Activity 'B' has shifted its resource from 4th day to 6th day using float days by one day increasing and having 9 days as total duration of the project. However, many trails were shown different results in genetic algorithm coding according to their float days changes, which having maximum fitness value by exceeding minimum daily requirement of resource utilization are not taken consideration. Resource allocation after leveling shown in Fig. 5, activity 'B' is denoted as noncritical activity, and Fig. 6 shows that resource profile histogram after resource leveling has done with minimum fitness value.

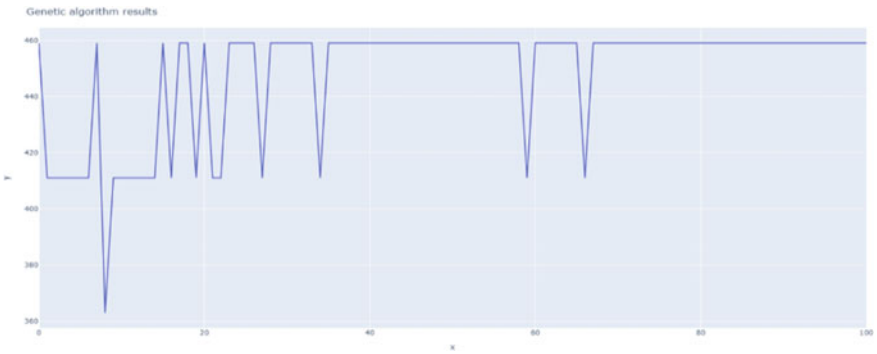

Fig. 4 Genetic algorithm result

Activity	After leveling-Duration (days)								
	1	2	3	4	5	6	7	8	9
A	5	5	5						
B(1)						6	6		
C				4	4	4			
D(2)				4					
E								6	6
Total	5	5	5	8	4	10	6	6	6
date	12-Mar	13-Mar	14-Mar	15-Mar	16-Mar	17-Mar	18-Mar	19-Mar	20-Mar

Fig. 5 Resource allocation after leveling

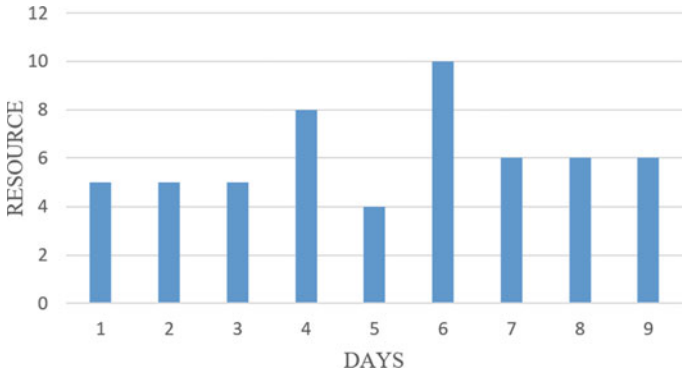

Fig. 6 Resource histogram after leveling

5 Conclusion

The proposed model is to solve resource leveling and resource-constrained project scheduling problems in real-time construction projects by interdepending both using a genetic algorithm approach. The effective schedule was created by simulating the data by their fitness function value and using random optimization technique to obtain better resource usage profile with some changes in total project duration. Considering real-time project data perform genetic algorithm due to many possible shifts in activity difficult to create chromosome structure, further study is to overcome this problem by taking crucial activities in resource usage where high to reduce the size of chromosome. By increasing the number of generation helps to achieve better results in getting minimum fitness value to obtain optimal solution in resource profile usage.

References

1. Hegazy T (1999) Optimization of resource allocation and leveling using genetic algorithms. Constr Eng Manage 125:167–175
2. Kim J, Kim K, Jee N, Yoon Y (2005) Enhanced resource leveling technique for project scheduling. J Asian Archit Build Eng: 461–466
3. Abdel-Basset M, Ali M, Atef A (2020) Resource levelling problem in construction projects under neutrosophic environment. J Supercomput 76(2):964–988. https://doi.org/10.1007/s11227-019-03055-6
4. Georgy ME (2008) Evolutionary resource scheduler for linear projects. Autom Constr 17:573–583. https://doi.org/10.1016/j.autcon.2007.10.005
5. Benjaoran V, Tabyang W, Sooksil N (2015) Precedence relationship options for the resource levelling problem using a genetic algorithm. Constr Manag Econ 33:711–723. https://doi.org/10.1080/01446193.2015.1100317
6. Li H, Wang M, Dong X (2019) Resource leveling in projects with stochastic minimum time lags. J Constr Eng Manage 145(4):04019015. https://doi.org/10.1061/(asce)co.1943-7862.0001635
7. Kastor A, Sirakoulis K (2009) The effectiveness of resource levelling tools for resource constraint project scheduling problem. Int J Proj Manage 27(5):493–500. https://doi.org/10.1016/j.ijproman.2008.08.006
8. Jun DH, Ph D, El-Rayes K, Asce M (2011) Multiobjective optimization of resource leveling and allocation during construction scheduling. J Constr Eng Manage 137:1080–1088. https://doi.org/10.1061/(ASCE)CO
9. Markou C, Koulinas GK, Vavatsikos AP (2017) Project resources scheduling and leveling using multi-attribute decision models: models implementation and case study. Expert Syst Appl 77:160–169. https://doi.org/10.1016/j.eswa.2017.01.035
10. Leu S, Hung T (2002) An optimal construction resource leveling scheduling simulation model. Can J Civ Eng 29:267–275. https://doi.org/10.1139/L02-007

Entrepreneurial Skills Among the Civil Engineering Students

K. Perumal and N. Pannirselvam

Abstract The capacity to analyze risk and launch construction and civil engineering enterprises that are at once hazardous and precisely suited to the shifting economic conditions is what is known as entrepreneurship. The promotion of entrepreneurship has recently risen to the top of the priority list for public policy in the majority of industrialized nations. Technical entrepreneurs with a solid education are crucial for the economic growth of any country. To maintain a competitive advantage in an innovation-driven global economy, it is crucial to nurture entrepreneurial skills. Students, policymakers, and educators are starting to realize the importance of high-quality entrepreneurship education and training in discovering and developing this entrepreneurial potential in young people. Younger generations are now showing a growing tendency and enthusiasm in starting their own businesses. However, our educational system is set up to produce more job seekers than job producers. A complicated phenomenon, entrepreneurial growth is the crystallization of a person's social milieu, family-ingrained views, caste system, educational attainment, parental income, occupation, and other factors. Additionally, educational institutions might encourage students to pursue self-employment in a good way. The goal of this study on the entrepreneurial spirit among civil engineering students is to determine the reasons why people choose entrepreneurship as a career and to look into the effects of various variables on students' preference for entrepreneurship. This study is based on the aforementioned context.

Keywords Employment · Entrepreneurship · Motivation · Skills · Students

K. Perumal · N. Pannirselvam (✉)
Department of Civil Engineering, Faculty of Engineering and Technology, SRM Institute of Science and Technology, Kattankulathur, Tamil Nadu 603203, India
e-mail: pannirsn@srmist.edu.in

K. R. Reddy et al. (eds.), *Recent Advances in Civil Engineering*, Lecture Notes in Civil Engineering 398, https://doi.org/10.1007/978-981-99-6229-7_49

1 Introduction

Entrepreneurship has been a buzzword in the twenty-first century, as more and more individuals strive to become self-reliant and create their own businesses. In recent times, entrepreneurship has become an important part of the curriculum in various academic institutions, including civil engineering schools [1]. Civil engineering students can benefit greatly from developing entrepreneurial skills, as they can help them create successful businesses and contribute to economic growth. This paper aims to explore the importance of entrepreneurial skills among civil engineering students, the challenges they face, and the strategies that can be implemented to enhance their entrepreneurial skills.

Importance of entrepreneurial skills among civil engineering students: Civil engineering students can benefit greatly from developing entrepreneurial skills [2]. These skills can enable them to create their own businesses and become self-reliant. Additionally, entrepreneurship can contribute to economic growth and job creation. Entrepreneurship has become an important driver of economic growth in many countries, and civil engineering students can contribute to this growth by creating innovative solutions to societal problems.

Entrepreneurship can also help civil engineering students to develop skills. In the civil engineering industry, as engineers are required to design, construct, and maintain infrastructure that meets the needs of society [3]. Moreover, entrepreneurial skills can help civil engineering students to become more adaptable and flexible in their thinking, which can help them navigate the changing demands of the industry.

Challenges faced by civil engineering students in developing entrepreneurial skills: Despite the importance of entrepreneurial skills, civil engineering students face several challenges in developing these skills. One of the major challenges is the lack of exposure to entrepreneurship [4]. Most civil engineering students are not exposed to entrepreneurship during their studies, which limits their ability to develop the necessary skills. Additionally, civil engineering students face the challenge of balancing their academic studies with entrepreneurship, as starting a business requires a significant amount of time and effort.

Another challenge faced by civil engineering students is the lack of resources and funding. Starting a business requires capital, and many civil engineering students may not have access to the necessary resources to start a business. Additionally, civil engineering students may not have the necessary business skills to manage a business, which can lead to failure [5].

Strategies to enhance entrepreneurial skills among civil engineering students: Several strategies can be implemented to enhance entrepreneurial skills among civil engineering students. One strategy is to incorporate entrepreneurship into the civil engineering curriculum [6]. This can be achieved by introducing courses that focus on entrepreneurship, innovation, and business management. Additionally, universities can organize workshops, hackathons, and competitions that encourage students to develop innovative solutions to societal problems.

Another strategy is to provide funding and resources to students who are interested in starting a business. Universities can provide funding through grants, scholarships, and venture capital funds [7]. Additionally, universities can provide students with access to business incubators and accelerators, which can provide them with the necessary resources and support to start a successful business.

2 Literature Review

The new enterprises are context-dependent and foster flourishing social processes, and their establishment contributes to the economic development of the society. The major factor in starting a business is discovered to be a person's skill or potential. Many startup hurdles and motivators have been examined [8]. The author looked into obstacles such a shortage of resources, including money, time, and human resources, as well as construction knowledge and owner decision-making skills [9]. Nader concentrated on effective lean building techniques and outlined a few key obstacles to beginning a new company. Since entrepreneurship is essential for sustainable development, research on sustainable economic development came to the conclusion that member participation, corporation, collaboration, and trust are crucial components of company growth.

Culture has a big impact on entrepreneurship, especially when it comes to motivating students to start businesses in Romania due to cultural differences [10]. The study emphasized numerous important driving forces behind motivation and obstacles in Romanian business. Two crucial factors for entrepreneurship are capital and human resources. It is sometimes suggested that those who are most likely to start their own businesses are more financially secure and have better human capital credentials than those who do not. In the context of entrepreneurs, a study looked at the causal connections between financial and human capital resources [11]. A major barrier to doing business is money, as are corrupt practices in government. Being independent is essential for being an entrepreneur.

People desire to start their own businesses because they want to be independent, have more control over their lives, and dislike having bosses over them, according to research. Money and personal safety are crucial factors in corporate operations. Finances and family security are the two most important business considerations. Business heavily depends on having the necessary experience. Business and experience have a significant relationship, according to number [12]. Little enterprises are the place where entrepreneurship begins. Finance, life stability, achievement, an easy schedule, experience, self-satisfaction, and the desire were identified to be the driving forces behind the self-employment according to a study on the drivers and barriers of smaller firms.

Several authors have researched the hard and soft skills that influence the growth of entrepreneurship. Hard talents are defined as business maturity and entrepreneurial qualification. Experience is frequently the best teacher of maturity. On the other hand, the soft skills are mostly connected to the emotional intelligence of business owners.

The aforementioned criteria show that entrepreneurs need to be capable of taking risks and can help strengthen risk-averting skills.

Running a business is somewhat dangerous, but a successful business owner will always accept the risk [13]. As a result of the owner's willingness to take calculated risks, the company benefits. Business market has two key effects on business: first, more entrepreneurs are produced as a result of increased competition, and second, it has a detrimental impact on the environment. A market failure can have a number of detrimental impacts. The employment security offered by being an entrepreneur is a significant factor. According to a new study, although entrepreneurship is extremely dangerous and unpredictable, it eventually becomes more dependable and secure [14].

Although there is a wealth of material on starting new businesses, there is less on construction. The two main topics of current research are business-related motives and impediments in the building industry. This study can close the knowledge gap and serve as a manual for recent graduates who want to start their own business in the construction sector.

2.1 Research Objectives

To reduce the unemployment rate for recently graduated engineers and architects, the goal of this essay is to highlight the importance of entrepreneurship in the construction sector. Based on critical literature, the study aims to illustrate the essential needs for a rookie to run a construction business. The primary causes of new business owners' lack of motivation to create their own construction company are examined in the second stage of this study. The ensuing goals are created in order to successfully accomplish the aforementioned goal:

1. Develop and improve your entrepreneurial spirit.
2. Learn about the resources for assistance and support available to launch a small business.
3. Obtain the managerial expertise required to manage the industrial unit.
4. Investigate the barriers to developing entrepreneurial skills.
5. Develop recommendations for improving entrepreneurship education for civil engineering students.

2.2 Research Methodology

The following methodology was used to accomplish all research goals:

1. Determine the research question.
2. Identify the target population.
3. Develop a survey or questionnaire: Some questions that could be included are:

(i) Have you ever started a business or been involved in an entrepreneurial venture?
(ii) What entrepreneurial skills do you think are important for civil engineers?
(iii) How do you rate your knowledge of business and entrepreneurship?
(iv) What resources do you need to develop your entrepreneurial skills?

4. Pilot the survey.
5. Administer the survey.
6. Analyze the data.
7. Draw conclusions and make recommendations: Finally, draw conclusions from the data and make recommendations for how civil engineering programs can better prepare students to be successful entrepreneurs.

3 Results and Discussions

Positive elements serve as motivators and are essential for starting a new business. The report highlights the top five elements as being essential aspects. The study's findings indicate that "financial resources of the owner" are considered to be the most important aspect by business owners. Owner does not require the first investment since financing is the most important requirement. The owner's financial assets act as a key to start the business.

The second-ranked aspect is "team collaboration," as managing a large company without effective teamwork is incredibly difficult for business owners. Successful teams collaborate to manage a business. The survey's third-ranked factor is "communication skills," as owning a business necessitates having good proficiency in this area. When interacting with the appropriate market stakeholders, business owners must possess good bargaining skills. The overall ranks of the factors are shown in Fig. 1.

Technical and leadership qualities in the owner are considered as the fourth and fifth most important factors, respectively. Again, having strong leadership qualities is essential to running a successful organization. This element may not be as crucial as finance, as is evident from the results, but it is still very important.

Barriers are obstacles that prevent a task from being completed successfully. Figure 2 lists the difficulties to starting a construction company or being an entrepreneur. According to the findings, the inflexible work schedule, government rules, a lack of social interaction, and narrow profit margins in the market are the biggest obstacles to starting a self-employed firm in the construction sector, followed by others depicted in the above figure.

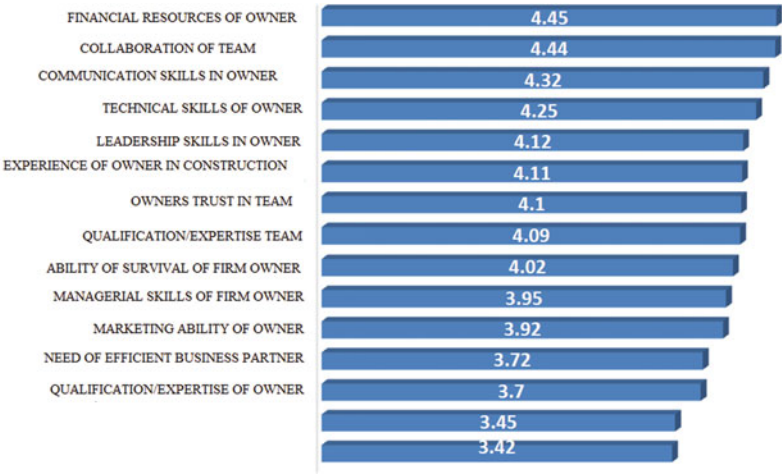

Fig. 1 Motivating factors for entrepreneurship

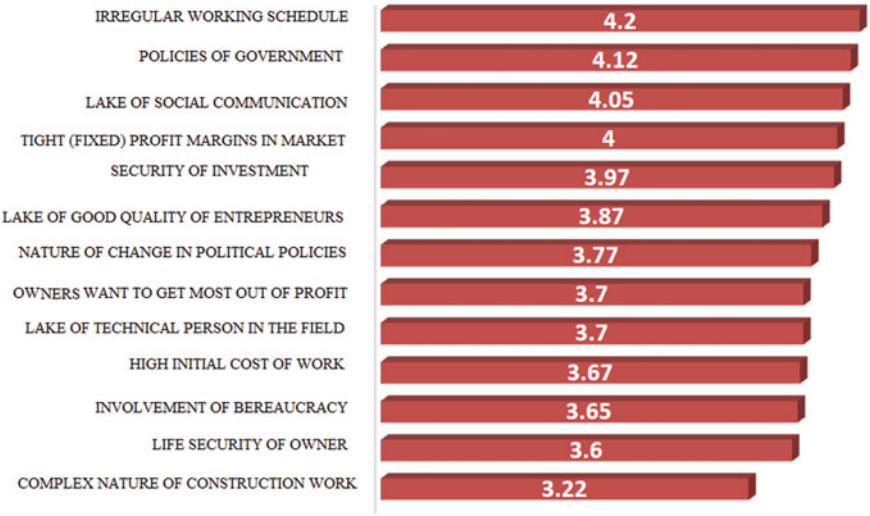

Fig. 2 Barriers for entrepreneurship

4 Conclusion

This study aims to advance understanding and knowledge of construction industry entrepreneurship. The unemployment rate is rising globally, and Pakistan is not an exception. To address this issue, entrepreneurship is essential. The introduction of innovative construction business startup techniques might lead to a variety of chances.

The issue can be solved by motivating recent graduates and giving them the knowledge and business opportunities they need. This essay focused on the main motivations and challenges for starting a new construction company. According to the study's results, teamwork, communication, technical knowledge, and the owner's leadership abilities are all essential for a successful construction business in addition to funds. Additionally, the paper makes the unsettling assertion that building entrepreneurship is feasible. Experts claim that other challenges include intense market rivalry and a hard work schedule. Many worry that working for this company will cut them off from society because fresh graduates are more gregarious. The scarcity of entrepreneurship education is the major obstacle that fresh graduates also see. The viewpoint presented in this paper can assist recent graduates in starting their own businesses. The report also advises considering these obstacles and looking for solutions to help the construction industry reach its full potential and improve the sector's health by reducing the unemployment rate.

References

1. Khoso AR, Siddiqui FH, Khahro SH, Akhund MA (2017) Entrepreneurship in construction industry: motives and barriers. Int J Civ Eng Technol 8(6):491–499
2. DeMonsabert S, Lanzarone J, Miller M, Liner B (2009) Educating federal engineers to be entrepreneurial thinkers and leaders who would have thought? In: ASEE annual conference exposition conference proceeding. https://doi.org/10.18260/1-2-5350
3. Oswald Beiler MR (2015) Integrating innovation and entrepreneurship principles into the civil engineering curriculum. J Prof Issues Eng Educ Pract 141(3):1–8. https://doi.org/10.1061/(ASCE)EI.1943-5541.0000233
4. Mayas N, Zabara H (2019) Types and importance of entrepreneurship and entrepreneurs done by: supervised by, Apr 2019 [online]. Available https://www.researchgate.net/publication/332709208
5. Looi KH, Khoo-lattimore C (2015) Undergraduate students' entrepreneurial intention: born or made? Undergraduate students' entrepreneurial intention: born or made? Kim Hoe Looi * Catheryn Khoo-Lattimore. Int J Entren Small Bus 26(1):1–20
6. Manokhoon K, Najafi FT (2005) Complementary courses: the public works management for civil engineers and the entrepreneurship for engineers, at the University of Florida. In: ASEE annual conference exposition conference proceeding, pp 2031–2036. https://doi.org/10.18260/1-2--14480
7. Clarke D, Reimer D, Ali A (2009) A structured approach to innovation: a classroom experience in inventive problem solving for an entrepreneurial program. In: ASEE annual conference exposition conference proceeding.https://doi.org/10.18260/1-2-5306
8. Zhu GX, Hong-Jie MA, Han Y (2019) Study the status and path of reform of innovation and entrepreneurship of civil engineering education system. IOP Conf Ser Earth Environ Sci 267(5). https://doi.org/10.1088/1755-1315/267/5/052053
9. Ortiz P, Pagán JI, Lopez I (2022) Entrepreneurship as a tool to facilitate job placement for civil engineering students. Int Symp Proj Approaches Eng Educ 12(2011):22–29. https://doi.org/10.5281/zenodo.6924017
10. Jensen MJ, Schlegel JL (2017) Implementing an entrepreneurial mindset design project in an introductory engineering course. In: ASEE annual conference exposition conference proceeding, vol 2017, June 2017. https://doi.org/10.18260/1-2--28480
11. Rusu S (2012) Entrepreneurship and entrepreneur: a review of literature concepts. Afr J Bus Manage 6(10):3570–3575. https://doi.org/10.5897/ajbm11.2785

12. Da Silva GB, Costa HG, De Barros MD (2015) Entrepreneurship in engineering education: a literature review. Int J Eng Educ 31(6):1701–1710
13. Lindsay E, Morgan JR (2016) The Charles Sturt University model—reflections on fast-track implementation. In: ASEE annual conference exposition conference proceeding, vol 2016, June 2016. https://doi.org/10.18260/p.26108
14. Welker AL, Sample-Lord KM, Yost JR (2017) Weaving entrepreneurially minded learning throughout a civil engineering curriculum. In: ASEE annual conference exposition conference proceeding, vol 2017, June 2017. https://doi.org/10.18260/1-2--29112

Identification of Factors Influencing Safety in South Indian Construction Projects

N. Pavithra, S. Manikandaprabhu, Sachikanta Nanda, and D. Harish

Abstract Safety in the construction industry has emerged as a key concern around the world. When compared to other industries, the construction industry has the highest proportion of injuries and fatalities among its employees. Compared to workers in other industries, construction workers are three times more likely to be injured in the workplace than their counterparts. A multitude of factors contributes to the poor safety performance of the workers, which is the leading cause of accidents. To enhance safety performance, it is necessary to study the possible reasons and contributing factors to construction accidents. The purpose of this study is to assess the relevant characteristics impacting safety performance in the construction process so as to decrease the probability of accidents. A diverse range of opinions from competent experts working on a variety of construction sites may be gathered via the use of a survey questionnaire. Using a relative importance index (RII) method, the most and least affecting factors of safety were identified.

Keywords Construction projects · Safety management · Factors influencing safety · Relative importance index · Quantitative survey

1 Introduction

In recent years, the worldwide construction sector has witnessed unprecedented expansion, according to industry experts. Despite the fast improvement of technology in many of these fields, building work is still a challenging task to complete. Construction safety management is a strategy for monitoring safety precautions on a construction site to order to provide a safe working environment. During the design and planning stages, decisions are taken that have a substantial influence on the overall safety of the construction project. According to the Bureau of Labour Statistics, it is the fourth most dangerous occupant, with the second-highest number of

N. Pavithra · S. Manikandaprabhu (✉) · S. Nanda · D. Harish
Department of Civil Engineering, SRM Institute of Science and Technology, Kattankulathur, Chengalpattu 603203, India
e-mail: saravanaprabhou@gmail.com

K. R. Reddy et al. (eds.), *Recent Advances in Civil Engineering*, Lecture Notes in Civil Engineering 398, https://doi.org/10.1007/978-981-99-6229-7_50

deaths, and the most dangerous occupation in general (BLS). Construction safety is a vital necessity, yet it is usually ignored on construction sites.

Construction workers have historically experienced more fatal and nonfatal injuries than workers in other sectors. A wide range of negative effects will always result from construction injuries, including human suffering for workers who are injured, project delays, reduced productivity suffered by the construction firm, higher insurance costs as a result of costly injuries, and the possibility of liability actions against all parties involved in the construction project [1]. There is a lack of proper training and education in safety measures, as well as a lack of carelessness and ignorance about the roles of both workers and managers, which results in the majority of construction-related fatalities. According to the study, the main causes of accidents are linked to different industrial environments, including human behaviour, challenging site conditions, and security abuses, all leading to risky operating practices, equipment, and processes [2]. The purpose of the study was to identify the critical safety factors influencing the success of a safety management system for construction sites.

1.1 Safety Management at the Construction Site

Accidents are unexpected occurrences that throw off the normal course of events. It has a negative impact on the company's production capacity. If the manufacturing process is constantly delayed, it will have a detrimental influence on the project's timeframe and on every area of construction [3]. On the basis of cost, quality, and time, projects have traditionally been negotiated and managed. Consequently, a lack of health and safety or an accident may have an indirect impact on costs, quality, and time. Behavioural change campaigns can help to minimize the number of accidents and deaths [4]. It is difficult to talk about human error without mentioning the importance of understanding and one's ability to take responsibility. All other departments in the firm should use a similar safety and health management approach. However, even though a comprehensive safety plan can help avoid or limit harm, not all contractors have adequate safety measures in place [5].

The occupational safety and health act (OSHA) and the regulations that regulate its execution have had a significant impact on the construction industry. Construction workers, more than any other group of government employees, have a higher risk of occupational sickness and injury than those in any other field [6]. Because of this, a site security management system is urgently needed to limit the number of accidents. To ensure that construction employees are safe at all times, construction safety management is used (CSM).

1.2 Literature Review

Nasrun et al. [7] says that a project's construction employees are among the most vulnerable members of the team, and they are constantly exposed to danger and risk. The Social Security Organization (SOSCO) reported in 2001 that the number of construction accidents went from 4406 in 1995 to 4654 in 2003, an increase of 5.6%. As a result, the death rate has risen from 60 to 95 instances since 1995 [7]. The number of fatalities at work shows that the construction industry is the most important one that needs to change its safety practices soon and in an efficient direction. Haslam et al. [8] the construction industry's poor safety performance has led to a variety of safety-related concerns being addressed at the worldwide level [8]. Usukhbayar and Choi [9] accidents, deaths, and injuries still occur on a daily basis at construction sites, in various attempts made over the last few decades to enhance the construction industry's safety record [9]. Giri [10] injury at work is 10–20 times more likely to happen in developing countries than in developed countries. This is due to the fact that the most of the workforce in emerging nations is engaged in smaller companies to medium level that does not follow the basic criteria and recommendations for occupational health and safety set by the WHO and the ILO [10]. Zhao et al. [11] there are three levels of elements that impact safety management at construction projects which are macro-levels, meso-levels, and micro-levels, which correspond to sector/country factors, organizational factors, and human factors [11]. Rivera et al. [12] discussed design safety in the construction industry, and an increasing number of innovative methods and technologies have been used by building companies, but the percentage of construction-related accidents has not decreased despite these advancements. Safety management has not been able to effectively respond to this long-standing issue, which has resulted in a lack of efficiency gains [12]. Therefore, a comprehensive comprehension of the issue is essential for enhancing risk management and lowering the number of accidents that occur in the construction industry. For this purpose, recognizing the elements that impact safety is the first step towards designing appropriate possible new solutions for the existing structure and, more crucially, for future situations in the construction field [13]. Khalid et al. [14] in order to maintain and improve a safety management system's effectiveness, it must be subject to ongoing safety monitoring and evaluation. Constant evaluation and change management have proven to be an essential component of the safety management strategy. A self-regulatory method for assessing safety performance is used by governments across the world, while construction industry experts urge a framework that measures individual safety performance [14].

2 Data Collection and Analysis

The quantitative surveys' section start with the demographic details of the responses which are distinguished by objective questions. Taking into account the findings of the literature review and pilot study, a questionnaire was created. A questionnaire is a resource consisting of a series of questions to collect data from respondents. In this study, a questionnaire was distributed to several construction firms in order to collect responses from construction experts. Using the Likert scale, each factor was given a score between 1 and 5, where 1 indicates minimal influence and 5 indicates a very strong impact on construction site safety. The qualifications held by the responding person include a diploma, an undergraduate degree, and a postgraduate degree. Sixty-six participants from the private sector and ten individuals from the public sector were replied. Seven important parameters were considered for research purposes and each major is comprised six sub-factors [15–18]. The seven major factors are technical factors, organizational factors, procedural factors, environmental factors, personal factors, psychological factors, and miscellaneous factor.

The 42 criteria which are discussed above are taken into account as considerations that have an influence on the safety of construction projects. The problems are organized into categories according to their classification as shown in Table 1.

Figure 1 represents the education qualification of the responded in four different categories. The response consists of a site engineer, supervisor, technical engineer, quantity surveyor, assistant engineer, owner, contractor, planning officers, a senior engineer, a project manager, and a designer.

Researchers in the fields of construction and project management commonly adopt a non-parametric method known as the relative importance index (RII) for the purpose of conducting data analysis on standardized questionnaire responses using ordinal measurements of opinions. For this study, 76 out of the 86 replies were found to be highly significant. The relative importance index, often known as RII, is the average of a component that defines how relevant the item is in the perspectives of respondents. RII stands for the acronym "Relative Importance Index." The five-point Likert scale was utilized for the analysis of the factors that influence safety, which was taken into consideration as shown in Table 2.

On the basis of this scale, respondents were required to answer questionnaires. In this study, the RII (Relative Significance Index) approach was used to estimate the relative importance of several factors impacting construction site safety [9]. The following formula was used for each respondent's response in order to determine the relative score of each response.

Relative importance index formula**:**

$$\mathrm{RII} = \sum W/A * N,$$

$$\mathrm{RII} = (5n5 + 4n4 + 3n3 + 2n2 + 1n1)/A * N.$$

Here, $\sum W$ indicates $= 5n5 + 4n4 + 3n3 + 2n2 + 1n1$,

where (1–5) is scale value $n1$, $n2$, $n3$, $n4$, $n5$.

Table 1 Factors influencing safety

Factors	Sub-factors
A. Technical factors	Unsafe mechanical design (A1)
	Hazardous arrangements (A2)
	Usage of defective devices (A3)
	Improper machine guarding (A4)
	Lack of scaffolding fixing and inspection (A5)
	Wrong choice of work equipment (A6)
	Communication gap among the workers (B1)
B. Organizational factors	Lack of safety officials on a site (B2)
	Poor worker-management relationship (B3)
	Discontinuity of regular workers (B4)
	Assigning overtime work (B5)
	Lack of safety instructions/indication (B6)
	Providing low standard PPE (C1)
C. Procedural factor	Issues of safety booklet (C2)
	Lack of training on the usage of safety clothing (C3)
	Lack of training on the usage of safety equipment (C4)
	Lack of adoption of advanced safety technologies (C5)
	Non-availability of the suitable safety accessories for hazards works (C6)
	Due to the location/region of the site (D1)
D. Environmental factor	Due to the layout of the plan (D2)
	Due to natural calamities (D3)
	Humidity causes uncomfortable (D4)
	Due to surrounding pollution (D5)
	Lack of proper ventilation (D6)
	Age and health of the employees (E1)
E. Personal factors	Education level of workers (E2)
	Improper attitude towards work (E3)
	Non-usage or improper use of safety devices (E4)
	Lack of skills of workers (E5)
	Involving in unknown/unfamiliar work (E6)
	Lack of involvement in work (F1)
F. Psychological factor	High anxiety level (F2)
	Due to supervisor's safety behaviour (F3)
	Due to workmate's safety behaviour (F4)
	Lack of personal care for the safety (F5)
	Working at unsafe speeds (F6)

(continued)

Table 1 (continued)

Factors	Sub-factors
	Lack of experts in construction safety management (G1)
G. Miscellaneous factors	Public policies in construction safety (G2)
	Local political pressures (G3)
	No proper penalty system for labour loss (G4)
	Due to language barriers (G5)
	Lack of motivation for labour (G6)

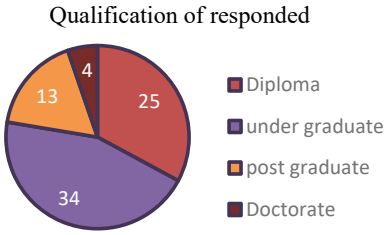

Fig. 1 Education qualification

Table 2 Variables and range

Strongly disagree	Disagree	Average	Agree	Strongly agree
1	2	3	4	5

A Response with the greatest possible score.
N Number of participants.

3 Factors Influencing Safety in Construction

According to Table 1, the factors that influence the level of safety at construction sites are shown in a graphical representation using the RII value. The sub-factors that have an effect on the overall safety of construction sites are presented in the form of a graph, organized according to the primary category of the key factors that they belong under.

In Fig. 2a, the technical factor demonstrates that the use of a defective device is seen as the most crucial component, while hazardous working arrangements are evaluated as the second most important factor 0.6263 and 0.6336, respectively. Within the technical sub-factors, the unsafe mechanical design with the lowest RII value (0.5973) is considered to have the least impact on safety.

In terms of the organizational factor, Fig. 2b shows the lack of safety officials at the construction site which was the most important factor that led to the accident, with an incidence rate ratio (RII) value of 0.6342. The communication gap between workers

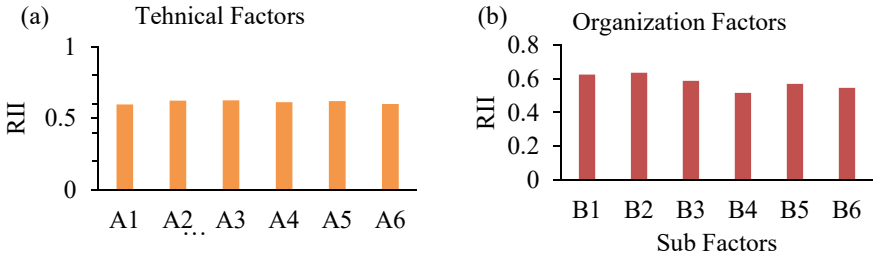

Fig. 2 **a** Technical factor; **b** organization factor

during the construction phase was the second most important factor that impacted worker safety, with an incidence rate ratio (RII) value of 0.6236. According to the response, discontinuity of regular work is observed as the factor that has the least impact on worker safety with the RII value of 0.5157.

In the procedural factor, the results indicate that the lack of proper safety accessories for hazardous work has the greatest impact on safety among the six sub-factors, with an RII of 0.6789, followed by the use of poor PPE in the workplace, which has an RII of 0.6657. In this procedural factor, the two sub-factors that have the identical RII value of 0.55 are regarded to be the least influential which are booklet problems and lack of training for safety equipment as shown in Fig. 3a Procedural factors; b environmental factors

Figure 3b demonstrates that the location or region of the site will cause safety issues during construction, as indicated by the highest RII value (0.6973), followed by the layout of the plan, which causes the second-highest RII value (0.6736) and thus causes safety issues for workers on the site. Moreover, among the six sub-factors, lack of ventilation contributes to fewer safety concerns than the other six sub-factors.

The RII rating of 0.7526 indicates that accidents or injuries are likely to occur on a construction site owing to the age and health of the employees, as determined by their responses to questions on personal variables. The improper or non-use of safety equipment in the workplace is the second leading cause of safety problems.

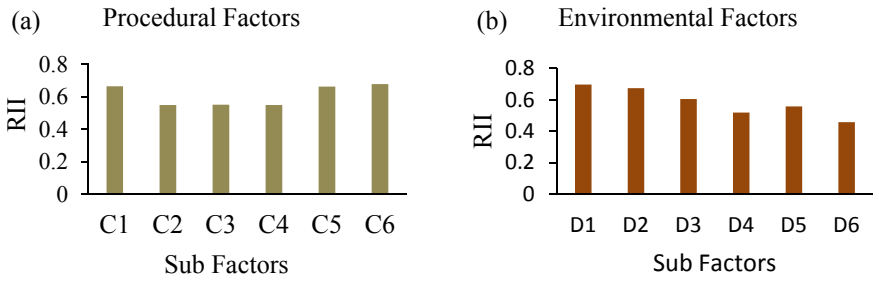

Fig. 3 **a** Procedural factors; **b** environmental factors

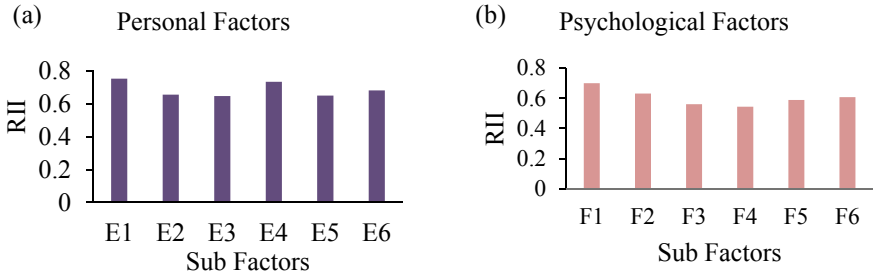

Fig. 4 **a** Personal factors; **b** psychological factors

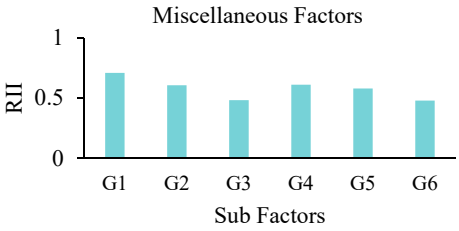

Fig. 5 Miscellaneous factors

With an RII of 0.6473, the incorrect attitude towards work is the least influential factor when compared to the other sub-factors which are shown in Fig. 4a.

According to the psychological factor Fig. 4b, a high level of anxiety among construction employees during working hours might have a significant impact on safety. The RII value for high levels of anxiety is 0.70. The lack of involvement in the work, with an RII value of 0.6351, is the second significant element that impacts the situation, and it has an effect on the employees' safety in the construction industry. Among other sub-factors, workmate behaviour is viewed as the least influential.

In various aspects, the lack of experts in construction safety management and improper plenty systems are considered to be the primary causes of the lack of safety in the construction industry, resulting in worker safety difficulties. These factors have RII values of 0.7078 and 0.6052 as it is shown in Fig. 5.

3.1 Critical Factor

The following graph illustrates RII and its position among the seven most important elements that contribute to unsafe working conditions on construction sites.

The age and health of the worker are considered to be the topmost significant of the 42 criteria shown in Fig. 6. Assuming that a worker is fit for work without understanding their condition may result in safety issues. The site's higher authorities, such as the site engineer, safety engineer, and supervisor, should assign responsibilities to

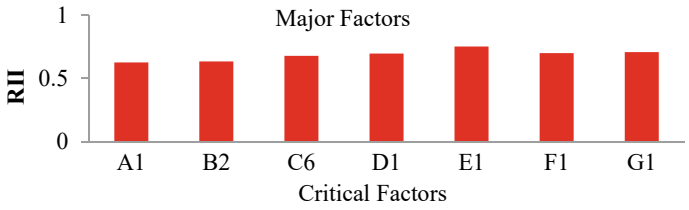

Fig. 6 Critical factors

workers based on the nature of the tasks. The majority of construction site accidents are caused by the non-availability of suitable safety accessories for hazardous works, and those who do not place a high priority on wearing guards enter the chance of being exposed to danger. Due to a lack of expertise in safety management, a number of construction companies lack in safety. This may result in time and expense issues for the firm. Without adequate guidance, projects may be plagued with numerous safety-related accidents. If workers are not involved in their work and if he/she is in high anxiety level, then this will negatively affect both the quality of their work and their fellow workers. Because the sluggish behavior of a single worker might have a psychological impact on the entire team schedule.

The working environment is the most significant factor for site safety. Insufficient site investigation prior to work is a primary cause of many accidental occurrences resulting from environmental circumstances. The work schedule should be created depending on the working location's and region's conditions. The appropriate number of safety authorities should be assigned based on the scope of the project. Otherwise, the project's overall design might be ruined by the amount of time spent on individual discussions, and safety concerns could arise more frequently. Even if it was used without their knowledge, an unsafe defective device can lead to major safety problems or even death. Complete device inspections are more likely to be performed for safety during significant activities. The study has determined that safety management is the most significant aspect of a construction project, as it maintains the health of workers on the construction site and avoids the development of various dangers and accidents. Within the scope of this study, the most significant factors impacting safety were investigated. To ensure safety, there should always be a safety engineer or officer on the construction site to inspect the application of safety measures. The management should mandate the use of safety equipment. To safeguard their own safety, all workers should be equipped with personal protective equipment. Every construction site should take the necessary precautions and treatments to prevent the occurrence of accidents.

4 Conclusion

The research highlighted the seven major types of accidents that may occur on construction sites, as well as the elements that can impact safety performance, and it suggested the techniques that can be taken to reduce the frequency of accidents that can be attributed to poor safety performance. The most major type of accident occurred as a result of the age and health of the workers on the construction site; however, this may be reduced by effective scheduling of workers to labour based on categories, and other causes such as a defective device, the location of the site, and a high degree of anxiety are produced by the construction personnel's lack of safety awareness, resulting in poor safety performance. So, from this research, it helps to find out that the solutions and makes awareness in the construction sector people. Therefore, determining the basic causes of accidents and taking preventative actions that are effective are the two most important things that can be done to reduce the number of times accidents take place on construction sites and to improve the overall level of safety performance among construction workers.

References

1. Shepherd R, Lorente L, Vignoli M, Nielsen K, Peiró JM (2021) Challenges influencing the safety of migrant workers in the construction industry: a qualitative study in Italy, Spain, and the UK. Saf Sci 142. https://doi.org/10.1016/j.ssci.2021.105388
2. Ahmed S (2019) Causes and effects of accident at construction site: a study for the construction industry in Bangladesh. Int J Sustain Constr Eng Technol 10(2):18–40. https://doi.org/10.30880/ijscet.2019.10.02.003
3. Deng L, Zhong M, Liao L, Peng L, Lai S (2019) Research on safety management application of dangerous sources in engineering construction based on BIM technology. Adv Civ Eng 2019. https://doi.org/10.1155/2019/7450426
4. Pereira E, Ahn S, Han S, Abourizk S (2018) Identification and association of high-priority safety management system factors and accident precursors for proactive safety assessment and control. J Manag Eng 34(1):04017041. https://doi.org/10.1061/(asce)me.1943-5479.0000562
5. Othman I, Shafiq N, Nuruddin MF (2018) Effective safety management in construction project. IOP Conf Ser Mater Sci Eng 291(1):832–836. https://doi.org/10.1088/1757-899X/291/1/012018
6. Rodrigues F, Coutinho A, Cardoso C (2015) Correlation of causal factors that influence construction safety performance: a model. Work 51(4):721–730. https://doi.org/10.3233/WOR-152030
7. Nasrun M, Nawi M, Ibrahim SH, Affandi R, Rosli NA (2016) Factor affecting safety performance construction industry, vol 6, pp 280–285
8. Haslam RA et al (2005) Contributing factors in construction accidents. Appl Ergon 36(4):401–415. https://doi.org/10.1016/j.apergo.2004.12.002
9. Usukhbayar R, Choi J (2020) Critical safety factors influencing on the safety performance of construction projects in Mongolia. J Asian Archit Build Eng 19(6):600–612. https://doi.org/10.1080/13467581.2020.1770095
10. Giri OP (2020) Factors causing health and safety hazards at construction sites. Tech J 2(1):68–74. https://doi.org/10.3126/tj.v2i1.32841
11. Zhao T, Kazemi SE, Liu W, Zhang M (2018) The last mile: safety management implementation in construction sites. Adv Civ Eng 2018:1. https://doi.org/10.1155/2018/4901707

12. La Rivera FM, Mora-Serrano J, Oñate E (2021) Factors influencing safety on construction projects (fSCPs): types and categories. Int J Environ Res Publ Health 18(20). https://doi.org/10.3390/ijerph182010884
13. Grabowski M, Ayyalasomayajula P, Merrick J, Harrald JR, Roberts K (2007) Leading indicators of safety in virtual organizations. Saf Sci 45(10):1013–1043. https://doi.org/10.1016/j.ssci.2006.09.007
14. Khalid U, Sagoo A, Benachir M (2021) Safety management system (SMS) framework development—mitigating the critical safety factors affecting health and safety performance in construction projects. Saf Sci 143:105402. https://doi.org/10.1016/j.ssci.2021.105402
15. Sawacha E, Naoum S, Fong D (1999) Factors affecting safety performance on construction sites. Int J Proj Manag 17(5):309–315. https://doi.org/10.1016/S0263-7863(98)00042-8
16. Meng X, Chan AHS, Lui LKH, Fang Y (2021) Effects of individual and organizational factors on safety consciousness and safety citizenship behavior of construction workers: a comparative study between Hong Kong and Mainland China. Saf Sci 135:105116. https://doi.org/10.1016/j.ssci.2020.105116
17. Khosravi Y, Asilian-Mahabadi H, Hajizadeh E, Hassanzadeh-Rangi N, Bastani H, Behzadan AH (2014) Factors influencing unsafe behaviors and accidents on construction sites: a review. Int J Occup Saf Ergon 20(1):111–125. https://doi.org/10.1080/10803548.2014.11077023
18. Chen Y, McCabe B, Hyatt D (2017) Impact of individual resilience and safety climate on safety performance and psychological stress of construction workers: a case study of the Ontario construction industry. J Safety Res 61:167–176. https://doi.org/10.1016/j.jsr.2017.02.014

Prediction of High-Performance Concrete Strength Using Python Programming

R. Rohithraman, N. Ganapathy Ramasamy, and P. R. Kannan Rajkumar

Abstract This paper seeks and brings up combination of computer programming and the concrete technology. The high-performance concrete acts as a core in construction of infrastructure. The high-performance concrete is made with the usage of basic concrete components and admixtures, and it is both mineral and chemical admixtures. The use of admixtures, either mineral or chemical, or even both, improves the performance of the concrete (Neville and Tcin in High Performance concrete—an overview, 1998, [1]). In this present study, the basic components of concrete are used with the addition of some mineral admixtures like Metakaolin and Alco fine, which are used for the concrete grades of M80 and M100 (cast and tested). High-performance concrete performs better than high-strength concrete considering the mechanical properties, which leads to a trend in the usage of HPC in infrastructure projects (Patel and Shah in Open J Civ Eng 03:69–79, 2013, [2]). Furthermore, Python programming is an evolving trend in the field of civil engineering. The Python programming language has majorly influenced its purpose in the design and estimation fields, as well as certain management-related computing tasks (Bengfort and Bilbro in J Open Source Softw 4:1075, 2019, [3]). However, when compared to other technologies, the evolution of the programming language in concrete technology is less. The primary goal of this research is to predict high-performance concrete strength using Python programming. The compressive strength of the concrete is determined by only experimental means. But, this experimental process is time-consuming and acts as a boon to further processes. This programming with the preloaded data and features will make it easy to predict the strength by just providing certain details like composition and ratio to be used for concrete. For each and every entity entered, the programming language does a graphical analysis, which in turn helps to iterate the required results for the respective grade of concrete. Based on the cast and the programmed results, the optimum grade was found.

R. Rohithraman · N. Ganapathy Ramasamy (✉) · P. R. Kannan Rajkumar
Department of Civil Engineering, Faculty of Engineering and Technology, SRM Institute of Science and Technology, Kattankulathur, Tamil Nadu 603203, India
e-mail: ganapatn@srmist.edu.in

K. R. Reddy et al. (eds.), *Recent Advances in Civil Engineering*, Lecture Notes in Civil Engineering 398, https://doi.org/10.1007/978-981-99-6229-7_51

Keywords High-performance concrete · Alco fine · Metakaolin · Python programming · Prediction of results · Graphical analysis · Material optimization · DOE

1 Introduction

In recent times, infrastructure development is at a rapid pace. The larger infrastructure is in the use of high-performance concrete. The initiation and implementation of the high-performance concrete involves various steps of casting and procedure. High-performance concrete is made of cementous binding material, fine aggregate, and coarse aggregate, along with certain mineral and chemical admixtures that can directly affect the mechanical properties of the concrete. This experimental investigation also involves understanding the behavior of the admixtures in the concrete based on the different compositions of the mixes involved in the casting. The strength of the high-performance concrete purely depends on the composition ratio and is also based on the specific type of material used [4]. From this virtue, this study further implements the Python program to predict the high-performance concrete strength by just certain provisions like the ratio or the composition of the material to be used. This project, in an overview, involves casting and testing of different ratios and grades of high-performance concrete and implementation of the results for the respective grades of concrete in programming. HPC is a type of concrete that is designed to be more durable and, if necessary, stronger than regular concrete [5]. High-performance concrete differs from high-strength concrete in most cases. The high-performance concrete is economical in nature considering the high-strength concrete. The high performance in the infrastructure is found to be economical as it may influence in reduction of the dimension of the structural member also influencing the reduction of reinforcement details of the member. The high-performance concrete also acts as an advantage on reducing the water–cement ratio hence enhancing a good cementitious content [6]. The top three picks from the optimal mix design are then put through more mechanical property tests to make sure they meet the needs of high-performance concrete with involving in the program for prediction analysis [7].

2 Material Characterization

The study initiates with the literature survey where the key insights of the various projects are observed. Based on the observation, the material to be implemented is characterized [8]. The design mix for the high-performance concrete is then made through the ACI 211-91 standards [9] based on the all the materials that are characterized [10]. After the attaining of the mix design of the mixes, the development of the project has categorized into two stages, one is with the casting of the specimens and the other is organized with the development of the programming language. The

casting and the programming are done simultaneously in a steady flow. After the casting, the specimens are subjected to testing on the respective 7th, 14th, and the 28th days of curing. On the other side, the program was developed and was subjected to the trial values run and the error decoding. After both the categorized tasks are completed, the program and the experimental are combined and the dataset is formed based on the program needs. The data are processed from the datasets and the final program is made to run, and the results of the test model are obtained in the form of the validation and the training score.

The casting of the high-performance concrete involves the materials for each entity, such as,

Cement:	Ordinary Portland Cement 53 grade.
Fine aggregate:	Manufactured sand.
Coarse aggregate:	Blue Metal of 10 mm (passing through 12.5).
Mineral admixture:	Alco fine, Metakaolin.
Chemical admixture:	SP 430.

In order to obtain the proper outcome of the product, each of the materials that are to be included should be tested. Since concrete is used in the critical areas, the material tests are must to be performed. The cement was subjected to the Vicat apparatus which was used to determine the initial and final setting times, and in inclusion, the density bottle for determining the specific gravity was also done and the values were in limit [11]. Similarly, the fine aggregate was determined the specific gravity and grading with the pycnometer and the sieve analysis [12]. The coarse aggregate was subjected to the Izod impact and sieve analysis to determine the impact resistance and grading of the aggregate [13].

3 Mix Design of HPC

The mix design for the high-performance concrete was obtained from the ACI 211-91. As per the standards, the mix design was prepared and done for M80 and M100 grades of concrete which are elaborated in Tables 1, 2, and 3.

The mix design for the M80 and M100 grades is composed of the basic concrete material. The admixtures of the Alco fine and the Metakaolin are replaced with

Table 1 Mix design ratio

S. No.	Description	Result	Units
M80 grade of concrete			
1	Admixture replacement	15	%
2	Mix ratio	1: 1.35: 2.19	–
M100 grade of concrete			
3	Admixture replacement	15	%
4	Mix ratio	1: 1.4: 1.76	–

Table 2 Parameters for M80 grade of concrete

Parameters		Variables		
		w/b	Material composition (Alco fine and Metakaolin)	Super plasticizers
Levels		*A*	*B*	*C*
Units		–	%	%
M80 grade	1	0.31	5 + 10	1.2
	2	0.34	7.5 + 7.5	1.1
	3	0.36	10 + 5	1

Table 3 Parameter for M100 grade of concrete

Parameters		Variables		
		w/b	Material composition (Alco fine and Metakaolin)	Super plasticizers
Levels		*A*	*B*	*C*
Units		–	%	%
M100 grade	1	0.29	5 + 10	1.2
	2	0.33	7.5 + 7.5 10 + 5	1.1
	3	0.34		1

the 15% of the total binder content. Further, the composition of the materials in association with the chemical admixture is discussed further below in this study.

3.1 Parameters Considered for Optimization of Material Composition

This study of two different mixes involves two different admixture and a chemical admixture which can directly influence the concrete with its characteristics. In order to obtain the best results, various combinations are to be tested. The parameters and variable chart form Taguchi method give an upper hand. Tables 4 and 5 matrices the parameters and the variables.

Table 4 Concrete mix combinations

Experimental trials	*A*	*B*	*C* (%)
M80 grade of concrete			
P1	0.31	5% + 10%	1.2
P2	0.31	7.5% + 7.5%	1.1
P3	0.34	5% + 10%	1
P4	0.34	7.5% + 7.5%	1.2
P5	0.34	10% + 5%	1.1
P6	0.36	5% + 10%	1.1
P7	0.36	7.5% + 7.5%	1
M100 grade of concrete			
R1	0.29	5% + 10%	1.2
R2	0.29	7.5% + 7.5%	1.1
R3	0.33	5% + 10%	1
R4	0.33	7.5% + 7.5%	1.2
R5	0.33	10% + 5%	1.1
R6	0.34	5% + 10%	1.1
R7	0.34	7.5% + 7.5%	1

Note The trials of the M80 and the M100 grades are represented in the letters P and R

Table 5 Mechanical property test results

S. No.	Description	Mix combinations	Water content	Split tensile (N/mm^2)	Flexural (N/mm^2)	Compressive strength (N/mm^2)
M80 grade of concrete						
1	P4	7.5% + 7.5%	0.34	5.99	9.10	90.3
2	P7	7.5% + 7.5%	0.36	5.81	8.50	89.3
3	P2	7.5% + 7.5%	0.31	5.5	8.10	87.3
M100 grade of concrete						
4	R4	7.5% + 7.5%	0.33	6.44	10.4	106.3
5	R7	7.5% + 7.5%	0.34	6.24	10.6	110.2
6	R2	7.5% + 7.5%	0.29	6.04	10.1	108.6

3.2 Design of Experiments (DOE)

In consideration with the above parameters, the different mix combinations were derived for the concrete [14]. The hard mix combinations were eliminated, whereas the proper and acceptable combinations were taken into account. Table 4 depicts the detailed mix proportion of the mixes.

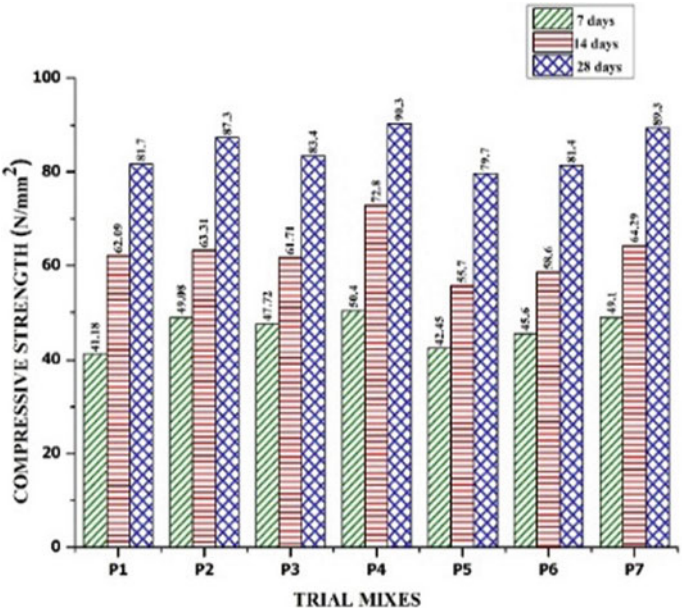

Fig. 1 Compressive test results for M80 grade of concrete

4 Experimental Investigations

The compression test is the vital experiment to determine the strength of the concrete based on their grade. The specimen was usually casted in a 100 mm × 100 mm × 100 mm cubical shape. Nine mixes of each combination were casted, and they were allowed to cure in water for respective 7, 14, and 28 days. The cured specimen is taken from curing dried and then later weighted and tested in the compression testing machine. The values denoted by the compression machine are taken and calculated. Figures 1 and 2 give the detailed values of the results. From the observation of the results, the P4, P2, P7 from the M80 grade and the trials R4, R7, R2 from M100 grade obtained the best results since the material composition of the admixture in mixes was of equal and better workability. The composition of the admixture in the equal quantity made sure to avoid irregular bonding or packing of the materials, which derived the better results.

5 Mechanical Property of Optimization Materials

Since the HPC are known for their best in their mechanical property. So, in order to satisfy the need of the mechanical property, the split tensile and flexure strength were carried out. To determine the tensile strength of hardened concrete, the splitting

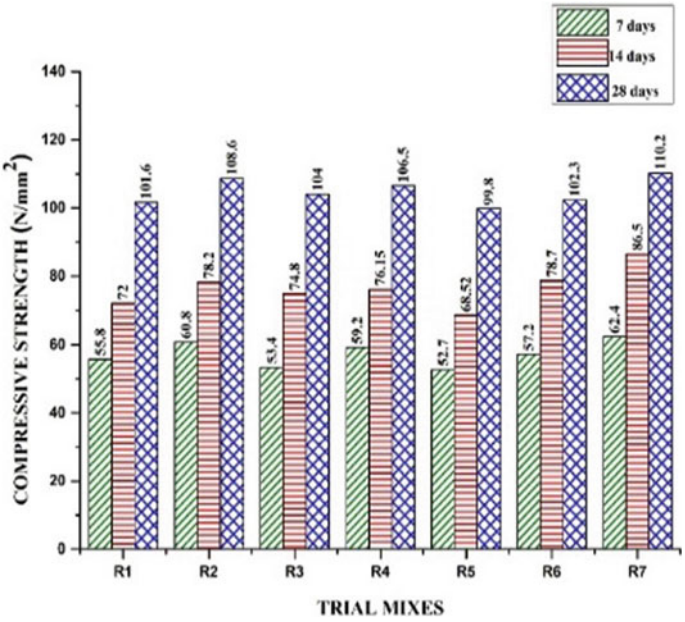

Fig. 2 Compressive test results for M100 grade of concrete

tensile strength test is utilized [15]. Minor changes in the water-to-cement ratio, component proportioning, slump growth, and other factors might affect the final concrete strength. As a result, the structural strength and stability are affected. The specimen was of 200 × 100 mm in which the diameter was of 200 mm and the test was carried out in compressive testing machine by keeping it in a transverse direction in the setup. The concrete members are more prone to the tensile load which influences the life cycle of concrete despite its strength [16]. The concrete member on tensile loads develops crack with respect to the deflection and the leads to failure. The flexure specimen is of dimensions 100 × 100 × 500 mm. The same procedure of concrete specimens is carried out for 28th day. The results obtained are tabulated in Table 5.

The concrete members are more prone to the tensile load which influences the life cycle of concrete despite its strength. The concrete member on tensile loads develops crack with respect to the deflection and the leads to failure. The flexure specimen is of dimensions 100 × 100 × 500 mm. The same procedure of concrete specimens is carried out for 28th day. The specimen is kept in the setup and subjected to a three-point loading.

6 Python in Civil Engineering

In the recent times, the programming language has immersed as a major aid in complex problem solving. Out of those, the trend has been reasonably more into the field of civil engineering solving complex problems in terms of the design criteria of the building and also to handle some of the management-related activities such as in terms of resource and manpower and other related activities [17]. It not only focuses Python in civil engineering but also it specifically uses in the field of the concrete technology [18]. Python programming is utilized in this concrete project to predict/forecast the compressive strength of high-performance concrete based on its composition and preload data gathered through the casting of desired and expected combinations of different ratios of high-performance concrete as derived from the ACI 211-91.

6.1 Syntax for Program

This program syntax involves the step-by-step process in the programming as shown in Fig. 3. The initialization was done with material characterization, mix design data, and the experimental load that was entered. The data (the coding) were done, and then, the data were processed [19]. During the process, the errors are encountered, and the loop is repeated to input of data after subjecting and completion of error decoding. In the positive result of the data processing, the model is validated and the results are obtained.

6.2 Data Input for Python

The dataset for the program has to done in order to process more data relative files is made. The dataset file usually helps to save the data in a tabular format in order to easy and quick processing of the data. The dataset file is the most suitable format for the program [20]. This dataset file contains all the material composition and the arrived results of the concrete through experimental investigations [21]. Table 6 shows the sample dataset file.

6.3 Cluster Analysis

Cluster analysis, frequently referred to as clustering, is an unsupervised machine learning technique for classifying unlabeled datasets [22]. It seeks to create clusters or groups from data points in a dataset with high intra-cluster and low inter-cluster

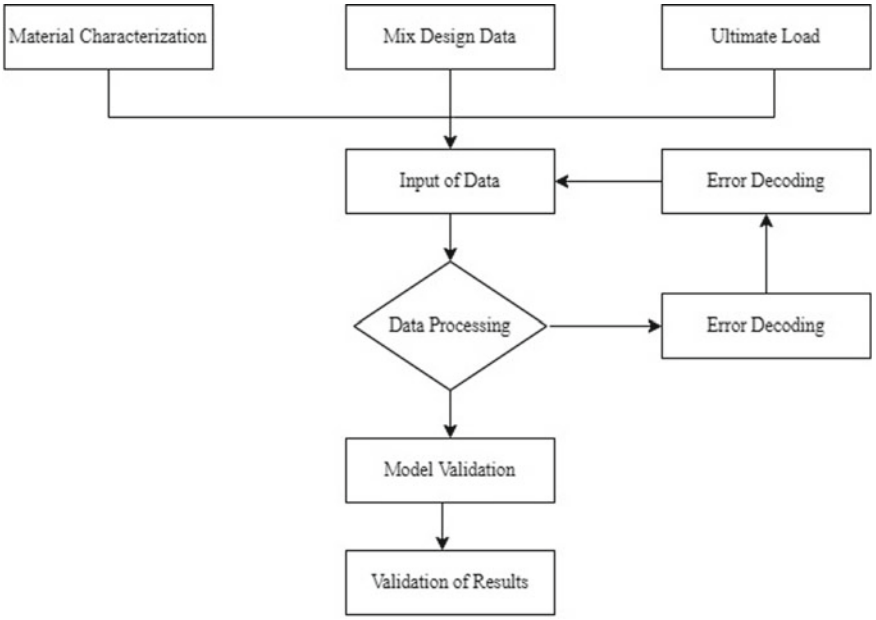

Fig. 3 Syntax of the program

Table 6 Sample dataset for the program

Trials	Cement	AF	Met	Water	S.P.	C.A.	F.A.	Age	Strength
P1	428	25.3	50.7	146	6.05	1108	683	28	81.7
P2	428	38	38	146	5.55	1108	683	28	87.3
P3	428	25.3	50.7	166	5.04	1108	683	28	83.4

similarity. In this program, the cluster distributes the dataset into four likely terms which influences the datasets' hierarchy and sections them. Here in this cluster, the specific elbow method is used [23]. When the distortions are plotted and the plot appears as an arm, the elbow (the point of inflection on the curve) is the best value of k derived. From Fig. 4, the elbow plots the cluster values lying in the k 2.0, 3.0, 4.0, 5.0 which are 30,236.40, 22,153.04, 16,396.34, and 14,122.14 corresponding to the cluster that the data points are evaluated.

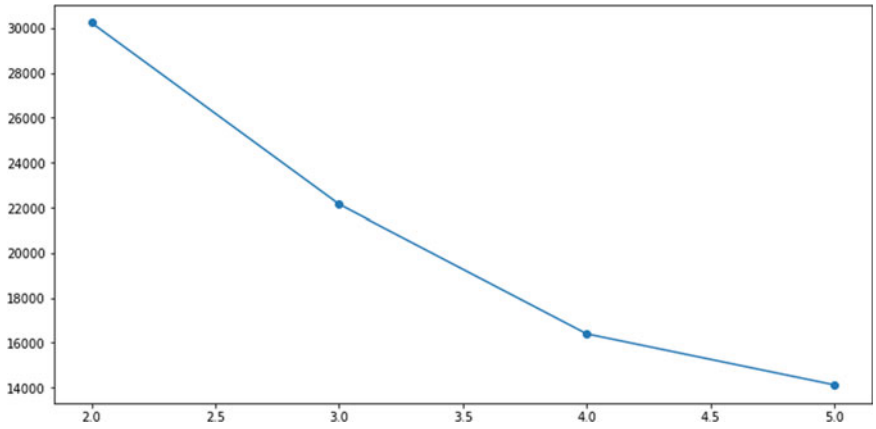

Fig. 4 Elbow plot of clusters

Table 7 Model validation results

Training score	Validation score	RMSE	*R* squared
0.975201	0.788662	0.286856	0.705639

6.4 Results from Python

The obtained compressive test result based on the mix proportion is made as a dataset and evaluated to the program. The regression of the results from the program was done through the random forest regressor. Random forest is an ensemble approach that solves regression and classification problems by combining many decision trees using the Bootstrap and Aggregation technique, often known as bagging. Instead, then relying on individual decision trees, the basic concept is to combine several decision trees to arrive at a final result. Random Forest uses a lot of decision trees as a basic learning model. For each model, we randomly choose rows and characteristics from the dataset to produce sample datasets. Bootstrap refers to this section, in which dataset leads to the Root Mean Squared Error (RMSE) [24]. In the analysis, the lowest validation, training, and RMSE were obtained for the 90-percentage confidence level in the validation for 70% of the values. In addition, the RMSE was also the lowest of 0.29. Table 7 shows the valuation of the model. Figure 5 shows the plot interval of 99.8% for confidence level of 95.

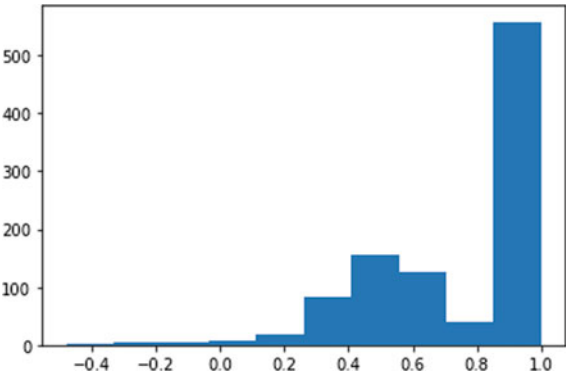

Fig. 5 Validation chart for confidence range

7 Conclusion

The trial mixes of the concrete were done for various combinations based on the admixture compositions [25]. The trial mixes were done accordingly to the composition and were experimentally investigated through compression test, and the results were obtained. The best three results of each grade were taken, and based on the mix of the specimens, the other mechanical property test like slit tensile and flexural test were carried out and results were obtained. The result from the program shows that the model obtained a 97% of success rate in the training session and the validation rate was obtained to be 78% with 80% split ups, while the RMSE has the least possible value of 0.29 and the whole some r squared value gives the accuracy of 70.56%.

References

1. Neville A, Tcin PCA (1998) High Performance concrete—an overview, vol 31
2. Patel V, Shah N (2013) A survey of high performance concrete developments in civil engineering field. Open J Civ Eng 03(02):69–79. https://doi.org/10.4236/ojce.2013.32007
3. Bengfort B, Bilbro R (2019) Yellowbrick: visualizing the Scikit-learn model selection process. J Open Source Softw 4(35):1075. https://doi.org/10.21105/joss.01075
4. Elbasha NM, Elbasha N (2013) High strength reinforced concrete beam and helix confinement. https://www.researchgate.net/publication/296945715
5. Wang D, Ju Y, Shen H, Xu L (2019) Mechanical properties of high performance concrete reinforced with basalt fiber and polypropylene fiber. Constr Build Mater 197:464–473. https://doi.org/10.1016/j.conbuildmat.2018.11.181
6. Chang PK (2004) An approach to optimizing mix design for properties of high-performance concrete. Cem Concr Res 34(4):623–629. https://doi.org/10.1016/j.cemconres.2003.10.010
7. Mo LT, Huurman M, Woldekidan MF, Wu SP, Molenaar AAA (2010) Investigation into material optimization and development for improved ravelling resistant porous asphalt concrete. Mater Des 31(7):3194–3206. https://doi.org/10.1016/j.matdes.2010.02.026
8. Thiyaneswaran MP, Revin Jenova L, Navaneethan KS (2021) Review paper on material properties of high performance concrete. IOP Conf Ser Mater Sci Eng 1055(1):012054. https://doi.org/10.1088/1757-899x/1055/1/012054

9. Dixon DE, Prestrera JR, George U, Burg SR et al (1991) Standard practice for selecting proportions for normal, heavyweight, and mass concrete (ACI 211.1-91) Chairman, Subcommittee A
10. Kibriya T, Tahir L (2017) Sustainable construction—high performance concrete containing limestone dust as filler. World J Eng Technol 05(03):404–411. https://doi.org/10.4236/wjet.2017.53034
11. IS: 12269-2013 (2013) Ordinary Portland cement, 53 grade-specification. Bureau of Indian Standards, New Delhi, India
12. IS (1963) IS 2386-1963 (part III): method of test for aggregates for concrete
13. IS (1970) 383 (1970) specification for coarse and fine aggregates from natural sources for concrete. Bureau of Indian Standards, New Delhi, India.
14. Yu R, Spiesz P, Brouwers HJH (2015) Development of an eco-friendly ultra-high performance concrete (UHPC) with efficient cement and mineral admixtures uses. Cem Concr Compos 55:383–394. https://doi.org/10.1016/j.cemconcomp.2014.09.024
15. Tanyildizi H (2009) Statistical analysis for mechanical properties of polypropylene fiber reinforced lightweight concrete containing silica fume exposed to high temperature. Mater Des 30(8):3252–3258. https://doi.org/10.1016/j.matdes.2008.11.032
16. Aïtcin PC (2003) The durability characteristics of high performance concrete: a review. Cem Concr Compos 25(4–5 SPEC):409–420. https://doi.org/10.1016/S0958-9465(02)00081-1
17. Quraishi MA, Dhapekar MNK (2021) Applicability of python in civil engineering: review. Int Res J Eng Technol. www.irjet.net
18. Hosseini R, Akhuseyinoglu K, Brusilovsky P et al (2020) Improving engagement in program construction examples for learning python programming. Int J Artif Intell Educ 30(2):299–336. https://doi.org/10.1007/s40593-020-00197-0
19. Sarvade Babasaheb Ambedkar S (2019) Use of python programming for interactive design of reinforced concrete structures load carrying capacity of cold formed steel using direct strength method. View project use of open source software in structural engineering. View project. https://www.researchgate.net/publication/334272564
20. Predicting high-performance concrete compressive
21. De Melo VV, Banzhaf W (2016) Predicting high-performance concrete compressive strength using features constructed by kaizen programming. In: Proceedings—2015 Brazilian conference on intelligent systems, BRACIS 2015. Institute of Electrical and Electronics Engineers Inc., 80–85. https://doi.org/10.1109/BRACIS.2015.56
22. Jagadale UT, Nayak CB, Mankar A, Thakare SB, Deulkar WN (2020) An experimental-based python programming for structural health monitoring of non-engineered RC frame. Innov Infrastructure Solutions 5(1). https://doi.org/10.1007/s41062-020-0260-x
23. Yeh IC (1998) Modeling of strength of high-performance concrete using artificial neural networks
24. Jain U, Sharma M, Tumrate CS (2021) A computational model to automate the design of reinforced concrete tee beam girder bridge using python ecosystem. IOP Conf Ser Mater Sci Eng 1099(1):012039. https://doi.org/10.1088/1757-899x/1099/1/012039
25. De Larrard F, Sedran T. Mixture-proportioning of high-performance concrete

Identification of the Lean Tools Used in the Tamil Nadu Construction Industry

M. Durai Aravindh, G. Nakkeeran, and L. Krishnaraj

Abstract Lean Tools and Methodologies are used in the construction sector to improve the workflow of a construction project. The purpose of this research is to identify the most important Lean Tools utilized in the construction sector in Tamil Nadu. The data is collected by issuing a structured questionnaire to the private and public construction organizations in Tamil Nadu. The most significant Lean Tools are identified from the list of 30 Lean Tools using mean of the responses and the Chi-square test is used to find the association between the Lean Tools and Respondent Profile. The ranking is executed based on responses given by the Respondents which implies that the ten significant Lean Tools are 5S, PDCA (plan do check act), FMEA (failure mode and effects analysis), JIT (just-in-time), LPS (last planner system), total productive maintenance, Kanban, 5 whys, VSM (value stream mapping), and root cause analysis. The significant Lean Tools can be adopted in construction projects to optimize the project workflow.

Keywords Lean tool · Statistical variance · Chi-square · Lean construction · Construction industry

1 Introduction

The value of the construction business may be increased via the use of various Lean technologies. It has proven to be challenging to execute the Lean strategy in the modern environment. It is of utmost importance to understand the Lean Tool and study how to successfully implement the Lean tools in construction projects to optimize the workflow and minimize waste. There are numerous works of literature that have studied and explored the Lean Tools and their application in various fields including the construction industry [1].

M. D. Aravindh · G. Nakkeeran · L. Krishnaraj (✉)
Department of Civil Engineering, Faculty of Engineering and Technology, SRM Institute of Science and Technology, Kattankulathur, Tamil Nadu 603203, India
e-mail: krishnal@srmist.edu.in

K. R. Reddy et al. (eds.), *Recent Advances in Civil Engineering*, Lecture Notes in Civil Engineering 398, https://doi.org/10.1007/978-981-99-6229-7_52

Construction waste kinds are evaluated according to their influence on time, cost, and the severity of their impact [2]. The implementation of suitable Lean Tools in the construction projects would minimize or eliminate these identified wastes. The lean wastes must be recognized and prioritized based on their impact, and then the best Lean Tool can be chosen from the offered alternative tool [3].

The importance of key parameters for successful 5S implementation is studied [4]. This research focuses on 5S as a concept, as well as the conditions for its holistic implementation, the interplay with other lean techniques, the benefits, success factors, and obstacles to 5S adoption [5]. The JIT philosophy's emphasis on quality, continuous improvement, and waste reduction may increase a company's competitiveness [6]. The customer's service-JIT delivery must also be taken into account for a long-term business. To put it another way, when policymakers assign weights to particular goals, they should take into account both the economic and environmental consequences [7]. Smooth work flow may be accomplished by reducing waste on site, regulating inventory movement into and within the site and limiting the use of automated plant and equipment [8]. Based on the root cause analysis findings, a heterogeneous biodiesel manufacturing process is built using Pareto Analysis and Fishbone diagrams. The process's long-term viability is evaluated in terms of its impact on the economy, the environment, society, and efficiency [9]. The instruments for root cause analysis must encourage discussion, be understandable when completed, and provide means for verifying the validity of group results [10]. To reduce the quantity of defective components, the PDCA cycle, Pareto charts, and flow chart are good quality tools [11]. Cost-effectiveness in offshore wind turbine systems will be greatly influenced by dependability, and the FMEA has the potential to improve the reliability of wind turbines [12]. Design improvements and concept selection may be aided by using life cost-based FMEA which can also be used to better plan component preventative and scheduled maintenance [13]. For manufacturers, the 5 whys analysis may be a powerful tool for eliminating or dramatically reducing defects via a reality and quite well approach to problem identification and solution [14]. System improvement processes may be analysed using a limited succession of Why questions [15]. The JIT-Kanban system and the variations of Kanban system were studied to better under the implementation effects and to find the difference between theoretical and practical application [16]. Design factors in a Kanban system like as sequencing rules and real lead times are evaluated using an experimental design [17]. Incorporating total productive maintenance (TPM) has a favourable impact on staff productivity and efficiency, as well as on the efficacy of the company's equipment [18]. The research explored for an efficient method of calculating costs in the study of underground pipeline building and value-added activities and time wastes throughout each construction stage were reduced using VSM [19]. From the literature study it can be identified that there are numerous Lean Tool that when successfully implemented can optimize the work flow and alter the project performance parameters.

Table 1 Identified Lean Tool

Key	Lean Tool	Key	Lean Tool
LT1	Andon	LT16	Visual management
LT2	Take time	LT17	Poka Yoke
LT3	JIT (Just-in-time)	LT18	Ishikawa diagram
LT4	VSM (value stream mapping)	LT19	Pareto analysis
LT5	Root cause analysis	LT20	5S
LT6	Kanban	LT21	Heijunka
LT7	LPS (last planner system)	LT22	A3 problem solving
LT8	Total productive maintenance	LT23	PDCA (plan do check act)
LT9	FMEA (failure mode and effects analysis)	LT24	Muda walk
LT10	5 whys	LT25	Six big losses
LT11	Kaizen	LT26	SMART goals
LT12	Jidoka	LT27	Standardized work
LT13	Concurrent engineering	LT28	Line balancing
LT14	Bottleneck analysis	LT29	Overall equipment effectiveness
LT15	Gemba	LT30	Statistical process control

2 Research Methodology

2.1 Questionnaire Design

A questionnaire based on a 5-point Likert scale is used to find the ten significant Lean Tools out of 30 Lean Tools based on their level of importance [3]. The 5-point Likert scale utilized is 1-Insignificant, 2-Minor, 3-Moderate, 4-Major, and 5-Severe. Table 1 represents the 30 Lean Tools selected for the study.

2.2 Data Collection and Validation

Data is collected by issuing around 50 questionnaires to private and public personnel in the Tamil Nadu construction industry. A total of 32 response was received in 30 days which is used for data analysis. Cronbach's Alpha is used to check the reliability of the data collection from the 32 Respondents [20]. Equation 1 is adopted to find the Alpha value.

$$\alpha = \frac{k}{k-1} \times \left(1 - \frac{\sum \sigma_i^2}{\sigma_x^2}\right), \tag{1}$$

Table 2 Cronbach's Alpha consistency benchmark

Cronbach's Alpha	< 0.5	0.5–0.6	0.6–0.7	0.7–0.8	0.8–09	≥ 0.9

where $\sum \sigma_i^2$= sum of variation scores; σ_x^2 = each factor's variation; K = number of factors.

The benchmark score for Cronbach's Alpha value [21] is represented in Table 2, and the Alpha score must be a minimum of 0.7 to deem the data collection acceptable in terms of consistency. Table 3 displays the averages, standard deviations, and Cronbach's Alpha values for each of the variables. With a Cronbach's Alpha score of 0.94, the results are very reliable, as seen in Table 2. This supports that the collected data is reliable and fit to proceed with data analysis.

2.3 Respondent Profile

The Respondent Profile is represented by Figs. 1, 2, 3, 4, and 5. One of the most significant findings from the survey is that more than half of respondents had obtained a bachelor degree (66%) as their highest level of education followed by a master degree (25%), diploma (6%), and finally a PhD (3%).

According to Fig. 2, 63% of the respondents have worked in the construction business for one to five years, followed by 28%with six to ten years of work experience, and 9% with more than 20 years of work experience.

Figure 3 represents that 41% of the Respondent organizations have 1 to 50 employees, 31% of the Respondents work in organizations with 51 to 100 employees, and 28% of the Respondent organizations are large in size with more than 100 employees. A majority of 81% are executing private contract works and 19% of Respondents execute public contract works as depicted in Fig. 4.

A majority of 69% of the Respondents work as engineer (assistant/associate) in their respective organizations, followed by 16% being supervisor, 6% being manager, 6% being contractor, and 3% are working as Researchers as represented in Fig. 5. Thus, the data has been collected across different Respondent and organization profile.

2.4 Data Analysis

2.4.1 Chi-Square Test

The Chi-square test measures the degree to which two categorical variables are connected statistically [22]. It is possible to utilize the Chi-square test in a wide range of situations where actual and theoretical frequencies are compared to assess

Table 3 Cronbach's Alpha value

Variable	Mean	Standard deviation	Cronbach's Alpha
5S	4.188	0.780	0.9441
PDCA (plan do check act)	4.094	0.856	0.9455
JIT (just-in-time)	4.031	0.782	0.9467
Root cause analysis	3.813	0.859	0.9441
FMEA (failure mode and effects analysis)	4.063	0.801	0.9451
5 whys	3.938	0.840	0.9443
LPS (last planner system)	4.000	0.762	0.9450
Total productive maintenance	3.969	0.647	0.9442
Kanban	3.969	0.822	0.9453
VSM (value stream mapping)	3.875	1.008	0.9452
Kaizen	2.938	0.801	0.9422
Jidoka	2.813	0.780	0.9422
Concurrent engineering	2.688	0.859	0.9426
Bottleneck	2.594	0.911	0.9431
Gemba	2.500	0.842	0.9420
Visual management	2.563	0.759	0.9421
Poka Yoke	2.250	0.880	0.9419
Ishikawa	2.750	0.880	0.9420
Pareto analysis	2.406	0.946	0.9419
Take time	2.438	0.914	0.9430
Heijunka	2.188	0.859	0.9410
A3 problem solving	2.250	0.842	0.9417
Andon	2.438	0.878	0.9429
Muda walk	2.438	0.801	0.9418
Six big losses	2.438	0.878	0.9414
SMART goals	2.406	0.837	0.9430
Standardized work	2.406	0.837	0.9423
Line balancing	2.469	0.879	0.9425
Overall equipment effectiveness	2.688	0.859	0.9416
Statistical process control	2.688	0.998	0.9423
Total	90.281	15.812	

a hypothesis [23]A Chi-square match to the total deviations is obtained by analysing the sum of cross products and their variance in light of all marginal totals [24].

The null hypothesis holds that there is no correlation between the variables, while the alternative hypothesis holds that there is a correlation. There is a 95% confidence interval for the significance level Alpha (α) value. If the p-value is more than 0.05,

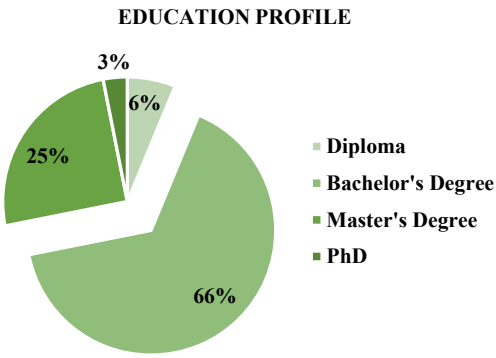

Fig. 1 Education profile—respondents

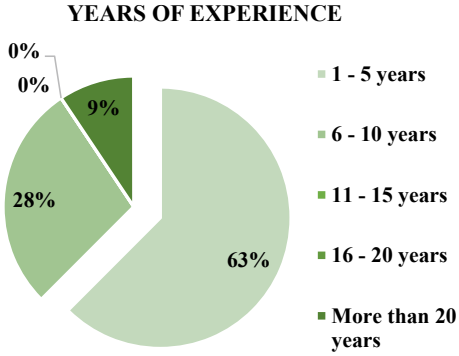

Fig. 2 Years of experience profile—respondents

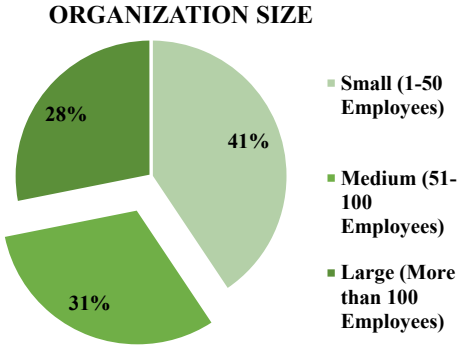

Fig. 3 Organization size profile—respondents

the null hypothesis is accepted, and if the p-value is less than 0.05, the alternative hypothesis is accepted.

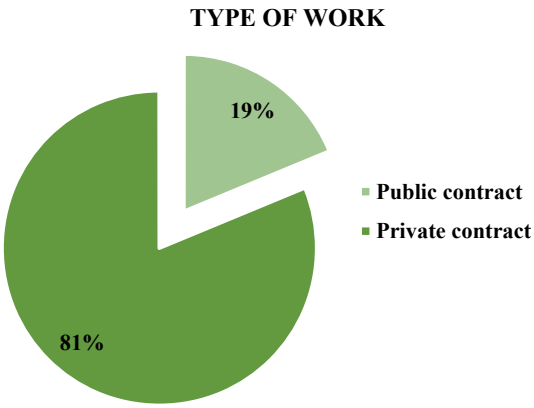

Fig. 4 Type of contract profile—respondents

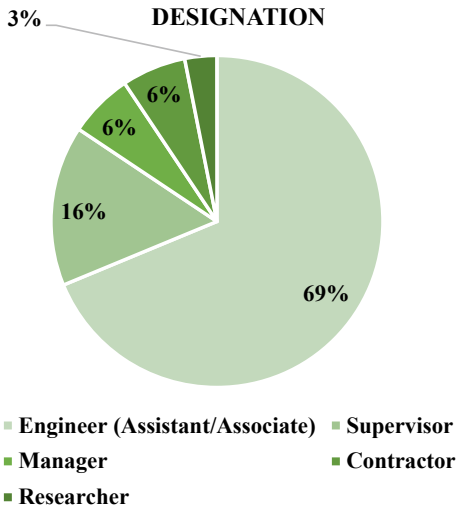

Fig. 5 Designation profile—respondents

3 Result and Discussion

3.1 Chi-Square Test

The Result from the Chi-square test as represented in Table 4 reveals that education qualification has an association with Concurrent Engineering, Pareto Analysis, Overall Equipment Efficiency, and Statistical Process Control. The Designation of the Respondents has an association with Pareto Analysis, Overall Equipment Efficiency, and Statistical Process Control. The type of work such as Private and Public do have an association with 5S. The size of the Respondent's Organization has no association

with any Lean Tool and the years of experience working in the construction industry have an association with muda walk and standardized work.

4 Conclusion

The study identifies the significant Lean Tools used in the Tamil Nadu construction industry from a list of 30 Lean Tools. The Lean Tools are ranked using the mean value from the observations. The association between the Respondent Profile and Lean Tools was explored using the Chi-square test.

- The ten significant Lean Tools used in the Tamil Nadu construction industry are 5S, PDCA (plan do check act), FMEA (Failure mode and effects analysis), JIT (Just-in-time), LPS (last planner system), total productive maintenance, Kanban, 5 whys, VSM (value stream mapping), and root cause analysis.
- The Chi-square test reveals that there is no association between the size of the organization and Lean Tools.
- The identified Lean Tools can be used in construction projects to improve the project characteristics.

Table 4 Pearson Chi-square test

Factors		Education qualification	Designation	Type of work	Size of organization	Years of experience
5S	Chi-square	5.629	9.198	8.369	4.526	2.121
	df	9	12	3	6	6
	Sig	0.776	0.686	0.039*	0.606	0.908
PDCA	Chi-square	4.775	11.458	5.357	5.007	5.590
	df	9	12	3	6	6
	Sig	0.853	0.490	0.147	0.543	0.471
JIT	Chi-square	7.407	18.901	1.003	9.469	2.326
	df	9	12	3	6	6
	Sig	0.595	0.091	0.801	0.149	0.887
Root cause analysis	Chi-square	5.657	12.703	2.872	2.569	6.080
	df	9	12	3	6	6
	Sig	0.774	0.391	0.412	0.861	0.414
FMEA	Chi-square	3.162	4.599	2.694	2.608	2.231
	df	6	8	2	4	4
	Sig	0.788	0.799	0.260	0.625	0.693
5 whys	Chi-square	6.193	14.982	2.826	5.017	2.530
	df	9	12	3	6	6
	Sig	0.720	0.242	0.419	0.542	0.865
LPS	Chi-square	4.038	11.098	3.035	4.895	2.725
	df	6	8	2	4	4
	Sig	0.672	0.196	0.219	0.298	0.605
Total productive maintenance	Chi-square	4.818	13.421	1.716	4.631	4.779
	df	9	12	3	6	6
	Sig	0.850	0.339	0.633	0.592	0.572
Kanban	Chi-square	3.253	15.635	0.690	3.693	3.011
	df	9	12	3	6	6
	Sig	0.953	0.209	0.875	0.718	0.807
VSM	Chi-square	8.245	14.024	1.941	3.982	12.301
	df	12	16	4	8	8
	Sig	0.766	0.597	0.747	0.859	0.138
Kaizen	Chi-square	10.540	15.010	6.369	6.262	3.907
	df	9	12	3	6	6
	Sig	0.309	0.241	0.095	0.394	0.689
Jidoka	Chi-square	8.390	8.190	4.181	4.884	9.128
	df	9	12	3	6	6
	Sig	0.495	0.770	0.243	0.559	0.167

(continued)

Table 4 (continued)

Factors		Education qualification	Designation	Type of work	Size of organization	Years of experience
Concurrent Engineering	Chi-square	21.640	19.572	3.647	7.930	4.931
	df	12	16	4	8	8
	Sig	0.042*	0.240	0.456	0.440	0.765
Bottleneck	Chi-square	9.916	10.749	4.060	7.239	14.222
	df	12	16	4	8	8
	Sig	0.623	0.825	0.398	0.511	0.076
Gemba	Chi-square	7.374	10.749	4.273	10.986	5.238
	df	9	12	3	6	6
	Sig	0.598	0.551	0.233	0.089	0.514
Visual management	Chi-square	9.424	15.386	5.692	3.852	9.370
	df	9	12	3	6	6
	Sig	0.399	0.221	0.128	0.697	0.154
Poka Yoke	Chi-square	8.564	13.472	0.847	8.209	5.924
	df	9	12	3	6	6
	Sig	0.478	0.336	0.838	0.223	0.432
Ishikawa diagram	Chi-square	19.844	15.103	3.556	5.417	12.753
	df	12	16	4	8	8
	Sig	0.070	0.517	0.469	0.712	0.121
Pareto Analysis	Chi-square	36.771	38.636	3.008	11.694	13.973
	df	12	16	4	8	8
	Sig	0.000*	0.001*	0.557	0.165	0.082
Take t time	Chi-square	7.851	8.128	6.619	5.344	5.179
	df	9	12	3	6	6
	Sig	0.549	0.775	0.085	0.501	0.521
Heijunka	Chi-square	8.065	8.869	2.785	3.807	7.636
	df	9	12	3	6	6
	Sig	0.528	0.714	0.426	0.703	0.266
A3 Problem solving	Chi-square	15.329	8.711	4.993	4.365	9.868
	df	9	12	3	6	6
	Sig	0.082	0.727	0.172	0.627	0.130
Andon	Chi-square	6.650	11.429	2.273	6.484	5.643
	df	9	12	3	6	6
	Sig	0.674	0.493	0.518	0.371	0.464
Muda walk	Chi-square	7.728	8.204	4.571	5.404	15.238
	df	9	12	3	6	6
	Sig	0.562	0.769	0.206	0.493	0.0188*

(continued)

Table 4 (continued)

Factors		Education qualification	Designation	Type of work	Size of organization	Years of experience
Six big losses	Chi-square	11.605	13.707	7.323	4.413	5.900
	df	9	12	3	6	6
	Sig	0.236	0.320	0.062	0.621	0.434
SMART goals	Chi-square	15.319	10.579	7.287	3.342	13.244
	df	9	12	3	6	6
	Sig	0.083	0.565	0.063	0.765	0.039*
Standardized work	Chi-square	10.236	8.764	2.355	2.043	7.962
	df	9	12	3	6	6
	Sig	0.332	0.723	0.502	0.916	0.241
Line balancing	Chi-square	9.284	11.893	4.321	8.970	9.841
	df	9	12	3	6	6
	Sig	0.412	0.454	0.229	0.175	0.132
Overall equipment effectiveness	Chi-square	42.771	39.648	5.883	12.314	8.951
	df	12	16	4	8	8
	Sig	0.000*	0.001*	0.208	0.138	0.346
Statistical process control	Chi-square	31.767	33.234	4.856	6.442	9.080
	df	12	16	4	8	8
	Sig	0.002*	0.007*	0.302	0.598	0.336

* The Chi-square statistic is significant at the 0.05 level

References

1. Bajjou MS, Chafi A, Ennadi A, EL Hammoumi M (2017) The practical relationships between lean construction tools and sustainable development: A literature review. J Eng Sci Technol Rev, Eastern macedonia and thrace institute of technology 10(4):170–177. https://doi.org/10.25103/jestr.104.20
2. Aravindh MD, Nakkeeran G, Krishnaraj L, Arivusudar N (2022) Evaluation and optimization of lean waste in construction industry. Asian J Civil Eng 2022 23:5 23(5):741–752. https://doi.org/10.1007/S42107-022-00453-9
3. Aravindh MD, Sriram NS, Nakkeeran G, Jayakeerti M, Velan C, Krishnaraj L (2023) Synergistic effect of alliance contract and lean methodology on project performance measures in the construction industry: SEM analysis. Technol Forecast Soc Change 192:122545. https://doi.org/10.1016/J.TECHFORE.2023.122545
4. Gapp R, Fisher R, Kobayashi K (2008) Implementing 5S within a Japanese context: an integrated management system. Manag Decis 46(4):565–579. https://doi.org/10.1108/00251740810865067/FULL/XML
5. Randhawa JS, Ahuja IS (2017) 5S—a quality improvement tool for sustainable performance: literature review and directions. Int J Qual Reliab Manage 34(3):334–361. https://doi.org/10.1108/IJQRM-03-2015-0045/FULL/XML
6. Fullerton RR, McWatters CS (2001) The production performance benefits from JIT implementation. J Oper Manag 19(1):81–96. https://doi.org/10.1016/S0272-6963(00)00051-6

7. Kong L, Li H, Luo H, Ding L, Zhang X (2018) Sustainable performance of just-in-time (JIT) management in time-dependent batch delivery scheduling of precast construction. J Clean Prod 193:684–701. https://doi.org/10.1016/J.JCLEPRO.2018.05.037
8. Pheng LS, Hui MS (2010) The application of JIT philosophy to construction: a case study in site layout. Constr Manage Econo 17(5):657–668. https://doi.org/10.1080/014461999371268
9. Jayswal A, Li X, Zanwar A, Lou HH, Huang Y (2011) A sustainability root cause analysis methodology and its application. Comput Chem Eng 35(12):2786–2798. https://doi.org/10.1016/J.COMPCHEMENG.2011.05.004
10. Doggett AM (2018) Root cause analysis: a framework for tool selection. Quality Manage J 12(4):34–45. https://doi.org/10.1080/10686967.2005.11919269
11. Realyvásquez-Vargas A, Arredondo-Soto KC, Carrillo-Gutiérrez T, Ravelo G (2018) Applying the plan-do-check-act (PDCA) cycle to reduce the defects in the manufacturing industry. A case study. Appl Sci 8(11):2181. https://doi.org/10.3390/APP8112181
12. Arabian-Hoseynabadi H, Oraee H, Tavner PJ (2010) Failure modes and effects analysis (FMEA) for wind turbines. Int J Electr Power Energy Syst 32(7):817–824. https://doi.org/10.1016/J.IJEPES.2010.01.019
13. Rhee SJ, Ishii K (2003) Using cost based FMEA to enhance reliability and serviceability. Adv Eng Inform 17(3–4):179–188. https://doi.org/10.1016/J.AEI.2004.07.002
14. Murugaiah U, Benjamin SJ, Marathamuthu MS, Muthaiyah S (2010) Scrap loss reduction using the 5-whys analysis. Int J Qual Reliab Manage 27(5):527–540. https://doi.org/10.1108/02656711011043517/FULL/XML
15. Myszewski JM (2013) On improvement story by 5 whys. TQM J 25(4):371–383. https://doi.org/10.1108/17542731311314863/FULL/XML
16. Lage Junior M, Godinho Filho M (2010) Variations of the kanban system: literature review and classification. Int J Prod Econ 125(1):13–21. https://doi.org/10.1016/J.IJPE.2010.01.009
17. AkturkMS, Erhun F (2010) An overview of design and operational issues of kanban systems. Int J Prod Res 37(17):3859–3881. https://doi.org/10.1080/002075499189808
18. Jain A, Bhatti R, Singh H (2014) Total productive maintenance (TPM) implementation practice: a literature review and directions. Int J Lean Six Sigma 5(3):293–323. https://doi.org/10.1108/IJLSS-06-2013-0032/FULL/XML
19. Gunduz M, Naser AF (2017) Cost based Value stream mapping as a sustainable construction tool for underground pipeline construction projects. Sustainability 9(12):2184. https://doi.org/10.3390/SU9122184
20. Cronbach LJ (1951) Coefficeint alpha and the internal struture of tests. Psychometrika 16(3):297–334. https://doi.org/10.1007/bf02310555
21. Taber KS (2018) The use of Cronbach's Alpha when developing and reporting research instruments in science education. Res Sci Educ 48(6):1273–1296. https://doi.org/10.1007/S11165-016-9602-2/TABLES/1
22. Ugoni A, Walker BF (1995) The chi Square test: an introduction. Comsig Rev 4(3):61. [Online]. Available: /pmc/articles/PMC2050386/?report=abstract. Accessed on 21 June 2022
23. Tallarida RJ, Murray RB (1987) Chi-square test. Manual Pharmacol Calculations 140–142. https://doi.org/10.1007/978-1-4612-4974-0_43
24. Mantel N (2012) Chi-square tests with one degree of freedom; extensions of the mantel-haenszel procedure. J Am Stat Assoc 58(303):690–700. https://doi.org/10.1080/01621459.1963.10500879

Analysis of Predisposition of Drivers to Cause Road Accidents in Guwahati Using a Neural Network

Surojit Das, Rakesh Sarma, and Rajashekar Hubballi

Abstract Need for the economic growth has resulted in the rapid development of road transportation facilities worldwide. This has resulted in the increase in the number of road accidents. These accidents are of global concern as they result in the loss of valuable lives of millions of people every year. These accidents also affect the economy of a country as they mainly affect the working class population. The number of road accidents are generally large in a developed city because of traffic congestion especially during morning and evening hours. Cities like Guwahati of North-eastern state Assam of India is witnessing large number of road accidents in the recent years. There are many factors contributing towards road accidents. These factors can be grouped in three categories as environmental characteristics, vehicular characteristics, and driver characteristics. In the present study, influences of these factors on the road traffic accidents are studied. The data related to driver characteristics are gathered through questionnaires survey, and the data related to environmental characteristics and vehicular characteristics are gathered through observations. The relationship between these factors and predisposition of drivers to cause road accidents is analysed through artificial neural network model. Sensitivity analysis is done to infer the extent of influence of each factor on the occurrence of an accident. From the analysis, it is observed that environmental characteristics have the highest influence on occurrence of an accident. This type of analysis can be used to take suitable measures to reduce the rate of accidents in Guwahati region.

Keywords Road traffic accident · Artificial neural network · Traffic safety · Driver characteristics · Vehicular characteristics · Environmental characteristics

S. Das · R. Sarma · R. Hubballi (✉)
Department of Civil Engineering, Central Institute of Technology, Kokrajhar, Assam, India
e-mail: rm.hubballi@cit.ac.in

S. Das
e-mail: u20cel2065@cit.ac.in

R. Sarma
e-mail: u20cel2072@cit.ac.in

K. R. Reddy et al. (eds.), *Recent Advances in Civil Engineering*, Lecture Notes in Civil Engineering 398, https://doi.org/10.1007/978-981-99-6229-7_53

1 Introduction

Many developing countries are facing road traffic accidents, and India is one of them. As per World Health Organization (WHO), road traffic accidents (RTAs) result in the death of around 1.3 million people every year. Under developed and developing nations account for 60% of world's vehicle but record 93% of world's road accident fatalities. Approximately, 3% of gross domestic product (GDP) is affected by RTAs in most of the countries [1]. The proper analysis of RTAs is very essential so that proper measures could be opt to reduce accidents. Such investigations are very rare in north-eastern states of India, and this has become one of the major motivations for this study. Researchers across the world have contributed in understanding the influence of several factors in occurrence of RTAs. Such as crash prediction model was prepared by using crash data obtained from police department for the Hyderabad region. The input parameters used for the model were road physical features, month of accident, and time of accident and characteristics of vehicles [2]. Analysis of the causes for road accidents was done for Kolkata region of West Bengal using crash data obtained by Kolkata traffic police. The relative importance of each independent variable in influencing the incident of accident is calculated [3]. Neural network model was used to study the influence of driver characteristics on RTAs for Peshawar region; but in this, the influence of environmental characteristics and vehicular characteristics were not considered. The relative importance of each factor on RTAs was not studied [4]. A case study on NH-544 was carried out to analyse the factors causing road fatalities and injuries using ANN but safety measures cannot be opt by analysing a single road network and model performance parameters were also not shown therefore the accuracy of models are not clear [5]. Influence of vehicular characteristics on RTAs was studied with three different algorithm for UK but other influencing factors were not studied which reduces the quality of the model [6]. Machine learning (ML) algorithm was used for determining the impact of meteorological parameters on RTAs and author has claimed that there are no significant limitations present in the developed models [7]. With the above-mentioned background, a methodology for analysing the impact of driver, vehicular, and environmental characteristics on RTAs is carried out using artificial neural network (ANN) for the Guwahati region of north-east India. The present study can help the traffic safety department of Guwahati to analyse the risk factors associated with RTAs to reduce the number of accidents in the city.

2 Indian RTAs Scenario

SaveLife Foundation has reported that in 2020 the road crash severity of India was 37.5 deaths per 100 crashes. In 2021, it was 38.6 deaths per 100 crashes which is higher than 2020. If the crash severity is high then the chances of road crash fatalities will be high [8]. It is found that the rate of accidents were higher in bad weather

conditions and working hours [9]. India accounts for approximately 11% of the total world road fatalities. Over the years there is steady increase in RTAs in India. RTAs resulted in the death of more than 1.5 lakh people in India in 2018 alone, and the count is increasing year after year. This is a staggering figure, and the volumes emphasis on the need for betterment of road safety in India [10].

3 Study Area

Guwahati is one of the major cities of north-east India. It is the central place for major economic activities in the Assam state. Because of large volume of traffic and less widen road, every inch of the road within the city is jam-packed with the vehicles for majority of duration of the day [11]. Indian National highways NH 31 and NH 37 connect the city with the rest of India. People from Bhutan, Bangladesh, and Nepal use these road networks to travel. All the cities of Assam are connected to these highways. These highways are also used for transporting the goods and supplies to Assam and other north eastern states of India [12].

4 Data Collection and Database Development

The data for the present study are collected through the questionnaire survey from the drivers of Guwahati city. A set of standard questions was prepared and posed to the drivers randomly and their response was noted. 1009 number of drivers were questioned face to face for the current study. The data pertaining to the following features were collected.

4.1 Driver Characteristics

The following driver characteristics has been taken for this study:

Vision. Clear vision enhances the driving performance. As vision deteriorates with age, it can be a reason for RTAs. Hence, a proper understanding of influence of vision on road accidents is essential. For this study, we have divided the vision problem into three categories: Myopia, Hyperopia, and Astigmatism.

Hearing Impairment. A driver with hearing impairment cannot take proper judgement for the vehicle in the traffic stream as sound from the other vehicles may not be clearly audible. A driver with the hearing loss greater than 100 decibels can hardly hear the traffic sound and can affect the traffic safety operations of motor vehicles [13].

Age. The age of the driver has direct influence on the RTAs. Majority numbers of drivers involved in RTAs are of younger age, the reason being lack of sufficient driving experience, and aggressive driving. The rate of RTAs decreases with the driver age beyond 60 [14]. Drivers of age 17–19 years are mostly involved in RTAs than drivers of age 20–25 years [15].

Gender. Many studies have concluded that female drivers are less involved in RTAs compared to male drivers [16]. The reason could be aggressive driving and lack of discipline during driving of the male drivers.

Driving Experience. More driving experience will give the improved understanding of the road and better control of the driving vehicle in the traffic stream. Hence, it will reduce the chances of RTAs. RTAs rate can be reduced from 15.90 to 3.13%, if the driving experience of drivers increases to 10 years or more [17]. With the driving experience, several driving skills such as processing of information, unwavering attention during driving, better control of vehicle in traffic stream and accurate knowledge of traffic rules will improve [19].

Education Level. A person with educational background can understand traffic rules and regulations much better than a person with no formal education. Hence, the chances of involvement of educated driver in RTAs are lower. For the survey, level of education is divided into four categories: Illiterate, Matric, Higher secondary, and Graduation.

Average KM Driven Per Day. The correlation between the frequency and magnitude of driving and the likelihood of being involved in an accident is well established. Prolonged driving can lead to decreased concentration, which increases the risk of accidents. Additionally, after extended periods of driving, drivers may become irritable and engage in dangerous behaviour such as speeding and neglecting to wear a seatbelt, further increasing their risk of an accident.

Break Time. Many drivers neglect to take breaks during their trips, leading to decreased concentration and an increased risk of accidents. This driver behaviour is one of the factors studied in the current research.

Driving School Trained or Not. Most drivers in the age group of 18–23 seem to have received training from a driving school. The training provided by driving experts results in a better understanding of driving control, traffic systems, and signals. Trained drivers are less likely to violate traffic rules, reducing the risk of road accidents.

Accused Alcoholic Status. The number of road accidents caused by alcohol has decreased significantly. Observations indicate that the impact of alcohol on road fatalities has stabilized. Drivers are taking more responsibility and refraining from excessive alcohol consumption, which is a positive trend for both traffic safety authorities and road users.

Use of Direction Indicator. Many serious road accidents occur due to the failure to use turn signals. Even experienced drivers sometimes neglect to use them, often due

to overconfidence. Such negligence can lead to serious accidents during overtaking, turning, and other scenarios.

4.2 Environmental Characteristics

Environmental characteristics play a significant role in RTAs. Driving in foggy weather is particularly challenging as it reduces visibility on the road, making it difficult for drivers to see other vehicles. In the present study, environmental characteristics are classified under four categories as: Rainy, Cold, Foggy, and Hot. The number of accidents is relatively low during the summer season. Accidents during hot weather are usually caused by tyre bursts, but this is a rare occurrence.

4.3 Vehicular Characteristics

The extensive study of the influence of vehicular characteristics on road crashes in the north-eastern part of India is limited. Type of vehicles plays a crucial role in road fatalities, with two-wheelers being the most commonly involved in fatal crashes compared to other types of vehicles. For the present study, vehicles are classified into four categories: light motor vehicles, heavy motor vehicles, heavy goods motor vehicles, and heavy transport vehicles.

5 Development of Artificial Neural Network Model

Artificial neural network mimics the working mechanism of human brain. It is a computational network which leverages the working mechanism of biological neural networks that forms the structure of the human brain. Just like the way human brain has neurons which are interconnected with each other, ANN also have neurons referred as nodes that are linked to each other in various layers of the networks. Equation (1) gives the general mathematical expression of an ANN [3].

$$A_N = \emptyset\left[b_o + \sum_{k=1}^{k=m} \{w_k \times \emptyset(b_k + \sum_{i=1}^{i=n} w_{ik} x_i)\} \right]. \tag{1}$$

Several models were tested using different optimizers and activation functions. Same model was tested with different number of neurons to obtain maximum accuracy. Dense layer was used as hidden layer. Only one hidden layer was used to avoid

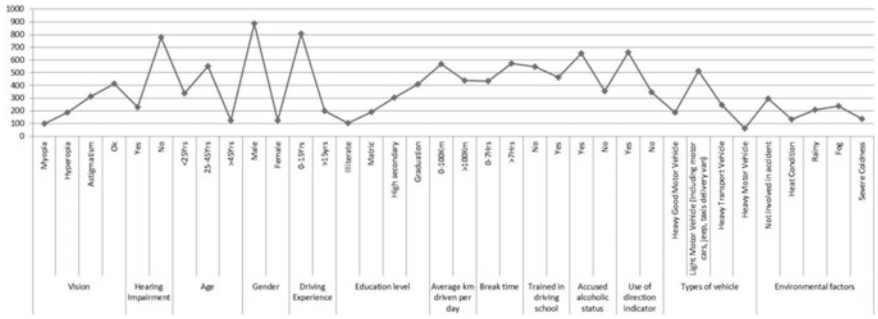

Fig. 1 Input variables used in ANN analysis

over fitting. Different types of optimizers used are Root Mean Square Propagation (RMSProp), Follow the Regularized Leader (FTRL), and Adaptive moment estimation (Adam). Activation functions (AF) used are TanH, Softmax, and ReLU.

6 Model Formulation

ANN model was formulated using keras NN toolkit in Python using the above-mentioned optimizers and activation functions. Firstly, the data shown in Fig. 1 were prepared in excel sheet, and the same was imported in Python using Google Colab. The inputs are the driver characteristics, vehicular characteristics, environmental characteristics, and the desired output will be the accident involvement. Total data set was divided into two parts. One part with 80% of data sets was used for training, and another part with remaining 20% of data sets was used for validation of ANN model (Fig. 2).

7 Model Performance

The performance of the ANN model depends on the activation function and optimizer adopted. Coding is done considering the input variables as shown in Fig. 1. Table 1 shows the performance of different ANN models in terms of accuracy. Based on Table 1, the following remarks can be made: optimizer FTRL with Softmax and ReLU as the activation function are the least accurate models with an accuracy of 70.79%. Adam optimizer gives the accuracy of 97.52, 96.53, and 98.01% with ReLU, TanH, and Softmax as activation functions, respectively. RMSProp gives the highest accuracy of 98.51% with Softmax as an activation function.

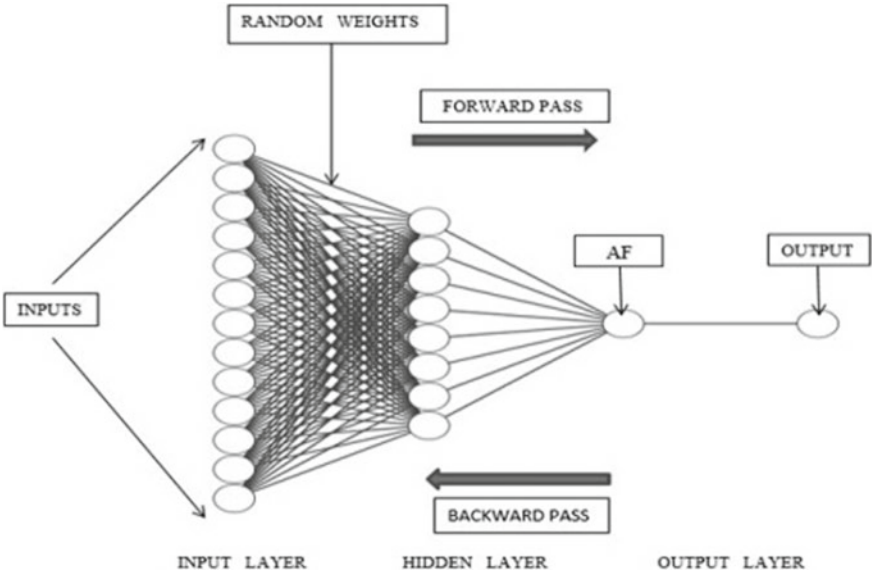

Fig. 2 Artificial neural network architecture

Table 1 Model performance parameters

AF	Optimizer	Loss function	Accuracy	Loss	MSE	RMSE	R^2
ReLU	RMSProp	Mean_ absolute_ error	0.9801	0.0783	0.0198	0.1407	0.9042
	Adam		0.9752	0.0739	0.0247	0.1573	0.8802
	FTRL		0.7079	0.2602	0.2920	0.5404	–0.4125
TanH	RMSProp		0.9603	0.1507	0.0396	0.1990	0.8084
	Adam		0.9653	0.0845	0.0346	0.1861	0.8324
	FTRL		0.9059	0.4660	0.0940	0.3066	0.5450
Softmax	RMSProp		0.9851	0.0287	0.0148	0.1218	0.9281
	Adam		0.9801	0.0375	0.0198	0.1407	0.9042
	FTRL		0.7079	0.4850	0.2920	0.5404	–0.4125

8 Sensitivity Analysis

Sensitivity analysis has been performed using Local Interpretable Model—Agnostic Explanation (LIME) as implemented by Ribeiro et al. [18]. LIME is compatible with all ML models [2]. Figure 3 shows the magnitude of influence of different factors on the occurrence of RTAs. As per the results of sensitivity analysis, environmental characteristics have the highest influence of 29.2% on the occurrence of RTAs followed

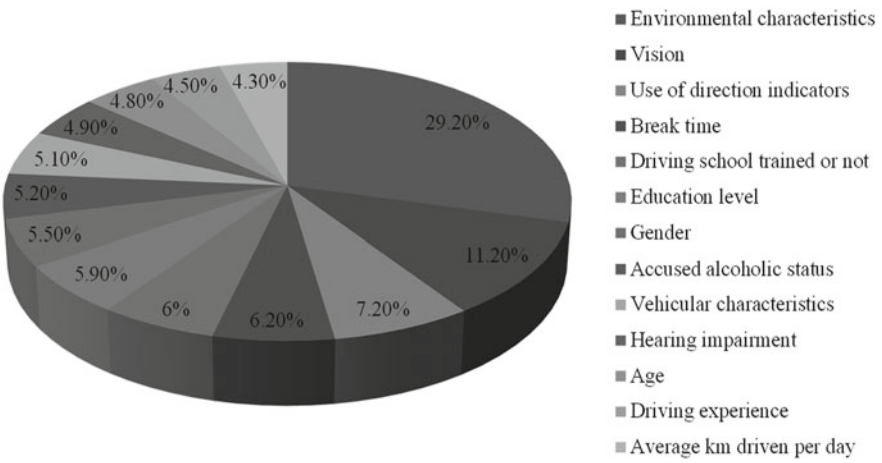

Fig. 3 Magnitude of influence of different factors on RTAs

by the vision of the driver which accounts for 11.2%. Average km driven per day has the least influence of 4.3%.

9 Conclusion

In the present study, crash prediction models were developed using ANN. ANN models were developed in Google Colab using Python programming language for predicting the influence of driver characteristics, environmental characteristics and vehicular characteristics on RTAs. LIME was used to perform sensitivity analysis to find the percentage of influence of each factor on RTAs. This can help the traffic safety department and local authorities to take proper safety measures to reduce the rate of RTAs.

References

1. World Health Organization (2023) https://www.who.int/news-room/fact-sheets/detail/road-traffic-injuries, Last accessed on 1 Feb 2023
2. Koramati S, Mukherjee A, Majumdar BB, Kar A (2023) Development of crash prediction model using artificial neural network (ANN): a case study of Hyderabad, India. J Inst Eng India Ser A 104(1):63–80
3. Chakraborty A, Mukherjee D, Mitra S (2019) Development of pedestrian crash prediction model for a developing country using artificial neural network. Int J Inj Contr Saf Promot 26(3):283–293

4. Ali A, Ud-Din S, Saad S, Ammad S, Rasheed K, Ahmad F (2021) Artificial neural network approach to study the effect of driver characteristics on road traffic accidents. In: 2021 international conference on data analytics for business and industry (ICDABI). pp 277–280, IEEE, Sakheer, Bahrain
5. Vishnuvardhan K, Muthukeerthana S, Muthuiswarya S, Ganesh VN, Rajkumar R (2023) Analysis of road traffic fatalities and injuries using artificial neural network: a case study on NH-544. AIP Conf Proc 2690(1)
6. Megnidio-Tchoukouegno M, Adedeji JA (2023) Machine learning for road traffic accident improvement and environmental resource management in the transportation sector. Sustainability 15(3):2014
7. Aleksić A, Ranđelović M, Ranđelović D (2023) Using machine learning in predicting the impact of meteorological parameters on traffic incidents. Mathematics 11(2):479
8. The Times of India (2023) https://timesofindia.indiatimes.com/india/why-indian-roads-are-deadly/articleshow/94022723.cms, Last accessed on 2 Feb 2023
9. Singh SK (2017) Road traffic accidents in India: issues and challenges. Transportation Research Procedia 25:4708–4719
10. Ministry of road transport and higways (2023) https://morth.nic.in/road-accident-in-india, Last accessed on 2 Feb 2023
11. Gplus (2023) https://www.guwahatiplus.com/guwahati/guwahati-traffic-becomes-nightmare-as-police-busy-chasing-violeters, Last accessed on 2 Feb 2023
12. Transport system in Guwahati (2023) https://www.guwahationline.in/city-guide/transport-in-guwahati, Last accessed on 2 Feb 2023
13. Picard M, Girard SA, Courteau M, Leroux T, Larocque R, Turcotte F, Lavoie M, Simard M (2008) Could driving safety be compromised by noise exposure at work and noise-induced hearing loss? Traffic Inj Prev 9(5):489–499
14. Kalyoncuoglu SF, Tigdemir M (2004) An alternative approach for modelling and simulation of traffic data: artificial neural networks. Simul Model Pract Theory 12(5):351–362
15. Clarke DD, Ward P, Bartle C, Truman W (2006) Young driver accidents in the UK: the influence of age, experience, and time of day. Accid Anal Prev 38(5):871–878
16. Al-Balbissi AH (2003) Role of gender in road accidents. Traffic Inj Prev 4(1):64–73
17. Moafian G, Aghabeigi MR, Hoseinzadeh A, Lankarani KB, Sarikhani Y, Heydari ST (2013) An epidemiologic survey of road traffic accidents in Iran: analysis of driver-related factors. Chinese Journal of Traumatology 16(3):140–144
18. Ribeiro MT, Singh S, Guestrin C (2016) Why should i trust you? Explaining the predictions of any classifier. In: Proceedings of the 22rd ACM SIGKDD international conference knowledge discovery data mining 137:1135–1144
19. Alfonsi R, Ammari A, Usami, DS (2018) Lack of driving experience, European Road Safety Decision Support System, developed by the H2020 project SafetyCube

An Integrated Management System Approach of QMS and OHSAS Risk Management in Oil and Gas Construction Project

A. R. Sivakumar and A. Arokiaprakash

Abstract Risk management in today's challenging environment requires more attention to provide value addition in terms of adoption of standards as per international organizations for standardization (ISO). This study evaluates various risk factors under QMS and OHSAS risk management with the help of questionnaire survey. Through qualitative and quantitative techniques, 53 risk identification factors were analysed and assessed, with recommended risk mitigation strategies. 105 responses were received and analysed for the risk index score (RI) by a risk matrix. Statistical analysis for data was done through frequency distribution, Cronbach's Alpha reliability analysis, regression analysis, and ANOVA. The results indicated a significant difference among working experience and job position of the responses with the risk factors. To achieve desired results, the organization must evaluate appropriate risk factors to successfully mitigate and manage risks in order to enhance profitability and productivity.

Keywords Risk management · Risk matrix · Risk index score · Quantitative analysis · Risk mitigation

1 Introduction

Risk assessment and analysis refer to the scientific process of identifying and managing/mitigating risks associated with EPC projects. In the customized approach, risk identification is the first process of recognizing potential hazards that could negatively affect the project outcomes [1, 2]. It helps the organization to determine and estimate the risks that could affect the process [3]. The organization then documents the characteristics of these risks and evaluates the relative significance of each [4]. Thereafter, severity analysis is conducted to determine the effect of the risks on the

A. R. Sivakumar · A. Arokiaprakash (✉)
Department of Civil Engineering, Faculty of Engineering and Technology, SRM Institute of Science and Technology, Kattankulathur, Tamil Nadu 603203, India
e-mail: arokipa@srmist.edu.in

K. R. Reddy et al. (eds.), *Recent Advances in Civil Engineering*, Lecture Notes in Civil Engineering 398, https://doi.org/10.1007/978-981-99-6229-7_54

project. Risk avoidance, risk acceptance, risk transference, and risk limitation are the four categories for managing these uncertain risks [5, 6]. With the help of the risk management process and framework, organizations can reduce the risk of incidents while increasing chances of success. By understanding the requirements of the quality management and OHSAS standards, they must explain how risks and opportunities are managed. During the risk assessment, the risks are classified, and their impact is evaluated [7–10]. Following that, mitigation measures and preventive with remedial techniques are adopted to reduce the risk level. Lastly, all stakeholders must cooperate with the management team for the effective implementation of the risk management system [11]. The customized risk management process helps in minimizing the possible risks by providing a systematical way to identify, evaluate, and mitigate them. As risks cannot completely be eliminated but through awareness and effective use of implements, organizations can successfully manage them and take informed decisions to lessen risks and losses from occurring [12, 13].

2 Objectives of Risk Management

The major objectives of this study is risk identification and data collection, identified risk factor measurement, analysis and assessment, and proposed risk mitigation strategy which affect the oil and gas construction projects are the primary goals of risk management process. The primary focus is on developing a comprehensive understanding of potential obstacles that may hinder the oil and gas construction processes. This involves evaluating the severity of each identified risk factor and assigning a significance level to effectively prioritize and address them. Investigating and determining the importance of the interaction between consistent risk management process by analysing the quantitative data evaluation in SPSS tools for risk analyses, evaluation and interpretation. Contemplating appropriate measures and applying suggested and recommended risk mitigation strategy in place as well as applying their knowledge to mitigate the impact of customized risk management process on construction projects by taking into account and addressing applicable QMS and OHSAS risk register. Figure 1 shows the integrated management systems: QMS, OHSAS, and RM Guidelines [14].

3 Methodology

This paper discusses the general methodology utilized to conduct the analysis, including how the questionnaire was constructed, sample selection, data collecting, and the analysis tools performed on the questionnaire data. The questionnaire involved descriptive questions about the possibility and impact of 53 risk identification indicators gathered from prior project risk registers and lesson learned registers using a qualitative and quantitative technique of assessing risk probability and impact.

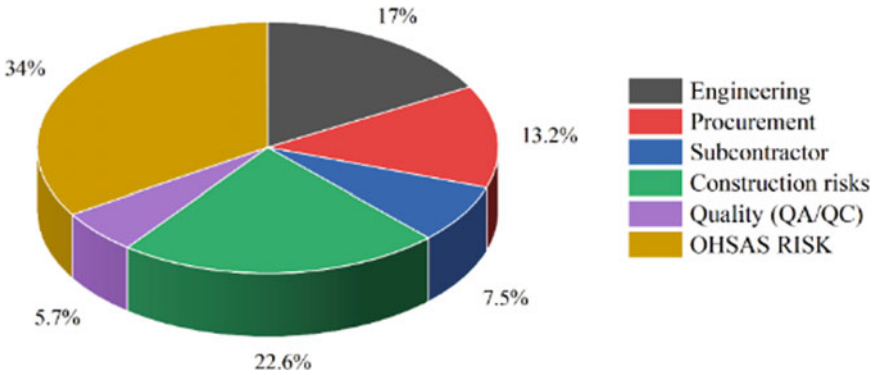

Fig. 1 Pie chart of QMS and OHSAS risks for oil and gas construction projects

The study depended on primary data collected from the various employees working under different oil and gas construction companies. The primary data was collected by sending google form link, in which the survey questionnaires were placed. The Statistical Package for Social Science version 24.0 (SPSS) was used for data analysis. Totally, Google Form link was sent to 300 members via email and via WhatsApp to the various employees working under different oil and gas construction companies. Finally, 105 response was received after screening and after eliminating the missing values. Thus, the study is further carried out with the 105 respondent's input.

4 Questionnaire Survey in Likert Scale

Among the topics covered in the survey are questions about respondents' demographics and risk factors under various fields. The distribution of risk factors with respect to the number of variables diagram is illustrated in Fig. 1. Table 1 shows the variables frame-QMS and OHSAS risks for oil and gas constructions. Sections of the final questionnaire include the following.

5 Results and Discussions

5.1 Risk Ranking and Risk Index

To apply the model, the opinion judgement scale needs to be converted into numerical scales. PMBOK (2021) suggested that the "extreme" takes a value of 0.9, and that "high", "moderate", and "low" take values of 0.7, 0.5, 0.3, respectively. A risk assessed by a respondent is called risk score and is calculated from the general model.

Table 1 Risk factors with description

Sl. No.	Risk code	Description of risks	
1	ER 1	Scope change	I Engineering
2	ER 2	Delay in document preparation/submission/approval cycles	
3	ER 3	Revision control and document mismatch	
4	ER 4	Unanticipated engineering and design changes during construction	
5	ER 5	As-built verification as per the client and project requirements	
6	ER 6	Design errors and poor engineering	
7	ER 7	Incomplete design	
8	ER 8	Technology changes	
9	ER 9	Complexity of design	
10	PR 1	Long lead item delivery at site	
11	PR 2	Price escalation	II Procurement:
12	PR 3	Clearance of material from port	
13	PR 4	Transit damage/loss of material during marine transport and road transport	
14	PR 5	Preservation and storage at vendor premises	
15	PR 6	Short ordered/supplied/received items	
16	PR 7	Unavailability or shortage of expected materials	
17	SCR 1	Delay in work order for subcontractors	
18	SCR 2	Awarding sub-contracts to in-competent/in-capable party contracts	III Subcontractor**:**
19	SCR 3	Unavailability of qualified subcontractors	
20	SCR 4	Delay in progress of subcontractors and poor response	
21	CR 1	Improper construction practices and workmanship leading to rework, repair and rejection	IV Construction risks
22	CR 2	Contractors' inability to complete the work package/ project	
23	CR 3	Changes in construction methods/techniques	
24	CR 4	Labour strikes	
25	CR 5	Drawing revision control and IDC	
26	CR 6	Conflicting interfaces of work items	
27	CR 7	Improper constructability	
28	CR 8	Site investigations were insufficient not in systematic way	
29	CR 9	Late construction site possession and progress	

(continued)

Table 1 (continued)

Sl. No.	Risk code	Description of risks	
30	CR 10	Ineffective control and management of change	
31	CR 11	Low labour productivity of local workforce	
32	CR 12	Equipment breakdown and downtime	
33	QR 1	Non-conformances/site observations issued by client	V Quality (QA/QC)
34	QR 2	Vendor supplied items rejection at project site	
35	QR 3	Project/corporate/client/TPI audit-based internal/ external non-conformances	
36	OHSAS 1	Epidemic and pandemic illness	VI Safety risk identification for construction projects
37	OHSAS 2	Elimination of work permits	
38	OHSAS 3	Construction-related near miss, mishaps, incidents and accidents	
39	OHSAS 4	Unsafe working conditions, unplanned precautions, or risky operations	
40	OHSAS 5	Damage to people, property, or materials as a result of the project's poor safety and health management	
41	OHSAS 6	Noncompliance with OHSAS standards	
42	OHSAS 7	Risk at working at height	
43	OHSAS 8	Worker safety laws or regulations have been changed	
44	OHSAS 9	Climbing on ladders	
45	OHSAS 10	Lifting operations	
46	OHSAS 11	Entry into excavations	
47	OHSAS 12	Failure to adhere housekeeping at project site	
48	OHSAS 13	Hydrogen Sulphide (H2S) prone areas	
49	OHSAS 14	Emergency evacuation	
50	OHSAS 15	Installation/replacement of electrical equipment's	
51	OHSAS 16	UV radiation and heat stroke at summer season	
52	OHSAS 17	Sand storm, dust, and illumination	
53	OHSAS 18	Ergonomic hazard	

Risk ranking was done based on the risk index score as given in Table 2. The 53 risk factors are used in order to easily interpret the risk ranking.

5.2 Reliability Testing

Cronbach's alpha is a test for the questionnaire's internal consistency. It can range from 0 to 1. The better the internal consistency of the items in the survey, the closer the alpha is to one. There is a total of 53 questions and 3 demographic factors in the survey. Using Cronbach's alpha test, we were able to determine how well the various risk factors are internally consistence. Using Cronbach's alpha, the maximum score was 0.963, obtained for construction risk (CR), all risk factors have the values more than 0.9 which shows a strong internal consistency except quality risk which has a moderate internal consistency with the alpha value of 0.869.

5.3 Multicollinearity

When more than one variable independently assesses the same item, we get multicollinearity. Each variable in Table 3 has a one-to-one association with every other variable, which is why their values are all listed as 1. The correlations between each item are computed to determine multicollinearity. That data set's "multicollinearity" issue is alleviated. All research elements are tested for multicollinearity. Table 4 represents the correlation between the variables, the results reveals that there exists a strong relationship among the variables correlation values are greater than 0.5.

5.3.1 Hypothesis Validation—Working Experience

The ANOVA results show the statistical values obtained between the working experience group and the risk factor. The p-values are less than 0.05 for all the variables which imply there is a discernible change and reject the null hypothesis risks factors. The p-values are more than 0.05 for all the variables which show that there is no discernible change among the selected parameter. The p-values are more than 0.05 the variables which imply that there is no discernible change among the selected parameter. Figure 2 explains the obtained results from the hypothesis 1.

5.3.2 Hypothesis Validation—Job Position

The ANOVA results show the statistical values obtained between the working experience group and the risk factor. The p-values are less than 0.05 for all the variables which imply there is a discernible change and reject the null hypothesis risks factors.

Table 2 Risk ranking and risk index

Risk code	Fr*Ir (low 0.3)	Fr*Ir (moderate 0.5)	Fr*Ir (high 0.7)	Fr*Ir (extreme 0.9)	Sum (Ri)	Ri/105	Risk ranking
ER1	2.7	10.5	35.7	21.6	70.5	0.671429	1
ER5	4.2	14	27.3	21.6	67.1	0.639048	2
OHSAS10	5.1	10.5	31.5	19.8	66.9	0.637143	3
OHSAS17	4.5	10	37.1	15.3	66.9	0.637143	4
PR3	5.1	10	33.6	18	66.7	0.635238	5
OHSAS1	6.9	9.5	23.1	27	66.5	0.633333	6
PR1	6	8	34.3	18	66.3	0.631429	7
OHSAS7	5.1	13	27.3	20.7	66.1	0.629524	8
PR2	4.5	11.5	36.4	13.5	65.9	0.627619	9
OHSAS16	4.5	12	35.7	13.5	65.7	0.625714	10
SCR4	4.8	14	28.7	18	65.5	0.62381	11
OHSAS5	7.2	7	32.9	18	65.1	0.62000	12
OHSAS11	4.8	14	30.8	15.3	64.9	0.618095	13
ER4	5.4	14.5	25.9	18.9	64.7	0.61619	14
ER2	5.1	12.5	33.6	13.5	64.7	0.61619	15
SCR1	5.7	12.5	30.1	16.2	64.5	0.614286	16
QR1	4.5	15.5	30.1	14.4	64.5	0.614286	17
CR1	5.7	14	28	16.2	63.9	0.608571	18
CR12	5.1	13	35	10.8	63.9	0.608571	19
PR7	5.1	14	32.2	12.6	63.9	0.608571	20
QR3	4.2	15	36.4	8.1	63.7	0.606667	21
CR11	5.7	14	29.4	14.4	63.5	0.604762	22
OHSAS6	5.7	14.5	28	15.3	63.5	0.604762	23
OHSAS13	9	8	23.1	23.4	63.5	0.604762	24
OHSAS14	5.7	15	26.6	16.2	63.5	0.604762	25
SCR3	6.6	10.5	33.6	12.6	63.3	0.602857	26
CR10	6	14.5	27.3	15.3	63.1	0.600952	27
OHSAS9	6.3	12	32.9	11.7	62.9	0.599048	28
OHSAS15	4.8	17	29.4	11.7	62.9	0.599048	29
PR6	5.1	16	30.8	10.8	62.7	0.597143	30
OHSAS4	6.6	11	34.3	10.8	62.7	0.597143	31
CR9	7.5	9.5	32.2	13.5	62.7	0.597143	32
ER6	7.5	12.5	24.5	18	62.5	0.595238	33
CR6	6.9	10	35.7	9.9	62.5	0.595238	34
OHSAS18	5.7	15	30.8	10.8	62.3	0.593333	35

(continued)

Table 2 (continued)

Risk code	Fr*Ir (low 0.3)	Fr*Ir (moderate 0.5)	Fr*Ir (high 0.7)	Fr*Ir (extreme 0.9)	Sum (Ri)	Ri/105	Risk ranking
OHSAS3	5.7	16	28.7	11.7	62.1	0.591429	36
CR5	6.3	15	28	12.6	61.9	0.589524	37
QR2	7.8	11.5	27.3	15.3	61.9	0.589524	38
SCR2	6.9	12.5	31.5	10.8	61.7	0.587619	39
ER9	6	17	25.9	12.6	61.5	0.585714	40
CR2	7.5	14.5	23.8	15.3	61.1	0.581905	41
CR8	6.9	14	29.4	10.8	61.1	0.581905	42
OHSAS12	5.7	17.5	28.7	9	60.9	0.58000	43
ER3	8.1	11	30.8	10.8	60.7	0.578095	44
PR4	8.1	10.5	32.2	9.9	60.7	0.578095	45
PR5	6	16.5	30.1	8.1	60.7	0.578095	46
ER8	7.2	15.5	25.9	11.7	60.3	0.574286	47
CR7	7.5	15	25.2	12.6	60.3	0.574286	48
CR3	8.1	12.5	29.4	9.9	59.9	0.570476	49
OHSAS2	9	11	28	11.7	59.7	0.568571	50
ER7	9	15	17.5	18	59.5	0.566667	51
OHSAS8	9.6	9.5	30.1	9.9	59.1	0.562857	52
CR4	10.8	13	22.4	9.9	56.1	0.534286	53

Table 3 Multicollinearity (correlations)

Correlations		ER	PR	SCR	CR	QR	OHSA
ER	Pearson correlation	1	0.845**	0.818**	0.865**	0.809**	0.804**
	Sig. (2-tailed)		0.000	0.000	0.010	0.000	0.000
PR	Pearson correlation	0.845**	1	0.861**	0.861**	0.863**	0.820**
	Sig. (2-tailed)	0.000		0.000	0.000	0.000	0.000
SCR	Pearson correlation	0.818**	0.861**	1	0.882**	0.880**	0.794**
	Sig. (2-tailed)	0.000	0.000		0.000	0.020	0.000
CR	Pearson correlation	0.865**	0.861**	0.882**	1	0.928**	0.832**
	Sig. (2-tailed)	0.010	0.000	0.000		0.000	0.000
QR	Pearson correlation	0.809**	0.863**	0.880**	0.928**	1	0.844**
	Sig. (2-tailed)	0.000	0.000	0.020	0.000		0.000
OHSA	Pearson correlation	0.804**	0.820**	0.794**	0.832**	0.844**	1
	Sig. (2-tailed)	0.000	0.000	0.000	0.000	0.000	

**. Correlation is significant at the 0.01 level (2-tailed)

Table 4 Model summary

Model	*R*	*R* square	Adjusted *R* square	Std. error of the estimate
1–ER1-ER9	0.602[a]	0.521	0.492	0.2388
1–PR1-PR7	0.866[a]	0.717	0.660	0.2297
1–SCR1-SCR4	0.544[a]	0.519	0.383	0.2400
1–CR1-CR12	0.841[a]	0.794	0.789	0.2392
1–QR1-QR3	0.402[a]	0.661	0.537	0.2329
1–OHSAS1-OHSAS18	0.714[a]	0.729	0.689	0.2257

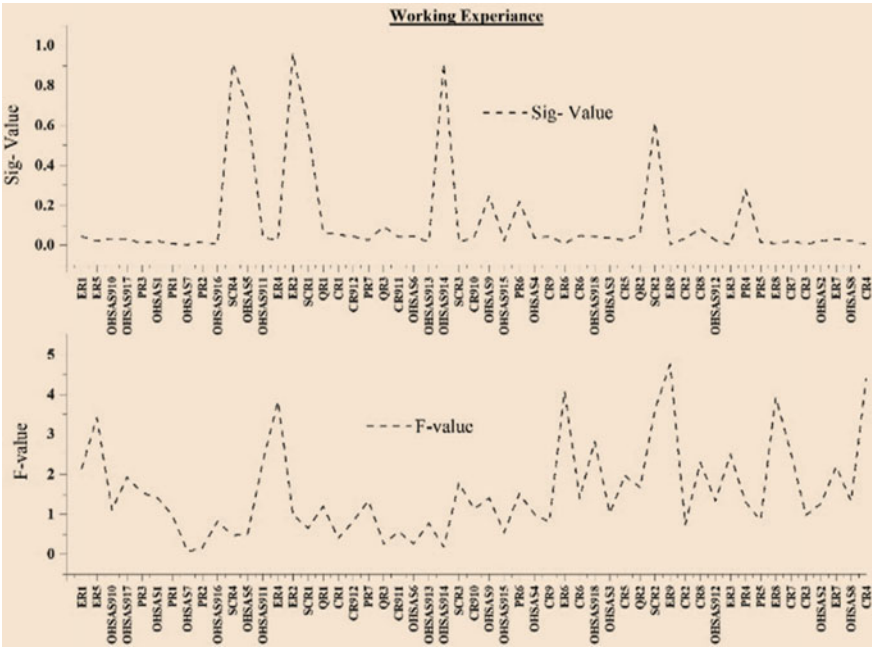

Fig. 2 Working experience ANOVA analysis results

The p-values are more than 0.05 for all the variables which show that there is no discernible change among the selected parameter. The p-values are more than 0.05 the variables which imply that there is no discernible change among the selected parameter. Figure 3 explains the obtained results from the hypothesis 2.

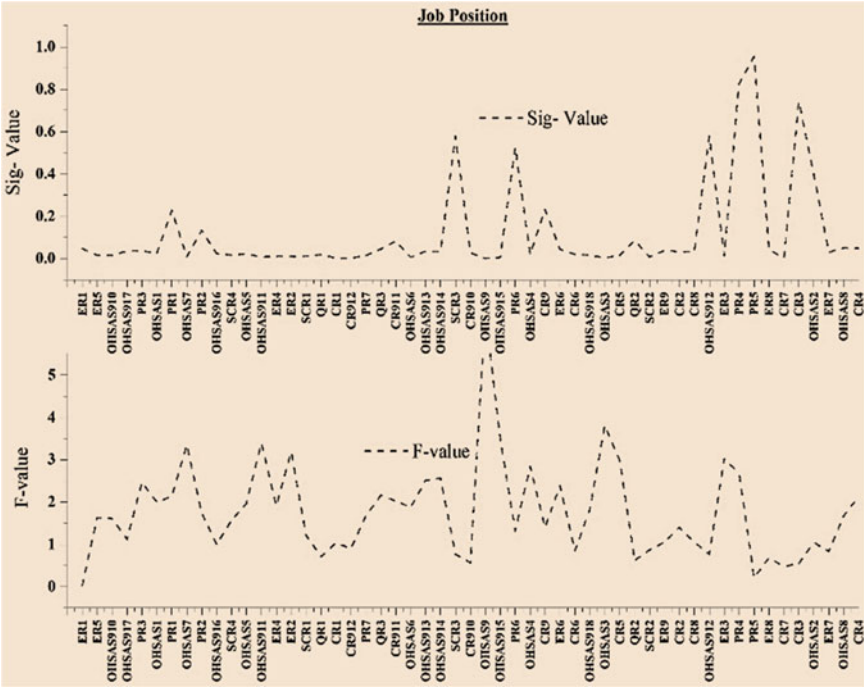

Fig. 3 Job position ANOVA analysis results

6 Linear Regression Analysis

In the linear regression analysis when the *R* score (Table 4) is reaching near to one is the most reliable and it increases the accuracy. ANNOVA (Table 5) is as a whole is highly discernible there is a substantial of "Impact of risk factors leads to delay in project completion" (Dependent Variables) by (Independent Variables).

7 Risk Register Model

The risk register model was created for all 53 risk factors, and top 5 risk factor's risk register was given in Table 6.

Table 5 ANOVA

Model		Sum of squares	df	Mean square	*F*	Sig.
Engineering risk factors	Regression	1.058	8	0.132	2.318	0.026[b]
	Residual	5.476	96	0.057		
	Total	6.533	104			
Procurement risk factors	Regression	1.416	7	0.202	3.835	0.001[b]
	Residual	5.117	97	0.053		
	Total	6.533	104			
Subcontractor risk factors	Regression	0.775	4	0.194	3.363	0.013[b]
	Residual	5.759	100	0.058		
	Total	6.533	104			
Construction risk factors	Regression	1.268	12	0.106	1.846	0.042[b]
	Residual	5.266	92	0.057		
	Total	6.533	104			
Quality risk factors	Regression	1.055	3	0.352	6.483	0.000[b]
	Residual	5.478	101	0.054		
	Total	6.533	104			
OHSAS risk factors	Regression	2.152	18	0.120	2.347	0.005[b]
	Residual	4.381	86	0.051		
	Total	6.533	104			

8 Conclusions

As an integrated management approach of QMS and OHSAS risk strategy, risk identification, risk analysis, risk assessment, and risk mitigation measures have been taken for the identified and shortlisted risks in terms of QMS and OHSAS-related risks. Applicable risks were identified, risk severity analysis was included, and the risk register was updated in order to mitigate the risk processes in a systematic manner. Totally, 53 risk factors were identified and ranked on the basis of risk index value. With the help of risk mitigation strategy, the risk register was generated for all risk factors in this study. Moreover, the hypothesis test was performed job position and work experience with respect to the risk factors. The findings of the study reveal the numerous risk variables that influence the construction of oil and gas projects. The risk register was contained the risk mitigation strategies for all risk factors. Furthermore, the study discovered that there is a substantial relationship between job position and work experience with risk variables.

Table 6 Risk register for top 5 risk factors

Sl. No.	Risk ID	Risk owner	Recommended risk mitigation strategy
1	ER1	PM and EM	(1) Capturing scope changes and securing end-client approvals on time (2) Using the scope matrix, identify the interface points, and acquire approval from the end customer
2	ER5	EM	(1) During the construction phase, design and engineering changes may be updated in the working design software on a regular basis in order to follow up on construction modifications via as-built drawing submission for future verification and project compliance
3	OHSAS10	CM, SE and SM	(1) A risk assessment for crane lifting activities must be performed, and the lifting area must be barricaded (2) Properly trained and competent workers must be available for lifting operations
4	OHSAS17	CM, SE and SM	(1) When feasible, control dust-raising components by enhancing natural vegetation. It helps with soil stability, sand dunes, and windbreak creation (2) Native plants and trees can be used as a buffer to minimize wind speed and sand drifts while boosting soil moisture
5	PR3	PCM and PDM	(1) Proper documentation must be kept for port clearance by the shipping information system (2) Material shipping navigation clearance assists in identifying the material with suitable care and timely delivery

References

1. Nabawy M, Khodeir L (2020) A systematic review of quantitative risk analysis in construction of mega projects. Ain Shams Eng J 11(4):1403–1410 (Elsevier)
2. Eskander PFA (2018) Risk assessment influencing factors for Arabian construction projects using analytic hierarchy process. Alexandria Eng J 57(4):4207–4218 (Elsevier)
3. Issa U, Mosaad S, Hassan MS (2020) Evaluation and selection of construction projects based on risk analysis. Structures 27:361–370 (Elsevier)
4. Siraj NB, Fayek AR (2019) Risk identification and common risks in construction: literature review and content analysis. J Constr Eng Manag 145(9):03119004. https://doi.org/10.1061/(ASCE)CO.1943-7862.0001685
5. Qazi A, Shamayleh A, EI-Sayegh S, Formaneck S (2021) Prioritizing risks in sustainable construction projects using a risk matrix-based Monte Carlo Simulation approach. Sustan Cities Soc 65:102576 (Elsevier)
6. Khalilzadeh M, Shakeri, S (2021) Risk identification and assessment with the fuzzy DEMATEL-ANP method in oil and gas projects under uncertainty. Procedia Comput Sci 181:277–284 (Elsevier)
7. Rakovic R (2021) Project of isms implementation in organization–aspects and practical experiences 11(1):20–30. https://doi.org/10.18485/epmj.2021.11.1.3
8. Rampini GHS, Berssaneti FT, Saut A, Henrique G, Rampini S, Saut AM (2019) Effect of ISO 9001, ISO 45001 and ISO 14000 toward financial performance of Indonesian manufacturing, researchgate.net vol 281, pp 209–221. https://doi.org/10.1007/978-3-030-14973-4_20

9. Vinnem JE (2010) Risk analysis and risk acceptance criteria in the planning processes of hazardous facilities—a case of an LNG plant in an urban area. Reliab Eng Syst Safety 95(6):662–670 (Elsevier)
10. Ramos D, Afonso P, Rodrigues MA (2020) Integrated management systems as a key facilitator of occupational health and safety risk management: a case study in a medium sized waste management firm. J Cleaner Prod 262:121346 (Elsevier)
11. Shammas-Toma M, Seymour D, Clark L (1998) Obstacles to implementing total quality management in the UK construction industry. Constr Manag Econ 16(2):177–192. https://doi.org/10.1080/014461998372475
12. Sayyed Y, Hatamleh MT, Alaya A (2021) Investigating the influence of procurement management in construction projects on the innovation level and the overall project performance in developing countries. Int J Constr Manag. https://doi.org/10.1080/15623599.2021.1889088
13. Kumar K, Narayanam R (2021) Review on construction risk and development of risk management procedural index–A case study from Chennai construction sector. Mater Today Proc 431141–1146 (Elsevier)
14. Rodney E, Ducq Y, Breysse D, Ledoux Y (2015) An integrated management approach of the project and project risks vol 48, pp 535–540 (Elsevier). https://doi.org/10.1016/j.ifacol.2015.06.136

Identification and Assessment of the Challenges Faced by the Construction Employees in Dubai

K. S. Anandh, D. Yuvaraj, Geever Alwin Ambaden, and K. Sri Chaitanya Reddy

Abstract The construction sector significantly contributes to the growth of the global economy by creating jobs and stimulating the economy. The industry provides jobs for many skilled and unskilled workers, including carpenters, electricians, engineers, and construction managers. While the construction industry in Dubai presents opportunities for employment and career growth, it also presents several challenges for construction employees. This study focuses on the major problems faced by the construction professionals in Dubai, like physical demands, health and safety concerns, stress and burnout, lack of job security, limited opportunities for career advancement, inadequate job training, low pay and benefits, superior-subordinate relationship, and language and cultural barriers. A quantitative analytical methodology was used for the study. The survey was conducted among 154 employees from various construction firms in Dubai using a structured questionnaire for this purpose. Descriptive statistics, independent samples t-tests, and one-way ANOVA were used to analyse the data. The results revealed that there exists a significant difference between the gender of the employees for the challenging factors except for physical demands, inadequate job training and superior-subordinate relationship. Addressing these challenges through proper regulations, improved working conditions, and fair compensation can lead to a more positive and sustainable work environment for construction employees in Dubai.

Keywords Challenges faced · Construction employees · Cultural barriers · Safety · Stress

K. S. Anandh (✉) · D. Yuvaraj · K. S. C. Reddy
Department of Civil Engineering, Faculty of Engineering and Technology, SRM Institute of Science and Technology, Kattankulathur, Tamil Nadu 603203, India
e-mail: anandhk@srmist.edu.in

G. A. Ambaden
Department of Civil Engineering, School of Engineering, Cochin University of Science and Technology, Eattappilly 686667, India

K. R. Reddy et al. (eds.), *Recent Advances in Civil Engineering*, Lecture Notes in Civil Engineering 398, https://doi.org/10.1007/978-981-99-6229-7_55

1 Introduction

The construction industry is a crucial component of the global economy, providing employment, infrastructure, and housing for billions of people worldwide. In recent years, the construction industry has experienced significant growth, driven by population growth, urbanization, and increasing investment in infrastructure. The construction industry depends more mainly on human resources than any other industry. According to a report by the International Labour Organization (ILO), more than 130 million people worldwide were employed in the construction sector in 2019 [1].

The construction sector in Dubai is expected to continue its growth trajectory, driven by the continued demand for infrastructure and real estate development, as well as the government's commitment to sustainability [2]. According to the Dubai Statistics Centre-Economic Survey 2021, nearly 600 thousand persons, including construction workers, engineers, architects, project managers, surveyors, and safety personnel, were employed in construction activities in Dubai in 2020 [3].

Construction employees play a critical role in building and shaping communities, but their work often comes with unique and challenging conditions. However, despite their essential role, construction employees often face various challenges in their daily work. From physically demanding labour [4] to hazardous working conditions [5] and limited job security [6], these challenges can have a significant impact on the health, safety, and well-being of construction employees. In Dubai, construction employees face challenges like working in hazardous conditions, lower wages, exploitation of migrant workers, and improper training leading to a lack of skilled labours. Understanding construction employees' challenges is crucial to support them in their work and ensure their safety and well-being. The previous studies focused only on a specific problem and lagged in collectively addressing the common problems. Therefore, this research aimed to identify the various challenges construction employees face.

Based on the literature study and interviews with the construction professionals, physical demands, health and safety concerns, stress and burnout, lack of job security, limited opportunities for career advancement, inadequate job training, low pay and benefits, superior-subordinate relationship, and language and cultural barriers were the significant challenges faced by the construction employees.

2 Literature Review

Construction work demands physical and ergonomic challenges [7], causing pain [8], and safety concerns [9]. Accidents occur due to inadequate OHS systems, despite significant investments in safety measures [10].

Project-based industries face pressures like unrealistic timeframes, budgets, and long working hours, causing stress and burnout in construction professionals [11]. Construction professionals face job security issues due to industry cyclicality, leading

to high turnover [12] and impacting employee health [13]. Limited career development also leads to high job mobility and increases the turnover of employees [14].

Highly skilled individuals are essential for an organization's success [15]; however, the lack of trained construction workers can affect productivity [16]. Construction workers' salaries and benefits are crucial for improving the company's productivity and the employees' livelihood [17].

The construction industry's superior-subordinate connection impacts individual performance [18], the productivity of the firm [19], and employee satisfaction, leading to absenteeism [20]. Construction workers also face language barriers, affecting communication between their superiors and co-workers [21].

Construction employees may face challenges influenced by regional and cultural considerations. For instance, foreign construction workers frequently encounter various cultural environments and struggle to connect with co-workers and adjust to the workplace in their new country [22].

3 Methodology

The first step in the research is identifying the major challenges construction employees face. This was achieved through a comprehensive literature study and interviews with construction professionals across Dubai. Professionals with more than 15 years of experience in the relevant field were considered for the interview process. The interview was done after selecting 12 professionals based on the above-mentioned criteria. A questionnaire survey was then administered to the construction employees to collect data on the challenges faced. There are two sections to the questionnaire. Part A consists of the demographic information of the respondent, including age, gender, marital status, designation, and work experience. The 74 items linked to the various challenges are found in Part B, and they were evaluated using a Likert scale with a 5-point scale from 1 to 5. A pilot study was carried out with 30 participants in Dubai to evaluate the questionnaire's reliability.

Further, 175 questionnaires were distributed randomly to construction employees in various construction firms in Dubai. 159 responses were received from the circulated questionnaire within the stipulated time. Due to missing data, five responses were rejected. Hence, 154 data were considered for the research work corresponding to a response rate of 88%. All respondents provided their written informed consent, and their confidentiality was upheld throughout the study. Table 1 displays the demographic profile of the respondents.

Table 1 Demographic profile

Demographic variable		Frequency	Percentage (%)
Gender	Male	117	76
	Female	37	24
Age (years)	18–29	48	31.2
	30–39	73	47.4
	40–49	24	15.6
	50 and above	9	5.8
Marital status	Married	94	61
	Unmarried	60	39
Educational qualification	Diploma	23	15
	Undergraduate	60	39
	Postgraduate	71	46
Current designation	Project manager	26	16.9
	Site engineer	77	50
	Design engineer	51	33.1
Total experience (years)	Less than 1	6	3.9
	1–5	89	57.8
	6–10	11	7.1
	More than 10	48	31.2

4 Data Analysis

The statistical package for social sciences (SPSS) software (version 23.0) was used to analyse the data that had been gathered. Cronbach's alpha test was used to evaluate the survey items' reliability based on the data gathered from the pilot study. Cronbach's alpha values for the study's challenging factors are given in Table 2. The table confirms that the factors' Cronbach's alpha values are higher than 0.7, which are acceptable.

4.1 Descriptive Statistics

Descriptive statistics summarize the features of the sample data with the help of frequency distribution, mean, median, mode, standard deviation, etc. The collected sample ($N = 154$) was analysed for descriptive statistics. From the analysis, it is identified that stress and burnout (Mean = 3.86) is the most challenging factor that a construction employee face in his/her work environment. It is then followed by low pay and benefits (Mean = 3.68) and lack of job security (Mean = 3.58). The least

Table 2 Reliability test

S. no	Factor	No. of items	Cronbach's alpha value
1	Physical demands	6	0.754
2	Health and safety concerns	9	0.842
3	Stress and burnout	9	0.898
4	Lack of job security	9	0.766
5	Limited opportunities for career advancement	8	0.754
6	Inadequate job training	9	0.811
7	Low pay and benefits	8	0.839
8	Superior-subordinate relationship	7	0.771
9	Language and cultural barrier	9	0.747

Table 3 Descriptive statistics ($N = 154$)

Variable	No. of items	Minimum	Maximum	Mean	Std. deviation
Physical demands	6	1.00	3.25	2.16	0.59
Health and safety concerns	9	2.40	4.40	3.51	0.55
Stress and burnout	9	1.60	4.80	3.86	0.67
Lack of job security	9	1.80	4.60	3.58	0.62
Limited opportunities for career advancement	8	1.40	3.80	3.14	0.45
Inadequate job training	9	2.20	3.65	3.25	0.53
Low pay and benefits	8	2.35	4.65	3.68	0.61
Superior-subordinate relationship	7	2.00	4.00	2.73	0.46
Language and cultural barrier	9	2.40	4.30	3.51	0.55

considered challenging factor is the physical demands, with a mean value of 2.16. The descriptive statistics for the data obtained are displayed in Table 3.

4.2 Inferential Analysis

Independent Sample t-test

Hypothesis-1

H0: There does not exist a significant difference between the employees' gender and the challenging factors faced by the construction employees.

H1: There exists a significant difference between the employees' gender and the challenging factors faced by the construction employees.

The findings of the independent sample t-test between gender and the challenging factors faced by construction workers are presented in Table 4.

At a 1% level of significance, the findings of the independent samples t-test show a significant difference between respondents' gender mean ratings of health and safety issues, stress, and burnout (P-value < 0.01). Whereas lack of limited opportunities for career advancement, job security, low pay and benefits, and language and cultural barrier were significant at 5%, i.e. P-value < 0.05. In the case of physical demands, inadequate job training and superior-subordinate relationship, the P-values were greater than the significance level of 5%, and hence, the null hypothesis was accepted for them.

Hypothesis-2

H0: There does not exist a significant difference between the employees' marital status and the challenging factors faced by the construction employees.

H1: There exists a significant difference between the employees' marital status and the challenging factors faced by the construction employees.

The findings of the independent sample t-test between marital status and the challenging factors faced by construction workers are presented in Table 5.

From Table 5, P-values concerning health safety and concerns, stress and burnout, lack of job security, and low pay and benefits were less than the significance level at 1%. Regarding limited opportunities for career advancement and language and cultural barriers, the P-values are less than 0.05, i.e. they are significant at 5% level. Hence, the null hypothesis is rejected for these factors. The null hypothesis is accepted

Table 4 Independent sample t-test between gender and challenging factors

Factors	Gender						t-value	P-value
	Male			Female				
	N	Mean	SD	*N*	Mean	SD		
Physical demands	117	2.75	0.45	37	2.70	0.50	0.548	0.585
Health and safety concerns	117	3.62	0.48	37	3.21	0.64	3.482	0.002**
Stress and burnout	117	3.78	0.63	37	2.87	0.44	3.907	0.000**
Lack of job security	117	3.75	0.43	37	3.44	0.51	3.489	0.020*
Limited opportunities for career advancement	117	3.54	0.72	37	4.13	0.46	2.407	0.018*
Inadequate job training	117	2.98	0.56	37	2.67	0.77	0.858	0.393
Low pay and benefits	117	3.56	0.54	37	3.14	0.66	3.031	0.030*
Superior-subordinate relationship	117	2.30	0.52	37	1.77	0.54	1.265	0.209
Language and cultural barrier	117	3.40	0.57	37	3.25	0.49	2.984	0.032*

*Level of significance = 5% and ** Level of significance = 1%

Table 5 Independent sample t-test between marital status and the challenging factors

Factors	Marital status						t-value	P-value
	Married			Unmarried				
	N	Mean	SD	*N*	Mean	SD		
Physical demands	94	3.18	0.95	60	2.80	1.64	−1.820	0.070
Health and safety concerns	94	3.44	0.48	60	3.15	0.75	− 2.928	0.003**
Stress and burnout	94	3.65	0.54	60	3.41	0.51	− 2.748	0.006**
Lack of job security	94	3.25	0.74	60	3.63	0.81	2.995	0.003**
Limited opportunities for career advancement	94	3.48	1.32	60	3.04	0.84	− 2.300	0.022*
Inadequate job training	94	3.11	0.56	60	3.27	0.63	1.646	0.101
Low pay and benefits	94	3.57	1.24	60	2.87	1.43	− 3.217	0.001**
Superior-subordinate relationship	94	2.97	0.48	60	3.01	0.46	0.512	0.609
Language and cultural barrier	94	3.10	0.59	60	3.35	0.77	2.273	0.024*

*Level of significance = 5% and ** Level of significance = 1%

for the factors, physical demands, inadequate job training, and superior-subordinate relationship as the P-values were greater than the significant level of 5%.

5 One-Way ANOVA

Hypothesis-3

H0: There does not exist a significant difference between employees' age groups and the challenging factors faced by the construction employees.

H1: There exists a significant difference between the employees' age groups and the challenging factors the construction employees face.

The findings of the one-way ANOVA between the age groups and the challenging factors are displayed in Table 6.

According to Table 6, the factors of low pay and benefits, lack of job security, stress and burnout, inadequate job training, health and safety concerns, and language and cultural barriers all have P-values that are less than the significant level at 5 and 1%, meaning that the null hypothesis can be rejected for each of these factors. Hence, a significant difference exists between the age groups and these factors. For the remaining factors, viz. physical demands, limited opportunities for career advancement, and superior-subordinate relationship, the null hypothesis is accepted as their P-values were greater than the significant level at 5%.

Table 6 One-way ANOVA between age groups and challenging factors

Factors	Age groups (years)								F-value	P-value
	18–29 ($n = 48$)		30–39 ($n = 73$)		40–49 ($n = 24$)		50 and above ($n = 9$)			
	Mean	SD	Mean	SD	Mean	SD	Mean	SD		
Physical demands	2.25	0.54	2.15	0.45	2.34	0.59	2.6	0.46	2.634	0.052
Health and safety concerns	3.26	0.63	3.55	0.41	3.38	0.79	3.1	0.81	3.371	0.020*
Stress and burnout	3.52	0.44	3.76	0.56	3.81	0.45	3.33	0.69	3.962	0.009**
Lack of job security	3.15	1.28	3.67	0.51	3.38	0.78	3.14	0.62	3.894	0.010**
Limited opportunities for career advancement	3.43	0.83	3.22	0.55	3.15	0.62	2.97	0.53	1.955	0.123
Inadequate job training	3.28	0.64	3.47	0.43	3.24	0.75	2.95	0.57	3.131	0.027*
Low pay and benefits	3.29	0.34	3.18	0.46	3.08	0.42	2.75	0.59	4.505	0.005**
Superior-subordinate relationship	2.93	0.58	3.15	0.50	3.18	0.49	3.08	0.68	1.949	0.124
Language and Cultural Barrier	3.33	0.64	3.12	0.56	2.96	0.52	3.01	0.47	2.671	0.050*

*Level of significance = 5% and ** Level of significance = 1%

Hypothesis-4

H0: There does not exist a significant difference between the educational qualification of the employees and the challenging factors faced by the construction employees.

H1: There exists a significant difference between the employees' educational qualification and the challenging factors the construction employees face.

The findings of the one-way ANOVA between educational qualification and the challenging factors are given in Table 7.

It is evident from Table 7 that the null hypothesis is accepted for the factors, physical demand and superior-subordinate relationship as their P-values were greater than 0.05. For the remaining factors, viz. health and safety concerns, stress and burnout, lack of job security, limited opportunities for career advancement, inadequate job training, low pay and benefits, and language and cultural barrier, the null hypothesis is rejected, and the alternate hypothesis is accepted as their P-values were lesser than the significant level of 5 and 1%.

Table 7 One-way ANOVA between educational qualification and the challenging factors

Factors	Educational qualification						F-value	P-value
	Diploma ($n = 23$)		Undergraduate ($n = 60$)		Postgraduate ($n = 71$)			
	Mean	SD	Mean	SD	Mean	SD		
Physical demands	3.40	0.58	3.44	0.65	3.28	0.35	1.615	0.202
Health and safety concerns	3.70	0.49	4.04	0.45	3.90	0.56	3.858	0.023*
Stress and burnout	3.80	0.23	3.60	0.58	3.35	0.55	7.579	0.001**
Lack of job security	2.96	0.54	3.65	0.89	3.51	1.03	4.750	0.010**
Limited opportunities for career advancement	3.33	0.41	3.10	0.29	3.25	0.53	3.104	0.048*
Inadequate job training	2.88	0.72	2.61	0.41	2.79	0.37	3.995	0.020*
Low pay and benefits	3.74	0.46	3.35	0.72	3.80	0.50	10.025	0.000**
Superior-subordinate relationship	2.87	0.78	2.99	0.83	2.64	1.01	2.455	0.089
Language and cultural barrier	1.87	0.38	2.20	0.54	2.16	0.59	3.213	0.043*

* Level of significance = 5% and ** Level of significance = 1%

6 Conclusion

Dubai's construction industry has seen significant growth and development over the years. However, this expansion has brought with it several challenges that have an impact on the well-being and job satisfaction of construction workers. These difficulties range from physical demands, health and safety concerns, and low wages to a lack of job security and inadequate opportunities for advancement. The government and construction companies must recognize and address these issues in order to ensure the health, safety, and satisfaction of the workers who contribute to the industry's growth and development. Implementing measures such as improving working conditions, providing fair wages, and providing opportunities for training and development can help mitigate the challenges construction employees face and enhance the industry's overall working environment. Self-report assessments and the study's limited sample size were the current study's limitations. Future research should include qualitative methods, stakeholder perspectives, and comparisons with other regions.

References

1. International Labour Organization (2023) Employment in the Construction Sector, https://www.ilo.org/global/topics/employment-in-the-construction-sector/lang--en/index.htm. Last accessed on 30 Jan 2023
2. Dubai Construction Sector (2023) A look into the Future. https://www2.deloitte.com/ae/en/pages/construction/articles/dubai-construction-sector-future.html. Accessed on 30 Jan 2023
3. Dubai Statistics Centre-Economic Survey 2021, https://dsc.gov.ae/Publications/Publications/Economic-Surveys/Economic-Survey-2021/Economic-Survey-2021.pdf. Last accessed on 30 Jan 2023
4. Abdelhamid TS, Everett JG (2002) Physiological demands during construction work. J Constr Eng Manag 128:427–437. https://doi.org/10.1061/(asce)0733-9364(2002)128:5(427)
5. Gupta RK (2021) A study on occupational health hazards among construction workers in India. Int J Enterp Netw Manag. 12:1. https://doi.org/10.1504/IJENM.2021.10039829
6. Sanyal S, Hisam MW, BaOmar ZA (2018) Loss of job security and its impact on employee performance—A study in sultanate of Oman. Int J Innov Res Growth 7. https://doi.org/10.26671/IJIRG.2018.6.7.101
7. Rodriguez FS, Spilski J, Hekele F, Beese NO, Lachmann T (2020) Physical and cognitive demands of work in building construction. Eng Constr Archit Manag 27:745–764. https://doi.org/10.1108/ECAM-04-2019-0211
8. Sundstrup E, Seeberg KGV, Bengtsen E, Andersen LL (2020) A systematic review of workplace interventions to rehabilitate musculoskeletal disorders among Employees with physical demanding work. J Occup Rehabil 30:588–612. https://doi.org/10.1007/s10926-020-09879-x
9. Lin J, Mills A (2001) Measuring the occupational health and safety performance of construction companies in Australia. Facilities 19:131–139. https://doi.org/10.1108/02632770110381676
10. Alhelo AA, Alzubaidi R, Rashid H (2023) A framework supporting health and safety practices in the United Arab Emirates' construction projects. Sustainability 15:1587. https://doi.org/10.3390/su15021587
11. Enshassi A, El-Rayyes Y, Alkilani S (2015) Job stress, job burnout and safety performance in the Palestinian construction industry. J Financ Manag Prop Constr 20:170–187. https://doi.org/10.1108/JFMPC-01-2015-0004
12. Shoss MK (2017) Job insecurity: an integrative Review and agenda for future research. J Manage 43:1911–1939. https://doi.org/10.1177/0149206317691574
13. Begum A, Shafaghi M, Adeel A (2022) Impact of job insecurity on work–life balance during COVID-19 in India. Vis J Bus Perspect 097226292110732. https://doi.org/10.1177/09722629211073278
14. Xie LL, Luo Z, Zhao X (2022) Critical factors of construction workers' career promotion: evidence from Guangzhou city. Eng Constr Archit Manag. https://doi.org/10.1108/ECAM-08-2021-0691
15. Tabassi AA, Ramli M, Hassan MAA, Bakar AHA (2011) Training and development of workforces in construction industry. Int J Acad Res 3:509–515
16. Sexton C, Zhang J (2022) Reducing harassment for women in the professional construction workplace with zero–tolerance and interventionist policies. In: Jazizadeh F, Shealy T, Garvin MJ (eds) Construction research congress 2022: health and safety, workforce, and education–selected papers from construction research congress 2022, Routledge, London, pp 376–385. https://doi.org/10.1080/01446193.2016.1277026
17. Poongavanam S, Viswanathan R (2017) Civil construction employees opinion on wage and benefits—A study. Int J Civ Eng Technol 8:1014–1019
18. Harish N, Anandh KS, Antony S (2019) Envisage on superior-subordinate in construction engineers pertaining to indian context. Int J Innov Technol Explor Eng 8:894–897
19. Anandh KS, Gunasekaran K, Sankar SS (2020) An envisage on emotional intelligence among superior-subordinate in construction sector of Chennai city, India. In: AIP conference proceedings, p 240012. https://doi.org/10.1063/5.0025223

20. Logo M, Hampton CT (2019) Supervisor-subordinate relationships and its effect on job satisfaction and job performance
21. Ne'Matullah KF, Pek LS, Roslan SA (2021) Investigating communicative barriers on construction industry productivity in Malaysia: an overview. Int J Eval Res Educ. 10:476. https://doi.org/10.11591/ijere.v10i2.21163
22. Kim S, Kim J-D, Shin Y, Kim G-H (2015) Cultural differences in motivation factors influencing the management of foreign laborers in the Korean construction industry. Int J Proj Manag 33:1534–1547. https://doi.org/10.1016/j.ijproman.2015.05.002

Artificial Neural Network and Multiple Linear Regression Approach for Optimization of Material Composition for Sustainable Super Capacitor

Kurupati Sireesha, Balasubramanian Murugesan, and P. T. Ravichandran

Abstract The proposed capacitor is made from natural materials like soil, river sand, and magnetite powder. The electrode is the capacitor's major component, acting like a conductor of electric storage. In this experimental investigation, sustainable materials are used as the substrates of electrodes to improvise and increase the efficiency of the capacitor. To optimize the ideal materials machine learning is brought into this study. Regression and ANN models are the most popular techniques for predicting values and identifying similarities that are used to optimize the ideal materials for manufacturing a sustainable capacitor. In preliminary tests, the soil capacitor device demonstrated the best electrochemical performance. Mix ratios were determined from the preliminary study conducted on the materials used as dielectrics and substrates in capacitors. These low-cost, high-performance capacitors' ideal combination was identified using the evolutionary algorithm. The optimization models were evaluated using matrix assessments such as MSE, and RMSE values. From the analysis, the optimization of materials, compositions, and performance were determined for the manufacturing of sustainable supercapacitors.

Keywords Electrode · Machine learning · Optimization · ANN · MLR · Material composition · Environment-friendly capacitor · Cost-effective capacitor · Sustainable super capacitor

1 Introduction

The use of nanoporous architectures in applications where the high specific area is essential, such as catalysis and energy storage devices, has become highly interesting [1]. Electrochemical supercapacitors have gained a lot of attention in the latter field as

K. Sireesha · B. Murugesan (✉) · P. T. Ravichandran
Department of Civil Engineering, Faculty of Engineering and Technology, SRM Institute of Science and Technology, Kattankulathur, Tamil Nadu 603203, India
e-mail: balasubm1@srmist.edu.in

K. R. Reddy et al. (eds.), *Recent Advances in Civil Engineering*, Lecture Notes in Civil Engineering 398, https://doi.org/10.1007/978-981-99-6229-7_56

a result of their higher power density, increased longevity, and capacity to withstand numerous charges and discharge cycles. Yet, these gadgets still don't have the same energy density as batteries. New electrode materials with the best characteristics must be developed to address this problem. Materials with the same physical and chemical properties are taken as an alternative for substrates for electrodes and dielectrics in capacitors which are flexible, low-cost, and sustainable [2, 3] in the environment. Supercapacitors are now one of the most intriguing technological developments. They have piqued the interest of scientists and engineers for since 2000 because of their quick charging and discharging capabilities, remarkable efficiency, high pulse power, and exceptionally extended cycle life. The combination of the following chemical and physical properties underlies the performance improvement of carbon-based electrode materials: moderately high surface area, high conductivity, high thermal stability, excellent corrosion resistance, and adequate compatibility with composite materials at a reasonable price and controlled pore size distribution [4].

However, a few experiments have found that increasing the micropore surface area reduces capacitance and power density. One of the issues could be that the micropores are inaccessible and testing whether the materials are having any electrical conductance values with some chemical solutions [5]. This exemplifies the difficulties encountered while researching the effect of pore size and quantity of the materials used for the overall performance of the EDLC. Optimizing the structural properties and mix ratio of electrode materials like soil, sand, and magnetite powder [6] increases the super capacitor performance and is an alternate way to boost specific capacitance. The optimization technique is done previously by many machine learning models for different parameters. The research study is now focused on the optimization of the mix ratio of materials for a better outcome and the development of the product [7]. Machine learning technique is used to run many models for predictions, optimization, simulation, and for accuracy. Another method based on artificial neural networks (ANN) is presently being developed. Furthermore, the ANN [8] can be applied to any linear or nonlinear system. The supercapacitor model uses a direct approach to linear regression for the best performance and optimization values of materials.

1.1 Literature Review

Using machine learning methods, Amit Gajurel et al. categorized whether a soil sample failed or passed specific threshold values based on the type and amount of treatment applied. Any studied classification model's "pass" prognosis can be utilized with greater assurance than "fail" prediction. Among all other classifiers, KNN has the most accurate prediction. Ladan Samadi et al., the soil was then classified using two machine learning classifiers: artificial neural network (ANN) and Nave Bayes. The testing data includes the remaining values of the other 34 data, which make up 70% of the remaining 70 data in the training data. Without using them in the design section, the remaining 30% of the data was also entered into

the modeling portion [9]. JanezTronteljml et al., in this study there is no uniform ML technique that can be utilized for several datasets and situations with the same accuracy. Nonetheless, the comparative analysis shows that least squares support vector machines and artificial neural network perform well on our research dataset [10]. MajedehGheytanzadeh et al., several physical characteristics, including specific surface area, derived pore size, intensity ratio of the *D* and *G* bands, applied potential window, and N-doping level were chosen as input parameters to investigate their influence on capacitances. The specific surface area of the supercapacitors has the biggest impact on the associated capacitance, according to sensitivity analysis, which was solely presented in this work. With an $R2$ value of 0.92, the suggested SVM-GWO outperformed all other developed ML models [11]. Yoichi Takagishi, et al., using the simulation results, regression models were developed utilizing ANN to predict the charge/discharge specific resistance from porous structural features [12]. Donal Finegan, et al., by combining data from various methodologies, AI has shown effective solutions for producing 3D multi-modal datasets. A literature survey of current improvements in lab-based characterization approaches for electrodes in this perspective was presented [13].

2 Experimental Section

Model-based and data-based approaches can both be used to forecast supercapacitor degradation. The model-based prediction describes the behavior and aging trend of the gadget using a conventional model depending on its mechanism [14]. In order to fill in the gaps and resolve the problems that previously existed, experimental investigations are being carried out to evaluate the impact of depth of discharge voltage on the lifecycle and charging-discharging currents of super capacitors. The experimental study focuses on the components of capacitors in order to lessen their impacts and improve their efficacy. The study is done to improvise the capacitors in the electronic industry with sustainability as a primary factor. Machine learning [15] is brought into the research for the prediction of performance analysis of materials and optimization Fig. 1. The linear regression model is taken for running the values.

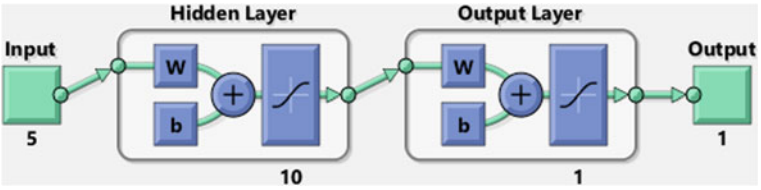

Fig. 1 Network diagram for prediction and performance evaluation

2.1 Parameters to Validate the Models

The ML models were developed using MATLAB software. The experimental values were used as input data, and manual literature extractions were also used to gather the data for the necessary parameters.

Mean Squared Error: Mean squared error is the commonly used evaluation metric which is the average squared difference between the actual value and the predicted value (as shown in Eq. (1)) [16].

$$\text{MSE} = (1/n) * \sum (yi - \hat{y}i)^2. \tag{1}$$

Mean absolute error (MAE): A metric to assess the degree to which predictions resemble actual values or outcomes. MAE $= 1\,n \sum ni = ||fi - yi|| = 1 \sum ni = 1||ei||$. Here, *fi* is the prediction value and *yi* stands for the actual results, and this is the average of the absolute errors (*ei*) for an overall MAE.

Root Mean Squared Error: The square root of the average of the squared difference between the actual and anticipated values (as stated in Eq. (2)) is a variation of the mean squared error (MSE) [17].

$$\text{RMSE} = \sqrt{(1/n * \sum (y - \hat{y}i))^2}. \tag{2}$$

Analysis and Evaluation by Machine learning models: Likewise, a super capacitor prototype performs by optimizing the binder (PVDF) content to 10%, the carbon-black content to 10%, and the remaining activated materials to 80%. This statistical approach allowed us to discover the best mix of the components with economized amounts of materials and time. [16–18]The primary goal of this study was to see if such a statistical and systematic technique could be used to identify the optimal proportion of supercapacitor component materials.

3 Performance Evaluation for Materials Used in Super Capacitor

3.1 Performance Evaluation for Soil

The linear regression model is taken for the validation, training, and performance analysis. Input parameters like current, voltage, temperature, no. of cycles, temperature, and capacitor retention are given, and the target is obtained as specific capacitance for soil (Fig. 2), magnetite powder (Fig. 5), and sand (Fig. 8). The correlation *r*

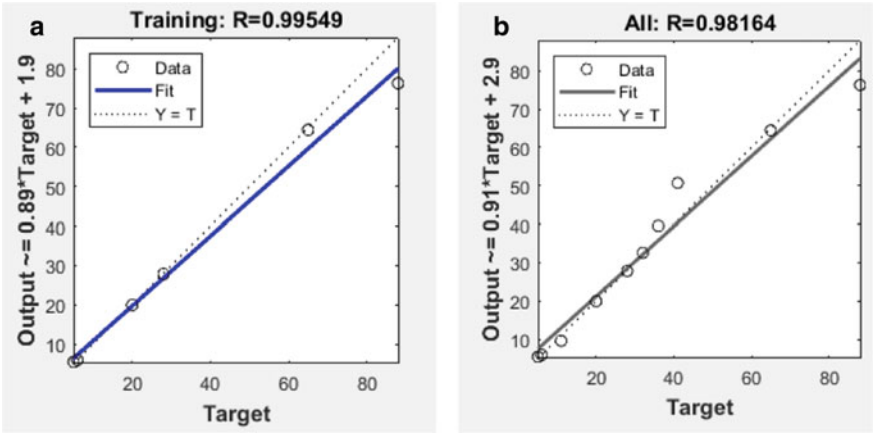

Fig.2 **a** Training model, **b** validation of values

in the linear regression model gauges the degree to which two quantitative variables are linearly related. From the inputs given in the model, the training value took the 5 most abundant values and R-value reached the maximum of 0.99.The validation is done through the model by taking inputs, training the model, and then obtaining the performance of the particular material and its efficiency which reached 0.98.

The graph Fig. 3 represents the best validation performance value by 12 hydrations or cycles, and for the 6th hydration, it gave the best performance value. Blue line shows training, green line shows validation, red line shows testing and imaginary lines represent the best coincident line. Through this performance analysis, we obtain a Mean Square Root (MSE) value of 2.88 for soil [19].

3.2 Performance Evaluation for Magnetite Powder

In this evaluation, the data division is done by random method, training of the model is done by Levenberg–Marquardt, and the performance is done by Mean Square Error (MSE). The training value obtained from the model is $R = 0.97$, and the validation value obtained is 0.99.

In Fig. 6, graph indicates that blue line shows training, green line shows validation, red line shows testing, and imaginary lines represent the best coincident line. Through this performance analysis, we obtain a Mean Square Root (MSE) value of 2.8 [9]. The best validation performance value was done for eight hydrations or cycles and for the 2nd hydration, it gave the best performance value. From the inputs provided for the model to run, we obtained an MSE value for magnetite material [20] as 2.68.

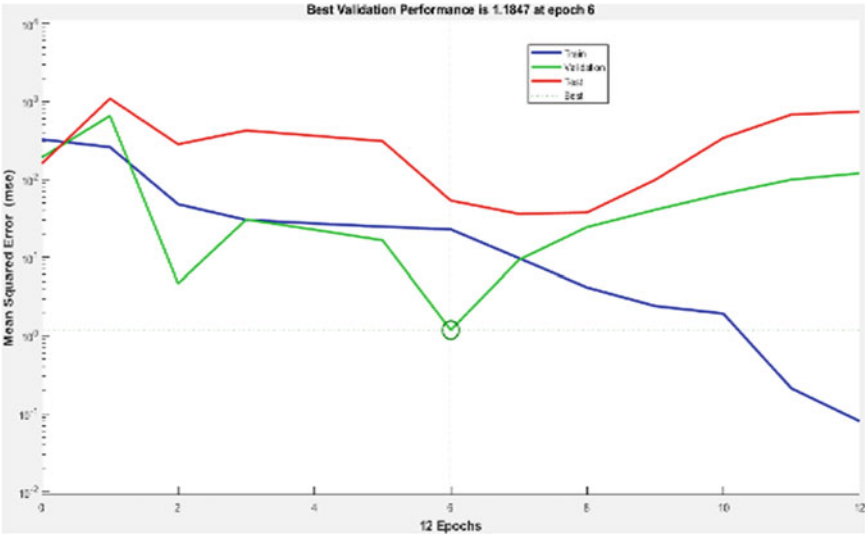

Fig.3 Best performance plot for soil

3.3 Performance Evaluation for Sand

Developing databases strategically is being examined. Lastly, there is experimental validation. This proof-of-concept work is anticipated to be helpful in assessing a novel material's (i) effectivity, (ii) practicability, and (iii) feasibility in a particular application. The research study is focused on the performance analysis and optimization of materials using regression analysis. The value while training the model is $R = 0.99$, and the validation data received is $R = 0.98$. Input parameters given for running the model are adequate to reach the target point.

By machine learning techniques, the linear regression model is taken into consideration, trained the models run, and validated it with the value obtained in the validation result. In this analysis mentioned, Fig. 9, the best validation performance value was done for 7 cycles, and for the 1st cycle or hydration, it gave the best performance value. MSE value obtained for sand as 1.90.

In this way, the performance and optimization are done for the three materials for better efficiency of the capacitor. Predictions are done for the capacitor by machine learning techniques to improve their life cycle and enhance their working of super capacitors in the electronic industry. The aging of super capacitors plays a crucial role in this environment. A path to super capacitors is being developed in these energy storage devices to increase the growth of the economy.

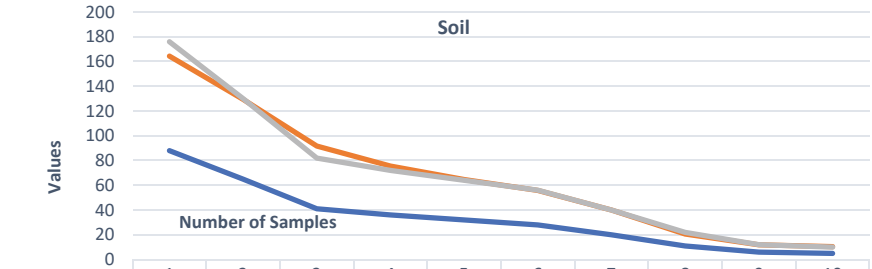

	1	2	3	4	5	6	7	8	9	10
Error	11.68863	0.561007	-9.71	-3.57197	-0.61095	0.160657	0.065299	1.412844	0.081259	-0.40313
Predicted	76.31137	64.43899	50.71	39.57197	32.61095	27.83934	19.9347	9.587156	5.918741	5.403127
Actual	88	65	41	36	32	28	20	11	6	5

Fig.4 Graphical representation for prediction analysis of soil material

4 Conclusion

An experimental validation of the material performance prediction is presented in this paper. ML models based on literature data are used to estimate specific capacitance and cyclic stability. MATLAB software uses the linear regression method to forecast the performance and optimization values of materials used in capacitors as super capacitors and dielectric substrates. The final prediction value is depending on the results of both the value and grade predictor models. MSE values obtained through this analysis are 2.88 for soil, 2.68 for magnetite [21], and 1.90 for sand. From this, we determine RMSE values for each material as given and mentioned above in this study. RMSE value for soil is 4.03, magnetite powder is 11.21, and 9.86 for sand. Among all materials, magnetite powder [22] is showing a higher performance index compared to soil and sand. But all three materials are reaching the validation value of giving the best performance value. So, all three materials are considered as high efficiency and optimum materials used as substrates of electrodes and dielectrics in capacitors in this electronics sustainable industry [23]. Figures 4, 7, and 10 represent the graphical representation for prediction analysis of soil, magnetite, and sand material, respectively. This study gave a conclusion for the sustainable and best-validating performance materials which are introduced in this experimental research study furthermore research can be carried out for the better outcome of other dielectric materials which are flexible, cost-effective, and eco-friendly [24] to this environment.

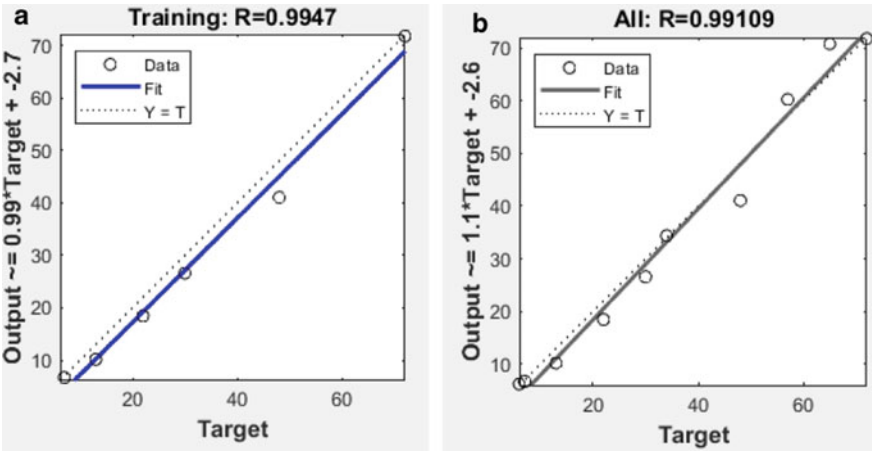

Fig. 5 **a** Training model, **b** validation graph

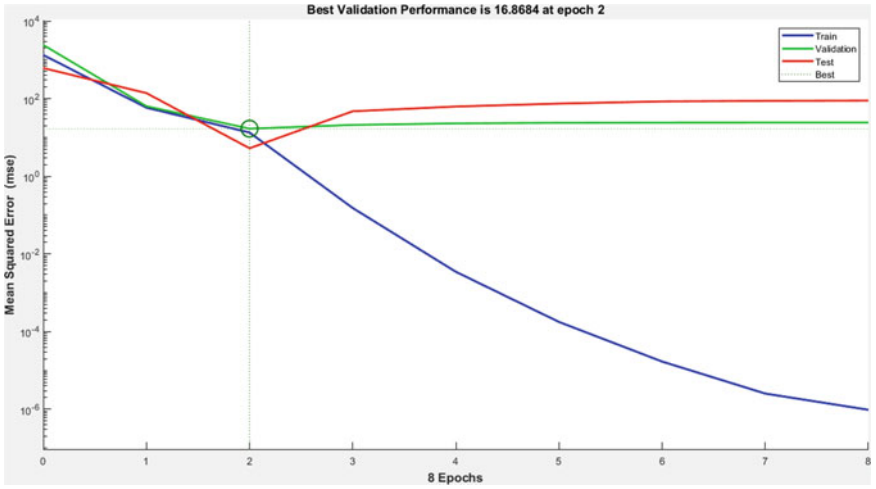

Fig. 6 Performance plot for magnetite material

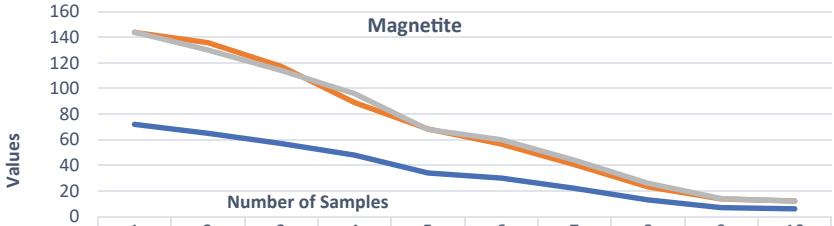

	1	2	3	4	5	6	7	8	9	10
Error	0.22124	-5.8042	-3.2272	6.9555	-0.3835	3.4115	3.5342	2.8129	0.27388	-0.22004
Predicted	71.7788	70.8042	60.2272	41.0445	34.3835	26.5885	18.4658	10.1871	6.7261	6.22
Actual	72	65	57	48	34	30	22	13	7	6

Fig. 7 Graphical representation for prediction analysis of magnetite material

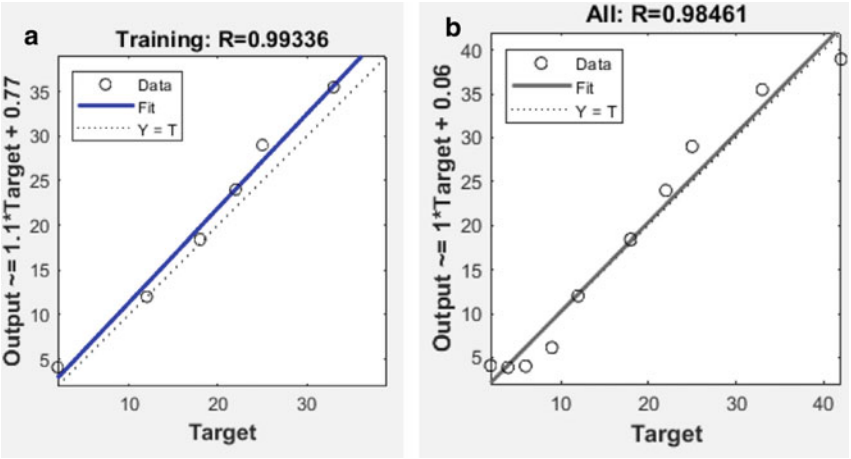

Fig. 8 **a** Training model, **b** validation model

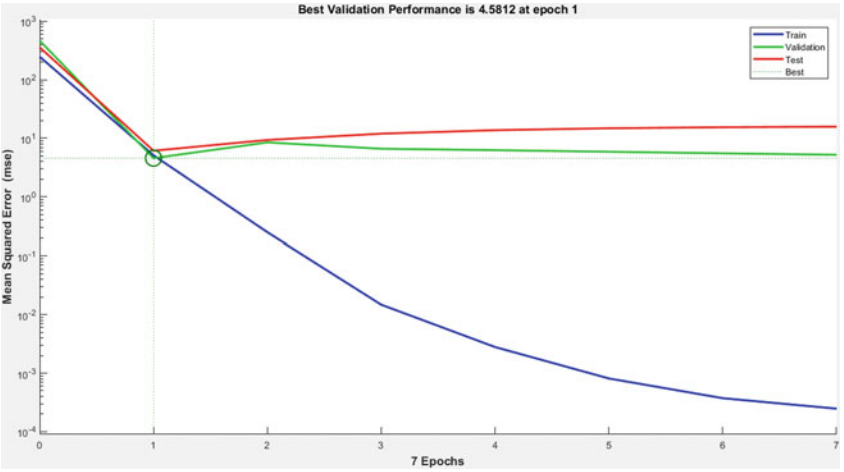

Fig. 9 Performance plot for sand materials

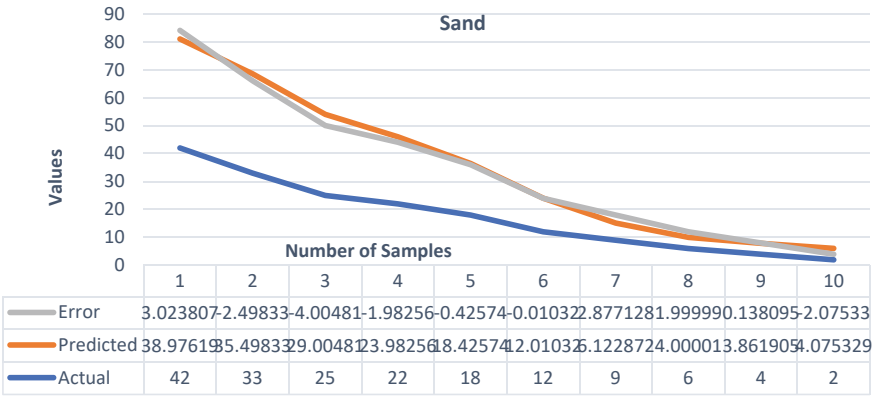

Fig. 10 Graphical representation for prediction analysis of sand material

References

1. Abbas Q (2019) Understanding the UV-vis spectroscopy for nanoparticles. J Nanomaterials Mol Nanotechnol 8:3. https://doi.org/10.4172/2324-8777.1000268
2. Kumar MSG, Balasubramanian M, Arul Jeya Kumar A (2020) Application of FGC blocks for sustainable infrastructure development. In: IOP conference series: materials science and engineering, IOP Publishing Ltd. https://doi.org/10.1088/1757-899X/912/6/062057
3. Raju SDK, Balasubramanian M, Kumar AAJ (2020) Experimental studies on replacement of steel stirrups by sisal fiber reinforced polymers. In: IOP conference series: materials science and engineering, IOP Publishing Ltd. https://doi.org/10.1088/1757-899X/912/6/062058
4. Reddy RA, Balasubramanian M, Selvam G (20202) Analysis of the effect of chromosome and generation count on genetic algorithm in construction projects: a case study. In: IOP conference

series: materials science and engineering, IOP Publishing Ltd. https://doi.org/10.1088/1757-899X/912/6/062056
5. Kim B, Koncar V, Devaux E (2004) Electrical properties of conductive polymers: pet-nano composites's fibres. http://www.autexrj.org/No1-2004/0081.pdf
6. Lennard JE, Jones I (1924) On the electrical conductivity of magnetite. Proc Royal Soc London. Series A. Containing pap math physical charact 105(731):334–345. https://doi.org/10.1098/rspa.1924.0023
7. Burke A, Miller M (2010) Testing of electrochemical capacitors: capacitance, resistance, energy density, and power capability. Electrochimica Acta. 7538–7548. https://doi.org/10.1016/j.electacta.2010.04.074
8. Marie-Françoise J-N, Gualous H, Berthon A (2004) Super capacitor modeling with artificial neural network (ANN)
9. Samadi H, Samadi L (2022) Soil classification modelling using machine learning methods. Database 9:11. https://www.researchgate.net/publication/359056095
10. TronteljMl J, Chambers O (2021) Machine learning strategy for soil nutrients prediction using spectroscopic method. Sensors 21(12). https://doi.org/10.3390/s21124208
11. Gheytanzadeh M, Baghban A, Habibzadeh S, Mohaddespour A, Abida O (2021) Insights into the estimation of capacitance for carbon-based supercapacitors. RSC Adv 11(10):5479–5486. https://doi.org/10.1039/d0ra09837j
12. Takagishi Y, Yamanaka T, Yamaue T (2019) Machine learning approaches for designing mesoscale structure of li-ion battery electrodes. Batteries 5(3). https://doi.org/10.3390/batteries5030054
13. Finegan DP, Squires I, Dahari A, Kench S, Jungjohann KL, Cooper SJ (2022) Machine-learning-driven advanced characterization of battery electrodes. ACS Energy Lett 7(12):4368–4378. https://doi.org/10.1021/acsenergylett.2c01996
14. Lee SD, Lee HS, Kim JY, Jeong J, Kahng YH (2017) A systematic optimization for graphene-based supercapacitors. Mater Res Express 4(8). https://doi.org/10.1088/2053-1591/aa8187
15. Gao T, Lu W (2021) iScience machine learning toward advanced energy storage devices and systems. https://doi.org/10.1016/j.isci
16. Ghosh S, Rao GR, Thomas T (2021) Machine learning-based prediction of supercapacitor performance for a novel electrode material: Cerium oxynitride. Energy Storage Mater 40:426–438. https://doi.org/10.1016/j.ensm.2021.05.024
17. Saad AG, Emad-Eldeen A, Tawfik WZ, El-Deen AG (2022) Data-driven machine learning approach for predicting the capacitance of graphene-based supercapacitor electrodes. J Energy Storage 55. https://doi.org/10.1016/j.est.2022.105411
18. Fromille S, Phillips J (2014) Super dielectric materials. Materials 7(12):8197–8212. https://doi.org/10.3390/ma7128197
19. Flogeac K et al (2005) Characterization of soil particles by X-ray diffraction (XRD), X-ray photoelectron spectroscopy (XPS), electron paramagnetic resonance (EPR) and transmission electron microscopy (TEM). Agron Sustain Dev 25(3):345–353. https://doi.org/10.1051/agro:2005037
20. Zaitsev VS, Filimonov DS, Presnyakov IA, Gambino RJ, Chu B (1999) Physical and chemical properties of magnetite and magnetite-polymer nanoparticles and their colloidal dispersions. http://www.idealibrary.com
21. Weidenfeller B, Höfer M, Schilling F (2020) Thermal and electrical properties of magnetite filled polymers. Compos Part A Appl Sci Manuf 33(8):1041–1053. www.elsevier.com/locate/compositesa
22. Fahlepy MR, Tiwow VA, Subaer (2018) Characterization of magnetite (Fe_3O_4) minerals from natural iron sand of Bonto Kanang Village Takalar for ink powder (toner) application. J Phys Conf Series, Institute of Physics Publishing. https://doi.org/10.1088/1742-6596/997/1/012036

23. Pershaanaa M, Bashir S, Ramesh S, Ramesh K (2022) Every bite of supercap: a brief review on construction and enhancement of supercapacitor. J Energy Storage 50. Elsevier Ltd. https://doi.org/10.1016/j.est.2022.104599
24. Vangari M, Pryor T, Jiang L (2013) Supercapacitors: review of materials and fabrication methods. J Energy Eng 139(2):72–79. https://doi.org/10.1061/(asce)ey.1943-7897.0000102

The Implementation of Integrated Mobility Planning: Navigating Challenges by Using Interpretive Structural Modeling (ISM) Approach

Rinkal Kishor Nakrani, Abishek Rauniyar, Peketi Sai Sasidhar Reddy, and B. Indhu

Abstract The implementation of integrated mobility planning in cities is a complex and crucial task, requiring the coordination of various stakeholders and the alignment of policies to ensure sustainable transportation solutions. The use of interpretive structural modeling (ISM) has been identified as a valuable tool in navigating these challenges. This study aimed to explore the potential of the ISM approach in the implementation of integrated mobility planning. Through a comprehensive literature review and case studies, the findings indicate that the ISM approach can be effectively utilized to identify and prioritize key issues, stakeholders, and strategies in the implementation process. By breaking down the problem into its constituent parts, the ISM approach provides a systemic understanding of the challenges faced in integrated mobility planning and facilitates the alignment of stakeholders and policies. The results of this study provide valuable insights for policymakers, urban planners, and transportation experts in their efforts to create comprehensive and sustainable mobility solutions for cities. The ISM approach has the potential to be a game-changer in the development of integrated mobility plans that are both efficient and effective, ensuring a better quality of life for urban residents.

Keywords Integrated mobility planning · Challenges · Interpretive structural modeling

1 Introduction

In today's rapidly changing world, cities are facing complex mobility challenges that require innovative and integrated solutions. The implementation of integrated mobility planning is gaining significance as a means of addressing these challenges

R. K. Nakrani · A. Rauniyar (✉) · P. S. S. Reddy · B. Indhu
Department of Civil Engineering, Faculty of Engineering and Technology, SRM Institute of Science and Technology, Kattankulathur, Tamil Nadu 603203, India
e-mail: rn6751@srmist.edu.in

K. R. Reddy et al. (eds.), *Recent Advances in Civil Engineering*, Lecture Notes in Civil Engineering 398, https://doi.org/10.1007/978-981-99-6229-7_57

and creating a more sustainable, equitable, and efficient transportation system [1]. This approach considers all modes of transportation, from traditional cars to public transit and active modes like biking and walking, and considers factors such as land use, economic development, and environmental impact [2]. However, the process of implementing integrated mobility planning is not without its difficulties, and navigating these challenges requires a combination of collaboration, creativity, and political will [3]. This study aims to provide insights and guidance on the journey toward successful implementation, exploring the successes and setbacks of real-life case studies and offering practical recommendations for overcoming obstacles along the way [4]. Integrated mobility planning (IMP) is a concept that encompasses the integration of various modes of transportation, including public transit, cycling, and walking, to create a sustainable and efficient transportation system [5]. This approach is critical in addressing the challenges faced by modern cities, such as congestion, air pollution, and increased energy consumption [6]. Despite its benefits, the implementation of IMP is a complex process that requires a significant amount of coordination and collaboration between multiple stakeholders, including government agencies, transportation providers, and the public. To address this challenge, the use of interpretive structural modeling (ISM) has emerged as a promising tool for integrated mobility planning [7].

ISM is a multi-disciplinary approach that can help to identify the relationships between the different components of a transportation system, as well as the interdependencies between them [4]. There are many roles to ISM. Among them are the process is systematic; the computer considers all possible pair-wise relationships in system elements, either directly or through transitive inference, by using transitive inference, you may be able to reduce the number of the required relational queries by 50–80% depending on the context, participants do not need to be cognizant of the underlying process; they only need to possess sufficient knowledge of the object system to be able to answer the various queries generated by the computer. A comprehensive and efficient method for guiding and recording the outcome of group deliberations on complex issues is provided. As a result, the original problem situation is better modeled or graphically represented so that it can be communicated more effectively. A focus on one specific question at a time allows participants to enhance interdisciplinary and interpersonal communication during the problem-solving process, the focus of the exercise is to enable participants to evaluate the suitability of a proposed system element or issue statement for illuminating a specific situation using issue statements and system elements. By forcing participants to examine and comprehend the significance and meaning of a particular list of elements, it serves as a learning tool. Participants can identify policy areas offering advantages or leverage for pursuing specified objectives using this tool, which provides action or policy analysis. And it can also help to identify the most critical issues that need to be addressed to achieve the desired level of integration. Furthermore, ISM can provide a framework for the development of strategies that can effectively address these issues and facilitate the implementation of IMP [8]. This research paper aims to provide a comprehensive examination of the challenges associated with the implementation of IMP and the use of ISM as a tool to navigate these

challenges [9]. The paper will begin by reviewing the background of IMP and its benefits, as well as the various challenges that are associated with its implementation [10].

2 Research Methods

Research objectives were achieved by following a three-step design (see Fig. 1). By conducting two rounds of systematic literature reviews, the implementation of integrated mobility planning for road transportation: Navigating challenges was prepared as a preliminary identification of barriers. To identify barriers specifically affecting the integrated mobility planning sector, questionnaire survey among industrial practitioners was conducted. To analyze the interrelationships between the identified barriers, an ISM-based model was developed. This step involved obtaining expert opinions about such challenges through semi-structured interviews with construction professionals. A hierarchical and logical order of expert opinions was then created using ISM.

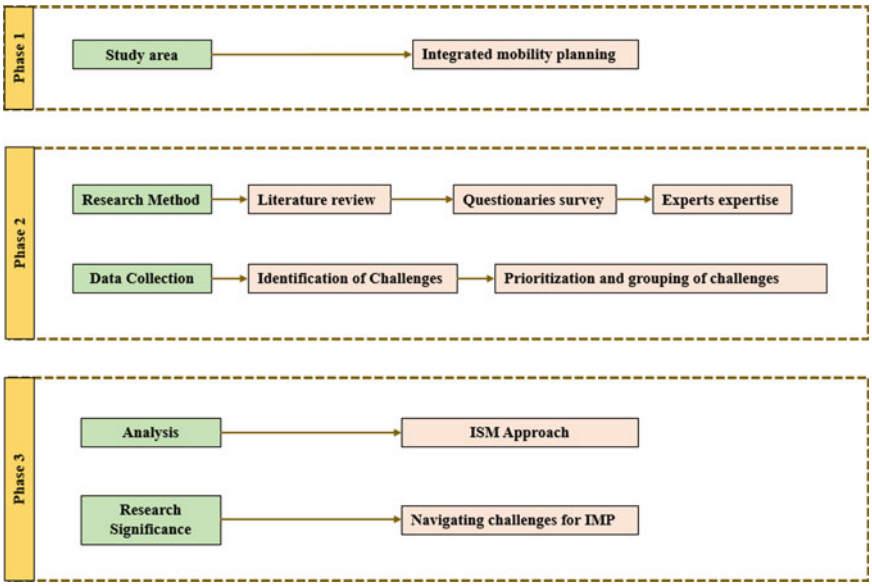

Fig. 1 Research methodology

2.1 Data Collection

Analyzing interrelationships among factors in complex systems can be done through techniques such as Analytical Network Process (ANP) and interpretive structural modeling (ISM). While ANP may not reveal all types of dependencies, ISM allows for insights into direct and indirect interrelationships with ranking and direction. ISM has been applied in construction management research to study productivity factors and design phase risks. In this study, ISM was used to map the interconnections of barriers to integrated mobility planning transportation in construction, following five essential steps of the ISM methodology shown in Fig. 1.

3 Preliminary Identification of Possible Challenges

Two phases were involved in this study's literature review. A Google Scholar search was conducted to identify relevant literature using keywords such as "challenges," "integrated mobility planning," and "implementation." A limited number of studies addressed the barriers to integrated mobility planning in road construction. An extensive literature review was conducted as a second step to determine all challenges associated with integrated mobility planning across all types of construction projects. ISM analysis search terms "challenges" and "integrated mobility planning" were used. To ensure a comprehensive search, the same keywords were utilized in both phases to gather relevant papers from both the ISI Web of Science and Scopus databases [20]. After the completion of the two-phase literature review, the authors screened each of the collected papers and recorded the key challenges identified b. Based on their frequency of occurrence and diversity of factors, a total of 14 challenges that could impact integrated mobility planning in the construction industry were identified and grouped into five main categories (as given in Table 2).

4 Results and Analysis

4.1 Defining the Correlation Framework

The study's authors conducted semi-structured interviews with experts to explore the interconnections among 15 challenges. It provides a means to integrate the diverse perceptions of participants in the interdisciplinary groups, is understandable by a variety of users, can handle many complex system components and relationships, can assess a model formulation's adequacy heuristically, and can provide insights into its behavior. Furthermore, ISM can be easily accessed by a wide variety of audiences and is easy to use. Consequently, ISM is widely used because of its features. They ensured that only professionals with robust expertise in integrated mobility

Table 1 Background information of interviewed experts

Expert expertise	Occupation	Employer	Education	Year of work experience	Years of experience in using integrated mobility planning
6	Researcher	Research institution	PhD	18	8
4	Engineer	Construction company	B-Tech	15	9
3	Manager	Construction company	M-Tech	13	7
4	Engineer	PWD	B-Tech	12	9
5	Architect	Design company	B-Tech	15	10

planning were included in the study by contacting fifteen eligible experts through LinkedIn and selecting five based on their professional profiles and services. Table 1 provides an overview of the selected experts. During the interviews, the experts were asked to comment on the relationship between each pair of challenges. The authors analyzed the responses and used the Structural Self-interaction Matrix (SSIM) to identify contextual interrelationships among the challenges. The authors employed four symbols to represent the interrelationship between challenges *i* and *j*, namely (1) *W* for "challenge *i* can result in challenge *j* but not vice versa," (2) *X* for "challenge *j* can lead to challenge *i* but not vice versa," (3) *Y* for "barriers *i* and *j* can lead to each other," and (4) *Z* for "challenge *i* and *j* are not related." The "minority gives way to the majority" principle was applied if different experts had divergent opinions on the relationship between two challenges.

The authors used the feedback from the interviewed experts to construct the contextual relationships among the fifteen challenges, as illustrated in Table 3. The table underscores the close interconnections among TB1, TB2, EB1, and RB3, which have frequent interactions with other challenges. Notably, the authors acknowledged that the interpretation of the collected answers was subjective, and therefore, subject to bias, as they utilized the SSIM to represent the interrelationships between the barriers. Nonetheless, the insights from the experts provided valuable information for the study, and their judgments offered valuable insights.

4.2 Reachability Matrix

The SSIM developed in the study was converted into a binary matrix and then analyzed using the substitution rule that was adopted for this research. This rule involves replacing the four symbols, V, A, X, and O, with 1 s and 0 s (Table 4). When

Table 2 Identification of possible challenges

Category	Challenges	Code	References
Organizational challenges (OB)	Lack of inter-departmental collaboration	OB1	[21–23]
	Resistance to change from stakeholders	OB2	[24, 25]
	Political will and support	OB3	[26–28]
Political challenges (PB)	Competition for funding with other public services and programs	PB1	[20, 29]
	Inadequate private investment in alternative transportation options	PB2	[6, 10]
	Limited public funding for transportation infrastructure and services	PB3	[28]
Technical challenges (TB)	Data availability and integration	TB1	[6, 9, 10]
	Insufficient public participation and engagement	TB2	[3, 7, 21]
	Inadequate public transportation infrastructure	TB3	[4, 22, 23]
Cultural challenges (CB)	Perception of individual car ownership as a symbol of status b	CB1	[1, 4, 21–24]
	Attitudinal resistance to alternative modes of transportation	CB2	[21, 22]
	Long-standing transportation habits and routines	CB3	[4, 23]
Regulatory challenges (RB)	Lack of comprehensive mobility planning guidelines and regulations	RB1	[5, 25]
	Inefficient land use planning policies	RB2	[4, 29]
	Limited enforcement of existing regulations	RB3	[23, 26, 27]

the correlation symbol is V, A, X, or O, the corresponding numbers are filled out in Table 5 to create a reachability matrix. The value in the reachability matrix (OB2, OB3) is zero if (OB2, OB3) in the SSIM is A and one if (PB2, PB3) is the case.

According to Table 2, the interrelationships between the 15 challenges are outlined in an initial reachability matrix. As given in Table 4, an analysis of power iterations was conducted to assess transitivity rules [20]. Transitivity is represented by entry a in Table 6. In the example above, (TB1, TB2) is 1a, meaning that there exists an indirect link between (RB1, RB2) which refers to insufficient dispute resolution mechanisms for integrated mobility planning.

Table 3 Structural Self-interaction Matrix (SSIM)

Variables	OB1	OB2	OB3	PB1	PB2	PB3	TB1	TB2	TB3	CB1	CB2	CB3	RB1	RB2	RB3
OB1		O	O	A	O	O	A	A	O	O	A	O	O	A	O
OB2			O	A	O	O	O	O	O	O	O	A	A	O	A
OB3				O	O	O	A	A	O	O	A	O	O	A	O
PB1					O	A	V	V	O	A	X	A	A	O	X
PB2						O	V	V	A	O	X	O	O	O	V
PB3							V	V	O	V	V	V	O	V	O
TB1								O	A	A	X	A	V	A	O
TB2									V	O	V	O	A	O	A
TB3										V	V	X	O	O	A
CB1											V	A	O	A	A
CB2												V	A	O	O
CB3													V	A	O
RB1														V	O
RB2															V

Table 4 Reachability matrix (RM)

Variables	OB1	OB2	OB3	PB1	PB2	PB3	TB1	TB2	TB3	CB1	CB2	CB3	RB1	RB2	RB3	Driving Power
OB1	1	0	0	0	0	0	0	0	0	0	0	0	0	0	0	1
OB2	0	1	0	0	0	0	0	0	0	0	0	0	0	0	0	1
OB3	0	0	1	0	0	0	0	0	0	0	0	0	0	0	0	1
PB1	1	1	0	1	0	0	1	1	0	0	1	0	0	0	1	7
PB2	0	0	0	0	1	0	1	1	0	0	1	0	0	0	1	5
PB3	0	0	0	1	0	1	1	1	0	1	1	1	0	1	0	8
TB1	1	0	1	0	0	0	1	0	0	0	1	0	1	0	0	5
TB2	1	0	1	0	0	0	0	1	1	0	1	0	0	0	0	5
TB3	0	0	0	0	1	0	1	0	1	1	1	1	0	0	0	6
CB1	0	0	0	1	0	0	1	0	0	1	1	0	0	0	0	4
CB2	1	0	1	1	1	0	1	0	0	0	1	1	0	0	0	7
CB3	0	1	0	1	0	0	1	0	1	1	0	1	1	0	0	7
RB1	0	1	0	1	0	0	0	1	0	0	1	0	1	1	0	6
RB2	1	0	1	0	0	0	1	0	0	1	0	1	0	1	1	7
RB3	0	1	0	1	0	0	0	1	1	1	0	0	0	0	1	6
Dependence pw	6	5	5	7	3	1	9	6	4	6	9	5	3	3	4	

Table 5 Substitution rule

SSIM	Reachability matrix	
(i, j)	(i, j)	(i, j)
V	1	0
A	0	1
X	1	1
O	0	0

4.3 Level Partitions

The final reachability matrix was utilized to determine the reachability and antecedent sets for each barrier, thereby creating level partitions. If any barriers are linked to the challenges, they would be included in the reachability set, while the antecedent set would contain additional challenges. All challenges are then examined based on the intersection of the reachability and antecedent sets, as depicted in Table 7. Using a hierarchical partitioning method (see Table 7), we identified a hierarchy of factors. In the final reachability matrix, antecedents and reachability are determined by casual factors, each with a value of 1. Similarly, factors of any type with a value of 1 in their column were included in the antecedent set. The levels of a different factor were determined by intersecting all factors. Reachability and intersection sets were the two common factors at the top of the ISM structure. Amounts I, II, and III are the levels at which casual factors barriers 1–15 fall. Any method will not be able to reach casual factors below the topmost factor. Iterations after the first will discard the factors at the top of the list. Determine the degree of casual factors by repeating the same steps. Challenges that have the same reachability set and intersection are likely to be impacted by other challenges, as they occupy the top level of the ISM hierarchy. Once the barrier at the top level is identified, the reachability set of other challenges is eliminated. This process is repeated to identify barriers at the subsequent level, and it continues until all barriers are accounted for Table 7 provides a breakdown of the level partitions.

4.4 Formation of ISM Diagraph and Model

In Table 7, the 15 challenges are shown in the chain of influence of challenges in the initial diagraph based on level partition results. This initial diagram illustrates how challenges are interrelated. A two-way arrow indicates a mutual influence between barrier i and challenges j. An arrow pointing from challenges i to challenges j indicates a possible result of barrier i. It includes both direct and indirect transitivity links between challenges; these relationships between barriers challenges are expressed by transitivity. By replacing the nodes with statements in Table 7, the diagraph was

Table 6 Final reachability matrix (FRM)

Variables	OB1	OB2	OB3	PB1	PB2	PB3	TB1	TB2	TB3	CB1	CB2	CB3	RB1	RB2	RB3	Driving power
OB1	1	0	0	0	0	0	0	0	0	0	0	0	0	0	0	1
OB2	0	1	0	0	0	0	0	0	0	0	0	0	0	0	0	1
OB3	0	0	1	0	0	0	0	0	0	0	0	0	0	0	0	1
PB1	1	1	1“*”	1	1“*”	0	1	1	1“*”	1“*”	1	1“*”	1“*”	1“*”	1	14
PB2	1“*”	1“*”	1“*”	1“*”	1	0	1	1	1“*”	1“*”	1	1“*”	1“*”	1“*”	1	14
PB3	1“*”	1“*”	1“*”	1	1“*”	1	1	1	1“*”	1	1	1	1“*”	1	1“*”	15
TB1	1	1“*”	1	1“*”	1“*”	0	1	1“*”	1“*”	1“*”	1	1“*”	1	1“*”	1“*”	14
TB2	1	1“*”	1	1“*”	1“*”	0	1“*”	1	1	1“*”	1	1“*”	1“*”	1“*”	1“*”	14
TB3	1“*”	1“*”	1“*”	1“*”	1	0	1	1“*”	1	1	1	1	1“*”	1“*”	1“*”	14
CB1	1“*”	1“*”	1“*”	1	1“*”	0	1	1“*”	1“*”	1	1	1“*”	1“*”	1“*”	1“*”	14
CB2	1	1“*”	1	1	1	0	1	1“*”	1“*”	1“*”	1	1	1“*”	1“*”	1“*”	14
CB3	1“*”	1	1“*”	1	1“*”	0	1	1“*”	1	1	1“*”	1	1	1“*”	1“*”	14
RB1	1“*”	1	1“*”	1	1“*”	0	1“*”	1	1“*”	1“*”	1	1“*”	1	1	1“*”	14
RB2	1	1“*”	1	1“*”	1“*”	0	1	1“*”	1“*”	1	1“*”	1	1“*”	1	1	14
RB3	1“*”	1	1“*”	1	1“*”	0	1“*”	1	1	1	1“*”	1“*”	1“*”	1“*”	1	14
Dependence power	13	13	13	12	12	1	12	12	12	12	12	12	12	12	12	

Table 7 Level partitioning iterations

Elements (Mi)	Reachability set R(Mi)	Antecedent set A(Ni)	Intersection set R(Mi) ∩ A(Ni)	Level
1	OB1	PB1, PB2, PB3, TB1, TB2, TB3, CB1, CB2, CB3, RB1, RB2, RB3		1
2	OB2	PB1, PB2, PB3, TB1, TB2, TB3, CB1, CB2, CB3, RB1, RB2, RB3		1
3	OB3	PB1, PB2, PB3, TB1, TB2, TB3, CB1, CB2, CB3, RB1, RB2, RB3		1
4	PB1, PB2, TB1, TB2, TB3, CB1, CB2, CB3, RB1, RB2, RB3	PB1, PB2, PB3, TB1, TB2, TB3, CB1, CB2, CB3, RB1, RB2, RB3	PB1, PB2, PB3, TB1, TB2, TB3, CB1, CB2, CB3, RB1, RB2, RB3	2
5	PB1, PB2, TB1, TB2, TB3, CB1, CB2, CB3, RB1, RB2, RB3	PB1, PB2, PB3, TB1, TB2, TB3, CB1, CB2, CB3, RB1, RB2, RB3	PB1, PB2, PB3, TB1, TB2, TB3, CB1, CB2, CB3, RB1, RB2, RB3	2
6	PB1, PB2, PB3, TB1, TB2, TB3, CB1, CB2, CB3, RB1, RB2, RB3	PB3	PB3	
7	PB1, PB2, TB1, TB2, TB3, CB1, CB2, CB3, RB1, RB2, RB3	PB1, PB2, PB3, TB1, TB2, TB3, CB1, CB2, CB3, RB1, RB2, RB3	PB1, PB2, PB3, TB1, TB2, TB3, CB1, CB2, CB3, RB1, RB2, RB3	2
8	PB1, PB2, TB1, TB2, TB3, CB1, CB2, CB3, RB1, RB2, RB3	PB1, PB2, PB3, TB1, TB2, TB3, CB1, CB2, CB3, RB1, RB2, RB3	PB1, PB2, PB3, TB1, TB2, TB3, CB1, CB2, CB3, RB1, RB2, RB3	2
9	PB1, PB2, TB1, TB2, TB3, CB1, CB2, CB3, RB1, RB2, RB3	PB1, PB2, PB3, TB1, TB2, TB3, CB1, CB2, CB3, RB1, RB2, RB3	PB1, PB2, PB3, TB1, TB2, TB3, CB1, CB2, CB3, RB1, RB2, RB3	2
10	PB1, PB2, TB1, TB2, TB3, CB1, CB2, CB3, RB1, RB2, RB3	PB1, PB2, PB3, TB1, TB2, TB3, CB1, CB2, CB3, RB1, RB2, RB3	PB1, PB2, PB3, TB1, TB2, TB3, CB1, CB2, CB3, RB1, RB2, RB3	2
11	PB1, PB2, TB1, TB2, TB3, CB1, CB2, CB3, RB1, RB2, RB3	PB1, PB2, PB3, TB1, TB2, TB3, CB1, CB2, CB3, RB1, RB2, RB3	PB1, PB2, PB3, TB1, TB2, TB3, CB1, CB2, CB3, RB1, RB2, RB3	2
12	PB1, PB2, TB1, TB2, TB3, CB1, CB2, CB3, RB1, RB2, RB3	PB1, PB2, PB3, TB1, TB2, TB3, CB1, CB2, CB3, RB1, RB2, RB3	PB1, PB2, PB3, TB1, TB2, TB3, CB1, CB2, CB3, RB1, RB2, RB3	2
13	PB1, PB2, TB1, TB2, TB3, CB1, CB2, CB3, RB1, RB2, RB3	PB1, PB2, PB3, TB1, TB2, TB3, CB1, CB2, CB3, RB1, RB2, RB3	PB1, PB2, PB3, TB1, TB2, TB3, CB1, CB2, CB3, RB1, RB2, RB3	2

(continued)

Table 7 (continued)

Elements (Mi)	Reachability set R(Mi)	Antecedent set A(Ni)	Intersection set R(Mi) ∩ A(Ni)	Level
14	PB1, PB2, TB1, TB2, TB3, CB1, CB2, CB3, RB1, RB2, RB3	PB1, PB2, PB3, TB1, TB2, TB3, CB1, CB2, CB3, RB1, RB2, RB3	PB1, PB2, PB3, TB1, TB2, TB3, CB1, CB2, CB3, RB1, RB2, RB3	2
15	PB1, PB2, TB1, TB2, TB3, CB1, CB2, CB3, RB1, RB2, RB3	PB1, PB2, PB3, TB1, TB2, TB3, CB1, CB2, CB3, RB1, RB2, RB3	PB1, PB2, PB3, TB1, TB2, TB3, CB1, CB2, CB3, RB1, RB2, RB3	2

converted to the ISM model. An ISM model was developed to separate the 15 challenges into six levels. The outcomes are presented in Table 7. The study suggests that the most fundamental challenge is the lack of research on the implementation of integrated mobility planning in cities as a complex issue (OB2), particularly with regards to making the implementation process feasible. Therefore, it is essential to consider China's distinct market environment when implementing integrated mobility planning in cities. Level V also pertains to the operation and technology support necessary to foster a suitable cooperative environment, as there is a dearth of mobility standards (B18) and domestic-oriented ISM tools (TB2). At Level IV, there are challenges associated with workflow and cooperation, such as a negative attitude toward collaboration (RB3) and underdeveloped dispute resolution mechanisms. In addition to OB1 and PB2, four more challenges must be overcome at Levels III, II, and I, which are largely related to the additional investment and effort required to implement integrated mobility planning in cities. These challenges include TB3 and RB1 at Level III, OB3 at Level II, and RB1 at Level I.

4.5 Differentiating of Challenges

The study used a MICMAC diagram (shown in Fig. 4) to categorize the fifteen challenges identified in Table 7. The challenges were divided into four groups: autonomous variables (with low driving and dependence powers), dependent variables (with high driving and dependence powers), driver variables (with high driving power and low dependence power), and linkage variables (with low driving and dependence powers) [8]. The results show that PB1 (lack of research on the implementation of integrated mobility planning) has the highest driving force but the lowest dependence power, indicating that it should be prioritized as the most important challenge to address as it has the potential to influence other challenges. On the other hand, CB1 (increased design costs) has the highest dependence power, which means that addressing this challenge is crucial in order to overcome other barriers. Although none of the challenges can be considered autonomous variables, they can all hinder the implementation of integrated mobility planning in some way. The study identified five challenges as linkage variables: TB2, TB3, RB1, RB2, and OB3. This

suggests that addressing any of these five challenges can have a positive feedback effect on other challenges.

5 Discussion

The findings of this research demonstrate the importance of using interpretive structural modeling (ISM) as a tool to navigate the challenges associated with the implementation of integrated mobility planning (IMP) [1]. The ISM approach provides a comprehensive framework for identifying the relationships between the various components of a transportation system and the interdependencies between them. This information can be used to identify the most critical issues that need to be addressed to achieve the desired level of integration. Furthermore, the ISM approach provides a means of developing strategies that can effectively address these issues and facilitate the implementation of IMP. The case study presented in this research highlights the practical application of ISM in the transportation sector and provides evidence of its effectiveness in facilitating the implementation of IMP. The results of the case study showed that the ISM approach helped to identify the critical issues that needed to be addressed and provided a framework for the development of strategies to address these issues. This highlights the importance of using ISM as a tool to navigate the challenges associated with the implementation of IMP and highlights the need for further research in this area.

6 Conclusion

This study examined the challenges associated with implementing integrated mobility planning (IMP) and the potential benefits of using interpretive structural modeling (ISM) to overcome them. As a result of this study, it can be demonstrated that the ISM framework provides a comprehensive framework for identifying the relationships among the different components of a transportation system, their interdependencies, as well as the critical issues that need to be addressed. ISM has also been found to effectively facilitate IMP implementation based on the results of the case study. These findings have important implications for transportation planners, policymakers, and researchers interested in improving transportation efficiency and sustainability. According to the findings of this study, ISM is an effective tool for navigating the challenges associated with the implementation of IMP, and further research in this area is needed to fully exploit its potential. This study is a valuable contribution to the field of transportation planning and shows how ISM can benefit implementation of IMP by navigating challenges associated with implementing IMP. This study aims to encourage further exploration of the potential applications of ISM in the transportation sector and contribute to the development of more sustainable and efficient transportation systems.

References

1. Wang Y, Zhu X, Li L, Wu B (2013) Integrated multimodal metropolitan transportation model. Proc Soc Behav Sci 96:2138–2146. https://doi.org/10.1016/j.sbspro.2013.08.241
2. Luo Q, Li S, Hampshire RC (2021) Optimal design of intermodal mobility networks under uncertainty: connecting micromobility with mobility-on-demand transit. EURO J Transp Logist 10(June):100045. https://doi.org/10.1016/j.ejtl.2021.100045
3. Yanocha D, Mason J, Hagen J (2021) Using data and technology to integrate mobility modes in low-income cities. Transp Rev 41(3):262–284. https://doi.org/10.1080/01441647.2020.1834006
4. Molenbruch Y, Braekers K, Hirsch P, Oberscheider M (2021) Analyzing the benefits of an integrated mobility system using a matheuristic routing algorithm. Eur J Oper Res 290(1):81–98. https://doi.org/10.1016/j.ejor.2020.07.060
5. Xu Z, Bai Q, Shao Y, Hu A, Dong Z (2022) A review on passenger emergency evacuation from multimodal transportation hubs. J Traffic Transp Eng 9(4):591–607. https://doi.org/10.1016/j.jtte.2022.02.001
6. Dawda NH, Joshi GJ, Arkatkar SS (2021) Synthesizing the evolution of multimodal transportation planning milestones in Indian cities. Proc Comput Sci 184:484–491. https://doi.org/10.1016/j.procs.2021.03.061
7. Hussin H, Osama A, El-Dorghamy A, Abdellatif MM (2021) Towards an integrated mobility system: the first and last mile solutions in developing countries; the case study of New Cairo. Transp Res Interdiscip Perspect 12(August):100469. https://doi.org/10.1016/j.trip.2021.100469
8. Sachan A, Mathew T (2020) Integrated multimodal transit route network design with feeder systems. Transp Res Proc 48(2019):756–763. https://doi.org/10.1016/j.trpro.2020.08.077
9. Chauhan V, Gupta A, Parida M (2021) Demystifying service quality of Multimodal Transportation Hub (MMTH) through measuring users' satisfaction of public transport. Transp Policy 102(December):47–60. https://doi.org/10.1016/j.tranpol.2021.01.004
10. Jha AP, Singh SK (2022) Future mobility in India from a changing energy mix perspective. Econ Anal Policy 73:706–724. https://doi.org/10.1016/j.eap.2021.12.022

Advanced Framed Structures

Study on the Seismic Performance of Multi-storey Reinforced Concrete Building with Dual Framed-Shear Wall System Considering Soft Storey

Mohanad Ali Ishaq Najajra, Taha Ahmed Ghaleb Mohammed, and Wesam Al Agha

Abstract A soft storey is an open space on the structure's first floor. This phenomenon might be attributed to the sudden variations in the lateral stiffness and strength of the building. The occurrence of a seismic event has the potential magnitude of extensive structural damage. Several studies have indicated that significant displacements caused by seismic lateral load are the primary factor in structural collapse. In cases where the preliminary design of a structure is intended to withstand horizontal loads, particularly respected to the building's structure, the deflection exhibited is more significant. Shear walls are inserted to enhance a structure's lateral stiffness, ductility, displacement, and stability. The seismic design of structures necessitates the crucial consideration of storey drift and lateral displacement. A shear wall is incorporated within the proposed building to mitigate seismic reactions and enhance the structure's rigidity. This study investigates the seismic performance of reinforced concrete structures with soft storey by applying seismic dissipation techniques as a shear wall structural system. The models examine the effects of shear walls installed at various positions within soft storey systems to contrast the behaviour of buildings. The 10-storey reinforced concrete building with a regular shape plan is located in Indian Zone V and subjected to distinct configurations, namely centre and corner. The analysis of models using ETABS 18.0.2 finite element software illustrated linear dynamic (response spectrum method) and nonlinear static (pushover analysis method). The Indian Standard 1893 (Part 1): 2016 is demonstrated to tabulate various parameters such as maximum storey displacement, drift, storey stiffness, and base shear. In conclusion, shear walls effectively improve structural rigidity and

M. A. I. Najajra · T. A. G. Mohammed
Department of Civil Engineering, Cyprus International University, via Mersin 10, Haspolat, North Cyprus, Turkey

W. Al Agha (✉)
Department of Civil Engineering, Delhi Technological University, Delhi 110042, India
e-mail: wesamalagha1@gmail.com; wesamalagha_2k21phdce16@dtu.ac.in; wesam.alagha@unich.it

Department of Engineering and Geology, University G. d'Annunzio of Chieti-Pescara, Pescara Viale Pindaro 42, 65127, Italy

K. R. Reddy et al. (eds.), *Recent Advances in Civil Engineering*, Lecture Notes in Civil Engineering 398, https://doi.org/10.1007/978-981-99-6229-7_58

reduce displacement. The incorporation of shear walls in buildings has demonstrated efficacy and ductility.

Keywords Shear wall · Storey displacement · Drift · Storey stiffness · Base shear · Pushover analysis · Response spectrum

1 Introduction

1.1 Design-Based Earthquake

Structural dynamic analysis is imperative to ensure structural integrity and investigate the structure's behaviour during earthquake effects. Additionally, it is essential to determine the optimal response to base shear where the structures are subjected to lateral loads induced by seismic activity, resulting in dynamic responses. In contrast to high-rise structures, low-rise buildings exhibit a significantly lower resistance towards energy dissipation [1]. The industrialization, economic considerations, population, and urban lifestyles might lead to tall buildings and structurally fragile construction. Since a structure is designed to withstand horizontal loads, particularly those imposed on the building, it is exhibited more deflection [2]. Installing structural shear walls is a practical approach for mitigating displacement caused by lateral loads. The construction has complied with the design-based earthquake (DBE) specifications.

Nevertheless, it exerted DBE force significantly [3]. A ductility-based design methodology in regions with high seismic activity is advisable as it reduces collapse [4]. The primary objective in designing seismic structures is to ensure sufficient ductility to withstand the potentially destructive forces of seismic activity. The presence of shear walls in the building guarantees protection against horizontal forces. Implementing shear walls in a building can effectively mitigate significant displacements and consequential structural damage [5]. The present investigation encompasses the evaluation of various parameters of soft floors and the positioning of shear walls [6].

Additionally, an examination will be conducted on the efficacy of employing uncomplicated reinforcement techniques to enhance the structural integrity of a building while minimising alterations to its architectural and functional requirements [7]. The initial analysis method pertains to a building with a soft storey configuration at the ground level [8]. During the second approach, the structural integrity of the building is evaluated using shear walls and the assessment of the soft storey located on the ground floor.

Response Spectrum Analysis

This methodology enables the consideration of various response modes in which a structure might react. The overall response is approximated by combining the

response corresponding to the modal frequency and modal mass for each mode, as extracted from the design spectrum. The subsequent are the diverse categories of amalgamation techniques [5, 9]. The maximum value is included by the Sum of Square Root Squares (SRSS) and the complete quadratic combination (CQC), which is a technique utilised to represent an enhancement in the square root of the sum of squares (SRSS) in modes.

1.2 Shear Wall

Shear walls are constructed to withstand seismic loads and provide the necessary rigidity and robustness to buildings when exposed to lateral loads. Shear walls are the most efficient lateral load resistance systems for tall structures. According to the IS13920:2016 standard, a shear wall is a vertical structural system designed to resist lateral forces, including axial, shear, and bending moments, primarily within its plane. According to the IS1893 (Part 1):2002 and ASCE 7–16 codes, stiffness irregularities are defined as follows: A storey can be classified as "soft" if its lateral stiffness is below 70% of the lateral stiffness subjected to storey directly above it, or since it is <80% of the average lateral stiffness of the above three storeys. A storey is considered extremely soft if its lateral stiffness is <60% of the lateral stiffness of the storey immediately above it or <70% of the average lateral stiffness of three storeys above it. The phenomenon is inconsistencies in the structural properties of stiffness and strength [10]. In the design process aimed at predicting the seismic response of high-rise buildings, it is crucial to ascertain the prerequisites for soft storeys and their consequential effects on the structure. A shear wall is a type of structural system comprising shear bases employed to reduce the effects of lateral loads on a building [4, 11]. The fundamental purpose of a shear wall, as Fig. 1, is to enhance the lateral load resistance rigidity and provide the structure with the requisite stiffness and strength. Shear walls are employed in buildings to alleviate the impact of lateral loads. These elements are supplied with the building's structural slabs, beams, and columns, imparting the necessary stiffness for residential towers. The calculation of structural elements dimensions such as beams and columns in tall buildings is substantial, and the reinforcement of beam-column connections is significant, leading to congestion at the joints [12]. Shear walls can be utilised as a fundamental mechanism to impart adequate stiffness for addressing these practical challenges.

In the view of shear wall geometry and location, it has a variety of cross sections, including rectangular and irregularly shaped cross sections like L, T, C, and U. A rectangular cross-section, that is, one dimension that is substantially greater than the other, is often utilised as an irregular cross-section. In order to withstand seismic forces, the shape and distribution of the shear wall have a significant effect on behaviour of the building. Shear walls are installed in the preferred position of the structure in order to build an effective lateral resistance system with minimal lateral

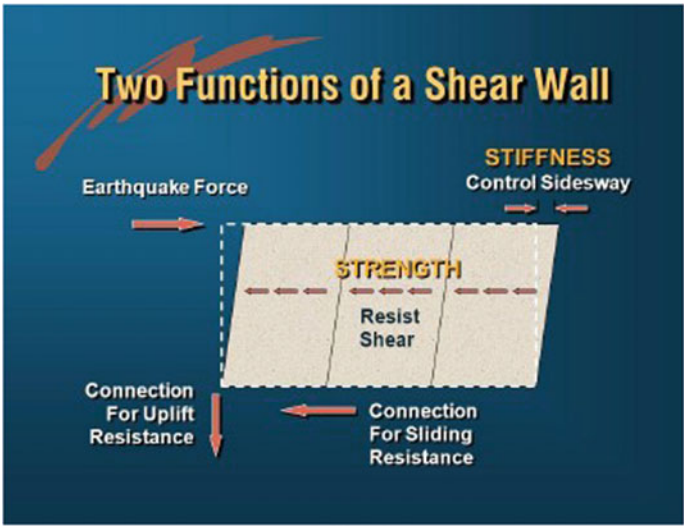

Fig. 1 Function of shear wall

displacement due to seismic loads. For the structure to be effective, the shear walls are placed symmetrically to reduce the effects of torsion.

1.3 Seismic Design Philosophy

The seismic evaluation was conducted to determine the resilience of existing buildings of designing structures to withstand potential earthquake forces, following the transition from a strength-oriented to a performance-oriented design standard. The present building codes encompass specific objectives for ensuring the stability of individuals, mitigating damage resulting from minor and moderate seismic activity, and averting structural collapse during major seismic events. The actual efficacy of the design in achieving its objective remains uncertain. The performance-based design of a new building is typically characterised by the recognition of a series of steps, which are abbreviated as follows. The investigation step is establishing the performance objectives for all the to-be-considered accounts. Commence the process by initiating the preliminary design. Subsequently, ensure that the projected results have been successfully attained. The performance level determination may be ascertained by utilising the guidelines outlined in FEMA 356. As shown in Fig. 2, it specified three different occupancy levels: Immediate Occupancy, Life Safety, and Collapse Prevention.

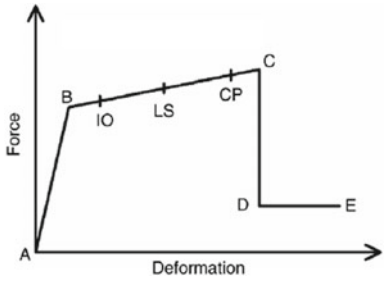

Fig. 2 Structural performance level (FEMA 356)

Immediate Occupancy (LO)

In the seismic magnitude effect, the building might be occupied. The structural integrity exhibits minor cracks, and no significant fractures are present. In the cracks, it is a minor effect. No structural deformation can result in the immediate occupation of a building subsequent to a sudden earthquake of this magnitude.

Life Safety Performance Level (LS)

The phenomenon is related to the reduction of the initial stiffness. The structural framework exhibits significant fractures. In contrast, the structure is capable of being repaired. In the event of restoration, a substantial amount of funds will be required.

Collapse Prevention Performance Level (CP)

The structure remains stable as it is not constructed to collapse. The damages occurred when a structure is exposed to excessive lateral loads, and the structure's rigidity is inadequate to resist the lateral stresses. Certain structural elements have experienced failure and subsequent collapse. The structure cannot be repaired or maintained.

2 Review of Literature

Kannan [13] shows that the G + 8 building has been designed using three different structural models: a frame, a frame with shear wall, and a frame with X bracing. These models were developed by altering the position of the soft floor across various floors. The impact of static analysis has been evaluated for the three models featuring zone IV and V, utilising Staad Pro-V8i software. The study's primary aim was to evaluate the influence of a soft floor throughout various seismic regions while also varying the effect of the soft floor from the first to the top floor and evaluating frames with distinct column shapes through seismic analyses in Staad Pro. The research outcomes of characteristics building models are based on variables such as storey displacement, storey drift, and storey base shear. Kanake [14] shows sudden reductions in stiffness might be avoided in newly constructed RC frame buildings. In order to mitigate this phenomenon, it is advisable to incorporate either masonry

walls or reinforced concrete shear walls in the lowermost storey. Infill walls are used to attain a more ductile structure effect between columns and beams, whereby force is transmitted from a node to another. The investigation examines the high-rise structure, taking into account the existence of infill walls and shear walls. The response spectrum investigation is conducted on a building that features an infill arrangement and reinforced concrete shear wall on an open ground storey. Abd-Alghany et al. [15] conducted a study using ETABS software to model and analyse a 20-storey soft storey building. The analysis was performed through linear static analysis and modal response spectrum techniques. The study incorporates parameters that consider the elevation of the soft storey, the dimensional irregularities of the structural plan, and the position of the soft storey throughout the height of the structure. A shear wall was implemented at the central location of the building to examine the alteration in relative stiffness. The findings centre on the effects of diverse parameters on horizontal displacement, comparative stiffness, and inter-storey deflection. The effectiveness of shear walls in enhancing stiffness irregularities and minimising displacement and drift has been well established. Furthermore, cross braces are a proficient and economical method while mitigating stiffness inconsistencies. Akhil Ahamad and Pratap [16], in 2020, aim to examine the implementation of shear walls in different seismic activity zones in ETABS software across 21 multi-storey buildings. The nature of structures exposed to seismic activity is being investigated by applying response spectrum analysis. This study examines the effects of storey drift, shear, higher permissible displacement, and twisting irregularities. The investigation of multi-storey buildings is being conducted. The utilisation of ETABS for structural analysis and modelling will be conducted across all earthquake zones stipulated by the IS 1893 code. This investigation aims to assess the performance of a multi-storey building system with and without the incorporation of shear walls and to analyse the outcomes of seismic zone assessments. Utilising the four-cornered shear wall configuration yielded superior base displacement, drift, and shear outcomes. Afghan et al. [17] utilised the seismic coefficient and dynamic response spectrum methods to assess the structural behaviour of G + 10 storey buildings featuring varying shear wall placements. The researchers investigated four distinct models of RCC structures, one lacking concrete structural walls while the other three featuring different configurations of structural wall construction. Among the four models that were analysed, it was found that the core shear wall model exhibited superior performance compared to the other models.

In conclusion, relevant studies are not considered widely on providing a shear wall in each direction of the building. The Indian standard code has also yet to include a detailed pushover analysis. Therefore, this study aims to assess the seismic performance of buildings considering soft storey configurations and examine the behaviour of such structures under earthquake conditions through dynamic and pushover analyses. The analysis of the structural characteristics, including base shear reaction, displacement, drift pattern, stiffness, and time period to mitigate the effects, it is recommended to identify the optimal placement of the soft storey throughout the vertical extent of the structure.

3 Materials and Modelling Structures

The study analysed 10-storey reinforced concrete frame structure (SMRF) with a soft storey inserted to plan by 36 × 36 m. The design of the models is executed through a two-case approach, whereby the initial case involves the modelling of the building with a soft storey located at the ground floor level [18]. During the second case, the structure of the building was designed to include shear walls and a soft storey in the ground floor [19]. ETABS is utilised to conduct a range of analyses, such as linear dynamic response spectra and nonlinear static pushover analysis. It is illustrated plan and 3D of two cases in Fig. 3.

Seismic analysis response spectra and pushover analyses were performed using IS 1893:2016 [20]. The structure and its specifications are designed according to IS 456:2000 [21]. The properties of the materials [22] (steel and concrete) in the building are presented in Table 1.

The nonlinear material properties of steel and concrete are used as per compression-strain and tension-strain, presented in Table 2. Stress–strain graph of steel and concrete is shown in Fig. 4.

ETABS presented the stress–strain plot of concrete M25 in Fig. 4a and illustrated the stress–strain plot Fe 500 in Fig. 4b.

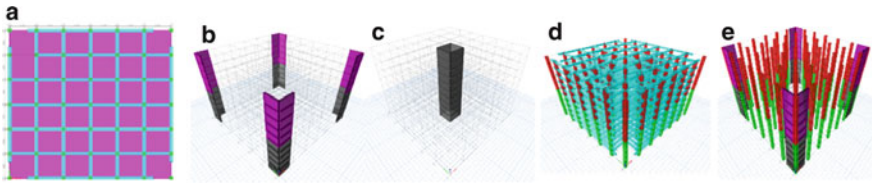

Fig. 3 Configuration of shear wall system. **a** Plan. **b** Corner shear wall. **c** Core shear wall. **d** Soft storey

Table 1 Properties of materials (steel and concrete)

Material	Steel	Concrete
Specific weight density	76.97 kN/m^3	25 kN/m^3
Specific mass density	7850 kg/m^3	2548 kg/m^3
Poisson's ratio (U)	0.3	0.2
Coefficient of thermal	0.0000117 1/0c	0.0000055 1/0c
Expansion (α)	80,769.23 MPa	10,416.67 MPa
Shear modulus (G)	210,000 MPa	25,000 MPa
Modulus of elasticity (E)	76.97 kN/m^3	25 kN/m^3
	Isotropic	Isotropic

Table 2 Properties of non-linear materials

Material	Steel	Compression–strain	Concrete	Compression– strain
IO	0.01	−0.005	0.01	−0.003
LS	0.02	−0.01	0.02	−0.006
CP	0.05	−0.02	0.05	−0.015

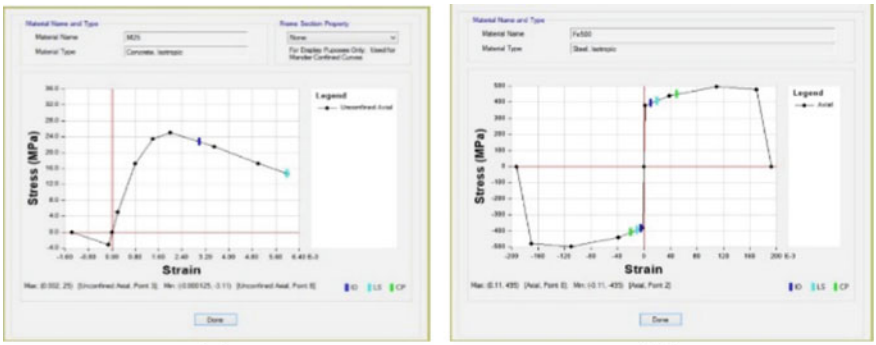

Fig. 4 Stress–strain plot of **a** concrete, **b** steel

4 Results

As a manual calculation of the stiffness in the case of the soft storey and validation using Indian standards, the stiffness is 21.6% compared with the second storey; therefore, the bottom storey has a lesser stiffness value. According to IS 1893 (Part 1):2016: "Soft floors have less lateral stiffness than upper floors." Therefore, the selected model has stiffness irregularity in the bottom storey. The process of RCC frame modelling and their analysis in the first case of response spectrum analysis for storey displacement, base shear, stiffness, and drift is presented in Fig. 5.

It is significant to explore in Fig. 5 that soft storey values are increased of storey displacement and storey drift; in the case without installing a shear wall, it presented higher values compared with shear wall usage in terms of storey shear and stiffness using response spectrum methods. The models of RC frame with a shear wall placed at four corners give the maximum base shear value of 9102.8 KN. The base shear increases by 80% and 114% when shear walls are placed at the core and four corners. Storey shear is more, i.e. 5206.9082 kN in the model with a corner shear wall compared to other models, while it is less in the case of the model with soft storey, i.e. 414.9 kN. The shear wall placed at all four corners gives a higher value of shear as compared to the shear wall placed at the core. Storey stiffness has a higher value of 4,790,126.626 kN/m in the case of the model having a corner shear wall compared to other models, while it is less in the case of the model with soft storey, i.e. 617,999.8 kN/m. Soft storey irregularity was reduced when the shear wall was

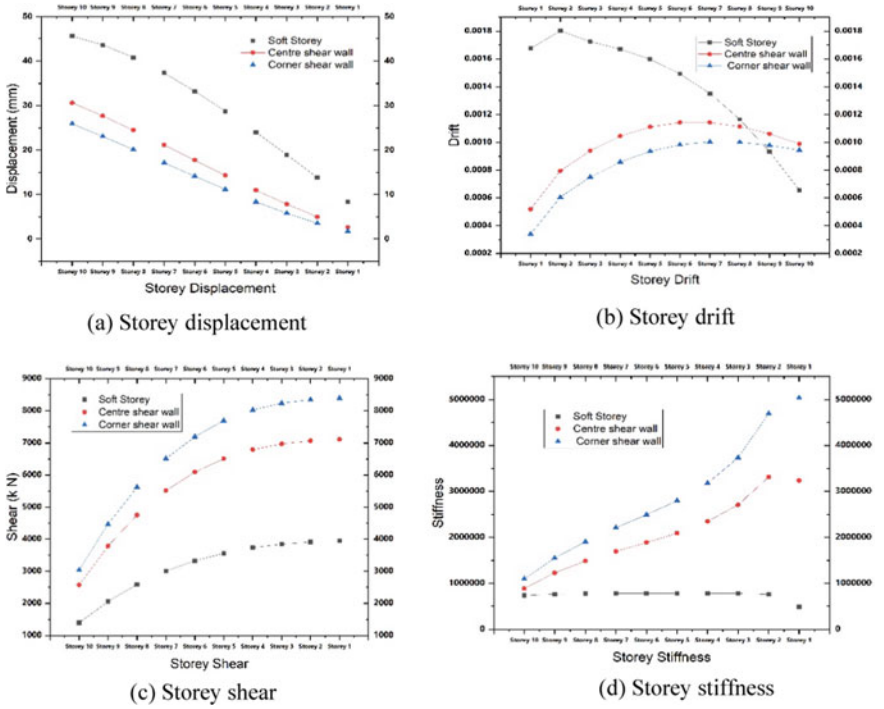

Fig. 5 Comparison results between soft storey and shear wall (centre and corner)

introduced in both corners and at the core, giving a maximum stiffness value in the first storey.

After analysing RSM and pushover analysis, the seismic performance parameters are varied to present as Fig. 6. The models with corner shear walls are illustrated a minimum vibration period of 0.795 s, while the model with soft storey has a maximum vibration period of 1.599 s.

The comparison between the response spectrum and pushover analysis in terms of maximum displacement, stiffness, base shear, and time period value is presented.

Response spectrum analysis has a higher storey drift value than pushover analysis. The models with shear walls installed at all four corners had the lowest drift values, as seen from both response spectra and pushover studies. Nonlinear time history analysis can be used to provide a more precise calculation of the structure's capacity and simulate a more realistic demand instance. Shear barriers can be built and examined in many different places.

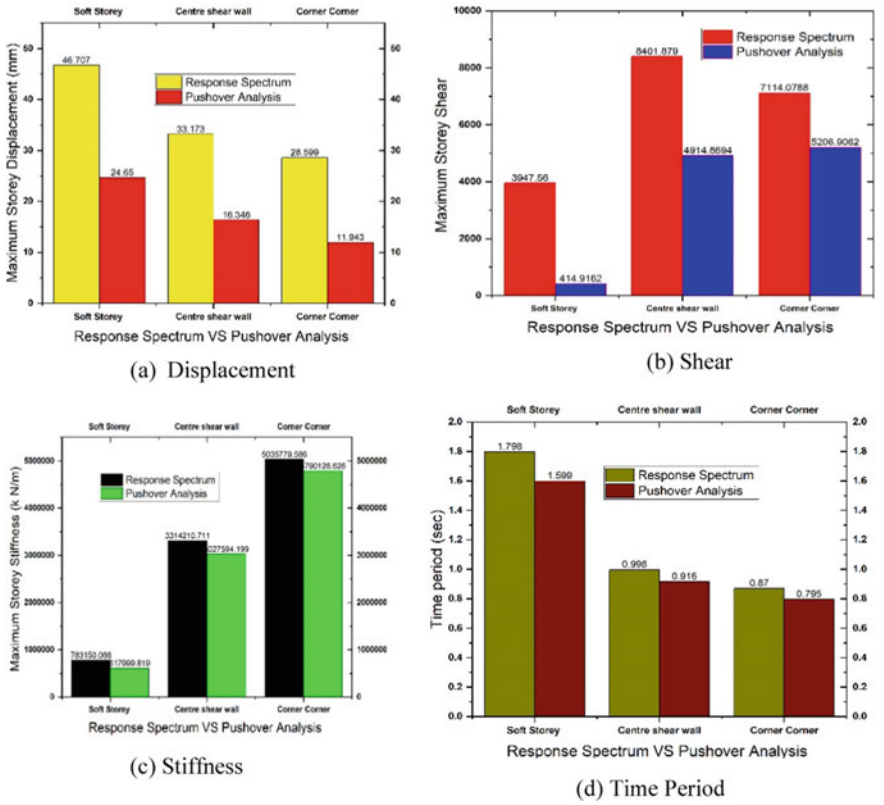

Fig. 6 Comparative results of response spectrum and pushover analysis

5 Conclusion

The models are analysed using the ETABS 18.0.2 programme and the IS 1893 (Part1): 2016 code. The seismic performance of soft-floor RC buildings is studied regarding maximum storey displacement, drift, storey stiffness, base shear value, and time period by performing linear dynamic analysis, the response spectrum method, nonlinear static analysis, or the pushover analysis method. It is concluded as the significant points of comparison as

- Response spectrum methods presented higher displacement values in the case without installing a shear wall compared with shear wall usage.
- The corner shear wall structure model shows high base shear indicating greater stiffness. The presence of a shear wall in the building strongly influences storey stiffness.
- The shear wall placed at all four corners gives a higher stiffness value than the shear wall at the core.

- Shear walls have demonstrated significant efficacy in enhancing soft storey irregularity and mitigating drift and displacement.
- The distribution of shear walls might be enhanced the structural efficacy of a building in the event of seismic activity-induced ground motion. The shear walls at the four corners have exhibited enhanced performance compared to those in the core.
- Pushover study showed larger base shear values than response spectrum analysis.
- All model displacements are within the maximum range allowed by IS 1893:2016. Comparing pushover analysis to response spectrum analysis, the maximum displacement result above is lower in the former. The models with shear walls in all four corners had the lowest displacement values throughout response spectra and pushover analyses.

Acknowledgements The authors would like to express appreciation to the Indian Council for Cultural Relations, India, and the INPS's social security contribution under separate management (CHIETI, IT), Italy.

References

1. Torelli G, D'Ayala D, Betti M, Bartoli G (2020) Analytical and numerical seismic assessment of heritage masonry towers. Bull Earthq Eng 18(3):969–1008. https://doi.org/10.1007/s10518-019-00732-y
2. Zaker Esteghamati M, Banazadeh M, Huang Q (2018) The effect of design drift limit on the seismic performance of RC dual high-rise buildings. Struct Design Tall Spec Build 27(8):e1464. https://doi.org/10.1002/tal.1464
3. Pertile V, Stella A, De Stefani L, Scotta R (2021) Seismic and energy integrated retrofitting of existing buildings with an innovative ICF-based system: design principles and case studies. Sustainability 13(16):9363. https://doi.org/10.3390/su13169363
4. Al Agha W, Umamaheswari N (2021) Analytical study of irregular reinforced concrete building with shear wall and dual framed-shear wall system by using equivalent static and response spectrum method. Mater Today Proc 43:2232–2241
5. Kant R, Al Agha W, Thakur MS, Umamaheswari N (2022) Comparative study on seismic performance of steel-concrete composite structure without and with buckling–restrained braces. Mater Today Proc 56:2134–2144. https://doi.org/10.1016/J.MATPR.2021.11.461
6. Di Sarno L, Manfredi G (2011) Seismic strengthening of an existing building with innovative materials and devices
7. Taranath BS (2016) Tall building design: steel, concrete, and composite systems. CRC Press, Boca Raton
8. Li Y, Ren J, Jing Z, Jianping L, Ye Q, Lv Z (2017) The existing building sustainable retrofit in China—a review and case study. Proc Eng 205:3638–3645. https://doi.org/10.1016/j.proeng.2017.10.224
9. Al Agha W, Umamaheswari N. Comparative study on seismic performance of reinforced concrete building with and without fluid viscous dampers. www.ijerm.com
10. Al Agha W, Alozzo Almorad W, Umamaheswari N, Alhelwani A (2021) Study the seismic response of reinforced concrete high-rise building with dual framed-shear wall system considering the effect of soil structure interaction. Mater Today Proc 43:2182–2188. https://doi.org/10.1016/J.MATPR.2020.12.111

11. Ravi K, Al Agha W, Thakur MS, Umamaheswari N (2021) Impact of the lead rubber base isolators on reinforced concrete building. IOP Conf Ser Mater Sci Eng 1026(1):012004. https://doi.org/10.1088/1757-899X/1026/1/012004
12. Kant R, Al Agha W, Alozzo Almorad W, Thakur MS, Umamaheswari N (2021) Study on seismic performance of reinforced concrete multi-storey building considering soil-structure interaction effect. Mater Today Proc. https://doi.org/10.1016/J.MATPR.2021.11.475
13. Kannan SS (2023) Seismic analysis of soft storey building in earthquake zones. In: IOP Conference Series: Earth and Environmental Science, Institute of Physics. https://doi.org/10.1088/1755-1315/1130/1/012023
14. Kanake S (2022) Seismic response of open ground multi-storey building retrootted with innll wall, shear wall and steel bracing. Shear Wall Steel Brac. https://doi.org/10.21203/rs.3.rs-2183625/v1
15. Abd-Alghany MM, El-Kashif KF, Abdalla HA (2021) Seismic response of multi-storey reinforced concrete buildings with soft floor. HBRC J 17(1):407–428. https://doi.org/10.1080/16874048.2021.1949690
16. Akhil Ahamad S, Pratap KV (2021) Dynamic analysis of G + 20 multi storied building by using shear walls in various locations for different seismic zones by using Etabs. Mater Today Proc 43:1043–1048. https://doi.org/10.1016/j.matpr.2020.08.014
17. Afghan MQ, Zazai N, Sediqi H (2020) Seismic response of multi-storeyed RC framed buildings with different location of shear walls. Int J Res Writings 2:1333. www.ijarw.com
18. IS: 456 (2000) Code of practice for plan and reinforced concrete (fourth revision). Bureau of Indian Standard, New Delhi
19. IS: 4326 (1993) Code of practice for earthquake resistant design and construction of buildings (second revision). Bureau of Indian Standard, New Delhi
20. IS 1893 (part1) (2016) Criteria for earthquake resistance design of structures; Part 1: GENERAL provisions and buildings. Bureau of Indian standards, New Delhi
21. IS: 875 Part 1–5 (1987) Code of practice for design load (other than earthquake) for buildings and structures. Bureau of Indian Standard, New Delhi
22. IS: 1893 Part I (2002) Code of practice for criteria for earthquake resistance design of structure: general provisions and building. Bureau of Indian Standard, New Delhi

Analytical Studies on the Progressive Collapse Behaviour of 2D RC Frames with Different Grades of Steel

P. Jagatheswari, R. Ramasubramani, and S. Durgadevagi

Abstract Progressive collapse is the structural failure whereas the initial failure occurs in the beam and column that results in a total failure of a structure, and one of the major failures that should be considered in a high-rise building is progressive collapse, in which minute damage occurs in an element like a beam or column that the local failure of a structure leads to a global one. It is a continuous chain of structural damage that leads to progressive collapse. In this present study, 2D two-bay 5-storey, 10-storey, 15-storey-reinforced concrete bare frame was analysed and their results were compared with different grades of steel such as Fe415, Fe500, and Fe550. A linear static analysis was carried out using finite element software for corner and middle column removal. Determination of demand capacity ratio (DCR) value for column and beam (axial force, bending moment, shear force), and displacement, was also determined to know the behaviour of progressive collapse of the structure. And the results show that moving to a higher grade of steel for analysis reduces the failure effect of the element when compared with the lower grade of steel and their values are checked according to the General Service Administration (GSA) guidelines.

Keywords Demand capacity ratio · Column · Beam · Displacement · Axial force

1 Introduction

In our overpopulated world due to the excess population, people were moving. To high-rise buildings, skyscrapers which require a limited area with easy livelihood, provide safety, basic needs, and procurement of the people. And when the buildings rise to a maximum height many challenges are faced. In this the important one that we should consider is structural design, material selection of the building and should satisfy the basic requirement such as fire safety, repair, and maintenance, efficiency

P. Jagatheswari · R. Ramasubramani (✉) · S. Durgadevagi
Department of Civil Engineering, Faculty of Engineering and Technology, SRM Institute of Science and Technology, Tamil Nadu, SRM Nagar, Kattankulathur 603203, India
e-mail: ramasubr@srmist.edu.in

K. R. Reddy et al. (eds.), *Recent Advances in Civil Engineering*, Lecture Notes in Civil Engineering 398, https://doi.org/10.1007/978-981-99-6229-7_59

plumbing system, basement provisions, geotechnical investigation, seismic resistance, every category should be considered while constructing the tall building, and if we fail to determine all this, failure may occur in this one of the major failures is progressive collapse. Where progressive collapse is a failure of a single member or part of the structure that results in the whole structural failure. In detail progressive collapse is a structural failure, whereas the initial failure occurs in a structure that results in a continuous chain of structural damage and at one stage whole structure tends to collapse. And the cause of the progressive collapse is because of the load that acts on the building, the load may be of impact load or pressure load on the building, such as gas explosions, due to bomb blast, winds, waves, etc., occur come under pressure load. And because seismic actions like an earthquake, foundation settlement, and vehicle collision all come under the impact load [1–4].

According to the General Service Administration (GSA) and Department of Defence (DOD), they have explained the detailed and stepwise procedure regarding the method to prevent the progressive collapse of the structure and they put forward one important concept, i.e. vertical structural elements and their load path is studied. In that column removal scenario is done to study the behaviour of the structure [5]. Several studies have been carried out in progressive collapse of column removal. Al-Al-Salloum et al. [6] present a progressive collapse of an RC; the building is analysed by considering the internal blasting alone, whereas in these two approaches that were involved, one is fluid–structure interaction and the other one is CONWEP. And the modelling of the structure is created by the FEM software, namely LS-DYNA which determines the time integration and algorithm solution; as a result of these concepts it reduces or prevents the progressive collapse of the structure by comparing the negligible similarity in the structure with the comparison of these two concepts [6]. Seetha Lakshmi et al. [7] present a comparative study between the bare and infill frame. In this, they consider a two-dimensional four-bay 5-storey RC frame in three conditions like bare frame, infill frame, and infill frames with openings. All these were considered to resist the structure and they have been analysed in a linear static method. All the conditions like shear force, bending moment, the deflection was found for both beams and columns. And the removal of the column resulted in a decrease at that moment, they observed a decrease in deflection in the case of the infilled frame when compared with the bare frame and they concluded that the progressive collapse was delayed due to the presence of infilled frame [7]. Gowtham et al. [8] investigated the two-dimensional 5-storey concrete bare frame with considering two bay. The analysis of the linear static and nonlinear dynamic is carried out, whereas in the nonlinear dynamic analysis time history method is used for the analysis purpose, were as the corner column and middle column removal scenario is done, and here they calculated the demand capacity ratio values and member acceptance criteria are calculated according to linear static analysis, maximum axial force, time vs displacement, bending moment were also determined to know the potential of a structure by progressive collapse [8]. Vieira et al. [9] present the TRT and NSM technique that were examined for the strengthening of structure when the structure tends to collapse. This strengthening process of the TRM technique increases the

bearing capacity of the structure and control the collapse, whereas the NSM technique controls the specimen from the ductility [9]. Huang et al. [10] present two-bay by 2-storey-reinforced concrete frames that were taken for the analysis with the loss of one corner column. Where it includes the strengthening of the high-performance ferrocement laminate as well as the bonded steel plates and strengthening effects is also determined, and it also investigates the crack development pattern, lateral deformation, load–displacement, load distribution and strengthening effects were also shown in figure. As initial stiffness and bearing capacity of the frame is strengthened after using the strengthening process [10].

This paper presents the study on two-dimensional RC behaviour of 5, 10, 15 storeys bare frame under the linear static condition which includes corner and middle column removal and to study on the RC frame with different grades of steel.

2 Analytical Details

The modelling and analysing of the structure were done using Abaqus (FEM software). This software accurately evaluates the results. Here analytical studies on the progressive collapse behaviour of 2D RC frames with different grades of steel were compared and the column removal scenario is done at the corner and middle level. For the given structure, the results taken are compared with different grades of steel with load versus deflection, demand capacity ratio (DCR) value for axial load for column and bending moment, and shear force for the beam is determined. The boundary condition of the RC frame is a fixed end condition for the linear static analysis.

3 Geometry of the Structure

Preliminary data of the two-dimensional RC frame structure with the three different storeys 5, 10, and 15 each storey consists of height 15, 30, 45 m, whereas no. of bay considered in these storeys are two bay and the height of each bay is 2.7 m and the width of each bay is 2.5 m. Cross-section of the beam is 0.3 m $\times$ 0.3 m and the cross-section of the column is 0.3 m $\times$ 0.45 m. Reinforcement details for the beam are the main bar 4 no. of 10 mm diameter with stirrups 8 mm diameter at 100 mm spacing and the clear cover is 25 mm overall the beam. Reinforcement details for the column are main bar 4 no. of 12 mm diameter along with ties 8 mm diameter at 150 mm spacing, the clear cover is 40 mm [8]. The loads that act on the structure are dead load, DL is automatically calculated by the Abaqus software and self-weight of the structure calculated is 15.39 kN/m, whereas the live load of the slab and floor finish is 3 and 1 kN/m, therefore the total load act on the structure is 19.4 kN/m for the linear static analysis. Figures 1, 2 and 3 show the 5-, 10-, 15-storey RC frame.

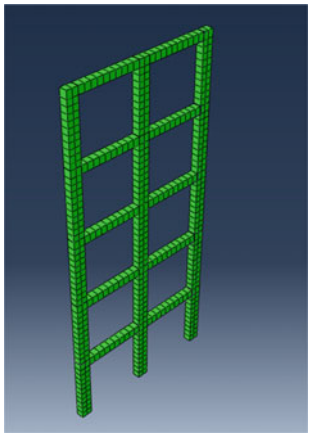

Fig. 1 5-storey RC frame

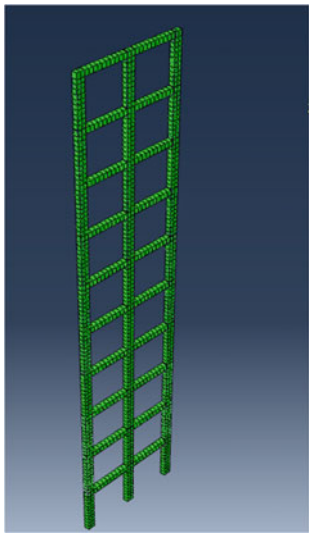

Fig. 2 10-storey RC frame

4 Material Properties

Material properties of the RC frame of different grades of steel and concrete was taken to compare the behaviour of steel at different storey levels and to give the better material for the frames and the properties are mentioned in Table 1.

Fig. 3 15-storey RC frame

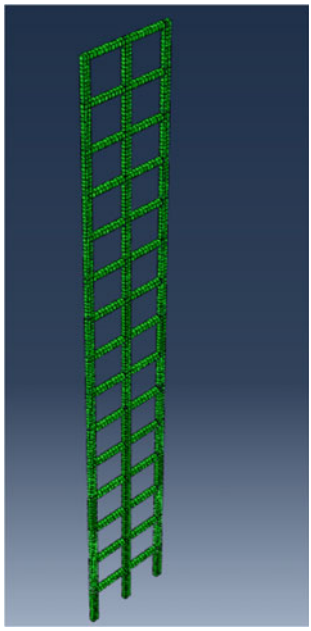

Table 1 Material properties of structure

Grade of steel	Grade of concrete	Poisson ratio of concrete	Poisson ratio of steel	Modulus of concrete (N/m^2)	Modulus of steel (N/m^2)
Fe415	M30	0.23	0.3	2×10^{10}	2×10^{11}
Fe500	M30	0.23	0.3	2×10^{10}	2×10^{11}
Fe550	M30	0.23	0.3	2×10^{10}	2×10^{11}

5 Element Property of the Structure

Automated type mesh was chosen for modelling the frame. Thus, modification of geometry will result in the change of mesh automatically. (C3D8R) Solid element of deformable type 8 node was taken as the type of element. Automated square mesh with the meshing size of 250 mm was taken. The stress–strain behaviour of Fe415, Fe500, and Fe550 have been referred from the material characteristics and design parameters for limit state method of design as per IS 456-2000 and IRC: 112-2011and the graph was shown in Fig. 4.

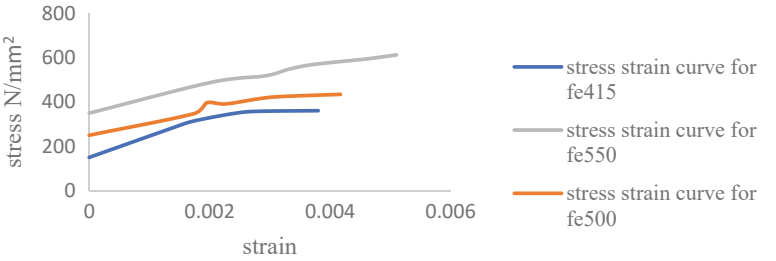

Fig. 4 Stress–strain curve for different grades of steel

6 Linear Static Analysis

Linear static analysis is performed to check the behaviour of a structure within its elastic limit under static loading conditions. It is the most general and basic analysis that we should consider for all types of structures. Linear means it deals with the response of displacement or stress at the elastic limit and it will not exceed beyond that is known as linear. Static means the applied load or force to a structure will determine the standard and does not vary with time [11, 12].

In this project, linear static analysis is to calculate the demand capacity ratio under an axial load of column, bending moment, and shear force for beam. The analysis is done for a bare frame of 27 models that have different grades of steel at the different storey levels, on the condition of column removal scenario at the corner and middle of an RC frame and the loads are considered as per the GSA guidelines and the DCR value should be within the limited range, and displacement of each frame is determined [5].

Procedure of Linear Static Analysis

- A bare frame model is created in Abaqus for different storey levels like 5, 10, 15 levels and the material properties, load cases, stress–strain behaviour for three different grades of steel were provided.
- The corner and middle column removal is carried over.
- The analysis is run and maximum axial force, bending moment, and shear force is determined.
- As per GSA guidelines, the DCR value is found for each model. According to Figs. 4, 5 and 6 the linear static analysis of RC frame of conventional, corner column removal, middle column removal was shown.

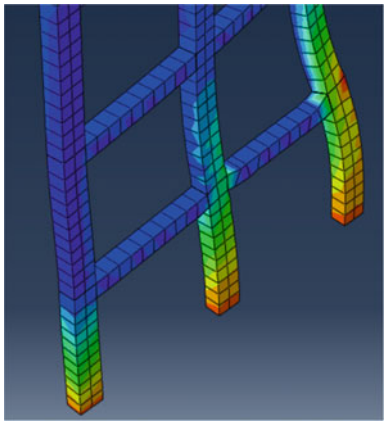

Fig. 5 Conventional frame

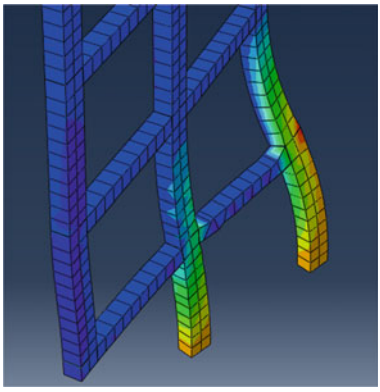

Fig. 6 Corner removal frame

7 Displacement

A displacement is a factor that takes in a structure due to applied load at a particular point. And here the displacement values are observed for different grades of steel at different storey levels concerning the time at the corner and middle column removal and at the different storey, levels were determined [13].

8 Demand Capacity Ratio (DCR)

As per the GSA guidelines, demand capacity ratio is defined as the ratio of acting force, i.e. determination of internal forces of the structure like an axial force of the column bending moment and shear force of a beam [14, 15]. Demand capacity ratio

(DCR) = Abaqus value/theoretical value. Condition to find DCR value as per GSA guidelines.

- If the demand capacity ratio (DCR) value is < 2 (as per GSA guidelines) the structure is safe.
- If the demand capacity ratio (DCR) value is > 2 (as per guidelines) the structure is failing.

9 Results and Discussion for Linear Static Analysis

The results analysed in the FEM was discussed below. There are three different storeys of buildings that were analysed for the linear static analysis and with different grades of steel that were used. The results were compared in terms of time and deflection and the corresponding values for each model were shown in Figs. 7, 8 and 9.

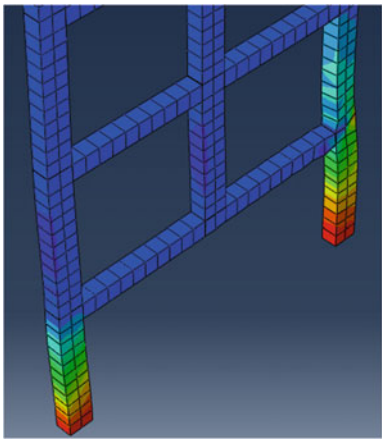

Fig. 7 Middle column removal of frame

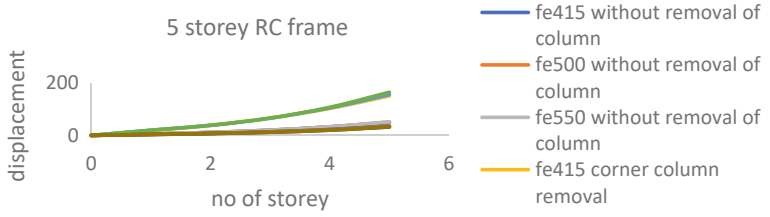

Fig. 8 Graph for a displacement of 5-storey RC frame for the different grades of steel such as FE415, FE500, FE550

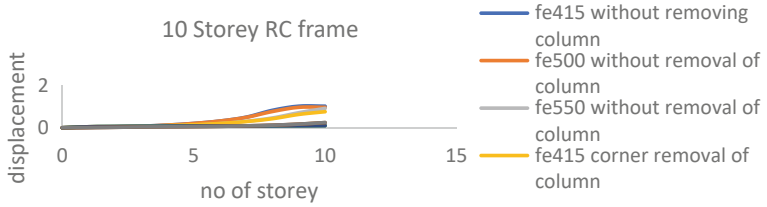

Fig. 9 Graph for the displacement of 10-storey RC frame for the different grades of steel such as FE415, FE500, FE550

Displacement of Linear Static Analysis

Displacement of 5-storey RC frames for the different grades of steel Fe415, Fe500, and Fe550, in this Fe415 grade of steel has 20% more displacement, when compared with the other two grades with the same load applied as the graph plotted in Fig. 8.

Displacement of 10-storey RC frame for the different grades of steel Fe415, Fe500, and Fe550, in this Fe415 grade of steel has 12% more displacement, when compared with the other two grades with the same load applied as the graph plotted in Fig. 9.

Displacement of 15-storey RC frame for the different grades of steel Fe415, Fe500, and Fe550, in this Fe415 grade of steel has 16% more displacement, when compared with the other two grades with the same load applied as the graph plotted in Fig. 10.

Results for Demand Capacity Ratio (DCR) of Column

According to Fig. 11, the demand capacity ratio of an axial load of column Fe415 at middle column removal has a higher DCR value of 0.016, when compared with the other two grades of steel and it is satisfying the DCR limit that should be < 2. According to the above bar chart, it shows that if we move for a higher grade of steel, the DCR value decreases.

According to Fig. 12, the demand capacity ratio of an axial load of column Fe415 at middle column removal has a higher DCR value of 0.018, when compared with the other two grades of steel and it is satisfying the DCR limit that should be < 2.

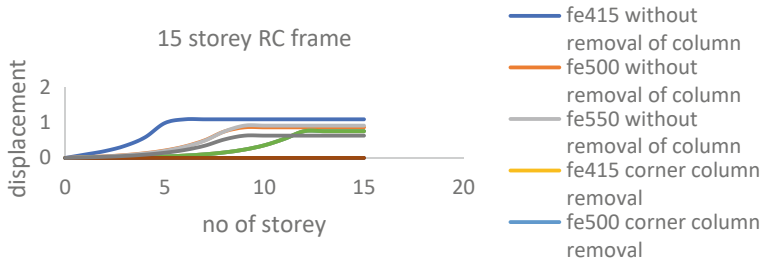

Fig. 10 Graph for a displacement of 15-storey RC frame for the different grades of steel such as FE415, FE500, FE550

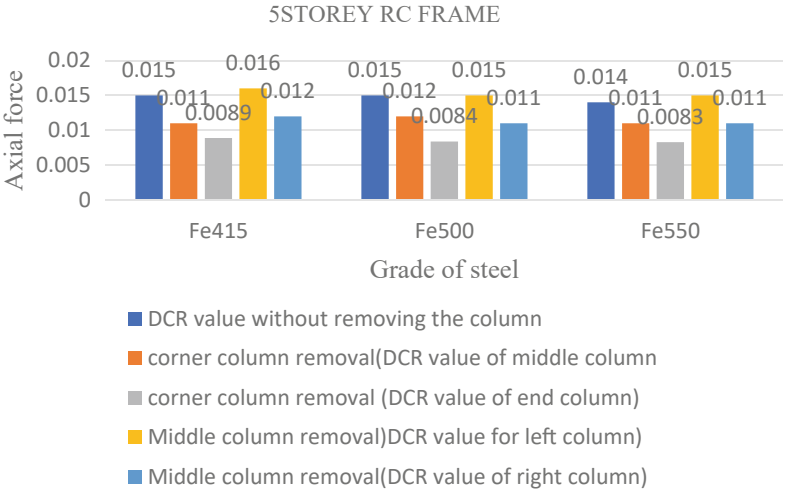

Fig. 11 DCR value of 5 storeys axial load of column

According to the above bar chart, it shows that if we move for a higher grade of steel the DCR value decreases.

According to Fig. 13, the demand capacity ratio of an axial load of column Fe415 at middle column removal has a higher DCR value of 0.019, when compared with the other two grades of steel and it is satisfying the DCR limit that should be < 2. According to the above bar chart, it shows that if we move for a higher grade of steel the DCR value decreases.

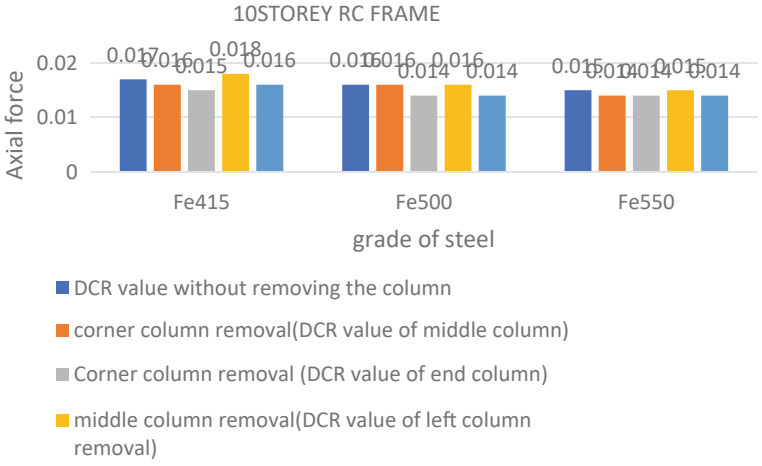

Fig. 12 DCR value of 10 storeys axial load of column

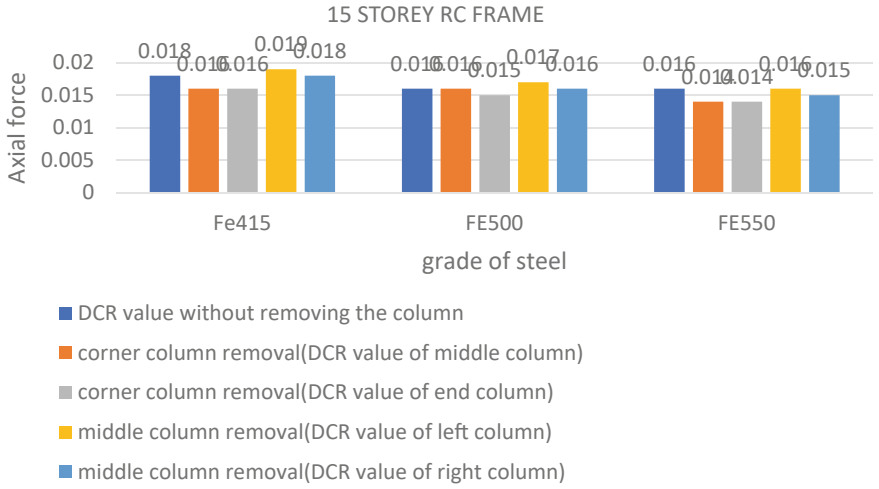

Fig. 13 DCR value of 15 storeys axial load of column

Results for Demand Capacity Ratio (DCR) of Beam

According to Fig. 14, the demand capacity ratio of bending moment of the beam of Fe500 at middle column removal has a higher DCR value of 0.0116, when compared with the other two grades of steel and it is satisfying the DCR limit that should be < 2.

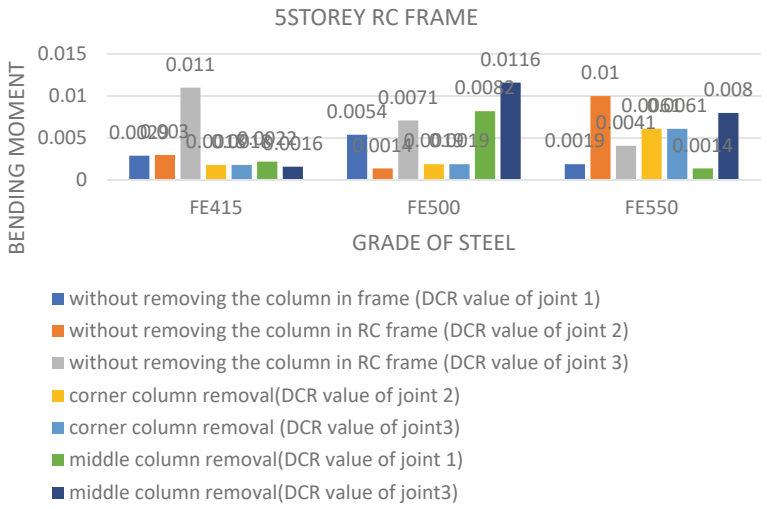

Fig. 14 DCR value of 5 storeys bending moment of beam

According to Fig. 15, the demand capacity ratio of bending moment of the beam of Fe500 without removing the column has a higher DCR value of 0.78, when compared with the other two grades of steel and it is satisfying the DCR limit that should be < 2.

According to Fig. 16, the demand capacity ratio of bending moment of the beam of Fe500 without removing the column has a higher DCR value of 0.85, when compared with the other two grades of steel and it is satisfying the DCR limit that should be < 2.

According to Fig. 17, the demand capacity ratio of bending moment of the beam of Fe500 without removing the column has a higher DCR value of 0.096, when

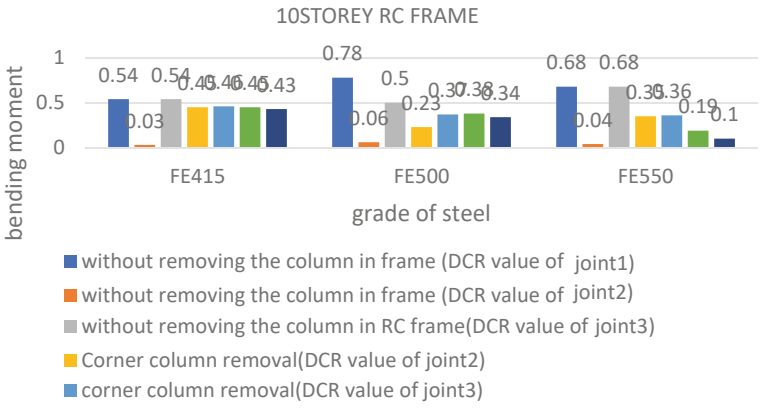

Fig. 15 DCR value of 10 storeys bending moment of beam

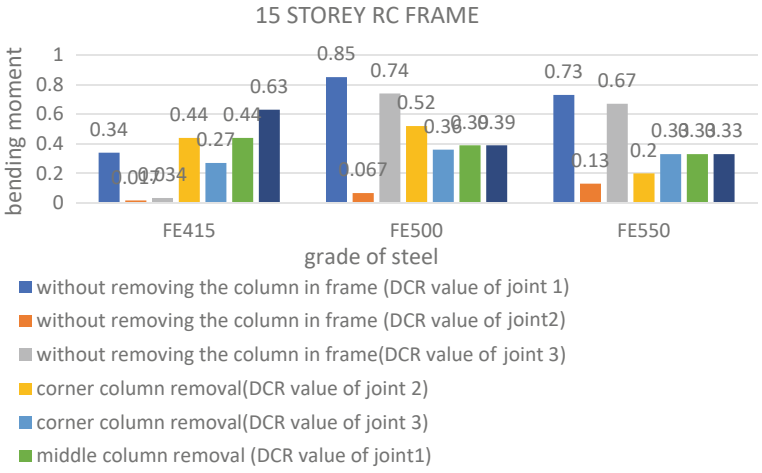

Fig. 16 DCR value of 15 storeys bending moment of beam

compared with the other two grades of steel and it is satisfying the DCR limit that should be < 2.

According to Fig. 18, the demand capacity ratio of bending moment of the beam of Fe500 without removing the column has a higher DCR value of 0.107, when compared with the other two grades of steel and it is satisfying the DCR limit that should be < 2.

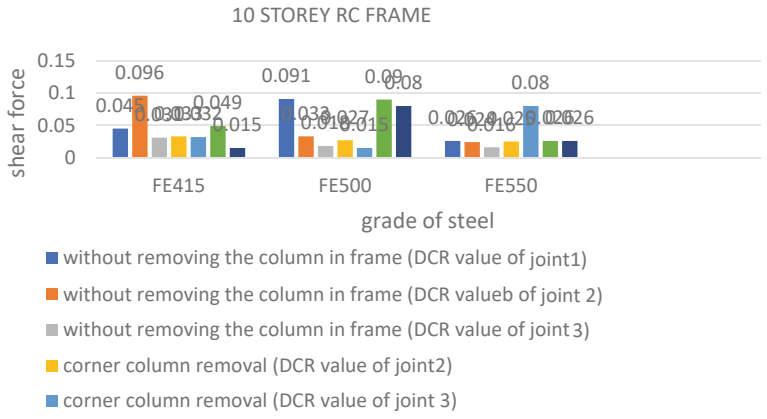

Fig. 17 DCR value of 10-storey shear force of the beam

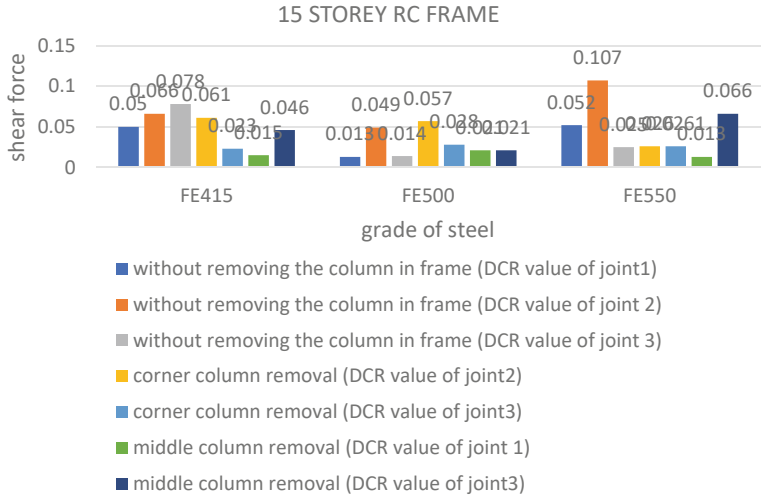

Fig. 18 DCR value of 15-storey shear force of the beam

10 Conclusion

- In this study, the behaviour of 5-storey, 10-storey, and 15-storey RC bare frame under the middle and corner column removal with a 2D finite element modelling software Abaqus was used. Based on this model, parametric studies like linear static analysis were done.
- According to the above analysis results, it shows that higher grades of steel have less DCR value when compared with lower grades of steel and it reduces some failure effects of the structure. As per GSA guidelines, the DCR value should be < 2 and the symmetrical structure determined is predicted correctly.

References

1. Starossek U (2009) Progressive collapse of structures, vol 153. London: Thomas Telford
2. Byfield M, Mudalige W, Morison C, Stoddart E (2014) A review of progressive collapse research and regulations. Proc Instit Civil Eng Struct Build 167(8):447–456
3. Marjanishvili SM (2004) Progressive analysis procedure for progressive collapse. J Perform Constr Facil 18(2):79–85
4. Bao Y, Kunnath SK, El-Tawil S, Lew HS (2008) Macro model-based simulation of progressive collapse: RC frame structures. J Struct Eng 134(7):1079–1091
5. General Service Administration Guidelines (2013) Alternate path analysis and design guidelines for progressive collapse resistance
6. Al-Salloum YA, Almusallam TH, Khawaji MY, Ngo T, Elsanadedy HM, Abbas H (2015) Progressive collapse analysis of RC buildings against internal blast. Adv Struct Eng 18(12):2181–2192
7. Seethalakshmi MS, Prakash M, Satyanarayanan KS, Thamilarasu V (2016) Effect of masonry infill structure with openings during progressive collapse by removing a middle column. Ind J Sci Technol 9:23
8. Gowtham S, Prakash M, Parthasarathi N, Satyanarayanan KS, Thamilarasu V (2018) 2D-Linear static and non-linear dynamic progressive collapse analysis of the reinforced concrete building. Mater Today Proc 5(2):8775–8783
9. Vieira ADA, Triantafyllou SP, Bournas DA (2020) Strengthening of RC frame subassemblies against progressive collapse using TRM and NSM reinforcement. Eng Struct 207:110002
10. Huang H, Huang M, Zhang W, Guo M, Chen Z, Li M (2021) Progressive collapse resistance of multistorey RC frame strengthened with HPFL-BSP. J Build Eng 43:103123
11. Marjanishvili S, Agnew E (2006) Comparison of various procedures for progressive collapse analysis. J Perform Constr Facil 20(4):365–374
12. Tsai MH, Huang TC (2009) Effect of interior brick-infill partitions on the progressive collapse potential of an RC building: linear static analysis results. Eng Technol 26:883–889
13. Li Y, Lu X, Guan H, Ye L (2014) An energy-based assessment on dynamic amplification factor for linear static analysis in progressive collapse design of ductile RC frame structures. Adv Struct Eng 17(8):1217–1225
14. Tsai MH, Lin BH (2008) Investigation of progressive collapse resistance and inelastic response for an earthquake-resistant RC building subjected to column failure. Eng Struct 30(12):3619–3628
15. Song BI, Sezen H (2013) Experimental and analytical progressive collapse assessment of a steel frame building. Eng Struct 56:664–672

Numerical Study on Strengthening of Brick Masonry Walls Using CFRP Strips

Shristi Sah and N. Umamaheswari

Abstract Structure constructed of brick masonry wall along with mud mortar has been used since long time in construction industry. It will get deteriorated due to various reasons and it is essential to find a method/material to strengthen it, since it is necessary to preserve values and culture of previous generation. Carbon fiber-reinforced polymer (CFRP) possesses essential properties and it has been tried and tested widely in structural repairs. The objective of the present study is to determine the effectiveness of using CFRP strips of varying thickness and width on enhancing load carrying capacity of brick masonry walls. Hence in the present numerical study, three sets of brick masonry wall models, each consisting of seven sample walls has been considered, modeled and strengthened using CFRP strips in various layouts. Increase in the thickness of strips had less impact on strength whereas increase in width of strips up to 240 mm provided considerable improvement in load resisting capacity of wall (up to 70%) along with reduction in strain in walls. Out of several layouts and dimensions of CFRP strips considered, combination of horizontal and vertical strips with thickness 3 mm and width 240 mm, respectively, is found to be more effective in terms of load resisting capacity and reduction in strain.

Keywords CFRP strengthening · Masonry wall · Failure pattern · Numerical study · Layout of CFRP

1 Introduction

It is found from history that brick masonry wall has been used as an essential building component in many parts of the world. The structures consisting of brick masonry elements are more prone to failure during earthquakes since less consideration is given for earthquake resistance during design. Strengthening of such walls protects identity of the place and also adds value to the existence of such structures.

S. Sah · N. Umamaheswari (✉)
Department of Civil Engineering, Faculty of Engineering and Technology, SRM Institute of Science and Technology, Kattankulathur, Tamil Nadu 603203, India
e-mail: umamahen@srmist.edu.in

K. R. Reddy et al. (eds.), *Recent Advances in Civil Engineering*, Lecture Notes in Civil Engineering 398, https://doi.org/10.1007/978-981-99-6229-7_60

Lignola et al. [1] investigated unreinforced masonry wall and then the retrofitted wall with diagonal and horizontal strips of FRP. Numerical, theoretical as well as experimental studies were carried out to find the effective method of providing FRP strips. It was observed that the diagonal FRP strips provided better improvement in terms of shear capacity and shear distribution. Also, FRP width increment was found to increase the performance of wall panel.

Willis et al. [2, 3] conducted a series of 29 pull-out tests to examine the use of externally bonded FRP strips over masonry walls. Study was focused on increasing bond strength in NSM specimens. The study highlighted that bond behavior and load transfer mechanism of FRP bonded with masonry were very similar to the bond between concrete and FRP strips.

Hamed and Rabinovitch [4] studied out-of-plane behavior of unreinforced masonry walls strengthened with FRP strips. Investigation for unreinforced masonry (URM) walls has been conducted analytically and flexural performance of the walls was observed. It was observed that the use of FRP strips decreased out-of-plane deflection. Results reflected that if coverage area of FRP strips in wall is more, the capacity of walls increased to a larger extent and depth of strips will have less impact only on strength of wall. Zhuge et al. [5] have presented the review of research in the area of strengthening of wall with FRP. Sheet FRP and strip FRP were arranged as a truss element in wall specimen. Strengthening wall with horizontal strips proved to be less effective in terms of shear and flexure capacity of walls. It was observed that provision of glass fiber in strengthening procedure induced shear failure. Mahmood et al. [6] studied the behavior of seventeen masonry walls retrofitted with CFRP and GFRP strips in order to study the shear strength mechanism of walls. It was observed that there was significant increase in ductility and toughness of walls. From the results of experiments, it was observed that larger increase in shear capacity up to 325% was obtained and provision of FRP strips only on one side of the wall itself was proven to be effective.

2 Use of CFRP for Strengthening of Masonry Walls

Carbon fiber-reinforced polymer (CFRP) has been extensively used in construction industry especially for repair and maintenance of existing structures [1]. CFRP application to strengthening of heritage buildings has been extensively increasing, because of its properties such as high fatigue strength, corrosion resistance, resistance to chemicals and high protective nature from electromagnetic radiation. CFRP application to masonry reduces cracks initiated during earthquake of high intensity [2, 3, 7]. Properties such as high strength to weight ratio and high tensile strength of CFRP make it as a feasible material for strengthening of masonry [8].

3 Numerical Investigation Using Finite Element Method (FEM)

Experimental study may not be feasible because of the following reasons, such as environmental conditions, time constraints, lack of availability of labor, material constraints, economic reasons, unavailability of specific testing machines and equipment for testing or for casting, error in mix design or material usage which can cause inadequate results [2, 3, 9]. Hence it is quite practical to go for numerical study.

FEM is quite popular and most widely used method to study the structure's behavior under applied load. It is a tool which saves time from forming experimental setup, reduce human error and provide quite accurate results with the constraint that effective input is given to get proper solution. FEM can be used to predict the behavior of complex model too, and is successful in generating accurate results. The concept of this method is dividing a structure into many numbers of elements and generating most accurate results as possible. The method can be used for both linear and nonlinear analysis of the structure. Complex geometry is broken down into parts and then analyzed for getting output. Its application is increasing day by day because of development of high engineering as well as computer knowledge among people.

In field, mostly the problems are nonlinear in nature and it is necessary to solve using nonlinear analysis (NLA) for obtaining good output. NLA can be complex depending upon the nature of material, extent of output, relationship of load and geometry, and these problems can be easily solved using finite element software [2, 3, 9]. ANSYS Workbench 2021 R2 2021 is excellent software operating to get viable outputs in the field of NLA. ANSYS runs and produces precise results based on criteria such as input material qualities, meshing, correct boundary conditions and material properties. In the current numerical study, an attempt was made to validate research work [8], by performing analysis using ANSYS Workbench 2021 R2 2021 for masonry wall joint using cement lime collar joint, and further analysis has been done as an extension for better understanding and presented in this paper.

3.1 Model Description

Three sets of brick masonry wall models Set 1, Set 2 and Set 3, each consisting of seven wall models from W1 to W7, W8 to W14 and W15 to W21, respectively, were simulated. The modeled walls were retrofitted with CFRP strips in different layouts. The geometrical and material properties of wall models of Set 1 have been given in Tables 1 and 2, respectively.

Compressive strength of the brick and mortar of wall models of Set 1 has been given in Table 3.

The geometry of walls of Set 2 was changed keeping the mechanical properties the same as that of Set 1 wall models. The geometrical properties of wall models of Set 2 have been given in Table 4.

Table 1 Geometrical properties of walls—Set 1

Dimensions of brick	Dimensions of wall specimen	Mortar
Length = 215 mm	Length = 900 mm	Thickness = 10 mm
Breadth = 102.5 mm	Width = 975 mm	Type = Type S and N mortar
Depth = 65 mm	Depth = 102.5 mm (single leaf), Depth = 215 mm (double leaf)	

Table 2 Material properties of walls—Set 1

Types of material	Compressive strength (N/mm^2)	Modulus of elasticity (N/mm^2)	Poisson's ratio
Brick	5.05	4300	0.238
Mortar	1.40	1170	0.147

Table 3 Compressive strength of the brick and mortar of walls—Set 1

Wall specimen	Wall type	Mortar type	Compressive strength of brick (MPa)	Compressive strength of mortar (MPa)
W1	Single-leaf	S	5.05	1.40
W2		S	7.6	1.64
W3		N	6.6	1.52
W4	Double-leaf	N	5.05	1.40
W5		N	7.6	1.64
W6	Single-leaf	N	6.6	1.52
W7	Double-leaf	N	6.6	1.52

Table 4 Geometrical properties of walls of Set 2

Wall specimen	Wall type	Mortar thickness (mm)	Brick dimension (l × b × h) (mm)	Panel dimension (l × b × h) (mm)
W8	Triple-leaf	20	205 × 135 × 60	1290 × 1260 × 445
W9	Double-leaf	20	205 × 135 × 60	1290 × 1260 × 290
W10	Quadruple-leaf	20	205 × 135 × 60	1290 × 1260 × 600
W11	Single-leaf	10	205 × 135 × 60	1290 × 1260 × 135
W12	Triple-leaf	10	215 × 102.5 × 65	900 × 975 × 327.5
W13	Quadruple-leaf	10	215 × 102.5 × 65	900 × 975 × 440
W14	Triple-leaf	10	215 × 102.5 × 65	1800 × 975 × 327.5

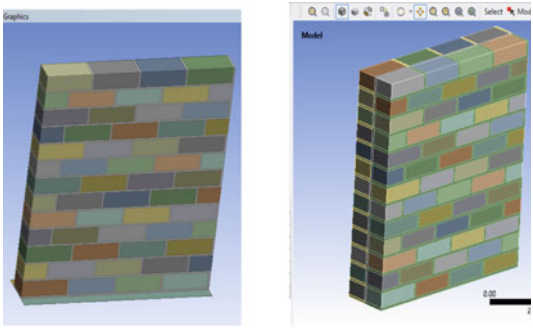

(a): Single Leaf wall **(b): Double Leaf wall**

Fig. 1 Wall models—Set 1

The geometry of walls of Set 3 was kept the same as that of Set 2 and the mechanical properties the same as that of Set 1 wall models.

3.2 Modeling of Walls

Masonry walls of types, single, double, triple and quadruple-leaf walls of varying height, width and length were modeled using ANSYS Workbench 2021 R2 under SpaceClaim and DesignModeler tabs under Static Structural project model. The modeled single and double-leaf walls of Set 1 are shown in Fig. 1a and b, respectively.

3.3 Meshing

Multi zone meshing with free mesh type as Hexa Core was used for wall models. Meshing of double, triple and quadruple-leaf walls is shown in Fig. 2a–c, respectively.

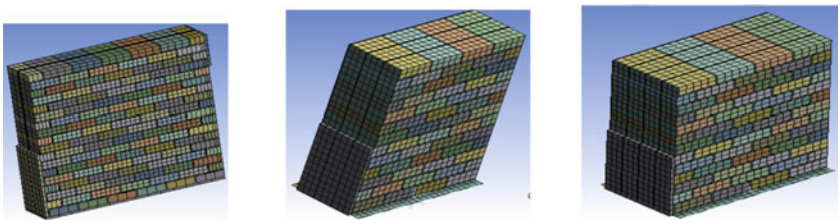

(a): Double Leaf Wall **(b): Triple Leaf Wall** **(c): Quadruple-leaf walls**

Fig. 2 Wall meshing

3.4 Loads and Boundary Conditions

The load application methods and support conditions are explained in this section. Horizontal loads are applied on three bricks on right side, vertical loads on two bricks in downward direction and compression only on support on the three bricks and mortar in opposite direction of load application. Displacement was found in the bottom bricks along z-direction.

4 Retrofitting of the Wall Models

Retrofitting of masonry walls using CFRP strips provided in different layouts was performed for three sets of wall models under consideration. CFRP strips used were connected to the masonry wall through 'bonded contact' in order to avoid slippage failure. Strips of constant thickness of 3 mm and varying width (between 50–2400 mm) were used for strengthening purpose. Mechanical properties of CFRP strips used for strengthening technique are given in Table 5.

4.1 Retrofitting of Wall Models of Set 1

Wall models of Set 1, W1–W7 were retrofitted using CFRP strips of thickness 3 mm and width varying between 50–70 mm. Layout of the CFRP in wall models of Set 1 consisted of combination of diagonal strips in different configurations like V and X-shaped. The layout of combination of CFRP strips used in the strengthening of wall models of Set 1, W1–W7 is shown in Fig. 3a–g, respectively.

4.2 Retrofitting of Wall Models of Set 2

Wall models of Set 2, W8–W14 were retrofitted using CFRP strips of thickness 3 mm and width varying between 70–140 mm. Layout of the CFRP in wall models of Set

Table 5 Mechanical properties of CFRP strips

Tensile strength	3500 MPa
Modulus of elasticity	220,000 MPa
Density	1500 kg/m^3
Poisson's ratio	0.3
Compressive strength	1400 MPa
Specific gravity	1.75 gr/cm^3

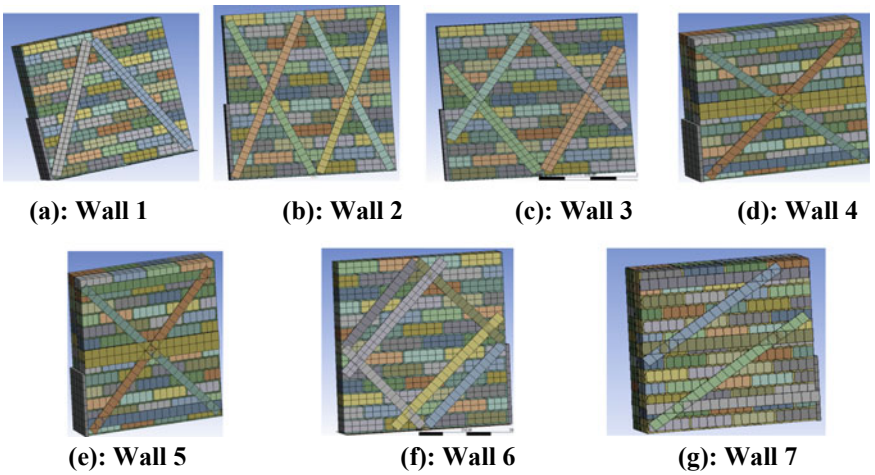

Fig. 3 Layout of CFRP strips for masonry walls of Set 1

2 consisted of combination of diagonal, horizontal and vertical strips in different configurations like Z- and H-shaped. The layout of combination of CFRP strips used in the strengthening of wall models of Set 2, W8–W14 is shown in Fig. 4a–g, respectively.

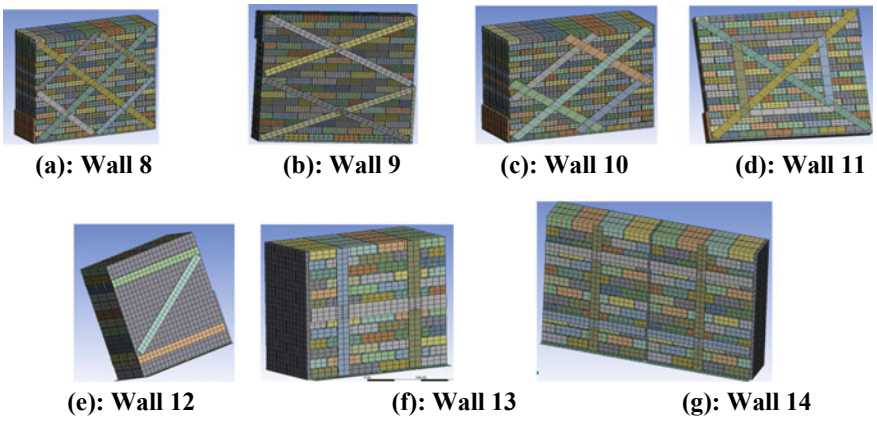

Fig. 4 Layout of CFRP strips for masonry walls of Set 2

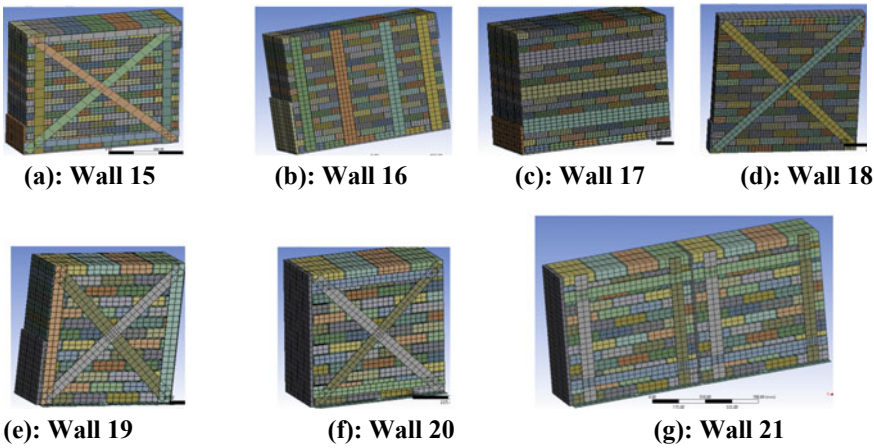

Fig. 5 Layout of CFRP strips for masonry walls of Set 3

4.3 Retrofitting of Wall Models of Set 3

Wall models of Set 3, W15 to W21, were retrofitted using CFRP strips of thickness 3 mm and width varying between 140–240 mm. Layout of the CFRP strips in wall models of Set 3 consisted of combination of diagonal, horizontal and vertical strips. The layout of combination of CFRP strips used in the strengthening of wall models of Set 3, W15–W21 is shown in Fig. 5a–g, respectively.

5 Results and Discussion

5.1 Load–Deflection Behavior

The three sets of unstrengthened wall models were modeled using ANSYS Workbench 2021 R2 and upon applying loading and boundary conditions, load–deflection plots were obtained and compared with strengthened walls. Load–deflection plots for unstrengthened walls for Set 1, 2 and 3 are shown in Fig. 6a–c, respectively.

From the plots obtained, it can be observed that for walls of Set 1, the maximum load resisting capacity was obtained in double-leaf wall W4, of 72 kN with corresponding deflection of 2.5 mm. Load deflection plots for strengthened walls for Set 1, 2 and 3 are shown in Fig. 7a–c, respectively.

From the plots obtained, it can be observed that for walls of Set 1, some increment in load resisting capacity and reduction in displacement was occurring due to strengthening procedure. From Set 1, for wall W4, the load resisting capacity

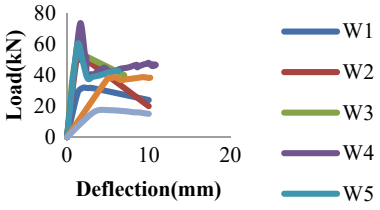

(a): Brick Masonry wall models-Set 1

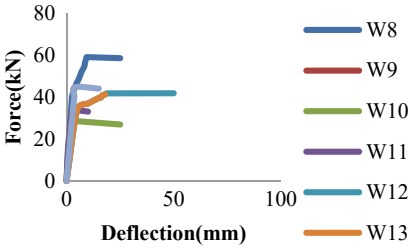

(b): Brick Masonry wall models-Set 2

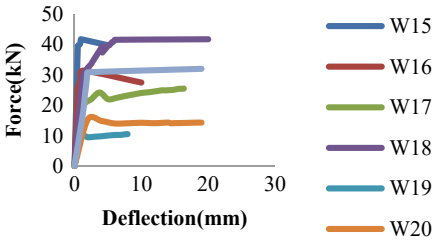

(c): Brick Masonry wall models-Set 3

Fig. 6 Load–deflection behavior of unstrengthened brick masonry wall models

has been increased from 72 to 101 kN which is 40.2% increment in load resisting capacity, similar to Lignola et al. [1] and Willis et al. [2, 3].

Of all the walls modeled and retrofitted, the increase in load resisting capacity was observed for all three sets which is given in Table 6.

5.2 Strain Diagram

Strain developed in unstrengthened masonry walls was taken by bricks and mortar, which ultimately resulted in crushing of the wall from point of load application to fixed support at the bottom. Strain in the brick masonry for walls of Set 1, 2 and 3 obtained (samples) was shown in Fig. 8a–c, respectively.

From the strain diagrams, it can be observed that strain in single-leaf wall was maximum at the point of application of vertical load, horizontal load and in fixed support, similar to Hamed and Rabinovitch [4] and Zhuge [5]. In the case of double- and triple-leaf wall, maximum strain appeared at top face of the brick masonry wall and minimum strain at fixed support.

Addition of CFRP strips as strengthening component in the brick masonry walls of Sets 1, 2 and 3 resulted in changes in strain pattern of walls which was shown in Fig. 9a–c respectively.

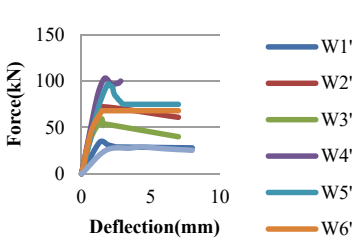

(a): Brick Masonry wall models-Set 1

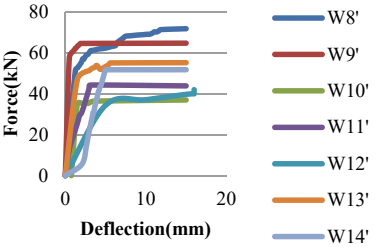

(b): Brick Masonry wall models-Set 2

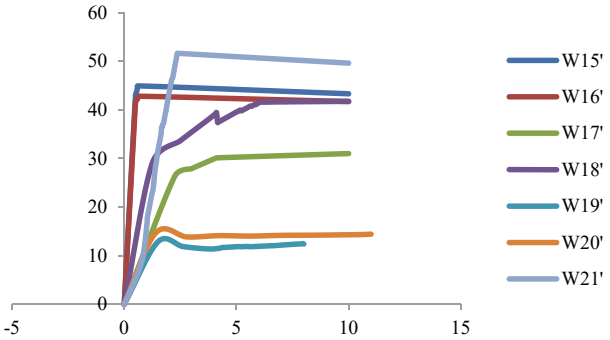

(c): Brick Masonry wall models-Set 3

Fig. 7 Load–deflection behavior of strengthened brick masonry wall models

Table 6 Increase in load resisting capacity after strengthening

Wall models—Set 1		Wall models—Set 2		Wall models—Set 3	
Wall specimen	Increase in load resisting capacity (%)	Wall specimen	Increase in load resisting capacity (%)	Wall specimen	Increase in load resisting capacity (%)
W1	9	W8	21	W15	12
W2	12	W9	23	W16	25
W3	22	W10	25	W17	25
W4	41	W11	32	W18	20
W5	54	W12	12	W19	30
W6	28	W13	37	W20	26
W7	52	W14	15	W21	70

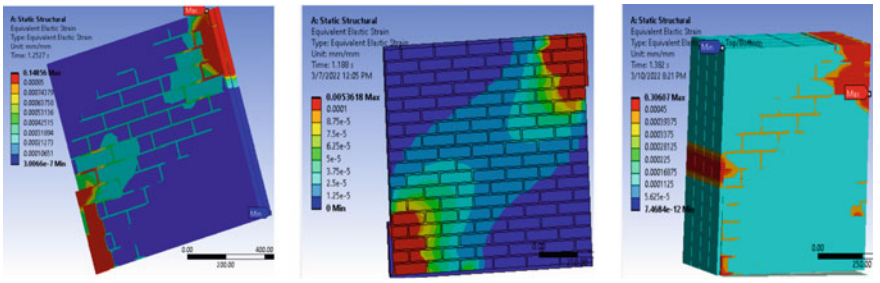

(a): Wall 4 (b): Wall 11 (c): Wall 20

Fig. 8 Failure pattern of sample walls before strengthening

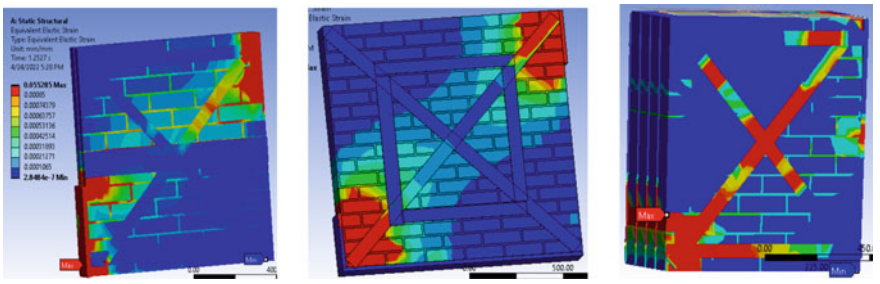

(a): Wall 4' (b): Wall 11' (c): Wall 20'

Fig. 9 Failure pattern of sample walls after strengthening

Failure pattern indicated that larger width of strips helped in decreasing strain to a greater extent. From model simulation, it was observed that maximum strains were undertaken by the CFRP strips and less impact had occurred in the brick masonry walls. For walls of Set 3, for model W20', strain was maximum at the area of provision of CFRP strips, which indicated strain was resisted by the strips to a larger extent protecting the masonry wall underneath. It can be concluded from present numerical study, CFRP strips strengthening can be largely used for load resisting purpose as well as protection of wall from excess deformation during earthquakes.

6 Conclusion

The present study is based on model creation of three sets of brick masonry wall samples along with varying pattern and appropriate layout of CFRP retrofitting strips over the masonry wall samples in order to obtain best results in terms of load resisting capacity and strain in the walls. Wall models were formed considering low quality

of brick and mud mortar to form a weaker masonry wall and then strengthened with CFRP strips if width ranging from 50 to 240 mm.

From the present numerical study, it was observed that the maximum strength increases as a result of strengthening of the walls that were found to be higher for when larger width of strips was provided. Thickness of CFRP strips was not showing much impact on the strength of masonry walls. Combination of diagonal and horizontal strips had shown high increase in strength and reduction in strain of the walls. Sample W21 of Set 3, maximum increase in load resisting capacity of 70% was obtained through the combination of horizontal and vertical strips of thickness 3 mm and width 200 mm.

It can be concluded that CFRP strengthening will be an applicable solution for protection of masonry wall against excessive deformation and crack due to earthquake.

Author Contribution All authors contributed to the study conception and design. Material preparation, data collection and numerical analysis were performed by Shristi Sah. The first draft of the manuscript was written by Shristi Sah and conceptualization and supervision, comments, writing, editing, corrections, checking results and discussions by N. Umamaheswari. All authors read and approved the final manuscript.

References

1. Lignola GP, Prota A, Manfredi G (2012) Numerical investigation on the influence of FRP retrofit layout and geometry on the in-plane behavior of masonry walls. J Compos Constr 16(6):712–723. https://doi.org/10.1061/(ASCE)CC.1943-5614.0000297
2. Willis CR, Yang Q, Seracino R, Griffith MC (2009) Bond behaviour of FRP-to-clay brick masonry joints. Eng Struct 31(11):2580–2587. https://doi.org/10.1016/j.engstruct.2009.10.015
3. Willis CR, Yang Q, Seracino R, Griffith MC (2009) Damaged masonry walls in two-way bending retrofitted with vertical FRP strips. Constr Build Mater 23(4):1591–1604. https://doi.org/10.1016/j.conbuildmat.2007.09.007
4. Hamed E, Rabinovitch O (2007) Out-of-plane behavior of unreinforced masonry walls strengthened with FRP strips. Compos Sci Technol 67(3–4):489–500. https://doi.org/10.1016/j.compscitech.2006.08.021
5. Zhuge Y (2010) FRP-retrofitted URM walls under in-plane shear: review and assessment of available models. J Compos Constr 14(6):743–753. https://doi.org/10.1061/(ASCE)CC.1943-5614.0000135
6. Mahmood H, Ingham JM (2011) Diagonal compression testing of FRP-retrofitted unreinforced clay brick masonry wallettes. J Compos Constr 15(5):810–820. https://doi.org/10.1061/(ASCE)CC.1943-5614.0000209
7. Willis CR, Seracino R, Griffith MC (2010) Out-of-plane strength of brick masonry retrofitted with horizontal NSM CFRP strips. Eng Struct 32(2):547–555. https://doi.org/10.1016/j.engstruct.2009.10.015
8. Su Y, Wu C, Griffth MC (2011) Modelling of the bond–slip behavior in FRP reinforced masonry. Constr Build Mater 25(1):328–334. https://doi.org/10.1016/j.conbuildmat.2010.06.021001
9. Li B, Qian K, Tran CTN (2013) Retrofitting earthquake-damaged RC structural walls with openings by externally bonded FRP strips and sheets. J Compos Constr 17(2):259–270. https://doi.org/10.1061/(ASCE)CC.1943-5614.0000336

Correction to: A Wastewater Reclamation Using Soil Aquifer Treatment (SAT) Technology to Enhance Groundwater Recharge

L. Chandrakanthamma and K. Prasanna

Correction to:
Chapter 36 in: K. R. Reddy et al. (eds.), *Recent Advances in Civil Engineering*, Lecture Notes in Civil Engineering 398, https://doi.org/10.1007/978-981-99-6229-7_36

In the original version of the book the following belated corrections were incorporated: In chapter 36, the affiliation of the author 'L. Chandrakanthamma' has been changed to "Department of Civil Engineering, Easwari Engineering College, Ramapuram, Chennai, India" and the affiliation of the author 'K. Prasanna' has been changed to "Department of Civil Engineering, Faculty of Engineering and Technology, SRM Institute of Science and Technology, Kattankulathur, Tamil Nadu, 603203, India". The book and the correction chapter have been updated with the changes.

The updated version of this chapter can be found at
https://doi.org/10.1007/978-981-99-6229-7_36

K. R. Reddy et al. (eds.), *Recent Advances in Civil Engineering*, Lecture Notes in Civil Engineering 398, https://doi.org/10.1007/978-981-99-6229-7_61